Investigating the regulation of DNA non-homologous end-joining through Ku70/80 interacting factors

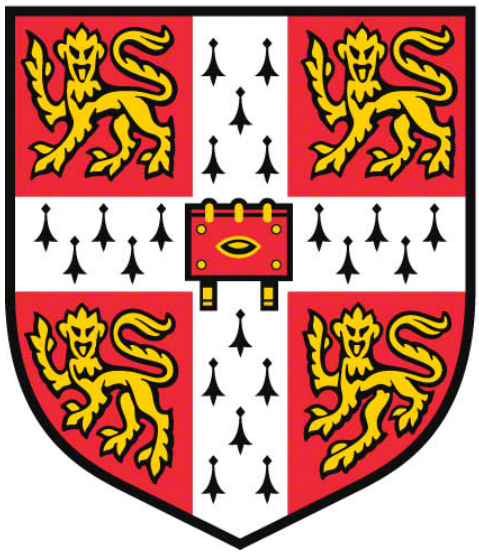

Rohan Sivapalan
University of Cambridge
Darwin College

This dissertation is submitted for the degree of Doctor of Philosophy

September 2018

Investigating the regulation of DNA non-homologous end-joining through Ku70/80 interacting factors

Summary

DNA double-strand breaks are the most deleterious type of DNA damage that cells experience, which makes the study of double-strand break repair extremely important. Unrepaired or aberrantly repaired DNA can result in changes to core genes with critical function and thus lead to multiple diseases. Two main repair pathways for double-strand breaks exist: homologous recombination (HR) and non-homologous end-joining (NHEJ). Whilst the regulation of HR has been heavily investigated, the regulation of NHEJ remains to be fully explored. The aim of this thesis is to investigate the regulation of DNA NHEJ through interacting factors of the core NHEJ protein heterodimer, Ku70/80 (Ku).

This thesis consists of three main research projects. The first, explores the potential role of the CUL4 substrate adaptor, WDR76, in the removal of Ku from sites of DNA damage. Data presented here highlight a role of WDR76 in the DNA damage response (DDR), and through effects on Ku removal kinetics, suggest a role for WDR76 in the regulating NHEJ.

The second research project investigates a potential cyclin-dependent kinase phosphorylation site on the protein paralog of XRCC4 and XLF (PAXX). As PAXX is a Ku interactor with a role in NHEJ, the effect of PAXX phosphorylation is investigated as a potential NHEJ regulatory system.

Lastly, I investigate the role of the RecQ helicase WRN, whose precise roles in the DDR are unclear. As an interactor of both HR and NHEJ proteins, WRN may affect the regulation of both pathways. WRN knockout cells were generated and a CRISPR-Cas9 screen performed to identify suppressors of WRN sensitivity to DNA damage. The targets identified offer insights into WRN function.

Rohan Sivapalan

September 2018

Preface

This dissertation is the result of my own work and includes nothing which is the outcome of work done in collaboration except as declared in the Preface and specified in the text.

It is not substantially the same as any that I have submitted, or, is being concurrently submitted for a degree or diploma or other qualification at the University of Cambridge or any other University or similar institution except as declared in the Preface and specified in the text. I further state that no substantial part of my dissertation has already been submitted, or, is being concurrently submitted for any such degree, diploma or other qualification at the University of Cambridge or any other University or similar institution except as declared in the Preface and specified text.

It does not exceed the prescribed word limit for the relevant Degree Committee.

Rohan Sivapalan
September 2018

Acknowledgements

I would like to thank a number of people and organisations, without whom this work would not have been possible. Firstly, I would like to thank Professor Steve Jackson. I am extremely grateful for the opportunity he has given me to be part of his lab, allowing me to experience a cutting-edge academic lab at the forefront of its field. I am also thankful for all his support and supervision over the years.

The Steve Jackson laboratory and the Gurdon Institute has been a great place to work in over the years. All the members who have overlapped with my time here have contributed to making it such a pleasant environment. In particular I thank my day to day supervisors in the lab, Andrew Blackford, Natalia Lukashchuk and Delphine Larrieu for their guidance, patience and support with everything. I will forever be grateful to them for taking the time to discuss and explain complex ideas with me and for their help with my relevant projects. In addition, I would like to thank Jessica Brown for her help early on in my studies and all the efforts of Kate Dry and Helen Reed in helping me with the admin throughout my studies. Dr Fabio Puddu and Iñigo Ayestaran have been instrumental in bioinformatics analysis of my data. Both of them are fantastic individuals who have performed and explained the analysis of my sequencing data. I particularly thank Fabio for teaching me some of the basics of coding (and not forgetting his help with my yeast work) in an enjoyable way. Julia Coates is the heart of the lab. Some of the most enjoyable times of my studies have been those spent working alongside her in the tissue culture lab. My lunch time buddies over the years: Linda, Sati, Julia, Matylda, Muku, Israel, Paco and Gonzalo have provided me with laughs, in-depth conversations and encouragement for which I am very appreciative.

I wish to thank the BBSRC and Horizon Discovery for their help in facilitating my studies; in particular Tom Henley and Rob Howes for all their support in the application process.

My family have shown interest and amazement in my work which has been inspiring and supportive. Many friends and family members have helped me along the way to get this far. To my two best PhD friends, Hanae Shimo and Wei Qiang Seow, we have been on a long

journey together over the years, and it has been great experiencing it together with the two of you. Throughout the highs and lows you have supported me along the way.

Last but not least, I would like to thank Gail for all her support before, during and hopefully after my studies. None of this would have been possible without her. She has embraced the journey together with me and words cannot describe my full admiration and gratitude towards her.

Table of Contents

Summary 2

Preface 3

Acknowledgements 4

Table of Figures 11

Table of Tables 13

Table of Appendices 13

List of Abbreviations 14

Chapter 1: Introduction 21

1. Introduction 22

1.1. The integrity of DNA 22

1.2. DNA repair pathways 23

1.2.1. Base excision repair and single-strand break repair 23

1.2.2. Mismatch repair 24

1.2.3. Nucleotide excision repair and inter-strand crosslink repair 24

1.2.4. Double strand breaks and their repair 25

1.3. Initial double strand break response 26

1.4. Roles of ATM/ATR in checkpoint signalling 27

1.5. Homologous recombination (HR) 28

1.6. Non-homologous end-joining (NHEJ) 31

1.7. Consequences of improper repair 34

1.8. Regulation of HR vs. NHEJ 36

1.9. The DSB repair protein, Ku 37

1.10. Regulation and Removal of Ku 39

1.11. Aims of projects in thesis 39

Chapter 2: Methods 41

2. Methods 42

2.1. Mammalian cell culture techniques 42

2.1.1. Cell culture maintenance 42

2.1.2. Mammalian cell stock freezing and revival 42

2.1.3. siRNA transfections 43

2.1.4. Plasmid transfections 43

2.1.5. Electroporation 43

2.1.6. Stable cell line generation 43

2.1.7. Cell cycle synchronisation 44

2.2. Survival Assays 45

2.2.1. Clonogenic cell survival assay 45

2.2.2. IncuCyte® cell growth assays 45

2.2.3. Hoechst 33342 staining cell survival assay 45

2.2.4. Crystal violet staining 46

2.3. Yeast work 46

2.3.1. Yeast culture 46

2.3.2. Yeast knockout generation 46

2.3.3. Yeast DNA damage sensitivity assays 46

2.4. Immunofluorescence 47

2.4.1. Persistence of Ku Foci by immunofluorescent staining 47

2.4.2. Laser line micro-irradiation 47

2.4.3. ClickiT EU – RNA imaging – transcription inhibition at sites of laser lines 48

2.5. Molecular biology techniques 48

2.5.1. Polymerase chain reaction (PCR) 48

2.5.2. Agarose gel electrophoresis 49

2.5.3. PCR purification 49

2.5.4. Immunoprecipitation 49

2.5.5. Protein extractions 50

2.5.6. Western blotting 50

2.5.7. Chromatin fractionation 51

2.5.8. Sample preparation for mass spectrometry 51

2.5.9. DNA Sequencing 51

2.6. Cloning techniques 52

2.6.1. Site directed mutagenesis 52

2.6.2. Guide RNA plasmid cloning 52

2.6.3. WDR76 targeting plasmid construction 52
2.6.4. Bacterial transformation 53
2.6.5. Plasmid Maxiprep 54

2.7. Virus work 54

2.7.1. Lentivirus generation 54
2.7.2. Virus titre determination 54

2.8. CRISPR-Cas9 genetic screen 55

2.8.1. Principle of the screen 55
2.8.2. Performing the CRISPR-Cas9 screen 56
2.8.3. gDNA extractions and library preparation 57
2.8.4. Sequencing 58
2.8.5. Bioinformatics analysis 59

Chapter 3: Investigating the role of WDR76 in the removal of Ku from DNA ends 60

3. Investigating the role of WDR76 in the removal of Ku from DNA ends 61

3.1. Introduction 61

3.1.1. Ubiquitylation in the DNA damage response 61
3.1.2. Cullin-RING ligases in the DNA damage response 63
3.1.3. The CUL4 complex and the DNA damage response 64
3.1.4. Investigating the role of WDR76 in the regulation of NHEJ 66

3.2. Results 69

3.2.1. WDR76 interacts with Ku70/Ku80 69
3.2.2. WDR76 localises to sites of DNA damage 70
3.2.3. WDR76 depletion does not increase persistence of NHEJ factors at sites of DNA damage 72
3.2.4. siRNA mediated knockdown of WDR76 leads to persistence of Ku foci after irradiation 74
3.2.5. Yeast *CMR1* knockout does not show sensitivity to DNA damaging agents 76
3.2.6. siRNA mediated depletion of WDR76 does not increase sensitivity of cells to irradiation 78
3.2.7. Human cell *WDR76* gene knockouts exhibit IR hypersensitivity 79
3.2.8. Mass spectrometry identifies interacting partners of WDR76 85
3.2.9. WDR76 knockout cells do not show increased sensitivity to heat shock 89
3.2.10. WDR76 knockout cells do not show increased sensitivity to UV 90
3.2.11. Assessing WDR76 protein levels throughout the cell cycle 93
3.2.12. WDR76 knockout cells do not show enhanced sensitivity to camptothecin 95
3.2.13. Transcription inhibition causes loss of WDR76 nucleolar localisation 97
3.2.14. Assessing whether WDR76 affects Ku ubiquitylation 99
3.2.15. Persistence of Ku on chromatin could not be detected in knockout cells 101

3.3. Discussion 103

3.3.1. WDR76 is involved in DNA repair 103

3.3.2. Other potential roles of WDR76 105

3.3.3. WDR76 concluding remarks 109

Chapter 4: Investigation of a potential CDK phosphorylation site on PAXX as a regulatory mechanism 110

4. Investigation of a potential CDK phosphorylation site on PAXX as a regulatory mechanism 111

4.1. Introduction 111

4.1.1. PAXX and the DDR 111

4.1.2. CDKs in the regulation of the DDR 113

4.1.3. PAXX contains a potential CDK phosphorylation site 114

4.2. Results 115

4.2.1. PAXX levels remain constant throughout the cell cycle 115

4.2.2. PAXX phosphorylation throughout cell cycle 117

4.2.3. Generation of PAXX point mutants 120

4.2.4. Testing IR sensitivity in cells expressing PAXX mutants 122

4.2.5. CDK inhibition and PAXX phosphorylation 123

4.3. Discussion 124

Chapter 5: Performing a CRISPR-Cas9 screen to investigate the role of WRN in the DDR 126

5. Performing a CRISPR-Cas9 screen to investigate the role of WRN in the DDR 127

5.1. Introduction 127

5.1.1. Werner syndrome 127

5.1.2. RecQ helicases 128

5.1.3. WRN structure 131

5.1.4. WRN binding partners 132

5.1.5. WRN in base excision repair 133

5.1.6. WRN at replication forks 134

5.1.7. WRN involvement in HR 135

5.1.8. WRN involvement in NHEJ 136

5.1.9. WRN at telomeres 136

5.1.10. WRN, G4 quadruplexes and transcription 137

5.1.11. Insights into WRN function from WRN knockout mice 137

5.1.12. WRN investigations herein 138

5.2. Results....140
5.2.1. Generation of RPE-1 *WRN* knockout....140
5.2.2. *WRN* knockout clones are hypersensitive to CPT....142
5.2.3. Generating stable Cas9 expressing cells for CRISPR genetic screen....146
5.2.4. CRISPR-Cas9 screen to identify suppressors of WRN-/- sensitivity to CPT....149
5.2.5. CRISPR-Cas9 screen results....152
5.3. WRN Discussion....159
5.3.1. p53 and p21 loss give growth advantage....160
5.3.2. *CAND1*, *KEAP1*, *RNF146*, *PTEN*, *SCAF4*, *CUL3* loss offers growth advantage....160
5.3.3. Hits that suppress CPT sensitivity in a WT background....162
5.3.4. Suppressors of CPT sensitivity in WRN-/- background....163
5.3.5. NBN1 as a dropout in WT cells....166
5.3.6. Dropouts specific to WRN-/- background....167
5.3.7. Limitations in the screening process....169
5.3.8. Concluding remarks....169
Chapter 6: Final Discussion....171
6. Final Discussion....172
7. References....175
8. Appendix....203

Table of Figures

Figure 1 Types of DNA damage 23
Figure 2 Initial double strand break response signalling 27
Figure 3 Homologous recombination pathway for double strand break repair (DSBR) 31
Figure 4 Non-homologous end-joining pathway 33
Figure 5 The ubiquitylation cascade and consequences of substrate ubiquitylation 63
Figure 6 WDR76 is a conserved substrate receptor of the CUL4 ubiquitin ligase 68
Figure 7 WDR76 interacts with Ku70, Ku80 and the CUL4 complex 70
Figure 8 WDR76 is recruited to sites of laser line induced DNA damage 71
Figure 9 siRNA depletion of WDR76 does not increase persistence of NHEJ factors after DNA damage in the chromatin fraction 73
Figure 10 WDR76 knockdown results in an increased persistence of Ku foci 75
Figure 11 S. cerevisiae cmr1 knockout does not show hypersensitivity to DNA damaging agents 77
Figure 12 siRNA mediated depletion of WDR76 does not increase sensitivity to irradiation 79
Figure 13 WDR76 knockout generation in RPE-1 cells 81
Figure 14 PCR screening of potential RPE-1 WDR76 knockouts 82
Figure 15 Validation of WDR76 knockouts 83
Figure 16 RPE-1 WDR76 knockouts show increased sensitivity to IR 84
Figure 17 WDR76 interacting partners identified by mass spectrometry 87
Figure 18 WDR76 knockouts are not sensitive to heat shock 90
Figure 19 WDR76 knockouts do not show increased sensitivity to UV 92
Figure 20 WDR76 protein levels throughout the cell cycle 94
Figure 21 WDR76 knockouts do not show increased sensitivity to camptothecin 96
Figure 22 Transcription inhibition at sites of DNA damage is intact in WDR76 knockout clones 98
Figure 23 Detection of Ku ubiquitylation in wildtype vs. WDR76 knockout cells 100
Figure 24 Chromatin fractionation in RPE-1 wildtype and WDR76-/- cells 102
Figure 25 PAXX contains a conserved phosphorylation site 112
Figure 26 Total PAXX levels throughout the cell cycle 116
Figure 27 PAXX phosphorylation throughout the cell cycle 119

Figure 28 PAXX mutant generation in RPE-1 cells 121
Figure 29 Clonogenic cell survival assays in RPE-1 PAXX mutant cell lines 122
Figure 30 Testing effects of CDK inhibitors on PAXX S148 phosphorylation 123
Figure 31 The RecQ helicases 131
Figure 32 WRN knockout generation 141
Figure 33 WRN knockout clones show sensitivity to camptothecin 144
Figure 34 WRN knockout cells show increased sensitivity to camptothecin 145
Figure 35 Testing Cas9 efficiency in cell lines for screen 148
Figure 36 Library Preparation for Illumina Sequencing 151
Figure 37 JACKS analysis plots of CRISPR screens performed in WT RPE-1 cells 154
Figure 38 JACKS analysis plots of analysis performed on individual WRN knockout clones 156
Figure 39 JACKS analysis plots of analysis performed on WRN knockout clones as biological replicates 157

Table of Tables

Table 1 Details of samples in screen and primers used for generating library for sequencing 58

Table 2 Human DDR CRISPR library 149

Table of Appendices

Appendix Table 1 List of primers used 203

Appendix Table 2 Sequences of gRNAs used 204

Appendix Table 3 List of antibodies used 205

Appendix Table 4 Raw data from JACKS analysis of RPE-1 WT 2nM CPT treated 207

Appendix Table 5 Raw data from JACKS analysis of RPE-1 WT 5nM CPT 218

Appendix Table 6 Raw data from JACKS analysis of RPE-1 WRN-/- G7-C5 2nM CPT treated 229

Appendix Table 7 Raw data from JACKS analysis of RPE-1 WRN-/- E5-C6 2nM CPT treated 240

Appendix Table 8 Raw data from JACKS analysis of combined WRN-/- clones 251

Appendix Table 9 List of genes showing greater enrichment in CPT treated samples than DMSO treated samples compared to the day 14 control (from related JACKS analysis). 262

List of Abbreviations

4NQO	4-nitroquinoline 1-oxide
53BP1	p53 binding protein 1
ADP	Adenosine diphosphate
AKT	AKT serine/threonine kinase 1
AT	Ataxia telangiectasia
ATM	Ataxia telangiectasia mutated
ATP	Adenosine triphosphate
ATR	Ataxia telangiectasia and Rad3 related
ATRIP	ATR interacting protein
BARD1	BRCA1 associated RING domain 1
BER	Base excision repair
BFP	Blue fluorescent protein
BGS	Baller Gerald syndrome
BLM	Bloom syndrome RecQ helicase
BRCA1	Breast and ovarian cancer susceptibility protein 1
BRCA2	Breast and ovarian cancer susceptibility protein 2
BrdU	Bromodeoxyuridine
BRG1	ATP-dependent chromatin remodeller SMARCA4
BSA	Bovine serum albumin
CAND1	Cullin associated NEDD8 dissociated protein 1
Cas9	CRISPR associated protein 9
CBX3	Chromobox 3
CCT	Chaperonin containing TCP1 complex
CDC25A	Cell division cycle 25A
CDC25C	Cell division cycle 25C
CDK	Cyclin dependent kinase
CDKN1A	Cyclin dependent kinase inhibitor 1A
CDT1	Chromatin licensing and DNA replication factor 1
CHEK2	Checkpoint kinase 2
CHFR	Checkpoint with forkhead and RING finger domains
CHK1	Checkpoint kinase 1
CHK2	Checkpoint kinase 2
CK2	Casein Kinase 2
Cmr1	Changed mutation rate
COP9	Constitutive photomorphogenesis 9
CPT	Camptothecin
CRISPR	Clustered regularly interspaced short palindromic repeats
CRL(s)	Cullin RING ligase(s)
CSA	Cockayne syndrome A

CSK	Cytoskeleton
CSN	COP9 signalosome
CSR	Class switch recombination
CtIP	C-terminal binding protein interacting protein
CUL1	Cullin 1
CUL3	Cullin 3
CUL4	Cullin 4
CUL9	Cullin 9
CUTs	Cryptic unstable transcripts
CycA	Cyclin A
DCAF(s)	DDB1 and CUL4 associated factor(s)
DDB1	DNA damage binding protein 1
DDB2	DNA damage binding protein 2
DDR	DNA damage response
diRNA	DNA damage induced RNA
DMEM	Dulbecco's Modified Eagle Media
DMSO	Dimethyl sulfoxide
DNA	Deoxyribonucleic acid
DNA lig III	DNA ligase III
DNA pol β	DNA polymerase β
DNA pol δ	DNA polymerase δ
DNA-PK	DNA dependent protein kinase
DNA2	DNA replication helicase/nuclease 2
DNAJA1	DNAJ homolog subfamily A member 1
DNAJC7	DNAJ homolog subfamily C member 7
DSB(s)	Double strand break(s)
DSBR	Double strand break repair
dsDNA	Double-stranded DNA
DUB(s)	Deubiquitylating enzyme(s)
E. coli	Escherichia coli
EDTA	Ethylenediaminetetraacetic acid
EGFP	Enhanced GFP
EME2	Essential meiotic structure specific endonuclease subunit 2
ERCC1	Excision repair cross complementing 1
ES	Embryonic stem
EtBr	Ethidium bromide
EU	Ethynyl Uridine
EXO1	Exonuclease I
FA	Fanconi anaemia
FACS	Fluorescence activated cell sorting
FBS	Foetal bovine serum
FBXW7	F-box and WD repeat domain containing 7

FDR	False discovery rate
FEN1	Flap endonuclease 1
G418	Geneticin
GAPDH	Glyceraldehyde 3-phosphate dehydrogenase
GFP	Green fluorescent protein
GG-NER	Global genome nucleotide excision repair
gRNA	Guide RNA
H2AX	H2A Histone family member X
H2O	Water
H3F3B	H3 Histone family member 3B
H3K36me3	Histone H3 trimethylation at lysine 36
HA-tagged	Human influenza hemagglutinin-tagged
HDAC1	Histone deacetylase 1
hDDR	Human DNA damage response
HEK293	Human embryonic kidney 293
HeLa	Henrietta Lacks
HELLS	Helicase lymphoid specific
HGPS	Hutchinson-Gilford progeria syndrome
Hoechst	Hoechst33342
HR	Homologous recombination
HRDC	Helicase and ribonuclease D C-terminal
HSD	High seeding density
HSP90AA1	Heat shock protein HSP 90-alpha
hTERT	Human telomerase reverse transcriptase
HU	Hydroxyurea
IC	Inhibitory concentration
ICL(s)	Interstrand crosslink(s)
IF	Immunofluorescence
IGEPAL	Octylphenoxypolyethoxyethanol
Indels	Insertions/deletions
IP(s)	Immuno-precipitation(s)
IR	Irradiation
JACKS	Joint analysis of CRISPR/Cas9 knockout screens
KAP1	KRAB-interacting protein
kDa	Kilodaltons
KEAP1	Kelch like ECH associated protein 1
LHA	Left homology arm
LIG4	Ligase IV
LP-BER	Long patch base excision repair
LSD	Low seeding density
MAPK	Mitogen-activated protein kinase 1
MAPK14	Mitogen-activated protein kinase 14

MDC1	Mediator of DNA damage checkpoint protein 1
$MgCl_2$	Magnesium chloride
MLH1	MutL homolog 1
MLNi	MLN4924
MMEJ	Microhomology-mediated end-joining
MMR	Mismatch repair
MMS	Methyl methanesulfonate
MOI	Multiplicity of infection
MOPS	3-(N-morpholino)propanesulfonic acid
MRE11	Meiotic recombination 11
MRN	MRE11, RAD50, NBS1
MSH2	MutS homolog 2
MSH3	MutS homolog 3
MSH6	MutS homolog 6
MUS81	MUS81 structure specific endonuclease subunit
NaCl	Sodium chloride
NAE1	Neddylation activating enzyme E1
NaF	Sodium fluoride
NBS1	Nijmegen breakage syndrome 1
NEB	New England Biolabs
NEDD8	Neural precursor cell expressed developmentally downregulated protein 8
NEIL1	Nei like DNA glycosylase 1
NER	Nucleotide excision repair
NHEJ	Non-homologous end-joining
NR	Non-released
NRF2	Nuclear factor erythroid 2-related factor 2
NT	Non-treated
OH	Hydroxyl
ORF	Open reading frame
p53	Tumour protein 53
PALB2	Partner and localiser of BRCA2
PAM	Protospacer adjacent motif
PAR	poly(ADP-ribose)
PARP1	Poly (ADP-ribose) polymerase 1
PAXX	Paralog of XRCC4 and XLF
PBRM1	Polybromo 1
PBS	Phosphate buffered saline
PCNA	Proliferating cell nuclear antigen
PCR	Polymerase chain reaction
PFA	Paraformaldehyde
PGK	Phosphoglycerate kinase

PIKK	Phosphatidylinositol 3-kinase-related kinase
PIPES	Piperazine-N,N'-bis(2-ethanesulfonic acid)
PISA	Present in SAS6
PLK1	Polo like kinase 1
PMS2	Postmeiotic segregation 1 homolog 2
POLR2A	RNA polymerase II subunit A
POT1	Protection of telomeres 1
PTEN	Phosphatase and tensin homolog
PTM(s)	Post translational modification(s)
qPCR	Quantitative PCR
RBX1	RING box protein 1
RCF	Relative centrifugal force
rDNA	Ribosomal DNA
RFC	Replication factor C
RFP	Red fluorescent protein
RHA	Right homology arm
RING	Really interesting new gene
RMI1	RecQ mediated genome instability 1
RMI2	RecQ mediated genome instability 2
RNA	Ribonucleic acid
RNA pol II	RNA polymerase II
RNF146	RING finger protein 146
RNF168	RING finger protein 168
RNF8	RING finger protein 8
ROS	Reactive oxygen species
RPA	Replication protein A
RPE-1	Retinal pigmented epithelial
RPS27L	Ribosomal protein S27 like
RQC	RecQ C-terminal
Rqh1	RecQ type DNA helicase
RTS	Rothmund Thompson syndrome
S. cerevisiae	Saccharomyces cerevisiae
S. pombe	Saccharomyces pombe
SAS6	Spindle assembly abnormal 6
SCAF4	SR-related CTD associated factor 4
SCAF8	SR-related CTD associated factor 8
SCF	SKP1, CUL1, F-Box protein
SCID	Severe combined immunodeficiency
SDS	sodium dodecyl sulphate
SEM	Standard error of the mean
SETD2	SET domain containing 2
Sgs1	Slow growth suppressor1

SILAC	Stable isotope labelling by amino acids in cell culture
siRNA	Small interfering RNA
SMARCA4	SWI/SNF related, matrix associated, actin dependent regulator of chromatin, subfamily A, member 4
SMARCC1	SWI/SNF related, matrix associated, actin dependent regulator of chromatin, subfamily C, member 1
SOC	Super optimal broth with catabolite repression
SOD1	Superoxide dismutase 1
SP-BER	Short patch base excision repair
SSB(s)	Single strand break(s)
SSBR	Single strand break repair
ssDNA	Single-stranded DNA
STUB1	STIP1 homology and U-box containing protein 1
TAE	Tris, acetic acid, EDTA
TBE	Tris borate EDTA
TBST	Tris buffered saline and Tween20
TC-NER	Transcription coupled nucleotide excision repair
TCEP	Tris(2-carboxyethyl) phoshphine
TCP1	T complex protein 1
TERC	Telomerase RNA component
TFIIH	Transcription factor II human
TOP1	Topoisomerase I
TOP3A	DNA topoisomerase III α
TP53	Tumour protein 53
TRF1	Telomeric repeat binding factor 1
TRF2	Telomeric repeat binding factor 2
Tris	Tris(hyrdoxymethyl)aminomethane
U2OS	U-2 osteosarcoma
Ub	Ubiquitin
UTR	Untranslated region
UV	Ultraviolet
V(D)J	Variable domain joining
VCP	Valosin-containing protein
WDR76	WD repeat domain 76
WRN	Werner syndrome protein
WS	Werner syndrome
WT	Wild-type
XLF	XRCC4-like factor
XPC	Xeroderma pigmentosum complementation group C
XRCC1	X-ray repair cross complementing 1
XRCC2	X-ray repair cross complementing 2
XRCC3	X-ray repair cross complementing 3

XRCC4	X-ray repair cross complementing 4
XRCC5	X-ray repair cross complementing 5 (Ku80)
XRCC6	X-ray repair cross complementing 6 (Ku70)
YPA	Yeast extract, peptone, adenine
ZDHHC16	Zinc finger DHHC-type containing 16

Chapter 1: Introduction

1. Introduction

1.1. The integrity of DNA

DNA is the code of life, the important data-store that encodes all the necessary components that maintain the function and progression of organisms. From the development in early life, right through to ageing, maintenance of these data is important to prevent loss of vital information that could compromise life.

The DNA in our cells is under constant threat throughout our daily lives, as we are exposed to a number of different factors that cause DNA damage. These can be exogenous, environmental factors, such as ultraviolet (UV) light from the sun or ionising radiation (IR) from radioactive materials that can both be natural or manmade. Exposure to other carcinogens, for example those found in tobacco products or everyday consumables including food can also lead to DNA damage[1,2]. Cells in our bodies are also susceptible to DNA damage caused by endogenous factors; these include DNA damage caused by reactive oxygen species (ROS), a natural product generated through normal cell metabolism, or damage that occurs through errors in DNA replication and repair during the cell cycle[3,4]. Constant DNA damage can lead to loss of DNA integrity through changes such as mutations, deletions, insertions and chromosomal rearrangements. This can be disastrous to cells and can compromise the life of organisms.

Despite this constant onslaught of DNA damage, organisms have a plethora of proteins involved in maintaining the integrity of the genome; these proteins are those involved in the DNA damage response (DDR). The activity of these proteins ultimately repair the DNA damage or target cells for destruction if the level of damage is beyond the threshold of repair[5].

DNA damage can occur in a variety of forms that can be broadly categorised into the following groups: single strand breaks (SSBs), crosslinks and bulky lesions, mismatches and base lesions, and double strand breaks (DSBs)[6] (Figure 1). Proteins involved in the DDR have evolved specific functions to combat these various forms of DNA damage and act through distinct cascades and mechanisms to ultimately aid in the repair of the damage.

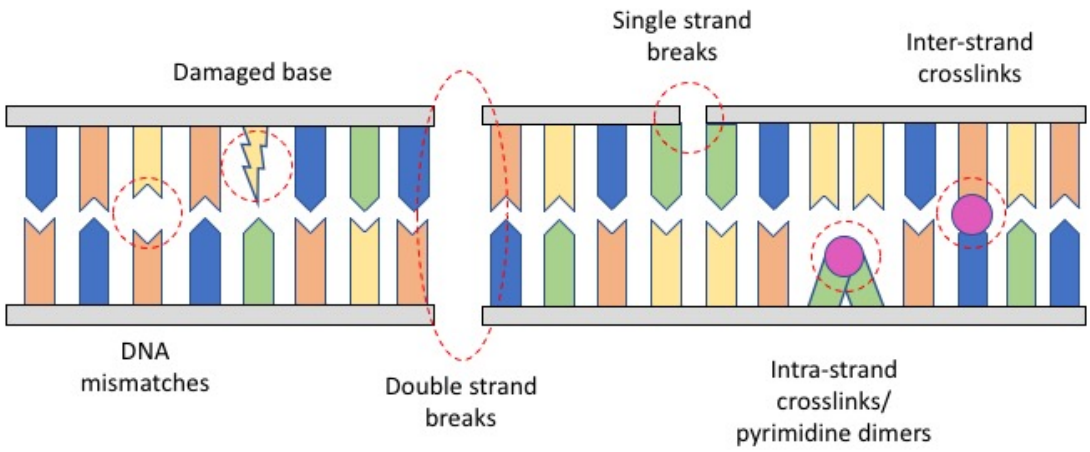

Figure 1 Types of DNA damage

Diagram showing the many types of DNA damage. The DNA backbone is in grey with the nucleotide bases indicated by the various colours. Types of DNA damage include DNA mismatches, damaged bases, DSBs, SSBs, pyrimidine dimers and inter-strand crosslinks. Pink circles mark bulkier DNA lesions which can cause distortion of the DNA double helix.

1.2. DNA repair pathways

1.2.1. Base excision repair and single-strand break repair

Single strand break repair (SSBR) refers to repair of DNA damage that occurs in one strand of the DNA backbone; specifically, in the sugar-phosphate bond form between adjacent DNA bases (Figure 1). SSBs are thought to be the most common type of DNA insult and occur more frequently than DSBs[7,8]. SSBs can occur directly or indirectly as a result of DNA base-excision repair (BER) intermediates[9]. As a result of the crossover between the two pathways SSBR is generally considered to be a sub-pathway of BER.

BER is the repair pathway which removes and replaces damaged bases that do not distort the DNA helix[10,11] (Figure 1). The process involves DNA glycosylases to recognise and remove the damaged base, creating an abasic site which is removed by endonucleases. This is a single strand nick, which is subsequently repaired by the proteins: DNA polymerase β (DNA polβ), x-ray cross complementing 1 (XRCC1) and DNA ligase III. If more than one base in a tract length is needed to be replaced DNA ligase I acts instead of DNA ligase III[11]. These downstream

proteins and mechanisms are common to BER and SSBR, however the recognition step in SSBR is different.

SSBs are primarily recognised by poly(ADP-ribose) polymerase 1 (PARP1), although activity of PARP1 can also be found at other types of DNA lesions[12,13]. Upon DNA-damage detection, PARP1 catalyses the synthesis of poly(ADP-ribose) (PAR) chains on itself and other proteins. This promotes the recruitment of XRCC1 and DNA ligase III which together repair the SSB[8,12,13].

1.2.2. Mismatch repair

The mismatch repair (MMR) pathway involves the recognition and resolving of base to base mismatches (Figure 1). MMR can repair both single base mismatches as well as larger stretches of base mismatch loops. The process of repairing these two types of mismatches are largely similar, although the initial recognition steps differ slightly. MMR recognition is performed by mutS homolog 2 (MSH2), which forms a heterodimer with MSH6 for the recognition of single base mismatches, and with MSH3 for the recognition of larger loop mismatches[14,15]. These heterodimer complexes form a ternary complex with mutL homolog 1 (MLH1) and postmeiotic segregation homolog 2 (PMS2). Endonuclease activity of PMS2 and recruitment and activity of exonucleases, such as exonuclease I (EXO1), results in degradation of bases and the associated phosphodiester DNA backbone, leading to a stretch of single stranded DNA. DNA polymerase δ, proliferating cell nuclear antigen (PCNA), replication factor C (RFC) and DNA ligase I subsequently synthesise the missing bases and maintain DNA integrity[16].

1.2.3. Nucleotide excision repair and inter-strand crosslink repair

Certain types of DNA damage can lead to bulkier base damage which causes distortion of the DNA helix. These include typical photoproducts such as cyclopyrimidine dimers produced by UV light (Figure 1). This type of DNA damage is repaired by a process called nucleotide excision repair (NER). NER is facilitated by the recognition of unstable duplex DNA through the protein xeroderma pigmentosum complementation group C (XPC) which binds the non-damaged strand opposite the lesion[17]. XPC then recruits a range of downstream proteins including transcription factor II human (TFIIH) and excision repair cross complementing 1 (ERCC1) to

facilitate the removal of damaged bases. Repair is then accomplished by DNA polymerases, XRCC1 and DNA ligases[17].

Inter-strand crosslinks (ICLs) can arise between opposite DNA strands usually as a result of mutagen exposure within the environment. This type of DNA damage can be particularly toxic as it creates a stable bond between complementary strands of DNA and thus inhibits DNA strand separation (Figure 1). This prevents the progression of processes like transcription and replication[18]. ICLs are repaired by proteins involved in the Fanconi anaemia (FA) pathway, named after the genetic disorder FA which is associated with increased sensitivity to ICLs[18]. Recognition of ICLs is performed by the protein FANCM and the rest of the FA complex (FANCA, B, C, E, F, G and L) [18]. This leads to the repair of ICLs through concerted efforts of nucleases and polymerases[18].

1.2.4. Double strand breaks and their repair

Double strand breaks (DSBs) (Figure 1) are the most toxic of DNA lesions as they require more coordination to repair since an undamaged intact strand is not immediately available[19]. DSBs can therefore result in the loss of genetic information if repaired incorrectly. DSBs can arise from the effects of ionising radiation (IR), which, amongst other types of DNA damage, can generate blunt ended DSBs. Additionally, two single strand breaks can be generated in close proximity also resulting in DSBs[20]. Naturally occurring developmental processes such as V(D)J (variable diversity joining) recombination and meiosis can also generate DSBs that require appropriate processing[21]. DSBs can also occur when there are blocks to the progression of the processes like replication and transcription and often single strand breaks can become converted into double strand breaks during these processes[22]. Cells overloaded with SSBs often carry over unrepaired SSBs into replication, thus resulting in DSBs. DNA damaging agents like camptothecin (CPT) work by causing double strand breaks specifically in S-phase. This happens as CPT inhibits the ligase activity, but not the initial cleavage activity, of topoisomerase 1 (TOP1). CPT thus causes a single strand break in DNA which is bound by TOP1. This complex creates collisions with the replication machinery in S-phase, causing replication forks to collapse and generating double strand breaks[23].

Two primary pathways exist to repair DSBs, these are homologous recombination (HR) and non-homologous end-joining (NHEJ). NHEJ is a process which directly ligates DSB ends together and is active throughout the cell cycle. HR on the other hand uses template DNA to restore information that is potentially lost during a DSB; this restricts repair by HR to S/G2 phases of the cell cycle when a sister chromatid is available. These two processes are described in more detail in sections 1.5 and 1.6.

1.3. Initial double strand break response

The initial response to DSBs and the chromatin signalling to mediate repair is coordinated by the phosphatidylinositol 3-kinase related kinases (PIKKs). These are ataxia telangiectasia mutated (ATM), ataxia telangiectasia and RAD3-related (ATR) and DNA-dependent protein kinase (DNA-PK). The main PIKK which mediates DNA-damage signalling in response to DSBs is ATM. ATM is recruited to DSBs through the meiotic recombination 11(MRE11)-RAD50-Nijmegen breakage syndrome 1 (NBS1) (MRN) complex which acts as a sensor of DSBs[24]. ATM phosphorylates histone H2AX on serine 139 which is referred to as γH2AX[25]. Production of γH2AX is one of the first things to occur in response to DNA damage and is thus used widely as a marker of DNA damage. Generation of γH2AX leads to the recruitment of mediator of DNA damage checkpoint protein 1 (MDC1) which is constitutively phosphorylated by casein kinase 2 (CK2), this results in the recruitment of more MRN and ATM[26]. This potentiates the DNA damage signalling pathway. MDC1 is also phosphorylated by ATM, which results in the recruitment and activation of the ubiquitin E3 ligases RING finger 8 (RNF8) and RING finger 168 (RNF168). RNF8/168 ubiquitylation of histones further potentiates the DNA damage signal on chromatin at and surrounding the site of DNA damage[27,28]. This recruits other proteins involved in the DDR including p53 binding protein 1 (53BP1) and breast and ovarian cancer susceptibility protein 1 (BRCA1); two proteins which are involved in the choice between double strand break repair (DSBR) through either HR or NHEJ (See section 1.8 for more) (Figure 2)[25,26].

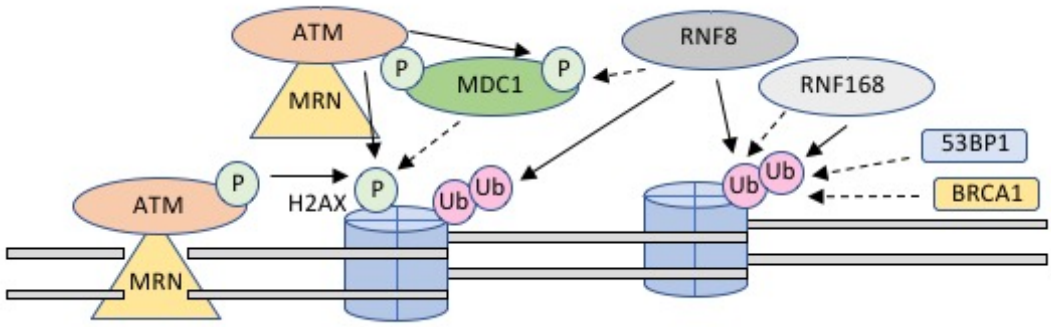

Figure 2 Initial double strand break response signalling

DSBs are recognised by the MRN complex which interacts with ATM mainly through the NBS1 subunit. Detection of DSBs results in auto-phosphorylation of ATM which promotes the phosphorylation of H2AX on ser139 (γH2AX). Blue cyclinders show nucleosomes with H2AX indicated. γH2AX recruits constitutively phosphorylated MDC1 which recruits more ATM, thus potentiating the signal further via γH2AX production. ATM phosphorylates MDC1 to promote the recruitment of the RNF8 E3 ligase. RNF8 ubiquitylates histones to promote the recruitment of RNF168. RNF8/168 together further ubiquitylate histones to expand the DNA damage signal resulting in recruitment of DNA damage proteins including 53BP1 and BRCA1. (Figure adapted from Panier and Boulton, 2014. Nature reviews[26]).

1.4. Roles of ATM/ATR in checkpoint signalling

The PIKKs, ATM and ATR are also responsible for checkpoint signalling through downstream kinases known as checkpoint kinase 2 (CHK2) and checkpoint kinase 1 (CHK1). These kinases phosphorylate further downstream factors and thus expands the number and diversity of factors affected by ATM and ATR[29]. The major functions of the checkpoint kinases are to cause cell cycle arrest and promote DNA repair, or in the presence of excessive DNA damage drive apoptosis or senescence[30]. The two main checkpoint pathways are the ATM-CHK2 and ATR-CHK1 responses.

ATM phosphorylates CHK2 on multiple sites, including on T68[29,31,32]. Activated CHK2 has a range of downstream targets which include DDR factors, cell cycle regulators as well as proteins involved in p53 signalling and apoptosis[33]. CHK2 can initiate both G1/S and G2/M

phase checkpoints by the phosphorylation of cell division cycle 25A (CDC25A) and cell division cycle 25C (CDC25C) respectively[34,35]. Phosphorylation of CDC25A leads to its degradation, which subsequently prevents the activation of cyclin dependent kinase 2 (CDK2), a step required for progression into S-phase[35]. In the case of the G2/M phase checkpoint, CHK2 mediated phosphorylation of CDC25C causes its translocation to the cytoplasm and thus CDC25C cannot activate cyclin dependent kinase 1 (CDK1) to allow for progression into mitosis[36,37]. CHK2 has also been linked to the activation of p53, although it has a potentially redundant role here with other p53 activators[30]. CHK2 has also been shown to be a driver of senescence and apoptosis as *CHK2-/-* mice were shown to be resistant to apoptosis after DNA damage exposure[38]. Furthermore, *CHK2-/-* mice also been shown to be cancer prone due to accumulation of DNA damage and apoptotic evasion[39].

The ATR-CHK1 checkpoint has overlapping functions with the ATM-CHK2 response[30] however the activation of the ATR-CHK1 pathway is predominantly due to replication stress[40,41]. ATR phosphorylates CHK1 on sites that include S345 to activate CHK1[42,43]. CHK1 promotes arrest of the cell cycle predominantly at the intra-S and G2/M checkpoint through similar mechanisms by which CHK2 prevents cell cycle progression[29]. CHK2 has been shown to phosphorylate CDC25A and CDC25C as well as the WEE1 kinase[44]. Phosphorylation activates WEE1 kinase activity, which results in the inhibitory phosphorylation of CDK1, and thus inhibits entry into mitosis[44–46].

1.5. Homologous recombination (HR)

HR involves the repair of DSBs through the use of a template DNA strand. This process is characterised by 5’ to 3’ DNA resection, which exposes single-stranded DNA (ssDNA), to allow for strand invasion into template DNA and subsequent repair (Figure 3). HR is mainly initiated by the MRN complex which recognises and binds DSBs[47]. Through interaction with NBS1, the C-terminal binding protein interacting protein (CtIP) protein is recruited to sites of DNA damage and is involved in the initiation of 5’ to 3’ resection to expose ssDNA. Whilst short range resection is promoted by CtIP, extensive long-range resection is promoted by EXO1[5]. This ssDNA is immediately coated by replication protein A (RPA), a heterotrimeric protein complex consisting of RPA1, RPA2 and RPA3. RPA binding to ssDNA stabilises it and prevents

its degradation. RPA is hyperphosphorylated in response to DNA damage by the PIKKs which is necessary for subsequent steps in HR[48]. RPA2 phosphorylation at serine 4/8 sites is often used as a readout of resection. ATR is recruited to RPA-coated ssDNA through ATR interacting protein (ATRIP), and is activated[49].

BRCA1 is a main coordinator of homologous recombination acting at multiple stages throughout the HR process[50]. BRCA1 together with BRCA1 associated RING domain 1 (BARD1) forms a complex to mediate ubiquitylation of substrates including BRCA1 itself, to promote complex assembly and protein stabilisation of proteins involved in HR[50]. BRCA1 also interacts breast and ovarian cancer susceptibility protein 2 (BRCA2) via the protein partner and localiser of BRCA2 (PALB2), to mediate downstream events in HR[50]. BRCA2 coordinates the unloading of RPA from ssDNA and replaces it with RAD51, resulting in RAD51 nucleofilament coated ssDNA[51]. This RAD51 coated ssDNA is key to homology search and strand invasion into template DNA which may require the RAD51 paralogs[52]. Strand invasion allows for replication of the resected DNA, which can create complex structures of intercalated DNA which include D-loops and double Holliday junctions. These are ultimately resolved by various helicases and nucleases which can result in either a crossover or a non-crossover event between the sister chromatids (Figure 3)[52].

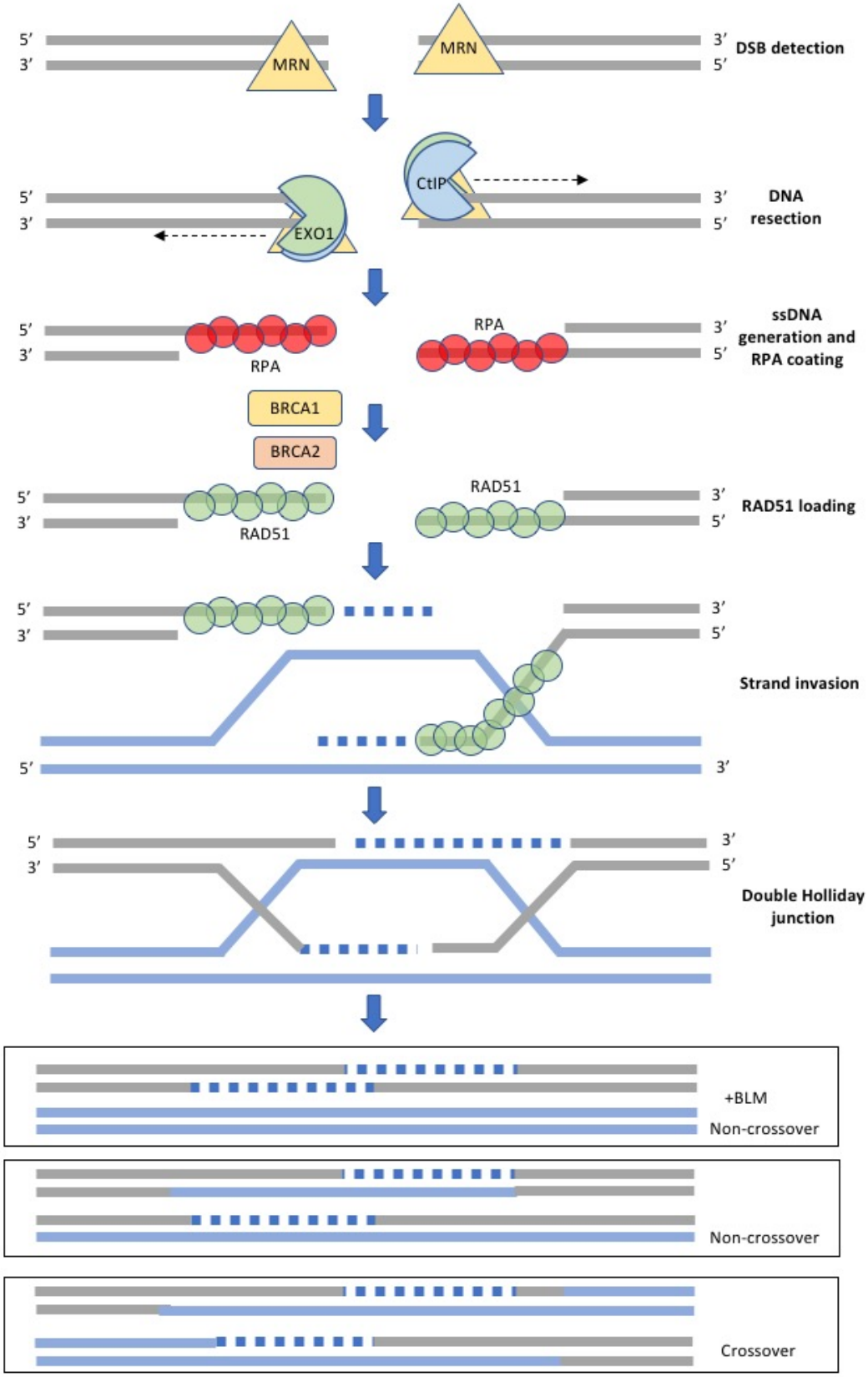
5′
3′
MRN
MRN
3′
5′
DSB detection
CtIP
EXO1
DNA resection
RPA
RPA
ssDNA generation and RPA coating
BRCA1
BRCA2
RAD51
RAD51
RAD51 loading
Strand invasion
Double Holliday junction
+BLM
Non-crossover
Non-crossover
Crossover

Figure 3 Homologous recombination pathway for double strand break repair (DSBR)

Homologous recombination pathway for DSBR. Double strand breaks are recognised by the MRN complex. CtIP is recruited by the MRN complex through direct interaction with NBS1. This promotes initiation of resection with EXO1 promoting long range resection. This generates ssDNA which is immediately coated by the multimeric RPA complex proteins (shown in red). Exchange of RPA coated ssDNA to RAD51 coated ssDNA is then mediated by the BRCA1 and BRCA2 proteins. RAD51 coated ssDNA drives homology search and strand invasion to form a D-loop structure and DNA synthesis. D-loop structures can be resolved by a process called synthesis dependent strand annealing where only one strand is used as a template before being resolved. Alternatively, double Holliday junctions are formed which can be subsequently resolved in a number of ways resulting in either crossovers or non-crossovers. The RecQ helicase BLM promotes Holliday junction dissolution to prevent crossovers. (Figure adapted from Panier and Boulton, 2014. Nature reviews[26])

1.6. Non-homologous end-joining (NHEJ)

Unlike HR, NHEJ is not restricted to S and G2 phases of the cell cycle as it does not require template DNA to initiate repair[53]. As a result, NHEJ is active throughout the cell cycle and is thought to be the main pathway of DSBR. NHEJ repairs DSBs that are generated by exogenous sources such as irradiation but is also important in repairing DSBs generated by the processes of (V(D)J) recombination and class-switch recombination (CSR). These recombination processes allow for the diverse production of antibodies in B-cells and the antigen binding domains of T-cells and is thus crucial to health[54,55].

DSB detection in the NHEJ pathway is performed by the Ku70/80 heterodimer (Ku), which is composed of a 70kDa and 80kDa protein respectively. Ku is able to bind a variety of DNA structures but has the highest affinity for DSB ends[56]. Two separate Ku molecules bind on both ends of a DNA DSB. This binding of Ku serves as a platform to recruit other downstream factors of the NHEJ pathway[56,57]. After initial detection and binding, Ku recruits DNA-PK catalytic subunit (DNA-PKcs), which together form the DNA-PK holoenzyme[58].

Depending on the nature of the DSB, DNA ends may need to be processed prior to final ligation step. Ku interacts with a number of proteins which may be involved in the processing

of DNA ends[57]. This includes the polynucleotide kinase/phosphatase, PNKP, which has 3' DNA phosphatase activity and 5' DNA kinase activity which can process incompatible DNA ends into compatible ends for ligation[59].

Aprataxin and PNKP-like factor (APLF) is another factor which interacts directly with Ku80 and has been reported to have nuclease activity[60–62]. In addition, APLF, through its interaction with Ku, promotes the recruitment of downstream factors and thus promotes NHEJ[60,61].

Artemis is another protein that forms a complex with DNA-PKcs and is involved in the processing of DNA termini prior to ligation[63,64]. The Artermis-DNA-PKcs complex is able to process DNA ends in a number of ways as it has 5' and 3' endonuclease activity, hairpin opening activity and Artermis alone has 5' exonuclease activity[64]. Ku can bind a number of duplex DNA end substrates, one of which is hairpin DNA ends[65,66].

NHEJ is said to be the more error prone of the two DSBR pathways. This is because insertions and deletions can occur at sites of DNA damage, largely as a result of DNA end processing activities[67]. Ku interacts with multiple other factors that may have a role in DNA end processing; this includes DNA polymerase μ and λ as well as the Werner's syndrome helicase (WRN) which will be discussed in more detail in chapter 5. DNA polymerase μ can add nucleotides in a template independent manner and DNA polymerase λ has also been shown to add nucleotides in a template independent manner in the presence of manganese[68–70]. Both DNA polymerase μ and λ also have a greater flexibility when using template DNA, with the ability to fold ssDNA back onto itself to prime DNA synthesis[68,69]. This results in short repeats, which are often seen at sites of DNA damage[70–72].

When DSBs have undergone DNA end processing, the DNA ends are ligated together in the final step of NHEJ. This happens through the recruitment of X-ray repair cross-complementing 4 (XRCC4) and XRCC4-like factor (XLF). Paralog of XRCC4 and XLF (PAXX) also promotes NHEJ and its function is discussed in more detail in chapter 4. These proteins aid in the recruitment of DNA ligase IV to the DSB which ultimately ligates the DNA ends together[57].

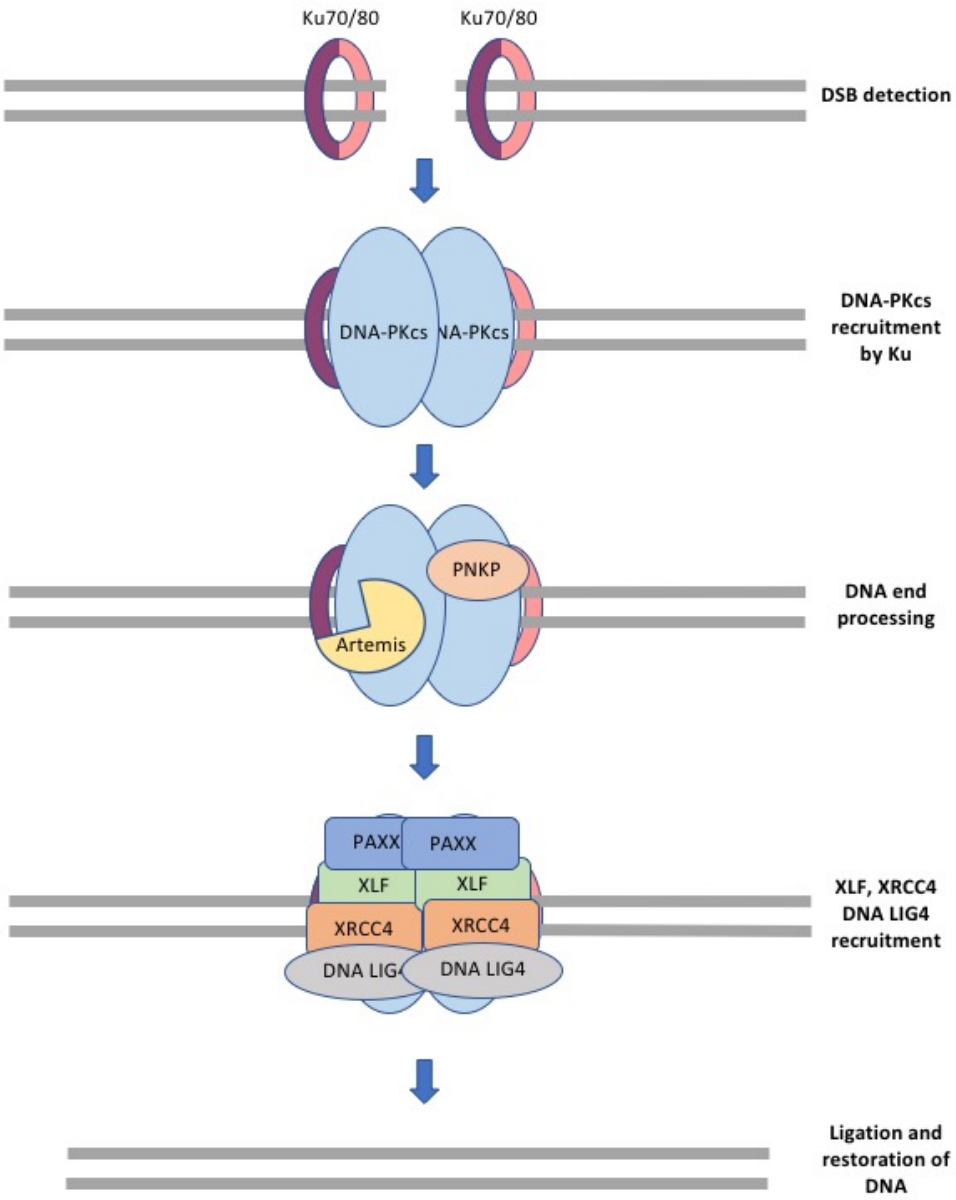

Figure 4 Non-homologous end-joining pathway

Non-homologous end-joining pathway for DSBR. DSBs are detected by the Ku heterodimer which has a high affinity for duplex DNA ends. Once bound, Ku recruits DNA-PKcs to form the DNA-PK holoenzyme. Depending on the nature of the break, DNA ends may need processing prior to ligation. Artemis has 5' exonuclease activity and when in complex with DNA-PKcs, 5' and 3' endonuclease activity, which process DNA ends. PNKP phosphatase and kinase activities ensure compatibility of DNA ends. PAXX, XRCC4, XLF and DNA LIG4 are recruited in a complex to finally ligate the DNA ends and repair the DSB.

1.7. Consequences of improper repair

The importance of DNA repair mechanisms is highlighted by the implication of DNA repair proteins in a variety of diseases such as immunodeficiency, infertility, cancer, premature ageing and neurodegeneration.

Ataxia-telangiectasia (AT) is an autosomal recessive disorder caused by mutations in ATM. Classical AT patients have frameshift mutations in ATM which result in loss of the protein, some patients exhibit a milder form of the disease which is usually associated with missense mutations resulting in partial ATM function[73–75]. The main characteristic of AT is progressive diffuse cerebellar atrophy, but about two thirds of patients also display abnormalities of the immune system[76,77]. This is at least partly due to the involvement of ATM in stabilising DSBs in V(D)J recombination[78]. AT is also associated with an increased sensitivity to radiation and an increased predisposition to a range of cancers[77].

Mutations in genes involved in NHEJ have also been linked to V(D)J recombination defects[79,80]. This has mainly been shown in mice containing mutations in DNA-PKcs which show developmental defects in B and T cells. DNA-PKcs null mice also display severe combined immunodeficiency (SCID)[81–83]. In addition, Lig4 syndrome is a rare human genetic disorder caused by hypomorphic mutations in *LIG4,* and is characterised by immunodeficiency[84].

Defects in DNA repair genes have been linked to male infertility[85]. Some men presenting with non-obstructive azoospermia have been shown to have defects in the MMR repair genes *MLH1* and *MSH2*. Cells from these patients also display microsatellite instability[85].

Defects in DNA repair genes have also been linked to neurodegenerative disorders such as Parkinson's disease and Alzheimer's disease[86]. Reduced levels of DNA-PKcs and the MRN complex as well as an increased level of DNA damage have also been shown in patients with Alzheimer's disease[87–89]. Similarly, an increased level of DNA damage, in particular oxidative DNA damage has been linked to the degeneration of dopaminergic neurons in Parkinson's disease[90,91].

Parkinson's disease is also connected to mitochondrial dysfunction, a process which can occur as a result of DNA damage to the mitochondrial DNA[92]. Mitochondrial DNA was thought to be maintained mainly by the BER pathway, however an increasing amount of evidence suggests that other DNA damage repair pathways are also active in mitochondria[93]. The importance of mitochondrial DNA maintenance can be exemplified by diseases such as Kearns-Sayre syndrome, which occurs as a result of deletions in mitochondrial DNA and results in drooping eyelids and lethargy. Furthermore, mice deficient in POLG, the mitochondrial DNA polymerase with proof-reading ability, show signs of premature ageing and a significantly reduced lifespan[94]. Other DNA repair proteins associated with premature ageing syndromes include the RecQ helicases; these will be discussed further in chapter 5.

Perhaps the most obvious connection DNA repair proteins have to disease is that with cancer. *p53* is the most commonly mutated gene in all cancers, these mutations can arise via the erroneous repair of DNA damage within the gene. Often there are underlying mutations in DNA repair genes which present prior to cancer inducing mutations. An example of this is in the mutations in the genes *BRCA1* and *BRCA2* which are particularly associated with breast and ovarian cancers[95]. BRCA1/2 have roles in DSBR by HR; defects in these proteins therefore can lead to error prone repair and are therefore drivers of cancer. Mutations in the mismatch repair genes *MSH2* and *MLH1* also have strong correlation with colorectal cancers[14].

The link between DNA damage/repair and cancer is also evident in the treatment of cancers as radiotherapy and many chemotherapies function by generating DNA damage in the quest to overload fast replicating cells with enough DNA damage to kill the cells[96]. The newly approved treatment of BRCA1 and BRCA2 mutant tumours using PARP inhibitors such as olaparib (Lynparza™- Astra Zeneca), exploits an HR deficiency in these tumours. Olaparib and other PARP inhibitors work by slowing down BER/SSBR and also by trapping PARP when it binds to SSBs; these structures are converted into DSBs when replication machinery encounters them. The HR deficiency in these tumour cells results in repair by NHEJ which leads to genetic instability and eventually death in these cells[97].

Due to the range of biological and medical impacts that DNA repair proteins have, it is extremely important to understand the mechanisms by which they mediate repair and also

the consequences of loss of DNA repair proteins in disease. Research further into these areas is extremely important to enhance the basic understanding of a multitude of diseases as well as offering potential therapeutic avenues for their treatment. This is particularly meaningful in the treatment of cancers which become resistant to chemotherapy, as understanding the mechanisms of resistance can offer new therapeutic targets to exploit the underlying genetics.

1.8. Regulation of HR vs. NHEJ

The type of DSB and the phase of the cell cycle it occurs in strongly influences the preferred method of repair[98]. HR requires template sister chromatid DNA and thus must be restricted to S and G2 phases of the cell cycle[98]. Initiation of HR without template DNA could result in loss of genetic information. NHEJ on the other hand is active throughout the cell cycle but is the more error prone of the two pathways[53]. Initiation of NHEJ in S and G2 phases during replication poses a threat to genome integrity as it may result in gross chromosomal rearrangements. As a result, there are mechanisms to control the type of DSBR initiated.

One of the major factors contributing to DSBR pathway choice is in the decision for cells to resect DNA[99]. Once extensive resection occurs at DSBs, cells become committed to repairing the DNA via HR. One of the ways of regulating this is through cyclin dependent kinases (CDKs) which can specifically promote HR in S and G2 phases[100]. A good example of this is in the phosphorylation at the threonine-847 CDK consensus site of CtIP. The phosphorylation of CtIP at this residue was specifically shown to enhance the ability of CtIP to promote DNA resection[101]. Interestingly cells expressing a phosphomimetic T847E mutant version of CtIP showed a decreased level of NHEJ, most likely as a result of resection occurring in G1. Additionally, other CDK phosphorylation sites on CtIP also promote HR by promoting interactions with other proteins involved in the same pathway; an example is the CDK mediated S347 phosphorylation that increases the interaction with BRCA1[102]. CDKs have also been implicated further downstream in the regulation of HR as CDK mediated BRCA2 phosphorylation promotes its interaction with RAD51 during S and G2 phases[103].

BRCA1 and 53BP1 promote HR and NHEJ respectively, and have antagonistic roles in the early DDR[104]. Both 53BP1 and BRCA1 are recruited to sites of DNA damage in an RNF8/168

dependent manner[105]. BRCA1 has been shown to promote HR, and importantly cells lacking BRCA1 show increased sensitivity to S-phase specific DNA damage. This sensitivity is partially suppressed by the 53BP1 depletion which shows the relevance of the interplay between the two proteins[106,107]. 53BP1 depletion alone results in hypersensitivity to IR in mouse cells, and B-cells from *53BP1* null mice exhibit CSR and V(D)J recombination defects[108–111], which is symptomatic of impaired NHEJ. 53BP1 has been shown to negatively regulate resection in the G1-phase of the cell cycle[112], as does yeast Rad9, which shares domain similarity with 53BP1[113].

BRCA1 together with BARD1 ubiquitylates CtIP which promotes its interaction with chromatin at sites of DNA damage; however CtIP driven resection does not require BRCA1[99]. Interestingly, super resolution microscopy showed that 53BP1 is enriched in foci in G0 and G1 cells, however BRCA1 pushes 53BP1 to the periphery of DNA damage foci in S-phase[114]. It is clear that BRCA1 and 53BP1 influence repair pathway choice however the exact mechanism by which BRCA1 and 53BP1 achieve this is still unclear.

The initial recognition of a DSB can also influence the repair pathway choice and therefore Ku and the MRN complex may compete for recognition and promotion of NHEJ and HR respectively. In line with this, Ku depletion can suppress the hypersensitivity of MRN/CtIP (mrx/sae2) null yeast mutants[115,116] and Ku loss increases the level of HR in mice cells[117,118]. Although the MRN and CtIP interaction seems to be positively regulated to promote HR during S and G2, DSBs formed during these phases would still be substrates for Ku binding. The MRN complex is far less abundant than Ku, and Ku binds DSB ends with high affinity; this suggests that Ku is first to bind DSBs and may therefore initiate NHEJ[119]. This raises the question of how NHEJ may be negatively regulated in these instances. Despite insights into the positive regulation of HR, the regulation mechanisms behind NHEJ are largely unexplored.

1.9. The DSB repair protein, Ku

Ku is the main protein involved in the NHEJ pathway, as it is the first responder to a DSB. Crystal structures of Ku alone and bound to DNA revealed that both Ku70 and Ku80

components are held together in a doughnut like shape[66]. The hole in the middle allows Ku to slide onto duplex DNA ends[66]. The structure of Ku and its nuclear abundance make it a great sensor of DNA DSBs[120]. This is because Ku has an extremely high affinity for double-stranded DNA ends[121]. Although Ku can bind a variety of DNA structures including double stranded DNA with short single stranded overhangs, its highest affinity is for blunt ended duplex DNA[120]. Ku has also been shown to bind RNA, although the significance of this is largely unexplored[122,123]. Ku outcompetes PARP1 in binding to DSB ends, although PARP1 dependent ribosylation of Ku can reduce its affinity for DNA[124]. DNA-PKcs itself does have some affinity for DNA, however this is greatly enhanced upon interaction with Ku and therefore makes Ku important in the assembly of the DNA-PK complex and subsequent recruitment of downstream proteins in the NHEJ pathway[125,126].

Ku has also been implicated in the maintenance of telomeres; this has been shown by the observation of shorter telomeres in *S. cerevisiae* strains containing a deletion in either of the Ku subunits compared to wildtype (WT)[127,128]. Ku deficient mice have also shown telomeric abnormalities, showing an increased level of telomere end to end fusions compared to WT[129,130]. Human cells with a Ku80 deletion have also been shown to have abnormal telomere structure and telomere loss ultimately resulting in cell death after a few cell divisions[131].

Ku interacts with the telomeric proteins including telomeric repeat binding factor 2 (TRF2) and it has been proposed that its role in telomere maintenance may be through these proteins[132]. Ku presence at telomeres serves to prevent loss of telomeric loops and prevent the generation of disjointed extrachromosomal telomere circles[131,133]. This happens by preventing recombination at telomeres and either happens through a direct action of Ku or an interactor of Ku. Some have proposed Ku's essentiality in humans may be as a result of its role in telomere maintenance rather than its role in NHEJ[133]. Clearly from phenotypes seen across a range of species Ku does have a role in telomere maintenance although the precise mechanism by which this is achieved is still unknown[131,133].

1.10.Regulation and Removal of Ku

The pivotal role Ku has in NHEJ makes it a likely target of regulation. Ku has been shown to be phosphorylated on various residues on both parts of the heterodimer however the significance of this is largely undetermined. Phosphorylation sites have been identified at S6 of Ku70 and S557, S580 and T715 of Ku80[134]. These phosphorylation sites were originally identified as DNA-PK phosphorylation sites in vitro but were shown to not be dependent on DNA-PK or ATM in vivo[134]. Furthermore, mutation of these residues to non-phosphorylatable alanine residues did not have an effect on NHEJ, as mutants were able to complement the IR sensitivity of Ku null mammalian cells[134]. Mutation of phosphorylation sites to alanine on Ku80 do not have obvious effects on Ku dynamics at laser line induced sites of DNA damage, however mutation of Ku70 phosphorylation sites resulted in significant retention of Ku at DNA damage sites[98]. The Ku70 phosphorylation sites at T305, S306, T307, S314 and T316 were shown to be necessary for retention of Ku and DSBs[135]. Conserved CDK phosphorylation sites have also been identified at T401 and T428 on Ku70[136]. Phosphorylation at these sites was shown to inhibit the interaction of Ku70 with Ku80 and inhibit the interaction of Ku with replication origin sites[137]. This modification of Ku was linked to its role in the initiation and stabilisation of replication but may also be significant to its roles in DNA damage.

The removal of Ku from DNA DSBs after completion of NHEJ has not been extensively studied, however a number of studies have implicated that ubiquitylation facilitates the removal of Ku. Work carried out in *Xenopus laevis* egg extracts showed that ubiquitylation of Ku80 promotes its removal from DNA[138]. In addition, multiple ubiquitin ligases have also been shown to be linked the removal of Ku[138–140] and the ubiquitin interacting protein valosin-containing protein (VCP)/p97 has also been linked to Ku removal[141]. The importance of Ku removal will be discussed in more detail in chapter 3.

1.11.Aims of projects in thesis

The overall aim of the work described in this thesis was to investigate the relatively unexplored mechanisms behind the regulation of NHEJ. This was carried out through investigating factors which interact with the core NHEJ heterodimer, Ku, and assessing how they influence DNA repair processes.

My thesis is broken down in to three projects. The first involves investigating the Ku interacting factor WDR76 for its potential involvement in the removal of Ku following DSBR.

The second involves investigating a potential CDK phosphorylation site on the NHEJ protein PAXX and its involvement in DSB repair pathway choice.

Lastly, I investigated the RecQ helicase linked to Werner syndrome (WS), WRN, and describe the results of a CRISPR-Cas9 screen that I performed to gain insights into its precise function(s) within the DDR.

Chapter 2: Methods

2. Methods

2.1. Mammalian cell culture techniques

2.1.1. Cell culture maintenance

All mammalian cell lines were grown in a 5% CO_2 humidified incubator at 37°C. HEK293, HeLa and U2OS cell lines were grown in Dulbecco's Modified Eagles Medium (DMEM) *(Sigma-Aldrich)* supplemented with 10% foetal bovine serum (FBS), 100U/ml penicillin, 100μg/ml streptomycin and 2mM L-glutamine. hTERT RPE-1 cells (RPE-1) were grown in DMEM/nutrient mixture F-12 Ham *(Sigma-Aldrich)* supplemented with 10% FBS, 100U/ml penicillin, 100μg/ml streptomycin and 2mM L-glutamine. Cells were split using trypsin *(Thermo Fischer Scientific)*.
The following cell lines were maintained in antibiotic selection as indicated:
HeLa green fluorescent protein (GFP)-WDR76 in 0.4mg/ml G418 (*Sigma Aldrich*).
RPE-1 *WDR76-/-* clones: 1G6,4B1,5B1,3H11 in 0.75mg/ml G418.
RPE-1 cell lines expressing WT, S148A and S148E mRuby2-PAXX in 0.6mg/ml Zeocin.
RPE-1 stable CRISPR associated protein 9 (Cas9) expressing clones: WT #28, *WRN-/-* E5-C6 and *WRN-/-* G7-C5 in 0.25mg/ml blasticidin.

2.1.2. Mammalian cell stock freezing and revival

Cells were washed in phosphate-buffered saline (PBS) and incubated at 37°C in trypsin (*Life Technologies*) to detach cells. Once detached, cells were resuspended in media and pelleted using a centrifuge at 300 RCF (relative centrifugal force) for 5 minutes. The supernatant was discarded. Cells were resuspended in freezing media (FBS containing 10% dimethyl sulfoxide (DMSO)) and aliquoted into cryovials (*Nunc®*); 1-2x10^6 cells in 1.5ml freezing media per cryovial. Cells were stored for 2 days at -80°C in an isopropanol chamber *(Thermo Fischer Scientific)* before being transferred into dewars containing liquid nitrogen.

Frozen cell stocks were revived by removing the cryovials from liquid nitrogen and thawing in a water bath at 37°C. Once defrosted, cells were quickly pipetted in a dropwise manner into a falcon tube containing 5ml of prewarmed media. Cells were then pelleted in a centrifuge (300 RCF for 5 minutes). The supernatant was discarded, cells resuspended in the relevant fresh medium and transferred to cell culture flasks.

2.1.3. siRNA transfections

siRNA transfections were performed using Lipofectamine® RNAiMAX reagent *(Invitrogen)* according to the manufacturer's protocol. Briefly, the siRNA and lipofectamine reagent were incubated in Opti-MEM™ (*Gibco®*) before being dosed dropwise onto cells in penicillin and streptomycin free media. The siRNA was incubated with cells for 6 hours and media was replaced with fresh media. Strong knockdown of protein levels was typically seen at 48/72 hours post transfection, as measured by Western blot. Typically, 20nM of siRNA was used unless stated otherwise in the figures (see figure details). siRNAs used: siWDR76-ORF 5'-GUA GAA GGU CAA CAA UGC GAU GAU UTT-3', siWDR76-UTR 5'- CCG CUA AGA AGC CGA AAG ATT-3', siWRN-ORF 5'-GGA UGA AUG UGC AGA AUA ATT-3', siATM 5'-GAC UUU GGC UGU CAA CUU UCG UU-3', siControl – 5'-CGU ACG CGG AAU ACU UCG AUU-3'.

2.1.4. Plasmid transfections

Plasmid transfections were performed using either Lipofectamine® 2000 transfection reagent *(Thermo Fischer Scientific)* or TransIT-LT1 transfection reagent *(Mirus)* according to the manufacturer's guidelines. See figure details for details of plasmid DNA concentrations used.

2.1.5. Electroporation

Plasmids used for generation of stable cell lines were introduced into cells via electroporation using a Neon transfection system (*Invitrogen*). Plasmids and cells were prepared according to the manufacturer's specifications and electroporated using the following protocol: 1 pulse at 1400V for 30ms.

2.1.6. Stable cell line generation

RPE-1 WDR76-/- and *WRN-/-* cell lines were made using clustered regularly interspaced short palindromic repeats (CRISPR) and CRISPR associated protein 9 (Cas9) (CRISPR/Cas9) technology derived from the bacteria *Streptococcus pyogenes*. Cas9 is a nuclease which can be targeted to genomic regions via a guide RNA (gRNA). Cas9 must be directed by the gRNA to a region of DNA which is 5' to a protospacer adjacent motif (PAM) sequence containing the

nucleotides NGG. Cas9 can then cut the DNA at these directed sites, thus generating a DSB[142]. Editing can occur at these sites as a result of natural erroneous repair mechanisms or can be specifically manipulated using exogenous constructs. Reduction of off target cutting can be achieved by directing a mutant nickase version of the Cas9 nuclease which only generates a SSB, this is Cas9 D10A[142].

RPE-1 *WDR76-/-* cells were generated using two gRNAs (gRNA25 and 26 in Appendix Table 1), Cas9D10A and a plasmid targeting construct (detailed in sections 2.6.3 and 3.2.7). RPE-1 *WRN-/-* cells were generated using two gRNAs, Cas9D10A and a plasmid targeting construct (5.2.1 and Appendix Table 2). Plasmids were electroporated in as described earlier.

RPE-1 cells stably expressing mRuby2 tagged WT and S148A/E mutant PAXX were generated by electroporation of plasmids into RPE-1 *PAXX -/-* cells generated by Ochi et al.[143]. Clones expressing mRuby2 PAXX versions were picked using zeocin antibiotic resistance selection and visually inspecting clones for nuclear mRuby2 using a fluorescent microscope.

2.1.7. Cell cycle synchronisation

Cell cycle synchronisation was performed using two different methods: double thymidine blocking and nocodazole treatment. For double thymidine blocking, cells were incubated in media containing 2.5mM thymidine *(Sigma-Aldrich)* for 18 hours followed by three PBS washes and fresh media added. Cells were left to recover for 10 hours and a second treatment of thymidine was added for a further 16 hours. Cells were washed with PBS and media replaced as before. Cells were harvested at relevant time points as indicated (see figures). For the non-released samples, cells were harvested immediately after washes. For nocodazole synchronisation, 100ng/ml of nocodazole was added for 18 hours to T175 flasks containing ~70% confluent cells. Mitotic cells were detached from the flasks by harsh tapping of the flask on a bench top. Cells were re-plated for subsequent recovery and time points taken (as indicated in the figures). For the non-released samples, cells were harvested immediately after the washes.

2.2. Survival Assays

2.2.1. Clonogenic cell survival assay

Cells were seeded onto plates/dishes at concentrations which allowed for good colony spacing and thus reliable counting after colony staining. Where indicated cells may have received siRNA mediated protein depletion prior to seeding and further treatment. For IR survivals, cells were irradiated at concentrations ranging from 1-4Gy using a CellRad® machine *(Faxitron®)*. Cells were then incubated as normal for around 10 days to obtain ideal colony densities for counting. Cells were washed with PBS and stained using a 20% ethanol solution containing 0.1% crystal violet. Colonies were counted manually, and a percentage of survival was calculated based on initial seeding densities and relative to untreated cells.

2.2.2. IncuCyte® cell growth assays

Cells were seeded onto 24 well plates at 1500 cells per well (triplicate wells per treatment). Treatments were added 24 hours after seeding and plates were placed inside the IncuCyte® ZOOM machine *(Essen Biosciences)* which captures images over time and calculates cell confluency. Cells were monitored over time and percentage confluence was measured using a confluence mask. Chronic treatments of camptothecin (CPT) were performed ranging from 1 – 10nM CPT. Cells were left inside the IncuCyte® machine for 6 -10 days to allow for untreated controls to become fully confluent. In some instances, at the end of the IncuCyte® incubation period, cells were stained with Hoechst as detailed below.

2.2.3. Hoechst 33342 staining cell survival assay

Cells were seeded into 24 well plates in triplicate at 1500 cells per well and drug treatments were added 24 hours later (as indicated in the figure legends). Cells were grown for 6 -10 days without letting cells become overconfluent. Cells were fixed and stained with Hoechst 33342 (Hoechst) *(Thermo Fischer Scientific)*. Images were taken on a fluorescent microscope and number of nuclei counted using ImageJ.

2.2.4. Crystal violet staining

Crystal violet staining was used to visualise colony survival for cells exposed to a range of DNA damaging agents including UV, CPT and heat-shock. Cells were washed with PBS and stained using a 20% ethanol solution containing 0.1% crystal violet. Colonies were counted manually, and the percentage survival was calculated based on initial seeding densities and relative to untreated cells.

2.3. Yeast work

2.3.1. Yeast culture

Yeast cells were grown on 2% agar plates containing yeast extract, peptone and glucose (prepared by the media kitchen at the Gurdon Institute) at 30°C. Cells were temporarily stored on plates at 4°C. Yeast strains were frozen in glycerol for long term storage at -80°C.

2.3.2. Yeast knockout generation

A stable *S. cerevisiae cmr1Δ* strain was generated by first PCR amplifying a kanamycin resistance gene with primers containing overhangs that were homologous to the flanking regions of the *Cmr1* gene (see Figure 11 and primers RS040 and RS041 in Appendix Table 1). This product was transformed into a K699 haploid strain of *S. cerevisiae*. Knockouts were identified by selecting single colonies grown on agar plates containing kanamycin resistance. Knockouts were confirmed for deletion of *Cmr1* by PCR.

2.3.3. Yeast DNA damage sensitivity assays

Yeast, peptone, adenine (YPA) agar plates containing 20% glucose and different concentrations of either hydroxyurea (HU), camptothecin (CPT), phleomycin or methyl-methanesulfonate (MMS) were used to measure the sensitivity of a cmr1 deletion strain (*cmr1Δ*) compared to a wildtype strain (*K699 wildtype*) and a DNA damage sensitive strain (*mec1Δsml1Δ*). 10µl drops of yeast strain culture were spotted onto plates at concentrations starting from 10^6 cells/ml and then descending 1:10 serial dilutions. Plates were incubated at 30°C and left for 2-3 days. Plates were then scanned using a scanner (*Epson*). For ultraviolet

(UV) sensitivity assays normal agar plates were used, and plates were exposed to 5-100 J/m^2 of UV using a UV microwave.

2.4. Immunofluorescence

2.4.1. Persistence of Ku Foci by immunofluorescent staining

Detection of Ku foci by immunofluorescence (IF) staining was performed as previously described by Britton et al[144]. Briefly, cells were treated with siRNA (as described earlier) and then reseeded onto cover slips. Cells were then irradiated at 10Gy using the CellRad (*Faxitron*®). 3μM MLN4924 was used 1 hour prior to irradiation of relevant samples. Cells were then pre-extracted in cytoskeleton (CSK) buffer (100mM NaCl, 300mM sucrose, 3mM MgCl2, 0.7% Triton X-100, 10mM PIPES pH7.0 with 0.3mg/ml RNase A) and cells were fixed, permeabilised and stained for Ku80, γH2AX and DAPI. Cover slips were mounted onto microscope slides and widefield images were taken using a DeltaVision (*GE Healthcare*) microscope. Quantification of Ku foci was performed using the program Volocity (*PerkinElmer*) and counting the number of foci per DAPI stained area.

2.4.2. Laser line micro-irradiation

Cells were seeded onto glass-bottomed dishes (*Wilco Wells*) and incubated with 10μM bromodeoxyuridine (BrdU) for 48 hours prior to laser micro-irradiation. Cells had their media changed into phenol-red free medium on the day of laser line micro-irradiation. Laser line micro-irradiation was performed on an *Olympus Inverted FV1000* confocal microscope with a 405nm laser. Images were taken before and after micro-irradiation and recruitment of proteins to sites of DNA damage visualised via GFP/RFP recruitment through either GFP-tagged proteins or by fixing, staining and IF afterwards.

2.4.3. ClickiT EU – RNA imaging – transcription inhibition at sites of laser lines

Cells were seeded and treated as described above for laser micro-irradiation. After laser micro-irradiation cells were allowed to recover for 10 minutes and then cells were incubated with 1mM 5-ethynyl uridine (EU) (*Invitrogen*) for 30 minutes. This was followed by fixation in 4% paraformaldehyde (PFA) in PBS for 15 minutes at room temperature followed by PBS washes. Permeabilisation was performed with 0.1% Triton X-100 in PBS for 15 minutes at room temperature. EU incorporation was detected using the Click-iT RNA Alexa Fluor 594 imaging kit (*Invitrogen*) according to the manufacturer's guidelines. Subsequent antibody labelling of γH2AX and DNA staining with Hoechst was performed. Cells were visualised on an Olympus Inverted FV-1000 confocal microscope and images taken.

2.5. Molecular biology techniques

2.5.1. Polymerase chain reaction (PCR)

Crude lysate, genomic DNA (gDNA) or plasmid DNA were used as templates for PCR reactions. Crude lysate was extracted from cells using Direct PCR lysis buffer *(Viagen Biotech)* containing 0.1mg/ml proteinase K *(Sigma-Aldrich)*. 5-10μl of trypsinised cells were taken into 30μl lysis mix. Lysis/cell mix was incubated at 55°C for 1 hour followed by 95°C for 30 minutes. 1-2μl of crude lysate was used as template for PCRs. gDNA extractions were performed using a DNeasy blood and tissue kit *(Qiagen)* according to the manufacturer's guidelines. 25-200ng of template gDNA were used for PCR reactions. 10-50ng of plasmid DNA was used as template for PCR reactions. PCRs were set up using Phusion high fidelity DNA polymerase *(New England Biolabs (NEB))* according to the manufacturer's protocol. See Appendix Table 1 for list of primers used. PCRs were set up in tubes/96W plates and performed in a Veriti^{TM} 96-well fast thermal cycler *(Thermo Fischer Scientific)* to the following protocol: 30 seconds at 98°C followed by 30 cycles of 10 seconds at 98°C, 30 seconds at 45-72°C (melting temperature) and 30 seconds per kilobase (kb) at 72°C then a final extension for 10 minutes at 72°C. Melting temperatures were adjusted based on the primers being used.

2.5.2. Agarose gel electrophoresis

Amplified PCR products had gel loading dye added and subsequently run on 1-2% agarose gels at 100-150 Volts in 1x Tris/acetic acid/EDTA (TAE) buffer. Samples were run with either a 100 base-pair (bp) or 1kb ladder *(NEB)*. DNA bands were visualised with a UV imager *(Biorad GelDoc)*.

2.5.3. PCR purification

PCR purifications were performed either directly on amplified products in solution or on bands excised from agarose gels. In both cases products were purified using a GeneJet PCR purification kit according to the manufacturer's guidelines (*Thermo Fischer Scientific*).

2.5.4. Immunoprecipitation

Cell lines expressing GFP tagged versions of proteins were cultured, expanded and harvested by washing cells twice in PBS and scraping cells into 1.5ml micro-centrifuge tubes. Cells were pelleted by centrifugation at 300 RCF for 5 minutes at 4°C and the supernatant removed. Pellets were resuspended and rotated for 30 minutes at 4°C in the following lysis buffer: 50mM Tris-HCl pH7.4, 100mM NaCl, 1mM $MgCl_2$, 10% glycerol, 5mM NaF, 0.2% Igepal CA-630, 1x EDTA-free protease inhibitor tablet (*Roche*) and 25U/ml Benzonase. NaCl and EDTA were then added to final concentrations of 200mM and 2mM respectively and vortexed briefly. Samples were rotated at 4°C for a further 10 minutes before being spun down at 3000 RCF for 5 minutes at 4°C. The supernatant was then transferred to fresh micro-centrifuge tubes. Samples were then spun hard at 20,000 RCF for 30 minutes at 4°C and the supernatant kept. A fraction of sample was kept for loading as inputs and the rest were incubated with GFP-trap beads *(ChromoTek)* for 3 hours on a rolling rotator at 4°C. Beads were then spun down, the supernatant discarded, and the beads washed with lysis buffer. Finally samples were eluted in Laemmli buffer (62.5mM Tris-HCl pH6.8, 2% SDS, 10% glycerol, 25mM tris(2-carboxyethyl)phosphine (TCEP)) and heated at 100°C for 5 minutes. Protein samples were subsequently used for Western blotting.

2.5.5. Protein extractions

Cell pellets were resuspended in 50-200μl of lysis buffer (50mM Tris-HCl pH7.4, 400mM NaCl, 10% glycerol, 1mM EDTA, 5mM NaF, 0.2% IGEPAL CA-630 and 1 protease inhibitor tablet *(Roche)*), put into micro-centrifuge tubes and vortexed briefly. Samples were then rotated at 4°C for 30 minutes followed by centrifugation at >20,000x g at 4°C for 30 minutes. Supernatants were transferred to fresh micro-centrifuge tubes.

In some cases, a sodium dodecyl sulphate (SDS) lysis buffer (4% SDS, 20% glycerol and 120mM Tris-HCl pH6.8) was used to prepare protein samples. Cell pellets were resuspended in 50-200μl of SDS lysis buffer, boiled for 5 minutes at 95°C and syringed 10 times with a 25-gauge needle.

2.5.6. Western blotting

Protein concentrations were determined by measuring the absorbance at a 280nm wavelength on a NanoDrop *(Thermo Fischer Scientific)*. Samples of equal concentration were made up by diluting in the same buffer as the protein extractions were performed. Gel loading dye containing 10% β-mercaptoethanol and 0.005% bromophenol blue was added, and samples were boiled for 5 minutes at 95°C. Samples were run on NuPAGE 4-12% Bis-Tris protein gels (*Invitrogen*) with a PageRuler (*Thermo Fischer Scientific*) Plus protein ladder in Novex gel running tanks (*Thermo Fischer Scientific*) with MOPS buffer. Protein was wet-transferred at 100V for 1 hour onto nitrocellulose membranes (GE Healthcare) in transfer buffer (1x protein running buffer (15g Tris, 72g glycine in 5L dH_20) and 20% methanol). Membranes were then stained with Ponceau solution (1% acetic acid, 0.1% Ponceau S) to check for correct transfer. Membranes were washed in distilled water to remove any remaining Ponceau and then membranes were blocked in tris-buffered saline and Tween20 (TBS-T) containing either 5% milk *(Marvel)* or 5% bovine serum albumin (BSA) *(Sigma-Aldrich)*, dependent on the downstream antibodies used. Membranes were blocked for 1-2 hours at room temperature on a shaker. Membranes were then incubated with primary antibody overnight at 4°C on a shaker. Membranes were washed 5 times in TBS-T and then incubated with the relevant horseradish peroxidase conjugated secondary antibodies. Protein bands were visualised using ECL reagent and Amersham Hyperfilm *(GE Healthcare*).

2.5.7. Chromatin fractionation

Cells were either left untreated or treated as detailed in the figures. Cells were harvested by first washing with PBS and subsequently pre-extracted twice (with PBS washes between each pre-extraction) for 3 minutes at 4°C with the following CSK buffer: 100mM NaCl, 300mM sucrose, 3mM MgCl2, 0.7% Triton X-100, 10mM PIPES pH7.0 with 0.3mg/ml RNase A. Cells were scraped into microcentrifuge tubes and protein extracted using Laemmli lysis buffer as described before. Western blotting was then performed as described earlier.

2.5.8. Sample preparation for mass spectrometry

HEK293 FT cells were transfected with either 10μg of a GFP-tagged WDR76 containing plasmid *(Genscript-WDR76cDNA pEGFP-C1*) or a GFP-only containing plasmid (pEGFP-C1), 48 hours prior to further treatment. Samples which received treatment had either 3μM of the neddylation inhibitor MLN4924 or 10μM of the proteasomal inhibitor MG132 added for 2 hours. Cells were then harvested and immunoprecipitation with GFP-trap beads performed as described earlier. A subset of eluted immunoprecipitated sample was run on a gel and stained with Coomassie to visualise banding patterns. Samples were sent to the Professor Benedikt Kessler lab (Target Discovery Institute, University of Oxford) for mass spectrometry analysis.

2.5.9. DNA Sequencing

Sequencing of DNA PCR fragments and plasmids was performed by the Department of Biochemistry Sequencing Facility, University of Cambridge. Relevant primers were provided. Alignments were carried out using either DNAdynamo DNA sequence analysis software (*Blue Tractor Software*) or SnapGene.

2.6. Cloning techniques

2.6.1. Site directed mutagenesis

Site directed mutagenesis was performed on a plasmid expressing mRuby2 tagged WT PAXX using a QuikChange site-directed mutagenesis kit (*Agilent*) according to the manufacturer's guidelines. Briefly, plasmids were amplified by PCR using forward and reverse primers which were designed to incorporate the coding sequences for the desired S148A, and S148E mutations (RS121, RS122, RS125, RS126 primers were used – see Appendix Table 1). The PCR product was *DpnI* digested, purified and transformed into chemically competent XL1-Blue bacteria (*Agilent*).

2.6.2. Guide RNA plasmid cloning

Guide RNA (gRNA) sequences were designed against exon 2 of human WDR76 using the Broad Institute gRNA design tool. Two gRNAs were used: a forward gRNA – TGTTGATGTGGAAAGTAGTC (gRNA25) and a reverse gRNA – CATCGCATCTGCCGTTCTCT (gRNA26). These were made by first annealing two oligos for each gRNA, RS095 and RS096 for the forward gRNA and RS097 and RS098 for the reverse gRNA. Annealing was accomplished by mixing equal volumes (1μl) of 100μM oligos with 98μl of annealing buffer (20mM Tris pH8.0 and 50mM NaCl) and heating to 96°C for 5 minutes followed by cooling down to 4°C at a rate of -1.5°C per minute. Heating and cooling were performed in a Veriti^{TM} 96-well fast thermal cycler *(Thermo Fischer Scientific).* Once annealed, gRNAs were cloned into an all-in-one Cas9D10A plasmid (this was performed by Matylda Sczaniecka-Clift and Siyue Wang in the Steve Jackson Lab). This was achieved by sequential restriction enzyme cutting of the plasmid and insertion of gRNAs through the restriction sites BsaI and BbsI.

2.6.3. WDR76 targeting plasmid construction

The targeting construct was made by cloning three fragments into a pUC19 plasmid backbone: a 5' left homology arm (LHA), a 3' right homology arm (RHA) and a positive selection cassette. Homology arms were designed to flank either side of the gRNA cut sites and generated via PCR. Due to the complexity of the overhangs on the primers needed for the cloning steps, the

fragments were amplified off of a template PCR product which was generated with less complex primers. These templates were generated by PCR amplification of RPE-1 (genomic DNA) gDNA using the primers RS051 and RS060 for the LHA template and RS058 and RS055 for the RHA template. The LHA fragment was generated using the primers RS083 and RS118, and the RHA fragment was generated using the primers RS140 and RS088. The positive selection cassette containing a neomycin resistance gene driven by a PGK promoter was amplified from plasmid pAAV0323 (*Horizon Discovery*) using the primers RS085 and RS119.

DNA fragments were cloned into a pUC19 vector backbone (*NEB*) between the XbaI and HindIII restriction sites using In-Fusion® cloning methods. The pUC19 vector backbone was linearised using XbaI and HindIII restriction enzymes and treated with Antarctic phosphatase (*NEB*) to prevent re-ligation of the backbone. Fragments and backbone were mixed at an equal ratio using 10-200ng of fragments in a 10μl reaction containing 2μl of 5X In-Fusion HD enzyme premix (*Takara-Clontech*). Ligations were performed by incubating the sample at 50°C for 15 minutes and then placing on ice. The ligated plasmid was then transformed into bacteria (see below).

2.6.4. Bacterial transformation

Ligated DNA fragments were transformed into chemically competent Stellar™ competent bacterial cells (*Takara-Clontech*). Stellar™ cells were thawed on ice and 50μl of cells aliquoted into pre-chilled Eppendorf tubes. 1μl (1-5ng) of DNA was added to the cells and left on ice for 30 minutes. Heat-shock was then performed by submerging the bottom half of the Eppendorf tubes into a water bath at 42°C for 45 seconds. Tubes were then placed back onto ice for 2 minutes. 500μl of super optimal broth with catabolite repression (SOC) medium (pre-warmed to 37°C) was then added and tubes incubated for 1 hour at 37°C with shaking (160-225rpm). Between 50 – 200μl of culture was then spread onto agar plates containing relevant antibiotic selection. Plates were incubated overnight at 37°C and then inspected for colonies. Colonies were picked for mini-prepping and confirmed for the correct constructs by restriction enzyme digestion and sequencing. Correct colonies were then maxiprepped to yield higher concentrations of plasmid DNA.

2.6.5. Plasmid Maxiprep

Bacterial colonies were picked and cultured in 200ml of LB medium in a conical flask. Cells were incubated overnight at 37°C with shaking. Cells were pelleted in a centrifuge (3000rpm for 20 minutes) and maxipreps were performed using a QIAGEN® plasmid maxi kit (*Qiagen*) according to the manufacturer's protocol.

2.7. Virus work

2.7.1. Lentivirus generation

Lentivirus carrying a CRISPR gRNA encoding library was produced by transfection of HEK293 Lenti-X cells with the human DDR (hDDR) plasmid library (made by Ramsay Bowden, Dr Yaron Galanty in the Prof Steve Jackson laboratory and Emmanouil Metzakopian at the Wellcome Trust Sanger Institute) and two packaging plasmids: psPAX2 (*Addgene ID12260*) and pMD2.G (*Addgene ID12259*). $3x10^6$ HEK-293 Lenti-X cells were seeded per 15cm dishes (4x dishes) in 25ml of penicillin and streptomycin free media. Plasmid transfections were performed the following day by mixing 7.5μg, 4μg and 18.5μg of the hDDR library, pMD2.G and psPAX2 plasmids respectively, in 1.6ml of Opti-MEM (*Gibco®*). Separately, 90μl of Lipofectamine LTX (*Thermo Fischer Scientific*) was mixed with 1.6ml Opti-MEM. Both Opti-MEM-plasmid and Opti-MEM-lipofectamine mixes were then pooled together and incubated at room temperature for 30 minutes. The mixture was then added to a 15cm dish containing cells in a dropwise manner, ensuring equal coverage across the dish (this was performed for each dish). Transfected cells were left for 54 hours before the supernatant media containing the virus was collected into 50ml falcon tubes. Tubes were spun at 300 RCF for 5 minutes and the supernatant passed through a 0.45μm filter using a syringe and collected. Virus was aliquoted into 5ml and 1ml volumes, snap frozen in an ethanol and dry-ice ice bath and stored at -80°C.

2.7.2. Virus titre determination

To determine the concentration of the hDDR library containing virus cells were infected with various dilutions of virus and fluorescence activated cell sorting (FACS) analysed for percentage of blue fluorescent protein (BFP) positive cells as follows. Two cell lines were used

for infection: an RPE-1 clone expressing Cas9 and an RPE-1 *WRN-/-* clone expressing Cas9 (which were used in the actual CRISPR screen). Measuring the titre in these cell lines most closely replicated screen conditions and thus gave the best determination of virus titre. Cells were seeded in 6cm dishes at $0.6x10^6$ cells per dish with a dish for each dilution of virus to be added as well as extra non-infected dishes: 1:250, 1:500, 1:2500, 1:5000, 1:25000 and 1:50000. 24 hours after seeding a dish from each cell line was used to count the number of cells at the time of infection using a Coulter counter. Virus was diluted, and relevant dishes infected. Cells were left for 5 days following infection and then harvested, fixed with 4% PFA and resuspended in PBS containing 1% BSA. Cells were measured for BFP expression by FACS, using a MoFlo Astrios (*Beckman Coulter*) cell sorter (excitation at 402nm, emission at 457nm). Virus titre was calculated using number of cells infected, dilution of virus used and percentage BFP expressed to give a final virus titre.

2.8. CRISPR-Cas9 genetic screen

2.8.1. Principle of the screen

The basic principle of a CRISPR-Cas9 screen is to identify genes, which when inactivated, alter an observed cellular phenotype. This is achieved by infecting cells expressing Cas9 with a library which contains gRNAs targeting Cas9 to different genes. The number of genes targeted depends on the design and size of the library. A population of cells where only one gRNA is expressed per cell can be achieved by controlling the multiplicity of infection (MOI). Once infected, gRNA mediated CRISPR-Cas9 generates genetic knockouts in a population of cells that represents the gRNA library. A given phenotype can be observed and changes to the phenotype can be traced back to the gRNA infected.

In this thesis, a CRISPR screen was set up to look for genes which when inactivate alter the hypersensitivity of *WRN-/-* cells to camptothecin (CPT). RPE-1 WT and *WRN-/-* clones expressing Cas9 were infected with a human DDR library and subject to CPT treatment at concentrations which kills the majority of cells. Genes which when inactivated give a growth advantage to cells can be identified at the end of the experiment by sequencing the

population and looking for gRNAs that are enriched compared to samples sequenced prior to treatment. In addition, genes which when inactivated, increase the sensitivity of cells to the treatment can be identified by looking at gRNAs which are reduced/dropout in the sequencing from samples after treatment compared to before.

The screen was performed with a focused human DDR library targeting 737 genes associated with the DDR. The library contained 11,281 gRNAs with an average number of 13 gRNAs targeting each gene to increase confidence in the data. In addition, the human DDR library also contained 1200 non-targeting gRNAs as negative controls. (See Appendix Table 4-Appendix Table 8 for list of genes).

2.8.2. Performing the CRISPR-Cas9 screen

The screen was performed in three separate Cas9 expressing cell lines: RPE-1 WT clone 28, RPE-1 *WRN-/-* E5-C6 and RPE-1 *WRN-/-* G7-C5. $28x10^6$ cells were seeded per T300 flasks (4x T300 flasks). 24 hours later cells were infected with the human DDR library containing virus at an MOI of 0.2. Cells were then bulk-sorted by FACS for blue fluorescent protein (BFP) positive cells ~72 hours after post infection to sort for positively infected cells. The number of cells sorted was enough to maintain a 500x library representation, meaning there are 500 cells for each gRNA. These cells were plated into fresh T300 flasks and cultured for 14 days maintaining sufficient cell numbers for 500x library representation of subsequent treatments. A fraction of the cell population was frozen down at this stage for subsequent gDNA extractions to be used as controls before the drug treatments.

$6x10^6$ cells were seeded into 2x T300 flasks per treatment; these were DMSO, 2nM CPT and 5nM CPT treatments for the RPE-1 WT cell line and a DMSO and 2nM CPT treatments for the *WRN-/-* clones. Treatments were performed by administering the CPT/DMSO 24 hours after seeding. Cells were left in the presence of the CPT/DMSO for 5 days, counted and reseeded. For the RPE-1 WT cells, 2nM CPT gave around an inhibitory constant 40 (IC40) and 5nM CPT gave around an IC70. For both *WRN-/-* clones 2nM CPT gave an IC60. Cells were grown to recover from the drug treatment for a further 6 days and samples frozen for subsequent gDNA extractions.

2.8.3. gDNA extractions and library preparation

$6x10^6$ cells per sample were used for gDNA extraction to ensure the 500x library representation was maintained. Cell were pelleted by centrifugation and washed twice in PBS. Cells were pelleted again, resuspended in 5ml of lysis buffer (17mM Tris pH7.5, 17mM EDTA, 170mM NaCl, 0.85% SDS and 1mg/ml proteinase K), and incubated overnight at 55°C with shaking. DNA was precipitated by adding 5ml isopropanol and inverting multiple times until a DNA precipitate was visible. DNA was pelleted in a centrifuge at full speed for 5 minutes. Pelleted DNA was washed three times in 70% ethanol before being resuspended in distilled water to a final DNA concentration of 200ng/μl as measured on a NanoDrop™.

For each sample, 48 initial PCR reactions were set up using 1μg of template DNA to ensure full representation of the experiment. This was to specifically amplify the gRNAs in the samples. PCRs were performed in 50μl in a 96 well plate using Q5 DNA polymerase (*NEB*) (10μl Q5 buffer, 2μl 10mM dNTPs, 0.5μl Q5 DNA polymerase, 2.5μl of 100μM primer (RS204 and RS208), 27.5μl H2O and 5μl (1μg) template DNA). PCRs were performed in a Veriti™ thermocycler at the following conditions: 1 minute at 95°C followed by 30 cycles of 30 seconds at 95°C, 30 seconds at 53°C and 30 seconds at 72°C then a final extension for 10 minutes at 72°C.

PCR reactions were pooled, and samples run on an agarose gel and bands gel purified. DNA concentrations were all around 200ng/μl. Purified products were then used for a second PCR to add Illumina® (Nextera with Truseq adaptors) sequencing specific overhangs, so that DNA samples could be sequenced, and gRNAs identified. 8x 50μl PCR reactions were set up using 1μg of template PCR product from the gel purified RS204/RS208 products. Primer RS217 was used as a forward primer and one of primers RS218 – RS227 was used as a reverse primer for each sample (Table 1). PCRs were performed in the same setup as before and products pooled and gel purified separately for each sample.

Sample ID	Sample detail	1st PCR primers	2nd PCR primers
SIV1	RPE-1 WT DMSO treated	RS204 – RS208	RS217 – RS218
SIV2	RPE-1 WT 2nM CPT treated	RS204 – RS208	RS217 – RS219
SIV3	RPE-1 WT 5nM CPT treated	RS204 – RS208	RS217 – RS220
SIV4	*WRN-/-* G7-C5 DMSO treated	RS204 – RS208	RS217 – RS221
SIV5	*WRN-/-* G7-C5 2nM CPT treated	RS204 – RS208	RS217 – RS222
SIV6	*WRN-/-* E5-C6 DMSO treated	RS204 – RS208	RS217 – RS223
SIV7	*WRN-/-* E5-C6 2nM CPT treated	RS204 – RS208	RS217 – RS224
SIV8	RPE-1 WT day 14 control	RS204 – RS208	RS217 – RS225
SIV9	*WRN-/-* G7-C5 day 14 control	RS204 – RS208	RS217 – RS226
SIV10	*WRN-/-* E5-C6 day 14 control	RS204 – RS208	RS217 – RS227

Table 1 Details of samples in screen and primers used for generating library for sequencing

Table shows the primers used for first and second PCRs for each sample sent for sequencing from the screen. Samples were given tracking IDs.

Gel purified products were run on a Tapestation2200 (*Agilent*) to verify product size. Purified PCR products were quantified using a Qubit™ double stranded DNA (dsDNA) high sensitivity assay kit (*Thermo Fischer Scientific*) and by quantitative PCR (qPCR) using an NEBNext® library quantification kit for Illumina® (*NEB*). Once quantified, 15nM of each PCR product was pooled together (multiplexed) and re-run by qPCR to verify concentration. The multiplexed sample was then submitted for Illumina® sequencing.

2.8.4. Sequencing

Sequencing was performed by Kay Harnish at the Gurdon Institute using an Illumina® Hi-Seq 1500. An Illumina® single read 22bp sequencing protocol was performed using RS228 as a sequencing primer. An average of $38x10^6$ reads matching gRNAs per sample was achieved.

2.8.5. Bioinformatics analysis

Sequence files were processed by Fabio Puddu in the Steve Jackson lab. Sequences were traced to original samples and matched to gRNAs and genes in the library. Joint analysis of CRISPR/Cas9 knockout screens (JACKS) was performed on the datasets from the screen by Iñigo Ayestaran in the Steve Jackson lab.

Chapter 3: Investigating the role of WDR76 in the removal of Ku from DNA ends

3. Investigating the role of WDR76 in the removal of Ku from DNA ends

3.1. Introduction

3.1.1. Ubiquitylation in the DNA damage response

Post translational modifications (PTMs) are a key method of regulating multiple biological processes[145] that involves the covalent attachment of molecules onto an existing protein. PTMs include processes like phosphorylation which covalently attaches a phosphate group onto amino acid residues within a protein; this can modify the structure or interaction capabilities of a protein thereby altering the role of that protein. Acetylation is another type of PTM which is often associated with modifying histones to regulate gene transcription[146]. Another common PTM is ubiquitylation. This involves the covalent attachment of a small, 76 amino acid protein called ubiquitin onto target proteins[147]. The attachment of ubiquitin happens in a three-step process that firstly involves the activation of ubiquitin through an E1 ubiquitin-activating enzyme. This first step is an adenosine triphosphate (ATP) dependent process and results in a covalent attachment between ubiquitin and the E1 enzyme. This now primed ubiquitin is then transferred onto an E2 ubiquitin-conjugating enzyme. Finally, through an interaction between the E2 enzyme and an E3 ubiquitin-ligase, the ubiquitin molecule is transferred onto a target substrate, usually with a bond forming between the C-terminus of ubiquitin and a lysine residue on the target protein[147,148] (Figure 5A).

Ubiquitylation of target proteins exists in multiple forms whereby ubiquitin can be attached to a substrate in different ways. Monoubiquitylation is when a single ubiquitin molecule is attached to an amino acid residue on a substrate. Substrates can also be multi-ubiquitylated, whereby multiple residues on a single protein are monoubiquitylated[149]. Substrates can also be polyubiquitylated; this involves the attachment of additional ubiquitin molecules onto existing ubiquitin, either through an N-terminal methionine (M1) or one of seven lysine residues (K6, K11, K27, K29, K33, K48, K63) on a ubiquitin moiety. This variety of ubiquitin conjugation creates a range of ubiquitin chain topologies, including ubiquitin branchings that have been linked to different types of protein regulation[148] (Figure 5B). The best described ubiquitylation process is K48 linked ubiquitylation which has been shown to be a major signal

driving degradation of proteins via the proteasome[150]. Additional research in the field has linked other types of ubiquitylation to distinct biological roles, such as K63 linked ubiquitin chains playing important roles in DNA damage signalling cascades. An example of this is in the initial DNA damage response to DSBs, where K63 ubiquitylation occurs on histones H1 and H2A by the RNF8 and RNF168 ubiquitin ligases respectively. This K63 ubiquitylation serves as a signal/platform for the downstream recruitment of DNA repair factors to sites of DNA damage[151].

Ubiquitylation is a dynamic process that is negatively regulated by enzymes which catalyse the removal of ubiquitin from substrates. These enzymes are known as deubiquitylating enzymes (DUBs)[152]. Since DNA damage is such a threat to organisms, the DNA repair machinery needs to be tightly coordinated and regulated. One of the ways in doing this is through the constant ubiquitylation and deubiquitylation of proteins involved in the DDR, which can affect their activity and recruitment/retention at sites of DNA damage[153].

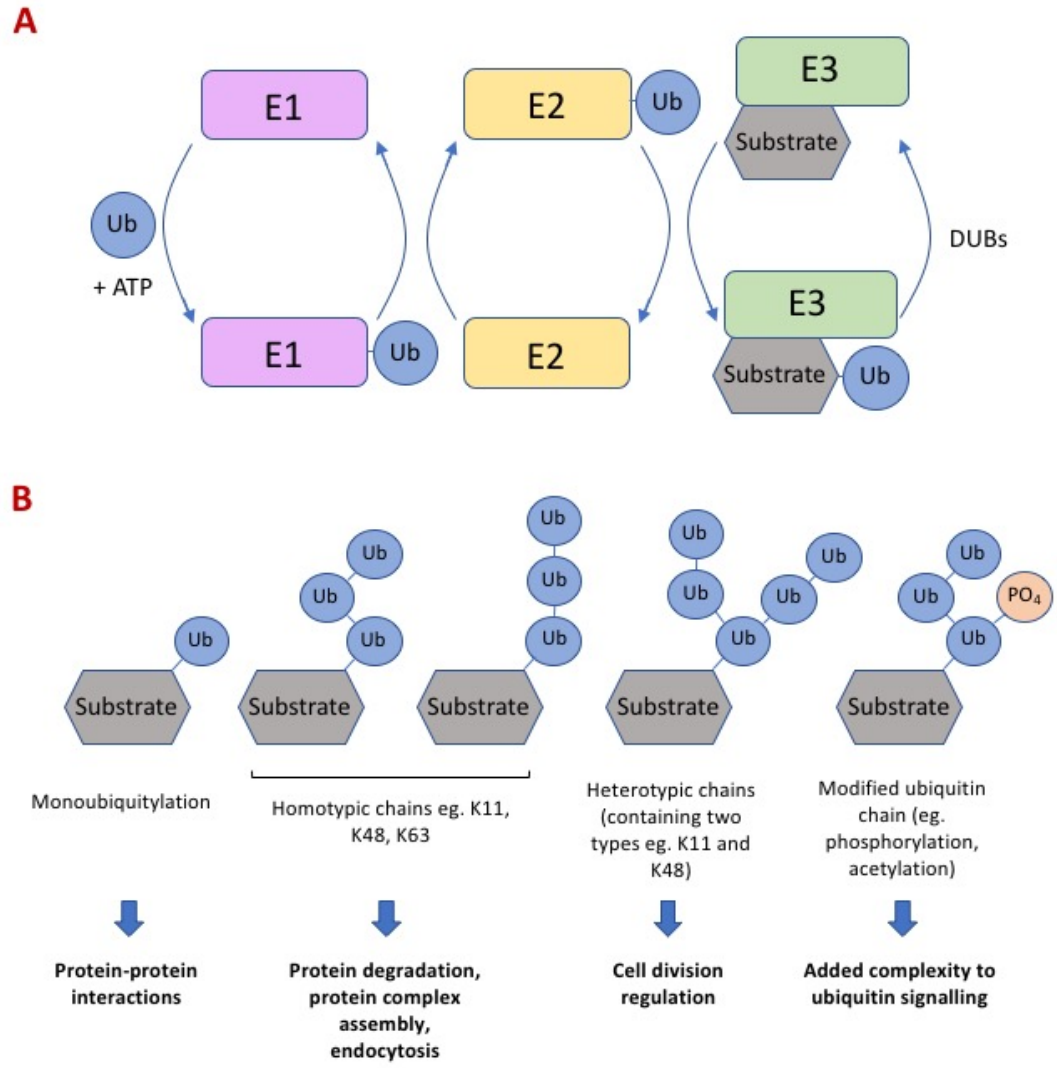

Figure 5 The ubiquitylation cascade and consequences of substrate ubiquitylation

(A) Simplified diagram of the activation and transfer of ubiquitin via E1, E2 and E3 enzymes onto substrates. **(B)** Ubiquitin can be conjugated in many forms which are linked to many different functions. Figure adapted from Rape. Nature Reviews 2018[148].

3.1.2. Cullin-RING ligases in the DNA damage response

The Cullin-RING ligases (CRLs) are a family of multi-subunit E3 ubiquitin ligases that comprise of a RING protein and a core scaffold Cullin protein, of which there are seven in humans: Cullin 1, 2, 3, 4A, 4A, 5 and 7 (CUL1, 2, 3, 4A, 4B, 5 and 7)[154]. The core Cullin scaffold protein has an elongated shape which allows for docking of an E2 conjugating enzyme through the RING protein at the C-terminal end of the Cullin. Binding of substrate adaptors and receptors is

mediated by the N-terminal end of the Cullin. CRLs are activated through a process called neddylation, which involves the attachment of the ubiquitin like protein NEDD8 (Neural Precursor Cell Expressed Down-Regulated 8) onto the Cullin. Neddylation is a multistep process which is very similar to the ubiquitin attachment cascade described earlier[155]. Only when CRLs are in their neddylated form, are they able to effectively facilitate the ligation of ubiquitin onto substrates[156].

As with ubiquitylation, neddylation is also a dynamic process and the CRLs are negatively regulated by the removal of NEDD8; a process referred to as de-neddylation. This is performed by the constitutive photomorphogenesis 9 (COP9) signalosome (CSN), a multi-subunit protein complex that directly interacts with CRLs and through isopeptidase activity, removes NEDD8 and thereby shifts CRLs into an inactive state[154,156].

Due to their ability to bind multiple substrate receptors, CRLs have multiple targets and therefore multiple functions. Additionally, CRL substrates are usually proteins that have already undergone PTMs and therefore the diversity and complexity of their functions are further increased[154]. The CRL with the strongest connection to DNA damage is the Cullin 4 (CUL4) complex[157].

3.1.3. The CUL4 complex and the DNA damage response

The CUL4 complex exists in two forms in mammals defined by the central backbone to the complex, either with CUL4A or CUL4B[158]. Despite high sequence similarity between the two paralogs, evidence suggests the two paralogs are not functionally redundant with each other. CUL4B plays an important role in embryonic development as indicated by the embryonic lethality of CUL4B knockout mice; CUL4A knockout mice in contrast, develop with no apparent defects[159–161].

The CUL4 complex is capable of the ubiquitylation of multiple target proteins. This is achieved through its binding of an adaptor protein, DNA damage binding protein 1 (DDB1) through the N-terminal end of CUL4. DDB1 subsequently has the ability to bind multiple different

substrate receptors; each substrate receptor binds specific substrates (Figure 6A)[162]. The substrate receptors bring potential substrates into close proximity to an E2 ligase which forms part of the complex by binding through a RING finger protein, RING box protein 1 (RBX1), located at the C-terminal region of CUL4. This then allows for transfer of ubiquitin onto a substrate. The substrate receptors are often referred to as DDB1-CUL4 associated factors (DCAFs). Many of these substrate receptor proteins are WD40 domain containing proteins. WD40 repeat domain containing proteins are able to fold into β-propeller structures allowing for large surfaces of interaction with potential substrates[163]. Many of the DCAFs have been identified through immunopurification techniques however a large proportion of them still have unknown functions and undefined substrates[162].

Due to its ability to bind multiple substrates, the CUL4 complex is involved in a number of biological processes including cell cycle regulation, transcription regulation, ribosome biogenesis, RNA splicing and histone modification [157,162]. In addition to these processes evidence suggests that the complex is involved in the DDR; this has been shown via its involvement in the nucleotide excision repair (NER) pathway and the response to UV damaged DNA. Two of the best characterised substrate receptors demonstrating the involvement of CUL4 in DNA repair are DNA damage binding 2 (DDB2) and Cockayne syndrome A (CSA)[164]. DDB1 and DDB2 are important components in the global genome NER (GG-NER) sub-pathway, which repairs bulky DNA adducts throughout the genome. Mutations in DDB1 or DDB2 result in xeroderma pigmentosum (XP), an autosomal recessive rare disease characterised by extreme sensitivity to sunlight[165,166]. One of the most common causes of death in XP patients is skin cancer[167]. CSA is involved in the transcription-coupled NER (TC-NER) sub-pathway, which acts solely on DNA damage that inhibits transcription[168]. Mutations in CSA result in Cockayne syndrome, a rare disease characterised by microcephaly and growth failure. This syndrome is also associated with increased sensitivity to sunlight[164].

Data published within the Steve Jackson laboratory clearly shows that neddylation occurs at sites of DNA damage as seen by recruitment of GFP-NEDD8 to sites of laser line induced DNA damage[169]. Furthermore, the level of GFP-NEDD8 recruitment was reduced upon siRNA mediated depletion of CUL4A/B, and both CUL4A and B themselves localise to sites of DNA damage. Inhibition of neddylation using MLN4924, an inhibitor of the NEDD8 activating

enzyme E1 (NAE1), resulted in an increased persistence of Ku foci after IR induced DNA damage[169]. One of the unanswered questions in the DNA damage field is how the Ku heterodimer is removed from the DNA after repair has taken place. The doughnut shaped structure of the heterodimer allows it to slide onto DNA ends; however when the break has been fixed by NHEJ, Ku could remain trapped on the DNA with the ability only to slide[66,170]. This would create potential problems by creating a barrier to transcription or replication and could lead to toxicity by creating more DNA damage. It is therefore likely that a method(s) exists for the removal of Ku from DNA. Postow et al.[138] showed that Ku80 can be removed from DNA via a K48-linked ubiquitin dependent pathway[138]. In addition, Brown et al[169] highlighted a role of Cullin mediated ubiquitylation in the removal of Ku after DNA damage and indicates the likely role of CUL4 specifically in the regulation of NHEJ. This raises the question: which substrate adaptor of the CUL4 complex is responsible for the ubiquitylation and subsequent removal of Ku?

3.1.4. Investigating the role of WDR76 in the regulation of NHEJ

WDR76 is a substrate receptor of the CUL4 complex but currently its substrate(s) is (are) unknown[162]. The implications of CUL4 in the regulation of Ku DNA binding make WDR76 an interesting protein to study, as it potentially has a role in the regulation of NHEJ.

WDR76 is a conserved protein from yeast to mammals and shows a high sequence similarity (18.97% sequence identity) between the human and *S. cerevisiae* orthologs (Figure 6B). This likely indicates that it has an important biological function(s). The *S. cerevisiae* ortholog of WDR76 is Cmr1. A number of groups have implicated Cmr1 in the DNA damage response[171–173]. Cmr1 has been shown to interact with several proteins involved in DDR processes, including the yeast orthologs of Ku70 and Ku80 as well as the yeast orthologs of the RPA complex[174,175]. Cmr1 has also been shown to directly bind both single-stranded DNA (ssDNA) and double-stranded DNA (dsDNA), with a slightly higher affinity for dsDNA over ssDNA[172]. In addition, Cmr1 showed preferential binding to UV damaged DNA which again suggests an involvement of WDR76 in the DNA repair process[172]. Studies in yeast have also identified Rtt101 as being the closest homolog to CUL4[176]. Interestingly *Rtt101* knockout strains are

hypersensitive to a range of DNA damaging agents including methyl methanesulfonate (MMS) and camptothecin[176,177].

More recently, two different groups showed via endogenous GFP-tagging that Cmr1 relocalises to form sub-nuclear foci under DNA damaging conditions[173,178]. In yeast, this is symptomatic of proteins involved in DDR processes. Gallina et al. also showed that human WDR76 interacts with Ku70/80 and alluded to a role in the cellular repair and recovery after DNA damage[173].

Despite these findings the precise role(s) of WDR76 within the DDR remains to be defined. This makes WDR76 an interesting target for investigation, as it has a potential role in the removal of Ku as well as in the regulation of NHEJ.

A

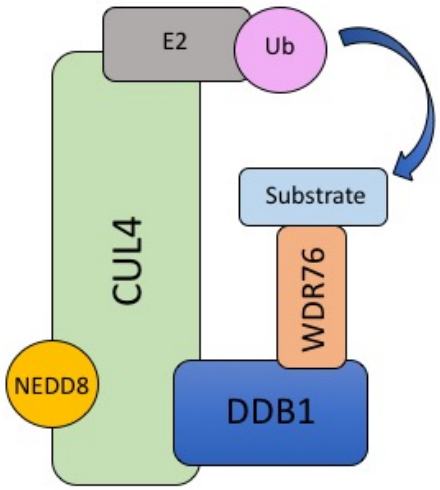

B

```
                                  WD4                                  WD5
Human, Homo sapiens               DARRLNSRR----------SQPLISLTEHTKSIASAYFSPLTGNRVVTTCA 516
Mouse, Mus musculus               DARFLKSRG----------SQPLISLTEHSKSIASAYFSPVTGNRVVTTCA 415
Duck, Anas platyrhynchos          DVRYLKSDG----------NKPVSTLNGHTKSVASAYFSPVTGNRVVTVCA 357
Chinese turtle, Pelodiscus sonensis DTRYLKPNG----------NKPILFLSGHTKSVASAYFSPITGHRVVTTCA 490
African clawed frog, Xenopus laevis DVRKLKQK----------AQPVLSLAGHSKSVASAYFSPVTGNRILTTCA 477
Zebrafish, Danio rerio            DLRHLKKRN----------SPAVCELYGHSRSTSSAFFSPLTGSRVLTTCM 446
Yeast, Saccharomyces cerevisiae   DTRNLVKKPEWSQYEDYPSHEIVSTYDSRLSVSAVSYSPTDG-TLVCNGY 410
                                  * * *                 :         * ::. :**  *  ::

                                  WD5                                  WD6
Human, Homo sapiens               DCNLRIFDSSC---ISSKIPLLTTIRHNTFTGRWLTRFQAMWDPKQEDCV 563
Mouse, Mus musculus               DCKLRVFDSSS---ISSQLPLLSTIRHNTVTGRWLTRFQAVWDPKQEDCF 462
Duck, Anas platyrhynchos          DDKLRVYDTSS---LSSTIAVLSTVRHNNNTGRWLTRFRAIWDPKQEDCF 404
Chinese turtle, Pelodiscus sonensis DDKLRVYDTSS---LSAAIPVVTAIRHNNNTGRWLTRFRAVWDPKQEDCF 537
African clawed frog, Xenopus laevis DDYIRVYDSSS---LSSASPLLTALRHNNNTGRWLTRFRAVWDPKQESCF 524
Zebrafish, Danio rerio            DDCIRVFDSSQ---IAGSIPALTSIRHNMQTGRWLSRLCAVWDPKHQECF 493
Yeast, Saccharomyces cerevisiae   DDTIRLFDVKSRDHLSAKLEPKLTIQHNCQTGRWTSILKARFKPNK-NVF 459
                                  *  :*::* .    ::.      :::**  **** : : * :.*:: . .
```

Sequence 1	Length (amino acids)	Sequence 2	Length (amino acids)	Percentage Identity (%)
Homo sapiens	626	*Mus musculus*	524	75.00
Homo sapiens	626	*Anas platyrhynchos*	465	53.76
Homo sapiens	626	*Pelodiscus sonensis*	584	43.15
Homo sapiens	626	*Xenopus laevis*	535	33.08
Homo sapiens	626	*Danio rerio*	598	51.67
Homo sapiens	626	*Saccharomyces cerevisiae*	522	18.97

Figure 6 WDR76 is a conserved substrate receptor of the CUL4 ubiquitin ligase

(A) Simplified diagram of the CUL4 ubiquitin ligase in its active, NEDD8 bound, form. The substrate adaptor DDB1 allows binding of the substrate receptor WDR76 to facilitate the ubiquitylation of a substrate. **(B)** Representative protein alignment comparing a section of WDR76 across a range of species. WD40 domains 4,5 and 6 of human WDR76 are highlighted and in orange text. Table shows sequence identity compared to human WDR76. * = single fully conserved residue, : = conservation between groups of strongly similar properties, . = conservation between groups of weakly similar properties.

3.2. **Results**

3.2.1. WDR76 interacts with Ku70/Ku80

If WDR76 is responsible in mediating the ubiquitylation of Ku, one would expect the two proteins to interact with each other. To first identify whether WDR76 interacts with the Ku70/80 heterodimer, immunoprecipitation assays (IPs) were set up. A plasmid construct expressing a GFP-tagged version of WDR76 in a pEGFP-C1 background was transfected into either human RPE-1 or HEK-293 cells and GFP-WDR76 captured using GFP trap beads. In both cell lines, WDR76 showed an interaction with Ku70 and Ku80 which was not seen in the GFP only transfected controls (Figure 7A/B). WDR76 also exhibited interactions with the substrate adaptor protein DDB1 and the CUL4A E3 ligase in both cell lines. As all IPs were performed in the presence of ethidium bromide (EtBr) and were benzonase treated, the likelihood of indirect interactions through DNA bridging was low.

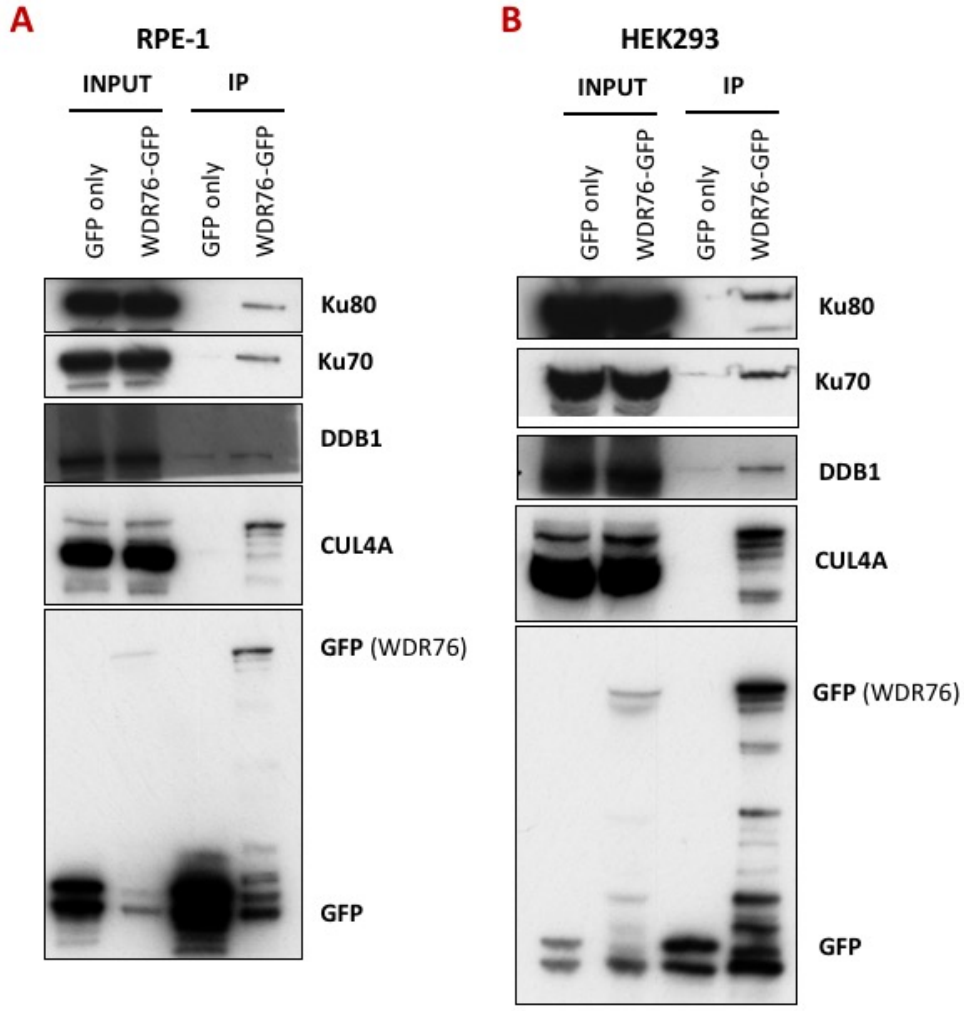

Figure 7 WDR76 interacts with Ku70, Ku80 and the CUL4 *complex*

Immunoprecipitation assays (IPs) showing pulldown of CUL4A, DDB1, Ku70 and Ku80 in RPE-1 cells **(A)** and HEK293 cells **(B)** expressing GFP-tagged WDR76 (WDR76-GFP). A plasmid expressing GFP only was used as a control. IPs were performed in the presence of EtBr (which intercalates with DNA) and benzonase (an endonuclease which digests DNA and RNA) to reduce the likelihood of DNA/RNA bridged interactions.

3.2.2. WDR76 localises to sites of DNA damage

As WDR76 appeared to interact with Ku, I next tested to see if WDR76 is recruited to sites of DNA damage. Live HeLa cells stably expressing a GFP tagged mouse version of WDR76 were used to visualise recruitment of the protein to sites of laser line induced DNA damage. Cells that had not undergone pre-treatment with BrdU showed no recruitment to UV lasered areas,

whereas cells pre-sensitised with BrdU did show obvious recruitment as seen by an enriched line of GFP in the lasered areas (Figure 8). This suggests that the recruitment of WDR76 is specific to DNA damage and not as a result of the laser itself. Recruitment of WDR76 to laser induced DNA damage appeared rapid, with clear GFP induction seen within a minute after damage. Recruitment appeared to fade around the 12-15 minute time points.

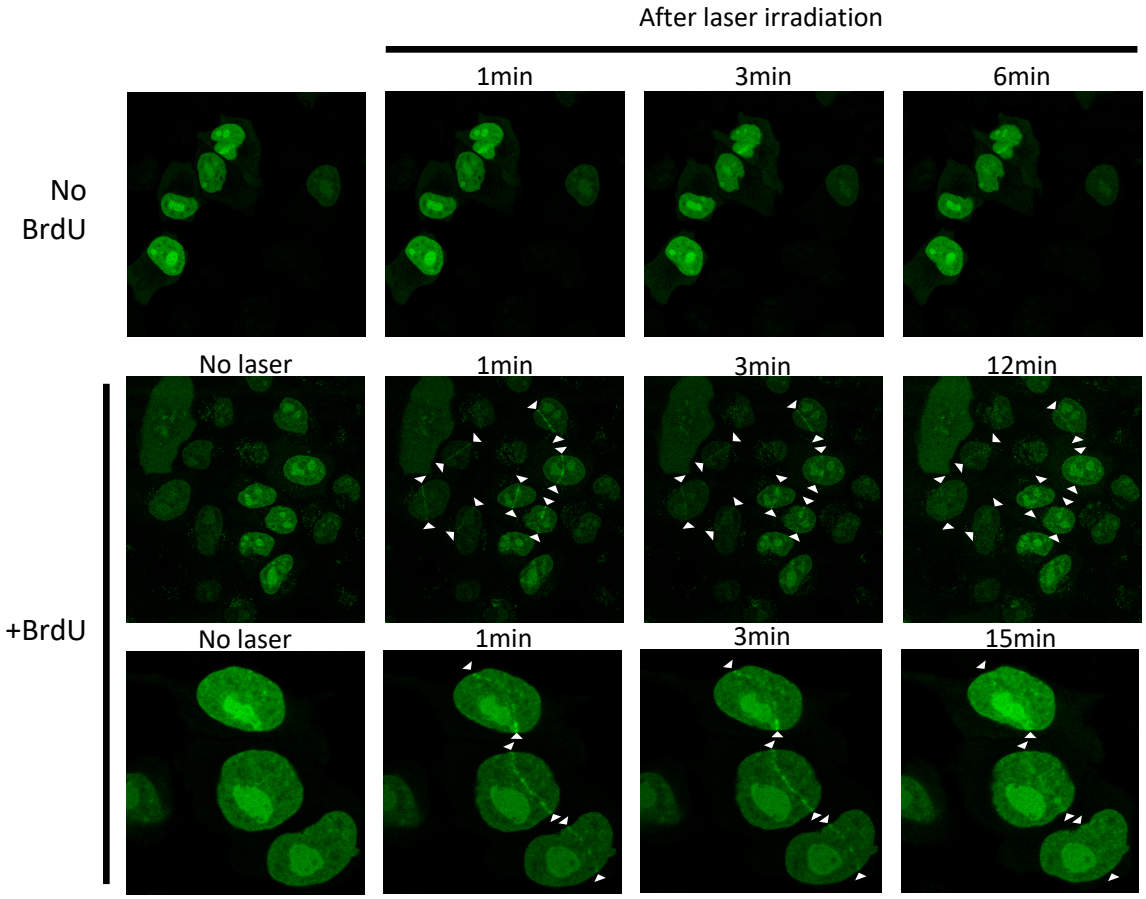

Figure 8 WDR76 is recruited to sites of laser line induced DNA damage

HeLa GFP-WDR76 expressing cells were either untreated (top panel) or pre-treated with BrdU (middle and bottom panels) prior to laser micro-irradiation and imaging to visualise recruitment of WDR76 to sites of DNA damage. Bottom panel shows zoomed in images of nuclei. White arrows indicate the positions of the start and end of lines.

3.2.3. WDR76 depletion does not increase persistence of NHEJ factors at sites of DNA damage

As explained earlier, neddylation, the process that activates Cullins, occurs at sites of DNA damage containing DSBs. Inhibition of this neddylation, using the small molecule drug MLN4924[179], results in an increase in persistence of the core NHEJ component Ku[169]. In light of this, investigations were carried out to see if siRNA mediated depletion of WDR76 resulted in persistence of Ku at sites of DNA damage. Chromatin fractionation was performed on WDR76 siRNA depleted and control cells before and after phleomycin treatment to see if NHEJ proteins were retained on chromatin after DNA damage. An siRNA against luciferase was used as a negative control (siControl). In undamaged control cells (siControl -0) there is a low level of the NHEJ factors Ku70, Ku80, XLF and XRCC4 on chromatin (Figure 9A). This level of these proteins on chromatin is induced upon DNA damage with phleomycin which can be seen strongly 1.5 hours after phleomycin treatment. The level of Ku80 on chromatin subsides 5.5 hours after phleomycin treatment. Two siRNAs against WDR76 were used, one against the open reading frame (ORF) (siWDR76 ORF) and one against the untranslated region (UTR) (siWDR76 UTR). Cells treated with siRNA against WDR76 show similar levels of NHEJ proteins on chromatin to the control cells; no obvious persistence of NHEJ factors on chromatin was detected relative to the control cells. Cells treated with MLN4924 did show an increased persistence of Ku80 compared to control siRNA treated cells, which is particularly evident in the 3.5 and 5.5 hours post phleomycin treatment samples (Figure 9B).

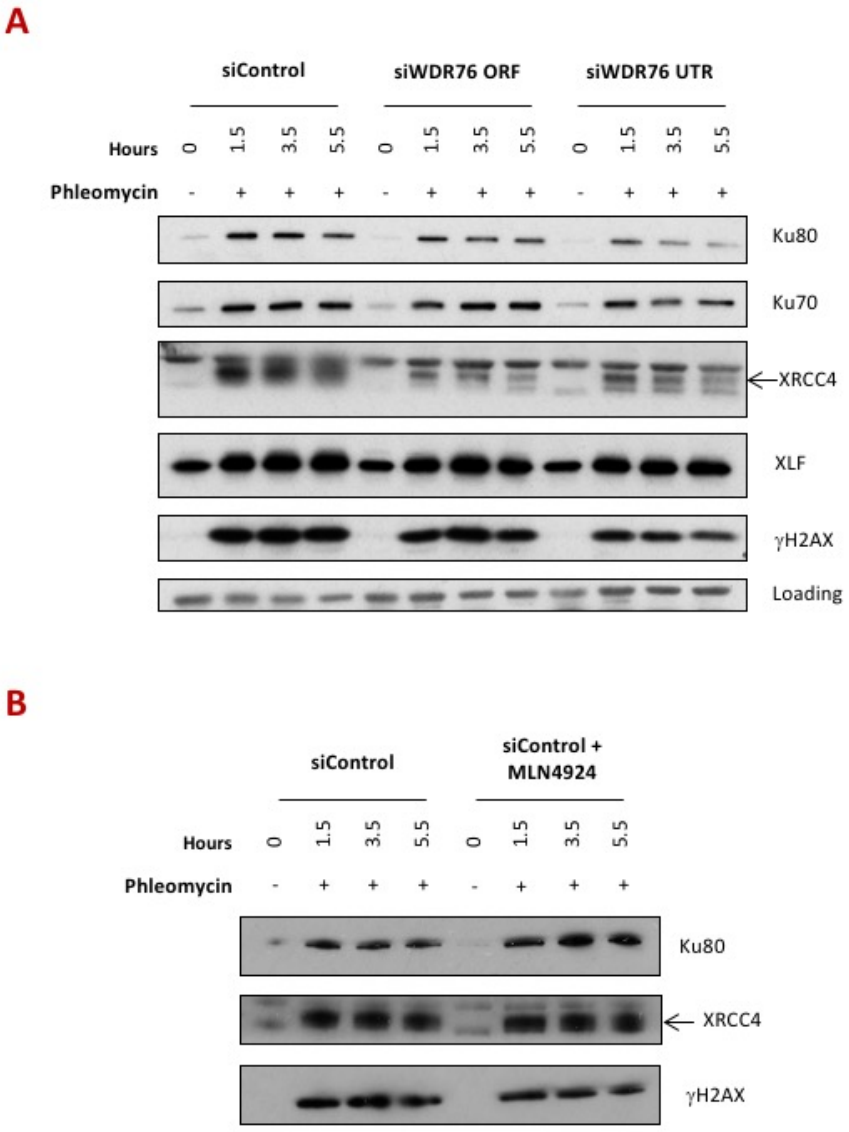

Figure 9 siRNA depletion of WDR76 does not increase persistence of NHEJ factors after DNA damage in the chromatin fraction

(A) U2OS cells were depleted with 20nM of either a negative control siRNA (siControl) or siRNA against either the ORF (siWDR76ORF) or UTR (siWDR76UTR) of WDR76. Cells were treated with 0.75mg/ml phleomycin and samples taken at 1.5, 3.5 and 5.5 hours of recovery. This was followed by chromatin fractionation and Western blotting. **(B)** Negative control siRNA treated cells were dosed with 3μM MLN4924 before chromatin fractionation and Western blot.

3.2.4. siRNA mediated knockdown of WDR76 leads to persistence of Ku foci after irradiation

Although an effect of WDR76 on persistence of Ku on chromatin after DNA damage was not detected by chromatin fractionation approaches, if WDR76 is involved in the ubiquitylation and subsequent removal of Ku from sites of DNA damage one would expect that WDR76 depletion might result in persistence of Ku foci after DNA damage. To test this, an established method to detect Ku foci by immunofluorescent (IF) staining was used (as described in the Methods section 2.4.1). U2OS cells were either transfected with a control siRNA or siRNA against WDR76. Cells treated with the control siRNA only have a relatively low number of Ku foci in undamaged cells (Figure 10A). This number increases sharply after irradiation with a peak in number of foci per nucleus 8 minutes after DNA damage. The number of foci then begin to drop with recovery time after irradiation, returning back to baseline level around 2 hours after the initial irradiation. Cells pre-treated with the neddylation inhibitor MLN4924 (MLNi), behave similarly to the control in non-irradiated cells and at the 8-minute after irradiation time-point. However, in these cells there is an increased persistence of Ku foci at the 1 hour and 2 hour after irradiation time-points compared to cells not treated with MLN4924 (Figure 10A/B). Cells treated with siRNA against WDR76 (si76ORF/si76UTR) show an increase in persistence of Ku foci at the 2-hour time-point compared to control siRNA treated cells at the same timepoint (Figure 10A/B).

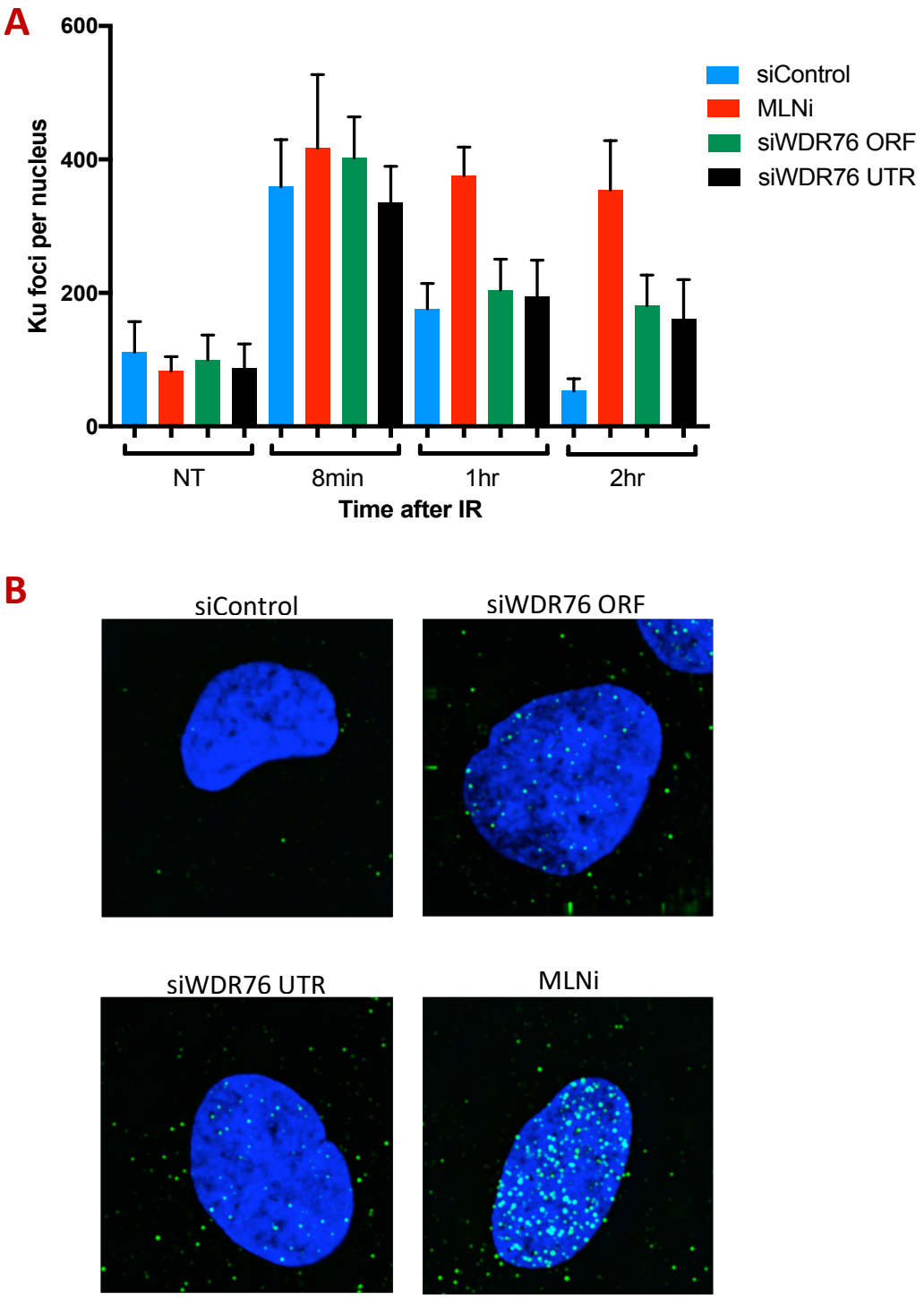

Figure 10 WDR76 knockdown results in an increased persistence of Ku foci

Non-treated (NT) and irradiated U2OS cells were pre-extracted with CSK buffer and stained by IF for Ku80 **(A)** Graph showing number of Ku foci before and after 10 Grays of irradiation. Negative control siRNA (siControl) or siRNA against either the ORF (siWDR76ORF) or UTR (siWDR76UTR) of WDR76 were used. MLNi = siControl cells pre-treated with 3μM MLN4924. N=3, error bars show SEM **(B)** Representative images of samples two hours after irradiation.

3.2.5. Yeast *CMR1* knockout does not show sensitivity to DNA damaging agents

As shown previously, WDR76 is conserved across a range of species (Figure 6B). In order to investigate its function in another model organism, a knockout in *S. cerevisiae* was generated in parallel to carrying out studies on mammalian cells. A knockout was made by first generating a PCR fragment containing a kanamycin resistance gene flanked by the genomic regions either side of the *CMR1* gene (Figure 11A). The *CMR1* deleted strain (*cmr1Δ*) was then tested for sensitivity to a range of different DNA damaging agents in comparison to a wildtype strain and a *mec1Δsml1Δ* strain that is hypersensitive to DNA damage. The *cmr1Δ* strain showed no detectable increase in sensitivity to HU, CPT, MMS, phleomycin or UV compared to the wildtype strain as can be seen from the similar growth in colonies across all drug doses. The *mec1Δsml1Δ* strain, as expected, showed increased sensitivity to all DNA damaging agents compared to the WT, thus showing that the drugs were working (Figure 11B).

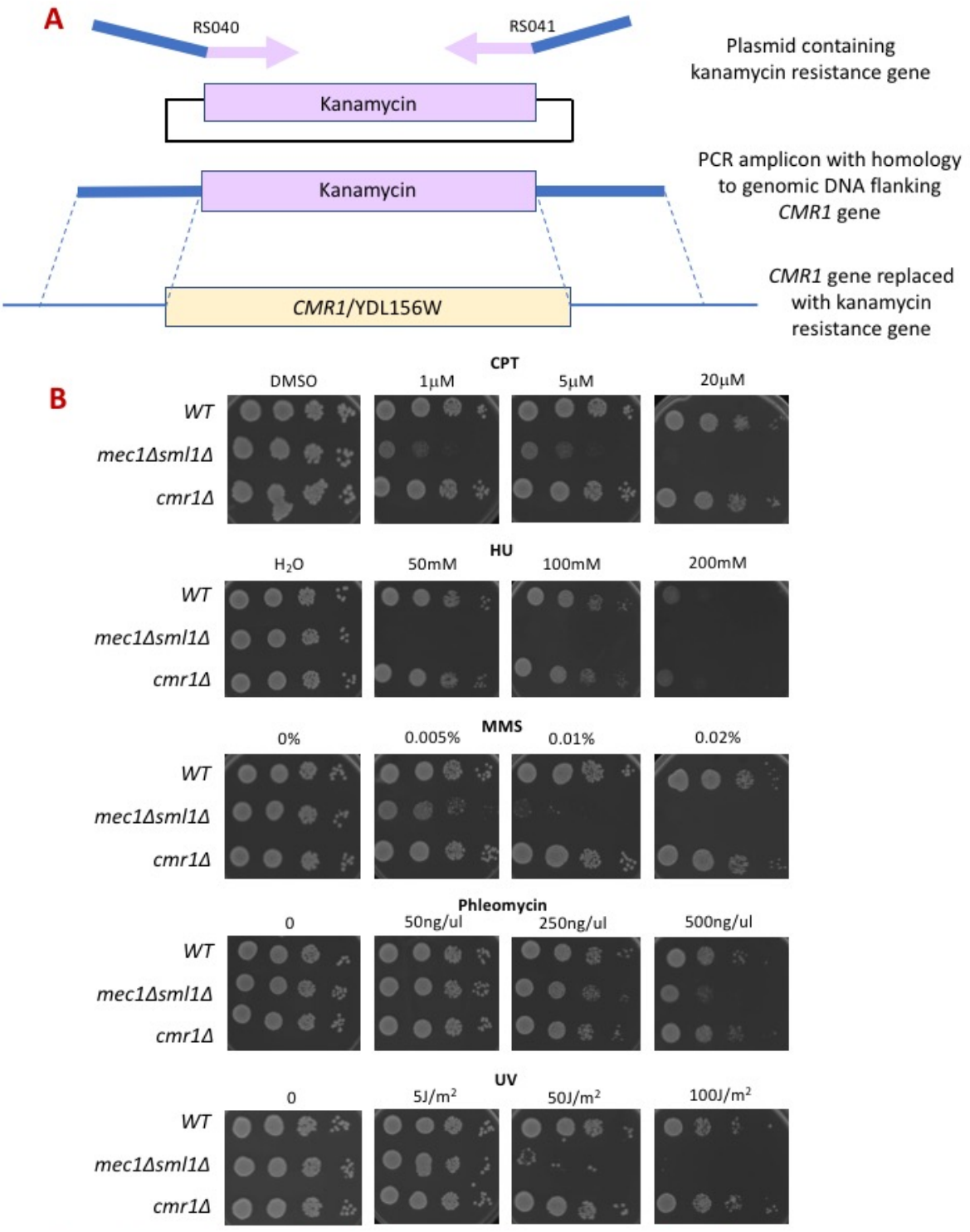

Figure 11 S. cerevisiae cmr1 knockout does not show hypersensitivity to DNA damaging agents

(A) Strategy used for the generation of cmr1 knockout in *S. cerevisiae*. **(B)** Sensitivity profile to indicated DNA damaging agents in WT = wildtype, *mec1Δsml1Δ* and *cmr1Δ* backgrounds.

3.2.6. siRNA mediated depletion of WDR76 does not increase sensitivity of cells to irradiation

As WDR76 was shown to be recruited to sites of DNA damage and may be influencing the ubiquitylation of Ku, I tested to see if siRNA mediated depletion of WDR76 renders cells more sensitive to DNA damage. To do this, clonogenic survival assays were performed in U2OS cells treated with increasing doses of irradiation. Control siRNA treated cells (siControl) showed a typical decline in percentage survival with increasing doses of irradiation (Figure 12). Cells treated with an siRNA against ATM (siATM), a central component of the DNA damage response, showed increased sensitivity to DNA damage by irradiation compared to the control. This is particularly evident at the 3 and 4 Gy doses. Cells treated with siRNA against WDR76 (siWDR76 ORF/UTR) did not show any significant difference in its DNA damage sensitivity profile from that of the control (Figure 12).

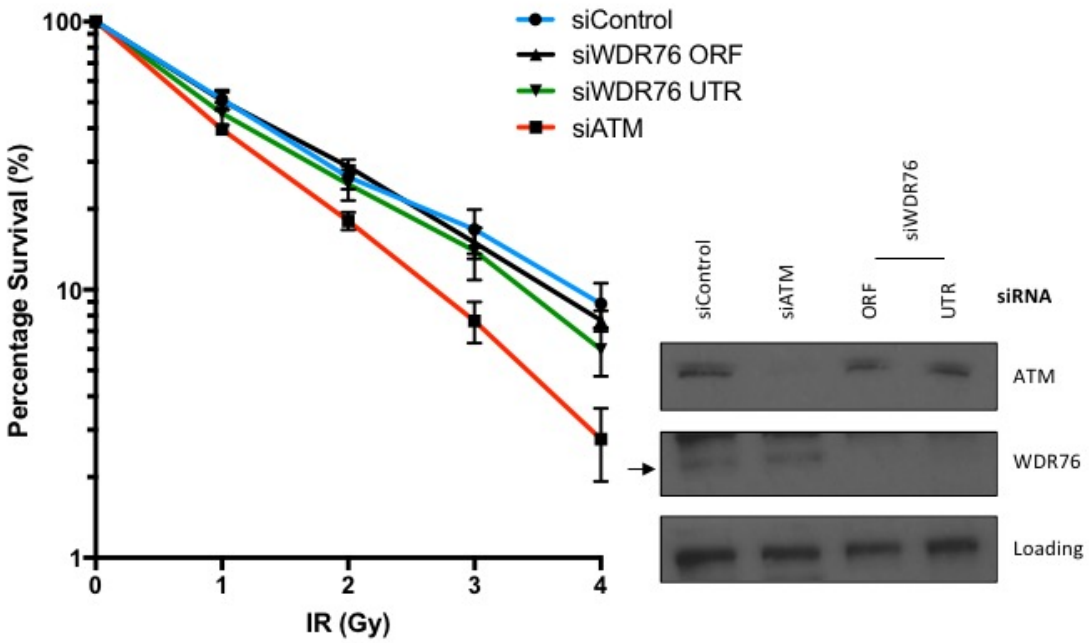

Figure 12 siRNA mediated depletion of WDR76 does not increase sensitivity to irradiation

U2OS clonogenic survival assay showing sensitivities of siRNA depleted cells to increasing doses of irradiation. N=3, error bars show SEM. Blots show depletion of relevant proteins in cells used in the assay.

3.2.7. Human cell *WDR76* gene knockouts exhibit IR hypersensitivity

My investigations into WDR76 thus far showed a link to the DDR via its interaction with Ku, effect on Ku foci after DNA damage and obvious localisation to sites of DNA damage. In order to further investigate the role of WDR76 within the DDR, isogenic knockouts were generated in human RPE-1 cells. It was expected that any phenotypes associated with WDR76 loss would be more apparent in a knockout background rather than by depletion with siRNA.

In order to generate knockouts, two CRISPR-Cas9 guide RNA (gRNA) targeting sites in exon 2 of the human WDR76 gene were determined using the Broad Institute gRNA design tool. These sequences were then cloned into an all-in-one plasmid backbone containing U6

promoters driving expression of each gRNA and a separate promoter driving Cas9D10A nickase expression. Using the Cas9D10A nickase causes ssDNA incisions at the gRNA targeted regions and thus reduces the potential of off-target editing. An enhanced GFP (EGFP) marker after a T2A linker from the nickase was also utilised to ensure plasmid entry upon targeting (Figure 13A). A targeting construct was also generated to make downstream validation of WDR76 knockouts easier. This was made by first generating PCR products of homology arms flanking the gRNA cut sites, and a PCR product of a positive selection cassette containing a neomycin resistance gene driven by a PGK promoter (Figure 13A). These PCR products were then cloned into a pUC19 backbone using InFusion® cloning techniques. Both plasmids were sequence validated to check for correct cloning.

Plasmids were electroporated into RPE-1 cells using a Neon nucleofector. 48 hours after electroporation, cells were single cell sorted by FACS into 96 well plates containing 0.75mg/ml G418. Colonies were grown and expanded whilst PCR validation was performed on potential knockout candidates (Figure 13B). An initial PCR screen was performed using a primer pair that allowed detection of insertions or deletions at the WDR76 exon 2 genomic locus as well as being able to visualise stable insertion of the targeting construct into cells. Colonies were picked where a PCR electrophoresis band showed an obvious variant to the WT control (Figure 14A). These colonies were then taken forward for further analysis to check for on target integration of the targeting construct by using primer pairs that contained one primer within the targeting construct itself and the second primer in the surrounding genomic locus. Products run by gel electrophoresis showed on-target integration of the targeting construct in multiple targeted colonies but not in untargeted WT cells (Figure 14B). Colonies were checked for insertions/deletions (indels) which put WDR76 out of frame by reducing the extension time of PCR cycles to specifically amplify the smaller of the two products. Sequence analysis revealed that clone 1G6 had a 142bp insertion and clone 3H11 had a 196bp insertion (Figure 15A). Both these insertions put WDR76 out of frame. Lastly, clones were confirmed for a WDR76 knockout on a protein level by Western blotting, once a reliable antibody was identified (Figure 15B).

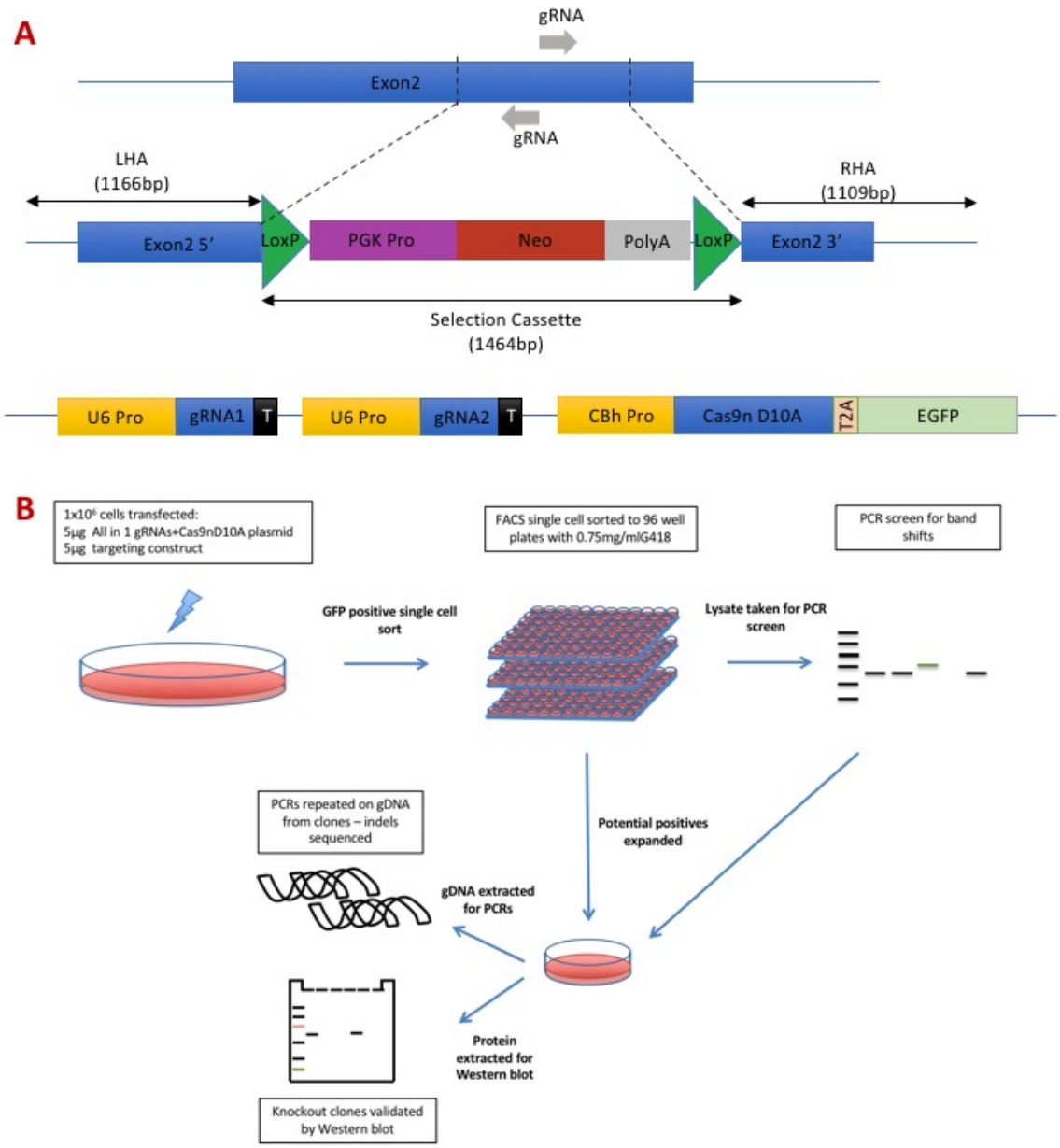

Figure 13 WDR76 knockout generation in RPE-1 cells

(A) Schematic of constructs used and design of gRNAs for the knockout strategy. Two gRNAs targeting exon2 of WDR76 were designed and cloned into an all-in-one plasmid containing a promoter driven Cas9D10A nickase. EGFP was also included via a T2A linker. A positive selection targeting plasmid containing a neomycin resistance gene (Neo) and homology arms flanking the gRNA cut-sites (LHA/RHA) was constructed. **(B)** Diagram showing overall knockout process from transfection through to validation. 5µg of targeting construct and all-in-one plasmid were transfected into RPE-1 cells and single cell sorted into 96W plates by FACS 48 hours after transfection. Single colonies were identified, and crude lysates taken for PCR validation. Potential knockout clones were expanded and validated by PCRs and Western blotting.

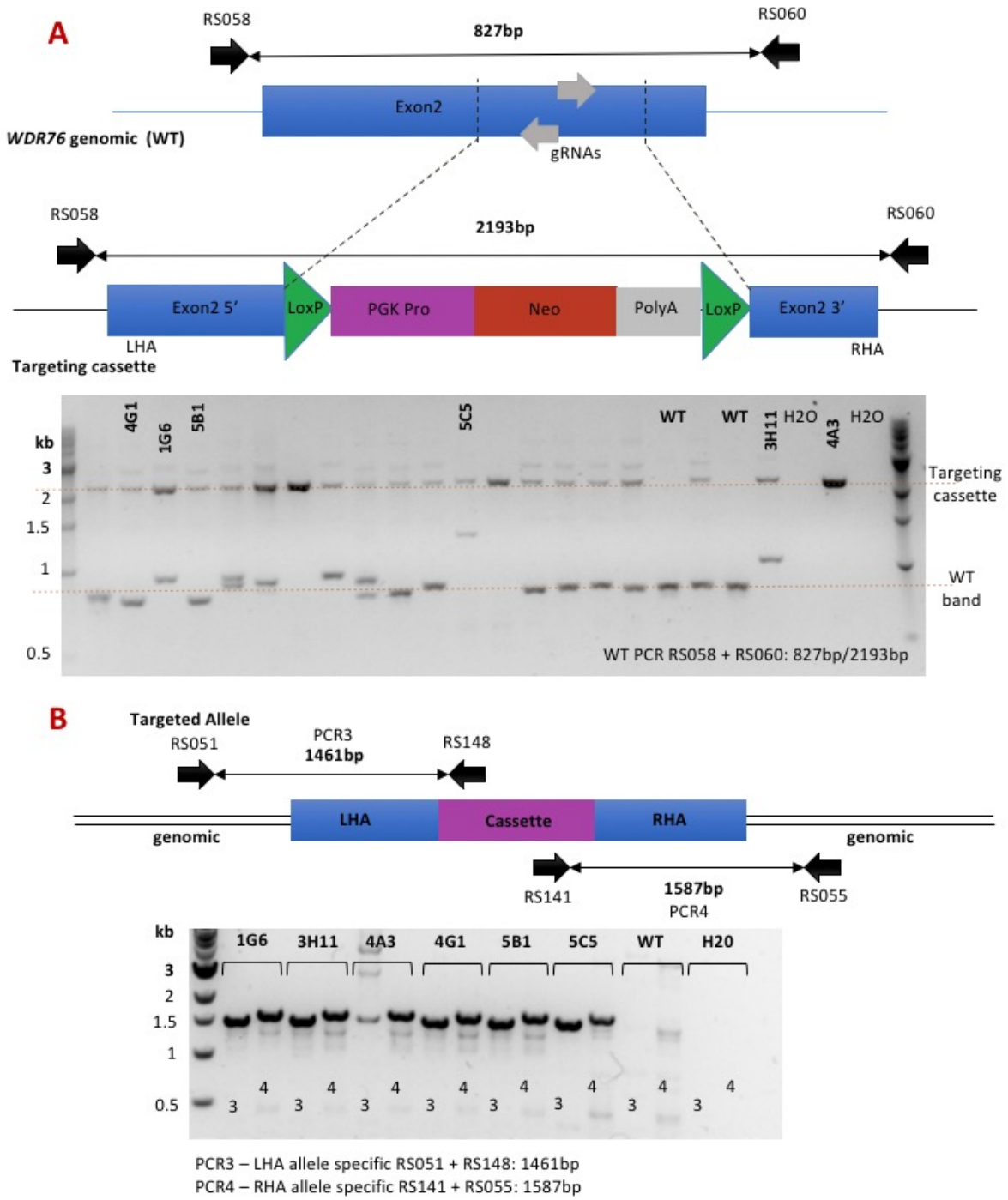

Figure 14 PCR screening of potential RPE-1 WDR76 knockouts

(A) Top shows the PCR screening strategy used to check for the introduction of the targeting cassette and indel incorporation using primer pair RS058/060. Bottom shows PCR gel; red dotted lines indicate size expected for product of targeting cassette incorporation and an unedited WT band. Bold annotations indicate clones taken forward for further validation. **(B)** PCR screen for the validation of on-target integration of the targeting cassette using two primer pair combinations.

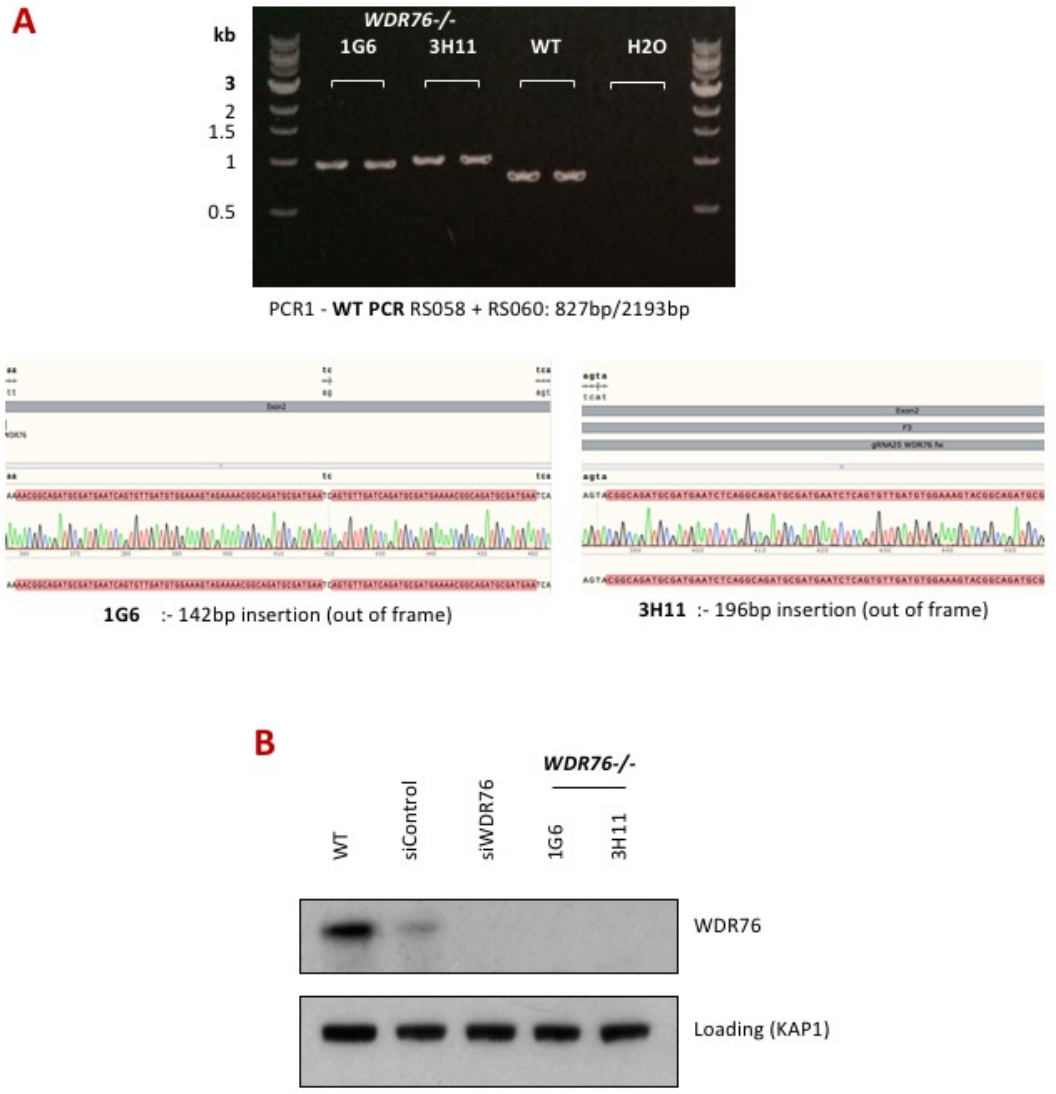

Figure 15 Validation of WDR76 knockouts

(A) Specific amplification of lower PCR product shown in Figure 14A for two potential *WDR76* knockouts (1G6 & 3H11). Sequencing of gel purified bands shows insertions occurring in WDR76 exon 2 locus. An 142bp insertion was seen in clone 1G6 and a 196bp insertion was seen in clone 3H11. **(B)** Western blot showing confirmation of *WDR76* knockouts, verified with an siRNA against WDR76.

Clonogenic survivals with four Western-blot confirmed WDR76 knockout cell lines were performed with wildtype RPE-1 cells as a control (Figure 16A/B). Three out of the four clones (1G6, 4G1 and 5B1) showed a lower percentage survival compared to the WT with increasing doses of IR (Figure 16A). This is particularly evident at the 3 and 4 Gy doses which show increased sensitivity to IR compared to the WT. Clones 1G6 and 4G1 showed a very similar profile of sensitivity to each other, while clone 5B1 showed a slightly milder sensitivity. Knockout clone 3H11 did not show an increased sensitivity to IR compared to the WT (Figure 16A).

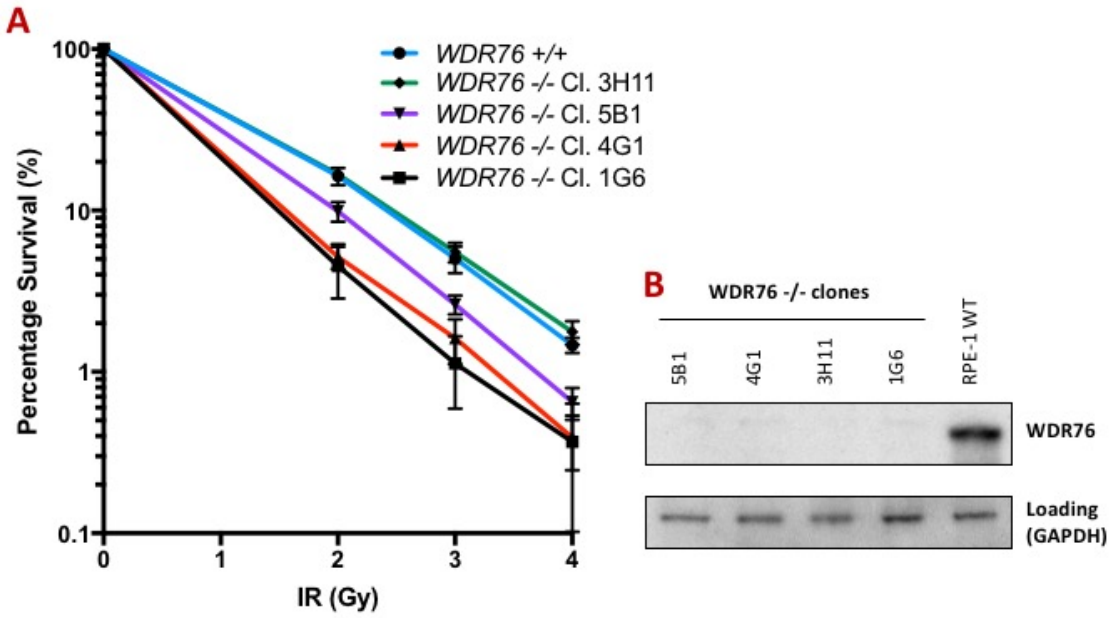

Figure 16 RPE-1 WDR76 knockouts show increased sensitivity to IR

(A) Clonogenic cell survival assays showing percentage survival to increasing doses of IR. N=3, error bars show SEM. **(B)** Western blot showing validation of knockout clones used.

3.2.8. Mass spectrometry identifies interacting partners of WDR76

Mass spectrometry was performed on immunoprecipitations in human HEK293-FT cells transfected with GFP-tagged WDR76 to identify proteins that WDR76 interacts with. This was in order to try to gain insight in to the function of WDR76 by looking at the functions and pathways of its binding partners. Four samples derived from cells that had been transfected with as plasmid directing the expression of GFP only or WDR76-GFP were sent for analysis. These were: a GFP only expressing sample, a WDR76-GFP only expressing sample, a WDR76-GFP expressing sample treated with the proteasomal inhibitor MG132 and a WDR76-GFP expressing sample treated with the neddylation inhibitor MLN4924 (Figure 17A). Gel staining showed the transfections worked efficiently, as there appears to be distinct bands present in WDR76-GFP transfected cells which correspond to the tagged protein, while the GFP-only transfected cells showed a strong band corresponding to GFP (Figure 17A). The immunoprecipitations also worked well as multiple other bands, corresponding to its binding partners, were present in WDR76-GFP transfected cells. GFP-only transfected cells did not produce many other bands and the banding pattern is distinctly different from the WDR76-GFP transfected cells. Samples were sent to Prof. Benedikt Kessler's lab (Target Discovery Institute, University of Oxford) for mass spectrometry analysis. Figure 17B displays the number of hits identified in each of the samples with everything that was present in the GFP only transfected sample removed, thus showing only protein interactors specific to WDR76 (Figure 17B). Comparing the three lists identified 32 proteins which were present in all three WDR76-GFP transfected samples but not GFP controls (Figure 17C).

Several DNA damage proteins appear in the list including DNA-PKcs (PRKDC), Ku70 (XRCC6) and Ku80 (XRCC5); all of which are components of the NHEJ machinery. PARP1, an enzyme involved in single strand break repair[12], also appears in the list. In addition to DNA damage repair proteins, WDR76 also seems to interact with several proteins involved in protein folding. This includes all components of the chaperonin complex containing T-complex protein 1 (TCP1) (CCT complex)[180]: CCT2, 3, 4, 5, 6A, 7, 8 and TCP1. Other chaperone proteins/proteins involved in protein folding that were identified from the mass spectrometry as WDR76 interactors include HSP90AA1, DNAJC7, DNAJA1 and STUB1. Other interactors identified by mass spectrometry include; HELLS, H3F3B and CBX3, which have roles in

chromatin regulation as well as a number of ribosomal protein subunits (RPS4X, RPL7, RPL3, RPS14, RPL18, RPL23, RPLP2, RPS21, RPL9, RPL24, RPL27A and RPL19)[181].

It was clear that there are a lower number of significant hits in the MG132 treated sample compared to the others. This may have been due to depletion of the ubiquitin pool as a result of the inability to recycle ubiquitin in MG132 treated cells[182]. To expand my search into other interactors of WDR76, I compared overlapping proteins across the NT and MLN4924 treated samples only (Figure 17D). This yielded a greater list of proteins which have roles in multiple processes including protein folding, ribosomal biogenesis, DNA repair, chromatin regulation, transcriptional regulation and RNA processing (See Discussion section 3.3 for more).

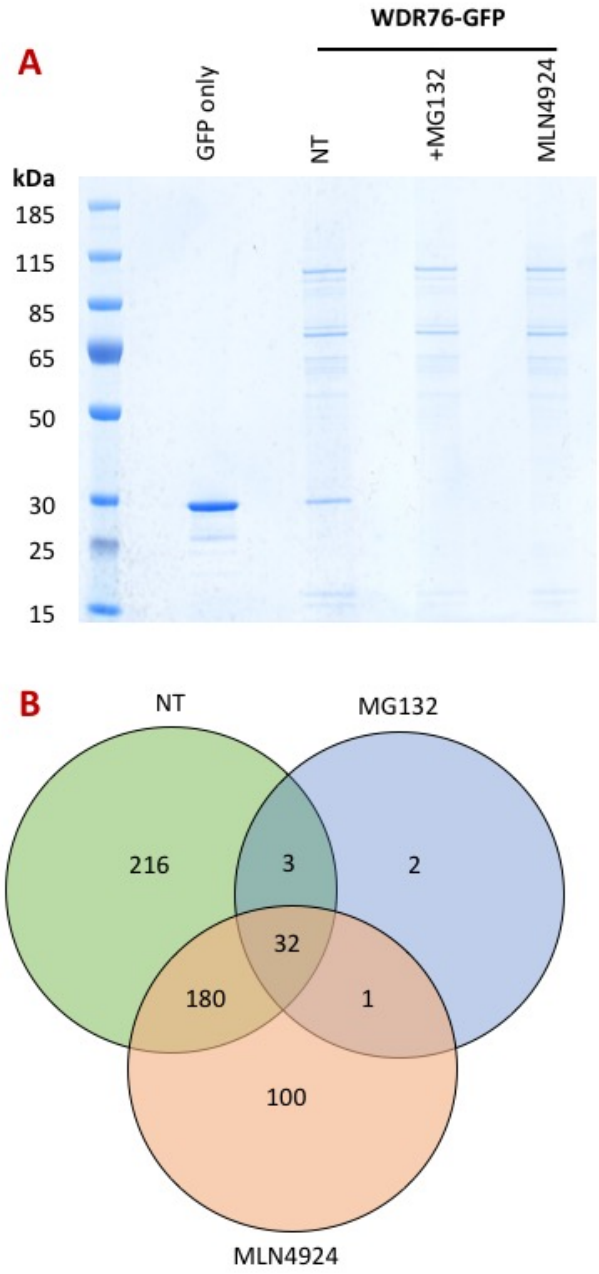

C

	Number of significant hits			
	NT	MG132	MLN4924	TOTAL
WDR76	44	20	20	**84**
PRKDC	38	4	37	**79**
CCT8	33	8	21	**62**
PARP1	39	3	19	**61**
CCT3	31	6	23	**60**
CCT2	33	1	14	**48**
CCT7	27	5	16	**48**
CCT5	28	5	14	**47**
CCT4	24	5	17	**46**
TCP1	24	5	15	**44**
CCT6A	27	4	12	**43**
HSP90AA1	21	3	10	**34**
XRCC6	25	1	7	**33**
HELLS	17	3	8	**28**
DNAJC7	13	3	11	**27**
XRCC5	15	1	6	**22**
DNAJA1	12	2	5	**19**
STUB1	9	1	5	**15**
RPS4X	6	2	6	**14**
RPL7	5	1	7	**13**
RPL3	8	1	3	**12**
RPS14	6	1	4	**11**
H3F3B	6	1	3	**10**
CBX3	6	1	2	**9**
RPL18	3	1	3	**7**
RPL23	2	2	3	**7**
RPLP2	2	1	3	**6**
RPS21	3	1	2	**6**
RPL9	3	1	1	**5**
RPL24	1	1	3	**5**
RPL27A	2	1	1	**4**
RPL19	1	1	1	**3**

Figure 17 WDR76 interacting partners identified by mass spectrometry

(A) IPs were performed on extracts from HEK293-FT transfected samples, run by SDS-PAGE and stained with Coomassie Blue. Samples transfected with 10μg of plasmids expressing either GFP only or WDR76-GFP containing plasmids. NT= non-treated, +MG132 = sample pre-treated with 10μM MG132 for 2 hours prior to IP, +MLN4924 = sample pre-treated with 3μM MLN4924 for 2 hours prior to IP. **(B)** Venn diagram showing overlapping proteins from mass spectrometry significant hits. Any hits present in GFP only sample were removed, and subsequent lists compared. **(C)** List of 32 proteins identified in all three samples.

D

	NT	MLN4924	Total
PRKDC	38	37	**75**
WDR76	44	20	**64**
PARP1	39	19	**58**
CCT3	31	23	**54**
CCT8	33	21	**54**
CCT2	33	14	**47**
CCT7	27	16	**43**
CCT5	28	14	**42**
CCT4	24	17	**41**
HSPH1	27	14	**41**
CCT6A	27	12	**39**
TCP1	24	15	**39**
XRCC6	27	7	**34**
HSP90AA1	21	10	**31**
HSPA2	19	10	**29**
TUBB4B	21	8	**29**
HELLS	17	8	**25**
TUBB2A	17	8	**25**
DNAJC7	13	11	**24**
HSPA4	15	8	**23**
SMARCA5	13	10	**23**
HUWE1	14	7	**21**
XRCC5	15	6	**21**
PABPC1	15	4	**19**
SNRPA1	13	5	**18**
STIP1	14	4	**18**
DNAJA1	12	5	**17**
RUVBL2	10	7	**17**
DICER1	9	6	**15**
TUBB6	11	4	**15**
STUB1	9	5	**14**
RFC1	5	8	**13**
SIRT1	7	6	**13**
RPL7	5	7	**12**
RPS4X	6	6	**12**
ANAPC1	8	3	**11**
DDB1	4	7	**11**
DNAJA2	8	3	**11**
IRS4	7	4	**11**
PPP2R1A	8	3	**11**
RBBP7	6	5	**11**
RPL3	8	3	**11**
HIST1H2BJ	6	4	**10**
PRDX4	5	5	**10**
RPS14	6	4	**10**
RPS9	6	4	**10**
SSBP1	7	3	**10**
TFAM	7	3	**10**

	NT	MLN4924	Total
DDX17	5	4	**9**
H3F3B	6	3	**9**
IGF2BP1	5	4	**9**
MATR3	5	4	**9**
RPS2	5	4	**9**
CBX3	6	2	**8**
CDC16	4	4	**8**
PSMD2	5	3	**8**
RPS16	5	3	**8**
RTCB	4	4	**8**
THBS1	5	3	**8**
CAD	2	5	**7**
CHD4	3	4	**7**
EIF3F	4	3	**7**
NUMA1	6	1	**7**
RFC5	3	4	**7**
RPL23A	3	4	**7**
BAG2	2	4	**6**
CBX5	5	1	**6**
CDC27	3	3	**6**
CDC73	2	4	**6**
FASN	3	3	**6**
GPRASP2	3	3	**6**
HP1BP3	4	2	**6**
HSPA4L	4	2	**6**
IPO7	3	3	**6**
KPNA2	2	4	**6**
LIG3	4	2	**6**
NAA10	4	2	**6**
PFDN2	2	4	**6**
PPP2CA	4	2	**6**
PPP3CA	4	2	**6**
RFC4	4	2	**6**
RPL18	3	3	**6**
RSF1	3	3	**6**
VCP	5	1	**6**
ANAPC7	4	1	**5**
BLM	1	4	**5**
CBX1	4	1	**5**
CCDC124	3	2	**5**
DDX21	4	1	**5**
DHX9	2	3	**5**
EIF3A	3	2	**5**
EIF3I	2	3	**5**
ELAVL1	2	3	**5**
GAN	3	2	**5**
HNRNPF	2	3	**5**
IMPDH2	4	1	**5**
NUP155	1	4	**5**
PARK7	3	2	**5**
PPP2R2A	4	1	**5**
PSME3	3	2	**5**
PURA	3	2	**5**
RPL23	2	3	**5**

Figure 17 (continued) WDR76 interacting partners identified by mass spectrometry

(D) List of 212 significant hits overlapping between NT and +MLN4924 samples.

3.2.9. WDR76 knockout cells do not show increased sensitivity to heat shock

Mass spectrometry analysis identified all components of the CCT complex as well as other chaperone proteins. Chaperone proteins are not only involved in promoting the correct folding of proteins but also the degradation of misfolded proteins[183]. One potential role of WDR76 could be the ubiquitylation and therefore targeting of misfolded proteins for proteasomal degradation. In order to see if accumulation of potential damaged/misfolded WDR76 substrates gives an increase in cell sensitivity to protein damage, *WDR76* knockout clones were tested for sensitivity to heat shock. WT and two *WDR76* knockout clones were subjected to short periods of time at higher temperatures before being placed back into 37°C incubators and left to recover. Crystal violet staining showed that all cells were sensitive to exposure at higher temperatures for extended periods of time. However, there was no dramatic differences between the WT and knockout clones with respect to survival (Figure 18).

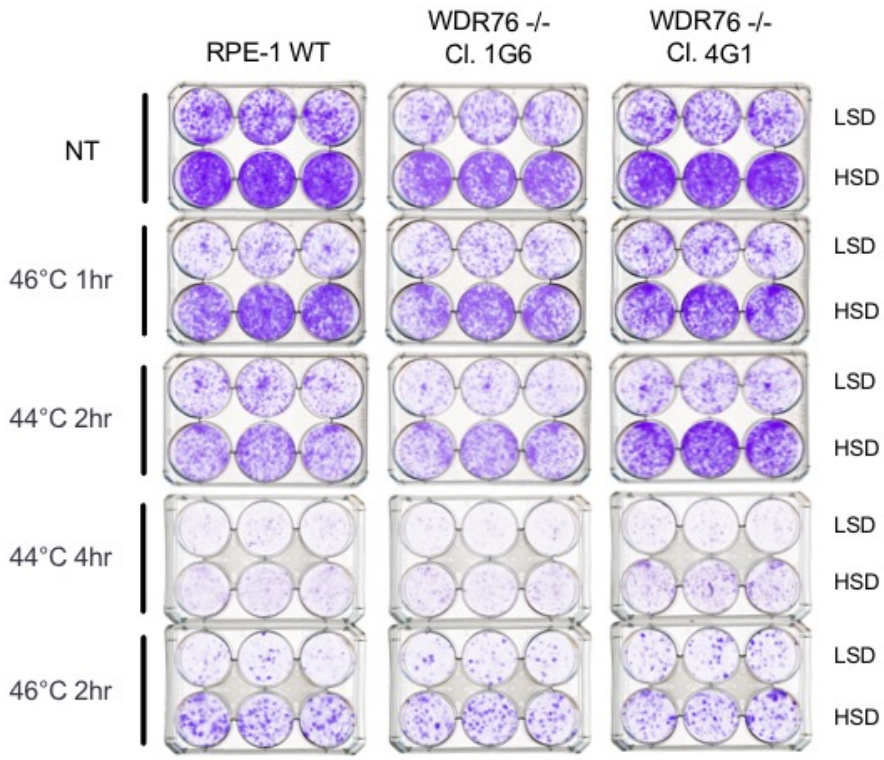

Figure 18 WDR76 knockouts are not sensitive to heat shock

Crystal violet staining of RPE-1 cell survival assays. Cells were seeded on day 1, heat shock performed on day 2 (at indicated temperature and time) and stained with crystal violet 6-10 days later. LSD refers to low seeding density used, HSD refers to a high seeding density used.

3.2.10. WDR76 knockout cells do not show increased sensitivity to UV

Chaperones and heat shock proteins have roles in protecting against UV induced DNA damage, and UV has also been shown to cause protein misfolding and protein damage[184]. In addition to assessing their ability to withstand heat shock, the *WDR76* knockout clones were tested for sensitivity to UV. This was to investigate if *WDR76* knockout clones were more sensitive to UV through either protein damage or DNA damage. The yeast homolog of WDR76, Cmr1, has previously been shown to bind UV damaged DNA[172] so one might expect the human protein to be involved in the DNA repair mechanism specific to UV damage. In addition, the CUL4 complex in association with different substrate receptors has also been shown to be implicated in the response to UV damaged DNA[185–187]. Crystal violet staining of cells exposed

to UV showed no discernible differences between WT and *WDR76* knockout clones when considering seeding densities (Figure 19A). Survival assays analysed by Hoechst staining also showed no detectable differences between the WT and knockout clones (Figure 19A). Therefore it was concluded that WDR76 knockout clones did not show any increase in sensitivity to UV damage compared to the WT control (Figure 19A,B).

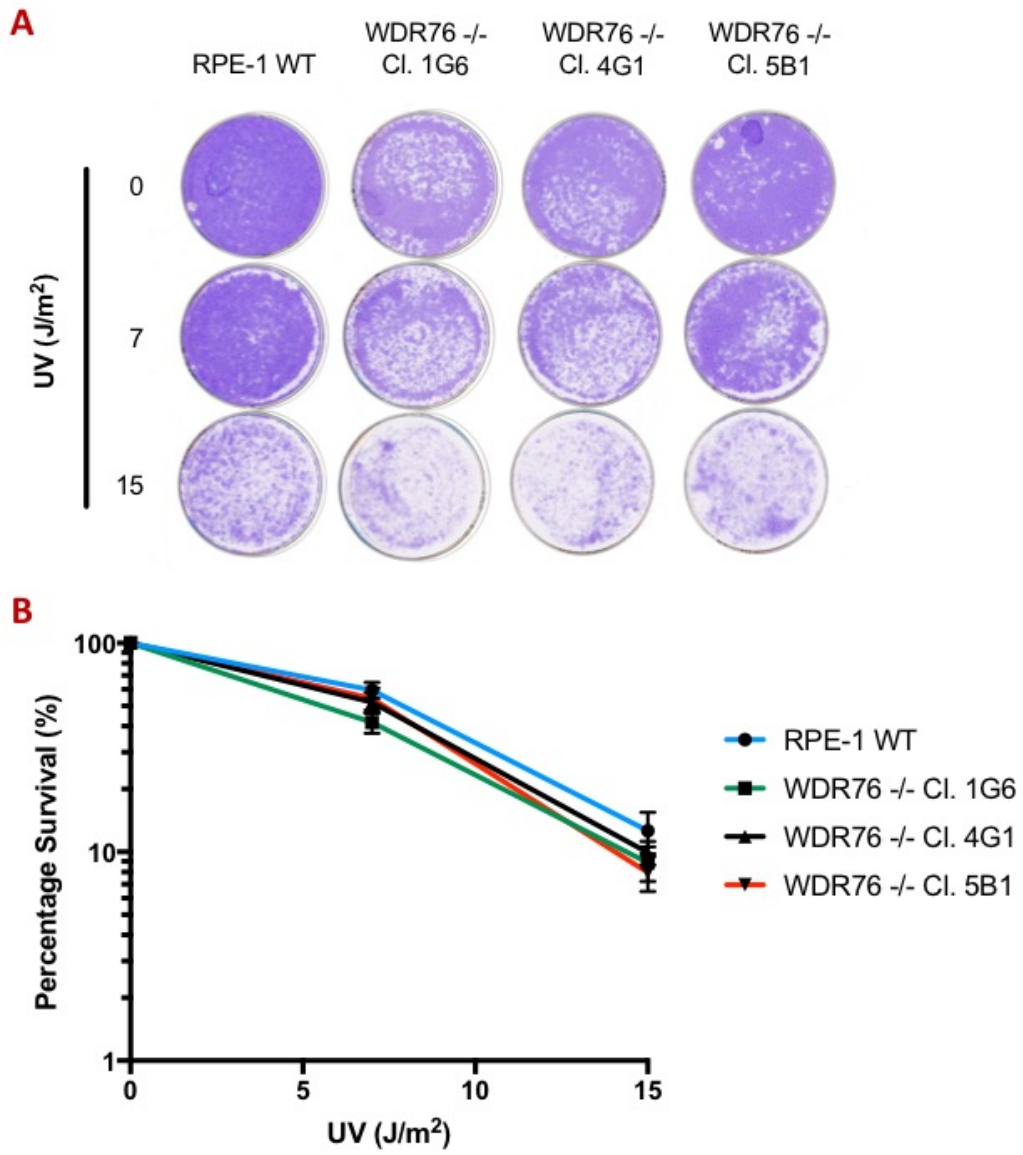

Figure 19 WDR76 knockouts do not show increased sensitivity to UV

(A) Crystal violet staining of cell survival from cells exposed to indicated doses of UV. Cells were seeded on day 1, UV dosed on day 2 and stained with crystal violet 6-10 days later. **(B)** Graph showing percentage survival relative to non-treated as measured by Hoechst staining and counting of nuclei. Clone numbers are indicated. Error bars show SEM.

3.2.11. Assessing WDR76 protein levels throughout the cell cycle

To investigate which DNA repair pathway WDR76 might be part of I looked to see if WDR76 itself is cell cycle regulated. For example, if WDR76 has a specific role in HR, one might expect the protein levels to be higher in the S/G2 phases of the cell cycle compared to rest of the cell cycle. U2OS cells were synchronised by double thymidine blocking to arrest cells in the G1 to S transition. Cells were then released from thymidine exposure and allowed to progress throughout the cell cycle. Protein samples were taken at various timepoints to achieve S and G2 populations. In addition, a separate population of cells were exposed to nocodazole to arrest cells in mitosis. Mitotic cells were recovered via shake off and then removed from the drug and allowed to progress through the cell cycle. This achieved samples from M phase and from the subsequent G1 phase.

In U2OS cells WDR76 levels seem to be highest in S and G2 phases of the cell cycle as seen by WDR76 protein levels correlating with that of Cyclin A (CycA) (Figure 20A). Conversely, WDR76 levels are reduced in mitotic cells (as indicated by sample with high phosphorylation of histone H3 at serine 10). WDR76 levels seem to decrease following release from nocodazole, suggesting lower levels of the protein in the G1 phase of the cell cycle (Figure 20A).

Despite the variations in WDR76 level in U2OS cells, the same trend is not seen in RPE-1 cells. WDR76 levels seem to be relatively stable in RPE-1 cells in both CycA positive and negative cells (Figure 20B).

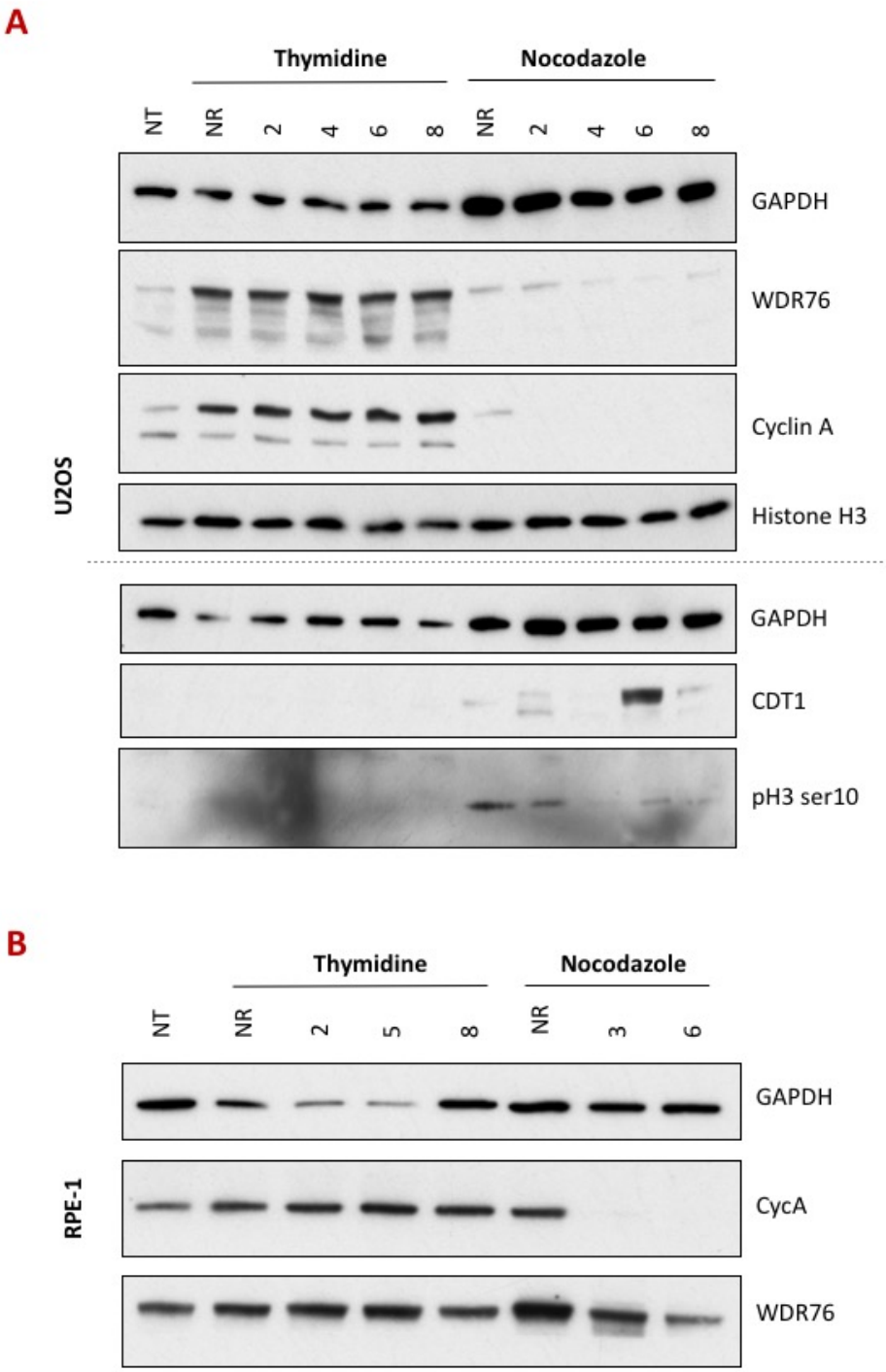

Figure 20 WDR76 protein levels throughout the cell cycle

Cells were synchronised by either double thymidine block or nocodazole treatment and released to allow progression through cell cycle. Samples were taken at time points to cover the cell cycle and Western blotting performed in **(A)** U2OS cells and **(B)** RPE-1 cells. NT = non-treated, NR = non-released from drug treatment, numbers indicate hours after drug release.

3.2.12. WDR76 knockout cells do not show enhanced sensitivity to camptothecin

Cell survival assays were set up to investigate if WDR76 knockouts were sensitive to S phase specific damage. Cells were seeded and exposed to chronic treatment of camptothecin (CPT). Cells were then stained with crystal violet 6 – 10 days after dosing. All cell lines showed sensitivity at 2nM CPT as seen by a decrease in observable colonies. There does not, however, appear to be increased sensitivity in the knockouts compared to the WT as when comparing differences in initial seeding densities the level of sensitivity to CPT looks the same across all cell lines (Figure 21A). To confirm sensitivity results, the same experiment was set up but instead of crystal violet staining, cell nuclei were stained with Hoechst and cell numbers counted from images taken under a fluorescent microscope. *WDR76-/-* cells do not differ drastically from WT cells. Perhaps a slight resistance is seen, as knockout clones show a higher percentage survival compared the WT at the 5nM CPT dose (Figure 21B).

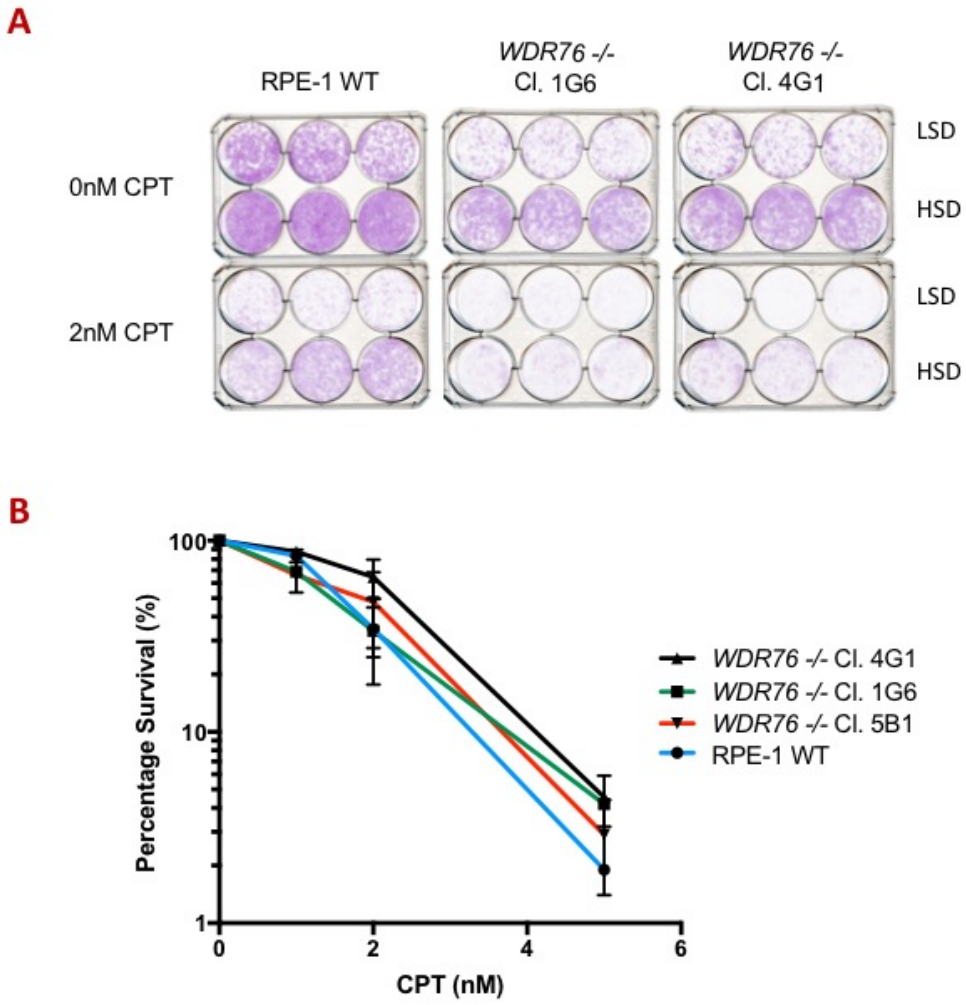

Figure 21 WDR76 knockouts do not show increased sensitivity to camptothecin

(A) Crystal violet staining of cell survival from cells exposed to indicated doses of camptothecin (CPT). Cells were seeded on day 1, drug administered on day 2 and stained with crystal violet 6-10 days later. Two different seeding densities were plated, a low/high seeding density (LSD/HSD). **(B)** Graph showing percentage survival as measured by Hoechst staining and counting nuclei relative to non-treated cells. Clone numbers indicated. N=2, error bars show SEM.

3.2.13. Transcription inhibition causes loss of WDR76 nucleolar localisation

One possibility of proteins localising to sites of DNA damage is to shutdown transcription and prevent further damage or impairment of DNA repair as a result of transcription machinery colliding with DNA damage sites[188]. Notably, CUL4 has been linked to transcriptional regulation[162,189] which raises the possibility of the substrate receptor WDR76 taking part in this process. To test if WDR76 is involved in inhibiting transcription at sites of DNA damage, I pre-treated cells with actinomycin D and then visualised recruitment of GFP-WDR76 to sites of laser line induced DNA damage as before. A low dose of actinomycin D was used to primarily inhibit RNA polymerase I mediated ribosomal DNA (rDNA) transcription. A higher dose was used to inhibit all transcription[190]. Recruitment of GFP-WDR76 was still seen in cells pre-treated with actinomycin-D at two different concentrations of the inhibitor (Figure 22A).

To subsequently test if WDR76 had an effect on transcription at sites of DNA damage, a Click-iT RNA imaging kit was used to visualise nascent RNA. WDR76-GFP expressing HeLa cells were subjected to laser induced DNA damage and allowed to recover whilst being incubated with EU. The EU incorporated with nascent RNA and could then be visualised by Click chemistry reactions. Under wildtype conditions transcription is inhibited in the vicinity of sites of damaged DNA, as seen from an exclusion of EU signal in areas with obvious γH2AX production. In both knockout clones the exclusion of EU can also be seen in areas with γH2AX staining, thus these cells behaved the same as the WT (Figure 22B).

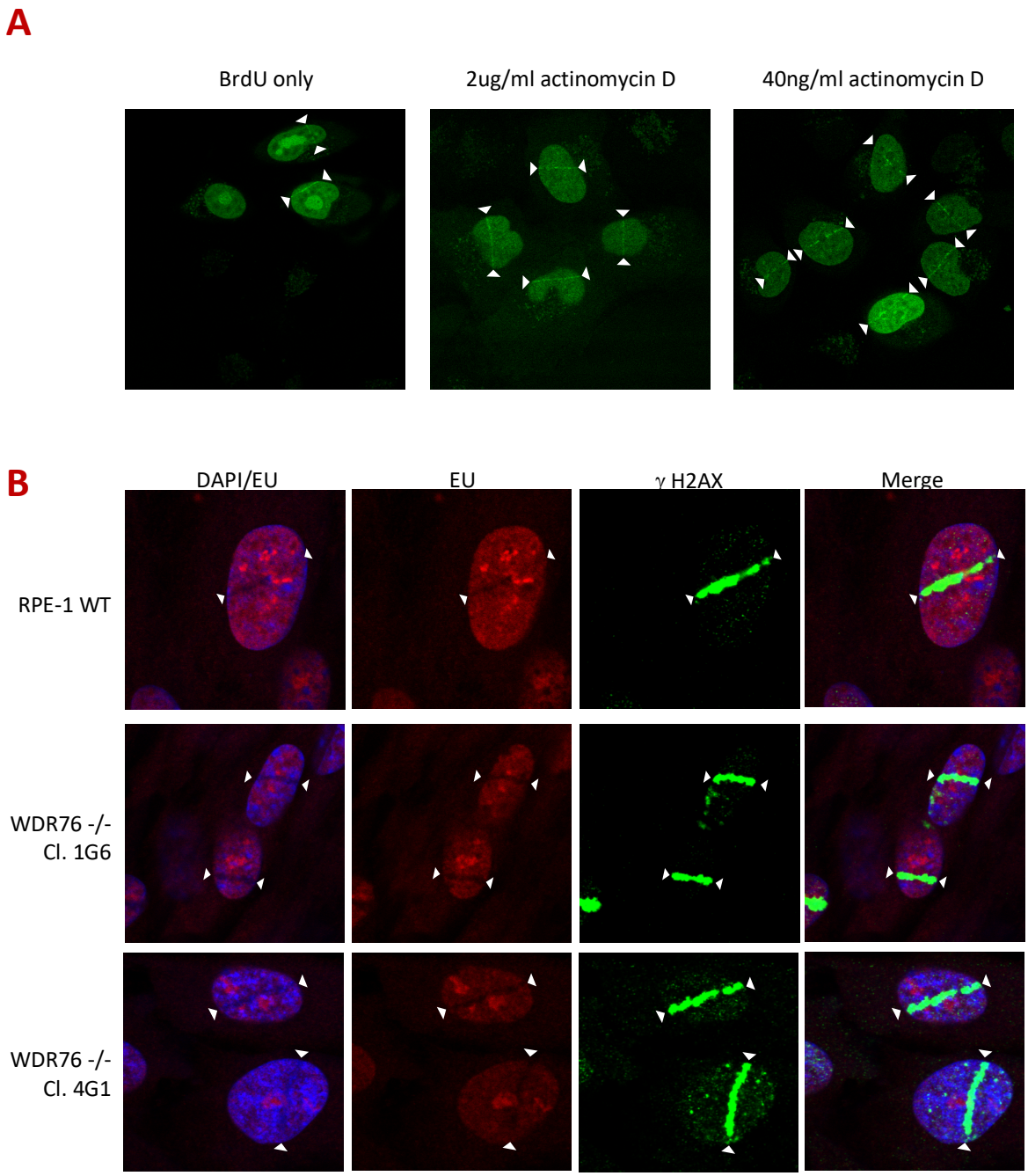

Figure 22 Transcription inhibition at sites of DNA damage is intact in WDR76 knockout clones

(A) Images in HeLa GFP-WDR76 cells showing recruitment of WDR76 to sites of laser line induced DNA damage. Indicated cells were pre-treated with actinomycin D for 1 hour prior to laser line micro-irradiation. **(B)** IF images after laser line micro-irradiation. Nascent RNA was visualised by a clickable reaction on EU incorporated after DNA damage as lines of damage can be seen from γH2AX staining as indicated by the white arrow-heads.

3.2.14. Assessing whether WDR76 affects Ku ubiquitylation

If Ku is a potential substrate of WDR76 and becomes ubiquitylated after DNA damage, one would expect to see a reduction of Ku ubiquitylation after DNA damage in *WDR76-/-* cell lines. IPs were set up initially on extracts derived from RPE-1 wildtype and knockout clones transfected with a GFP-Ku80 expressing plasmid. Cells were harvested immediately after IR induced DNA damage. Despite good detection of GFP-tagged Ku80, detection of ubiquitylation via the FK2 antibody was not strong, with it detecting no obvious higher molecular weight bands; however, suggestive of Ku80 ubiquitylation, the smear detected with the FK2 antibody does appear to be stronger in damaged versus undamaged cells. No clear differences can be seen between WT and knockout clones (Figure 23A). In an attempt to ensure detection of ubiquitin a subset of samples were also transfected with a plasmid expressing human influenza hemagglutinin (HA-tagged) ubiquitin. A corresponding shift can be seen in the FK2 smear compared to samples transfected with the plasmid expressing GFP-Ku80 only, but again the poor level of detection and lack of sensitivity by this method made it difficult to conclude any effects on Ku ubiquitylation.

IPs were also performed on samples transfected with a plasmid expressing GFP-Ku70. Levels of ubiquitylation detected by FK2 antibody appear to be higher in all samples from damaged cells compared to undamaged cells, although no obvious differences between the WT and knockouts can be detected when compared to the loading controls (Figure 23B). RPE-1 cells proved to be challenging to work with when performing transfections and thus made this type of assay difficult.

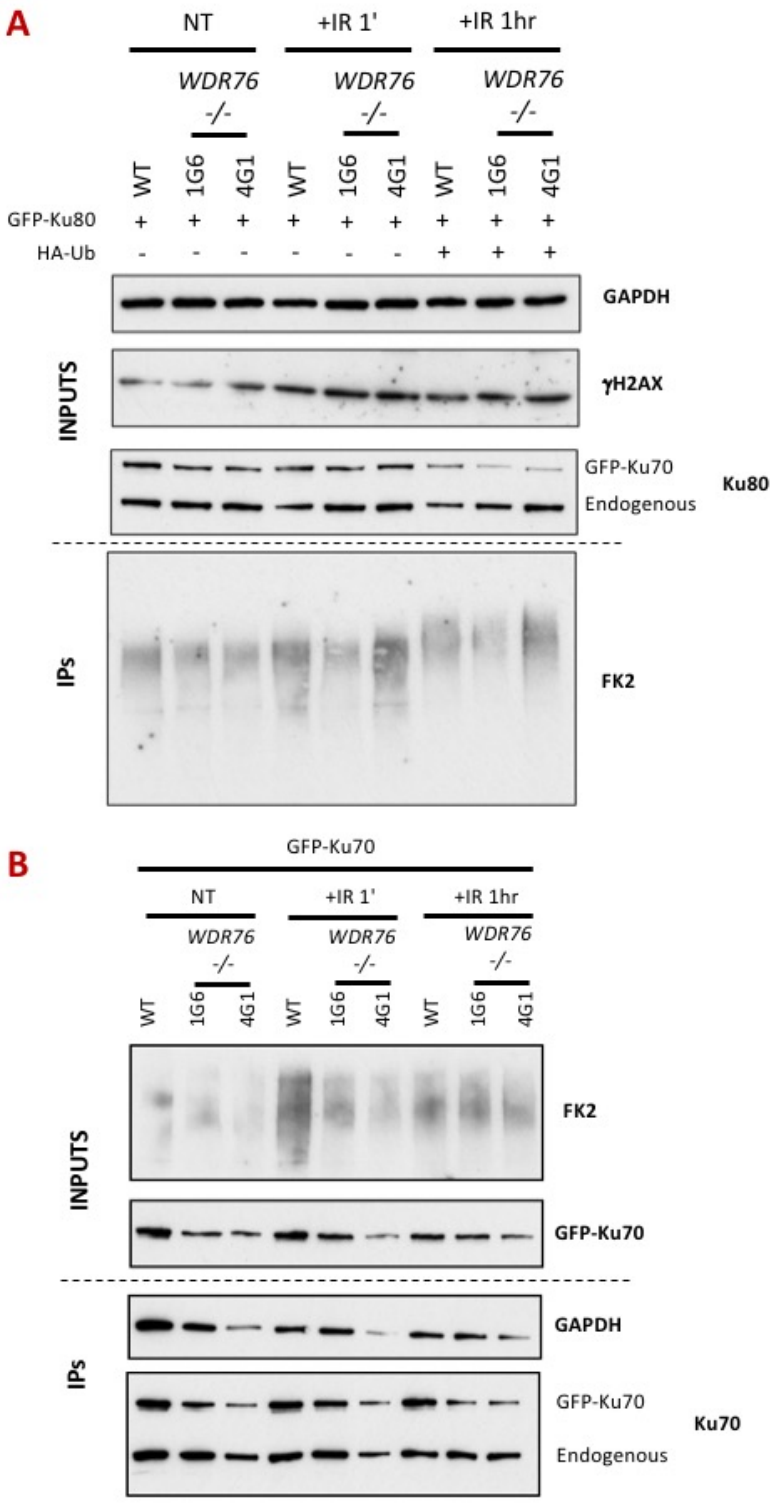

Figure 23 Detection of Ku ubiquitylation in wildtype vs. WDR76 knockout cells

IPs performed in RPE-1 wildtype vs. *WDR76* knockout cells transfected with plasmids expressing **(A)** GFP-Ku80 and HA-tagged ubiquitin (HA-Ub) and **(B)** GFP-Ku70. Cells were irradiated with 10Gy IR and samples taken either 1min (1') or 1hr after irradiation as indicated.

3.2.15. Persistence of Ku on chromatin could not be detected in knockout cells

siRNA mediated depletion of WDR76 in U2OS cells did not show and increased persistence of NHEJ factors on chromatin (Figure 9A). In an attempt to detect retention of NHEJ factors on chromatin, similar experiments were performed but in the RPE-1 *WDR76-/-* cells. Ku80 levels were stable across all cell lines and treatment conditions. This was unexpected as one would normally expect there to be an increase in Ku accumulation on chromatin following DNA damage[169]. This indicated a problem with the assay. The same issue was apparent when blotting for Ku70 and the other NHEJ factors (XLF and XRCC4) as no radiation-induced recruitment on chromatin was detected. As expected an increase in γH2AX was seen in all cell lines after DNA damage with no increased persistence of γH2AX in the *WDR76-/-* clones. One noticeable difference was the increased levels of phosphorylated ATM at S1981 (pATM) in the WDR76 knockouts compared to the wildtype. This was apparent in all timepoints after DNA damage. A higher amount of pATM in undamaged WDR76 knockout cells compared to wildtype cells was also observed in a higher exposure (Figure 24). Neither chromatin fractionation nor Ku foci experiments were technically possible in RPE-1 cells. This issue was also experienced by other members in the lab and meant performing these experiments to detect persistence of Ku was unfortunately not technically achievable.

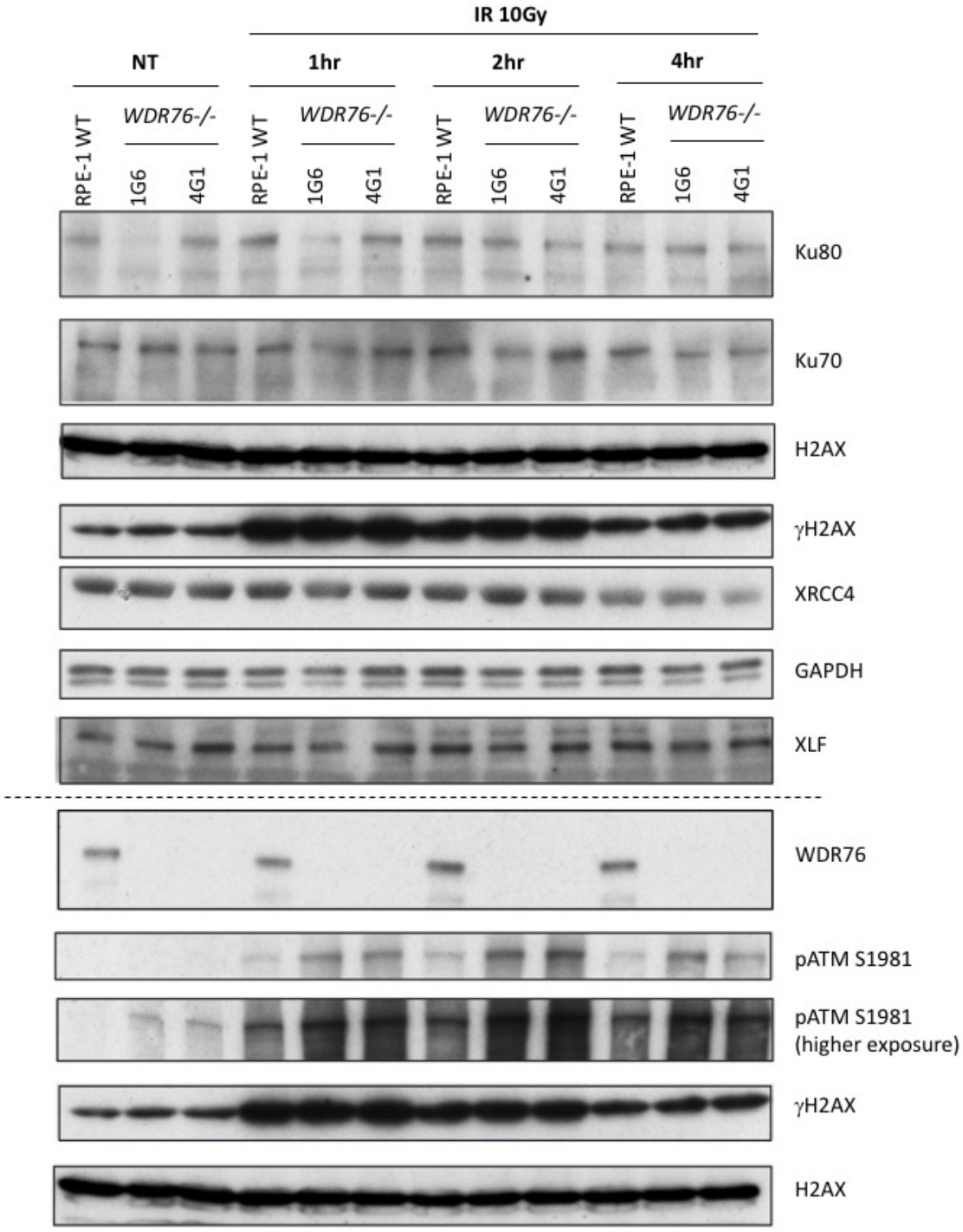

Figure 24 Chromatin fractionation in RPE-1 wildtype and WDR76-/- cells

Chromatin fractionation on wildtype (RPE-1-WT) and two *WDR76-/-* clones (1G6 & 4G1) before and after DNA damage by 10 Gy of irradiation. Western blotting was performed and probed for indicated proteins. Duplicate probes show different exposures as labelled. Dotted line indicates blots performed on separate gel.

3.3. Discussion

3.3.1. WDR76 is involved in DNA repair

Overall the data presented here does implicate WDR76 within the DDR. Initial IPs performed on cells expressing GFP-WDR76 show that WDR76 interacts directly with CUL4A and DDB1 which corroborates with existing literature (Figure 7)[162,191]; this suggests WDR76 is a DCAF and thus confirms that it is a component of the CUL4A E3 ligase. Both CUL4A and DDB1 are known to have roles within the DDR[192,193]. IPs also confirmed an interaction with the DNA damage specific Ku70/80 heterodimer (Ku) (Figure 7), and therefore suggests Ku as a potential substrate of WDR76. The fact that WDR76 localises to sites of DNA damage also implicate it within the DDR. Recruitment was seen very rapidly after DNA damage induction (Figure 8), which might suggest that WDR76 plays a role in the early response to DNA damage. Ku itself is also known to be recruited quickly and with high affinity to double-strand breaks which encourages the possibility of functional interactions occurring between WDR76 and Ku[56,121]. The dependency of WDR76 to be recruited to sites of DNA damage in the absence of Ku could not be tested due to the essentiality of Ku in human cells.

Persistence of NHEJ factors was not detected by Western blot in the chromatin fraction of WDR76 siRNA depleted U2OS cells as compared to controls (Figure 9), however a persistence of Ku foci was seen by IF after DNA damage in WDR76 siRNA depleted cells compared to control siRNA treated cells (Figure 10). This may be because subtle changes in overall protein levels are harder to detect by the chromatin fractionation approach; even cells treated with MLN4924, which cause a dramatic increase in persistence of Ku foci after DNA damage, only led to a moderate increase in chromatin persistence on a Western blot level (Figure 9 & Figure 10). Furthermore, WDR76 depletion caused increased persistence of Ku80 foci relative to the wildtype 2 hours after DNA damage, which is further evidence highlighting a link between WDR76 and the DDR through regulation of Ku (Figure 10). The level of persistence in WDR76 depleted cells was not as great as the level of persistence seen in MLN4924 treated cells. This could be due to inefficient depletion of the protein by siRNA but could also suggest that there are other neddylation dependent mechanisms regulating Ku after DNA damage. This might be in the form of other substrate adaptors of CUL4 but could also be other members of the

Cullin E3 ligase family or even unknown targets of the MLN4924 inhibitor. The fact that WDR76 depletion did increase persistence of Ku foci might imply that it is responsible for the removal of Ku after DNA damage, although the possibility of Ku ubiquitylation being a method for positively regulating NHEJ cannot be ruled out. While the CRL family of E3 ligases are normally associated with ubiquitylation of targets for proteasomal degradation, there are examples of CRL dependent ubiquitylation that regulates substrates in a non-proteolysis driven manner[194].

Proteins involved in promoting NHEJ often show an increase in sensitivity to IR when depleted or deleted in cell lines[195]. Although siRNA mediated depletion of WDR76 in U2OS cells did not lead to an increase in sensitivity to IR (Figure 12), RPE-1 WDR76-/- cells did show an increase in sensitivity to IR in clonogenic survival assays (Figure 16). Three out of four clones tested showed an increase in IR sensitivity while knockout clone 3H11 did not show an increased sensitivity, potentially due to clonal variation/selection and perhaps an unintended off-target effect of the knockout process in that particular clone. The increased sensitivity to IR in knockout clones again suggests that WDR76 has a role that affects the DDR. In addition, chromatin fractionation experiments showed an increase in pATM in *WDR76-/-* cells compared to WT cells in both damaged and undamaged conditions (Figure 24). This may be due to increased DNA damage as a result of inefficient repair occurring in a *WDR76-/-* background.

S. cerevisiae cells with a *Cmr1* deletion did not show sensitivity to a broad range of DNA damaging agents (Figure 11B), a phenotype which is also stated in other publications[172,173]. Although at first these findings might argue against a role of the protein in the DDR, it may also be because yeast cells replicate and divide quickly and do not spend much time in G1; a phase when cells are more reliant on NHEJ as a means of double strand break repair. Furthermore, yeast cells predominantly repair via HR and therefore proteins affecting NHEJ may not show a clear phenotype in this background. Even *S. cerevisiae* cells with a yeast Ku70 (*yKu70*) deletion, do not show increased sensitivity to IR[196]. Yeast cells with mutations in both *yKu70* and *rad52 do* enhance the IR and MMS sensitivity of *rad52* mutants alone, and so generating triple mutants with a *Cmr1 deletion* could be a means of investigating this further[127,196]. This could further support a role of WDR76 specifically in the NHEJ pathway of

DNA repair, or could also imply an evolutionarily distinct development of WDR76 (over other CUL4 substrate receptors) from the yeast ortholog. Additionally, when testing my human WDR76 knockout cells for sensitivity to camptothecin, a drug which causes S-phase specific damage, I did not see a change in sensitivity compared to WT cells (Figure 21).

Mass spectrometry analysis identified Ku70, Ku80 and DNA-PKcs as potential interactors of WDR76 (Figure 17), which again points to a role of WDR76 in the NHEJ pathway. Interactions between the proteins were present in undamaged cells, so it would be interesting to see if there is enhancement in these interactions when DNA damage is administered, or whether WDR76 interacts with additional DNA damage related proteins in this scenario. In the future, performing a SILAC based mass spectrometry analysis in damaged versus undamaged cells would be a good way of doing this.

3.3.2. Other potential roles of WDR76

Mass spectrometry revealed a diverse range of proteins with which WDR76 interacts. These interactors could explain the potential mechanisms through which WDR76 affects DNA repair or alternatively may reveal additional, diverse functions of WDR76.

3.3.2.1. Involvement of WDR76 in protein folding

The interaction of WDR76 with Ku was also seen by Gallina et al.[173], as was the interaction between WDR76 and the CCT complex that I also identified through mass spectrometry (Figure 17). The CCT complex is a chaperone complex that is involved in the folding of around 10% of the proteome[180]. Many of the proteins that associate with the CCT complex do so upon translation[197] which might suggest a role of WDR76 in the folding of newly translated proteins. WDR76 also interacts with ribosomal proteins and RNA modifiers and is enriched in the nucleolus (Figure 8 & Figure 22), which may also imply it has a role in protein assembly and folding.

The CCT complex has also been linked to the folding and assembly of oligomeric protein structures[197]. This raises the possibility that WDR76 through its association with multiple proteins by means of its WD40 domains, is capable of creating protein complexes. It is tempting to speculate whether WDR76 aids in the coordination of the NHEJ proteins to promote a stable complex to initiate DNA repair. This could be through the coordinated binding of the Ku heterodimer and CCT complex to then promote the stable assembly of the downstream NHEJ machinery. In this regard, binding Ku may be particularly important as, due to its high affinity for dsDNA ends, it is the first protein recruited to double strand breaks.

Alternatively, the interaction between WDR76 and the CCT complex could purely be for the folding of WDR76 itself. Proteomic approaches have identified WD proteins that form β-propeller domains as CCT complex substrates[198]. One example of this is in the activation of the anaphase-promoting complex (APC/C) through the correct folding of the WD40 domain containing protein CDC20.[199]

3.3.2.2. WDR76 and ribosome biogenesis

From localisation studies, WDR76 is a nuclear protein but a large accumulation of WDR76 appears to be nucleolar (Figure 8 & Figure 22). The nucleolus is the centre of ribosome subunit biogenesis[200], which might suggest that WDR76 plays a part in this process. Indeed, a large number of ribosomal proteins were also identified as interactors of WDR76 (Figure 17). Additionally, a loss of WDR76 from nucleoli was seen upon transcription inhibition suggesting its role in nucleoli is transcription dependent. This could mean it is involved in the correct folding of the ribosome through its interaction with ribosomal proteins and newly transcribed ribosomal DNA (rDNA).

The CUL4 complex has also been associated in ribosome biogenesis, as an RNAi based screen performed by Badertscher et al[201] showed that CUL4 and DDB1 are required for ribosome maturation. Interestingly the publication revealed 302 proteins required for 40S subunit production, which included the CCT complex, as well as other proteins identified as interactors of WDR76. Although WDR76 itself was not identified in this screen, the

involvement of its interactors in addition to the data presented here might suggest its involvement in ribosome biogenesis.

3.3.2.3. WDR76 and transcription

Data presented here points to a potential link between WDR76 and transcription regulation however it is difficult to specify its exact role within this process. Due to the density of WDR76 in the nucleolus one might speculate its involvement in the transcription of rDNA. When transcription was inhibited, WDR76 was no longer concentrated in nucleoli (Figure 22). WDR76 could either be a positive regulator of transcription, or an inhibitor of transcription and thus is no longer concentrated in the nucleolus when transcription is inhibited.

Despite the interaction with multiple proteins that could be linked to transcriptional regulation, transcription inhibition at sites of DNA damage was still seen in *WDR76-/-* cells. This suggests that local inhibition of transcription at sites of DNA damage is still intact and not affected by WDR76 loss.

Recruitment of GFP-WDR76 to laser induced DNA damage was also seen in the presence of transcription inhibition. This does not necessarily mean that WDR76 is not involved in transcription inhibition, as it could be redundant over other proteins or could be that its recruitment is specific to DNA damage and/or recruitment of Ku regardless of downstream function.

In the future, performing RNA-seq in WT versus *WDR76-/-* cells might enable identification of role of WDR76 in transcription and would also establish which genes WDR76 may be regulating.

3.3.2.4. WDR76 and chromatin regulation

When comparing the non-treated and MLN4924 treated samples only and looking at a larger list of interacting partners, a number of proteins involved in chromatin remodelling are

present. These include: SMARCA5, SIRT1, HIST1H2BJ, H3F3B, HP1BP3, RBBP7, CBX1, CBX3, and CBX5. This might suggest an involvement of WDR76 in nucleosome remodelling. Again, this could be linked to transcriptional regulation as all of the aforementioned proteins have roles modulating gene expression through mechanism connected to histone modifications. The increased pATM levels in *WDR76-/-* cells previously mentioned could also be linked to the chromatin state in these cells as hyperacetylated DNA, commonly associated with increased transcription, causes an increase in ATM activation[202,203]. The interactions with chromatin regulators could also be directly linked to the early DNA repair process, and the potentiation of DNA damage signalling and opening of chromatin to allow DNA repair factors access to DNA lesions. Despite efforts to detect changes in histone modifications by Western blotting, I was unable to interrogate variance in histone modifications between WT and *WDR76-/-* cells.

3.3.2.5. WDR76 and RNA processing

The WDR76 interactome also identified a number of proteins involved in RNA related processes including splicing, folding and resolution of RNA secondary structure. Whilst this could again point to roles of WDR76 in transcriptional and translational regulation it also raises the possibility of a role connecting RNA and the DDR. An increasing field of investigation in the DDR points to roles of RNAs in the maintenance of genome stability[204,205]. Notably, WDR76 interacts with both DNA repair factors and RNA processing factors. Some of these include RNA helicases such as DHX9 and DDX17. This could implicate WDR76 in the resolution of dsRNA or even in the resolution of DNA-RNA hybrids. These DNA-RNA hybrids naturally arise as a result of transcription, creating R-loops which can pose a threat to an efficient DNA repair if left unresolved.

Another possibility is that WDR76 is involved in the generation of DNA damage-induced small RNAs (diRNAs). These diRNAs are produced at sites of DSBs and although not involved in the initial recognition of DSBs seem to be required for proficient DNA repair[206]. This could fit data generated here, in that Ku loading and recruitment of γH2AX to sites of DNA damage seems to be unaffected, although there is an increased persistence of Ku foci which might suggest a

delay in the completion of NHEJ (potentially through reduced recruitment of downstream NHEJ factors).

The endoribonuclease DICER, which was identified as an interactor of WDR76 (Figure 17D), has also been implicated in the generation of small non-coding RNAs to mediate the DDR[207,208]. The exact mechanisms by which RNA and associated proteins coordinate DNA repair is still largely unexplored. One theory is the utilisation of RNA as a template for DNA repair which has been demonstrated in both yeast and human cells[209–211].

3.3.3. WDR76 concluding remarks

Overall, I have shown that WDR76 does appear to have a role(s) in the DDR but have been unable to identify the exact substrate(s) and mechanism(s) by which it affects DNA repair and perhaps other DDR processes. Given the range of interactors of WDR76, its fast localisation to sites of DNA damage and IR sensitivity seen in *WDR76* knockouts one might speculate that its role is in the initial stages of the DDR and may influence repair through chromatin regulation and processing of RNA. The depletion of WDR76 results in a persistence of Ku foci but not a delay in Ku loading to DNA-damage sites, suggesting it may be involved in the removal of Ku or completion of NHEJ through the recruitment of downstream factors. In summary my data has revealed interesting insights into the largely unknown role(s) of WDR76 in the DDR.

Chapter 4: Investigation of a potential CDK phosphorylation site on PAXX as a regulatory mechanism

4. Investigation of a potential CDK phosphorylation site on PAXX as a regulatory mechanism

4.1. Introduction

4.1.1. PAXX and the DDR

A new player involved in NHEJ was identified relatively recently by several groups through both bioinformatic and proteomic approaches[143,212,213]. This originally undefined protein, C9orf142, was shown to be a paralog of XRCC4 and XLF and was hence named PAXX (also known as XLS). PAXX was shown to contain a 'present in SAS6' (PISA) motif, a motif that is conserved throughout the XRCC4 superfamily [143,214]. Similarly to XLF and XRCC4, PAXX contains a head domain (within which lies the PISA motif), followed by an α helical domain[214] (Figure 25A). This helical domain is required for the formation of a coiled-coil with another PAXX monomer to form a homodimer. PAXX and XLF differ from XRCC4 in that they have a relatively short coiled-coil region which is unable to bind LIG4 directly [215,216]. The C-terminal section of PAXX contains a highly conserved unstructured region, with the extreme C-terminus containing a region required for Ku binding (Figure 25A). PAXX itself cannot bind DNA but is recruited swiftly to sites of laser line induced DNA damage and co-localises with Ku. This interaction with Ku is extremely important to PAXX function; mutation of residues within this region, result in loss of Ku binding and an increased cellular sensitivity to DNA damage. Total PAXX loss results in the same phenotype. This suggests PAXX's involvement in NHEJ is directly linked to its interaction with Ku.

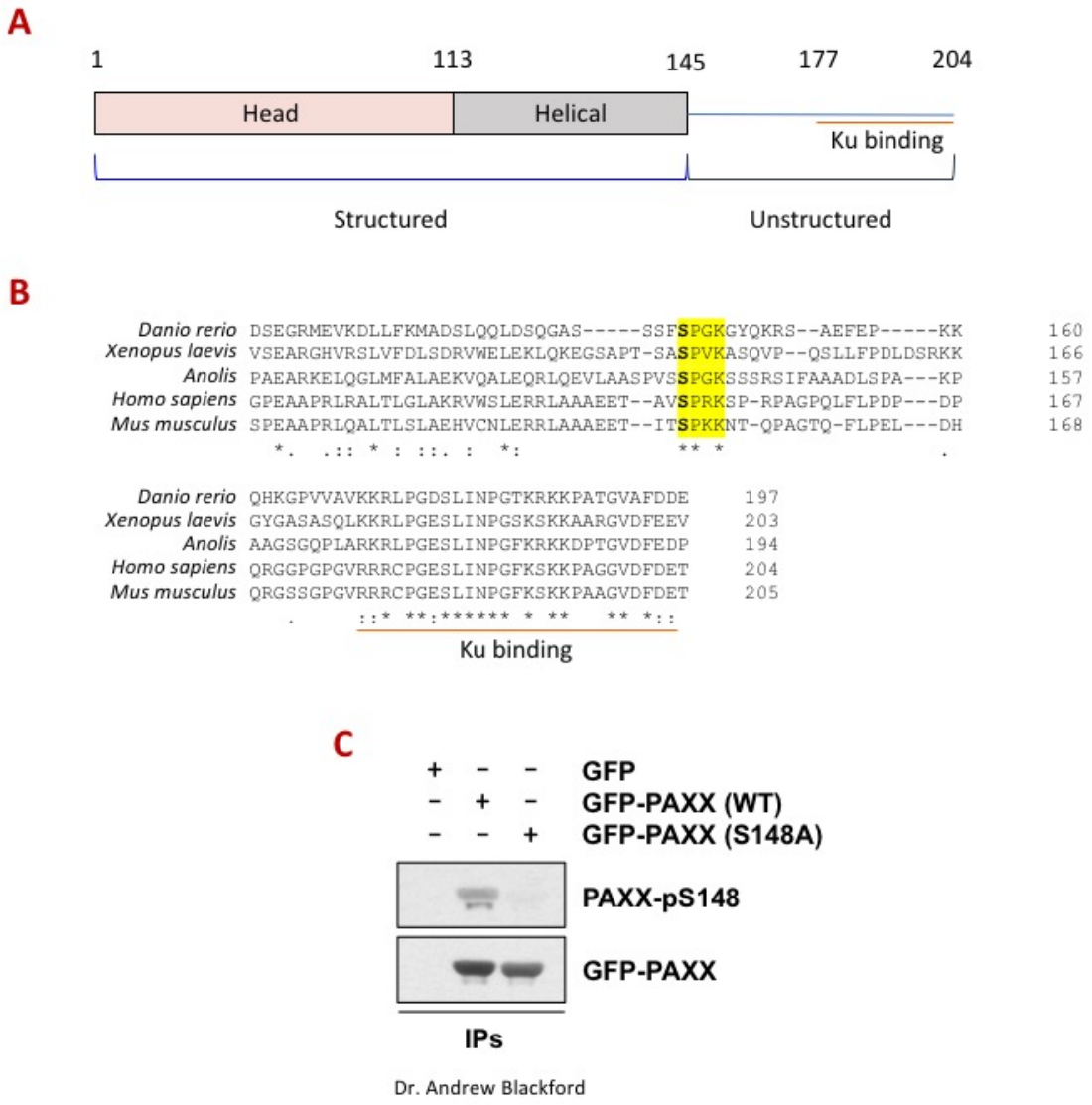

Figure 25 PAXX contains a conserved phosphorylation site

(A) PAXX contains a structured N terminal section required for dimerisation and an unstructured C-terminal section required for Ku binding. **(B)** PAXX contains a conserved CDK phosphorylation site as shown by the pS/T-P-X-R/K motif highlighted in yellow. *Danio rerio* (zebrafish), *Xenopus laevis* (frog), *Anolis* (anole lizard), *Homo sapiens* (human), *Mus musculus* (mouse) **(C)** PAXX phosphorylation at S148 can be detected in WT PAXX expressing cells but not in cells expressing a S148A mutant (performed by Dr. Andrew Blackford)

Since my studies began, PAXX has been deemed as an accessory canonical NHEJ factor as it has many similarities to XLF[217]. Both proteins have some overlapping functions and evidence exists suggesting largely redundant functions. *PAXX-/-* cells and *XLF-/-* cells both show increased sensitivity to IR (compared to WT cells) to a fairly similar level; double knockout cells show an even greater level of sensitivity to IR[218,219] and double knockout mice were embryonic lethal[218,220]. Neither PAXX loss or XLF loss individually result in impaired V(D)J recombination, however a double XLF/PAXX knockout does result in V(D)J recombination defects. This suggests functional redundancy between the two proteins. Despite this, *ATM-/- XLF-/-* cells show significantly greater defects in end-joining compared to *ATM-/- PAXX-/-* cells[219]. Importantly, overexpression of PAXX did not rescue end-ligation defects in *ATM-/- XLF-/-* cells[219]. These findings suggest PAXX and XLF do seem to have some distinct functions. Furthermore, loss of PAXX results in reduced Ku recruitment to laser induced DSBs; a phenotype not seen with XLF loss[218]. PAXX therefore seems to mediate its role in NHEJ through direct association with Ku and may be involved in the stabilisation of Ku at DSBs. XLF on the other hand seems to have a role in NHEJ that is mainly mediated by its interaction with XRCC4, allowing for efficient DNA-damage recruitment of LIG4[221]. Another possibility could be that PAXX and XLF have cell cycle specific differences and roles. More research is needed in order to define the specific functions of the two proteins and potential redundancies between them.

4.1.2. CDKs in the regulation of the DDR

CDKs have influential roles in the DDR, and their inhibition is important in the arrest of the cell cycle which facilitates repair of damaged DNA. In addition to this important function, CDKs are also thought to act further upstream in the choice of DNA repair pathways [222]. This has been shown through their roles in controlling the initiation of resection; for example, in the CDK mediated phosphorylation of CtIP and NBS1[101,223,224]. In addition, multiple other proteins involved in HR such as RPA and BRCA1 have been documented to contain CDK phosphorylation sites that influence their activity during repair [223,225,226]. Despite the positive regulation of HR by CDKs, there is a lack of information on how they may influence NHEJ. One theory is that CDKs may act to dampen NHEJ during the S-phase of the cell cycle; a time when

replication fork problems occur and HR is the favoured DNA repair choice [227]. NHEJ occurring at these types of DNA insults could lead to error-prone repair and unwanted translocations of DNA, which could be toxic to cells.

4.1.3. PAXX contains a potential CDK phosphorylation site

Within the highly conserved C-terminal tail of PAXX, there is a potential CDK phosphorylation site, just upstream of the region necessary for Ku binding. This is at serine 148 (position in human) which fits the consensus pS/T-P-X-R/K. The serine, proline and lysine residues are all conserved amongst vertebrates (Figure 25B). This conservation and the close proximity of the site relative to the Ku binding region raises the possibility of a regulatory mechanism of PAXX which may be performed by CDKs. Unpublished data by a previous postdoc in the lab, Dr. Andrew Blackford showed via immunoprecipitation and a phospho-specific antibody that PAXX phosphorylation is detected at S148 in cells expressing WT PAXX but not in cells containing a S148A mutation (Figure 25C).

Since PAXX is involved at the very early stages of NHEJ and contains a CDK phosphorylation site, one might speculate that PAXX is a potential candidate for CDK regulation and thus a way of regulating NHEJ. A hypothesis that was explored in this project was that CDK mediated phosphorylation of PAXX is a mechanism of down-regulating NHEJ in order to promote HR.

4.2. Results

4.2.1. PAXX levels remain constant throughout the cell cycle

One possibility regarding CDK regulation of PAXX is that phosphorylation of PAXX results in loss of PAXX protein. This could occur by phosphorylation targeting the protein for ubiquitylation and proteasomal degradation. This principle is found in other regulatory systems, and multiple proteins have been identified as being more likely to be ubiquitylated after phosphorylation [228]. In the human form of PAXX, there appears to be a potential CDK-targeted F-box and WD repeat domain containing 7 (FBXW7) degron[229,230] at the same site. This is a site recognised by an F-box protein of the SCF (SKP1-CUL1-FBox) complex which ubiquitylates and targets proteins for proteasomal degradation. Often these substrates are phosphorylated, which promotes FBXW7 binding and subsequent degradation [230]. To test whether PAXX is targeted for degradation in a cell cycle dependent manner, cell cycle synchronisation and release was performed, and samples were taken throughout various stages for Western blotting. PAXX levels did not vary discernibly throughout the cell cycle and there were no time points that showed a loss of PAXX (Figure 26). PAXX levels were relatively constant throughout S and G2 phases, as indicated by CycA levels, and remained essentially constant through M phase as indicated by increased levels of phosphorylated histone 3 at serine 10 (pH3 ser10). PAXX levels remained similar in G1 phase as indicated by a lack of CycA and lower pH3 ser10 levels. PAXX and XLF levels were similar throughout the cell cycle (Figure 26).

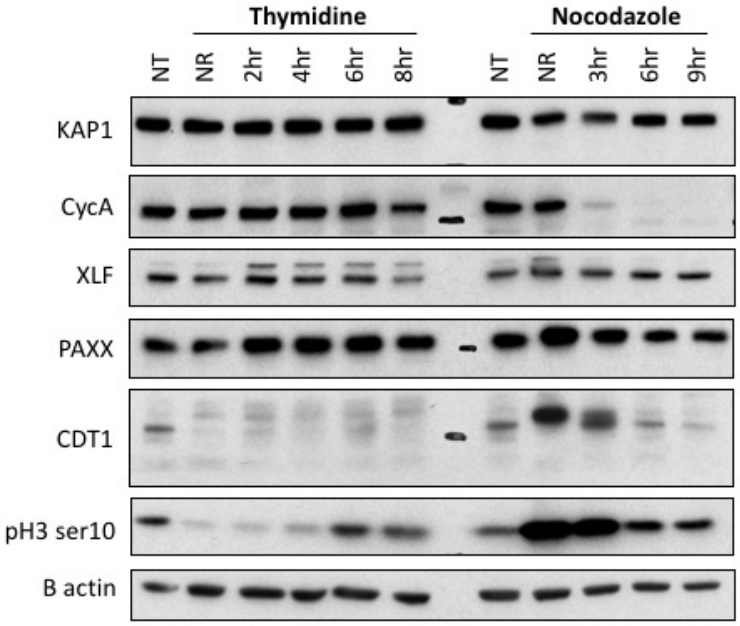

Figure 26 Total PAXX levels throughout the cell cycle

Cell synchronisation with thymidine block and nocodazole treatment was performed in human RPE-1 cells. Cells were treated with either thymidine or nocodazole to synchronise cell cycle timings and then released. Samples were taken at different timepoints and Western blotting performed. NT=non-treated (asynchronous cells), NR=non-released from drug, hr=time sample collected after release and recovery from drug in hours. pH3 ser10=phosphorylated histone 3 at serine 10.

4.2.2. PAXX phosphorylation throughout cell cycle

Although total PAXX levels did not vary throughout the cell cycle, it is important to assess if PAXX phosphorylation at S148 varies. To test this, U2OS cells were transfected with a GFP-PAXX construct and protein levels were monitored throughout cell cycle via Western blot. PAXX phosphorylation, as detected with an antibody generated against the S148 phospho-site, did not show any detectable changes throughout the cell cycle (Figure 27A).

In order to test PAXX phosphorylation levels throughout the cell cycle in a different way, IPs were performed in cells overexpressing GFP-PAXX and probed with an MPM2 antibody; an antibody shown to specifically recognise phospho-serine/threonine-proline sites. This revealed a slight variation in phospho-PAXX levels with a detectable increase at the 6-hour and 9-hour time-points after thymidine release (Figure 27B). This seems to correlate with CycA levels, and importantly total PAXX levels appear to be relatively constant.

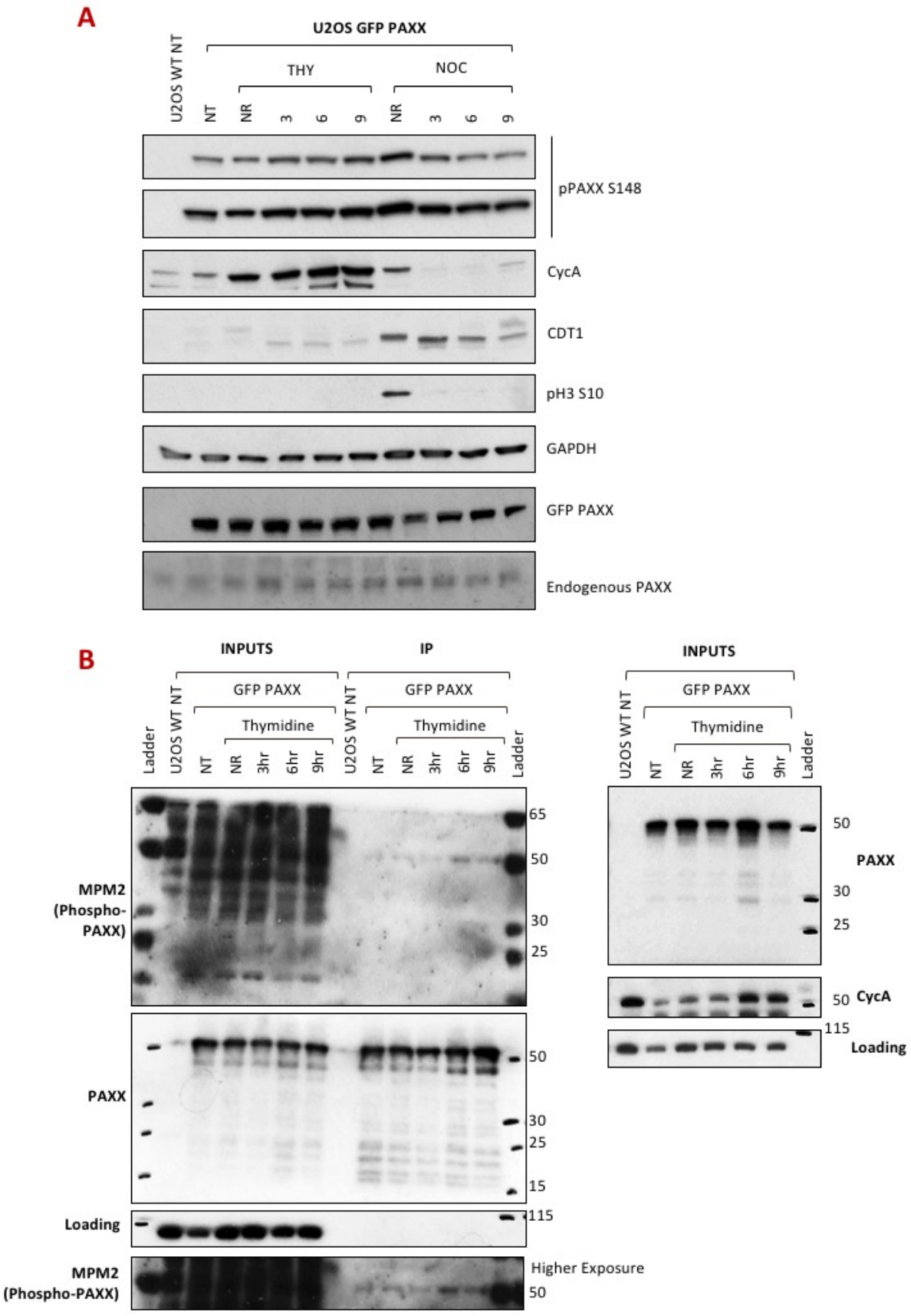
A
U2OS GFP PAXX
U2OS WT NT
THY
NOC
NT
NR
3
6
9
NR
3
6
9
pPAXX S148
CycA
CDT1
pH3 S10
GAPDH
GFP PAXX
Endogenous PAXX
B
INPUTS
IP
INPUTS
GFP PAXX
Thymidine
Ladder
U2OS WT NT
NT
NR
3hr
6hr
9hr
MPM2 (Phospho-PAXX)
PAXX
Loading
MPM2 (Phospho-PAXX)
Higher Exposure
65
50
30
25
15
115

Figure 27 PAXX phosphorylation throughout the cell cycle

(A) U2OS cells were transfected with GFP-PAXX and synchronised using thymidine or nocodazole. Cells were released, and samples taken throughout the cell cycle. Western blotting was performed to look at phosphorylation of PAXX S148. **(B)** U2OS cells were transfected with GFP-PAXX and immunoprecipitation performed using GFP-trap beads. Blots were stained with an MPM2 antibody to look at phosphorylation of PAXX throughout the cell cycle (left). Inputs are shown on right. WT = wildtype, NT=non-treated (asynchronous cells), NR=non-released from drug, hr=time sample collected after release and recovery from drug in hours. pH3 ser10=phosphorylated histone 3 at serine 10.

4.2.3. Generation of PAXX point mutants

To investigate the potential roles of the phosphorylation site at serine 148 in PAXX, PAXX mutant cell lines were generated. This was achieved by site directed mutagenesis of a plasmid construct expressing mRuby2 tagged PAXX and subsequent stable integration in RPE-1 *PAXX-/-* cells. Clones were selected based on zeocin resistance and cells expressing nuclear mRuby2, since PAXX is a nuclear protein (Figure 28A). Two types of PAXX mutants were made; S148A and S148E mutants. Mutating a serine residue to an alanine removes the hydroxyl (OH) group on the side chain of serine and thus leaves a residue that is unable to be phosphorylated. Conversely mutating the serine to a glutamic acid adds a carboxyl group creating a negatively charged side chain, which can mimic phosphorylation.

Cell lines were verified via Western blotting to visualise expression of mRuby2 tagged PAXX. Blotting with an antibody against PAXX revealed a higher molecular weight band corresponding to the mRuby2 tagged version (Figure 28B). Blotting with an antibody specific to the S148 phosphorylation site on PAXX showed a band present just below a non-specific band in WT mRuby2-PAXX samples only. This band is not seen in the S148A/E mutants as the antibody binding site is disrupted (Figure 28B). Although the antibody did not work particularly well (because of the non-specific band) it does show the expected trend with regard to the WT and mutant clones.

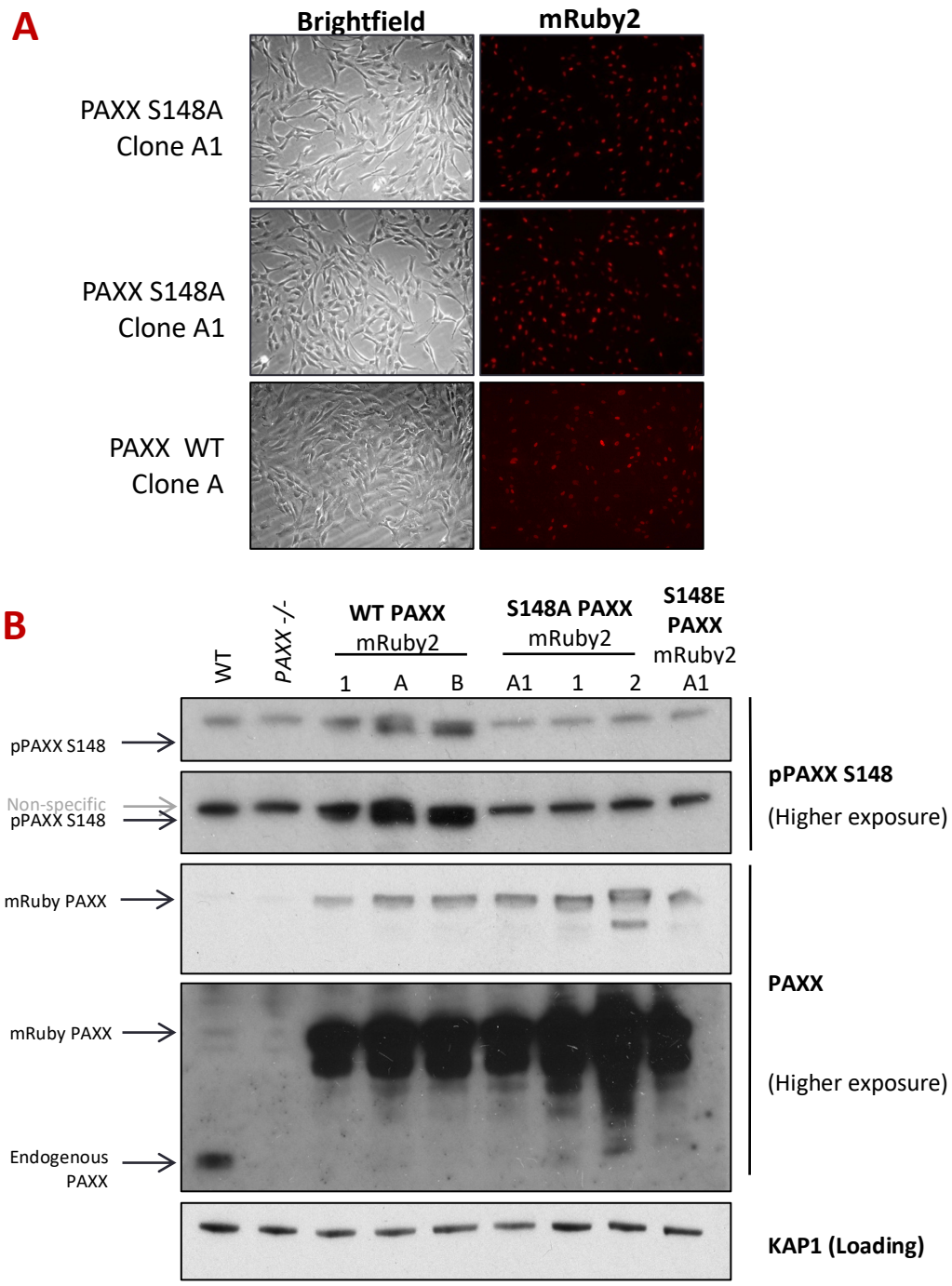

Figure 28 PAXX mutant generation in RPE-1 cells

(A) Microscope images of cell lines generated by random plasmid integration of mRuby2 expressing PAXX mutants. Mutant clones show nuclear expression of mRuby2-PAXX **(B)** Western blot showing detection of tagged PAXX. Endogenous PAXX can be seen in WT cells only whereas a mRuby2-tagged PAXX is seen in stable cell lines generated. Detection of phosphorylation at S148 can be seen in cells complemented with WT PAXX only (As indicated just below non-specific band). Clone numbers are indicated.

4.2.4. Testing IR sensitivity in cells expressing PAXX mutants

PAXX-/- cells have already been shown to have an increased sensitivity to IR compared to WT cells[143,213]. If PAXX phosphorylation at serine 148 has a significant impact on PAXX function, changes in sensitivity to IR may be detectable when this site is mutated. Clonogenic survivals reproduced the increased sensitivity to IR seen in *PAXX-/-* cells as compared to WT cells (Figure 29). Complementation of *PAXX-/-* cells by expressing WT PAXX (+PAXX WT), however, did not rescue sensitivity back to the same level as the WT cells. The clone expressing the PAXX S148A mutant (+PAXX S148A) showed similar levels of sensitivity to the PAXX knockout (*PAXX-/-)*. The clone expressing PAXX S148E (+PAXX S148E) showed a similar trend to the WT PAXX complement cells (+PAXX WT). None of the complemented clones showed much variation from each other and none of them rescued sensitivity of the knockout clone (*PAXX-/-)* to levels seen in WT cells (*PAXX +/+*) (Figure 29).

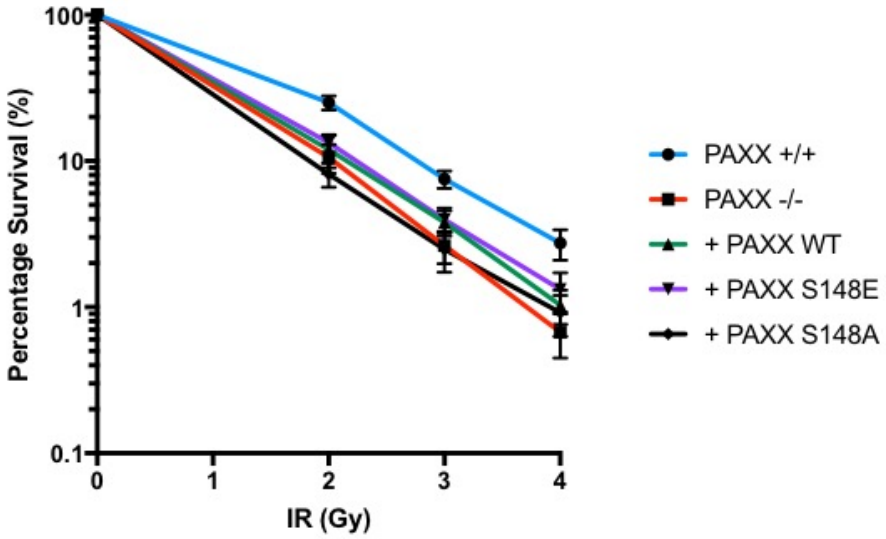

Figure 29 Clonogenic cell survival assays in RPE-1 PAXX mutant cell lines

Clonogenic cell survival assays of RPE-1 PAXX mutant cell lines to increasing doses or irradiation. RPE-1 WT cells = PAXX +/+, RPE-1 PAXX knockout = PAXX -/-. + PAXX WT/S148E/S148A = RPE-1 PAXX -/- cells complemented with stable WT/S148E/S148A mRuby2 tagged PAXX, respectively. Error bars show SEM, n=4.

4.2.5. CDK inhibition and PAXX phosphorylation

Since no obvious differences in IR sensitivity phenotypes were detectable between PAXX-/- cells containing WT of S148 mutated PAXX derivatives, I wanted to check phospho-PAXX S148 levels when inhibiting CDKs, in order to test if a reduction could be seen. Cells expressing GFP-tagged PAXX were subjected to three different CDK inhibitors (CDK1/2 inhibitor III, Flavopiridol and RO-3306) and blotted using an anti pPAXX-S148 antibody. Although CDK inhibition was observed, as seen by a reduction in many bands detected by with the MPM2 antibody, no changes in the level of pPAXX could be detected by this method (Figure 30).

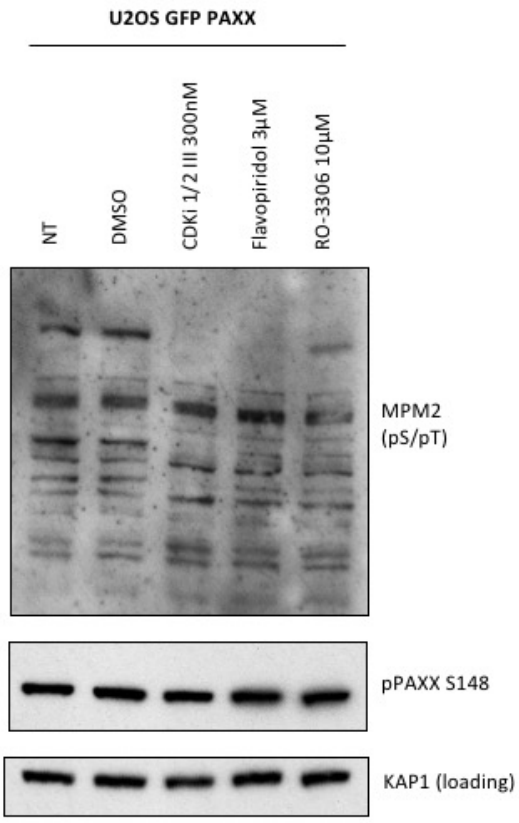

Figure 30 Testing effects of CDK inhibitors on PAXX S148 phosphorylation

U2OS cells were transfected with GFP PAXX and treated with various CDK inhibitors. CDKi 1/2 III was dosed for 2 hours at 300nM. Flavopiridol was dosed for 2 hours at 3μM. RO-3306 was dosed for 8 hours at 10μM. DMSO treatment was used as a control. Samples were harvested without recovery and blots were performed to detect PAXX S148 phosphorylation.

4.3. Discussion

Results presented here suggest PAXX is not a target for cell cycle dependent degradation, as total PAXX levels remained essentially constant throughout the cell cycle (Figure 26). This makes the possibility of PAXX phosphorylation targeting the protein for proteasomal degradation through a FBXW7 degron highly unlikely. PAXX seems to be phosphorylated at serine/threonine sites, as a noticeable band was detected via MPM2 probing in IPs that correlate with GFP-tagged PAXX (Figure 27B). This is not specific to S148 however and could be detecting other potential phosphorylation sites on PAXX. From my data PAXX does seem to be phosphorylated on S148 which was detectable with a specific antibody against that residue in U2OS cells over expressing GFP PAXX (Figure 27A). Although the antibody used did not seem to work brilliantly in RPE-1 cells, there does appear to be a band present in cells expressing mRuby2 tagged WT PAXX compared to cells expressing S148A/E variant of PAXX (Figure 28B). This suggests that mutating these residues results in loss of phosphorylation at this site. The online tool, PhosphoSitePlus®[231], also indicates that PAXX is indeed phosphorylated at S148.

By creating point mutants of PAXX S148, I explored potential effects that this site and its phosphorylation may have on PAXX function. Point mutants did not show much variation from each other in terms of sensitivity to IR. Unexpectedly, mRuby2 tagged WT PAXX complemented cells did not rescue the sensitivity seen in *PAXX-/-* cells back to the level of WT cells (Figure 29). This may indicate problems with the cells to tolerate overexpression of PAXX or potentially problems with the tagging of the protein. PAXX is a relatively small protein and both the N-terminal and C-terminal regions of the protein are highly important for PAXX function. mRuby2 was tagged at the N-terminal side of PAXX to prevent any disruption to the C-terminal interaction with Ku. The N-terminal head domain of PAXX is required for PAXX dimerization[143] and it is possible that fluorescent N-terminal tagging may have interfered with this.

In the interest of time, cell lines were generated by stable random plasmid integration which overexpressed variants of mRuby2 tagged PAXX in an already established RPE-1 *PAXX-/-* background. A better, more reliable model to use, would have been by generating point mutants of S148 at the endogenous PAXX locus by CRISPR-Cas9 mediated mutagenesis.

Nevertheless, this approach would have also had its limitations as a reliable antibody to detect phosphorylation at S148, especially in the context of endogenous PAXX protein levels was not available. The antibody used here gave mixed results in the two different cell lines chosen for experiments. When the antibody was tested to see if the band detected by it was depleted upon CDK inhibition, a reduction was not observed (Figure 30). CDK inhibition was occurring as validated by a loss of bands detected by the MPM2 antibody (Figure 30). This either suggests that the phospho-PAXX S148 antibody is not specific to that site, or the phosphorylation is not CDK dependent. This raises the intriguing possibility that PAXX S148 phosphorylation may be mediated via a distinct kinase whose identity remains to be determined.

Clonogenic survival assays performed with the PAXX mutants generated did not show obvious differences compared to *PAXX-/-* cells, furthermore WT PAXX complemented *PAXX-/-* cells did not rescue IR hypersensitivity to the same level as WT cells. This might suggest that the level of PAXX expression in these cells was not at the level needed to rescue sensitivity and perhaps overexpression in these cell lines is almost as toxic as total loss of the protein.

The difficulties encountered, and lack of appropriate tools to study PAXX S148 phosphorylation, coupled with the fact that there were no detectable changes in IR sensitivity phenotype between mutants meant that the project was put on hold.

Chapter 5: Performing a CRISPR-Cas9 screen to investigate the role of WRN in the DDR

5. Performing a CRISPR-Cas9 screen to investigate the role of WRN in the DDR

5.1. Introduction

5.1.1. Werner syndrome

Otto Werner, a medical student, first identified patients presenting with bilateral cataracts and scleroderma-like skin in 1904[232]. The disease has since been referred to as 'Werner Syndrome' (WS).

WS is a progeroid syndrome as it is mainly characterised by accelerated ageing. Symptoms that WS patients express are signs of premature ageing which include greying and loss of hair, bilateral cataracts, skin atrophy and loss of muscle and fat[233,234]. Unlike classical progeria syndromes such as Hutchinson-Gilford progeria syndrome (HGPS), WS patients seem to develop normally with no obvious abnormalities throughout childhood; however, they often miss their pubertal growth spurt during their teenage years[235,236]. WS syndrome patients only begin to show obvious premature ageing symptoms in their 20s-30s, typically showing an early onset of cataracts, osteoporosis, hypergonadism, diabetes mellitus, neoplasms and atherosclerosis[236,237]. The life span of WS patients is severely reduced with an average life expectancy of around 45-47 years[238]. The most common forms of death in WS patients are myocardial infarction and death from malignant cancers. Despite the link to cancer and neoplasms there are variations in the type of cancers that develop and ultimately, WS patients present with a diverse range of tumours. One study of literature case-reports found there to be a 1:1 ratio of epithelial to non-epithelial cancers in WS patients compared to a normal ratio of 10:1[239]. Others have reported an increased incidence of cancers of mesenchymal origin including an increased incidence of osteosarcoma[240].

WS is a rare autosomal recessive disorder which has an estimated incidence of 1:380,000 – 1:1,000,000; however the Japanese population has a greater incidence of around 1:20,000 – 1:40,000[241–243].

WS is solely caused by mutations at the *WRN* locus on chromosome 8. The gene spreads across ~140kb of genomic DNA and contains 35 exons (34 coding exons) which code for the WRN protein. A range of mutations have been identified in WS patients, with mutations occurring throughout the gene with no particular clustering in any one domain. Whilst some mutations appear to generate a truncated protein, all mutations result in loss of functional WRN[237]. WRN is a ~160kDa nuclear protein which is a member of the RecQ DNA helicase family[244].

5.1.2. RecQ helicases

Escherichia coli (*E. coli*) contains a single RecQ helicase, RecQ, which has been shown to be involved in plasmid recombination and in the recovery of replication fork stalling at sites of UV-induced DNA damage[245–247]. Mutations in *E. coli RecQ* result in increased illegitimate recombination in both untreated and UV damaged backgrounds[248]. *S. cerevisiae* and *S. pombe* also contain a single RecQ helicase; Sgs1 and Rqh1 respectively, which are homologous to *E. coli RecQ*. Sgs1 and Rqh1 are also involved in the responses to DNA damage. Despite knockout strains being viable, both Sgs1 and Rqh1 deficiency show a hypersensitivity to DNA damaging agents and an increase in chromosomal abnormalities[249,250]. *Sgs1* deletion also results in a decreased number of total cell divisions[251,252]. Sgs1 has been shown to be particularly involved in HR, as levels of the protein are increased in S-phase and deletion of *Sgs1* results in a reduced rate of DNA resection at double strand break ends[253]. The RecQ helicases have therefore been shown to be involved in DNA repair and the maintenance of genome stability, in both bacteria and fungi.

In humans, there are five known RecQ helicases: RECQ1, BLM, WRN, RECQ4 and RECQ5 which have evolved from a single ancestral gene to have specialised functions[254]. The RecQ helicases all contain a highly conserved helicase domain and are known to be involved in maintenance of genome stability. Three of the five human helicases are associated with rare genetic diseases; these are RECQ4, BLM and WRN. Mutations in *RECQ4* have been linked to three disorders: RAPADILINO syndrome, Rothmund-Thomson syndrome (RTS) and Baller-Gerold

syndrome (BGS). These three disorders are distinct disorders although they have some similarities in their symptoms which include skeletal malformation.

RAPADILINO is an acronym for the pathological features presented in patients with this syndrome; RA (radial ray malformation), PA (patella and palate abnormalities), DI (diarrhoea and dislocated joints), LI (limb abnormalities and little size) and NO (slender nose and normal intelligence)[255]. RAPADILINO has a higher incidence in Finland and characterisation of Finnish patients shows that they all carry at least one allele with a splice site mutation in intron 7 which results in an in-frame deletion of exon 7[254].

RTS is mainly characterised by poikiloderma, a skin condition featuring hypo/hyper pigmentation and atrophy which usually presents on the face and neck. Juvenile cataracts are also evident in patients with RTS in addition to some overlapping features described earlier. RTS is associated with an increased risk of developing osteosarcomas[256].

BGS is the least well studied of the three disorders due to the low incidence, predicted to be rarer than 1:1,000,000. Less than 40 cases of BGS have been reported in medical literature[255,257]. It has overlapping clinical features with RAPADILINO but also is characterised by poikiloderma which usually occurs within the first few months of life [254].

Mutations in *BLM* give rise to the rare genetic disorder Bloom syndrome (BS). BS patients typically have a significantly smaller body size than average which is evident in both young and adult patients[258,259]. Again, BS shares many of the symptoms of RTS, however the most striking and distinct phenotype of BS is an extreme sensitivity to sunlight which manifests in children between 1 and 2 years old. This usually presents on the faces of patients. The most common cause of death in BS is as a result of cancer which occurs at a much earlier average age than normal; 23, relative to 66 respectively. The average age of death in BS is below 30[260,261]. Despite similarities between BLM and WRN, BS is not a premature ageing syndrome and patients do not exhibit the typical accelerated ageing phenotypes associated with WS[260].

Of the RecQ helicases, BLM is the most well studied. The most distinct phenotype in cells lacking BLM is a large increase in sister chromatid exchanges[254,260,262]. These can be visualised

in chromosome spreads by labelling with BrdU, Hoechst and Giemsa. Chromosomes from wildtype cells usually show chromatid arms in one colour. Cells from BS show alternating colours within chromatid arms as a result of sister chromatid exchanges[262]. This occurs as a result of crossovers between nascent DNA and template DNA during DNA damage at replication forks, when strand invasion of the damaged DNA uses the sister chromatid as a template for repair[260]. BLM has specifically been implicated in preventing crossovers and has been shown to bind Holliday junctions[263–265]. BLM forms a complex with DNA topoisomerase III α (TOP3A), RecQ mediated genome instability 1 (RMI1), and RecQ mediated genome instability 2 (RMI2), which together resolve Holliday junctions[266,267]. BLM is specifically important in the HR pathway of DSBR and has a role in the promotion of long-range resection through its interaction with the exonucleases DNA replication helicase/nuclease 2 (DNA2) and EXO1[268–270]. BLM has some functional redundancies with WRN but also has non-redundant functions, this can be evidenced by differences in cell sensitivities between single and double knockouts to DNA damaging agents and differences in chromosome aberrations[271].

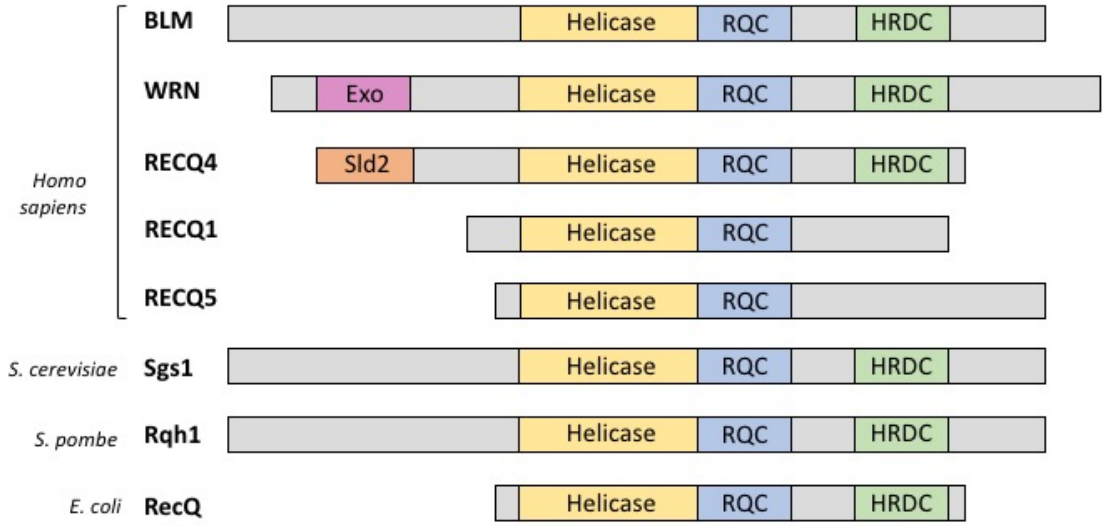

Figure 31 The RecQ helicases

Diagram showing RecQ helicases in bacteria, fungi and humans. *E. coli*, *S. cerevisiae* and *S. pombe* contain a single RecQ helicase whereas humans have 5 RecQ helicases: BLM, WRN, RECQ4, RECQ1 and RECQ5. All proteins contain a conserved helicase domain (yellow) and RecQ C-terminal (RQC) domain (blue). Helicase-and-ribonuclease D-C-terminal (HRDC) domains have also been highlighted (green). RECQ4 contains a Sld-2 like domain (orange) and WRN contains an exonuclease domain (pink). Domain sizes are not to scale. Figure adapted from W. Chu & I. Hickson, Nature Reviews Cancer, 2009[254].

5.1.3. WRN structure

WRN possesses a conserved helicase domain just like the other RecQ helicases and, like BLM, contains a RecQ C-terminal (RQC) domain and a helicase-and-ribonuclease D-C-terminal (HRDC) domain (Figure 31).

The helicase domain is essential for ATP binding and hydrolysis and serves as an ATP-dependent mode of DNA translocation to allow for the subsequent DNA helicase activity of the protein[272]. Despite the name the helicase domain alone cannot unwind DNA and requires a concerted effort with the RQC domain to have helicase activity[273].

The RQC domain folds into a winged-helix motif, which is a motif that is known to bind double stranded DNA[273]. Structural insights into the WRN RQC domain showed binding of the RQC domain onto duplex DNA, and specifically with blunt ended DNA[273,274].

The HRDC domain is unique to WRN and BLM amongst the other RecQ helicases. HRDC domains have typically been associated with structure specific DNA binding activity and the HRDC domain present in Sgs1 has been shown to have DNA binding activity for both ssDNA and partial duplex DNA[275,276]. The WRN HRDC domain has controversial reports on its activity; some suggest it has no DNA binding activity whilst others suggest it binds Holliday junctions and forked DNA but not ssDNA[273,277]. The HRDC domain function in WRN therefore remains unclear but is potentially involved in the binding of DNA and in particular, in the binding of DNA secondary structures. Another possibility is that it is involved in protein-protein interactions. The HRDC domain is connected to the RQC domain via a linker; this linker is longer in WRN than in BLM and likely to be unstructured. One proposed theory is that this distance between the two may be beneficial to aid interactions with other proteins; this could be with other DNA damage related proteins[273,278].

Although the BLM and WRN proteins contain many of the same domains the sequence identity between them varies; the helicase domain shares ~30%, the RQC shares around ~10% and the HRDC ~20% identity[273]. This may explain some of the functional differences in the two proteins and the clinical differences between the two syndromes. One unique feature of WRN compared to other RecQ helicases is its N-terminal exonuclease domain, which, like its helicase activity, acts in a 3' to 5' direction. WRN exonuclease activity is stimulated by Ku and LIG4/XRCC4[279]. Interestingly Ku, LIG4 and XRCC4 do not stimulate WRN helicase activity and thus suggests that WRN exonuclease activity is perhaps specific to NHEJ (discussed further in section 5.1.8). Recently, WRN was identified to contain two Ku binding motifs, one at the N-terminus next to the exonuclease domain and another at the C-terminus. Both the Ku binding motifs and the exonuclease domain are required for efficient DSBR in irradiated cells[280].

5.1.4. WRN binding partners

WRN interacts with a diverse range of proteins and has thus been implicated in a range of biological processes including replication, base excision repair (BER), DSBR, transcription and

telomere maintenance. The binding partners and relevant pathways WRN has a potential role in are discussed below.

5.1.5. WRN in base excision repair

WRN has been linked to BER through its interaction with other proteins involved in the same pathway. These include flap endonuclease 1 (FEN1), DNA polymerase β (DNAPolβ) and the DNA glycosylase, Nei like DNA glycosylase 1 (NEIL1)[281].

BER is a DNA repair process that results in the removal and replacement of damaged bases. BER exists in two forms: short patch BER (SP-BER) and long patch BER (LP-BER). SP-BER involves the removal and replacement of a single nucleotide base of DNA and is the more frequently used of the two processes. LP-BER involves the removal and replacement of more than one nucleotide[282].

BER begins by the recognition of damaged bases through damage-specific DNA glycosylases. These glycosylases cleave the N-glycosylic bond and thus detach the base from the sugar phosphate backbone. There are several DNA glycosylases, each of which recognises a specific type of base damage[282]. NEIL1 is a DNA glycosylase that recognises a number of base lesions including formamido-pyrimidine (fapy) lesions[283]. WRN interacts with NEIL1 both in vivo and in vitro and the binding between the two is enhanced upon oxidative stress[284,285]. WRN has been shown to stimulate the ability of NEIL1 to excise oxidative lesions from DNA substrates[284]. Consistent with this, WRN depleted cells accumulate oxidative damage[284].

The abasic site created after excision via the glycosylase in BER is processed to create a single strand break (SSB). DNAPolβ then catalyses the addition of nucleotide bases and the DNA is ligated via the XRCC1-DNA ligase IIIα complex[286,287]. WRN also interacts with DNAPolβ and stimulates its activity thus confirming its role in BER[288].

WRN has also been implicated in LP-BER through its interaction with FEN1. FEN1 has 5’ exonuclease activity and is thought to bind DNA containing 5’ ssDNA flaps[289]. This activity of

FEN1 is involved in LP-BER but it also functions at replication forks, particularly in the processing of Okazaki fragments[289]. WRN has been shown to stimulate FEN1 cleavage of 5' flap DNA. This functional interaction between the two also applies to the processing of DNA replication and repair intermediates[290].

5.1.6. WRN at replication forks

WRN has been linked to DNA replication through a number of interactors; these include RPA, DNAPolδ, PCNA and, as previously mentioned, FEN1[291,292]. The *Xenopus* ortholog of WRN, Ffa-1, was originally identified in the replication initiation complex and has been shown to be required for replication foci formation[293] which suggests a role for WRN in the DNA replication process. WRN promotes the activity of DNAPolδ, however WRN helicase and exonuclease activities are not enhanced by this interaction[292]. This might suggest that the role of WRN during replication is non-enzymatic. Interestingly, WRN also enables DNAPolδ to overcome DNA secondary structures, to perform DNA replication[294]. This may indicate that one of the main roles of WRN at replication forks is to resolve DNA secondary structures that create a potential block to replication fork progression. In concordance with this, WRN binds a range of DNA secondary structures, particularly those which are likely to form at replication forks[277]. Specific domains within WRN have been shown to have preferred secondary structure specificity; for example, the exonuclease domain preferentially binds forked DNA structures and 5' overhang duplex DNA whereas the HRDC domain shows a greater preference for Holliday junctions[295,296].

WRN has been implicated in promoting replication fork restart after fork stalling and fork collapse. Multiple groups have demonstrated this link by showing an increased sensitivity of WS cells to drugs that induce replication fork stalling[297–299]. This includes an increased sensitivity of WRN deficient cells to HU, a drug that induces replication fork stalling by depleting the dNTP pool. WRN depleted cells showed a delay in cell cycle progression when treated with HU and also showed an impaired ability in replication fork elongation, as measured by DNA fibre analysis[298]. Furthermore, WRN depleted cells showed an increased S-

phase arrest in cells treated with the TOP1 inhibitor topotecan[300]. This suggests an inability of replication fork restart after collapse in WRN depleted cells.

Despite extensive research in this area, the precise mechanisms by which WRN functions to prevent replication fork collapse is still debated.

5.1.7. WRN involvement in HR

There is strong evidence to suggest WRN is involved in DSBR as it accumulates at sites of laser induced DNA damage and interacts with proteins from both the HR and NHEJ pathways[281,301]. This consequently makes WRN an interesting protein with regards to regulation of DSBR pathway choice.

WRN interacts with some of the key components of the HR pathway and importantly has been shown to colocalise with RPA and RAD51, both of which are essential for HR[302]. The physical interaction of RPA and WRN has been shown to promote WRN helicase activity and therefore a potential role of WRN is in promoting DNA resection. Consistent with this WRN inhibition results in a decrease in pRPA following DNA damage which may be due to impaired resection[303]. Furthermore, WRN and DNA2 interact and together promote 5'-3' DNA resection as stimulated by RPA. The significance of this function of WRN may be redundant as BLM also performs this function and can perhaps compensate for any lack of WRN, with BLM being the more important RecQ helicase in this process in humans[304].

The involvement of WRN in HR is also apparent from the kinetics downstream of DNA resection. Cells from WS patients show increased levels of RAD51 foci compared to control cells, suggesting defects at the strand invasion stage of HR[305,306]. Consistent with this, WRN also interacts with RAD52 and RAD54 which both have roles in promoting recombination[307,308]. The hypersensitivity that WRN depleted cells show to DNA damaging agents that induce HR is further evidence of WRN functioning in HR[271,305].

5.1.8. WRN involvement in NHEJ

WRN is also implicated in NHEJ and has been shown to interact with DNA-PKcs, Ku, XRCC4 and DNA ligase IV. Similarly to Ku, XRCC4 and DNA ligase IV stimulate the exonuclease activity of WRN[279,309,310]. This suggests that WRN may have a role in processing DNA ends for NHEJ to take place. DNA-PKcs on the other hand is reported to have an inhibitory effect on WRN exonuclease activity in the presence of Ku[311]. The opposing effects of the NHEJ components on WRN suggest that the WRN activity in NHEJ is tightly controlled. WS cells only show a mild increase in sensitivity to IR compared to the core NHEJ factors, but this sensitivity is rescued by overexpression of WRN[312].

Recently, WRN has been linked to NHEJ pathway choice through promotion of canonical NHEJ versus alternative NHEJ. WRN appears to specifically inhibit alternative NHEJ by inhibiting resection, this was shown to occur via a mechanism which results in reduced recruitment of MRE11 and CtIP in G1 cells[313]. This reported inhibition of resection perhaps contradicts the functions of WRN proposed in promoting HR but may imply that WRN function is regulated throughout the cell cycle.

5.1.9. WRN at telomeres

WRN interacts with several components of the Shelterin complex including telomere repeat-binding factor 1 (TRF1), telomere repeat-binding factor 2 (TRF2) and protection of telomeres 1 (POT1). All of these factors are responsible for the recognition of TTAGGG repeats found at telomeric DNA[314,315]. The Shelterin complex acts to shape telomere secondary structures and protect the DNA ends from aberrant processing by DNA repair[316–318]. WRN might be involved in the resolution of DNA secondary structures at telomeres to enable efficient and successful telomere elongation. T-loops and D-loops are both substrates of WRN and both occur at Shelterin bound telomeres. In vitro experiments implicate WRN exonuclease activity in the resolution of telomeric D-loops by removing the homologous region of the 3’ invading strand that forms the D-loop[319]. Several DNA damage proteins, which are also interactors of WRN, associate with telomeres[320]. These aid in the repair and maintenance of telomeres and perhaps achieve this through their interaction with WRN. Repetitive sequences of triple

guanines in telomeric DNA make it prone to oxidative DNA damage and telomere shortening. This type of DNA damage is repaired by the BER pathway, which, as described earlier, WRN has been implicated in.

5.1.10. WRN, G4 quadruplexes and transcription

Telomeric TTAGGG sequences can also form G4 quadruplexes, a DNA secondary structure that is a preferential substrate of WRN[319,321,322]. Whilst telomeric G4 quadruplexes exist, the vast majority of G4 forming DNA regions are non-telomeric. G4 quadruplexes can be formed in both DNA and RNA. A large number of G4 quadruplexes are found in promoter regions and have been linked in regulating transcription in addition to their roles in regulating replication and telomere maintenance[323]. WRN has also been linked to transcription and has been shown to be a highly nucleolar protein. Nucleolar intensity of WRN is lost upon actinomycin-D treatment suggesting an involvement in rDNA transcription[324]. WRN helicase activity is also functional on RNA-DNA heteroduplexes. Cells from patients with WS also show a 40-60% reduction in the level of transcription compared to cells from normal individuals[325]. These results suggest WRN is involved in transcription and might suggest that the overall decrease in transcription in WS patients leads to the decline of cell fitness and hence premature ageing phenotypes.

5.1.11. Insights into WRN function from WRN knockout mice

Studies in patient cells and human cells depleted for WRN have offered insights into WRN function but its precise roles are still to be identified. Mouse models have been generated as a means to explore WRN function but unfortunately have not been able to establish any exact mechanisms. Neither *WRN* null mice nor mice containing an in-frame deletion of the helicase domain present the same clinical premature ageing phenotypes associated with WS[326,327]. Cells taken from *WRN* null mice did not show an increased sensitivity to CPT or 4-nitroquinoline 1-oxide (4NQO) contrary to cells taken from WS patients and contrary to embryonic stem (ES) cells derived from the helicase deleted mouse[326]. Despite the lack of physical clinical manifestations of mice harbouring only *WRN* defects, late generation mice

that are *WRN* and telomerase RNA component (*TERC*) null do show signs of premature ageing. *WRN-/- TERC-/-* mice were smaller in size compared to controls and showed a reduced lifespan. These mice also presented kyphotic stature, greying of hair and alopecia as well as cataracts, all of which can be linked to WS[328]. This might suggest that WRN function and the phenotypes presented in WS are a result of improper telomere maintenance and telomere shortening.

5.1.12. WRN investigations herein

Literature on WRN suggest it has a variety of possible functions, and publications convey a number of conflicting and contradictory results (as described above). The fact that WRN is involved in DNA repair and seems to have functions in both HR and NHEJ mechanisms of DSBR make it an interesting protein that may influence and regulate DSBR pathway choice. In order to further investigate WRN and interrogate its function, two main areas of research were pursued.

The main area of research involved using a generated isogenic WRN knockout cell line as a tool, to perform a CRISPR-Cas9 gene inactivation screen to look for suppressors of WRN specific DNA damage sensitivity. This was performed with the aim of identifying genetic interactors that could offer mechanistic insights into the functions of WRN within the DDR.

The second aspect of my research was to utilise the knockout cell line to investigate mutational signatures that accumulate over time. WS is a premature ageing syndrome which gives an increased predisposition to cancers. Little is known about why this might be the case. Performing mutational signatures analysis might give insights into multiple questions regarding the involvement of WRN in maintaining genome stability. This includes information like the number and types of indels and single nucleotide polymorphisms, as well as the location of any mutations. This will reveal which genetic areas are prone to mutations and may allow us to link it to other features such as DNA secondary structure or highly transcribed areas. Unfortunately, the sequencing data is still in a pipeline for bioinformatic analysis and therefore has not been fully interrogated. As a result, it will not be presented in this thesis.

5.2. Results

5.2.1. Generation of RPE-1 *WRN* knockout

In order to better study the functions and roles of WRN, I first generated a *WRN* gene knockout in RPE-1 cells. This gave me a novel system to study WRN, as previously published reports on WRN have typically been focused using patient derived fibroblasts taken from patients towards the later stages of their lives, or mouse and chicken cell lines. Knockouts were generated by the process detailed in Figure 32A, which began with the electroporation of RPE-1 cells with four separate plasmids. This included two encoding gRNAs targeting Exon 12 of WRN (Figure 32B), one encoding a Cas9 nickase and one carrying a targeting cassette containing a puromycin resistance gene and GFP (targeting cassette and gRNA plasmids were obtained from Sasa Svikovic in the Julian Sale lab, Laboratory of Molecular Biology, Cambridge). The RPE-1 cells used already contained a puromycin resistance gene and thus the knockouts were generated using GFP as a selection marker; cells were FACS bulk sorted initially in order to select for positively transfected cells. These cells were split into two populations and plated back onto dishes and left to recover. Cells were then FACS single cell sorted into 96 well plates for cells still expressing GFP. This enabled selection of stable integration of the targeting cassette. Plates were monitored over the next 10 days and inspected under a microscope to ensure only wells which contained single colonies were taken forward. Crude lysate was extracted from potential positive clones and PCR screened for bands shifts. Bands shifts differing from the WT product correspond to insertions or deletions at the locus. Clones were expanded and then verified for loss of WRN by Western blot. Four clones tested showed complete loss of WRN with no evidence of truncated products (Figure 32C). For the duration of my studies I used these four clones (E5, F11, G7 & 1A6).

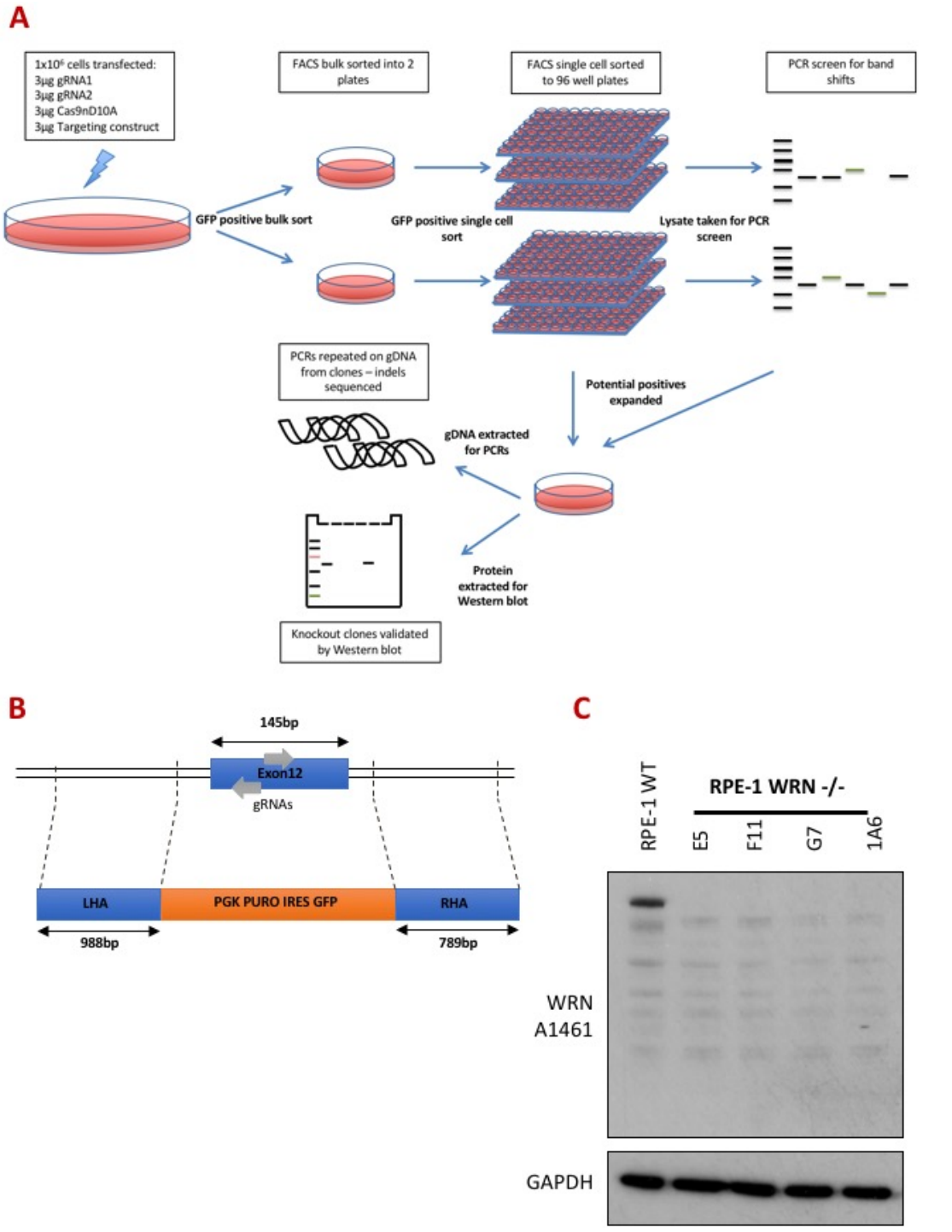

Figure 32 WRN knockout generation

(A) Schematic showing the *WRN* knockout generation process. RPE-1 cells were transfected with gRNAs, Cas9nickase and a targeting construct (3µg each plasmid). Positively transfected cells were selected by FACS bulk sorting for GFP and split into two populations. Subsequent populations were single cell GFP sorted by FACS for stable integration of the targeting construct. Clones were then screened by PCR and Western blotting to confirm knockout **(B)** Diagram of targeting construct designed against Exon12 of *WRN*. **(C)** Western Blot validation of knockout clones generated.

5.2.2. *WRN* knockout clones are hypersensitive to CPT

Previous literature has shown that WRN deficient cells exhibit an increased sensitivity to drugs that interfere with DNA replication, such as hydroxyurea (HU) and camptothecin (CPT)[271,305]. I tested this in my knockout cell lines to see if they showed the same phenotype to allow for direct comparison and were a reliable cellular model of the disease. Growth assays were set up with chronic treatment of CPT at 2nM, and growth monitored by percentage confluence using an IncuCyte® ZOOM system. There was a slower increase in percentage confluence over time when comparing 2nM CPT treated to the non-treated (NT) in the *WRN-/-* clones (NT) (Figure 33A). Importantly the WT clone does not show the same level of increased CPT sensitivity (as measured by percentage confluence) at this concentration. Knockout clones G7, E5 and 1A6 all showed an increased sensitivity to CPT compared to WT cells. Clone F11, by contrast, did not show the same increase in sensitivity at this concentration of CPT.

I next tested to see if an increase in CPT sensitivity could be seen in WRN siRNA depleted cells. This was to verify if depletion of WRN showed the same hypersensitivity to CPT phenotype as the majority of the *WRN-/-* clones tested. Depletion of WRN protein with siRNA was seen at both 24 hours and 96 hours after transfection (Figure 33B). This meant that protein levels were efficiently depleted at the time the CPT was administered (48 hours after transfection). WRN depleted cells did show an increased sensitivity to 2nM CPT compared to cells transfected with the control siRNA (Figure 33C).

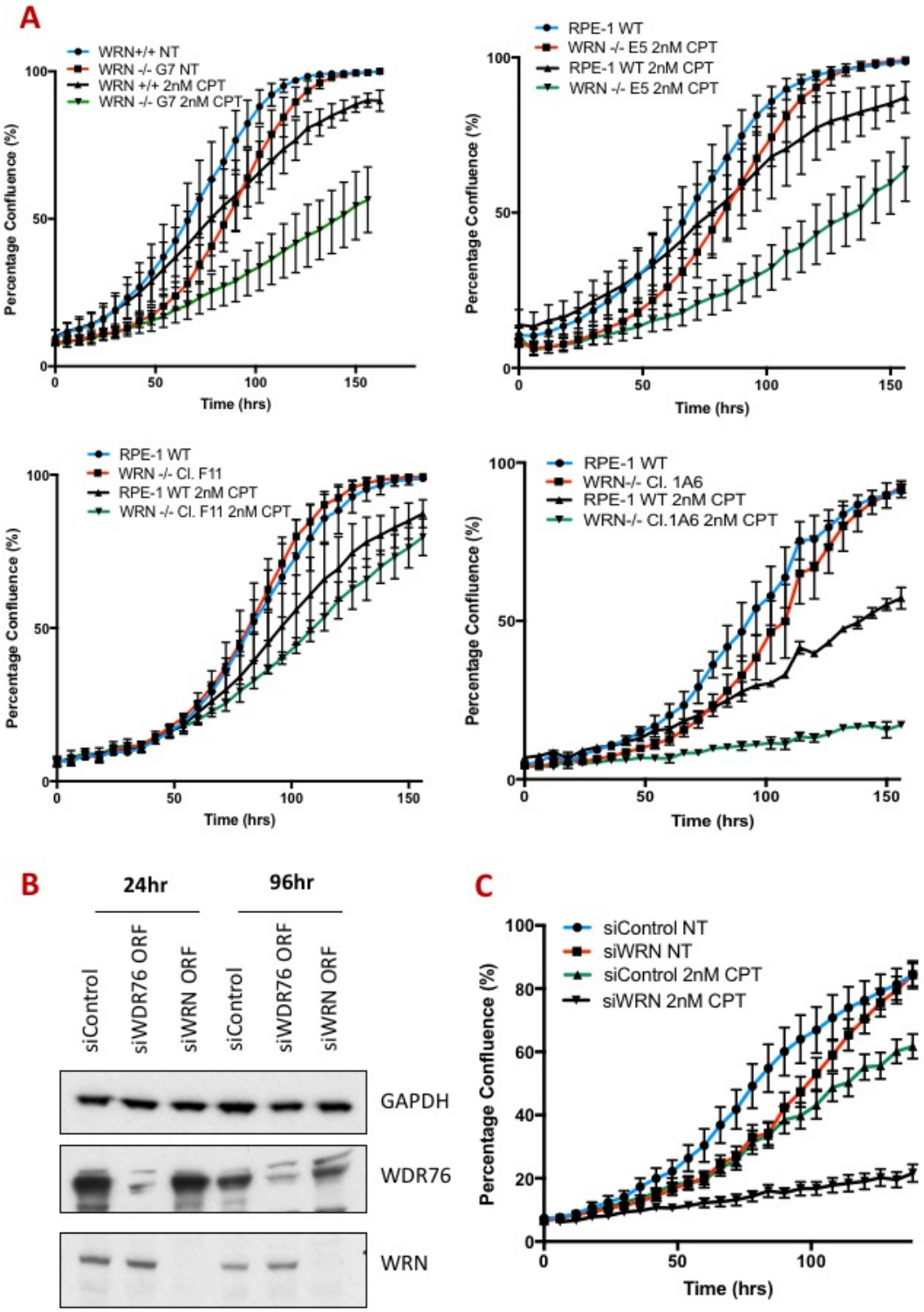
A
WRN+/+ NT
WRN -/- G7 NT
WRN +/+ 2nM CPT
WRN -/- G7 2nM CPT
Percentage Confluence (%)
Time (hrs)
RPE-1 WT
WRN -/- E5 2nM CPT
RPE-1 WT 2nM CPT
WRN -/- E5 2nM CPT
RPE-1 WT
WRN -/- Cl. F11
RPE-1 WT 2nM CPT
WRN -/- Cl. F11 2nM CPT
RPE-1 WT
WRN-/- Cl. 1A6
RPE-1 WT 2nM CPT
WRN-/- Cl.1A6 2nM CPT
B
24hr
96hr
siControl
siWDR76 ORF
siWRN ORF
GAPDH
WDR76
WRN
C
siControl NT
siWRN NT
siControl 2nM CPT
siWRN 2nM CPT

Figure 33 WRN knockout clones show sensitivity to camptothecin

(A) Graphs of Incucyte® growth assays performed in RPE-1 WT and *WRN* knockout clones (G7,E5,F11,1A6), showing percentage confluence in untreated and 2nM CPT treated samples. Each graph shows a different *WRN* knockout clone tested as indicated in the key. Error bars show SEM, n≥2. **(B)** Western blot showing validation of siRNA mediated WRN depletion relevant to **(C)** Graph of Incucyte® growth assay shown in performed in WT and WRN siRNA depleted cells. (siRNA against WDR76 was used as a control in (B)).

Upon performing the survival assays, I noticed a tendency for the RPE-1 cells to senesce when exposed to high levels of DNA damage. This was particularly noticeable in the RPE-1 *WRN-/-* knockout clones used. Senescent cells, although not continuing to divide, maintain adherence to cell culture plates and expand in size. Both the nucleus size and the cytoplasmic size increase in senescent cells. The confluence mask used in the IncuCyte® assays does take this into account, however at higher levels of senescence, the software struggles to distinguish alive, proliferative confluent cells from large expanding senescent cells. This could have therefore led to overestimates of the level of survival following CPT treatment seen in the *WRN-/-* compared to WT cells, thereby underestimating the CPT hypersensitivity of *WRN-/-* cells.

To overcome this potential issue, plates were stained with the DNA stain Hoechst, at the end point of experiments and images taken under a fluorescent microscope. NT WT cells and NT *WRN-/-* cells grow normally and cells become compact and highly confluent. In WT cells treated with 2nM CPT, there is a mixture of cells which correspond to both proliferative and senescent cells. This can be seen by the mixture of densely packed smaller nuclei (proliferative cells) as well as swollen nuclei with few nuclei surrounding them (senescent cells) (Figure 34A). *WRN-/-* cells treated with 2nM CPT show an almost complete loss of proliferative cells, with the majority of cells showing swollen nuclei. The number of nuclei in a given field therefore correlate to the level of cell survival. Multiple images were taken from triplicate wells and nuclei numbers counted using ImageJ software. The three WRN knockout clones showed an increase in sensitivity to 2nM CPT giving 4-7.5% survival. WT cells in contrast were much less affected at this concentration of CPT, showing around 30% survival (Figure 34B).

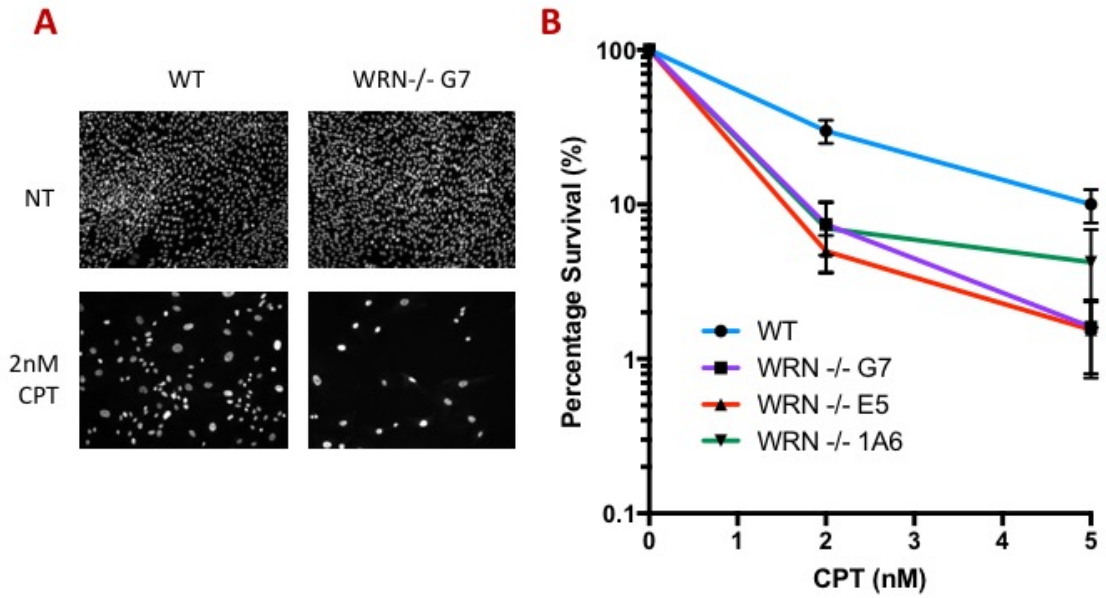

Figure 34 WRN knockout cells show increased sensitivity to camptothecin

(A) Cell survival assays were performed in non-treated (NT) or chronic 2nM CPT treated (2nM CPT) WT or *WRN-/-* RPE-1 cells. Cells were stained 6-10days after dosing and stained with Hoechst. Images of Hoechst staining from cell survival assays can be seen. **(B)** Images of Hoechst stained cells were quantified using ImageJ and percentage survival measured relative to non-treated. Error bars show SEM, n=4.

5.2.3. Generating stable Cas9 expressing cells for CRISPR genetic screen

Having established a defined window of sensitivity between WT and *WRN-/-* cells to CPT, I set out to explore functional mechanisms behind the sensitivity. To do this, a CRISPR-Cas9 screen to look for potential suppressors was performed. In order to setup a screen, I first had to generate *WRN-/-* cells stably expressing Cas9. This was done by lentiviral infection of the already validated *WRN-/-* clones (E5,G7,F11 & 1A6) with a plasmid containing WT Cas9 and a blasticidin resistance gene. Once infected, cells were selected using blasticidin and resistant clones picked (Figure 35A). Clones then had to be tested to ensure that Cas9 was active in these cells. This was performed using a lentiviral vector expressing both blue fluorescent protein (BFP) and GFP as well as a gRNA targeting GFP (Figure 35B). The principle behind this system is that cells infected with the lentivirus that do not express Cas9 would express both BFP and GFP; conversely lentiviral infection in cells expressing Cas9 would result in largely BFP only as the GFP sequence would be cut and mutated by Cas9/gRNA complex. This is the case that can be seen in RPE-1 WT cells (Figure 35C top panel); non-treated cells are non-fluorescent, lentiviral infected cells without Cas9 show both BFP and GFP, and lentiviral infected cells containing Cas9 show mostly BFP only cells.

The *WRN-/-* cells that were generated already contained GFP in them as a result of the targeting construct used to make them, and thus gating had to be adjusted accordingly (Figure 35C bottom panel). An obvious shift can still be seen when comparing lentiviral infected cells with and without Cas9 (Figure 35C bottom panel, middle and right). Efficiency of the Cas9 cutting was quantified by FACS and measured by percentage of GFP remaining (Figure 35D). All Cas9 expressing clones exhibited a dramatic reduction in GFP to below or around 10% GFP remaining therefore showing good Cas9 efficiency. This is probably an underestimate of Cas9 efficiency in *WRN-/-* Cas9 clones as they contained two copies of GFP (one from the original knockout generation).

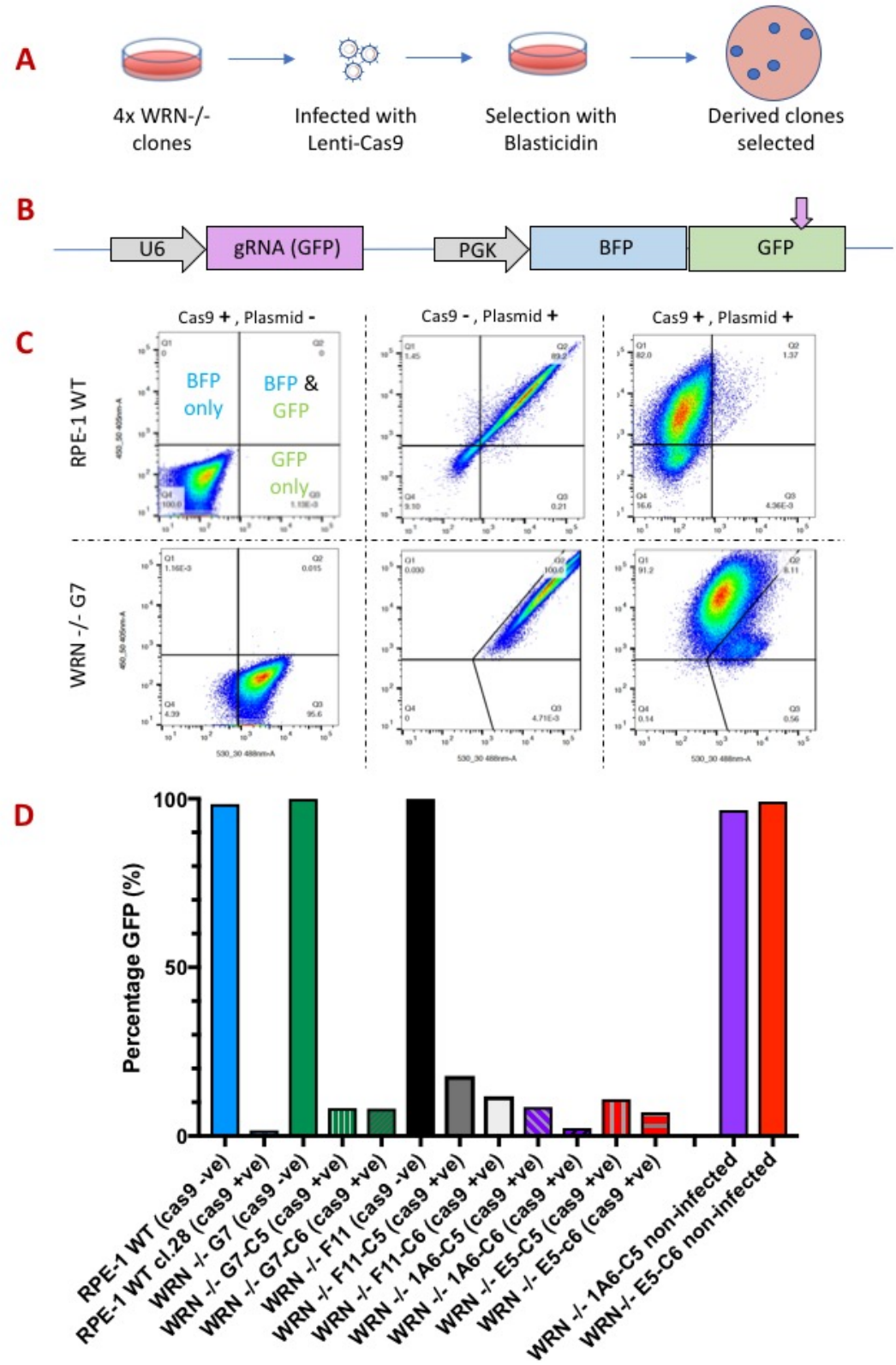
A
4x WRN-/- clones
Infected with Lenti-Cas9
Selection with Blasticidin
Derived clones selected
B
U6
gRNA (GFP)
PGK
BFP
GFP
C
Cas9 + , Plasmid -
Cas9 - , Plasmid +
Cas9 + , Plasmid +
RPE-1 WT
WRN -/- G7
BFP only
BFP & GFP
GFP only
D
Percentage GFP (%)
100
50
0
RPE-1 WT (cas9 -ve)
RPE-1 WT cl.28 (cas9 +ve)
WRN -/- G7 (cas9 -ve)
WRN -/- G7-C5 (cas9 +ve)
WRN -/- G7-C6 (cas9 +ve)
WRN -/- F11 (cas9 -ve)
WRN -/- F11-C5 (cas9 +ve)
WRN -/- F11-C6 (cas9 +ve)
WRN -/- 1A6-C5 (cas9 +ve)
WRN -/- 1A6-C6 (cas9 +ve)
WRN -/- E5-C5 (cas9 +ve)
WRN -/- E5-c6 (cas9 +ve)
WRN -/- 1A6-C5 non-infected
WRN-/- E5-C6 non-infected

Figure 35 Testing Cas9 efficiency in cell lines for screen

(A) Diagram showing generation of *WRN-/-* cells stably expressing Cas9. Knockout clones were infected with lentivirus carrying Cas9 and placed under blasticidin selection. Resistant clonal colonies were picked. **(B)** Map of lentiviral Cas9 test plasmid which contains BFP and GFP driven by a PGK promoter and a U6 promoter driving a gRNA targeting the GFP. **(C)** FACS plots of Cas9 testing. Top row shows WT cells and bottom row shows WRN knockout clone G7. Left column shows cells expressing Cas9 but without infection with test plasmid. Middle column shows cells not expressing Cas9 but infected with the test plasmid. Right column shows cells expressing Cas9 and infected with test plasmid. Column titles denote presence of Cas9/test plasmid as denoted by Cas9+/- and Plasmid+/-. **(D)** Graph showing quantification of Cas9 gene mutation efficiency testing as measured by percentage GFP. Clones are indicated below bars with indication of Cas9 status. Two non-infected clones as controls are plotted on the far right.

5.2.4. CRISPR-Cas9 screen to identify suppressors of WRN-/- sensitivity to CPT

A CRISPR-Cas9 screen was performed in three cell lines: the RPE-1 WT background and two knockout clones (all expressing Cas9). *WRN-/-* clones G7-C6 and E5-C5 were chosen as they showed good Cas9 cutting efficiency and both showed an increased sensitivity to CPT compared to WT cells (Figure 33A, Figure 34B, Figure 35D). The screen was performed with a focused human DDR CRISPR library targeting a total of 737 genes (Table 2).

Total number of guides	11281
Number of DDR target genes	737
Number of targeting guides	10081
Number of non-targeting guides	1200
Average number of guides per gene	13.68

Table 2 Human DDR CRISPR library

Information on the content of the human DDR CRISPR (hDDR) library. Non-targeting guides contained sequences which do not match human genomic DNA and thus do not target the genome. The human DDR CRISPR library contained multiple gRNAs targeting each gene with an average of ~13 gRNAs per gene. For full list of genes in the library see Appendix Table 4.

All cell lines were infected with a 0.2 multiplicity of infection (MOI) with enough cells to get a 500x cells per guide library representation (Figure 36A). Infecting at this MOI reduced the likelihood of single cells being targeted with more than one guide. Positively targeted cells were selected for BFP expression by FACS, as again the resistance in the hDDR library was puromycin (a resistance gene already present in the clones used) (Figure 36B). Cells were then cultured for 14 days to allow for removal of cells mutated in essential genes. Cells were treated with 2nM CPT and left in the drug for 5 days before being washed and allowed 6 days recovery. At all stages throughout the screen, cell numbers were maintained to give 500 times representation for each guide in the starting library (Figure 36A).

PCR library preparation was performed in two stages with an initial PCR to generate a product which includes the gRNA 'barcode' for the guide present in the cell (Figure 36B). This PCR product was then purified and used as templates to generate PCR products containing adaptors for Illumina sequencing (Figure 36C). These products were quantified by Qubit and qPCR before being pooled and submitted for sequencing.

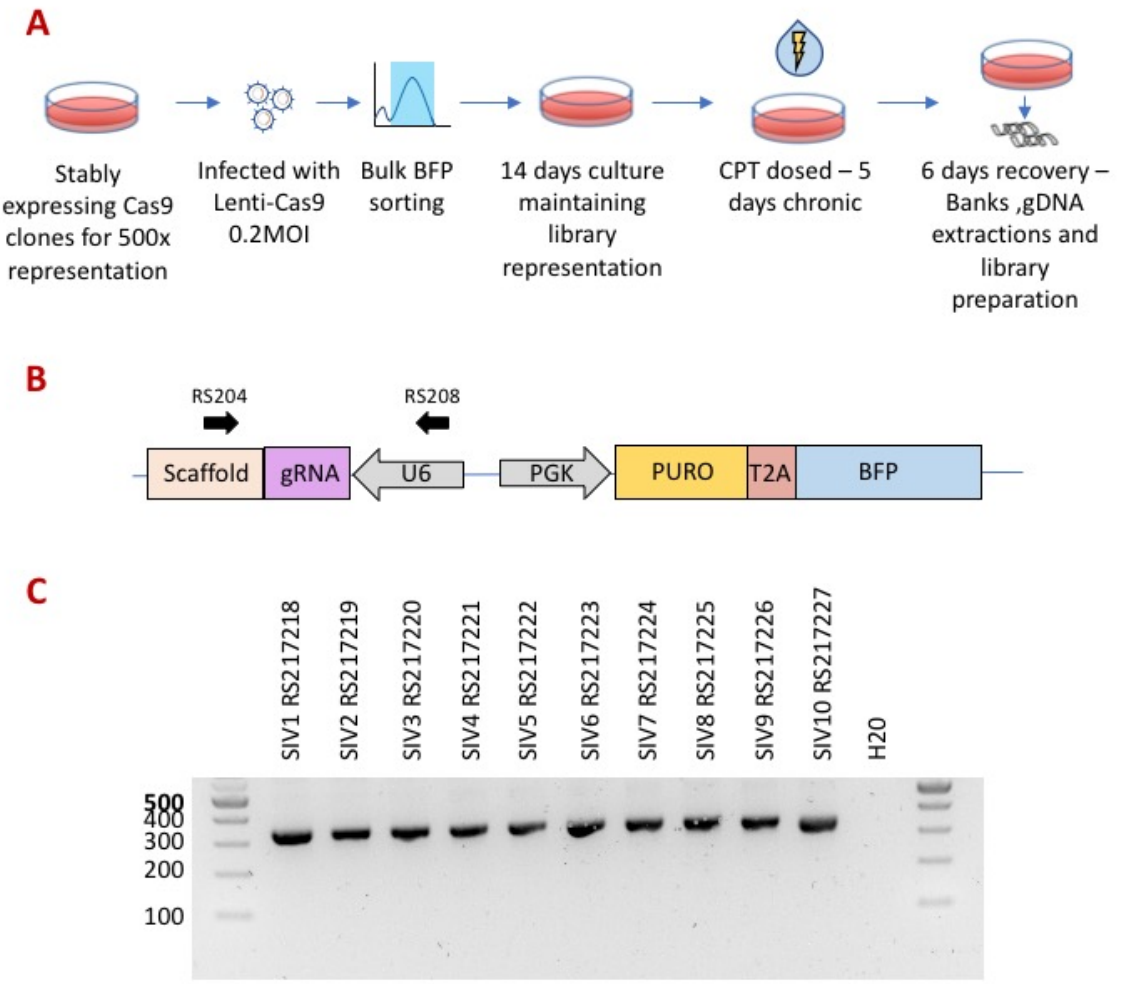

Figure 36 Library Preparation for Illumina Sequencing

(A) Schematic of the CRISPR-Cas9 screen process. Stably expressing Cas9 clones were infected with a 0.2MOI to gain a 500x representation. Targeted cells were BFP sorted and cultured in flasks for 14 days, splitting and maintaining cell numbers for 500x library representation. Cells were chronically treated with DMSO or CPT at either 2nM or 5nM for 5 days. Cells were allowed to recover, and samples taken for library preparation. **(B)** Map of gRNA lentivirus containing a gRNA driven by a U6 promoter and a puromycin and BFP driven by a PGK promoter. Black arrows annotated RS204 and RS208 indicated the primers used for the first PCR which was used as a template for subsequent PCRs in library preparation **(C)** PCR products of second PCR to add Illumina sequencing specific adaptors. Sample labels SIV1-10 were used for the 10 samples and primers indicated (RS***) (see Table 1 and Appendix Table 1 for details). These samples were pooled and sequenced.

5.2.5. CRISPR-Cas9 screen results

5.2.5.1. Suppressors in the WT background

CRISPR screen analysis was performed by comparing DMSO treated and CPT treated endpoint samples (after treatment and recovery) to the day 14 control (prior to treatments) for each cell line included in the screen. This was done using joint analysis of CRISPR/Cas9 knock-out screens (JACKS)[329] and performed by Iñigo Ayestaran in the Jackson Lab. This allowed a comparison of changes in gRNA sequence counts between CPT treated and DMSO treated cells, which allowed for identification of suppressors specific to the DNA damage treatment. By comparing the lists of genes between the cell lines used, suppressors specific to the *WRN-/-* background could be identified. Figure 37A/B shows a comparison of the level of enrichment of DMSO treated and CPT treated cells compared to the day 14 control in WT RPE-1 cells. Two concentrations of CPT were used in the WT background: 2nM which gave an IC40 and 5nM which gave an IC70. The non-targeting guides present in the DDR library have been randomly clumped into groups of 15 and plotted in red on the graphs. They tend to localise close to the XY intersect which reflects little enrichment or loss from the day14 control. The blue dotted line is plotted where X=Y and thus reflects the position where enrichments are equal in the DMSO and CPT treated samples.

gRNAs against *TP53* showed the greatest enrichment in both samples but shows a comparatively greater enrichment of around 6-fold increase in the CPT treated sample compared to a 3.5-fold increase in the DMSO treated sample (Figure 37A/B). gRNAs against *CDKN1A* showed the next greatest enrichment in the CPT treated sample. Other gRNA targets that showed a greater enrichment in the CPT mediated DNA damage samples include: *NEDD8*, *CHEK2*, *SOD1,* and *POLR2A* (Figure 37A/B).

A number of targets were identified which showed a greater enrichment in DMSO treated samples compared to CPT treated samples in the WT background. These can be seen by points that have a positive value for enrichment in DMSO treated samples but fall below the blue dotted line. These include *RNF146*, *KEAP1*, *CAND1*, *UBE2F*, *PTEN*, *SCAF4* and *CUL3* (Figure 37A/B).

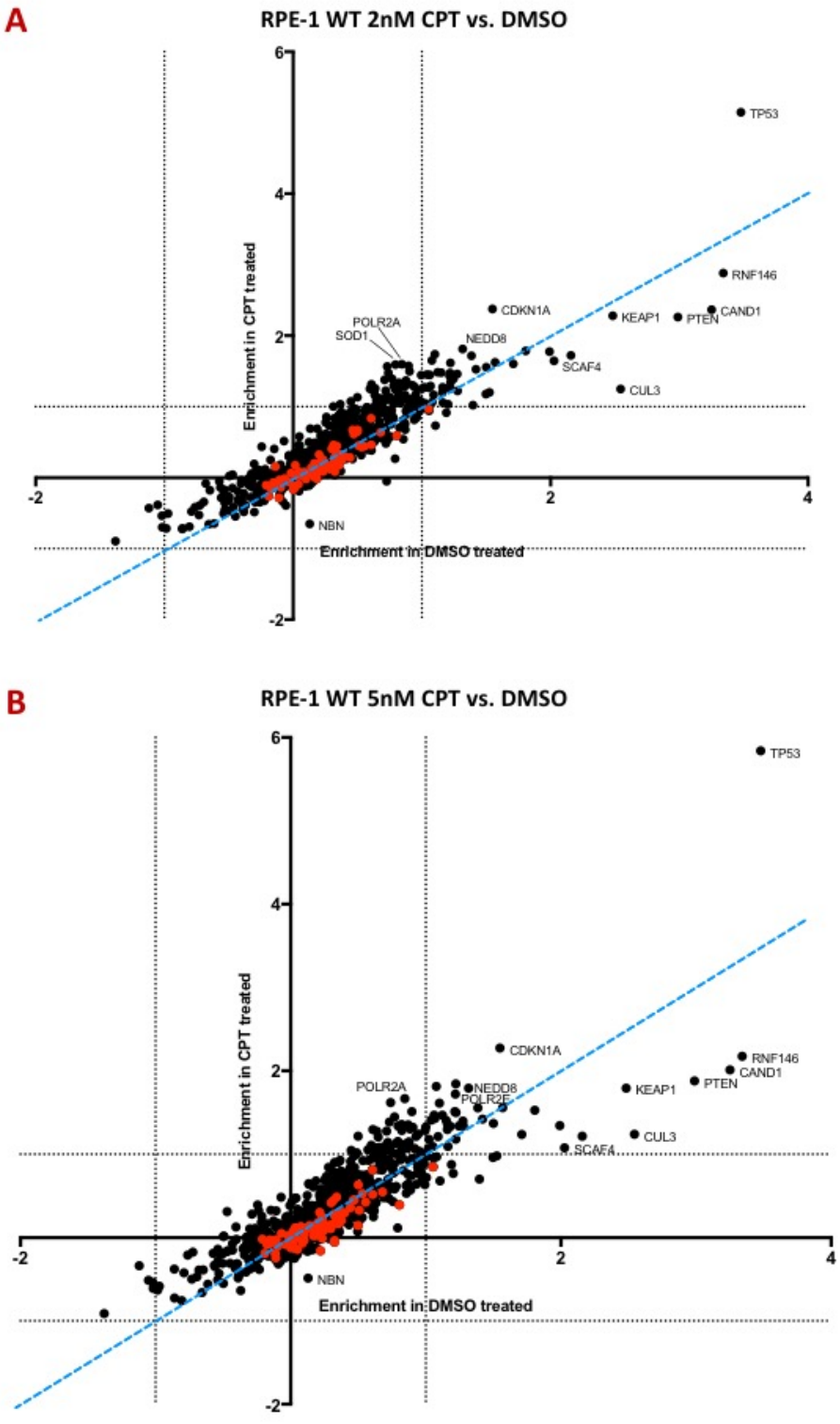
A
RPE-1 WT 2nM CPT vs. DMSO
Enrichment in CPT treated
Enrichment in DMSO treated
TP53
RNF146
CDKN1A
KEAP1
PTEN
CAND1
POLR2A
SOD1
NEDD8
SCAF4
CUL3
NBN
B
RPE-1 WT 5nM CPT vs. DMSO
Enrichment in CPT treated
Enrichment in DMSO treated
TP53
CDKN1A
RNF146
CAND1
POLR2A
NEDD8
POLR2E
KEAP1
PTEN
CUL3
SCAF4
NBN

Figure 37 JACKS analysis plots of CRISPR screens performed in WT RPE-1 cells

Plot of JACKS analysis showing fold enrichment of grouped gRNAs in DMSO treated samples versus CPT treated samples compared to the day 14 control in WT cells. Red dots indicate non-targeting guides. All black dots indicate the gene target of gRNAs, which have been grouped. Some have been indicated. The blue dotted line represents x=y where enrichments in DMSO and CPT treated samples are equal. The black dotted line shows enrichments at +/- 1. **(A)** Plot of DMSO treated vs. 2nM CPT treated **(B)** Plot of DMSO treated vs. 5nM CPT. (Raw data in Appendix Table 4 & Appendix Table 5)

5.2.5.2. Suppressors in WRN-/- background

gRNAs enriched in both CPT and DMSO treated samples were also the same in both *WRN-/-* clones compared to WT RPE-1 cells and included gRNAs targeting *RNF146*, *KEAP1*, *CAND1*, *PTEN*, *SCAF4* and *CUL3* as before (Figure 38A/B). The two strongest suppressors of CPT sensitivity in both *WRN-/-* clones screened were also TP53 and CDKN1A, thus matching the strongest suppressors in the WT background (Figure 38A/B).

When looking at the raw numbers from the JACKS analysis for the E5 WRN knockout clone, other suppressors which showed greater suppression in the CPT treated versus the DMSO treated were identified. These hits were picked by looking at the fold difference between the two samples and taking hits which showed a difference greater than 0.3 and a false discovery rate (FDR) less than 10% (Appendix Table 7 & Appendix Table 9). This identified the other targets *CHEK2*, *SMARCC1*, *POLD3*, *EME2* and *MAPK14* (highlighted in the plots) in addition to *TP53* and *CDKN1A* (Figure 38A).

The same analysis was performed for the G7 WRN knockout clone which identified the following suppressors specific to CPT treatment: *MAPK14*, *TP53*, *ENDOV*, *CDKN1A*, *CUL3*, *DNTT*, *SHFM1*, *DCLRE1A*, *CDC25A*, *APEX1*, *GADD45G*, *MLH3* and *PBRM1* (Appendix Table 6 & Appendix Table 9) (Figure 38B).

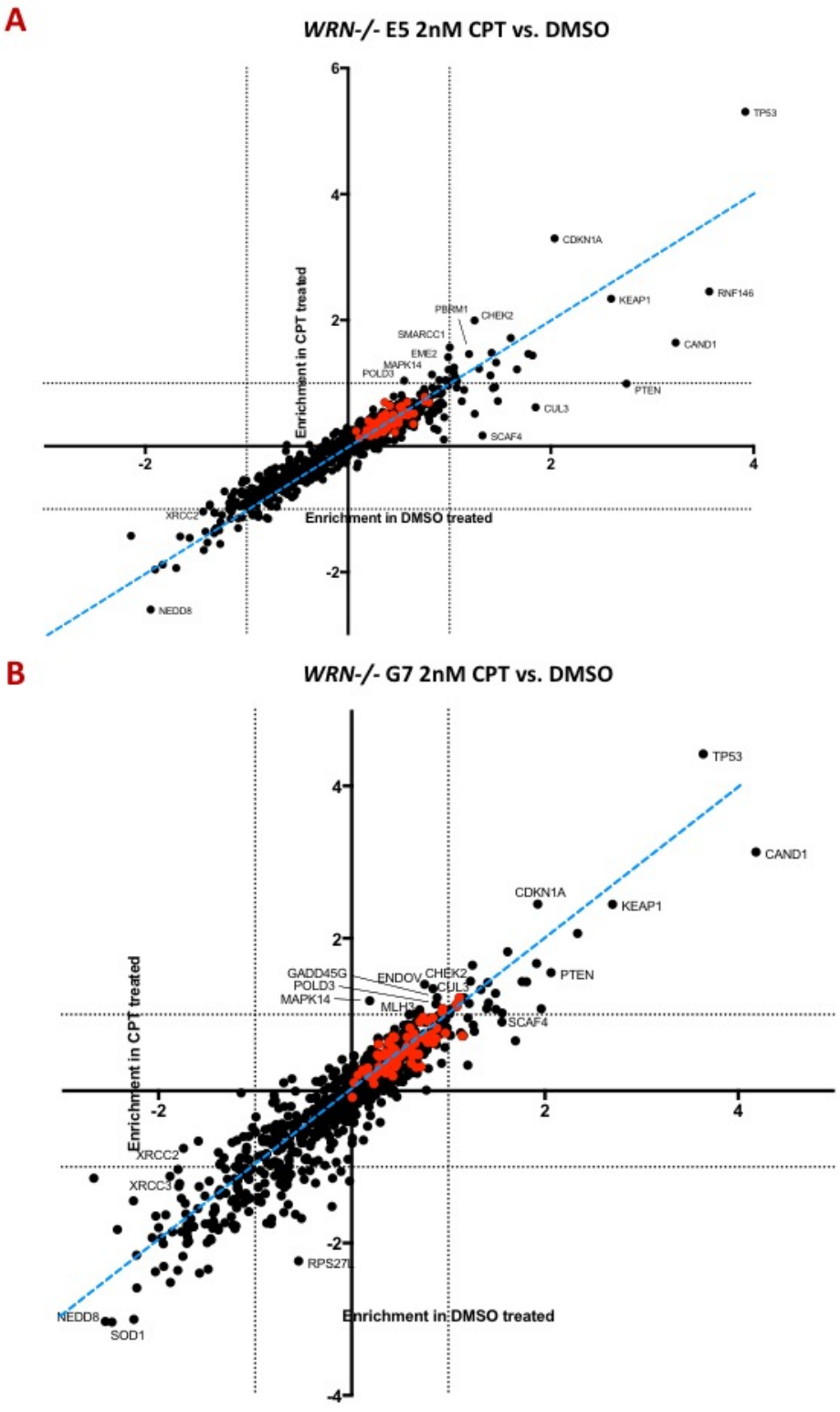
A
WRN-/- E5 2nM CPT vs. DMSO
Enrichment in CPT treated
Enrichment in DMSO treated
TP53
CDKN1A
RNF146
KEAP1
PBRM1
CHEK2
SMARCC1
CAND1
EME2
MAPK14
POLD3
PTEN
CUL3
SCAF4
XRCC2
NEDD8
B
WRN-/- G7 2nM CPT vs. DMSO
Enrichment in CPT treated
Enrichment in DMSO treated
TP53
CAND1
CDKN1A
KEAP1
GADD45G
ENDOV
CHEK2
POLD3
CUL3
PTEN
MAPK14
MLH3
SCAF4
XRCC2
XRCC3
RPS27L
NEDD8
SOD1

Figure 38 JACKS analysis plots of analysis performed on individual WRN knockout clones

Plot of JACKS analysis showing fold enrichment of grouped gRNAs in DMSO treated samples versus CPT treated samples compared to the day 14 control in *WRN-/-* cells. Red dots indicate non-targeting guides. All black dots indicate the gene target of gRNAs, which have been grouped. Some have been indicated. The blue dotted line represents x=y where enrichments in DMSO and CPT treated samples are equal. The black dotted line shows enrichments at +/- 1. Plot of screen performed in WRN-/- clone **(A)** E5 and **(B)** G7. (Raw data in Appendix Table 6 & Appendix Table 7)

An advantage of performing the screen in two independent WRN knockout clones was that it allowed JACKS analysis to be performed by combining both biological replicates (Figure 39). gRNAs enriched in the CPT treated versus DMSO treated samples were identified as before. This revealed a selection of target genes which included *TP53*, *CDKN1A*, *MAPK14*, *CHEK2*, *ZDHCC16*, *POLD3*, *SMARCC1*, *PBRM1*, *CHFR*, *EME2* and *SETD2* (Figure 39).

When comparing gRNAs enriched in the CPT treated samples between WT and *WRN-/-* clones, unique genes were identified which were specific to the *WRN-/-* background. These were: *CHFR*, *EME2*, *MAPK14*, *PBRM1*, *SETD2*, *SMARCC1* and *ZDHHC16*.

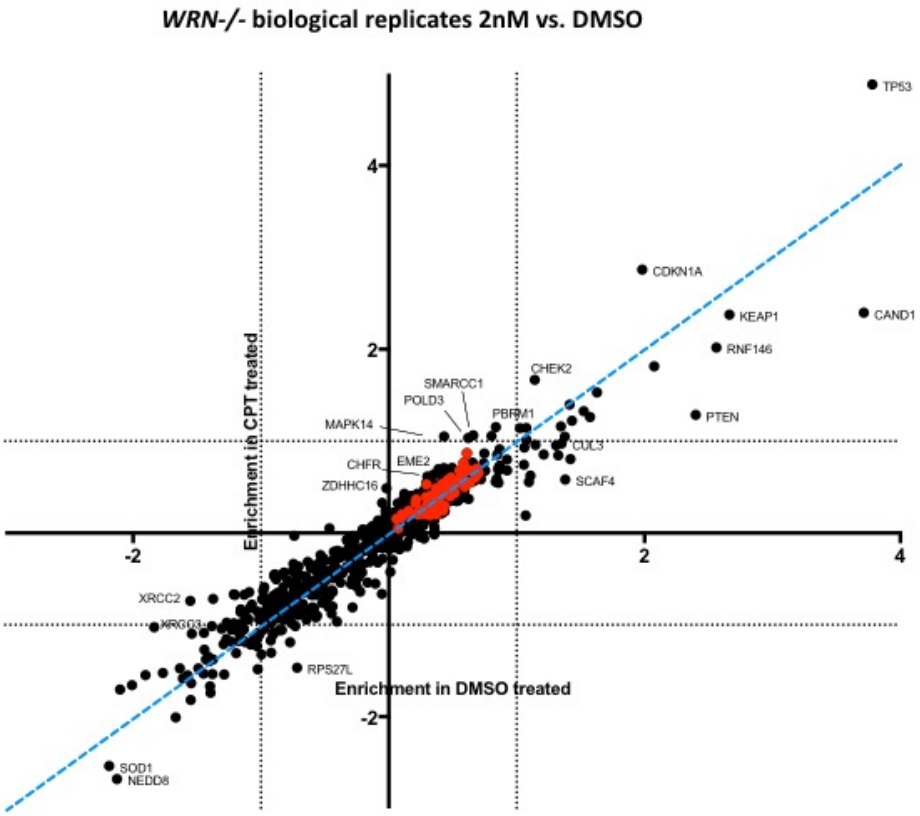

Figure 39 JACKS analysis plots of analysis performed on WRN knockout clones as biological replicates

Plot of JACKS analysis showing fold enrichment of grouped gRNAs in DMSO treated samples versus CPT treated samples compared to the day 14 control in *WRN-/-* clones treated as biological replicates. Red dots indicate non-targeting guides. All black dots indicate the gene target of gRNAs, which have been grouped. Some have been indicated. The blue dotted line represents x=y where enrichments in DMSO and CPT treated samples are equal. The black dotted line shows enrichments at +/- 1. (Raw data in Appendix Table 8)

5.2.5.3. Dropouts in a WRN-/- background

In addition to suppressors, the screen can also identify factors that when lost, increase the sensitivity of cells either to CPT treatment or DMSO treatment alone. These can be seen by points that show a negative value for enrichment. The WT clone did not really show any genes which when lost conferred a greater sensitivity to CPT compared to DMSO. This can be seen by the lack of data points below the X axis and below the blue dotted line. One possible exception is *NBN* (aka *NBS1*) (Figure 37A/B). *NBN* appears as a dropout in the screens

performed at both concentrations of CPT, however it does not have an FDR value of less than 10% in both sets of analysis (Figure 37A/B and Appendix Table 4 & Appendix Table 5). From the plots of the analysis performed on individual WRN knockout clones, there is a noticeably greater number of genes which show a negative fold change compared to the WT clone (Figure 38A/B). WRN knockout clone G7 has more of these compared to the E5 clone (Figure 38A/B). When considering both sets of data as biological replicates, two target genes which show the greatest loss of gRNA representation compared to day 14 are *SOD1* and *NEDD8* (Figure 39). gRNAs against *SOD1* and *NEDD8* also show a slightly greater loss in the CPT treated sample over the DMSO treated sample. These two genes are enriched however in the WT screens as can be seen in the table of data (Appendix Table 4 & Appendix Table 5). gRNAs against *RPS27L* show a greater loss which is specific to CPT induced DNA damage in *WRN-/-* samples (Figure 39). Again, when looking at the table of results, *RPS27L* is enriched in the WT cells in both treatments of CPT and in DMSO treated cells compared to the day 14 control (Appendix Table 4 & Appendix Table 5).

The results also show genes which are lost without the presence of DNA damage in a *WRN-/-* background. These can be seen by the points which drop down into the negative enrichment in DMSO treated but remain above the dotted blue line. The factors which dropout the most in the DMSO treated samples only include *XRCC2* and *XRCC3* (Figure 39).

5.3. WRN Discussion

WRN function has been largely debated and its precise functions and roles within the DDR are still not clearly defined. Until now, most studies have been conducted in either WS patient cells, which may have already undergone significant genetic alteration, or in non-human mammalian knockout cells, which may not properly reflect the function of WRN and the human specific syndrome. Generating an isogenic WRN knockout in RPE-1 cells allowed the study of WRN in a novel way.

WRN knockouts were generated using CRISPR-Cas9 nickase technology to ensure minimal off-target effects of gRNA targeted cutting[330,331]. Western blotting showed that there was complete loss of WRN in the clones selected and that there was no detection of any truncated products (Figure 32C). This meant that WRN was completely absent and therefore there was no possibility of retained function through its exonuclease/helicase domains.

Three of the four knockout clones tested showed an increased sensitivity to CPT when measured by two independent methods (Figure 33A & Figure 34B). Interestingly clone F11 did not show an increased sensitivity to CPT despite showing complete loss of WRN (Figure 33A). The growth rate of this clone does not vary from that of the WT and thus shows that the lack of sensitivity is not as a result of a slower cell cycle turnover (Figure 33A). The lack of sensitivity in this clone could be due to a genetic alteration occurring in the clone which has compensated for the loss of WRN. The sensitivity seen in the other three WRN knockout clones was also seen when depleting WT cells for WRN with siRNA (Figure 33C). Multiple independent groups have also shown that WRN deficient cells show an increase in sensitivity to CPT and thus the bulk of the results shown here corroborate this phenotype[271,305]. It would be interesting to test the sensitivity of WRN knockout clones to other types of DNA damage since the literature on WS cells has some conflicting reports of sensitivity.

5.3.1. p53 and p21 loss give growth advantage

Testing both WT and WRN knockout clones in a CRISPR-Cas9 screen using a DDR focused library allowed me to search for DDR components whose loss might suppress CPT sensitivity in a WT background as well as in a *WRN-/-* specific background. The strongest suppressors of CPT sensitivity in all backgrounds were *TP53* and *CDKN1A* (Figure 37, Figure 38 & Figure 39). Unsurprisingly *TP53*, the gene coding for p53, was the strongest hit, as it is a strong tumour suppressor involved in cell cycle arrest, cell senescence and apoptosis in response to cellular stresses[332]. *TP53* is the most common gene mutated in cancer and loss of p53 function is common in progressive tumours[332]. Loss of *TP53* in the screen therefore presumably offers a growth advantage to cells as it allows cells to survive even after sustaining high levels of DNA damage. This is evident as gRNAs targeting *TP53* were enriched in both DMSO treated and CPT treated samples in both WT and *WRN-/-* backgrounds (Figure 37, Figure 38 & Figure 39). This also shows that p53 loss offers a growth advantage even in a *WRN-/-* background.

CDKN1A is the gene responsible for the p21 protein. p21 is a direct target of p53 and is responsible for the inhibition of CDK1, CDK2 and CDK4/6 [333,334]. p21 acts downstream of p53 as a cell cycle regulator to prevent cell cycle progression after a cell stress response and in particular in response to DNA damage[333,334]. Again, it is therefore not surprising that gRNAs targeting this gene were enriched in all cell backgrounds and conditions tested (Figure 37, Figure 38 & Figure 39).

Interestingly, in all cases, loss of p53 or loss of p21 resulted in a greater level of suppression to CPT compared to DMSO treated cells. This may have been due to a comparatively better growth advantage of these targets over others in CPT treated cells which might have dominated the total cell populations faster.

5.3.2. *CAND1*, *KEAP1*, *RNF146*, *PTEN*, *SCAF4*, *CUL3* loss offers growth advantage

Other strong suppressors that were not specific to the cell background included the genes *CAND1*, *KEAP1*, *RNF146*, *PTEN*, *CUL3* and *SCAF4* (Figure 37, Figure 38 & Figure 39). gRNAs targeting

these genes were enriched in DMSO treated cells as well as CPT treated cells but showed a greater level of suppression in DMSO treated cells. This suggests that loss of these factors offers cells a growth advantage that is not changed by loss of *WRN*.

KEAP1 (Kelch like ECH associated protein 1) is a substrate adaptor of the CUL3 (Cullin3) complex which is responsible for the degradation of nuclear factor erythroid 2-related factor (NRF2), a transcription factor that is responsible for the induction of cytoprotective proteins. NRF2 has been shown to enhance the survival of normal cells but also accumulates in and promotes survival of cancer cells[335]. It is possible that both gRNAs against *CUL3* and *KEAP1* are enriched as a result of their effects on NRF2. CUL3 however, does bind other substrate adaptors and may therefore act through a different mechanism. Interestingly gRNAs targeting *NRF2* (labelled as *NFE2L2*) are lost in all backgrounds and treatments compared to the day 14 controls (Appendix Table 4 & Appendix Table 8). This fits the suggested mechanism by which KEAP1 and CUL3 loss, and subsequent stabilisation of NRF2 confers a growth advantage to cells.

Cullin associated NEDD8 dissociated protein 1 (CAND1) is also linked to the regulation of Cullins, as it binds Cullins in their deneddylated state and promotes the assembly of the full complex which includes the substrate adaptors and receptors[336]. This has mainly been shown to be the case in the assembly of the SKP1-CUL1-FBox complex but CAND1 is thought to also promote the assembly of the other CRL complexes. This could mean that CAND1 loss functions in the same pathway as KEAP1 and CUL3 and results in increased NRF2 thus resulting in increased survival. Alternatively, CAND1 could also be involved through the regulation of a separate CRL complex and interestingly gRNAs targeting *NEDD8* were also enriched in the WT samples. The lack of enrichment in other components of CRL complexes however, makes CUL3 the likely mode of function.

PTEN gRNAs were also enriched in all samples and conditions compared to the day 14 control. *PTEN* is another well-known tumour suppressor gene that is involved in the regulation of a wide number of biological processes. PTEN inhibits AKT serine/threonine kinase 1 (AKT) through its phosphatase activity and thus inhibits the cell proliferative and anti-apoptotic functions of AKT[337]. *PTEN*, like p53, is one of the most frequently mutated or lost genes in

several cancers[332,338]. It is therefore not surprising that cells which lose PTEN are enriched in all endpoint samples compared to the earlier day 14 sample.

RNF146 is a RING finger E3 ubiquitin ligase that can specifically bind PARP1 dependent poly ADP-ribosylated (PARsylated) proteins[339]. RNF146 ubiquitylates several PARsylated proteins involved in the DDR including XRCC1, PARP1, DNA Ligase III and Ku70[339,340]. RNF146 has also been shown to be a positive regulator of the Wnt signalling pathway and therefore may promote apoptosis[341]. Since RNF146 loss provides a growth advantage in both CTP and DMSO treated samples it is likely that the mechanism of resistance is through its effects on apoptosis rather than through regulation of DNA damage proteins.

SCAF4 is an SR-like CTD-associated (splicing factor serine/arginine rich like carboxy terminal domain associated) factor with a largely undefined function, however it is structurally similar to SCAF8, and therefore is predicted to have a similar function[181]. SCAF8 binds to the CTD of the largest subunit of RNA polymerase II (RNA pol II), a region which is thought to act as the main regulatory site of RNA pol II mediated transcription. SCAF8 colocalises with sites of transcription and is predicted to have a role in splicing. The yeast paralog of SCAF4 and SCAF8 is *nrd1* which may be involved in RNA pol II termination and in the regulation of cryptic unstable transcripts (CUTs)[342]. CUTs are thought to play a role in the control of gene expression[343]. Based on the limited understanding of SCAF4's function it is difficult to explain why SCAF4 loss might increase cell survival, but one hypothesis could be that it influences expression of genes involved in cell proliferation and apoptosis.

5.3.3. Hits that suppress CPT sensitivity in a WT background

Suppressors specific to the DNA damage treatment were identified by looking specifically at gRNAs enriched in the CPT treated samples. Interestingly guides against multiple subunits of RNA pol II were more enriched in the CPT treated samples compared to the DMSO treated samples. These included gRNAs targeting *POLR2A, POLR2G, POLR2D and POLR2L*. This suggests that loss of RNA pol II activity increased resistance of WT cells to CPT.

RNA pol II is responsible for the transcription of DNA into mRNA. CPT works by preventing the religation step of topoisomerase I (TOPI) activity, creating a ternary complex with TOP1 and nicked DNA. This primarily causes S-phase specific damage due to collisions of the replication machinery with DNA SSBs and subsequent generation of DSBs. Another cause of CPT toxicity is due to DSBs caused by the transcription machinery colliding with DNA nicks and ternary TOP1-DNA complexes[23]. RNA pol II loss resulted in a resistance to CPT which may most likely be due to a reduction in RNA pol II mediated transcription occurring and thus a reduction in the cytotoxic effects of the TOP1-DNA complexes.

5.3.4. Suppressors of CPT sensitivity in WRN-/- background

Multiple genes were identified as suppressors of CPT sensitivity in a WRN-/- specific background. These include: *CHFR, EME2, MAPK14, PBRM1, SETD2, SMARCC1 and ZDHHC16*. Of these, *MAPK14* showed the greatest difference in enrichment in CPT treated compared to DMSO treated samples. The *MAPK14* gene codes for one of four members of the p38 mitogen-activated protein kinases (MAPKs), specifically p38α. The p38 MAPKs are collectively known as stress activated protein kinases[344]. p38α is involved in a variety of processes which perhaps most significantly include the regulation of apoptosis, cellular senescence and the cell cycle[345,346]. Interestingly, p38α seems to initiate the G2/M checkpoint after UV induced DNA damage as inhibition of p38α resulted in a loss of this checkpoint[347]. This however, does not explain the suppression of sensitivity to CPT, as one would expect that cells progressing into mitosis prematurely after suffering CPT induced DNA damage would die of mitotic catastrophe due to unrepaired DNA. Another role of p38α is in growth inhibition as a result of contact inhibition[345]. Conditions of the screen may have therefore given these cells a growth advantage as flasks may have been densely populated at certain times in the screen. Loss of contact inhibition would allow the cells to continue to grow whereas other cells in the population could not. Although p38α was identified as a suppressor specific to CPT treatment in a *WRN-/-* background, the diverse functions of the protein make it difficult to fully understand potential mechanisms behind it. Clearly, further research needs to be conducted to validate this target and identify its mechanism of suppression.

CHFR (Checkpoint with FHA and RING finger domains) is an E3 ubiquitin ligase whose targets include polo like kinase 1 (PLK1) and Aurora kinase A[181]. CHFR targets PLK1 and Aurora kinase A for degradation and thus prevents cells from entering into mitosis. CHFR therefore functions in the antephase checkpoint and delays entry into mitosis. Loss of CHFR should therefore promote mitotic entry of cells[181,348]. This seems counterintuitive to causing CPT resistance, as one would expect that delaying entry into mitosis and prolonging S and G2 phase, would enable cells more time to repair damaged DNA. One possible explanation is that these cells would initially divide faster and, if the level of DNA damage sustained is not significant enough to kill the cell, they would continue to grow at an accelerated rate. Another of CHFR's targets is histone deacetylase 1 (HDAC1) which downregulates transcription[349]. CHFR ubiquitylates and downregulates HDAC1, and thus loss of CHFR would result in an increase in HDAC1 levels and subsequently a reduction in transcription. A reduction in transcription would increase resistance to CPT due to a reduction in DSBs caused by progression of the transcription machinery, as described earlier.

SMARCC1 and *PBRM1* both code for proteins which make up the SWI/SNF complex[350]. This complex is an ATP dependent chromatin remodelling complex[351,352]. Loss of ATP-dependent chromain remodeller SMARCA4 (BRG1), the main component of the SWI/SNF complex, has been linked to increased sensitivity to DSBs associated with replication fork collapse. The opposite effect was seen in a *WRN-/-* background which could suggest interplay between WRN and the SWI/SNF complex. WRN has been linked to heterochromatin organisation through its interaction with other heterochromatin proteins and the irregular nuclei often seen in WRN deficient cells. It is possible that WRN and the SWI/SNF complex together regulate chromatin remodelling in response to DNA damage and that loss of WRN destabilises this regulation. Loss of the SWI/SNF complex may therefore counterbalance the loss of WRN.

Interestingly, the SWI-SNF complex has also been shown to be required for the recruitment of TOP1 to chromatin[351,352]. This could explain why loss of the complex increases resistance to CPT, as potentially less TOP1 becomes inhibited and bound to chromatin. This would ease the toxicity of CPT induced DNA damage from replication fork and transcription machinery collisions. This mechanism however should also apply to CPT sensitivity in a WT background;

whilst SMARCC1 and PBRM1 gRNAs are enriched in CPT treated samples, they are also enriched in DMSO treated samples to a similar extent (Appendix Table 4 & Appendix Table 5).

EME2 (essential meiotic structure specific endonuclease subunit 2) forms a heterodimer with MUS81, a structure specific endonuclease that plays a role in DNA secondary structure resolution[181]. The MUS81-EME2 heterodimer seems to be important for replication fork restart and unlike the MUS81-EME1 heterodimer is not required for Holliday junction. MUS81 depletion causes a decrease in the number of DSBs created after HU as does depletion of EME2. This is not the case for EME1 depletion [353]. Potentially in a *WRN-/-* background, activity of MUS81-EME2 specifically, causes the generation of double strand breaks at sites of CPT induced replication stress and thus leads to cytotoxicity. This might suggest that WRN also acts to compete with and suppress inappropriate repair of collapsed replication forks by MUS81-EME2[354]. It would be interesting to investigate the potential interplay between MUS81 and WRN further and in particular tease out the differences in their roles in response to HU versus CPT.

ZDHHC16 (zinc finger DHHC-type containing 16) is a palmitoyl acyltransferase that is involved in heart development and cardiac function as well as being linked to eye development[181]. Recently ZDHHC16 has been linked to the DDR as inhibition of palmitoylation, and specifically depletion of ZDHHC16, resulted in impaired activation of ATM[355]. The exact function and mechanisms of ZDHHC16 in the DDR are still unknown, but ZDHHC16 could potentially affect proteins that stimulate ATM activation or be involved in remodelling of chromatin. The interplay between ATM and ATR at sites of replication stress is an extremely important and tightly regulated process, timely ATM inactivation could potentially promote HR repair and an ATR dominant replication fork restart process[29,40]. Interestingly WS is associated with increased heart defects as well as premature cataracts; whether there is link between these phenotypes and the processes ZDHHC16 is involved in is unknown but could be an interesting area of research.

SETD2 (SET domain containing 2) is a histone methyltransferase that is responsible for the trimethylation of Histone3 at K36 (H3K36me3)[356]. H3K36me3 is a marker of transcriptional activation but has also been linked to the promotion of HR via CtIP, RPA and RAD51

recruitment[356]. As discussed previously, inhibiting transcription reduces the effects of CPT due to a reduction in DSBs generated by collision with active transcription complexes and thus may explain the effect of SETD2 loss on CPT resistance. The link H3K36me3 has to HR however makes it is more complicated to explain a functional mechanism. One explanation could be that since loss of WRN results in the inability to restart collapsed replication forks efficiently or results in improper resolution of Holliday junctions; inhibiting HR and extensive resection therefore may allow cells to repair the damage by alternative methods such as microhomology-mediated end-joining (MMEJ).

The next steps would be to validate these targets to see if they are indeed suppressors of CPT sensitivity and if they are indeed specific to a *WRN-/-* background. The best way to do this would be to perform survival assays in WT and *WRN-/-* cells with siRNA depletion of the potential suppressors. Once confirmed, experiments to investigate mechanisms can be pursued. This could be in the form of looking at kinetics at the replication fork by DNA fibre techniques or investigating recruitment of factors involved in HR such as RPA or RAD51.

5.3.5. NBN1 as a dropout in WT cells

The screen in WT cells did not reveal strong factors which dropout specifically in the CPT treated samples versus the DMSO treated. This may be due to the essentiality of genes involved in promoting HR[357]. gRNA read counts for these genes may therefore have already been low at the day 14 sample making identifying dropouts difficult. One potential dropout identified however, was *NBN*. *NBN* is the gene responsible for NBS1, a component of the MRN complex. Since the MRN complex is critical to the repair of DSBs by HR it is logical that loss of NBS1 and subsequently loss of the MRN complex causes increased sensitivity to a DNA damaging drug that induces S-phase specific damage which has to be repaired by HR. Interestingly NBN appears to be an essential gene and this might suggest that it somehow did not get eliminated after 14 days or could mean that the gRNAs targeting this gene did not efficiently eliminate the protein and led to a truncated protein or a protein with an in-frame indel with some retained functions.

5.3.6. Dropouts specific to WRN-/- background

Screen results in *WRN-/-* cells showed a greater number of genes which were lost from the day 14 control in both CPT and DMSO treated samples. This might suggest WRN is synthetic lethal/sick with a number of genes or could suggest that the factors that gave *WRN-/-* cells a growth advantage took over sample populations and thus skewed results. The fact that a large number of factors were depleted from day 14 controls made it difficult to identify dropouts. Two genes which showed the greatest loss were *NEDD8* and *SOD1*. Interestingly these genes were enriched in the WT cells and this therefore suggests that the loss of either of the two genes is particularly cytotoxic in a WRN knockout background. NEDD8 as previously discussed (3.1.2), is the protein which binds to and thus activates all Cullins. Due to the diversity of functions of Cullins it is difficult to speculate by which mechanism this synthetic lethality/sickness occurs. Out of the Cullins in the DDR library, only CUL1 and CUL9 showed a mild decrease from the day 14 control.

SOD1 encodes for superoxide dismutase 1 (SOD1) whose main function is to convert superoxide radicals into less harmful substances. Most studies investigating SOD1 are based on its mutations which link it to amyotrophic lateral sclerosis, however there is some evidence that suggests it is linked to the DNA damage response and inhibition of apoptosis through p53[358]. Loss of SOD1 might therefore be as a result of induced apoptosis in response to a greater accumulation of DNA damage in *WRN-/-* cells compared to WT cells.

gRNAs targeting the *RAD51* paralogs *XRCC2* and *XRCC3*, dropout in *WRN-/-* cells in both DMSO treated and CPT treated cells, although there seems to be a greater decrease in the DMSO treated samples. This suggest that there might be synthetic lethality/sickness between WRN and the RAD51 paralogs that occurs overtime in these cells. gRNAs against *XRCC2* and *XRCC3* did not dropout to the same extent in WT cells, suggesting a specific lethality in WRN knockout cells only. Both these RAD51 paralogs form a complex with RAD51C, which is also a dropout in *WRN-/-* cells, but to a less significant extent. The RAD51 paralogs do not currently have robustly defined functions but are involved in the HR pathway and have been linked to the strand invasion process of RAD51 coated single stranded DNA into the sister chromatid[52].

They have also been linked to DNA repair and maintenance of telomeres[359]. XRCC2 and XRCC3 in particular have also been shown to prevent long tract gene conversions and *WRN-/- XRCC3-/-* DT40 cells display an increased sensitivity to MMS compared to *WRN-/-* or *XRCC3-/-* DT40 cells alone[360,361]. Since WRN has been shown to be involved in the resolution of D-loops one might hypothesise that the increased sensitivity in the double knockout is as a result of a greater length of D-loop at Holliday junction formed by HR. This enhanced length coupled with the inability to resolve the D loop may lead to cytotoxicity. Potentially BLM may help resolve these types of extended Holliday junctions in the absence of WRN as triple knockout (*WRN-/-*, *XRCC3-/-*, *BLM-/-*) DT40 cells show an even greater sensitivity to MMS[361].

This points to a function for WRN in the later stages of HR after resection in a manner dependent on RAD51 and RAD51 paralogs. Interestingly sensitivity of WRN cells to DNA damage has been shown to be suppressed by expression of a dominant negative form of RAD51[362], which also implies a role for WRN in the later stages of HR. Again, further investigation of these genetic interactions will need to be carried out in order to validate the results of the screen.

RPS27L was identified as a dropout in *WRN-/-* cells and showed a greater loss in CPT treated samples compared to DMSO treated samples. In addition, RPS27L did not show a loss in a WT background in either treatments. This suggests that the loss of *RPS27L* results in cell toxicity in *WRN-/-* cells which is enhanced by DNA damage with CPT. *RPS27L* encodes for a ribosomal protein with similarity to the ribosomal protein S27 (RPS27), hence the name ribosomal protein S27-like protein (RPS27L)[181]. RPS27L has been shown to be involved in the DDR through direct interaction with p53[363,364]. The exact function or RPS27L with respect to DNA damage is unclear, however one report suggests that RPS27L disruption leads to p53 activation[365]. Loss of RPS27L may therefore result in cell death following DNA damage as a result of increased p53 activity. Having said this, loss of RPS27L did not seem to have the same effect in WT cells and therefore could suggest functional overlap/interactions with WRN. Interestingly, an interaction between WRN and p53 has also been shown to exist[281,366,367]. This could suggest that RPS27L and WRN both have functions that maintain genome stability by coordinating the DDR through interactions with p53. Loss of RPS27L in addition to loss of WRN may result in genome instability that may result in apoptosis or senescence of cells. The

interplay between senescence and apoptosis by p53 could be governed by RPS27L and WRN. It would be interesting to explore these potential functional interactions further in both p53 proficient and p53 null backgrounds.

5.3.7. Limitations in the screening process

One of the main advantages of performing the CRISPR screen with a DDR focused library was that the number of cells required were much more manageable than if the screen had been performed with the same level of representation using a whole genome library. This did however create some complications when analysing the data as it is difficult to define cut-offs of significance. Since all the guides apart from the non-targeting guides in the library targeted DDR genes, it makes it difficult to identify real hits from false positive hits as they can perhaps all be justified in some way or another as to why they might increase or decrease sensitivity. The DDR library could therefore be improved by incorporating some control gRNAs that still target genes, but simply genes which are not linked to the DDR and therefore are unlikely to influence cell survival after DNA damage. This would make it easier to set cut-offs and focus on the true hits. A new human DDR library incorporating these features has since recently been generated by the Steve Jackson Lab.

The strongest hit in all screens was *TP53*. Although this is explainable and is evidence of the screen working properly, it does potentially mask the enrichment of other genes due to these cells dominating the total cell population. Performing the screen in a p53 null background therefore would enhance the detection of other factors that suppress CPT sensitivity.

5.3.8. Concluding remarks

Generating a WRN knockout in human primary cells has allowed me to research into WRN function in a novel way. Utilising the cell lines, sensitivity to the DNA damaging drug CPT was established and a screen set-up in the search for suppressors of sensitivity. This has identified potential suppressors of CPT sensitivity in *WRN-/-* cells and also suppressors of *WRN-/-* cell toxicity in undamaged cells. Continued investigation can be pursued by interrogating the data

further as well as validating potential targets by methods discussed earlier. This would allow insights into the specific function of WRN in response to DNA damage.

Research can be continued by defining other sensitivities in the WRN knockout cells generated and performing further screens with different DNA damaging agents or even with drugs which stabilise DNA secondary structures that might be potential substrates of WRN.

Serially passaging WRN knockout cells and looking for accumulation of mutational signatures over time may allow me to gain insights into why WS patients might show premature ageing phenotypes and why they have a higher predisposition to cancers. Again, interrogating this data by cross-referencing it with other data such as with replication origins, highly transcribed regions or regions of high DNA secondary structure might establish a greater understanding of WRN function.

Altogether I believe that the work shown here offers a good foundation for further investigation into the precise function of WRN in the DDR.

Chapter 6: Final Discussion

6. Final Discussion

The main aim of the work described in this thesis was to investigate the regulation of NHEJ through Ku interacting factors. This has been performed by looking at three factors which have been shown here or elsewhere to be interactors of Ku.

The first part of this thesis investigated the protein WDR76. WDR76 was shown to be a Ku interacting factor and whilst its precise function was not identified, it clearly plays a part in the DDR. This was strongly evidenced by the increased sensitivity of WDR76 knockout cells to IR. Depletion of WDR76 resulted in an increased persistence of Ku on chromatin, suggesting a role of WDR76 in the removal of Ku following DNA damage. Whether this is due to WDR76 mediated ubiquitylation of Ku itself or other proteins remains to be determined.

Ubiquitylation of Ku has been implicated in its removal from DNA in a number of publications[138–140,169,368]. Most recently, the E3 ligase RNF126 was shown to be involved in the ubiquitylation of Ku80, and depletion of RNF126 resulted in persistence of Ku on chromatin[368]. In addition, RNF8 has also been shown to promote Ku80 ubiquitylation and removal with RNF8 depletion also resulting in a persistence of Ku at damage sites [139]. Interestingly, Ismail et al.[140] confirmed the ability of RNF8 to ubiquitylate Ku80, however they showed that this ability is restricted to G1. Ismail et al. also describe a mechanism whereby RNF138 ubiquitylates Ku80 to facilitate its removal prior to NHEJ initiation to promote HR[140]. This work demonstrates that ubiquitylation of Ku is a complex process that can affect the regulation of NHEJ in many scenarios, likely depending on the location, timing, and type of ubiquitylation on Ku. WDR76 can therefore be another factor that regulates NHEJ through Ku. WDR76 may also be involved in the ubiquitylation of Ku70 specifically, as opposed to the majority of publications describing Ku80 ubiquitylation[138–140,368].

My continued research into WDR76 highlighted other potential roles of WDR76 in the DDR. Further investigation to identify the specific substrate(s) of WDR76 and the residues it ubiquitylates will help define its precise role in the DDR.

The second part of my work described in this thesis showed that PAXX is phosphorylated on S148 in human cell lines. Whilst S148 was initially identified as a potential CDK phosphorylation site through sequence analysis, my data raises the possibility of other kinases mediating this phosphorylation. The proximity of this phosphorylation site to the Ku binding domain of PAXX raises the possibility of this site being involved in the regulation of NHEJ by modulating the PAXX-Ku interaction. Interestingly, the lysine residue at position 151 (K151) is also conserved, encouraging the potential for an additional level of regulation at this site, perhaps by ubiquitylation. The functional relevance of S148 phosphorylation however remains to be defined, and further work is needed to explore the significance of this modification.

In the last part of my research, WRN knockouts were generated by CRISPR-Cas9 in RPE-1 cells to use as tools for investigating WRN function. The sensitivity of the knockout to CPT was determined and the data I generated were consistent with previous reports of CPT sensitivity seen in WS cells. Despite the knowledge of CPT sensitivity, the mechanism by which WRN loss creates sensitivity is still unclear. A CRISPR-Cas9 based genetic screen was performed to look for suppressors and dropouts in order to gain insights into the function of WRN.

WRN-/- hypersensitivity to CPT has been shown to be suppressed by loss of Ku70 in chicken DT40 cells[369], which raised the possibility of gRNAs targeting factors promoting NHEJ being enriched in my screen. Ku is essential in humans cells in culture, so unsurprisingly it did not come out as a suppressor of *WRN-/-* CPT sensitivity in my screen; nevertheless, neither did any other factors that positively regulate NHEJ, despite them not being essential for cell viability in WT cells. This might suggest that WRN does not have a role in downregulating NHEJ during S-phase or is redundant with other mechanisms that downregulate NHEJ; perhaps its roles in NHEJ are not significant with respect to CPT induced damage.

The increased CPT sensitivity of *WRN-/-* cells compared to WT cells reinforces the conclusion that WRN has a role(s) in HR. Many of the suppressors identified were targets that promote transcription, and therefore may be a reflection of the CPT induced DNA damage treatment rather than the genetic background. Despite this, the dropouts specific to a *WRN-/-* background, XRCC2 and XRCC3, may imply a role of WRN in the later processes of HR,

downstream of DNA resection and at the level of RAD51 loading/recombination. Suppressors and dropouts identified in the screen will need to be validated and further experiments pursued (as described in section 5.3) in order to help understand the exact mechanisms by which WRN promotes DNA repair. Once generated, sequence analysis data from the mutational signatures aspect of my research may also yield novel insights into the functions of WRN in the maintenance of genome stability.

In summary this thesis has identified some potential regulatory mechanisms of NHEJ, and has offered insights into the functions and regulation of the Ku interactors: WDR76, PAXX and WRN that will hopefully be explored further by ensuing studies.

7. References

1. Jackson, S. P. & Bartek, J. The DNA-damage response in human biology and disease. *Nature* **461,** 1071–1078 (2009).
2. Wogan, G. N., Hecht, S. S., Felton, J. S., Conney, A. H. & Loeb, L. A. Environmental and chemical carcinogenesis. *Semin. Cancer Biol.* **14,** 473–486 (2004).
3. Cadet, J. & Wagner, J. R. DNA Base Damage by Reactive Oxygen Species,Oxidizing Agents, and UV Radiation. *Cold Spring Harb. Perspect. Biol.* **5,** 1–16 (2013).
4. Valko, M., Rhodes, C. J., Moncol, J., Izakovic, M. & Mazur, M. Free radicals, metals and antioxidants in oxidative stress-induced cancer. *Chem. Biol. Interact.* **160,** 1–40 (2006).
5. Ciccia, A. & Elledge, S. J. The DNA damage response: making it safe to play with knives. *Mol. Cell* **40,** 179–204 (2010).
6. Hoeijmakers, J. H. J. Genome maintenance mechanisms for preventing cancer. *Nature* **411,** 366–374 (2001).
7. Bradley, M. O. & Kohn, K. W. X-ray induced DNA double strand break production and repair in mammalian cells as measured by neutral filter elution. *Nucleic Acids Res.* **7,** 793–804 (1979).
8. Caldecott, K. W. Single-strand break repair and genetic disease. *Nat. Rev. Genet.* **9,** 619–631 (2008).
9. Hegde, M. L., Hazra, T. K. & Mitra, S. Early steps in the DNA base excision/single-strand interruption repair pathway in mammalian cells. *Cell Res.* **18,** 27–47 (2008).
10. Boiteux, S. & Radicella, J. P. Base excision repair of 8-hydroxyguanine protects DNA from endogenous oxidative stress. *Biochimie* **81,** 59–67 (1999).
11. Krokan, H. E. & Bjoras, M. Base Excision Repair. *Cold Spring Harb. Perspect. Biol.* **5,** a012583–a012583 (2013).
12. D'Amours, D., Desnoyers, S., D'Silva, I. & Poirier, G. G. Poly(ADP-ribosyl)ation reactions in the regulation of nuclear functions. *Biochem. J.* **342 (Pt 2,** 249–68 (1999).
13. Amé, J. C., Spenlehauer, C. & De Murcia, G. The PARP superfamily. *BioEssays* **26,** 882–893 (2004).
14. Jiricny, J. The multifaceted mismatch-repair system. *Nat. Rev. Mol. Cell Biol.* **7,** 335–346 (2006).

15. Jun, S. H., Kim, T. G. & Ban, C. DNA mismatch repair system: Classical and fresh roles. *FEBS J.* **273,** 1609–1619 (2006).
16. Hsieh, P. & Yamane, K. DNA mismatch repair: Molecular mechanism, cancer, and ageing. *Mech. Ageing Dev.* **129,** 391–407 (2008).
17. Scharer, O. D. Nucleotide Excision Repair in Eukaryotes. *Cold Spring Harb. Perspect. Biol.* **5,** a012609–a012609 (2013).
18. Deans, A. J. & West, S. C. DNA interstrand crosslink repair and cancer. *Nat. Rev. Cancer* **11,** 467–480 (2011).
19. Giglia-Mari, G., Zotter, A. & Vermeulen, W. DNA damage response. *Cold Spring Harb. Perspect. Biol.* **3,** 1–19 (2011).
20. Jackson, S. P. Sensing and repairing DNA double-strand breaks. *Carcinogenesis* **23,** 687–96 (2002).
21. O'Driscoll, M. & Jeggo, P. A. The role of double-strand break repair - Insights from human genetics. *Nat. Rev. Genet.* **7,** 45–54 (2006).
22. Kuzminov, A. Single-strand interruptions in replicating chromosomes cause double-strand breaks. *Proc. Natl. Acad. Sci.* **98,** 8241–8246 (2001).
23. LIU, L. F. *et al.* Mechanism of Action of Camptothecin. *Ann. N. Y. Acad. Sci.* **922,** 1–10 (2006).
24. Falck, J., Coates, J. & Jackson, S. P. Conserved modes of recruitment of ATM, ATR and DNA-PKcs to sites of DNA damage. *Nature* **434,** 605–611 (2005).
25. Lukas, J., Lukas, C. & Bartek, J. More than just a focus: The chromatin response to DNA damage and its role in genome integrity maintenance. *Nat. Cell Biol.* **13,** 1161–1169 (2011).
26. Panier, S. & Boulton, S. J. Double-strand break repair: 53BP1 comes into focus. *Nat. Rev. Mol. Cell Biol.* **15,** 7–18 (2014).
27. Kolas, N. K. *et al.* Orchestration of the DNA-damage response by the RNF8 ubiquitin ligase. *Science (80-.).* **318,** 1637–1640 (2007).
28. Doil, C. *et al.* RNF168 Binds and Amplifies Ubiquitin Conjugates on Damaged Chromosomes to Allow Accumulation of Repair Proteins. *Cell* **136,** 435–446 (2009).
29. Blackford, A. N. & Jackson, S. P. ATM, ATR, and DNA-PK: The Trinity at the Heart of the DNA Damage Response. *Mol. Cell* **66,** 801–817 (2017).
30. Bartek, J. & Lukas, J. Chk1 and Chk2 kinases in checkpoint control and cancer. *Cancer*

Cell **3,** 421–429 (2003).

31. Ahn, J. Y., Schwarz, J. K., Piwnica-Worms, H. & Canman, C. E. Threonine 68 phosphorylation by ataxia telangiectasia mutated is required for efficient activation of Chk2 in response to ionizing radiation. *Cancer Res.* **60,** 5934–6 (2000).
32. Matsuoka, S. *et al.* Ataxia telangiectasia-mutated phosphorylates Chk2 in vivo and in vitro. *Proc. Natl. Acad. Sci. U. S. A.* **97,** 10389–94 (2000).
33. Zannini, L., Delia, D. & Buscemi, G. CHK2 kinase in the DNA damage response and beyond. *J. Mol. Cell Biol.* **6,** 442–457 (2014).
34. Matsuoka, S., Huang, M. & Elledge, S. J. Linkage of ATM to cell cycle regulation by the Chk2 protein kinase. *Science (80-.).* **282,** 1893–1897 (1998).
35. Falck, J., Mailand, N., Syljuåsen, R. G., Bartek, J. & Lukas, J. The ATM-Chk2-Cdc25A checkpoint pathway guards against radioresistant DNA synthesis. *Nature* **410,** 842–847 (2001).
36. Dalal, S. N., Schweitzer, C. M., Gan, J. & DeCaprio, J. A. Cytoplasmic localization of human cdc25C during interphase requires an intact 14-3-3 binding site. *Mol. Cell. Biol.* **19,** 4465–79 (1999).
37. Takizawa, C. G. & Morgan, D. O. Control of mitosis by changes in the subcellular location of cyclin-B1-Cdk1 and Cdc25C. *Curr. Opin. Cell Biol.* **12,** 658–665 (2000).
38. Takai, H. *et al.* Chk2-deficient mice exhibit radioresistance and defective p53-mediated transcription. *EMBO J.* **21,** 5195–5205 (2002).
39. Hirao, A. *et al.* Chk2 Is a Tumor Suppressor That Regulates Apoptosis in both an Ataxia Telangiectasia Mutated (ATM)-Dependent and an ATM-Independent Manner. *Mol. Cell. Biol.* **22,** 6521–6532 (2002).
40. Yan, S., Sorrell, M. & Berman, Z. Functional interplay between ATM/ATR-mediated DNA damage response and DNA repair pathways in oxidative stress. *Cell. Mol. Life Sci.* 3951–3967 (2014). doi:10.1007/s00018-014-1666-4
41. Harper, J. W. & Elledge, S. J. The DNA Damage Response: Ten Years After. *Mol. Cell* **28,** 739–745 (2007).
42. Guo, Z. Requirement for Atr in phosphorylation of Chk1 and cell cycle regulation in response to DNA replication blocks and UV-damaged DNA in Xenopus egg extracts. *Genes Dev.* **14,** 2745–2756 (2000).
43. Zhao, H. & Piwnica-Worms, H. ATR-Mediated Checkpoint Pathways Regulate

Phosphorylation and Activation of ATR-Mediated Checkpoint Pathways Regulate Phosphorylation and Activation of Human Chk1. *Mol. Cell. Biol.* **21,** 4129–4139 (2001).

44. Zhang, Y. & Hunter, T. Roles of Chk1 in cell biology and cancer therapy. *Int. J. Cancer* **134,** 1013–1023 (2014).
45. Rhind, N., Furnari, B. & Russell, P. Cdc2 tyrosine phosphorylation is required for the DNA damage checkpoint in fission yeast. *Genes Dev.* **11,** 504–511 (1997).
46. O'Connell, M. J., Raleigh, J. M., Verkade, H. M. & Nurse, P. Chk1 is a wee1 kinase in the G2 DNA damage checkpoint inhibiting cdc2 by Y15 phosphorylation. *EMBO J.* **16,** 545–54 (1997).
47. Williams, R. S., Williams, J. S. & Tainer, J. A. Mre11–Rad50–Nbs1 is a keystone complex connecting DNA repair machinery, double-strand break signaling, and the chromatin templateThis paper is one of a selection of papers published in this Special Issue, entitled 28th International West Coast Chromatin a. *Biochem. Cell Biol.* **85,** 509–520 (2007).
48. Liu, S. *et al.* Distinct roles for DNA-PK, ATM and ATR in RPA phosphorylation and checkpoint activation in response to replication stress. *Nucleic Acids Res.* **40,** 10780–94 (2012).
49. Zou, L. & Stephen J, E. ATRIP Recognition of RPA-ssDNA. *Science (80-.).* **300,** 1542–1548 (2003).
50. Prakash, R., Zhang, Y., Feng, W. & Jasin, M. Homologous recombination and human health: the roles of BRCA1, BRCA2, and associated proteins. *Cold Spring Harb. Perspect. Biol.* **7,** a016600 (2015).
51. Jensen, R. B., Carreira, A. & Kowalczykowski, S. C. Purified human BRCA2 stimulates RAD51-mediated recombination. *Nature* **467,** 678–683 (2010).
52. Jasin, M. & Rothstein, R. Repair of strand breaks by homologous recombination. *Cold Spring Harb. Perspect. Biol.* **5,** 1–18 (2013).
53. Mao, Z., Bozzella, M., Seluanov, A. & Gorbunova, V. DNA repair by nonhomologous end joining and homologous recombination during cell cycle in human cells. *Cell Cycle* **7,** 2902–6 (2008).
54. Roth, D. B. V(D)J Recombination: Mechanism, Errors, and Fidelity. *Microbiol. Spectr.* **2,** 313–324 (2014).
55. Stavnezer, J., Guikema, J. E. J. & Schrader, C. E. Mechanism and regulation of class

switch recombination. *Annu. Rev. Immunol.* **26,** 261–92 (2008).

56. Downs, J. a & Jackson, S. P. A means to a DNA end: the many roles of Ku. *Nat. Rev. Mol. Cell Biol.* **5,** 367–378 (2004).
57. Radhakrishnan, S. K., Jette, N. & Lees-Miller, S. P. Non-homologous end joining: Emerging themes and unanswered questions. *DNA Repair (Amst).* 1–7 (2014). doi:10.1016/j.dnarep.2014.01.009
58. Yin, X., Liu, M., Tian, Y., Wang, J. & Xu, Y. Cryo-EM structure of human DNA-PK holoenzyme. *Cell Res.* **27,** 1341–1350 (2017).
59. Weinfeld, M., Mani, R. S., Abdou, I., Aceytuno, R. D. & Glover, J. N. M. Tidying up loose ends: The role of polynucleotide kinase/phosphatase in DNA strand break repair. *Trends Biochem. Sci.* **36,** 262–271 (2011).
60. Shirodkar, P., Fenton, A. L., Meng, L. & Koch, C. A. Identification and functional characterization of a ku-binding motif in aprataxin polynucleotide kinase/phosphatase-like factor (APLF). *J. Biol. Chem.* **288,** 19604–19613 (2013).
61. Grundy, G. J. *et al.* APLF promotes the assembly and activity of non-homologous end joining protein complexes. *EMBO J.* **32,** 112–125 (2013).
62. Li, S. *et al.* Polynucleotide kinase and aprataxin-like forkhead-associated protein (PALF) acts as both a single-stranded DNA endonuclease and a single-stranded DNA 3' exonuclease and can participate in DNA end joining in a biochemical system. *J. Biol. Chem.* **286,** 36368–77 (2011).
63. Lieber, M. R., Ma, Y., Pannicke, U. & Schwarz, K. Mechanism and regulation of human non-homologous DNA end-joining. *Nat. Rev. Mol. Cell Biol.* **4,** 712–20 (2003).
64. Ma, Y., Pannicke, U., Schwarz, K. & Lieber, M. R. Hairpin opening and overhang processing by an Artemis/DNA-dependent protein kinase complex in nonhomologous end joining and V(D)J recombination. *Cell* **108,** 781–794 (2002).
65. Andrews, B. J., Lehman, J. A. & Turchi, J. J. Kinetic analysis of the Ku-DNA binding activity reveals a redox-dependent alteration in protein structure that stimulates dissociation of the Ku-DNA complex. *J. Biol. Chem.* **281,** 13596–13603 (2006).
66. Walker, J. R., Corpina, R. A. & Goldberg, J. Structure of the Ku heterodimer bound to dna and its implications for double-strand break repair. *Nature* **412,** 607–614 (2001).
67. Rodgers, K. & McVey, M. Error-Prone Repair of DNA Double-Strand Breaks. *J. Cell. Physiol.* **231,** 15–24 (2016).

68. Ramadan, K., Shevelev, I. V., Maga, G. & Hübscher, U. De Novo DNA synthesis by human DNA polymerase λ, DNA polymerase μ and terminal deoxyribonucleotidyl transferase. *J. Mol. Biol.* **339,** 395–404 (2004).
69. Ramadan, K. *et al.* Human DNA polymerase λ possesses terminal deoxyribonucleotidyl transferase activity and can elongate RNA primers: Implications for novel functions. *J. Mol. Biol.* **328,** 63–72 (2003).
70. Lieber, M. R. The Mechanism of Double-Strand DNA Break Repair by the Nonhomologous DNA End-Joining Pathway. *Annu. Rev. Biochem.* **79,** 181–211 (2010).
71. Roth, D. B. & Wilson, J. H. Nonhomologous recombination in mammalian cells: role for short sequence homologies in the joining reaction. *Mol. Cell. Biol.* **6,** 4295–304 (1986).
72. Roth, D. B., Chang, X. B. & Wilson, J. H. Comparison of filler DNA at immune, nonimmune, and oncogenic rearrangements suggests multiple mechanisms of formation. *Mol. Cell. Biol.* **9,** 3049–57 (1989).
73. Gilad, S. *et al.* Genotype-Phenotype Relationships in Ataxia-Telangiectasia and Variants. *Am. J. Hum. Genet.* **62,** 551–561 (1998).
74. McConville, C. M. *et al.* Mutations associated with variant phenotypes in ataxia-telangiectasia. *Am. J. Hum. Genet.* **59,** 320–30 (1996).
75. Savitsky, K. *et al.* A single ataxia telangiectasia gene with a product similar to PI- 3 kinase. *Science (80-.).* **268,** 1749–1753 (1995).
76. Nowak-Wegrzyn, A., Crawford, T. O., Winkelstein, J. A., Carson, K. A. & Lederman, H. M. Immunodeficiency and infections in ataxia-telangiectasia. *J. Pediatr.* **144,** 505–511 (2004).
77. Rothblum-Oviatt, C. *et al.* Ataxia telangiectasia: A review. *Orphanet J. Rare Dis.* **11,** 1–21 (2016).
78. Bredemeyer, A. L. *et al.* ATM stabilizes DNA double-strand-break complexes during V(D)J recombination. *Nature* **442,** 466–470 (2006).
79. Gennery, A. R., Cant, A. J. & Jeggo, P. A. Immunodeficiency associated with DNA repair defects. *Clin. Exp. Immunol.* **121,** 1–7 (2000).
80. Hakem, R. DNA-damage repair; the good, the bad, and the ugly. *EMBO J.* **27,** 589–605 (2008).
81. Blunt, T. *et al.* Defective DNA-dependent protein kinase activity is linked to V(D)J

recombination and DNA repair defects associated with the murine scid mutation. *Cell* **80,** 813–823 (1995).

82. Bosma, G. C., Custer, R. P. & Bosma, M. J. A severe combined immunodeficiency mutation in the mouse. *Nature* **301,** 527–530 (1983).
83. Kirchgessner, C. U. *et al.* DNA-dependent kinase (p350) as a candidate gene for the murine SCID defect. *Science (80-.).* **267,** 1178–1183 (1995).
84. Taccioli, G. E. *et al.* Impairment of V (D) J Recombination in Double-Strand Break Repair Mutants. *Science (80-.).* **260,** 207–210 (1993).
85. Mukherjee, S., Ridgeway, A. D. & Lamb, D. J. DNA mismatch repair and infertility. *Curr. Opin. Urol.* **20,** 525–532 (2010).
86. Madabhushi, R., Pan, L. & Tsai, L. H. DNA damage and its links to neurodegeneration. *Neuron* **83,** 266–282 (2014).
87. Shackelford, D. A. DNA end joining activity is reduced in Alzheimer's disease. *Neurobiol. Aging* **27,** 596–605 (2006).
88. Adamec, E., Vonsattel, J. P. & Nixon, R. A. DNA strand breaks in Alzheimer's disease. *Brain Res.* **849,** 67–77 (1999).
89. Jacobsen, E., Beach, T., Shen, Y., Li, R. & Chang, Y. Deficiency of the Mre11 DNA repair complex in Alzheimer's disease brains. *Mol. Brain Res.* **128,** 1–7 (2004).
90. Ogino, M. *et al.* Roles of PTEN with DNA repair in Parkinson's disease. *Int. J. Mol. Sci.* **17,** (2016).
91. Li, D.-W., Li, G.-R., Zhang, B.-L., Feng, J.-J. & Zhao, H. Damage to dopaminergic neurons is mediated by proliferating cell nuclear antigen through the p53 pathway under conditions of oxidative stress in a cell model of Parkinson's disease. *Int. J. Mol. Med.* **37,** 429–35 (2016).
92. Winklhofer, K. F. & Haass, C. Mitochondrial dysfunction in Parkinson's disease. *Biochim. Biophys. Acta - Mol. Basis Dis.* **1802,** 29–44 (2010).
93. Wisnovsky, S., Jean, S. R. & Kelley, S. O. Mitochondrial DNA repair and replication proteins revealed by targeted chemical probes. *Nat. Chem. Biol.* **12,** 567–573 (2016).
94. Kujoth, G. C. Mitochondrial DNA Mutations , Oxidative Stress , and Apoptosis in Mammalian Aging. **481,** 481–484 (2007).
95. Lord, C. J. & Ashworth, A. The DNA damage response and cancer therapy. *Nature* **481,** 287–294 (2012).

96. Jackson, S. P. & Bartek, J. The DNA-damage response in human biology and disease. *Nature* **461,** 1071–1078 (2010).

97. O'Connor, M. J. Targeting the DNA Damage Response in Cancer. *Mol. Cell* **60,** 547–560 (2015).

98. Shrivastav, M., De Haro, L. P. & Nickoloff, J. a. Regulation of DNA double-strand break repair pathway choice. *Cell Res.* **18,** 134–47 (2008).

99. Chapman, J. R., Taylor, M. R. G. & Boulton, S. J. Playing the End Game: DNA Double-Strand Break Repair Pathway Choice. *Mol. Cell* **47,** 497–510 (2012).

100. Trovesi, C., Manfrini, N., Falcettoni, M. & Longhese, M. P. Regulation of the DNA damage response by cyclin-dependent kinases. *J. Mol. Biol.* **425,** 4756–4766 (2013).

101. Huertas, P. & Jackson, S. P. Human CtIP mediates cell cycle control of DNA end resection and double strand break repair. *J. Biol. Chem.* **284,** 9558–9565 (2009).

102. Yu, X. & Chen, J. DNA Damage-Induced Cell Cycle Checkpoint Control Requires CtIP , a Phosphorylation-Dependent Binding Partner of BRCA1 C-Terminal Domains DNA Damage-Induced Cell Cycle Checkpoint Control Requires CtIP , a Phosphorylation-Dependent Binding Partner of BRCA1. *Mol. Cell. Biol.* **24,** 9478–9486 (2004).

103. Esashi, F. *et al.* CDK-dependent phosphorylation of BRCA2 as a regulatory mechanism for recombinational repair. *Nature* **434,** 598–604 (2005).

104. Daley, J. M. & Sung, P. 53BP1, BRCA1, and the Choice between Recombination and End Joining at DNA Double-Strand Breaks. *Mol. Cell. Biol.* **34,** 1380–1388 (2014).

105. Mailand, N. *et al.* RNF8 Ubiquitylates Histones at DNA Double-Strand Breaks and Promotes Assembly of Repair Proteins. *Cell* **131,** 887–900 (2007).

106. Cao, L. *et al.* A Selective Requirement for 53BP1 in the Biological Response to Genomic Instability Induced by Brca1 Deficiency. *Mol. Cell* **35,** 534–541 (2009).

107. Bunting, S. F. *et al.* 53BP1 inhibits homologous recombination in brca1-deficient cells by blocking resection of DNA breaks. *Cell* **141,** 243–254 (2010).

108. Morales, J. C. *et al.* Role for the BRCA1 C-terminal repeats (BRCT) protein 53BP1 in maintaining genomic stability. *J. Biol. Chem.* **278,** 14971–14977 (2003).

109. Ward, I. M., Minn, K., Deursen, J. Van & Chen, J. p53 Binding Protein 53BP1 Is Required for DNA Damage Responses and Tumor Suppression in Mice These include : p53 Binding Protein 53BP1 Is Required for DNA Damage Responses and Tumor Suppression in Mice. **23,** 2556–2563 (2003).

110. Manis, J. P. *et al.* 53BP1 links DNA damage-response pathways to immunoglobulin heavy chain class-switch recombination. *Nat. Immunol.* **5,** 481–487 (2004).

111. Ward, I. M. *et al.* 53BP1 is required for class switch recombination. *J. Cell Biol.* **165,** 459–464 (2004).

112. Bothmer, A. *et al.* 53BP1 regulates DNA resection and the choice between classical and alternative end joining during class switch recombination. *J. Exp. Med.* **207,** 855–865 (2010).

113. Lazzaro, F. *et al.* Histone methyltransferase Dot1 and Rad9 inhibit single-stranded DNA accumulation at DSBs and uncapped telomeres. *EMBO J.* **27,** 1502–1512 (2008).

114. Chapman, J. R., Sossick, A. J., Boulton, S. J. & Jackson, S. P. BRCA1-associated exclusion of 53BP1 from DNA damage sites underlies temporal control of DNA repair. *J. Cell Sci.* **125,** 3529–3534 (2012).

115. Tomita, K. *et al.* Competition between the Rad50 complex and the Ku heterodimer reveals a role for Exo1 in processing double-strand breaks but not telomeres. *Mol. Cell. Biol.* **23,** 5186–97 (2003).

116. Limbo, O. *et al.* Ctp1 Is a Cell-Cycle-Regulated Protein that Functions with Mre11 Complex to Control Double-Strand Break Repair by Homologous Recombination. *Mol. Cell* **28,** 134–146 (2007).

117. Bunting, S. F. *et al.* BRCA1 Functions Independently of Homologous Recombination in DNA Interstrand Crosslink Repair. *Mol. Cell* **46,** 125–135 (2012).

118. Pierce, A. J., Hu, P., Han, M., Ellis, N. & Jasin, M. Ku DNA end-binding protein modulates homologous repair of double-strand breaks in mammalian cells service Ku DNA end-binding protein modulates homologous repair of double-strand breaks in mammalian cells. *Genes Dev.* 3237–3242 (2001). doi:10.1101/gad.946401

119. Chang, H. H. Y., Pannunzio, N. R., Adachi, N. & Lieber, M. R. Non-homologous DNA end joining and alternative pathways to double-strand break repair. *Nat. Rev. Mol. Cell Biol.* **18,** 495–506 (2017).

120. Grundy, G. J., Moulding, H. a, Caldecott, K. W. & Rulten, S. L. One ring to bring them all-The role of Ku in mammalian non-homologous end joining. *DNA Repair (Amst).* **17,** 30–8 (2014).

121. Blier, P. R., Griffith, A. J., Craft, J. & Hardin, A. Binding of Ku Protein to DNA. *J. Biol. Chem.* **268,** 7594–7601 (1993).

122. Dalby, A. B., Goodrich, K. J., Pfingsten, J. S. & Cech, T. R. RNA recognition by the DNA end-binding Ku heterodimer. *Rna* **19,** 841–851 (2013).
123. Yoo, S. & Dynan, W. S. Characterization of the RNA binding properties of Ku protein. *Biochemistry* **37,** 1336–1343 (1998).
124. Li, B., Navarro, S., Kasahara, N. & Comai, L. Identification and Biochemical Characterization of A Werner's Syndrome Protein Complex with Ku70/80 and Poly(ADP-ribose) Polymerase-1. *J. Biol. Chem.* **279,** 13659–13667 (2004).
125. Suwa, A. *et al.* DNA-dependent protein kinase (Ku protein-p350 complex) assembles on double-stranded DNA. *Proc. Natl. Acad. Sci.* **91,** 6904–6908 (1994).
126. West, R. B., Yaneva, M. & Lieber, M. R. Productive and nonproductive complexes of Ku and DNA-dependent protein kinase at DNA termini. *Mol. Cell. Biol.* **18,** 5908–20 (1998).
127. Boulton, S. J. & Jackson, S. P. Identification of a Saccharomyces cerevisiae Ku80 homologue: roles in DNA double strand break rejoining and in telomeric maintenance. *Nucleic Acids Res.* **24,** 4639–48 (1996).
128. Gravel, S., Larrivée, M., Labrecque, P. & Wellinger, R. J. Yeast Ku as a regulator of chromosomal DNA end structure. *Science (80-.).* **280,** 741–744 (1998).
129. D'Adda di Fagagna, F. *et al.* Effects of DNA nonhomologous end-joining factors on telomere length and chromosomal stability in mammalian cells. *Curr. Biol.* **11,** 1192–1196 (2001).
130. Samper, E., Goytisolo, F. A., Slijepcevic, P., Van Buul, P. P. W. & Blasco, M. A. Mammalian Ku86 protein prevents telomeric fusions independently of the length of TTAGGG repeats and the G-strand overhang. *EMBO Rep.* **1,** 244–252 (2000).
131. Wang, Y., Ghosh, G. & Hendrickson, E. A. Ku86 represses lethal telomere deletion events in human somatic cells. *Proc. Natl. Acad. Sci.* **106,** 12430–12435 (2009).
132. Ribes-Zamora, A., Indiviglio, S. M., Mihalek, I., Williams, C. L. & Bertuch, A. A. TRF2 Interaction with Ku Heterotetramerization Interface Gives Insight into c-NHEJ Prevention at Human Telomeres. *Cell Rep.* **5,** 194–206 (2013).
133. Indiviglio, S. M. & Bertuch, A. a. Ku's essential role in keeping telomeres intact. *Proc. Natl. Acad. Sci. U. S. A.* **106,** 12217–8 (2009).
134. Douglas, P., Gupta, S., Morrice, N., Meek, K. & Lees-Miller, S. P. DNA-PK-dependent phosphorylation of Ku70/80 is not required for non-homologous end joining. *DNA*

Repair (Amst). **4,** 1006–18 (2005).

135. Lee, K. J. *et al.* Phosphorylation of Ku dictates DNA double-strand break (DSB) repair pathway choice in S phase. *Nucleic Acids Res.* **44,** 1732–1745 (2015).
136. Mukherjee, S., Chakraborty, P. & Saha, P. Phosphorylation of Ku70 subunit by cell cycle kinases modulates the replication related function of Ku heterodimer. *Nucleic Acids Res.* **44,** 7755–7765 (2016).
137. Novac, O., Matheos, D., Araujo, F. D., Price, G. B. & Zannis-Hadjopoulos, M. In vivo association of Ku with mammalian origins of DNA replication. *Mol. Biol. Cell* **12,** 3386–3401 (2001).
138. Postow, L. *et al.* Ku80 removal from DNA through double strand break-induced ubiquitylation. *J. Cell Biol.* **182,** 467–79 (2008).
139. Feng, L. & Chen, J. The E3 ligase RNF8 regulates KU80 removal and NHEJ repair. *Nat. Struct. Mol. Biol.* **19,** 201–6 (2012).
140. Ismail, I. H. *et al.* The RNF138 E3 ligase displaces Ku to promote DNA end resection and regulate DNA repair pathway choice. *Nat. Cell Biol.* **17,** (2015).
141. van den Boom, J. *et al.* VCP/p97 Extracts Sterically Trapped Ku70/80 Rings from DNA in Double-Strand Break Repair. *Mol. Cell* **64,** 189–198 (2016).
142. Sander, J. D. & Joung, J. K. CRISPR-Cas systems for editing, regulating and targeting genomes. *Nat. Biotechnol.* **32,** 347–350 (2014).
143. Ochi, T. *et al.* PAXX, a paralog of XRCC4 and XLF, interacts with Ku to promote DNA double-strand break repair. *Science (80-.).* **347,** 185–188 (2015).
144. Britton, S., Coates, J. & Jackson, S. P. A new method for high-resolution imaging of Ku foci to decipher mechanisms of DNA double-strand break repair. *J. Cell Biol.* **202,** 579–95 (2013).
145. Deribe, Y. L., Pawson, T. & Dikic, I. Post-translational modifications in signal integration. *Nat. Struct. Mol. Biol.* **17,** 666–672 (2010).
146. Drazic, A., Myklebust, L. M., Ree, R. & Arnesen, T. The world of protein acetylation. *Biochim. Biophys. Acta - Proteins Proteomics* **1864,** 1372–1401 (2016).
147. Brinkmann, K., Schell, M., Hoppe, T. & Kashkar, H. Regulation of the DNA damage response by ubiquitin conjugation. *Front. Genet.* **6,** 1–15 (2015).
148. Rape, M. Post-Translational Modifications: Ubiquitylation at the crossroads of development and disease. *Nat. Rev. Mol. Cell Biol.* **19,** 59–70 (2018).

149. Sadowski, M. & Sarcevic, B. Mechanisms of mono- and poly-ubiquitination: Ubiquitination specificity depends on compatibility between the E2 catalytic core and amino acid residues proximal to the lysine. *Cell Div.* **5,** 1–5 (2010).
150. A. Hershko, C. C. The ubiquitin system. *Annu. Rev. Biochem.* **67,** 425–79 (1998).
151. Lee, B. L., Singh, A., Mark Glover, J. N., Hendzel, M. J. & Spyracopoulos, L. Molecular Basis for K63-Linked Ubiquitination Processes in Double-Strand DNA Break Repair: A Focus on Kinetics and Dynamics. *J. Mol. Biol.* **429,** 3409–3429 (2017).
152. Jacq, X., Kemp, M., Martin, N. M. B. & Jackson, S. P. Deubiquitylating Enzymes and DNA Damage Response Pathways. *Cell Biochem. Biophys.* **67,** 25–43 (2013).
153. Brown, J. S. & Jackson, S. P. Ubiquitylation, neddylation and the DNA damage response. *Open Biol.* **5,** 150018–150018 (2015).
154. Petroski, M. D. & Deshaies, R. J. Function and regulation of cullin-RING ubiquitin ligases. *Nat. Rev. Mol. Cell Biol.* **6,** 9–20 (2005).
155. Rabut, G. & Peter, M. Function and regulation of protein neddylation. 'Protein modifications: beyond the usual suspects' review series. *EMBO Rep.* **9,** 969–976 (2008).
156. Bosu, D. R. & Kipreos, E. T. Cullin-RING ubiquitin ligases: Global regulation and activation cycles. *Cell Div.* **3,** 1–13 (2008).
157. Sharma, P. & Nag, A. CUL4A ubiquitin ligase: a promising drug target for cancer and other human diseases. *Open Biol.* **4,** 130217–130217 (2014).
158. Jackson, S. & Xiong, Y. CRL4s: the CUL4-RING E3 ubiquitin ligases. *Trends Biochem. Sci.* **34,** 562–570 (2010).
159. Jiang, B. *et al.* Lack of Cul4b, an E3 ubiquitin ligase component, leads to embryonic lethality and abnormal placental development. *PLoS One* **7,** (2012).
160. Liu, L. *et al.* CUL4A Abrogation Augements DNA Damage Response and Protection Against Skin Carcinogenesis. *Mol. Cell* **34,** 451–460 (2010).
161. Manuscript, A. & Structures, T. Cul4A is Essential for Spermatogenesis and Male Fertility. *Dev. Biol.* **352,** 278–287 (2011).
162. Lee, J. & Zhou, P. DCAFs, the missing link of the CUL4-DDB1 ubiquitin ligase. *Mol. Cell* **26,** 775–80 (2007).
163. Xu, C. & Min, J. Structure and function of WD40 domain proteins. *Protein Cell* **2,** 202–214 (2011).

164. Scrima, A. *et al.* Detecting UV-lesions in the genome: The modular CRL4 ubiquitin ligase does it best! *FEBS Lett.* **585,** 2818–2825 (2011).

165. Kapetanaki, M. G. *et al.* The DDB1-CUL4ADDB2 ubiquitin ligase is deficient in xeroderma pigmentosum group E and targets histone H2A at UV-damaged DNA sites. *Proc. Natl. Acad. Sci.* **103,** 2588–2593 (2006).

166. Tang, J. Xeroderma pigmentosum complementation group E and UV-damaged DNA-binding protein. *DNA Repair (Amst).* **6,** 601–616 (2002).

167. Lehmann, A. R., McGibbon, D. & Stefanini, M. Xeroderma pigmentosum. *Orphanet J. Rare Dis.* **6,** 70 (2011).

168. Vermeulen, W. & Fousteri, M. Mammalian transcription-coupled excision repair. *Cold Spring Harb. Perspect. Biol.* **5,** 1–16 (2013).

169. Brown, J. S. *et al.* Neddylation Promotes Ubiquitylation and Release of Ku from DNA-Damage Sites. *Cell Rep.* 704–714 (2015). doi:10.1016/j.celrep.2015.03.058

170. Postow, L. Destroying the ring: Freeing DNA from Ku with ubiquitin. *FEBS Lett.* **585,** 2876–82 (2011).

171. Gilmore, J. M. *et al.* WDR76 Co-Localizes with Heterochromatin Related Proteins and Rapidly Responds to DNA Damage. *PLoS One* **11,** e0155492 (2016).

172. Choi, D.-H., Kwon, S.-H., Kim, J.-H. & Bae, S.-H. Saccharomyces cerevisiae Cmr1 protein preferentially binds to UV-damaged DNA in vitro. *J. Microbiol.* **50,** 112–8 (2012).

173. Gallina, I. *et al.* Cmr1/WDR76 defines a nuclear genotoxic stress body linking genome integrity and protein quality control. *Nat. Commun.* **6,** 1–16 (2015).

174. Gilmore, J. M. *et al.* Characterization of a Highly Conserved Histone Related Protein, Ydl156w, and Its Functional Associations Using Quantitative Proteomic Analyses. *Mol. Cell. Proteomics* **11,** M111.011544 (2012).

175. Abu-Jamous, B., Fa, R., Roberts, D. J. & Nandi, A. K. Yeast gene CMR1/YDL156W is consistently co-expressed with genes participating in DNA-metabolic processes in a variety of stringent clustering experiments. *J. R. Soc. Interface* **10,** 20120990 (2013).

176. Zaidi, I. W. *et al.* Rtt101 and Mms1 in budding yeast form a CUL4DDB1-like ubiquitin ligase that promotes replication through damaged DNA. *EMBO Rep.* **9,** 1034–1040 (2008).

177. Luke, B. *et al.* The Cullin Rtt101p Promotes Replication Fork Progression through

Damaged DNA and Natural Pause Sites. *Curr. Biol.* **16,** 786–792 (2006).

178. Tkach, J. M. *et al.* Dissecting DNA damage response pathways by analysing protein localization and abundance changes during DNA replication stress. (2012). doi:10.1038/ncb2549
179. Soucy, T. A. *et al.* An inhibitor of NEDD8-activating enzyme as a new approach to treat cancer. *Nature* **458,** 732–736 (2009).
180. Leitner, A. *et al.* The molecular architecture of the eukaryotic chaperonin TRiC/CCT. *Structure* **20,** 814–825 (2012).
181. Stelzer, G. *et al.* in *Current Protocols in Bioinformatics* 1.30.1-1.30.33 (John Wiley & Sons, Inc., 2016). doi:10.1002/cpbi.5
182. Dantuma, N. P., Groothuis, T. A. M., Salomons, F. A. & Neefjes, J. A dynamic ubiquitin equilibrium couples proteasomal activity to chromatin remodeling. *J. Cell Biol.* **173,** 19–26 (2006).
183. Saibil, H. Chaperone machines for protein folding, unfolding and disaggregation. *Nat. Rev. Mol. Cell Biol.* **14,** 630–642 (2013).
184. Trautinger, F., Kindås-Mügge, I., Knobler, R. M. & Hönigsmann, H. Stress proteins in the cellular response to ultraviolet radiation. *J. Photochem. Photobiol. B.* **35,** 141–148 (1996).
185. Sugasawa, K. *et al.* UV-induced ubiquitylation of XPC protein mediated by UV-DDB-ubiquitin ligase complex. *Cell* **121,** 387–400 (2005).
186. Wang, H. *et al.* Histone H3 and H4 Ubiquitylation by the CUL4-DDB-ROC1 Ubiquitin Ligase Facilitates Cellular Response to DNA Damage. *Mol. Cell* **22,** 383–394 (2006).
187. Nishitani, H. *et al.* CDK Inhibitor p21 Is Degraded by a Proliferating Cell Nuclear Antigen-coupled Cul4-DDB1 ^{Cdt2} Pathway during S Phase and after UV Irradiation. *J. Biol. Chem.* **283,** 29045–29052 (2008).
188. Adam, S. & Polo, S. E. Blurring the line between the DNA damage response and transcription: The importance of chromatin dynamics. *Exp. Cell Res.* **329,** 148–153 (2014).
189. Higa, L. A. *et al.* CUL4-DDB1 ubiquitin ligase interacts with multiple WD40-repeat proteins and regulates histone methylation. *Nat. Cell Biol.* **8,** 1277–1283 (2006).
190. Bensaude, O. Inhibiting eukaryotic transcription: Which compound to choose? How to evaluate its activity? *Transcription* **2,** 103–108 (2011).

191. Gilmore, J. M. *et al.* Characterization of a highly conserved histone related protein, Ydl156w, and its functional associations using quantitative proteomic analyses. *Mol. Cell. Proteomics* **11,** M111.011544 (2012).

192. Li, J. *et al.* DNA damage binding protein component DDB1 participates in nucleotide excision repair through DDB2 DNA-binding and cullin 4a ubiquitin ligase activity. *Cancer Res.* **66,** 8590–8597 (2006).

193. Chu, G. & Yang, W. Here Comes the Sun: Recognition of UV-Damaged DNA. *Cell* **135,** 1172–1174 (2008).

194. Petroski, M. D. & Deshaies, R. J. Function and regulation of cullin-RING ubiquitin ligases. *Nat. Rev. Mol. Cell Biol.* **6,** 9–20 (2005).

195. Zdzienicka, M. Z. Mammalian mutants defective in the response to ionizing radiation-induced DNA damage. *Mutat. Res.* **336,** 203–213 (1995).

196. Boulton, S. J. & Jackson, S. P. Saccharomyces cerevisiae Ku70 potentiates illegitimate DNA double-strand break repair and serves as a barrier to error-prone DNA repair pathways. *EMBO J.* **15,** 5093–103 (1996).

197. Yam, A. Y. *et al.* Defining the TRiC/CCT interactome links chaperonin function to stabilzation of newly-made proteins with complex topologies. *Nat. Struct. Mol. Biol.* **15,** 1255–1262 (2008).

198. Spiess, C., Meyer, A. S., Reissmann, S. & Frydman, J. Mechanism of the eukaryotic chaperonin: Protein folding in the chamber of secrets. *Trends Cell Biol.* **14,** 598–604 (2004).

199. Camasses, A., Bogdanova, A., Shevchenko, A. & Zachariae, W. The CCT chaperonin promotes activation of the anaphase-promoting complex through the generation of functional Cdc20. *Mol. Cell* **12,** 87–100 (2003).

200. Boisvert, F. M., Van Koningsbruggen, S., Navascués, J. & Lamond, A. I. The multifunctional nucleolus. *Nat. Rev. Mol. Cell Biol.* **8,** 574–585 (2007).

201. Badertscher, L. *et al.* Genome-wide RNAi Screening Identifies Protein Modules Required for 40S Subunit Synthesis in Human Cells. *Cell Rep.* **13,** 2879–2891 (2015).

202. Kaidi, A. & Jackson, S. P. KAT5 tyrosine phosphorylation couples chromatin sensing to ATM signalling. *Nature* **498,** 70–4 (2013).

203. Ura, K., Kurumizaka, H., Dimitrov, S., Almouzni, G. & Wolffe, A. P. Histone acetylation: influence on transcription, nucleosome mobility and positioning, and linker histone-

dependent transcriptional repression. *EMBO J.* **16,** 2096–107 (1997).

204. Naro, C., Bielli, P., Pagliarini, V. & Sette, C. The interplay between DNA damage response and RNA processing: The unexpected role of splicing factors as gatekeepers of genome stability. *Front. Genet.* **6,** 1–10 (2015).
205. Hawley, B. R., Lu, W.-T., Wilczynska, A. & Bushell, M. The emerging role of RNAs in DNA damage repair. *Cell Death Differ.* **24,** 580–587 (2017).
206. Wei, W. *et al.* A role for small RNAs in DNA double-strand break repair. *Cell* **149,** 101–112 (2012).
207. Francia, S., Cabrini, M., Matti, V., Oldani, A. & d'Adda di Fagagna, F. DICER, DROSHA and DNA damage response RNAs are necessary for the secondary recruitment of DNA damage response factors. *J. Cell Sci.* **129,** 1468–1476 (2016).
208. Burger, K. *et al.* Nuclear phosphorylated Dicer processes doublestranded RNA in response to DNA damage. *J. Cell Biol.* **216,** 2373–2389 (2017).
209. Ohle, C. *et al.* Transient RNA-DNA Hybrids Are Required for Efficient Double-Strand Break Repair. *Cell* **167,** 1001–1013.e7 (2016).
210. Keskin, H. *et al.* HHS Public Access. *Nature* **515,** 436–439 (2016).
211. Chakraborty, A. *et al.* Classical non-homologous end-joining pathway utilizes nascent RNA for error-free double-strand break repair of transcribed genes. *Nat. Commun.* **7,** 1–12 (2016).
212. Xing, M. *et al.* Interactome analysis identifies a new paralogue of XRCC4 in non-homologous end joining DNA repair pathway. *Nat. Commun.* **6,** 6233 (2015).
213. Craxton, a *et al.* XLS (c9orf142) is a new component of mammalian DNA double-stranded break repair. *Cell Death Differ.* **22,** 890–897 (2015).
214. Leidel, S., Delattre, M., Cerutti, L., Baumer, K. & Gönczy, P. SAS-6 defines a protein family required for centrosome duplication in C. elegans and in human cells. *Nat. Cell Biol.* **7,** 115–125 (2005).
215. Sibanda, B. L. *et al.* Crystal structure of an Xrcc4-DNA ligase IV complex. *Nat. Struct. Biol.* **8,** 1015–1019 (2001).
216. Bryans, M., Valenzano, M. C. & Stamato, T. D. Absence of DNA ligase IV protein in XR-1 cells: Evidence for stabilization by XRCC4. *Mutat. Res. - DNA Repair* **433,** 53–58 (1999).
217. Tadi, S. K. *et al.* PAXX Is an Accessory c-NHEJ Factor that Associates with Ku70 and Has

Overlapping Functions with XLF. *Cell Rep.* **17,** 541–555 (2016).

218. Liu, X., Shao, Z., Jiang, W., Lee, B. J. & Zha, S. PAXX promotes KU accumulation at DNA breaks and is essential for end-joining in XLF-deficient mice. *Nat. Commun.* **8,** 13816 (2017).
219. Lescale, C. *et al.* Specific Roles of XRCC4 Paralogs PAXX and XLF during V(D)J Recombination. *Cell Rep.* **16,** 2967–2979 (2016).
220. Balmus, G. *et al.* Synthetic lethality between PAXX and XLF in mammalian development. *Genes Dev.* **30,** 2152–2157 (2016).
221. Riballo, E. *et al.* XLF-Cernunnos promotes DNA ligase IV-XRCC4 re-adenylation following ligation. *Nucleic Acids Res.* **37,** 482–492 (2009).
222. Luo, K. *et al.* CDK-mediated RNF4 phosphorylation regulates homologous recombination in S-phase. *Nucleic Acids Res.* **43,** 5465–5475 (2015).
223. Ferretti, L. P., Lafranchi, L. & Sartori, A. a. Controlling DNA-end resection: A new task for CDKs. *Front. Genet.* **4,** 1–7 (2013).
224. Falck, J. *et al.* CDK targeting of NBS1 promotes DNA-end resection, replication restart and homologous recombination. *EMBO Rep.* **13,** 561–568 (2012).
225. Oakley, G. G. *et al.* RPA phosphorylation in mitosis alters DNA binding and protein-protein interactions. *Biochemistry* **42,** 3255–3264 (2003).
226. Ruffner, H., Jiang, W., Craig, a G., Hunter, T. & Verma, I. M. BRCA1 is phosphorylated at serine 1497 in vivo at a cyclin-dependent kinase 2 phosphorylation site. *Mol. Cell. Biol.* **19,** 4843–4854 (1999).
227. Arnaudeau, C., Lundin, C. & Helleday, T. DNA double-strand breaks associated with replication forks are predominantly repaired by homologous recombination involving an exchange mechanism in mammalian cells. *J. Mol. Biol.* **307,** 1235–1245 (2001).
228. Willems, a R. *et al.* SCF ubiquitin protein ligases and phosphorylation-dependent proteolysis. *Philos. Trans. R. Soc. Lond. B. Biol. Sci.* **354,** 1533–1550 (1999).
229. Wertz, I. E. *et al.* Sensitivity to antitubulin chemotherapeutics is regulated by MCL1 and FBW7. *Nature* **471,** 110–114 (2011).
230. Welcker, M. & Clurman, B. E. FBW7 ubiquitin ligase: a tumour suppressor at the crossroads of cell division, growth and differentiation. *Nat. Rev. Cancer* **8,** 83–93 (2008).
231. Hornbeck, P. V *et al.* PhosphoSitePlus, 2014: mutations, PTMs and recalibrations.

Nucleic Acids Res. **43,** D512-20 (2015).

232. Werner, O. On cataract associated in conjunction with scleroderma. *Doctoral Dissertation* (Kiel University, Schmidt and Klauning, Kiel, 1904).
233. Goto, M. Hierarchical deterioration of body systems in Werner's syndrome: Implications for normal ageing. *Mech. Ageing Dev.* **98,** 239–254 (1997).
234. Epstein, C. J., Martin, G. M., Schultz, A. . & Motulsky, A. G. Werner syndrome. A review of its symptomatology, natural history, pathologic features, genetics and relationship to the natural aging process. *Medicine (Baltimore).* **45,** 177–221 (1966).
235. Hennekam, R. C. M. Hutchinson-Gilford Progeria Syndrome: Review of the Phenotype. *Am. J. Med. Genet. A* **140A,** 2603–2624 (2006).
236. Muftuoglu, M. *et al.* The clinical characteristics of Werner syndrome: molecular and biochemical diagnosis. *Hum. Genet.* **124,** 369–377 (2008).
237. Huang, S. *et al.* The spectrum of WRN mutations in Werner syndrome patients. *Hum. Mutat.* **27,** 558–567 (2006).
238. Chun, S. G., Shaeffer, D. S. & Bryant-Greenwood, P. K. The Werner's Syndrome RecQ helicase/exonuclease at the nexus of cancer and aging. *Hawaii Med. J.* **70,** 52–5 (2011).
239. Goto, M., Miller, R. W., Ishikawa, Y. & Sugano, H. Excess of Rare Cancers in Werner Syndrome (Adult Progeria). *Cancer Epidemiol. Biomarkers Prev.* **5,** 239–246 (1996).
240. Chu, W. K. & Hickson, I. D. RecQ helicases: multifunctional genome caretakers. *Nat. Rev. Cancer* **9,** 644–654 (2009).
241. Oshima, J., Martin, G. M. & Hisama, F. M. in *GeneReviews(®)* (2014).
242. Satoh, M., Imai, M., Sugimoto, M., Goto, M. & Furuichi, Y. Prevalence of Werner's syndrome heterozygotes in Japan. *Lancet* **353,** 1766 (1999).
243. Yamaga, M. *et al.* Recent Trends in WRN Gene Mutation Patterns in Individuals with Werner Syndrome. *J. Am. Geriatr. Soc.* **65,** 1853–1856 (2017).
244. Oshima, J., Sidorova, J. M. & Monnat, R. J. Werner syndrome: Clinical features, pathogenesis and potential therapeutic interventions. *Ageing Res. Rev.* **33,** 105–114 (2017).
245. Bernstein, D. A. & Keck, J. L. Domain mapping of Escherichia coli RecQ defines the roles of conserved N- and C-terminal regions in the RecQ family. *Nucleic Acids Res.* **31,** 2778–2785 (2003).

246. Courcelle, J. & Hanawalt, P. C. RecQ and RecJ process blocked replication forks prior to the resumption of replication in UV-irradiated Escherichia coli. *Mol. Gen. Genet.* **262,** 543–551 (1999).

247. Kolodner, R., Fishel, R. A. & Howard, M. Genetic recombination of bacterial plasmid DNA: Effect of RecF pathway mutations on plasmid recombination in Escherichia coli. *J. Bacteriol.* **163,** 1060–1066 (1985).

248. Hanada, K. *et al.* RecQ DNA helicase is a suppressor of illegitimate recombination in Escherichia coli. *Proc. Natl. Acad. Sci. U. S. A.* **94,** 3860–3865 (1997).

249. Watt, P. M., Hickson, I. D., Borts, R. H. & Louis, E. J. SGS1, a homologue of the Blooms and Werner's syndrome genes, is required for maintenance of genome stability in Saccharomyces cerevisiae. *Genetics* **144,** 935–945 (1996).

250. Stewart, E., Chapman, C. R., Al-Khodairy, F., Carr, A. M. & Enoch, T. rqh1^{+}, a fission yeast gene related to the Bloom's and Werner's syndrome genes, is required for reversible S phase arrest. *EMBO J.* **16,** 2682–2692 (1997).

251. Sinclair, D., Mills, K. & Guarente, L. Aging in Saccharomyces cerevisiae. *Annu. Rev. Microbiol.* **52,** 533–560 (1998).

252. Frei, C. & Gasser, S. M. RecQ-like helicases: the DNA replication checkpoint connection. *J. Cell Sci.* **113 (Pt 1,** 2641–2646 (2000).

253. Zhu, Z., Chung, W.-H., Shim, E. Y., Lee, S. E. & Ira, G. Sgs1 helciase and two nucleases Dna2 and Exo1 resect DNA double strand break ends. *Cell* **134,** 981–994 (2008).

254. Chu, W. K. & Hickson, I. D. RecQ helicases: Multifunctional genome caretakers. *Nat. Rev. Cancer* **9,** 644–654 (2009).

255. Mo, D., Zhao, Y. & Balajee, A. S. Human RecQL4 helicase plays multifaceted roles in the genomic stability of normal and cancer cells. *Cancer Lett.* **413,** 1–10 (2018).

256. Larizza, L., Roversi, G. & Volpi, L. Rothmund-Thomson Syndrome. *Orphanet J. Rare Dis.* **5,** (2010).

257. Kaneko, H. *et al.* Nationwide survey of Baller-Gerold syndrome in Japanese population. *Mol. Med. Rep.* **15,** 3222–3224 (2017).

258. Keller, C., Keller, K. R., Shew, S. B. & Plon, S. E. Growth deficiency and malnutrition in Bloom syndrome. *J. Pediatr.* **134,** 472–479 (1999).

259. German, J. Bloom's syndrome. I. Genetical and clinical observations in the first twenty-seven patients. *Am. J. Hum. Genet.* **21,** 196–227 (1969).

260. Renty, C. de & Ellis, N. A. Bloom's Syndrome: Why Not Premature Aging? *Ageing Res. Rev.* (2016). doi:10.1016/j.arr.2016.05.010

261. Sanz, M. M., German, J. & Cunnif, C. Bloom's Syndrome. *GeneReviews(®)* (2016).

262. Chaganti, R. S., Schonberg, S. & German, J. A manyfold increase in sister chromatid exchanges in Bloom's syndrome lymphocytes. *Proc. Natl. Acad. Sci. U. S. A.* **71,** 4508–12 (1974).

263. Wu, L. *et al.* The HRDC domain of BLM is required for the dissolution of double Holliday junctions. *EMBO J.* **24,** 2679–2687 (2005).

264. MacHwe, A., Karale, R., Xu, X., Liu, Y. & Orren, D. K. The Werner and Bloom syndrome proteins help resolve replication blockage by converting (regressed) Holliday junctions to functional replication forks. *Biochemistry* **50,** 6774–6788 (2011).

265. Karow, J. K., Constantinou, A., Li, J. L., West, S. C. & Hickson, I. D. The Bloom's syndrome gene product promotes branch migration of holliday junctions. *Proc. Natl. Acad. Sci. U. S. A.* **97,** 6504–8 (2000).

266. Wu, L. & Hickson, I. O. The Bloom's syndrome helicase suppresses crossing over during homologous recombination. *Nature* **426,** 870–874 (2003).

267. Liu, Y. & West, S. C. More complexity to the Bloom's syndrome complex. *Genes Dev.* **22,** 2737–2742 (2008).

268. Nimonkar, A. V., Ozsoy, A. Z., Genschel, J., Modrich, P. & Kowalczykowski, S. C. Human exonuclease 1 and BLM helicase interact to resect DNA and initiate DNA repair. *Proc. Natl. Acad. Sci.* **105,** 16906–16911 (2008).

269. Nimonkar, A. V. *et al.* BLM, DNA2, RPA, MRN and EXO1, BLM, RPA, MRN constitute two DNA end resection machineries for human DNA break repair. *Genes Dev.* **25,** 350–362 (2011).

270. Gravel, S., Chapman, J. R., Magill, C. & Jackson, S. P. DNA helicases Sgs1 and BLM promote DNA double-strand break resection. *Genes Dev.* **22,** 2767–2772 (2008).

271. Imamura, O. *et al.* Werner and Bloom helicases are involved in DNA repair in a complementary fashion. *Oncogene* **21,** 954–963 (2002).

272. Swan, M. K. *et al.* Structure of human Bloom's syndrome helicase in complex with ADP and duplex DNA. *Acta Crystallogr. Sect. D Biol. Crystallogr.* **70,** 1465–1475 (2014).

273. Kitano, K. Structural mechanisms of human RecQ helicases WRN and BLM. *Front.*

Genet. **5,** 1–11 (2014).

274. Kitano, K., Kim, S. Y. & Hakoshima, T. Structural Basis for DNA Strand Separation by the Unconventional Winged-Helix Domain of RecQ Helicase WRN. *Structure* **18,** 177–187 (2010).
275. Morozov, V., Mushegian, A. R., Koonin, E. V. & Bork, P. A putative nucleic acid-binding domain in Bloom's and Werner's syndrome helicases. *Trends Biochem. Sci.* **22,** 417–418 (1997).
276. Sattler, M. The three-dimensional structure of the HRDC domain and implications for the Werner and Bloom syndrome proteins Z Liu , MJ Macias , MJ Bottomley , G Stier , JP Linge , M Nilges , P Bork. 1557–1566
277. von Kobbe, C., Thomä, N. H., Czyzewski, B. K., Pavletich, N. P. & Bohr, V. A. Werner Syndrome Protein Contains Three Structure-specific DNA Binding Domains. *J. Biol. Chem.* **278,** 52997–53006 (2003).
278. Kitano, K., Yoshihara, N. & Hakoshima, T. Crystal structure of the HRDC domain of human Werner syndrome protein, WRN. *J. Biol. Chem.* **282,** 2717–2728 (2007).
279. Cooper, M. P. *et al.* Ku complex interacts with and stimulates the Werner protein. *Genes Dev.* **14,** 907–912 (2000).
280. Grundy, G. J. *et al.* The Ku binding Motif is a conserved module for recruitment and stimulation of non-homologous end-joining proteins. *Nat. Commun.* 1–11 (2016). doi:10.1038/pj.2016.37
281. Lachapelle, S. *et al.* Proteome-wide Identification of WRN-Interacting Proteins in Untreated and Nuclease-Treated Samples. *J. Proteome Res.* **10,** 1216–1227 (2011).
282. Dianov, G. L. & Hübscher, U. Mammalian base excision repair: The forgotten archangel. *Nucleic Acids Res.* **41,** 3483–3490 (2013).
283. Singh, P. K. & Mistry, K. Human NEIL1 DNA glycosylase: Structure, function and polymorphisms. *Meta Gene* **11,** 49–57 (2017).
284. Das, A. *et al.* The human Werner syndrome protein stimulates repair of oxidative DNA base damage by the DNA glycosylase NEIL1. *J. Biol. Chem.* **282,** 26591–602 (2007).
285. Sidorova, J. M. Roles of the Werner syndrome RecQ helicase in DNA replication. *DNA Repair (Amst).* **7,** 1776–1786 (2008).
286. Cappelli, E. *et al.* Involvement of XRCC1 and DNA ligase III gene products in DNA base excision repair. *J. Biol. Chem.* **272,** 23970–23975 (1997).

287. Caldecott, K. W., Tucker, J. D., Stanker, L. H. & Thompson, L. H. Characterization of the XRCC1-DNA ligase III complex in vitro and its absence from mutant hamster cells. *Nucleic Acids Res.* **23,** 4836–4843 (1995).

288. Harrigan, J. A. *et al.* The Werner syndrome protein stimulates DNA polymerase β strand displacement synthesis via its helicase activity. *J. Biol. Chem.* **278,** 22686–22695 (2003).

289. Zheng, L. *et al.* Functional regulation of FEN1 nuclease and its link to cancer. *Nucleic Acids Res.* **39,** 781–794 (2011).

290. Brosh, R. M., Driscoll, H. C., Dianov, G. L. & Sommers, J. A. Biochemical characterization of the WRN-FEN-1 functional interaction. *Biochemistry* **41,** 12204–12216 (2002).

291. Lebel, M., Spillare, E. A., Harris, C. C. & Leder, P. The Werner syndrome gene product co-purifies with the DNA replication complex and interacts with PCNA and topoisomerase I. *J. Biol. Chem.* **274,** 37795–37799 (1999).

292. Kamath-Loeb, A. S., Johansson, E., Burgers, P. M. & Loeb, L. A. Functional interaction between the Werner Syndrome protein and DNA polymerase delta. *Proc. Natl. Acad. Sci. U. S. A.* **97,** 4603–8 (2000).

293. Yan, H., Chen, C. Y., Kobayashi, R. & Newport, J. Replication focus-forming activity 1 and the Werner syndrome gene product. *Nat. Genet.* **19,** 375–8 (1998).

294. Kamath-Loeb, A. S., Loeb, L. A., Johansson, E., Burgers, P. M. J. & Fry, M. Interactions between the Werner Syndrome Helicase and DNA Polymerase δ Specifically Facilitate Copying of Tetraplex and Hairpin Structures of the d(CGG)n Trinucleotide Repeat Sequence. *J. Biol. Chem.* **276,** 16439–16446 (2001).

295. Von Kobbe, C. *et al.* Colocalization, physical, and functional interaction between Werner and Bloom syndrome proteins. *J. Biol. Chem.* **277,** 22035–22044 (2002).

296. Shen, J. C. & Loeb, L. a. Werner syndrome exonuclease catalyzes structure-dependent degradation of DNA. *Nucleic Acids Res.* **28,** 3260–3268 (2000).

297. Rodriguez-Lopez, A. M., Jackson, D. A., Iborra, F. & Cox, L. S. Asymmetry of DNA replication fork progression in Werner's syndrome. *Aging Cell* **1,** 30–39 (2002).

298. Sidorova, J. M., Li, N., Folch, A. & Monnat, R. J. The RecQ helicase WRN is required for normal replication fork progression after DNA damage or replication fork arrest. *Cell Cycle* **7,** 796–807 (2008).

299. Dhillon, K. K. *et al.* Functional role of the Werner syndrome RecQ helicase in human fibroblasts. *Aging Cell* **6,** 53–61 (2007).
300. Christmann, M. *et al.* WRN protects against topo I but not topo II inhibitors by preventing DNA break formation. *DNA Repair (Amst).* **7,** 1999–2009 (2008).
301. Lan, L. *et al.* Accumulation of Werner protein at DNA double-strand breaks in human cells. *J. Cell Sci.* **118,** 4153–62 (2005).
302. Lee, M. *et al.* Multiple RPAs make WRN syndrome protein a superhelicase. *Nucleic Acids Res.* **46,** 4689–4698 (2018).
303. Wang, A. T. *et al.* A Dominant Mutation in Human RAD51 Reveals Its Function in DNA Interstrand Crosslink Repair Independent of Homologous Recombination. *Mol. Cell* **59,** 478–490 (2015).
304. Sturzenegger, A. *et al.* DNA2 cooperates with the WRN and BLM RecQ helicases to mediate long-range DNA end resection in human cells. *J. Biol. Chem.* **289,** 27314–27326 (2014).
305. Pichierri, P., Franchitto, A., Mosesso, P. & Palitti, F. Werner's syndrome protein is required for correct recovery after replication arrest and DNA damage induced in S-phase of cell cycle. *Mol. Biol. Cell* **12,** 2412–21 (2001).
306. Rossi, M. L., Ghosh, A. K. & Bohr, V. a. Roles of Werner syndrome protein in protection of genome integrity. *DNA Repair (Amst).* **9,** 331–344 (2010).
307. Baynton, K. *et al.* WRN interacts physically and functionally with the recombination mediator protein RAD52. *J. Biol. Chem.* **278,** 36476–36486 (2003).
308. Otterlei, M. *et al.* Werner syndrome protein participates in a complex with RAD51, RAD54, RAD54B and ATR in response to ICL-induced replication arrest. *J. Cell Sci.* **119,** 5215–5215 (2006).
309. Kusumoto, R. *et al.* Werner protein cooperates with the XRCC4-DNA ligase IV complex in end-processing. *Biochemistry* **47,** 7548–56 (2008).
310. Li, B. & Comai, L. Functional interaction between Ku and the werner syndrome protein in DNA end processing. *J. Biol. Chem.* **275,** 28349–28352 (2000).
311. Karmakar, P. *et al.* Werner protein is a target of DNA-dependent protein kinase in vivo and in vitro, and its catalytic activities are regulated by phosphorylation. *J. Biol. Chem.* **277,** 18291–18302 (2002).
312. Yannone, S. M. *et al.* Werner Syndrome Protein Is Regulated and Phosphorylated by

DNA-dependent Protein Kinase. *J. Biol. Chem.* **276,** 38242–38248 (2001).

313. Shamanna, R. A. *et al.* WRN regulates pathway choice between classical and alternative non-homologous end joining. *Nat. Commun.* **7,** 1–12 (2016).
314. Palm, W. & de Lange, T. How Shelterin Protects Mammalian Telomeres. *Annu. Rev. Genet.* **42,** 301–334 (2008).
315. O'Sullivan, R. J. & Karlseder, J. Telomeres: Protecting chromosomes against genome instability. *Nat. Rev. Mol. Cell Biol.* **11,** 171–181 (2010).
316. De Lange, T. Shelterin: The protein complex that shapes and safeguards human telomeres. *Genes Dev.* **19,** 2100–2110 (2005).
317. d'Adda di Fagagna, F. *et al.* A DNA damage checkpoint response in telomere-associated senescence. *Nature* **426,** 194–198 (2003).
318. D'Adda Di Fagagna, F., Teo, S. H. & Jackson, S. P. Functional links between telomeres and proteins of the DNA-damage response. *Genes Dev.* **18,** 1781–1799 (2004).
319. Opresko, P. L. *et al.* The Werner syndrome helicase and exonuclease cooperate to resolve telomeric D loops in a manner regulated by TRF1 and TRF2. *Mol. Cell* **14,** 763–74 (2004).
320. Brosh, R. M. & Bohr, V. A. Human premature aging, DNA repair and RecQ helicases. *Nucleic Acids Res.* **35,** 7527–7544 (2007).
321. Brosh, R. M., Opresko, P. L. & Bohr, V. A. Enzymatic Mechanism of the WRN Helicase/Nuclease. *Methods Enzymol.* **409,** 52–85 (2006).
322. Li, J. L. *et al.* Inhibition of the Bloom's and Werner's syndrome helicases by G-quadruplex interacting ligands. *Biochemistry* **40,** 15194–15202 (2001).
323. Rhodes, D. & Lipps, H. J. G-quadruplexes and their regulatory roles in biology. *Nucleic Acids Res.* **43,** 8627–8637 (2015).
324. Shiratori, M. *et al.* WRN helicase accelerates the transcription of ribosomal RNA as a component of an RNA polymerase I-associated complex. *Oncogene* **21,** 2447–2454 (2002).
325. Balajee, A. S. *et al.* The Werner syndrome protein is involved in RNA polymerase II transcription. *Mol. Biol. Cell* **10,** 2655–68 (1999).
326. Lombard, D. B. *et al.* Mutations in the WRN gene in mice accelerate mortality in a p53-null background. *Mol. Cell. Biol.* **20,** 3286–3291 (2000).
327. Lebel, M. & Leder, P. A deletion within the murine Werner syndrome helicase induces

sensitivity to inhibitors of topoisomerase and loss of cellular proliferative capacity. *Proc. Natl. Acad. Sci. U. S. A.* **95,** 13097–102 (1998).

328. Chang, S. *et al.* Essential role of limiting telomeres in the pathogenesis of Werner syndrome. *Nat. Genet.* **36,** 877–82 (2004).
329. Allen, F. *et al.* JACKS : joint analysis of CRISPR / Cas9 knock-out screens. *BioRxiv* (2018).
330. Wang, X. *et al.* Unbiased detection of off-target cleavage by CRISPR-Cas9 and TALENs using integrase-defective lentiviral vectors. *Nat. Biotechnol.* **33,** 175–179 (2015).
331. Frock, R. L. *et al.* Genome-wide detection of DNA double-stranded breaks induced by engineered nucleases. *Nat. Biotechnol.* **33,** 179–86 (2015).
332. Bieging, K. T., Mello, S. S. & Attardi, L. D. Unravelling mechanisms of p53-mediated tumour suppression. *Nat. Rev. Cancer* **14,** 359–70 (2014).
333. Abbas, T. & Dutta, A. P21 in Cancer: Intricate Networks and Multiple Activities. *Nat. Rev. Cancer* **9,** 400–414 (2009).
334. Karimian, A., Ahmadi, Y. & Yousefi, B. Multiple functions of p21 in cell cycle, apoptosis and transcriptional regulation after DNA damage. *DNA Repair (Amst).* **42,** 63–71 (2016).
335. Jaramillo, M. & Zhang, D. The emerging role of the Nrf2–Keap1 signaling pathway in cancer. *Genes Dev.* **27,** 2179–2191 (2013).
336. Chua, Y. S., Boh, B. K., Ponyeam, W. & Hagen, T. Regulation of cullin ring e3 ubiquitin ligases by cand1 in vivo. *PLoS One* **6,** e16071 (2011).
337. Worby, C. A. & Dixon, J. E. Pten. *Annu. Rev. Biochem.* **83,** 641–669 (2014).
338. Song, M. S., Salmena, L. & Pandolfi, P. P. The functions and regulation of the PTEN tumour suppressor. *Nat. Rev. Mol. Cell Biol.* **13,** 283–296 (2012).
339. Zhou, Z., Chan, C. H., Xiao, Z. & Tan, E. Ring finger protein 146/Iduna is a poly(ADP-ribose) polymer binding and PARsylation dependent E3 ubiquitin ligase. *Cell Adh. Migr.* **5,** 463–71 (2011).
340. Kang, H. C. *et al.* Iduna is a poly(ADP-ribose) (PAR)-dependent E3 ubiquitin ligase that regulates DNA damage. *Proc. Natl. Acad. Sci.* **108,** 14103–14108 (2011).
341. Zhang, Y. *et al.* RNF146 is a poly(ADP-ribose)-directed E3 ligase that regulates axin degradation and Wnt signalling. *Nat. Cell Biol.* **13,** 623–629 (2011).
342. Becker, R., Loll, B. & Meinhart, A. Snapshots of the RNA processing factor SCAF8

bound to different phosphorylated forms of the carboxyl-terminal domain of RNA polymerase II. *J. Biol. Chem.* **283,** 22659–22669 (2008).

343. Colin, J., Libri, D. & Porrua, O. Cryptic Transcription and Early Termination in the Control of Gene Expression. *Genet. Res. Int.* **2011,** 1–10 (2011).
344. Cuenda, A. & Rousseau, S. p38 MAP-Kinases pathway regulation, function and role in human diseases. *Biochim. Biophys. Acta - Mol. Cell Res.* **1773,** 1358–1375 (2007).
345. Coulthard, L. R., White, D. E., Jones, D. L. & Mcdermott, M. F. Europe PMC Funders Group p38 MAPK : stress responses from molecular mechanisms to therapeutics. **15,** 369–379 (2011).
346. Plotnikov, A., Zehorai, E., Procaccia, S. & Seger, R. The MAPK cascades: Signaling components, nuclear roles and mechanisms of nuclear translocation. *Biochim. Biophys. Acta - Mol. Cell Res.* **1813,** 1619–1633 (2011).
347. Itoh, M. *et al.* Nuclear Export of Glucocorticoid Receptor is Enhanced by c-Jun N-Terminal Kinase-Mediated Phosphorylation. *Mol. Endocrinol.* **16,** 2382–2392 (2002).
348. Privette, L. M. & Petty, E. M. CHFR: A Novel Mitotic Checkpoint Protein and Regulator of Tumorigenesis. *Transl. Oncol.* **1,** 57–64 (2008).
349. Oh, Y. M. *et al.* Chfr is linked to tumour metastasis through the downregulation of HDAC1. *Nat. Cell Biol.* **11,** 295–302 (2009).
350. Tang, L., Nogales, E. & Ciferri, C. Structure and function of SWI / SNF chromatin remodeling complexes and mechanistic implications for transcription. *Prog. Biophys. Mol. Biol.* **102,** 122–128 (2010).
351. Dykhuizen, E. C. *et al.* BAF complexes facilitate decatenation of DNA by topoisomerase IIα. *Nature* **497,** 624–627 (2013).
352. Husain, A. *et al.* Chromatin remodeller SMARCA4 recruits topoisomerase 1 and suppresses transcription-associated genomic instability. *Nat. Commun.* **7,** 1–15 (2016).
353. Pepe, A. & West, S. C. MUS81-EME2 promotes replication fork restart. *Cell Rep.* **7,** 1048–1055 (2014).
354. Franchitto, A. *et al.* Replication fork stalling in WRN-deficient cells is overcome by prompt activation of a MUS81-dependent pathway. *J. Cell Biol.* **183,** 241–252 (2008).
355. Cao, N. *et al.* A potential role for protein palmitoylation and zDHHC16 in DNA damage response. *BMC Mol. Biol.* **17,** 12 (2016).

356. Pfister, S. X. *et al.* SETD2-Dependent Histone H3K36 Trimethylation Is Required for Homologous Recombination Repair and Genome Stability. *Cell Rep.* **7,** 2006–2018 (2014).

357. Hart, T. *et al.* High-Resolution CRISPR Screens Reveal Fitness Genes and Genotype-Specific Cancer Liabilities. *Cell* **163,** 1515–26 (2015).

358. Barbosa, L. F. *et al.* Increased SOD1 association with chromatin, DNA damage, p53 activation, and apoptosis in a cellular model of SOD1-linked ALS. *Biochim. Biophys. Acta - Mol. Basis Dis.* **1802,** 462–471 (2010).

359. Suwaki, N., Klare, K. & Tarsounas, M. RAD51 paralogs: Roles in DNA damage signalling, recombinational repair and tumorigenesis. *Semin. Cell Dev. Biol.* **22,** 898–905 (2011).

360. Nagaraju, G., Hartlerode, A., Kwok, A., Chandramouly, G. & Scully, R. XRCC2 and XRCC3 Regulate the Balance between Short- and Long-Tract Gene Conversions between Sister Chromatids. *Mol. Cell. Biol.* **29,** 4283–4294 (2009).

361. Seki, M., Otsuki, M., Ishii, Y., Tada, S. & Enomoto, T. RecQ family helicases in genome stability: Lessons from gene disruption studies in DT40 cells. *Cell Cycle* **7,** 2472–2478 (2008).

362. Saintigny, Y. *et al.* Homologous Recombination Resolution Defect in Werner Syndrome Homologous Recombination Resolution Defect in Werner Syndrome. *Mol. Cell. Biol.* **22,** 6971–6978 (2002).

363. He, H. & Sun, Y. Ribosomal protein S27L is a direct p53 target that regulates apoptosis. *Oncogene* **26,** 2707–2716 (2007).

364. Li, J. *et al.* Ribosomal protein S27-like, a p53-inducible modulator of cell fate in response to genotoxic stress. *Cancer Res.* **67,** 11317–26 (2007).

365. Xiong, X. *et al.* Ribosomal protein S27-like is a physiological regulator of p53 that suppresses genomic instability and tumorigenesis. *Elife* **3,** e02236 (2014).

366. Sommers, J. A. *et al.* p53 modulates RPA-dependent and RPA-independent WRN helicase activity. *Cancer Res.* **65,** 1223–1233 (2005).

367. Blander, G. *et al.* Physical and functional interaction between p53 and the Werner's syndrome protein. *J. Biol. Chem.* **274,** 29463–9 (1999).

368. Ishida, N. *et al.* Ubiquitylation of Ku80 by RNF126 Promotes Completion of Nonhomologous End Joining-Mediated DNA Repair. *Mol. Cell. Biol.* **37,** 1–16 (2017).

369. Otsuki, M. *et al.* WRN counteracts the NHEJ pathway upon camptothecin exposure. *Biochem. Biophys. Res. Commun.* **355,** 477–482 (2007).

8. Appendix

Appendix Table 1 List of primers used

Primer ID	Primer Sequence
RS040	TTAGTACGGCAATTAAAAGAAAGCTGCTTTTCAGTCAAGACGGATCCCCGGGTTAATTAA
RS041	GGAGAGAAAAAAGGCAGTGCGGGTAACTGAGATGTTTTCAGAATTCGAGCTCGTTTAAAC
RS051	AGCCGAAAGATGTCCAGGTC
RS055	GCTAGGCTCTCAACCCCAAG
RS058	GGCACAGGACTTGGAGTTCT
RS060	GGTCAGTCAATACCATGTCCCA
RS083	AGCTCGGTACCCGGGGATCCTCTAGAGGCGCGCCCGACCCCAGATGAAGGTGAG
RS085	AAAATTCATCCGGTACCATAACTTCGTATAATGTATGCTATACGAAGTTATAATTCTACCGGGTAGGGGAGGCG
RS088	GCTATGACCATGATTACGCCAAGCTTGCGGCCGCTACCCCATGCTGTCCCACTA
RS095	ACCGTGTTGATGTGGAAAGTAGTC
RS096	AAACGACTACTTTCCACATCAACA
RS097	ACCGCATCGCATCTGCCGTTCTCT
RS098	AAACAGAGAACGGCAGATGCGATG
RS118	TGACCATGATTACGCCAAGCTTGGTACCGGATGAATTTTGCAGCGTGGA
RS119	TGACCATGATTACGCCAAGCTTGTCGACATAACTTCGTATAGCATACATTATACGAAGTTATCACACAAAAAACCAACACACAGATCC
RS121	GACAGCTGTCGCCCCGAGGAAGA
RS122	TCTTCCTCGGGGCGACAGCTGTC
RS125	GACAGCTGTCGAACCGAGGAAGA
RS126	TCTTCCTCGGTTCGACAGCTGTC
RS140	TACGAAGTTATGTCGACAAGTGAAGATACCACACCATCCCTG
RS141	GATCAGGATGATCTGGACGAA
RS148	GGGGAACTTCCTGACTAGGG
RS204	TCAAGTTGATAACGGACTAGCCT
RS208	TTTCTTGGGTAGTTTGCAGTTTT
RS217	AATGATACGGCGACCACCGAGATCTACACTCTTTCCCTACACGACGCTCTTCCGATCTTCAAGTTGATAACGGACTAGCCT
RS218	CAAGCAGAAGACGGCATACGAGATGACGTCGAGTGACTGGAGTTCAGACGTGTGCTCTTCCGATCTTTT

	CTTGGGTAGTTTGCAGTTTT
RS219	CAAGCAGAAGACGGCATACGAGATTAGCTGCAGTGACTGGAGTTCAGACGTGTGCTCTTCCGATCTTTTC TTGGGTAGTTTGCAGTTTT
RS220	CAAGCAGAAGACGGCATACGAGATTAGCGAGTGTGACTGGAGTTCAGACGTGTGCTCTTCCGATCTTTT CTTGGGTAGTTTGCAGTTTT
RS221	CAAGCAGAAGACGGCATACGAGATGTAGCTCCGTGACTGGAGTTCAGACGTGTGCTCTTCCGATCTTTTC TTGGGTAGTTTGCAGTTTT
RS222	CAAGCAGAAGACGGCATACGAGATTACTACGCGTGACTGGAGTTCAGACGTGTGCTCTTCCGATCTTTTC TTGGGTAGTTTGCAGTTTT
RS223	CAAGCAGAAGACGGCATACGAGATGCAGCGTAGTGACTGGAGTTCAGACGTGTGCTCTTCCGATCTTTT CTTGGGTAGTTTGCAGTTTT
RS224	CAAGCAGAAGACGGCATACGAGATCTGCGCATGTGACTGGAGTTCAGACGTGTGCTCTTCCGATCTTTTC TTGGGTAGTTTGCAGTTTT
RS225	CAAGCAGAAGACGGCATACGAGATGAGCGCTAGTGACTGGAGTTCAGACGTGTGCTCTTCCGATCTTTT CTTGGGTAGTTTGCAGTTTT
RS226	CAAGCAGAAGACGGCATACGAGATCGCTCAGTGTGACTGGAGTTCAGACGTGTGCTCTTCCGATCTTTTC TTGGGTAGTTTGCAGTTTT
RS227	CAAGCAGAAGACGGCATACGAGATACTGATCGGTGACTGGAGTTCAGACGTGTGCTCTTCCGATCTTTTC TTGGGTAGTTTGCAGTTTT
RS228	AGCCTTATTTAAACTTGCTATGCTGTTTCCAGCATAGCTCTTAAAC

Appendix Table 2 Sequences of gRNAs used

gRNA ID	**Description**	**Sequence**
gRNA25	WDR76 knockout forward	TGTTGATGTGGAAAGTAGTC
gRNA26	WDR76 knockout reverse	CATCGCATCTGCCGTTCTCT
WRN gRNA1	WRN knockout forward	GTTCTACCGTGCCACTATTG
WRN gRNA2	WRN knockout reverse	TTAAAAATGGAAAGAAATCT

Appendix Table 3 List of antibodies used

All antibodies were diluted in 5% Milk in TBST.

Antibody	**Dilution**	**Species**	**Supplier**	**Catalog number**
GFP	1:2000	Mouse	Roche	11814460001
Ku80	1:2000	Mouse	Fischer Scientific worldwide	MS-285-P1
Ku70	1:400	Mouse	Abcam	ab3114
DDB1		Goat	Abcam	ab9194
CUL4A	1:20000	Rabbit	Abcam	ab92554
XRCC4	1:3000	Rabbit	Abcam	ab145
XLF	1:500	Rabbit	Abcam	ab33499
γH2AX	1:1000	Mouse	Merck-Millipore	05-636
GAPDH	1:30000	Mouse	Millipore	MAB374
WDR76	1:250	Rabbit	Atlas	HPA039804
ATM	1:5000	Rabbit	Abcam	ab32420
Cyclin A	1:5000	Rabbit	Santa Cruz Biotechnology	sc-751
Histone H3	1:500	Rabbit	Abcam	ab1791
CDT1	1:1000	Rabbit	Abcam	ab70829
pH3 ser10	1:5000	Mouse	Abcam	ab14955
FK2	1:1000	Mouse	Enzo Life Sciences	BML-PW8810
pATM S1981	1:1000	Rabbit	Epitomics	2152-1
H2AX	1:5000	Rabbit	Abcam	ab11175
pPAXX S148	1:200	Rabbit	Peptide1510021	1510021
PAXX	1:100	Goat	Abcam	ab126353
KAP1	1:5000	Rabbit	Abcam	ab10483
β-actin	1:5000	Mouse	Abcam	ab8226
MPM2	1:500	Mouse	Millipore	05-368
WRN	1:1000	Mouse	Abcam	ab66601

Anti-Goat IgG-HRP Secondary	1:10000	Donkey	Santa Cruz Biotechnology	sc-2020
Anti-Mouse IgG-HRP Secondary	1:10000	Donkey	Santa Cruz Biotechnology	sc-2314
Anti-Rabbit IgG-HRP Secondary	1:10000	Donkey	Santa Cruz Biotechnology	sc-2313

Appendix Table 4 Raw data from JACKS analysis of RPE-1 WT 2nM CPT treated

RPE-1 WT – DMSO and 2nM CPT treated enrichments compared to the day 14 control. fdr=false discovery rate.

Gene	Enrichment in DMSO	neg_fdr1	pos_fdr1	Enrichment in 2nM CPT	neg_fdr2	pos_fdr2	Difference in Enrichment
TP53	3.478343858	1	7.03E-10	5.147071467	1	0	1.668727609
RNF146	3.342174495	1	1.14E-08	2.8817172	1	4.63E-07	-0.460457294
CDKN1A	1.548402497	1	0.006661002	2.376541374	1	1.45529E-04	0.828138878
CAND1	3.251324882	1	9.85E-09	2.365157013	1	2.27E-05	-0.886167869
KEAP1	2.483000039	1	2.16E-05	2.280486616	1	5.60E-05	-0.202513423
PTEN	2.989153557	1	6.03E-08	2.262925838	1	5.59E-05	-0.726227719
NEDD8	1.316840385	0.997608314	0.052826231	1.812477712	0.997608314	0.012511861	0.495637327
H2AFZ	1.807149541	1	0.001542282	1.785069837	1	0.001542282	-0.022079704
RNF7	1.992484214	1	8.41E-05	1.774221477	1	3.96237E-04	-0.218262737
TINF2	1.100595288	0.999707723	0.033739	1.737620654	0.999707723	0.002630496	0.637025365
UBE2F	2.157784094	1	1.41307E-04	1.723118723	1	0.001928239	-0.43466537
NHP2	1.38567457	0.999210651	0.017170615	1.716903398	0.999210651	0.007104141	0.331228828
UBC	1.078420637	0.999658144	0.051744941	1.650039221	0.999658144	0.003275532	0.571618585
SCAF4	2.027124007	1	1.12026E-04	1.645565814	1	0.00093256	-0.381558193
ARID2	1.568928223	1	0.002943369	1.624229057	1	0.002943369	0.055300834
BRD7	1.222877703	1	0.02120377	1.617141085	1	0.010066749	0.394263382
DCUN1D3	1.710527193	1	0.00108847	1.603044843	1	0.002242041	-0.107482351
POLR2A	0.844985861	0.999743729	0.089551101	1.596495305	0.999743729	0.001625139	0.751509443
SOD1	0.795714541	0.995957182	0.297691842	1.592816233	0.995957182	0.03638536	0.797101691
THOC2	0.897782531	0.99942868	0.091272149	1.573142302	0.99942868	0.004594557	0.675359772
RPS27L	0.730379459	0.994490993	0.325118111	1.565018071	0.994490993	0.04729164	0.834638612
USP28	1.501057011	1	0.001295878	1.554639146	1	0.001113677	0.053582135
XRCC6	1.420821193	0.996425727	0.017788114	1.526103333	0.996425727	0.017788114	0.10528214
POLR2D	0.904087783	0.998352112	0.086472326	1.497041302	0.998352112	0.014830995	0.592953519
UPF1	1.123865534	0.99939939	0.019163465	1.483303992	0.99939939	0.003314716	0.359438458
HNRNPK	1.151021266	0.998457502	0.034694387	1.479347922	0.998457502	0.010137349	0.328326656
UBE2D3	0.74016914	0.996663275	0.319471661	1.476491438	0.996663275	0.026958571	0.736322298
POLR2E	1.219824327	0.999348419	0.037929435	1.474218168	0.999348419	0.013286426	0.25439384
BABAM1	1.274140118	1	0.0052029	1.461341137	1	0.002744091	0.187201019
POLR2G	1.040481506	0.998702537	0.047424725	1.453004293	0.998702537	0.008032543	0.412522788
CHEK2	1.061693034	1	0.018781658	1.446294455	1	0.003834671	0.38460142
CCNH	0.994625196	0.998363641	0.064727007	1.443935545	0.998363641	0.014727233	0.449310348
VCP	1.21433551	0.999408308	0.01031894	1.436229522	0.999408308	0.003025065	0.221894012
FANCD2	0.768656194	0.998603983	0.173537091	1.392286169	0.998603983	0.009756588	0.623629975
SUPT5H	1.246177214	0.999366891	0.00543512	1.390878121	0.999366891	0.003472975	0.144700906
MDM2	0.709913641	0.999296181	0.079859685	1.378700445	0.999296181	0.004918483	0.668786804
NPM1	0.877513543	0.987281768	0.202109067	1.367397953	0.987281768	0.114464086	0.489884411
PARG	1.224402373	0.995565538	0.042044953	1.346138689	0.995565538	0.03872594	0.121736316
MASTL	0.883977082	0.997129735	0.081320799	1.335632111	0.997129735	0.016672547	0.451655028
CCND1	0.823227575	0.996336636	0.12009587	1.335270642	0.996336636	0.027245401	0.512043067
RRM1	0.820813157	0.994380199	0.17057678	1.324012755	0.994380199	0.026712064	0.503199598
PPP4C	0.609274956	0.995421926	0.347698274	1.314252945	0.995421926	0.021822068	0.704977989
COPS4	0.927344964	0.996519824	0.081713373	1.301229451	0.996519824	0.025235778	0.373884487
PPP4R2	0.861925299	0.992153067	0.150266243	1.298020327	0.992153067	0.0706224	0.436095028
TICRR	0.780954623	0.998537571	0.104551121	1.296869578	0.998537571	0.013161865	0.515914955
TRIP13	1.067703935	0.996766587	0.066606999	1.290225504	0.996766587	0.020665527	0.222521569
CDK4	0.866901776	0.994950855	0.125128634	1.285271644	0.994950855	0.045442305	0.418369868
H2AFX	0.944368353	0.998598322	0.040684137	1.278443754	0.998598322	0.009308027	0.334075401
SMC4	1.019371979	0.997535657	0.029737842	1.27160191	0.997535657	0.022179091	0.252229931
POLR2I	1.161224126	0.999089699	0.013897347	1.27097241	0.999089699	0.006941804	0.109748284
SMC1A	1.051782928	0.992995034	0.063262757	1.26811206	0.992995034	0.063044692	0.216329132
DKC1	0.83340222	0.996300223	0.126259375	1.268096083	0.996300223	0.033297997	0.434693863
WAPL	1.22277863	0.991839751	0.028081849	1.262117555	0.991839751	0.028081849	0.039338925
SMC2	1.180896449	0.99918801	0.008957961	1.260094844	0.99918801	0.005367751	0.079198395
PCNA	0.638126227	0.996830336	0.244456705	1.257174987	0.996830336	0.015933777	0.619048761
UBE2I	1.001190375	0.996570528	0.060585709	1.250888446	0.996570528	0.023703545	0.249698072
GPS1	0.596238841	0.991719994	0.35462115	1.24984891	0.991719994	0.07316407	0.653610069
CUL3	2.544711008	1	5.87E-08	1.249203857	1	0.011268217	-1.295507151
RAD21	0.793491497	0.992826602	0.169308031	1.243742132	0.992826602	0.063919118	0.450250635
COPS6	0.812914627	0.995788736	0.12361223	1.228463324	0.995788736	0.037901373	0.415548697
USP7	0.630685863	0.997173314	0.210344337	1.224209893	0.997173314	0.025440178	0.59352403
PLK1	0.719615666	0.998089148	0.117179068	1.223724497	0.998089148	0.014438922	0.504108831
ASCC1	1.277043384	0.999128493	0.00594499	1.222664549	0.999128493	0.008071274	-0.054378835
STAG2	1.526033493	0.999999998	0.003144522	1.202067732	0.999999998	0.016716466	-0.323965761
SFPQ	1.159703742	0.997777455	0.014166462	1.201488627	0.997777455	0.014166462	0.041784886
CUL5	1.497920684	1	0.00186744	1.176298984	1	0.009052039	-0.3216217
ATR	0.954095586	0.99380791	0.074905632	1.170592214	0.99380791	0.055728814	0.216496628
ERCC6L	1.09147551	0.995790705	0.024750777	1.166766388	0.995790705	0.024750777	0.075290878
SMC5	0.633037318	0.99410568	0.265722904	1.165491358	0.99410568	0.053048884	0.53245404
MDM4	0.869317978	0.999708607	0.027373616	1.163158198	0.999708607	0.005709912	0.29384022
POLR2H	0.815835883	0.997758477	0.068571978	1.155606006	0.997758477	0.020173711	0.339770123
PNN	0.834358345	0.997902515	0.044707643	1.140491177	0.997902515	0.012646814	0.306132832
TERF2	0.731185088	0.977439919	0.275266616	1.134441037	0.977439919	0.116369333	0.40325595

POLD3	0.750650972	0.999843055	0.023063205	1.133748119	0.999843055	0.005585801	0.383097148
APEX2	0.499736041	0.993601958	0.427304879	1.132355275	0.993601958	0.045902673	0.632619234
USP37	0.651572418	0.993616294	0.19983209	1.13051416	0.993616294	0.042914486	0.478941742
TEP1	0.934910019	0.9949726	0.039248942	1.12147119	0.9949726	0.039248942	0.186561172
DCLRE1B	0.69692639	0.987281035	0.235747477	1.113693131	0.987281035	0.063407231	0.416766741
CHAF1A	0.873093909	0.995065372	0.06059186	1.1107891	0.995065372	0.035416204	0.237695191
POLR2L	0.678906203	0.987939077	0.225688715	1.109801638	0.987939077	0.084695833	0.430895435
POLA1	0.902565703	0.992727618	0.06890491	1.104647162	0.992727618	0.065451436	0.202081459
USP5	0.647932938	0.993647465	0.192219458	1.103328188	0.993647465	0.031033385	0.455395249
RUVBL1	0.683546411	0.990871965	0.212939865	1.097113419	0.990871965	0.082152319	0.413567009
UBE2T	0.732915298	0.982067098	0.269670205	1.096963692	0.982067098	0.104776972	0.364048394
TOP1	0.794316168	0.995683636	0.098703312	1.094202873	0.995683636	0.026655039	0.299886705
MAPK8	0.987010362	0.999525364	0.041435367	1.081846805	0.999525364	0.041435367	0.094836442
RPAIN	0.660322488	0.993352226	0.180150532	1.076282899	0.993352226	0.031759254	0.41596041
DNAJC2	0.64827602	0.994253356	0.253706572	1.073528365	0.994253356	0.060616228	0.425252345
TTI2	0.448339822	0.98798189	0.494958822	1.072509602	0.98798189	0.057028021	0.62416978
UBA3	1.080529152	0.994051665	0.028282293	1.063243401	0.994051665	0.028282293	-0.017285751
CHD3	0.995587622	0.991912216	0.028208578	1.056403021	0.991912216	0.028208578	0.0608154
TP53BP1	1.164112135	1	0.019079977	1.054676479	1	0.022022593	-0.109435656
APAF1	0.9340822	0.999769105	0.045435651	1.050455264	0.999769105	0.039783768	0.116373064
NCAPD2	0.835052204	0.993107623	0.091277018	1.047960492	0.993107623	0.062031394	0.212908288
POLL	1.023597645	0.995018218	0.033412652	1.047835562	0.995018218	0.033412652	0.024237917
BRCA2	0.692271982	0.996405184	0.056377273	1.045421976	0.996405184	0.016202843	0.353149994
SMG1	0.778542329	0.987292224	0.1227647	1.041164829	0.987292224	0.067803378	0.2626225
HDAC3	0.367283077	0.973752172	0.721775953	1.03407496	0.973752172	0.185745615	0.666791883
BRE	1.202639487	0.999999447	0.016665748	1.03378383	0.999999447	0.031759935	-0.168855657
PPP4R3B	0.917753086	0.993541008	0.043391854	1.026217236	0.993541008	0.038987578	0.10846415
SENP8	1.397902065	1	0.018598027	1.021660563	1	0.071898413	-0.376241502
ASF1A	1.004582547	0.992322994	0.034672897	1.016567014	0.992322994	0.034672897	0.011984467
THRAP3	0.993672044	1	0.049885242	1.009470709	1	0.049885242	0.015798665
KAT8	0.313370111	0.971895592	0.732243619	1.003058995	0.983369007	0.149678934	0.689688884
SCAF11	0.893994862	0.986336654	0.065113885	0.99912987	0.986336654	0.065113885	0.105135008
APC	0.950329669	1	0.018941734	0.99843253	1	0.018941734	0.04810286
TONSL	0.65221681	0.984422249	0.217480272	0.994617799	0.984422249	0.100426795	0.342400989
POLE2	0.627275302	0.995019808	0.177439228	0.994443602	0.995019808	0.047078383	0.3671683
CHEK1	0.571655384	0.980397889	0.380679277	0.991814227	0.980397889	0.117866344	0.420158843
XAB2	0.57591632	0.992620544	0.216069106	0.985814455	0.992620544	0.047838964	0.409898135
NCAPD3	0.466598138	0.985103036	0.277419456	0.979018278	0.985103036	0.070961265	0.51242014
SUPT4H1	0.701185205	0.980619787	0.277921111	0.973487398	0.980619787	0.137983536	0.272302193
HDAC9	1.004834047	0.999999739	0.031717342	0.969455487	0.999999739	0.031717342	-0.03537856
NonTargetingC	1.053700789	0.99999303	0.044109855	0.968743708	0.99999303	0.046400078	-0.08495708
MAPKAPK2	1.052642319	1	0.033510011	0.968173121	1	0.043107646	-0.084469198
RUVBL2	0.488938307	0.995203032	0.311492839	0.965287131	0.995203032	0.035371872	0.476348824
RBX1	0.939828133	0.98131896	0.097311233	0.961247747	0.98131896	0.097311233	0.021419614
XRCC5	0.678004709	0.986959415	0.107422336	0.960492843	0.986959415	0.073694186	0.282488135
CDK9	0.647511273	0.974297575	0.326920002	0.950730783	0.974297575	0.190145135	0.30321951
GTF2H1	0.765687306	0.985989059	0.114474111	0.950198189	0.985989059	0.090181841	0.184510883
DCLRE1A	1.055831103	0.999578127	0.037537926	0.942722577	0.999578127	0.037537926	-0.113108526
POLR2K	0.553599397	0.950612481	0.466559829	0.940169905	0.950612481	0.444487672	0.386570508
RNF126	0.729115717	0.98261248	0.109412227	0.938872003	0.98261248	0.083640997	0.209756286
UBE2W	0.876941483	0.991327705	0.029246599	0.937995468	0.991327705	0.029246599	0.061053985
MTA2	0.966456629	0.999859602	0.040785377	0.935385156	0.999859602	0.040785377	-0.031071473
BCLAF1	0.931145382	1	0.096179445	0.934032771	1	0.096179445	0.002887389
BCCIP	0.444198368	0.971715887	0.516373643	0.926439007	0.971715887	0.145883047	0.482240638
SMARCB1	0.37323629	0.958125566	0.727687149	0.926300262	0.958125566	0.376869904	0.553063973
EP300	0.972588809	1	0.040019774	0.919751529	1	0.040019774	-0.05283728
PHIP	1.190806885	1	0.018075463	0.916246583	1	0.037564294	-0.274560302
ACD	0.61831279	0.982712271	0.265566728	0.907540729	0.982712271	0.126892223	0.28922794
POLD1	0.665823754	0.975782143	0.189344575	0.907308826	0.975782143	0.120412834	0.241485072
DNA2	0.483948473	0.973856355	0.488303297	0.903913057	0.973856355	0.160991679	0.419964584
SPTBN1	0.886349276	1	0.039491377	0.899216561	1	0.039491377	0.012867285
TAF1	0.559692212	0.960873048	0.35466535	0.893400403	0.960873048	0.352142565	0.333708191
SPRTN	0.720521563	0.991903735	0.092452466	0.89119599	0.991903735	0.043053879	0.170674427
UBA2	0.394634327	0.971728077	0.574803006	0.888609157	0.971728077	0.25444731	0.493974829
PPM1D	0.356217552	0.978428922	0.656240543	0.881960648	0.978428922	0.097824862	0.525743097
MMS22L	0.443912075	0.993358946	0.316429493	0.877973182	0.993358946	0.059769482	0.434061107
DTX4	0.768386081	0.999941958	0.048127349	0.87394936	0.999941958	0.039358656	0.10556328
COPS3	0.644020139	0.988603626	0.215172887	0.871858795	0.988603626	0.1339793	0.227838656
PCID2	0.448915706	0.967975412	0.478618712	0.870158424	0.967975412	0.153627593	0.421242718
GAR1	0.607701084	0.971597461	0.245209734	0.857451133	0.971597461	0.139906761	0.249750049
RAD51	0.346951985	0.961409067	0.70174548	0.856107413	0.961409067	0.237484521	0.509155428
ERCC3	0.259299845	0.90174041	0.895939043	0.853554863	0.951370037	0.387855137	0.594255018
SF3B1	0.396857231	0.985254946	0.167453355	0.850707806	0.985254946	0.055963987	0.453850575
PRPF19	0.368630712	0.975059426	0.572795487	0.850436497	0.975059426	0.163494597	0.481805785
TET2	0.961352491	0.999998163	0.053624086	0.848471352	0.999998163	0.056909985	-0.112881138
RPA1	0.442165533	0.95627332	0.541128882	0.844467171	0.95627332	0.225500397	0.402301638
CCND3	0.780095793	0.99943543	0.03918954	0.839555006	0.99943543	0.035744217	0.059459213
UCHL3	0.734197915	0.990060866	0.101431848	0.839358628	0.990060866	0.101431848	0.105160714
NCAPH2	0.319972736	0.958320243	0.757017051	0.836749467	0.958320243	0.375117812	0.516776731
COPS8	0.535714299	0.942254364	0.547492294	0.83530871	0.942254364	0.355310586	0.299594411
NonTargetingC	0.606066621	0.99983586	0.147679814	0.834837094	0.99983586	0.071219003	0.228770473
PNKP	0.6016236	0.986698291	0.237818407	0.831435941	0.986698291	0.10674828	0.229812341

DAXX	0.457122673	0.973070034	0.417385363	0.827398984	0.973070034	0.125803507	0.370276311
NCAPG2	0.353751211	0.964674732	0.648837051	0.823715714	0.964674732	0.248514921	0.469964503
HUWE1	0.334594436	0.973696627	0.616699647	0.817591211	0.973696627	0.236730356	0.482996775
UBA1	0.473635204	0.978447394	0.374095522	0.817093032	0.978447394	0.109264778	0.343457828
DDX11	0.940904613	0.977610396	0.148517407	0.813717107	0.977610396	0.148517407	-0.127187505
L3MBTL1	0.854595326	0.999081574	0.034925472	0.80787945	0.999081574	0.038363016	-0.046715876
ACTL6A	0.358286421	0.970335202	0.609068499	0.807417912	0.970335202	0.221222324	0.449131491
GADD45G	0.767118456	0.999993748	0.109459973	0.807414798	0.999993748	0.109459973	0.040296343
SUPT6H	0.474132851	0.974460321	0.366703068	0.79248361	0.974460321	0.229857111	0.318350758
ABL1	0.672014131	0.999996573	0.098284978	0.791247889	0.999996573	0.087390741	0.119233758
WEE1	0.600200634	0.971297942	0.233526736	0.790030705	0.971297942	0.233526736	0.189830071
ALKBH2	0.746975538	0.987312972	0.123447394	0.786951639	0.987312972	0.123447394	0.039976101
XRCC2	0.467780347	0.962583472	0.408856284	0.785919281	0.962583472	0.336748755	0.318138935
GTF2H3	0.252724093	0.928549406	0.83338472	0.776053402	0.95911275	0.292084438	0.523329309
RFC2	0.468266061	0.937529267	0.519520376	0.763744928	0.937529267	0.394048838	0.295478867
FANCI	0.451293692	0.938329569	0.525008094	0.763430898	0.938329569	0.347230403	0.312137205
SSBP3	0.869913407	0.993437983	0.124852644	0.755743977	0.993437983	0.124852644	-0.11416943
STN1	0.385883857	0.96521081	0.525693718	0.753858085	0.96521081	0.177040794	0.367974228
EYA1	0.760901764	0.990056724	0.085153923	0.751386126	0.990056724	0.085153923	-0.009515637
POLR2F	0.430626457	0.963045892	0.427068794	0.749887627	0.963045892	0.305987292	0.319261171
BRCA1	0.550838477	0.955113721	0.283203934	0.748118653	0.955113721	0.262227722	0.197280176
RPA3	0.334188058	0.948213769	0.69465913	0.745662903	0.948213769	0.251679352	0.411474845
CSNK1D	0.582612508	0.998727585	0.105453163	0.744974884	0.998727585	0.105453163	0.162362376
THOC1	0.376679817	0.977654268	0.511834518	0.737540124	0.977654268	0.158664095	0.360860307
MNAT1	0.326048196	0.937788527	0.811826771	0.733528547	0.953900783	0.37848029	0.407480351
GTF2H4	0.447515912	0.960760387	0.388348798	0.73321825	0.960760387	0.223851421	0.285702338
BRCC3	1.10574645	0.99999999	0.063021436	0.732261474	0.99999999	0.129582776	-0.373484975
NOP10	0.280743976	0.943532357	0.798424501	0.731713087	0.972454592	0.234961302	0.450969111
COPS2	0.568854641	0.972442529	0.21942953	0.730050177	0.972442529	0.21942953	0.161195536
ATMIN	0.504352778	0.945798935	0.407700882	0.729387177	0.945798935	0.392876994	0.225034399
SERBP1	0.531703972	0.936111565	0.358438756	0.719040141	0.936111565	0.358438756	0.18733617
SMARCE1	0.656105281	0.953730866	0.239854599	0.71802606	0.953730866	0.239854599	0.06192078
SCAF8	0.490131615	0.997827855	0.175836763	0.715460582	0.997827855	0.162676815	0.225328967
MTOR	0.367836152	0.97405185	0.483736938	0.712015585	0.97405185	0.233533351	0.344179434
POLR2J	0.718039456	0.996488758	0.151021882	0.711130105	0.996488758	0.151021882	-0.006909352
OR1E1	0.493094137	0.985974094	0.248132441	0.703764693	0.985974094	0.248132441	0.210670556
GTF2H2	0.825960389	0.983875327	0.298260716	0.703362831	0.983875327	0.298260716	-0.122597559
POLM	0.707251649	0.999967463	0.066705271	0.703353604	0.999967463	0.066705271	-0.003898045
PMS2	0.67722614	0.962221154	0.15340566	0.694324152	0.962221154	0.15340566	0.017098012
CSNK2A2	0.50986497	0.999868116	0.163497721	0.693841516	0.999868116	0.122707864	0.183976546
RAD54L2	0.528436525	0.99939853	0.175195409	0.691670814	0.99939853	0.162887868	0.163234289
YBX1	0.13271515	0.743065398	0.999992389	0.69050688	0.840390641	0.795249761	0.55779173
NSMCE1	0.187589796	0.867557448	0.975699288	0.689956778	0.955246461	0.204691963	0.502366982
PRMT1	0.376784763	0.954860129	0.508823395	0.689413228	0.954860129	0.304772787	0.312628466
CCNB3	0.717691187	0.999788155	0.076506761	0.68796922	0.999788155	0.078724611	-0.029721968
ECT2	0.514413137	0.945441559	0.314002487	0.683651823	0.945441559	0.278317049	0.169238686
PMP22	0.633250013	0.999994455	0.152606457	0.683306967	0.999994455	0.152606457	0.050056954
MCRS1	0.579872089	0.962567628	0.238472544	0.681185755	0.962567628	0.237193944	0.101313666
RECQL	0.870503241	0.991266977	0.106949165	0.675834637	0.991266977	0.149410788	-0.194668604
RAD1	0.323759743	0.901107482	0.81722643	0.672641228	0.901107482	0.447352348	0.348881485
NonTargetingC	0.462116891	0.998943602	0.209028753	0.671242646	0.998943602	0.192844466	0.209125755
NonTargetingC	0.500963774	0.995789702	0.150159785	0.670490353	0.995789702	0.150159785	0.169526579
CHD4	0.349677869	0.948970665	0.557518574	0.665545924	0.948970665	0.318866757	0.315868055
USP51	0.515818535	0.999505252	0.193741697	0.662421834	0.999505252	0.162255581	0.146603299
BCAS2	0.393516836	0.952015502	0.519345734	0.658760236	0.952015502	0.321132075	0.2652434
NUDT1	0.514664269	0.946357521	0.256553735	0.658263215	0.946357521	0.243187598	0.143598947
LIG1	0.408442556	0.95099314	0.546549017	0.649189796	0.95099314	0.396067329	0.24074724
SETX	0.638301636	0.956660985	0.104585117	0.648472029	0.956660985	0.104585117	0.010170393
NonTargetingC	0.499186756	0.999991775	0.217961669	0.646419952	0.999991775	0.168050263	0.147233196
RBBP8	0.501838356	0.96332858	0.333322767	0.644656332	0.96332858	0.290947083	0.142817976
NonTargetingC	0.67970672	0.999344463	0.161848152	0.637643683	0.999344463	0.161848152	-0.042063037
SIRT6	0.580681507	0.933946592	0.319914192	0.630212922	0.933946592	0.319914192	0.049531415
KMT5B	0.648701797	0.999968266	0.103565356	0.625871686	0.999968266	0.103565356	-0.022830111
CHFR	0.405361716	0.999662265	0.215805398	0.625034354	0.999662265	0.171961903	0.219672638
PBRM1	0.687943917	1	0.135051244	0.624538789	1	0.135202919	-0.063405128
POLD2	0.256301144	0.945471268	0.733883653	0.616060847	0.945471268	0.428514497	0.359759703
CDCA5	0.471446315	0.953015111	0.410465928	0.615861184	0.953015111	0.355940538	0.144414869
SUMO4	0.463018295	0.958853859	0.212663185	0.615268418	0.958853859	0.153849462	0.152250124
NonTargetingC	0.471570905	0.999257052	0.158280513	0.614000768	0.999257052	0.158280513	0.142429863
NOTCH3	0.629412445	0.994536715	0.114422057	0.608581735	0.994536715	0.114422057	-0.02083071
APOBEC2	0.606607318	0.999739009	0.145825187	0.608502379	0.999739009	0.145825187	0.001895062
PPP6C	0.216168934	0.901738276	0.895944022	0.60778159	0.927447893	0.543269057	0.391612655
KMT5C	0.619178579	0.999795972	0.133164186	0.606664817	0.999795972	0.133164186	-0.012513762
NFATC2IP	0.464750009	0.947512601	0.218206324	0.600491592	0.947512601	0.218206324	0.135741583
BRD4	0.366077075	0.954687836	0.459386861	0.598675345	0.954687836	0.228469914	0.23259827
SMARCA4	0.37031933	0.921918975	0.347630633	0.595859949	0.921918975	0.339227283	0.22554062
INO80E	0.599795954	0.915057453	0.305161286	0.593057419	0.915057453	0.305161286	-0.006738535
TERF1	0.300716598	0.891230903	0.881866827	0.592116642	0.891230903	0.686687749	0.291400044
NonTargetingC	0.804925962	0.999981145	0.09448797	0.591144854	0.999981145	0.137054504	-0.213781108
SIRT5	0.510897261	0.999831869	0.149802239	0.589844187	0.999831869	0.149802239	0.078946926
DMC1	0.73527993	0.999556483	0.074692826	0.58979586	0.999556483	0.127130625	-0.14548407
ANKRD52	0.392471217	0.919276861	0.538245639	0.587931635	0.919276861	0.36346902	0.195460418

POLN	0.60916456	0.999765812	0.160303789	0.579903119	0.999765812	0.160303789	-0.029261441
USP15	0.757389347	1	0.065138382	0.579781047	1	0.109662027	-0.177608301
NSMCE3	0.048877426	0.698453842	0.999991203	0.577917855	0.898066455	0.917401907	0.529040428
GPI	0.215464397	0.999992441	0.31817114	0.577055642	0.999992441	0.178502918	0.361591244
DUT	0.532754467	0.963292454	0.264972384	0.575518723	0.963292454	0.264972384	0.042764256
WDR70	0.274001952	0.919984796	0.444759693	0.575203873	0.919984796	0.444759693	0.30120192
NEIL1	0.414464269	0.967157443	0.197009555	0.573720389	0.967157443	0.189189276	0.15925612
TIMELESS	0.402455917	0.904159214	0.506353162	0.570079166	0.904159214	0.453628084	0.167623249
USP11	0.538775995	0.977479353	0.153262321	0.558588707	0.977479353	0.153262321	0.019812712
APOBEC3C	0.651966331	0.995992372	0.161640284	0.556137138	0.995992372	0.161640284	-0.095829193
TRIP12	0.509089587	0.999977382	0.190500439	0.556077224	0.999977382	0.190500439	0.046987636
CDC25A	0.355230262	0.999910282	0.237963608	0.555564563	0.999910282	0.191855954	0.200334301
PHF11	0.5548391	0.968480013	0.214912858	0.554665489	0.968480013	0.214912858	-1.73611E-04
KAT2B	0.68996412	0.998273194	0.149539643	0.552755272	0.998273194	0.190016003	-0.137208848
COL1A1	0.366080096	0.911479638	0.541344177	0.549337967	0.911479638	0.460714715	0.183257871
PHF3	0.455625991	0.999371961	0.143769059	0.547359659	0.999371961	0.143769059	0.091733668
CUL9	0.419968504	0.91141591	0.465315529	0.542160285	0.91141591	0.465315529	0.12219178
CIB1	0.618150028	0.992548413	0.139868079	0.541860811	0.992548413	0.139868079	-0.076289217
UBE2R2	0.855975926	1	0.067788305	0.54117677	1	0.145224292	-0.314799156
UBE2D1	0.526864285	0.999939613	0.17954647	0.53876379	0.999939613	0.17954647	0.011899504
SMARCD1	0.525308641	0.999812917	0.137079121	0.536070378	0.999812917	0.137079121	0.010761737
MGMT	0.499961864	0.992856975	0.198492016	0.535517934	0.992856975	0.198492016	0.035556071
CHD1L	0.280722827	0.999838881	0.293622209	0.533575535	0.999838881	0.232137854	0.252852709
XPC	0.499630599	0.991484933	0.201804197	0.532741316	0.991484933	0.201804197	0.033110717
NOTCH4	0.534518463	0.977380485	0.170484673	0.531290536	0.977380485	0.170484673	-0.003227928
APOBEC1	0.734016869	0.956864874	0.234856141	0.530697279	0.956864874	0.234856141	-0.20331959
HNRNPUL1	0.391382272	0.981160424	0.318235111	0.522569156	0.981160424	0.318235111	0.131186884
KAT5	0.255786644	0.939740242	0.67560114	0.520305005	0.939740242	0.347298061	0.26451836
MCM10	0.464674147	0.90263807	0.293246413	0.519972377	0.90263807	0.293246413	0.05529823
RAD54B	0.632748934	0.984425058	0.210337492	0.518024866	0.984425058	0.227586521	-0.114724068
CDK7	-0.071350577	0.578927962	0.999996104	0.516500541	0.819337633	0.882138893	0.587851118
TPP1	0.473110787	0.998535295	0.168111978	0.514244703	0.998535295	0.168111978	0.041133916
TRRAP	0.328885638	0.881436828	0.64564017	0.511185861	0.881436828	0.64564017	0.182300223
RNF138	0.457038629	0.999989483	0.198265834	0.510371562	0.999989483	0.198265834	0.053332933
MORF4L1	0.563658653	0.994177809	0.199108881	0.508717093	0.994177809	0.199873662	-0.05494156
UBE2V2	0.423879572	0.999897557	0.188967762	0.504683589	0.999897557	0.183107207	0.080804018
UBE2D4	0.462303142	0.907990743	0.308397143	0.503777345	0.907990743	0.308397143	0.041474203
RAG2	0.626378518	0.937786552	0.240309256	0.500639592	0.937786552	0.240309256	-0.125738926
CBX5	0.366269036	0.913303254	0.48031268	0.500353207	0.913303254	0.48031268	0.134084171
RECQL4	0.613534021	0.880369061	0.595715041	0.498982489	0.880369061	0.595715041	-0.114551532
CTCF	0.122634174	0.784405204	0.999918614	0.498400393	0.868529592	0.614396517	0.375766219
NOTCH2	0.510715064	0.91600724	0.344733419	0.496378634	0.91600724	0.344733419	-0.01433643
SMC6	0.167952582	0.820466401	0.999345574	0.49276331	0.886668239	0.684501774	0.324810728
EME1	0.526170666	0.900026124	0.209613513	0.492227079	0.900026124	0.209613513	-0.033943587
HELB	0.568693343	0.99823044	0.173793352	0.490040257	0.99823044	0.173793352	-0.078653086
MORF4L2	0.399172218	0.909420079	0.401249076	0.482280869	0.909420079	0.401249076	0.083108651
ATXN3	0.298619174	0.999887003	0.248271682	0.482053423	0.999887003	0.235765562	0.183434249
NEK9	0.476432151	0.99995695	0.192826201	0.48160664	0.99995695	0.192826201	0.005174489
SKP1	0.72028588	0.9118113	0.411038191	0.480008109	0.9118113	0.55250199	-0.240277771
REV3L	0.210023169	0.868753474	0.932761344	0.477629597	0.868753474	0.788736013	0.267606428
FBXO18	0.529714634	0.999245999	0.182890444	0.475887294	0.999245999	0.182890444	-0.05382734
FAM175A	0.475283203	0.987271407	0.244612063	0.472513313	0.987271407	0.244612063	-0.002769891
USP47	0.446509119	0.996708864	0.31463378	0.469347993	0.996708864	0.31463378	0.022838874
HPF1	0.396970933	0.942247654	0.482518472	0.468252681	0.942247654	0.482518472	0.071281748
NonTargetingC	0.607242373	0.999896743	0.199662611	0.46347788	0.999896743	0.199662611	-0.143764493
WRNIP1	0.32049541	0.995688479	0.305766406	0.461251274	0.995688479	0.230312625	0.140755864
MVP	0.316961898	0.881549393	0.324692981	0.460545732	0.881549393	0.324692981	0.143583834
NonTargetingC	0.314520653	0.999748986	0.285754435	0.458787573	0.999748986	0.239880679	0.14426692
POLD4	0.325040377	0.846632852	0.684444735	0.457087069	0.846632852	0.684444735	0.132046692
RRM2	0.04018955	0.686176125	0.999998419	0.456028331	0.837413672	0.82022985	0.415838781
DDB1	0.051937277	0.703881747	1	0.453515238	0.843925082	0.986091054	0.40157796
NONO	0.317595834	0.924561884	0.677445624	0.451928718	0.924561884	0.647037783	0.134332884
NonTargetingC	0.50853398	0.999346524	0.207882263	0.451307325	0.999346524	0.207882263	-0.057226655
RNF2	0.427654003	0.999627895	0.27250104	0.450762275	0.999627895	0.27250104	0.023108272
CBX1	0.233113527	0.818043684	0.73796149	0.447070827	0.818043684	0.73796149	0.2139573
CSNK2B	0.267964331	0.925706318	0.814131287	0.446772199	0.925706318	0.779983575	0.178807867
PDS5A	0.223515701	0.881387988	0.943428028	0.446355887	0.903669151	0.747192437	0.222840186
RFC1	0.418056179	0.870530865	0.493337784	0.445726261	0.870530865	0.493337784	0.027670082
C9orf142	0.431925396	0.955815087	0.345532622	0.445515319	0.955815087	0.345532622	0.013589923
RAD51D	0.324252353	0.892670296	0.59099305	0.445427251	0.892670296	0.524784962	0.121174897
NonTargetingC	0.340278519	0.999944922	0.231304551	0.44316637	0.999944922	0.17984537	0.102887851
SIRT1	0.31689217	0.999600581	0.201449853	0.441973199	0.999600581	0.161515408	0.125081028
NEIL2	0.473125247	0.900745624	0.319866714	0.441030147	0.900745624	0.319866714	-0.0320951
NonTargetingC	0.554486916	0.999963084	0.155978914	0.440316589	0.999963084	0.155978914	-0.114170327
SFR1	0.401276155	0.81670404	0.6184974	0.438317301	0.81670404	0.6184974	0.037041146
CBX3	0.373231435	0.85241978	0.418979627	0.438278363	0.85241978	0.418979627	0.065046929
NABP2	0.592938669	0.995463463	0.162132468	0.438202643	0.995463463	0.238488437	-0.154736025
TOP3A	0.319739642	0.888644981	0.617350779	0.437836922	0.888644981	0.617350779	0.118097279
NELFB	0.326455677	0.92473282	0.614812545	0.436821867	0.92473282	0.614812545	0.11036619
COPS5	-0.244384407	0.404433415	0.999999992	0.436111781	0.812575703	0.961241786	0.680496188
ALDH2	0.537953486	0.97275521	0.275798753	0.434771805	0.97275521	0.275798753	-0.10318168
CUL7	0.546102568	0.999988816	0.163441994	0.433301867	0.999988816	0.182839298	-0.112800701

NonTargetingC	0.531076367	0.999999115	0.15579312	0.430043927	0.999999115	0.196061195	-0.101032441
DLGAP5	0.480816324	0.886341913	0.404700279	0.427621779	0.886341913	0.404700279	-0.053194545
DTX3L	0.495498776	0.99393549	0.250939498	0.422698428	0.99393549	0.25449819	-0.072800349
BRAT1	0.192455024	0.764885569	1	0.4189431	0.777359531	1	0.226488075
APTX	0.33897098	0.902305794	0.297388906	0.416739487	0.902305794	0.297388906	0.077768507
POT1	0.320688413	0.855717782	0.689061257	0.413581495	0.855717782	0.689061257	0.092893082
HDAC2	0.402738613	0.869520373	0.350883165	0.408529961	0.869520373	0.350883165	0.005791348
APLF	0.171434195	0.999572699	0.363502534	0.407066343	0.999572699	0.27377354	0.235632149
SIRT7	0.247455597	0.999664558	0.268494609	0.407006824	0.999664558	0.184380409	0.159551227
NonTargetingC	0.298967265	0.999895055	0.275815284	0.405983974	0.999895055	0.246418794	0.107016709
MAU2	-0.147011198	0.476696072	0.999999903	0.404915335	0.829245983	0.999999903	0.551926532
RNF111	0.504709692	0.999944988	0.188176928	0.402843904	0.999944988	0.194413077	-0.101865787
RNF8	0.16014603	0.802892438	0.996162079	0.401770936	0.802892438	0.960191821	0.241624906
PLRG1	0.309439362	0.857516336	0.68552123	0.401213084	0.857516336	0.68552123	0.091773722
MSH4	0.364146544	0.993583438	0.259161096	0.398148732	0.993583438	0.259161096	0.034002187
APOBEC3B	0.495681136	0.999967008	0.236724223	0.397779226	0.999967008	0.236724223	-0.097901909
RIF1	0.050419085	0.70734721	0.999998123	0.396552768	0.837438824	0.999998123	0.346133683
RAD51AP1	0.456931665	0.853380663	0.405176852	0.395344894	0.853380663	0.405176852	-0.061586771
SIRT4	0.257673676	0.909510653	0.374848148	0.395260671	0.909510653	0.309220548	0.137586995
ETAA1	0.322595837	0.999902643	0.221874002	0.394671315	0.999902643	0.221874002	0.072075478
RNF40	0.172548026	0.729677955	0.999986349	0.393773291	0.799178389	0.999986349	0.221225265
CDKN1B	0.32112048	0.999985514	0.28000831	0.393384972	0.999985514	0.277651111	0.072264492
FBXW7	0.574566033	0.999999997	0.085417617	0.39336848	0.999999997	0.155916677	-0.181197552
UNG	0.505883328	0.879170242	0.711741337	0.393148198	0.879170242	0.711741337	-0.11273513
PMS2P5	0.138202807	0.642106223	0.567006492	0.389535249	0.642106223	0.567006492	0.251332441
POLB	0.43192381	0.978148625	0.284457033	0.389073775	0.978148625	0.284457033	-0.042850035
UBE2V1	0.246067744	0.994675609	0.311815552	0.386276349	0.994675609	0.311815552	0.140208605
NSMCE4A	0.16462439	0.797276073	0.999942809	0.383594015	0.797276073	0.999942809	0.218969626
SETMAR	0.328957864	0.987364155	0.317835521	0.382624947	0.987364155	0.317664523	0.053667084
ATXN7	0.608538726	0.999322392	0.185430777	0.38193821	0.999322392	0.272883116	-0.226600516
OPRM1	0.401464041	0.999960465	0.208737076	0.379630819	0.999960465	0.208737076	-0.021833222
CLSPN	0.352877128	0.890889164	0.569936767	0.379519881	0.890889164	0.569936767	0.026642754
SSBP2	0.477726997	0.999223979	0.29651219	0.377744276	0.999223979	0.29651219	-0.099982721
POLI	0.458026212	0.870502638	0.359127809	0.377006201	0.870502638	0.359127809	-0.081020012
NonTargetingC	0.327835915	0.999999893	0.249756542	0.37420295	0.999999893	0.247258081	0.046367035
EP400	0.507184212	0.878030871	0.605255147	0.371851363	0.878030871	0.605255147	-0.13533285
PML	0.317368004	0.999831852	0.230662228	0.36918379	0.999831852	0.230662228	0.051815786
UBE2D2	0.393105956	0.926997804	0.271229486	0.369012697	0.926997804	0.271229486	-0.024093259
XRCC3	0.05203835	0.701483566	1	0.368384689	0.80264027	1	0.316346339
CCNB2	0.364482867	0.989274411	0.262865149	0.366758019	0.989274411	0.262865149	0.002275152
USP20	0.347646686	0.997002414	0.283895858	0.365057578	0.997002414	0.283895858	0.017410892
H3F3B	0.341607808	0.771063803	0.762949784	0.362618926	0.771063803	0.762949784	0.021011118
UBE2K	0.253967734	1	0.303014228	0.358417001	1	0.255826373	0.104449267
WDR76	0.279239542	0.892541247	0.274239745	0.358202341	0.892541247	0.274239745	0.078962799
SMARCA5	0.01820058	0.665372902	0.999784118	0.358129132	0.804649048	0.999784118	0.339928553
EXO5	0.193381234	0.775154374	0.966614507	0.357571894	0.798456092	0.966614507	0.16419066
CDC25B	0.342002859	0.844476651	0.635585585	0.356930621	0.844476651	0.635585585	0.014927762
SKIV2L2	0.10922438	0.791033887	0.788549952	0.35581037	0.791033887	0.788549952	0.24658599
DCUN1D2	0.333394694	0.967274579	0.312938999	0.355547276	0.967274579	0.312938999	0.022152582
FEN1	0.123433362	0.79899342	0.999973193	0.353708615	0.799238777	0.914509293	0.230275253
RAD9B	0.460246134	0.907235566	0.334368469	0.353457765	0.907235566	0.334368469	-0.106788369
RING1	0.420651615	1	0.220555776	0.352031738	1	0.239150381	-0.068619876
MSH3	0.349040835	0.986451479	0.310510777	0.351101713	0.986451479	0.310510777	0.002060879
HELLS	0.179866498	0.807778785	0.971985663	0.345545562	0.807778785	0.914990729	0.165679064
TOP2A	0.130692025	0.810893181	0.622751665	0.343851907	0.810893181	0.622751665	0.213159882
UBE2NL	0.309468499	0.944566022	0.338582809	0.343317528	0.944566022	0.338582809	0.03384903
FANCE	0.089604266	0.750727108	0.999512955	0.34310645	0.785751133	0.999512955	0.253502184
CDC34	0.234787574	0.943082939	0.317670536	0.341898512	0.943082939	0.317670536	0.107110937
MAPK14	0.27530326	0.999999645	0.374315111	0.339959188	0.999999645	0.366488828	0.064655928
HLTF	0.416922155	0.842836197	0.400106702	0.339439261	0.842836197	0.400106702	-0.077482894
ALKBH1	0.349034622	0.999961205	0.247811976	0.338390595	0.999961205	0.247811976	-0.010644027
TDG	0.248283136	0.776038219	0.622908194	0.332695013	0.776038219	0.622908194	0.084411878
NonTargetingC	0.202147548	0.999854713	0.331837147	0.325800654	0.999854713	0.282497522	0.123653106
NonTargetingC	0.366537602	0.999451714	0.280807461	0.325557884	0.999451714	0.280807461	-0.040979718
TNP1	0.361322998	0.962981376	0.371141252	0.322803806	0.962981376	0.371141252	-0.038519192
NonTargetingC	0.359949368	0.999534742	0.252566243	0.322587255	0.999534742	0.252566243	-0.037362113
ANKRD28	0.344712209	0.964281934	0.377704218	0.322374739	0.964281934	0.377704218	-0.022337469
CCNA2	0.005150099	0.649111021	0.999949601	0.322195777	0.775593239	0.999949601	0.317045679
CETN2	0.297006696	0.995655769	0.37745133	0.320840127	0.995655769	0.37745133	0.023833432
USP13	0.344368252	0.999322517	0.2603818	0.320760623	0.999322517	0.2603818	-0.023607629
CUL1	0.281142958	0.852117278	0.817536936	0.319596005	0.852117278	0.817536936	0.038453047
OTUD7B	0.297632198	0.966178755	0.309427349	0.319494057	0.966178755	0.309427349	0.021861859
OR6B1	0.369405735	0.780133397	0.543041925	0.318227732	0.780133397	0.543041925	-0.051178003
RMI1	0.088313273	0.779794902	0.999979412	0.316949368	0.821870283	0.951183412	0.228636096
HMGB2	0.529962903	0.999925107	0.189092663	0.316944303	0.999925107	0.267173602	-0.2130186
POLE	0.005568224	0.65044863	0.865959085	0.31659369	0.791463212	0.865959085	0.311025466
BOD1L1	-0.032829853	0.60517879	0.999999296	0.315338604	0.752132281	0.999999296	0.348168457
ARID1B	0.359173691	0.970376264	0.301973032	0.314414093	0.970376264	0.301973032	-0.044759598
PIF1	0.289386808	0.789502562	0.452710548	0.313727119	0.789502562	0.452710548	0.024340311
CHTF18	0.356636942	0.982124975	0.28965022	0.31168448	0.982124975	0.28965022	-0.044952462
PRKCG	0.307436638	0.999019977	0.26646088	0.311334514	0.999019977	0.26646088	0.003897877
INO80B	0.116820451	0.761572409	0.998019997	0.311157558	0.789809779	0.998019997	0.194337107

CDC5L	0.137101956	0.81731613	0.999999994	0.308150876	0.81731613	0.94976868	0.17104892
KLHL15	0.269454997	0.992613477	0.306523469	0.308016192	0.992613477	0.306523469	0.038561196
NonTargetingC	0.399940064	0.99906883	0.28639908	0.301261661	0.99906883	0.28639908	-0.098678403
TERF2IP	0.239063688	0.747038604	0.740824367	0.299921602	0.747038604	0.740824367	0.060857914
SMC1B	0.274894788	0.999741633	0.333848527	0.299534361	0.999741633	0.333848527	0.024639572
NCAPG	-0.034200251	0.598434212	0.999983682	0.298910212	0.775976151	0.999983682	0.333110463
MBD4	0.346396449	0.99826714	0.294597572	0.297892135	0.99826714	0.294597572	-0.048504314
FAN1	0.289960407	0.997111193	0.267264115	0.297545282	0.997111193	0.267264115	0.007584876
SMARCAL1	0.286381239	0.760780742	0.748013154	0.290849365	0.760780742	0.748013154	0.004468126
CSNK1E	0.284173167	0.996433343	0.282415934	0.288234273	0.996433343	0.282415934	0.004061106
HFM1	0.349526351	0.993815046	0.276872453	0.28630904	0.993815046	0.276872453	-0.063217311
EID3	0.170894052	0.993920362	0.38559444	0.285562109	0.993920362	0.368745894	0.114668057
NonTargetingC	0.326262759	0.999829527	0.263208602	0.285278571	0.999829527	0.265679618	-0.040984188
SCAI	0.398552836	0.999862613	0.216875457	0.283933362	0.999862613	0.238601495	-0.114619474
SMG6	-0.005461663	0.636351351	0.975220406	0.28335194	0.812123968	0.975220406	0.288813603
MUM1	0.314494111	0.998613554	0.275787866	0.282557534	0.998613554	0.275787866	-0.031936577
NonTargetingC	0.323106605	0.993980969	0.287545259	0.28242709	0.993980969	0.287545259	-0.040679515
NonTargetingC	0.442509568	0.860063864	0.436971171	0.28195196	0.860063864	0.436971171	-0.160557608
UBE2A	0.242774433	0.966338213	0.370554378	0.281604175	0.966338213	0.370554378	0.038829742
TRAIP	0.031801186	0.679698557	0.999999649	0.280776687	0.824114734	0.999999649	0.248975502
MLH3	0.347832787	0.999862757	0.264575591	0.279756127	0.999862757	0.288765802	-0.06807666
SLBP	0.144814752	0.84926528	0.520300724	0.278865115	0.84926528	0.520300724	0.134050364
ALKBH3	0.204496952	0.999874058	0.340861998	0.276096839	0.999874058	0.315633542	0.071599888
SIRT2	0.281448634	0.996559267	0.27428979	0.275800353	0.996559267	0.27428979	-0.00564828
PRDM9	0.232303207	0.943546646	0.367872819	0.275581963	0.943546646	0.367872819	0.043278756
CASP3	0.107890271	0.92594083	0.520395807	0.275472279	0.92594083	0.457113336	0.167582008
PARP4	0.287562937	0.999779181	0.272654857	0.273920536	0.999779181	0.272654857	-0.013642401
MDC1	0.321779889	0.7975822	0.732251606	0.271832818	0.7975822	0.732251606	-0.049947072
PPP6R2	0.154498939	0.793930204	0.51836679	0.270382552	0.793930204	0.51836679	0.115883613
INO80D	0.264091668	0.995796808	0.322263207	0.267929607	0.995796808	0.322263207	0.003837939
PPP5C	0.041976523	0.956631895	0.457858901	0.267103018	0.956631895	0.442428591	0.225126496
HMGB1	0.791723087	0.994845796	0.425398111	0.265316598	0.994845796	0.469061389	-0.526406489
DCUN1D1	0.413050362	0.999999878	0.314919159	0.263746526	0.999999878	0.314919159	-0.149303835
DCUN1D5	0.461718052	0.999889397	0.278144345	0.260858082	0.999889397	0.293437971	-0.200859971
RPA4	0.269746202	0.926587876	0.347017442	0.260189787	0.926587876	0.347017442	-0.009556415
PARK2	0.159903876	0.744557492	0.508448011	0.256986054	0.744557492	0.508448011	0.097082178
NonTargetingC	0.231527536	0.999971612	0.299195533	0.256408871	0.999971612	0.299195533	0.024881335
APOBEC3F	0.223065013	0.96743583	0.474663017	0.256227324	0.96743583	0.474663017	0.033162311
NonTargetingC	0.379861196	0.998153711	0.268790737	0.255508604	0.998153711	0.294528743	-0.124352592
COPS7A	0.160935669	0.999970404	0.376272799	0.25157948	0.999970404	0.349247598	0.090643811
MMS19	-0.176260766	0.438297367	0.99999986	0.25089863	0.725648182	0.99999986	0.427159396
NonTargetingC	0.376914598	0.990797611	0.311783685	0.25000042	0.990797611	0.311783685	-0.126914178
SMARCAD1	0.336684001	0.902049214	0.473019693	0.249663968	0.902049214	0.473019693	-0.087020033
PRDM10	0.113669381	0.750825113	0.67521091	0.248892747	0.750825113	0.67521091	0.135223366
HDAC1	0.238744524	0.853806783	0.358107678	0.246846989	0.853806783	0.358107678	0.008102465
CCND2	0.291705106	0.999700615	0.311027717	0.245587653	0.999700615	0.311027717	-0.046117453
PER3	0.330918674	0.849608299	0.489903783	0.244607421	0.849608299	0.489903783	-0.086311253
REV1	0.083720514	0.951147894	0.418264435	0.244472601	0.951147894	0.357975676	0.160752088
ERCC8	0.151748201	0.716506865	0.709966902	0.243551989	0.716506865	0.709966902	0.091803788
USP45	0.290465849	0.96395309	0.348616929	0.242891058	0.96395309	0.348616929	-0.047574791
PRIMPOL	0.233167036	0.97661071	0.334150094	0.240746414	0.97661071	0.334150094	0.007579379
USP3	0.352998415	0.90412076	0.449800464	0.240588624	0.90412076	0.449800464	-0.112409791
BARD1	0.109171041	0.778589206	0.99981174	0.238214266	0.778589206	0.99981174	0.129043225
RNF169	0.171406662	0.972630813	0.445966562	0.23646796	0.972630813	0.445966562	0.065061297
TIPIN	0.245494149	0.889867239	0.384848746	0.235940062	0.889867239	0.384848746	-0.009554088
PARK7	0.197329461	0.994823768	0.356819735	0.235497583	0.994823768	0.356819735	0.038168122
WHSC1	0.090989869	0.984510192	0.423713962	0.233962446	0.984510192	0.423713962	0.142972577
APOBEC3H	0.170452151	0.843921742	0.402261229	0.23169574	0.843921742	0.402261229	0.061243589
SALL4	0.364380296	0.991028909	0.305548539	0.231390359	0.991028909	0.311969916	-0.132989936
PARP14	0.128894718	0.999626837	0.470970352	0.230040427	0.999626837	0.422550735	0.101145709
UIMC1	0.225093982	0.861488402	0.390302293	0.228886826	0.861488402	0.390302293	0.003792844
BAZ1A	0.145901898	0.733462775	0.45138603	0.228754412	0.733462775	0.45138603	0.082852514
NABP1	0.284152881	0.959632317	0.345913405	0.228583251	0.959632317	0.345913405	-0.055569631
NonTargetingC	0.214876411	0.999999994	0.31495842	0.228260974	0.999999994	0.31495842	0.013384562
MPZ	0.233931752	0.783285652	0.514905795	0.228142454	0.783285652	0.514905795	-0.005789298
SUV39H2	0.17767884	0.994902355	0.317153685	0.227178699	0.994902355	0.317153685	0.049499858
MSH6	0.336586656	0.807076469	0.633023141	0.226628693	0.807076469	0.633023141	-0.109957962
HNRNPUL2	0.19112298	0.999853973	0.361544483	0.22618309	0.999853973	0.361544483	0.03506011
ATP23	0.28894874	0.941599552	0.436241072	0.223659635	0.941599552	0.436241072	-0.065289105
H2AFY	0.176274938	0.985621785	0.372894174	0.222470159	0.985621785	0.370549484	0.046195221
RECQL5	0.364150897	0.807844349	0.447635835	0.221373398	0.807844349	0.447635835	-0.142777498
PINK1	0.133626093	0.859205561	0.480296597	0.221259381	0.859205561	0.480296597	0.087633288
PIAS2	0.174949454	0.972756723	0.373570722	0.220125931	0.972756723	0.373570722	0.045176478
RHO	0.159588291	0.867938538	0.43694721	0.218766147	0.867938538	0.43694721	0.059177856
ATF2	0.204044217	0.990828682	0.307924958	0.217369987	0.990828682	0.307924958	0.013325769
BTG2	0.262777446	0.999849211	0.355808262	0.216477214	0.999849211	0.355808262	-0.046300232
RAD18	0.268618645	0.998249125	0.318397932	0.216165221	0.998249125	0.318397932	-0.052453424
NonTargetingC	0.31815717	0.999245228	0.296567827	0.21581919	0.999245228	0.341736188	-0.102337979
CDK12	0.20957843	0.699279618	0.972174261	0.214489017	0.699279618	0.972174261	0.004910587
NonTargetingC	0.235156649	0.998153433	0.304050787	0.21387682	0.998153433	0.304050787	-0.021279829
TREX1	0.193696223	0.968436391	0.370772458	0.213614082	0.968436391	0.370772458	0.019917859
DTX1	0.234206059	0.802545681	0.457077757	0.210779801	0.802545681	0.457077757	-0.023426259

POLH	0.147576642	0.817609978	0.414541812	0.208411394	0.817609978	0.414541812	0.060834752
PAGR1	0.198099944	0.703693388	0.916817828	0.208019419	0.703693388	0.916817828	0.009919475
RAP1A	0.19255877	0.998612783	0.393863608	0.207691058	0.998612783	0.393863608	0.015132289
SUMO3	0.223064655	0.994900124	0.328498082	0.207681549	0.994900124	0.328498082	-0.015383107
SMARCC1	0.022106108	0.999999991	0.479243695	0.207346811	0.999999991	0.360935491	0.185240703
NonTargetingC	0.248073406	0.998182876	0.349017695	0.206145606	0.998182876	0.351532207	-0.0419278
TCEB3	0.04505574	0.60703653	0.990465878	0.205402993	0.67279111	0.990465878	0.160347252
LIG3	0.011577723	0.999904028	0.489055158	0.204636395	0.999904028	0.353746338	0.193058672
DCAF11	0.34057827	0.900717935	0.386361477	0.202973579	0.900717935	0.386361477	-0.137604691
NonTargetingC	0.165686803	0.939658178	0.359655223	0.201764959	0.939658178	0.359655223	0.036078156
NonTargetingC	0.220282152	0.995046821	0.372114596	0.201558503	0.995046821	0.372114596	-0.018723649
MEN1	-0.020974036	0.619235737	0.983314517	0.201416625	0.712323746	0.983314517	0.222390661
BEND3	0.126494563	0.782060364	0.418467606	0.20107894	0.782060364	0.418467606	0.074584377
ANP32E	0.156182167	0.877808356	0.388795789	0.200921799	0.877808356	0.388795789	0.044739633
MBTD1	0.330697551	0.982125174	0.388244541	0.198373223	0.982125174	0.47602617	-0.132324328
RBBP7	0.288182063	0.976664116	0.416652738	0.197204719	0.976664116	0.416652738	-0.090977344
APBB1	0.072882493	0.998373594	0.421358868	0.196774435	0.998373594	0.368351676	0.123891943
CDK2	-0.302984953	0.355245308	0.991668433	0.193277469	0.67768649	0.991668433	0.496262422
MRE11	0.30082283	0.806380107	0.999979051	0.192502245	0.78700842	0.999979051	-0.108320585
CLK2	0.071729317	0.937955813	0.53407626	0.191250954	0.937955813	0.496150193	0.119521638
GEN1	0.276229726	0.754153117	0.671192216	0.18926765	0.754153117	0.671192216	-0.086962076
ERCC5	0.172530907	0.788299656	0.480513536	0.188525406	0.788299656	0.480513536	0.015994499
PARP2	0.301501907	0.943985904	0.309226463	0.18782285	0.943985904	0.309226463	-0.113679057
SUMO1	0.188213129	0.848506551	0.352701213	0.18761212	0.848506551	0.352701213	-6.01009E-04
KMT5A	0.044776008	0.741562051	0.574073591	0.186486525	0.741562051	0.574073591	0.141710516
PIAS1	0.239954108	0.730146097	0.478187399	0.185935985	0.730146097	0.478187399	-0.054018124
BLM	0.137441067	0.840181435	0.470355048	0.185412032	0.840181435	0.470355048	0.047970965
GABBR1	0.152584097	0.830415951	0.443223333	0.185070399	0.830415951	0.443223333	0.032486301
PPP6R3	0.198306861	0.99966489	0.346160016	0.183797564	0.99966489	0.346160016	-0.014509297
NIPBL	0.306525747	0.754348284	0.998963233	0.183584703	0.754348284	0.998963233	-0.122941045
NonTargetingC	0.245055782	0.999117535	0.350377074	0.183534855	0.999117535	0.362643208	-0.061520927
DCUN1D4	0.203768083	0.997906465	0.37770114	0.183367651	0.997906465	0.37770114	-0.020400432
NonTargetingC	0.223745852	0.999998311	0.370998384	0.183183379	0.999998311	0.370998384	-0.040562472
SMC3	-0.098608192	0.532186486	0.999896419	0.182902796	0.66233072	0.999896419	0.281510989
TP73	0.228221807	0.721214667	0.496816724	0.182709884	0.721214667	0.496816724	-0.045511923
SENP2	0.235677481	0.974847315	0.384750348	0.182241795	0.974847315	0.384750348	-0.053435686
H2AFY2	0.186008731	0.763884749	0.465235999	0.181804571	0.763884749	0.465235999	-0.004204161
RRM2B	0.137291676	0.999997564	0.374142036	0.180935333	0.999997564	0.374142036	0.043643657
NonTargetingC	0.248671566	0.995299415	0.370924813	0.180822056	0.995299415	0.370924813	-0.06784951
USP44	0.151529559	0.66852974	0.962981781	0.177587397	0.66852974	0.962981781	0.026057838
POLR2C	0.127829777	0.757168982	0.999999547	0.175616697	0.757168982	0.999999547	0.04778692
NonTargetingC	0.01743834	0.999049499	0.483241338	0.173702573	0.999049499	0.431120013	0.156264233
NEIL3	0.262646778	0.830465663	0.459576238	0.172120323	0.830465663	0.459576238	-0.090526454
UHRF2	0.150949908	0.933087821	0.456677267	0.17195469	0.933087821	0.456677267	0.021004781
TOPBP1	0.172817156	0.749373197	0.999999996	0.171156489	0.749373197	0.999999996	-0.001660668
NonTargetingC	0.355351287	0.999695194	0.275977059	0.170233569	0.999695194	0.34865466	-0.185117718
NonTargetingC	0.296627755	0.999974703	0.315982043	0.168711352	0.999974703	0.387102264	-0.127916402
PRMT6	0.001627464	0.998934623	0.498427432	0.168487541	0.998934623	0.437978699	0.166860077
ZRANB3	0.179837509	0.858872109	0.384695382	0.168383431	0.858872109	0.384695382	-0.011454078
PPM1G	0.127716356	0.727096542	0.977161392	0.16793244	0.727096542	0.977161392	0.040216084
NonTargetingC	0.233662123	0.9463425	0.377586763	0.164364524	0.9463425	0.377586763	-0.069297598
APOBEC3G	0.172558944	0.800085083	0.404673257	0.164281887	0.800085083	0.404673257	-0.008277057
DTX3	0.098059875	0.999520968	0.402899465	0.162838927	0.999520968	0.388267478	0.064779052
SHFM1	0.06493968	0.999991064	0.45381777	0.160719437	0.999991064	0.446457726	0.095779757
CCNO	0.112287059	0.98679286	0.393804847	0.160042715	0.98679286	0.393804847	0.047755656
CUL4B	-0.107486351	0.99947849	0.586378269	0.155337833	0.99947849	0.421662709	0.262824184
NonTargetingC	-0.138457431	0.99999849	0.618000193	0.154563035	0.99999849	0.469625734	0.293020466
BAZ1B	0.196188049	0.677081241	0.831773684	0.150708868	0.677081241	0.831773684	-0.04547918
TOP2B	0.100925367	0.894281573	0.517418298	0.150633053	0.894281573	0.517418298	0.049707686
NUDT16L1	0.132170695	0.821254066	0.439119507	0.149468792	0.821254066	0.439119507	0.017298097
PAPD7	0.026422408	0.791645969	0.607132583	0.147663324	0.791645969	0.529345001	0.121240916
NonTargetingC	0.236617153	0.975822499	0.356101424	0.147135705	0.975822499	0.356101424	-0.089481447
SLF2	0.017301604	0.968887803	0.484472338	0.146587878	0.968887803	0.484472338	0.129286273
NOTCH1	0.161498064	0.99799131	0.40855067	0.145092521	0.99799131	0.40855067	-0.016405543
PARPBP	0.230639358	0.997597669	0.369543954	0.141320756	0.997597669	0.408838675	-0.089318602
KAT2A	0.056820247	0.699444162	0.992094734	0.140128499	0.699444162	0.992094734	0.083308252
STAG1	0.227472047	0.723799903	0.633347551	0.138820487	0.723799903	0.633347551	-0.08865156
NonTargetingC	0.140635653	0.998830219	0.372629334	0.135891673	0.998830219	0.372629334	-0.00474398
TYMS	0.162326344	0.989232021	0.373620608	0.133733068	0.989232021	0.373620608	-0.028593276
SLX4	0.134821732	0.708659367	0.999341474	0.129582422	0.708659367	0.999341474	-0.005239311
PPP4R4	0.285672558	0.999944276	0.376532614	0.127561827	0.999944276	0.423630814	-0.158110731
ASF1B	0.03716606	0.852870623	0.49571593	0.127174211	0.852870623	0.479460419	0.090008151
USP4	0.281471169	0.805362863	0.589526684	0.126714937	0.805362863	0.589526684	-0.154756232
ESCO2	0.017999061	0.582427273	0.992629276	0.126411988	0.620304456	0.992629276	0.108412928
EXD2	0.195805746	0.986875983	0.445430619	0.126293251	0.986875983	0.445430619	-0.069512495
USP22	0.156814152	0.642641712	0.653544646	0.126189276	0.642641712	0.653544646	-0.030624876
AICDA	0.030042485	0.884412741	0.47259631	0.124504585	0.884412741	0.47259631	0.0944621
TDP2	0.069773341	0.674335764	0.917993286	0.124434523	0.674335764	0.917993286	0.054661182
POLE4	-0.041769721	0.59141024	0.999981281	0.122363122	0.609192821	0.999981281	0.164132843
NonTargetingC	0.285915648	0.998539304	0.315053553	0.122197702	0.998539304	0.38688018	-0.163717947
NonTargetingC	0.18444402	0.965584874	0.434281159	0.120852342	0.965584874	0.434281159	-0.063591678
RASSF7	0.188515544	0.997777622	0.450251198	0.12080156	0.997777622	0.450251198	-0.067713984

IGHMBP2	0.074253192	0.733461585	0.477616102	0.119984305	0.733461585	0.477616102	0.045731113
POLR2B	-0.216481377	0.468988107	0.998193741	0.119559141	0.659020709	0.998193741	0.336040518
USP26	0.152007057	0.977805328	0.439122437	0.118891348	0.977805328	0.439122437	-0.033115709
CCNA1	0.034679891	0.810951228	0.598707029	0.118001615	0.810951228	0.598707029	0.083321725
NonTargetingC	0.222434374	0.999989034	0.374467506	0.117216961	0.999989034	0.433866013	-0.105217413
SENP7	0.171343024	0.8161503	0.467620277	0.115805524	0.8161503	0.467620277	-0.0555375
TRIM29	0.189422766	0.983559316	0.416560922	0.115623442	0.983559316	0.433498953	-0.073799324
SET	-0.084422359	0.548548085	0.9998963	0.113341157	0.635075834	0.9998963	0.197763516
MCPH1	-0.015420607	0.586576959	0.999999494	0.109815508	0.586576959	0.999999494	0.125236116
SENP6	-0.286711438	0.322686644	0.99993276	0.10923331	0.673046944	0.99993276	0.395944748
INO80C	0.245621527	0.99225101	0.408909174	0.109177858	0.99225101	0.442737388	-0.136443669
CSNK2A1	-0.262970831	0.59893175	0.749365565	0.107247143	0.59893175	0.744935698	0.370217974
NEK8	0.188480188	0.999004224	0.410909534	0.106848452	0.999004224	0.443480968	-0.081631736
PXMP2	0.128311372	0.923308842	0.444325346	0.106613449	0.923308842	0.444325346	-0.021697924
GADD45A	0.161994458	0.999990609	0.449042256	0.105183684	0.999990609	0.450984945	-0.056810774
APOBEC3A	0.178830077	0.949371552	0.402239037	0.105069457	0.949371552	0.402239037	-0.073760619
NonTargetingC	0.178838353	0.997641235	0.416399926	0.104253997	0.997641235	0.416399926	-0.074584356
OGG1	-0.008340151	0.848582944	0.508307522	0.101833594	0.848582944	0.508307522	0.110173745
H3F3A	0.226807795	0.576658748	0.533961199	0.097575286	0.576658748	0.533961199	-0.129232509
APOBEC3D	0.211079234	0.974141819	0.417259904	0.096799085	0.974141819	0.441172526	-0.114280148
FANCM	-0.026907834	0.605209051	0.999902234	0.096339987	0.681682742	0.999902234	0.12324782
PSIP1	0.160209525	0.882014247	0.407987723	0.095908711	0.882014247	0.407987723	-0.064300813
SLF1	0.105642745	0.957297648	0.419842852	0.09586278	0.957297648	0.419842852	-0.009779965
ANKRD44	0.066732909	0.998536699	0.477003499	0.095281797	0.998536699	0.477003499	0.028548888
PARP9	0.370294465	0.997612841	0.358199205	0.091615008	0.997612841	0.469345243	-0.278679457
RFC3	0.014504918	0.572970282	0.999999623	0.090764508	0.572970282	0.999999623	0.07625959
ORC2	-0.106338257	0.481268607	0.87352768	0.089482728	0.594049264	0.87352768	0.195820985
UVSSA	0.097944023	0.69812623	0.613241301	0.088044628	0.69812623	0.613241301	-0.009899394
NonTargetingC	0.17001704	0.999998025	0.445386196	0.087685697	0.999998025	0.470948554	-0.082331343
NonTargetingC	0.233506459	0.999999634	0.388790269	0.08762825	0.999999634	0.472359523	-0.145878209
SHPRH	0.098958681	0.726763686	0.552152367	0.085941728	0.726763686	0.552152367	-0.013016953
IP6K3	0.12028865	0.985510177	0.420443513	0.085326357	0.985510177	0.420443513	-0.034962294
NonTargetingC	0.042761908	0.998422901	0.457736564	0.084930323	0.998422901	0.457736564	0.042168415
NonTargetingC	0.323773806	0.997856576	0.39414485	0.084896178	0.997856576	0.47694779	-0.238877628
PMS2P3	0.113501082	0.943456195	0.540776061	0.084254463	0.943456195	0.540776061	-0.029246619
SIRT3	0.044493062	0.979592947	0.513082548	0.083043652	0.979592947	0.513082548	0.03855059
MSH2	0.269148225	0.974192869	0.401188919	0.081460828	0.974192869	0.41836272	-0.187687397
RAD17	-0.12485428	0.503630424	0.99993315	0.079799946	0.571729947	0.99993315	0.204654226
NonTargetingC	0.085174159	0.963105599	0.474021678	0.077697425	0.963105599	0.474021678	-0.007476735
POLQ	0.206025128	0.707187804	0.452518333	0.076248616	0.707187804	0.452518333	-0.129776512
ERCC6	0.038199894	0.742080257	0.463305052	0.073180462	0.742080257	0.463305052	0.034980568
PMS1	0.210088274	0.958274699	0.395162706	0.07287396	0.958274699	0.471369499	-0.137214314
KDM1A	-0.079761611	0.935769267	0.576498871	0.07053469	0.935769267	0.48560199	0.1502963
NonTargetingC	0.050549676	0.850087936	0.533634841	0.066427097	0.850087936	0.533634841	0.015877421
NonTargetingC	0.122333369	0.99991058	0.441098104	0.065607588	0.99991058	0.441098104	-0.056725781
NonTargetingC	-0.016312358	0.995893787	0.516918944	0.0632195	0.995893787	0.516918944	0.079531857
NonTargetingC	0.186983093	0.9999448	0.437487325	0.061103154	0.9999448	0.47723812	-0.125879939
ADH5	0.217448393	0.997682785	0.454255411	0.058970422	0.997682785	0.454255411	-0.158477971
NonTargetingC	0.10721369	0.999028141	0.437768735	0.057022269	0.999028141	0.437768735	-0.050191421
DDX1	-0.23667862	0.387931432	1	0.056399734	0.617503473	1	0.293078354
NonTargetingC	0.074845753	0.999499894	0.446367433	0.056313317	0.999499894	0.446367433	-0.018532436
OR1E2	-0.179013757	0.776359	0.646068915	0.056121642	0.776359	0.639285089	0.235135399
RAD51C	-0.323902805	0.39136104	0.997588655	0.055625962	0.551480941	0.997588655	0.379528766
CENPS	0.210625614	0.809540827	0.504680041	0.055454275	0.809540827	0.504680041	-0.155171339
BMI1	0.072267586	0.997754667	0.473439774	0.055185658	0.997754667	0.473439774	-0.017081928
OTUB1	-0.253278478	0.59043536	0.800128386	0.054321437	0.59043536	0.800128386	0.307599915
PINX1	-0.12540294	0.4890233	0.974286015	0.051980864	0.617505364	0.974286015	0.177383804
HDAC10	0.045044759	0.997973562	0.508985692	0.051578709	0.997973562	0.508985692	0.00653395
MUS81	0.262045319	0.73378913	0.99287909	0.048414443	0.612924944	0.99287909	-0.213630876
CCNB1	0.137667683	0.634479609	0.998111376	0.047336718	0.634018473	0.998111376	-0.090330965
PARP15	0.062636979	0.998960655	0.514397665	0.046850503	0.998960655	0.514397665	-0.015786476
CHRAC1	-0.165555297	0.470805861	0.883613746	0.046486978	0.542804673	0.883613746	0.212042276
SWI5	-0.168908419	0.998147498	0.639690468	0.045976221	0.998147498	0.590926446	0.214884639
MUTYH	0.114817047	0.663194739	0.683401713	0.045906624	0.663194739	0.683401713	-0.068910423
FIGNL1	-0.016811797	0.606793026	0.998935428	0.043612545	0.606793026	0.998935428	0.060424343
NonTargetingC	0.100703259	0.999838243	0.461086203	0.040599676	0.999838243	0.461086203	-0.060103583
RAD9A	-0.470775683	0.2339057	0.999222767	0.040428024	0.597972542	0.999222767	0.511203707
HINFP	-0.289465065	0.315293475	0.999999995	0.03964153	0.536356119	0.999999995	0.329106594
SETDB1	-0.024883536	0.99959465	0.588933526	0.037964137	0.99959465	0.588933526	0.062847673
EYA3	-0.248226171	0.490007368	0.978716184	0.037752302	0.537003538	0.978716184	0.285978473
MPG	0.02048292	0.678395155	0.64260504	0.036954883	0.678395155	0.64260504	0.016471963
NonTargetingC	0.033124009	0.999960589	0.470147617	0.036333663	0.999960589	0.470147617	0.003209654
CDKN2A	0.323500887	0.999994328	0.26627578	0.036127171	0.999994328	0.462717073	-0.287373716
MLH1	0.005062914	0.942751324	0.556658798	0.035771369	0.942751324	0.556658798	0.030708455
NonTargetingC	0.011664054	0.998717176	0.549290299	0.035265353	0.998717176	0.549290299	0.023601299
ZDHHC16	-0.15006496	0.956923154	0.713194275	0.035241763	0.956923154	0.713194275	0.185306723
SETD2	-0.179302521	0.99309399	0.672358721	0.032913054	0.99309399	0.665279736	0.212215574
TNKS	0.126349217	0.667495342	0.844252915	0.030902122	0.667495342	0.844252915	-0.095447096
XPA	0.198370699	0.954356687	0.473829968	0.029963138	0.954356687	0.473829968	-0.16840756
NFRKB	-0.066215911	0.57136474	0.983903022	0.029184497	0.57136474	0.983903022	0.095400409
RNF168	0.106702335	0.686855358	0.768789476	0.029128936	0.686855358	0.768789476	-0.077573399
NLK	0.207005543	0.981217976	0.473667152	0.028220016	0.981217976	0.473667152	-0.178785527

MCM3AP	-0.286180313	0.308827261	0.973219488	0.027255652	0.535656581	0.973219488	0.313435966
NonTargetingC	0.067907148	0.99999086	0.476318929	0.027057008	0.99999086	0.476318929	-0.04085014
HUS1B	0.128084867	0.999041355	0.489202098	0.026226417	0.999041355	0.529101758	-0.10185845
RHNO1	-0.11414187	0.976984352	0.598425131	0.024436133	0.976984352	0.538649728	0.138578004
PER2	-0.097272424	0.999727149	0.594350844	0.024410667	0.999727149	0.535196289	0.121683091
ERCC2	-0.49491335	0.187000355	1	0.024161957	0.520286283	1	0.519075307
HDAC4	0.101608408	0.952460343	0.448885076	0.023891255	0.952460343	0.476704027	-0.077717153
SMARCA2	-0.028202709	0.964445153	0.590235601	0.021566155	0.964445153	0.590235601	0.049768863
RBM7	-0.098994913	0.988203047	0.584967972	0.019306575	0.988203047	0.579838284	0.118301488
CENPX	0.127619606	0.828940722	0.621083846	0.018985371	0.828940722	0.621083846	-0.108634234
NonTargetingC	0.094635038	0.999971942	0.477072241	0.016076044	0.999971942	0.485077387	-0.078558993
PIAS3	-0.017344841	0.955902472	0.518574108	0.015993308	0.955902472	0.518574108	0.033338149
SPO11	0.026064919	0.999054627	0.522824139	0.010489267	0.999054627	0.522824139	-0.015575653
DNTT	0.020176515	0.999905117	0.539049228	0.010206846	0.999905117	0.539049228	-0.009969669
NTHL1	0.115199037	0.931538222	0.496313114	0.009576491	0.931538222	0.507212164	-0.105622546
NonTargetingC	0.1619288	0.999975913	0.446068832	0.00887581	0.999975913	0.49157035	-0.15305299
UVRAG	-0.111994747	0.432851819	0.999970332	0.007630585	0.508010662	0.999970332	0.119625333
PALB2	-0.149867519	0.501162855	0.956352073	0.007270902	0.507357419	0.956352073	0.157138421
COPS7B	-0.028425894	0.999189187	0.530865771	0.007238785	0.999189187	0.530865771	0.03566468
OTUB2	0.00231718	0.999750694	0.497927565	0.00372368	0.999750694	0.497927565	0.0014065
RPA2	-0.21376361	0.432295693	0.999999998	0.003205153	0.565554219	0.999999998	0.216968764
EXO1	0.079384069	0.626652201	0.875452844	0.00281363	0.626652201	0.875452844	-0.076570439
RAD52	0.069762424	0.728971579	0.559429461	-0.001573154	0.728971579	0.559429461	-0.071335577
NSMCE2	-0.197583236	0.402159958	0.996527617	-0.002159382	0.560190778	0.996527617	0.195423854
PER1	0.098799031	0.990077097	0.514606643	-0.003420442	0.990077097	0.566483139	-0.102219473
RFC5	-0.343450701	0.321844312	1	-0.005498219	0.495744537	1	0.337952481
MAD2L2	-0.310795125	0.337235147	0.999997565	-0.006598738	0.494569072	0.999997565	0.304196387
ACTR8	0.022464979	0.520837149	0.99999942	-0.007928963	0.520837149	0.99999942	-0.030393941
CRY2	0.081785464	0.8956699	0.466013717	-0.010492581	0.8956699	0.511204189	-0.092278045
NonTargetingC	-0.068327269	0.984970515	0.567578657	-0.01381773	0.984970515	0.567578657	0.054509538
POLG2	-0.189875925	0.981114272	0.681840553	-0.014193983	0.981114272	0.661018285	0.175681941
NonTargetingC	0.184370111	0.99994745	0.42039104	-0.017767165	0.99994745	0.515896423	-0.202137276
NonTargetingC	0.099973709	0.999999492	0.516849778	-0.018795528	0.999999492	0.530138163	-0.118769237
TREX2	0.049093165	0.89181467	0.589818312	-0.024080832	0.89181467	0.589818312	-0.073173997
UBE2B	0.01174031	0.967780942	0.537212607	-0.024198357	0.967780942	0.537212607	-0.035938667
NonTargetingC	-0.107054688	0.999999992	0.59688114	-0.032660436	0.999999992	0.59618914	0.074394253
PPP4R1	-0.014994947	0.856665652	0.662714626	-0.032874046	0.856665652	0.662714626	-0.017879099
FAAP100	-0.23706679	0.348324268	0.999216741	-0.035921977	0.464012593	0.999216741	0.201144813
BUB1B	-0.402122358	0.336105544	0.999987313	-0.037794211	0.539107392	0.999987313	0.364328147
AMN1	-0.090166737	0.99801046	0.637246295	-0.039194926	0.99801046	0.637246295	0.050971811
TCEB1	0.160536218	0.600507844	1	-0.041932886	0.532691408	1	-0.202469104
DNMT1	-0.323635804	0.309144761	0.999965741	-0.043745922	0.494476034	0.999965741	0.279889882
RTEL1	-0.330234985	0.248836053	0.999998909	-0.048697101	0.448818801	0.999998909	0.281537884
EME2	-0.058043618	0.998886994	0.583093659	-0.048859987	0.998886994	0.583093659	0.009183631
DCLRE1C	-0.115781035	0.999665045	0.605788186	-0.048911512	0.999665045	0.605788186	0.066869523
WRN	0.131974248	0.936131005	0.479474015	-0.050541125	0.936131005	0.550005563	-0.182515373
MYBBP1A	-0.197797672	0.40555722	1	-0.051011087	0.453187843	1	0.146786585
ATM	0.726936134	1	0.168865327	-0.051079994	1	0.540250304	-0.778016128
TTI1	-0.573352558	0.174725054	1	-0.051534449	0.459057262	1	0.521818109
CRY1	-0.083618706	0.920529515	0.580422196	-0.054556645	0.920529515	0.580422196	0.029062061
NonTargetingC	-0.038938678	0.999287288	0.584495058	-0.056571933	0.999287288	0.584495058	-0.017633255
MTA3	-0.030980498	0.998930186	0.547359712	-0.056767954	0.998930186	0.547359712	-0.025787456
TOP3B	-0.079061265	0.997428561	0.650585715	-0.064227809	0.997428561	0.650585715	0.014833456
ATAD5	-0.227787361	0.639201937	0.719766489	-0.066667093	0.639201937	0.719766489	0.161120268
SMARCC2	0.003612468	0.997555566	0.581758943	-0.067593746	0.997555566	0.581758943	-0.071206214
NonTargetingC	-0.154190756	0.999962639	0.639036963	-0.069608901	0.999962639	0.633891715	0.084581856
NonTargetingC	-0.114289432	0.999823905	0.686442141	-0.072605257	0.999823905	0.686442141	0.041684175
MTA1	-0.212200519	0.620309887	0.799156054	-0.072957811	0.620309887	0.740035073	0.139242709
ERCC6L2	-0.08184418	0.872367225	0.646306863	-0.074131153	0.872367225	0.646306863	0.007713027
RMI2	-0.165800103	0.436135851	0.971086796	-0.076239009	0.475123909	0.971086796	0.089561095
WDR48	0.143072651	0.618490932	0.999368917	-0.076297641	0.561616446	0.999368917	-0.219370292
HES1	-0.027615052	0.76809946	0.612258629	-0.07793616	0.76809946	0.612258629	-0.050321108
RNF20	-0.351332795	0.230650755	0.999999519	-0.079758738	0.412755965	0.999999519	0.271574056
TP63	-0.037612615	0.982719463	0.659207594	-0.079866567	0.982719463	0.659207594	-0.042253952
TCEB2	-0.67807386	0.220472453	1	-0.082553511	0.455251704	1	0.59552035
HELQ	-0.028334907	0.53104413	0.86709702	-0.083141766	0.53104413	0.86709702	-0.054806859
UCHL5	-0.404248878	0.236702792	0.999999896	-0.08322925	0.469946513	0.999999896	0.321019628
DDB2	-0.132236323	0.968589624	0.712817449	-0.085578697	0.968589624	0.712817449	0.046657625
HMGN1	-0.068084139	0.991290138	0.570215911	-0.091942925	0.991290138	0.570215911	-0.023858786
NonTargetingC	0.042081856	0.999913624	0.572381097	-0.092458187	0.999913624	0.587576554	-0.134540043
SPIDR	-0.06379337	0.476235924	0.816668104	-0.096322472	0.476235924	0.816668104	-0.032529102
RFC4	-0.325879669	0.291544092	0.999840568	-0.10281324	0.458601295	0.999840568	0.223066429
BRIP1	-0.141799403	0.47669902	0.882716175	-0.103561987	0.47669902	0.882716175	0.038237416
RNF4	-0.341582966	0.51553963	0.863172383	-0.106123524	0.51553963	0.863172383	0.235459443
PARP3	-0.189061477	0.999043034	0.676938494	-0.107608136	0.999043034	0.676938494	0.081453341
NonTargetingC	-0.208488508	0.99765574	0.693830415	-0.107801495	0.99765574	0.679276228	0.100687013
TCEA1	-0.032200996	0.635881387	0.597959364	-0.108261557	0.635881387	0.597959364	-0.076060561
SUV39H1	-0.240812088	0.686927959	0.727706492	-0.109176985	0.686927959	0.727706492	0.131635103
CUL4A	-0.252242157	0.655076567	0.74258042	-0.110353907	0.655076567	0.689545238	0.14188825
PAXIP1	0.124689613	0.640313842	0.733419247	-0.112534594	0.640313842	0.733419247	-0.237224208
RAG1	0.0278725	0.998190338	0.609191893	-0.115658459	0.998190338	0.684703167	-0.143530959
CCNE1	-0.087163357	0.972601188	0.624351389	-0.116624211	0.972601188	0.624351389	-0.029460854

RFWD3	-0.165143786	0.445843971	0.946496535	-0.117231705	0.445843971	0.946496535	0.047912081
CDKN2D	-0.075545086	0.997688613	0.685570329	-0.117830575	0.997688613	0.685570329	-0.042285489
NonTargetingC	0.001714446	0.878180299	0.628679769	-0.118381474	0.878180299	0.628679769	-0.12009592
POLK	-0.190678596	0.999979036	0.682608088	-0.119929539	0.999979036	0.682608088	0.070749057
PPP6R1	0.094075231	0.772941429	0.646705834	-0.121460479	0.772941429	0.696452101	-0.215535709
TRIM28	-0.318105925	0.696727965	0.791868369	-0.123519183	0.696727965	0.743038716	0.194586742
RAD23A	-0.281339552	0.635087306	0.805323122	-0.123569515	0.680085256	0.805323122	0.157770037
NonTargetingC	-0.151836407	0.999427371	0.645580156	-0.12665433	0.999427371	0.645580156	0.025182076
COL21A1	-0.079655005	0.921825514	0.629774398	-0.132640326	0.921825514	0.629774398	-0.052985321
APEX1	-0.164506127	0.975643502	0.654696958	-0.134801239	0.975643502	0.654696958	0.029704888
RAD54L	-0.067512892	0.553927821	0.930512659	-0.134807884	0.553927821	0.930512659	-0.067294992
MSH5	-0.185385827	0.738573839	0.706570482	-0.134822708	0.738573839	0.706570482	0.05056312
INO80	-0.316400948	0.26996301	0.998880602	-0.136755865	0.378822049	0.998880602	0.179645083
NonTargetingC	-0.095008934	0.966309425	0.627350751	-0.137119687	0.966309425	0.627350751	-0.042110753
PDS5B	-0.564826034	0.164773	0.997655936	-0.137473178	0.375233179	0.997655936	0.427352856
KDM4D	-0.099761613	0.999517962	0.626749494	-0.138722503	0.999517962	0.626749494	-0.03896089
FANCG	-0.471611377	0.19714898	0.999845823	-0.145802356	0.374626323	0.999845823	0.325809021
SMUG1	-0.241451733	0.926775706	0.722752663	-0.146968892	0.926775706	0.722752663	0.094482841
NonTargetingC	0.011533528	0.980263038	0.59738111	-0.147028836	0.980263038	0.643751122	-0.158562364
ARID1A	-0.26679015	0.459801678	0.960738841	-0.153405917	0.460648157	0.960738841	0.113384233
NonTargetingC	-0.174044727	0.985115366	0.664975186	-0.153847782	0.985115366	0.664975186	0.020196945
RAD23B	-0.203060898	0.726194025	0.689054646	-0.161824982	0.726194025	0.689054646	0.041235915
USP1	-0.178477004	0.590243354	0.848664132	-0.165343827	0.590243354	0.848664132	0.013133176
NonTargetingC	0.002317818	0.999999721	0.640099925	-0.16833555	0.999999721	0.650712797	-0.170653367
WRAP53	-0.530918051	0.206508048	0.999668421	-0.171619034	0.346982738	0.999668421	0.359299017
CTC1	-0.646536128	0.171305894	0.999977979	-0.176956051	0.398744547	0.999977979	0.469580077
PIAS4	-0.091510459	0.530232231	0.788581482	-0.183930595	0.530232231	0.788581482	-0.092420136
FAAP20	0.04531898	0.545811951	0.704574993	-0.191146335	0.529341341	0.704574993	-0.236465315
ATRIP	-0.430669068	0.203753298	0.998218448	-0.191529181	0.343011224	0.998218448	0.239139886
DTX2	-0.216824845	0.671581355	0.696367427	-0.196863007	0.671581355	0.696367427	0.019961838
ENDOV	-0.20974255	0.999296873	0.717721773	-0.203881355	0.999296873	0.717721773	0.005861196
NCAPH	-0.538643734	0.127392844	0.99898725	-0.204687572	0.33424038	0.99898725	0.333956161
UHRF1	-0.384034522	0.261600482	0.99999626	-0.220104155	0.337463247	0.99999626	0.163930368
TADA3	-0.102741899	0.433691801	0.915647428	-0.221515107	0.433691801	0.915647428	-0.118773208
MPLKIP	-0.281904592	0.417071503	0.839815793	-0.22373901	0.417071503	0.839815793	0.058165582
HUS1	-0.231085161	0.3202775	0.999975309	-0.242631865	0.3202775	0.999975309	-0.011546704
ZSWIM7	-0.211411608	0.735231576	0.724270237	-0.247060996	0.735231576	0.724270237	-0.035649388
NFE2L2	-0.251395388	0.300917887	0.994462838	-0.250111291	0.300917887	0.994462838	0.001284098
KDM4A	-0.53778644	0.166800392	0.999685556	-0.259415828	0.261393687	0.999685556	0.278370612
NonTargetingC	-0.189504919	0.999999932	0.720769173	-0.262059244	0.999999932	0.720769173	-0.072554325
FANCB	-0.496912034	0.256489302	0.995133965	-0.270325579	0.334949315	0.995133965	0.226586455
GTF2H5	-0.329634928	0.299807685	0.999989346	-0.27587607	0.299807685	0.999989346	0.053758858
XRCC1	-0.106298568	0.503469724	0.83560372	-0.280389207	0.443528978	0.83560372	-0.174090638
KDM2A	-0.558518598	0.434804887	0.910732661	-0.283781803	0.434804887	0.910732661	0.274736795
NonTargetingC	-0.110602421	0.999988159	0.74150653	-0.284517369	0.999988159	0.74150653	-0.173914947
POLE3	-0.236645108	0.308110286	0.999987142	-0.294164681	0.308110286	0.999987142	-0.057519573
FANCL	-0.396020418	0.280568326	0.999999866	-0.297233892	0.280568326	0.999999866	0.098786525
FANCA	-0.503828788	0.209442566	0.968847838	-0.306267119	0.212293296	0.968847838	0.197561669
SSBP1	-0.24047795	0.828033245	0.768758977	-0.307391809	0.828033245	0.768758977	-0.06691386
TDP1	-0.296059632	0.743472684	0.813004354	-0.312638648	0.743472684	0.813004354	-0.016579015
CUL2	-0.43007583	0.180360854	0.999999866	-0.314123621	0.241613681	0.999999866	0.115952209
ATRX	-0.223235115	0.584883682	0.796610207	-0.32493211	0.584883682	0.796610207	-0.101696995
RAD51B	-0.504569208	0.161939293	0.9999845	-0.326316295	0.235724626	0.9999845	0.178252913
UBB	-0.408509311	0.712171643	0.810120028	-0.326993265	0.712171643	0.810120028	0.081516046
ACTR5	-0.280987237	0.309331697	0.999664378	-0.329951219	0.309331697	0.999664378	-0.048963982
CCNC	-0.079634918	0.999898713	0.643277447	-0.340115894	0.999898713	0.784447098	-0.260480977
XRCC4	-0.692794146	0.091989725	0.983404757	-0.34197341	0.175353771	0.983404757	0.350820737
CNOT7	-0.295707409	0.288024187	0.942650234	-0.34487223	0.288024187	0.942650234	-0.049164821
FAAP24	-0.258183287	0.289786957	0.999280513	-0.348474845	0.262097914	0.999280513	-0.090291558
DSCC1	-0.531996416	0.140551596	0.999994766	-0.355920038	0.210479682	0.999994766	0.176076378
ERCC4	-0.398931986	0.252285106	0.999998625	-0.369082173	0.252285106	0.999998625	0.029849814
PRKDC	-1.052365726	0.107027335	0.997540738	-0.384213058	0.283092828	0.997540738	0.668152668
ZMPSTE24	-0.369169724	0.278722686	0.99078592	-0.386573497	0.278722686	0.99078592	-0.017403773
CEP57	-0.724040032	0.081750529	0.999999863	-0.389291065	0.225622191	0.999999863	0.334748967
SUMO2	-0.055497564	0.592600641	0.874235475	-0.391802644	0.592600641	0.874235475	-0.336305079
NAE1	-0.464061867	0.106455892	0.999999565	-0.41210036	0.128353976	0.999999565	0.051961507
ERCC1	-0.761019077	0.121299122	0.999920277	-0.41620847	0.231041197	0.999920277	0.344810607
TERT	-1.120561076	0.043657438	0.999994311	-0.429838048	0.242057508	0.999994311	0.690723029
FZR1	-0.388999548	0.182286415	1	-0.441190194	0.167080847	1	-0.052190646
CREBBP	-0.529525138	0.200253782	0.977017433	-0.450868105	0.200253782	0.977017433	0.078657033
PARP1	-0.497157357	0.279310195	0.90920163	-0.470447165	0.279310195	0.90920163	0.026710192
TELO2	-0.789127642	0.081905094	0.999999997	-0.476377261	0.176882663	0.999999997	0.312750381
POLG	-0.383028325	0.400960382	0.874455448	-0.481244409	0.400960382	0.874455448	-0.098216083
TFPT	-0.301295778	0.297516508	0.890885344	-0.485778145	0.297516508	0.890885344	-0.184482367
FANCF	-0.540715666	0.115596019	0.999997085	-0.505680481	0.115596019	0.999997085	0.035035184
ENY2	-0.971981534	0.148082476	0.971646103	-0.50606681	0.218434077	0.971646103	0.465914724
NHEJ1	-0.731347402	0.121990341	0.989815203	-0.528542438	0.18793881	0.989815203	0.202804964
LMNA	-1.019814402	0.106849512	0.988127832	-0.539154303	0.183523833	0.988127832	0.4806601
SIN3A	-0.448706121	0.136922181	0.999999614	-0.546778344	0.119723101	0.999999614	-0.098072224
RAD50	-0.612330237	0.043572166	0.999999891	-0.646348762	0.037270877	0.999999891	-0.034018525
NBN	0.129128469	0.797503888	0.750377074	-0.650386391	0.561989758	0.937556694	-0.77951486
FANCC	-0.655601424	0.084856054	0.999998236	-0.657318106	0.084856054	0.999998236	-0.001716682

LIG4	-0.80476088	0.089990965	0.997992962	-0.690597891	0.093721735	0.997992962	0.114162988
UBE2N	-1.016751085	0.01951038	0.999808198	-0.69824877	0.068995853	0.999808198	0.318502315
UBE2M	-0.859090131	0.119797607	0.99993481	-0.713969218	0.119797607	0.99993481	0.145120913
RNASEH2A	-0.985021172	0.059056933	0.999838311	-0.714404668	0.074537796	0.999838311	0.270616503
BAP1	-0.861019258	0.06781337	0.991006485	-0.721855485	0.073380185	0.991006485	0.139163773
TEN1	-1.379092553	0.007574556	1	-0.895302063	0.048887649	1	0.48379049

Appendix Table 5 Raw data from JACKS analysis of RPE-1 WT 5nM CPT

RPE-1 WT DMSO and 5nM CPT treated enrichments compared to the day 14 control. fdr=false discovery rate

Gene	Enrichment in DMSO treated	neg_fdr1	pos_fdr1	Enrichment in 5nM CPT treated	neg_fdr2	pos_fdr2	Difference in Enrichment
TP53	3.478343858	1	7.03E-10	5.839756226	1	0	2.361412369
CDKN1A	1.548402497	1	0.006661002	2.273239869	1	2.21007E-04	0.724837372
RNF146	3.342174495	1	1.14E-08	2.174441437	1	7.45E-05	-1.167733057
CAND1	3.251324882	1	9.85E-09	2.011668366	1	1.36765E-04	-1.239656516
PTEN	2.989153557	1	6.03E-08	1.879284785	1	6.11774E-04	-1.109868773
BRD7	1.222877703	1	0.02120377	1.843158685	1	0.006609599	0.620280981
UBC	1.078420637	0.999658144	0.051744941	1.814365861	0.999658144	0.003076703	0.735945224
KEAP1	2.483000039	1	2.16E-05	1.792946949	1	9.67406E-04	-0.69005309
NEDD8	1.316840385	0.997608314	0.052826231	1.791081182	0.997608314	0.012511861	0.474240798
POLR2E	1.219824327	0.999348419	0.037929435	1.720186375	0.999348419	0.005864225	0.500362047
POLR2A	0.844985861	0.999743729	0.089551101	1.666908986	0.999743729	0.001625139	0.821923125
UBE2D3	0.74016914	0.996663275	0.319471661	1.620742576	0.996663275	0.026958571	0.880573436
TINF2	1.100595288	0.999707723	0.033739	1.613741623	0.999707723	0.003422671	0.513146335
ARID2	1.568928223	1	0.002943369	1.558508326	1	0.002943369	-0.010419896
NHP2	1.38567457	0.999210651	0.017170615	1.556318991	0.999210651	0.007662606	0.170644422
H2AFZ	1.807149541	1	0.001542282	1.528441243	1	0.00422173	-0.278708298
THOC2	0.897782531	0.99942868	0.091272149	1.51225068	0.99942868	0.004594557	0.61446815
VCP	1.21433551	0.999408308	0.01031894	1.511640768	0.999408308	0.003025065	0.297305259
PARG	1.224402373	0.995565538	0.042044953	1.500145721	0.995565538	0.03872594	0.275743348
UPF1	1.123865534	0.99939939	0.019163465	1.46767638	0.99939939	0.003314716	0.343810846
CHEK2	1.061693034	1	0.018781658	1.467617967	1	0.003619417	0.405924933
FANCD2	0.768656194	0.998603983	0.173537091	1.446919576	0.998603983	0.009756588	0.678263383
TRIP13	1.067703935	0.996766587	0.066606999	1.429255489	0.996766587	0.020665527	0.361551554
XRCC6	1.420821193	0.996425727	0.017788114	1.422047939	0.996425727	0.017788114	0.001226746
POLR2G	1.040481506	0.998702537	0.047424725	1.408427396	0.998702537	0.008032543	0.367945891
HNRNPK	1.151021266	0.998457502	0.034694387	1.404507885	0.998457502	0.010137349	0.253486619
BABAM1	1.274140118	1	0.0052029	1.397745839	1	0.004027136	0.123605721
RPS27L	0.730379459	0.994490993	0.325118111	1.386822746	0.994490993	0.04729164	0.656443286
USP28	1.501057011	1	0.001295878	1.370255485	1	0.002906934	-0.130801526
RRM1	0.820813157	0.994380199	0.17057678	1.357438986	0.994380199	0.026712064	0.536625829
POLR2I	1.161224126	0.999089699	0.013897347	1.35641392	0.999089699	0.006941804	0.195189794
MDM4	0.869317978	0.999708607	0.027373616	1.352583504	0.999708607	0.002622541	0.483265526
RNF7	1.992484214	1	8.41E-05	1.343416666	1	0.004618119	-0.649067548
ASCC1	1.277043384	0.999128493	0.00594499	1.34012311	0.999128493	0.00594499	0.063079726
SOD1	0.795714541	0.995957182	0.297691842	1.338386072	0.995957182	0.064629127	0.54267153
SUPT5H	1.246177214	0.999366891	0.00543512	1.338379085	0.999366891	0.003472975	0.092201871
SMC2	1.180896449	0.99918801	0.008957961	1.333491509	0.99918801	0.005367751	0.15259506
UBE2I	1.001190375	0.996570528	0.060585709	1.326586404	0.996570528	0.023703545	0.32539603
POLR2D	0.904087783	0.998352112	0.086472326	1.321755405	0.998352112	0.019059897	0.417667622
MASTL	0.883977082	0.997129735	0.081320799	1.30211832	0.997129735	0.016672547	0.418141238
PPP4C	0.609274956	0.995421926	0.347698274	1.296997829	0.995421926	0.021822068	0.687722873
SFPQ	1.159703742	0.997777455	0.014166462	1.296373927	0.997777455	0.014166462	0.136670185
CCNH	0.994625196	0.998363641	0.064727007	1.284025028	0.998363641	0.014954456	0.289399831
CCND1	0.823227575	0.996336636	0.12009587	1.28380045	0.996336636	0.027245401	0.460572875
MDM2	0.709913641	0.999296181	0.079859685	1.277644984	0.999296181	0.006781752	0.567731342
PCNA	0.638126227	0.996830336	0.244456705	1.274937065	0.996830336	0.015933777	0.636810838
H2AFX	0.944368353	0.998598322	0.040684137	1.241928704	0.998598322	0.009308027	0.297560351
CUL3	2.544711008	1	5.87E-08	1.238580416	1	0.007455089	-1.306130592
DCUN1D3	1.710527193	1	0.00108847	1.237979875	1	0.010333614	-0.472547319
APEX2	0.499736041	0.993601958	0.427304879	1.215845994	0.993601958	0.045902673	0.716109953
UBE2F	2.157784094	1	1.41307E-04	1.215510244	1	0.012666928	-0.942273849
COPS4	0.927344964	0.996519824	0.081713373	1.213089334	0.996519824	0.025235778	0.28574437
ERCC6L	1.09147551	0.995790705	0.024750777	1.210834785	0.995790705	0.024750777	0.119359275
DNAJC2	0.64827602	0.994253356	0.253706572	1.205720221	0.994253356	0.051719793	0.557444201
WAPL	1.22277863	0.991839751	0.028081849	1.180023786	0.991839751	0.028081849	-0.042754843
POLL	1.023597645	0.995018218	0.033412652	1.178551061	0.995018218	0.033412652	0.154953416
TOP1	0.794316168	0.995683636	0.098703312	1.151808487	0.995683636	0.026655039	0.357492319
NPM1	0.877513543	0.987281768	0.202109067	1.147659741	0.987281768	0.118981516	0.270146198
PLK1	0.719615666	0.998089148	0.117179068	1.143492521	0.998089148	0.014438922	0.423876855
RAD21	0.793491497	0.992826602	0.169308031	1.140657841	0.992826602	0.063919118	0.347166345
CDK4	0.866901776	0.994950855	0.125128634	1.138345958	0.994950855	0.052846951	0.271444181
TICRR	0.780954623	0.998537571	0.104551121	1.128696793	0.998537571	0.021453942	0.34774217
DKC1	0.83340222	0.996300223	0.126259375	1.115466371	0.996300223	0.047331321	0.282064151
PNN	0.834358345	0.997902515	0.044707643	1.107816816	0.997902515	0.012646814	0.273458471
GPS1	0.596238841	0.991719994	0.35462115	1.10737099	0.991719994	0.07316407	0.511132149
DCLRE1B	0.69692639	0.987281035	0.235747477	1.094696472	0.987281035	0.063407231	0.397770081
SMC1A	1.051782928	0.992995034	0.063262757	1.092997799	0.992995034	0.063262757	0.041214871
TP53BP1	1.164112135	1	0.019079977	1.092823541	1	0.019079977	-0.071288594
CHAF1A	0.873093909	0.995065372	0.06059186	1.086233694	0.995065372	0.035416204	0.213139785
RPAIN	0.660322488	0.993352226	0.180150532	1.080845942	0.993352226	0.031759254	0.420523453
CDK9	0.647511273	0.974297575	0.326920002	1.078854698	0.974297575	0.190145135	0.431343424
SCAF4	2.027124007	1	1.12026E-04	1.075727298	1	0.016190019	-0.951396708

TERF2	0.731185088	0.977439919	0.275266616	1.075640205	0.977439919	0.116369333	0.344455118
POLE2	0.627275302	0.995019808	0.177439228	1.073688898	0.995019808	0.044821728	0.446413597
USP37	0.651572418	0.993616294	0.19983209	1.070266226	0.993616294	0.042914486	0.418693808
PPP4R2	0.861925299	0.992153067	0.150266243	1.069577908	0.992153067	0.107289101	0.207652609
PPP4R3B	0.917753086	0.993541008	0.043391854	1.06908882	0.993541008	0.038987578	0.151335734
SMC4	1.019371979	0.997535657	0.029737842	1.068668444	0.997535657	0.029737842	0.049296464
USP5	0.647932938	0.993647465	0.192219458	1.061146175	0.993647465	0.031033385	0.413213236
BRCA2	0.692271982	0.996405184	0.056377273	1.061041532	0.996405184	0.016202843	0.36876955
UBE2T	0.732915298	0.982067098	0.269670205	1.055115303	0.982067098	0.104776972	0.322200005
CHEK1	0.571655384	0.980397889	0.380679277	1.053877128	0.980397889	0.117866344	0.482221744
TTI2	0.448339822	0.98798189	0.494958822	1.04460211	0.98798189	0.057028021	0.596262288
SUPT4H1	0.701185205	0.980619787	0.277921111	1.042314235	0.980619787	0.137983536	0.34112903
POLR2H	0.815835883	0.997758477	0.068571978	1.035831304	0.997758477	0.026870878	0.219995422
ATR	0.954095586	0.99380791	0.074905632	1.033238588	0.99380791	0.061476743	0.079143002
POLD3	0.750650972	0.999843055	0.023063205	1.021940896	0.999843055	0.009074953	0.271289925
RUVBL2	0.488938307	0.995203032	0.311492839	1.016593204	0.995203032	0.035371872	0.527654897
CHD3	0.995587622	0.991912216	0.028208578	1.007993134	0.991912216	0.028208578	0.012405512
SMG1	0.778542329	0.987292224	0.1227647	1.004357639	0.987292224	0.067803378	0.22581531
POLR2L	0.678906203	0.987939077	0.225688715	1.003353616	0.987939077	0.084695833	0.324447413
COPS3	0.644020139	0.988603626	0.215172887	0.999708537	0.988603626	0.102567369	0.355688397
DNA2	0.483948473	0.973856355	0.488303297	0.99511301	0.973856355	0.160991679	0.511164536
ACD	0.61831279	0.982712271	0.265566728	0.989564378	0.982712271	0.126892223	0.371251589
RUVBL1	0.683546411	0.990871965	0.212939865	0.985105621	0.990871965	0.084279367	0.30155921
STAG2	1.526033493	0.999999998	0.003144522	0.978755894	0.999999998	0.039133738	-0.547277599
NCAPD3	0.466598138	0.985103036	0.277419456	0.976242641	0.985103036	0.070961265	0.509644502
UBA3	1.080529152	0.994051665	0.028282293	0.969169561	0.994051665	0.039658077	-0.111359591
ASF1A	1.004582547	0.992322994	0.034672897	0.966979981	0.992322994	0.034672897	-0.037602566
SMC5	0.633037318	0.99410568	0.265722904	0.963304287	0.99410568	0.089447773	0.330266969
USP7	0.630685863	0.997173314	0.210344337	0.962179313	0.997173314	0.061423531	0.331493451
CUL5	1.497920684	1	0.00186744	0.960426739	1	0.024218267	-0.537493945
GTF2H2	0.825960389	0.983875327	0.298260716	0.95895141	0.983875327	0.298260716	0.132991021
DCLRE1A	1.055831103	0.999578127	0.037537926	0.956168668	0.999578127	0.037537926	-0.099662434
POLA1	0.902565703	0.992727618	0.06890491	0.949316331	0.992727618	0.06890491	0.046750628
PNKP	0.6016236	0.986698291	0.237818407	0.948148714	0.986698291	0.10674828	0.346525114
TEP1	0.934910019	0.9949726	0.039248942	0.942649291	0.9949726	0.039248942	0.007739273
COPS6	0.812914627	0.995788736	0.12361223	0.933218399	0.995788736	0.094114131	0.120303772
HDAC3	0.367283077	0.973752172	0.721775953	0.928694708	0.973752172	0.185745615	0.561411631
RNF126	0.729115717	0.98261248	0.109412227	0.927822192	0.98261248	0.083640997	0.198706475
TONSL	0.65221681	0.984422249	0.217480272	0.927009537	0.984422249	0.100426795	0.274792727
XAB2	0.57591632	0.992620544	0.216069106	0.926118368	0.992620544	0.047838964	0.350202049
SPRTN	0.720521563	0.991903735	0.092452466	0.924683153	0.991903735	0.043053879	0.204161589
COPS8	0.535714299	0.942254364	0.547492294	0.922210493	0.942254364	0.355310586	0.386496195
UBE2W	0.876941483	0.991327705	0.029246599	0.922045832	0.991327705	0.029246599	0.045104349
XRCC5	0.678004709	0.986959415	0.107422336	0.915847692	0.986959415	0.073694186	0.237842984
BCCIP	0.444198368	0.971715887	0.516373643	0.913936038	0.971715887	0.145883047	0.469737669
PPM1D	0.356217552	0.978428922	0.656240543	0.906157907	0.978428922	0.097824862	0.549940356
APAF1	0.9340822	0.999769105	0.045435651	0.90294845	0.999769105	0.061545504	-0.031133751
MNAT1	0.326048196	0.937788527	0.811826771	0.901423732	0.953900783	0.37848029	0.575375535
TET2	0.961352491	0.999998163	0.053624086	0.893825353	0.999998163	0.056907656	-0.067527137
MAPK8	0.987010362	0.999525364	0.041435367	0.88305418	0.999525364	0.045106756	-0.103956182
GTF2H1	0.765687306	0.985989059	0.114474111	0.881601836	0.985989059	0.090181841	0.11591453
POLD1	0.665823754	0.975782143	0.189344575	0.874987941	0.975782143	0.120412834	0.209164186
PHIP	1.190806885	1	0.018075463	0.874902793	1	0.037564294	-0.315904092
UCHL3	0.734197915	0.990060866	0.101431848	0.872106967	0.990060866	0.101431848	0.137909053
SMARCE1	0.656105281	0.953730866	0.239854599	0.861437311	0.953730866	0.239854599	0.20533203
MAPKAPK2	1.052642319	1	0.033510011	0.851037319	1	0.05758942	-0.201605001
DMC1	0.73527993	0.999556483	0.074692826	0.850885468	0.999556483	0.051355478	0.115605538
NonTargetingCo	1.053700789	0.99999303	0.044109855	0.846338936	0.99999303	0.06474499	-0.207361852
RBX1	0.939828133	0.98131896	0.097311233	0.844051172	0.98131896	0.097311233	-0.095776961
UBA1	0.473635204	0.978447394	0.374095522	0.843628437	0.978447394	0.109264778	0.369993232
NOP10	0.280743976	0.943532357	0.798424501	0.843174956	0.972454592	0.234961302	0.562430979
RPA1	0.442165533	0.95627332	0.541128882	0.839408621	0.95627332	0.225500397	0.397243089
DAXX	0.457122673	0.973070034	0.417385363	0.833865452	0.973070034	0.125803507	0.376742779
PCID2	0.448915706	0.967975412	0.478618712	0.833852664	0.967975412	0.153627593	0.384936958
GAR1	0.607701084	0.971597461	0.245209734	0.819809848	0.971597461	0.139906761	0.212108764
KMT5B	0.648701797	0.999968266	0.103565356	0.816092391	0.999968266	0.064170549	0.167390594
NonTargetingCo	0.606066621	0.99983586	0.147679814	0.812723289	0.99983586	0.071219003	0.206656668
PMS2	0.67722614	0.962221154	0.15340566	0.808713668	0.962221154	0.15340566	0.131487528
NCAPD2	0.835052204	0.993107623	0.091277018	0.803877949	0.993107623	0.105431735	-0.031174255
KAT8	0.313370111	0.971895592	0.732243619	0.796492949	0.983369007	0.211176027	0.483122838
PRPF19	0.368630712	0.975059426	0.572795487	0.793369921	0.975059426	0.163494597	0.424739209
THOC1	0.376679817	0.977654268	0.511834518	0.793190054	0.977654268	0.158664095	0.416510237
MTA2	0.966456629	0.999859602	0.040785377	0.789321014	0.999859602	0.072500219	-0.177135615
GADD45G	0.767118456	0.999993748	0.109459973	0.78463892	0.999993748	0.109459973	0.017520464
LIG1	0.408442556	0.95099314	0.546549017	0.781347689	0.95099314	0.396067329	0.372905134
DDX11	0.940904613	0.977610396	0.148517407	0.778629729	0.977610396	0.148517407	-0.162274884
EYA1	0.760901764	0.990056724	0.085153923	0.777243836	0.990056724	0.085153923	0.016342072
RAD51	0.346951985	0.961409067	0.70174548	0.773769458	0.961409067	0.237484521	0.426817473
BRE	1.202639487	0.999999447	0.016665748	0.770327538	0.999999447	0.082524807	-0.43231195
STN1	0.385883857	0.96521081	0.525693718	0.765795192	0.96521081	0.177040794	0.379911336
APC	0.950329669	1	0.018941734	0.764133153	1	0.032557745	-0.186196517
SF3B1	0.396857231	0.985254946	0.167453355	0.758708257	0.985254946	0.055963987	0.361851025

HELB	0.568693343	0.99823044	0.173793352	0.757672203	0.99823044	0.106849088	0.18897886
SSBP3	0.869913407	0.993437983	0.124852644	0.757239201	0.993437983	0.124852644	-0.112674206
RBBP8	0.501838356	0.96332858	0.333322767	0.75516921	0.96332858	0.290947083	0.253330854
CDCA5	0.471446315	0.953015111	0.410465928	0.753898202	0.953015111	0.355940538	0.282451887
DUT	0.532754467	0.963292454	0.264972384	0.748134956	0.963292454	0.264972384	0.21538049
SCAF11	0.893994862	0.986336654	0.065113885	0.740654074	0.986336654	0.106747942	-0.153340788
MCRS1	0.579872089	0.962567628	0.238472544	0.735886139	0.962567628	0.237193944	0.15601405
CSNK2B	0.267964331	0.925706318	0.814131287	0.735265482	0.925706318	0.668643136	0.46730115
NCAPG2	0.353751211	0.964674732	0.648837051	0.734059972	0.964674732	0.248514921	0.38030876
MMS22L	0.443912075	0.993358946	0.316429493	0.724518392	0.993358946	0.095969568	0.280606317
FANCI	0.451293692	0.938329569	0.525008094	0.72082028	0.938329569	0.347230403	0.269526587
HDAC9	1.004834047	0.999999739	0.031717342	0.719837671	0.999999739	0.061757606	-0.284996376
ERCC3	0.259299845	0.90174041	0.895939043	0.712533846	0.951370037	0.387855137	0.453234001
POLR2K	0.553599397	0.950612481	0.466559829	0.709769291	0.950612481	0.450585517	0.156169894
UBA2	0.394634327	0.971728077	0.574803006	0.706488579	0.971728077	0.306140555	0.311854252
RPA3	0.334188058	0.948213769	0.69465913	0.701548343	0.948213769	0.251679352	0.367360285
SENP8	1.397902065	1	0.018598027	0.700992654	1	0.124909829	-0.696909411
ACTL6A	0.358286421	0.970335202	0.609068499	0.698453741	0.970335202	0.221222324	0.34016732
SKP1	0.72028588	0.9118113	0.411038191	0.697838812	0.9118113	0.411038191	-0.022447068
TERF1	0.300716598	0.891230903	0.881866827	0.696338881	0.891230903	0.686687749	0.395622283
EP300	0.972588809	1	0.040019774	0.693616665	1	0.07019854	-0.278972144
NEIL1	0.414464269	0.967157443	0.197009555	0.690933754	0.967157443	0.189189276	0.276469485
CSNK1D	0.582612508	0.998727585	0.105453163	0.688091773	0.998727585	0.105453163	0.105479265
GTF2H3	0.252724093	0.928549406	0.83338472	0.685450757	0.95911275	0.292084438	0.432726664
BRCC3	1.10574645	0.99999999	0.063021436	0.67906394	0.99999999	0.129582776	-0.42668251
BRCA1	0.550838477	0.955113721	0.283203934	0.67890862	0.955113721	0.262227722	0.128070143
NSMCE1	0.187589796	0.867557448	0.975699288	0.678901025	0.955246461	0.204691963	0.491311228
HUWE1	0.334594436	0.973696627	0.616699647	0.669553069	0.973696627	0.246624112	0.334958633
RFC2	0.468266061	0.937529267	0.519520376	0.668029589	0.937529267	0.394048838	0.199763528
APOBEC3C	0.651966331	0.995992372	0.161640284	0.662949724	0.995992372	0.161640284	0.010983394
GTF2H4	0.447515912	0.960760387	0.388348798	0.65946552	0.960760387	0.223851421	0.211949608
RAD1	0.323759743	0.901107482	0.81722643	0.651998964	0.901107482	0.447352348	0.328239221
YBX1	0.13271515	0.743065398	0.999992389	0.647495605	0.840390641	0.795249761	0.514780456
RECQL	0.870503241	0.991266977	0.106949165	0.643391453	0.991266977	0.149410788	-0.227111788
SETX	0.638301636	0.956660985	0.104585117	0.642760559	0.956660985	0.104585117	0.004458923
BCLAF1	0.931145382	1	0.096179445	0.640527458	1	0.160306515	-0.290617924
PMS2P5	0.138202807	0.642106223	0.567006492	0.637981541	0.642106223	0.567006492	0.499778734
THRAP3	0.993672044	1	0.049885242	0.634770018	1	0.137171968	-0.358902026
NonTargetingCo	0.500963774	0.995789702	0.150159785	0.632748896	0.995789702	0.150159785	0.131785122
PRMT1	0.376784763	0.954860129	0.508823395	0.632347451	0.954860129	0.304772787	0.255562688
POLR2J	0.718039456	0.996488758	0.151021882	0.628387265	0.996488758	0.151021882	-0.089652192
NOTCH3	0.629412445	0.994536715	0.114422057	0.625477466	0.994536715	0.114422057	-0.00393498
POLR2F	0.430626457	0.963045892	0.427068794	0.624330295	0.963045892	0.305987292	0.193703839
SUPT6H	0.474132851	0.974460321	0.366703068	0.623610778	0.974460321	0.275097337	0.149477927
ECT2	0.514413137	0.945441559	0.314002487	0.623015299	0.945441559	0.278317049	0.108602162
L3MBTL1	0.854595326	0.999081574	0.034925472	0.622960338	0.999081574	0.086390665	-0.231634988
CBX5	0.366269036	0.913303254	0.48031268	0.621978365	0.913303254	0.48031268	0.255709329
SUMO4	0.463018295	0.958853859	0.212663185	0.619458656	0.958853859	0.153849462	0.156440361
CUL1	0.281142958	0.852117278	0.817536936	0.618087586	0.910397649	0.806421161	0.336944628
WEE1	0.600200634	0.971297942	0.233526736	0.61679714	0.971297942	0.233526736	0.016596506
CCND3	0.780095793	0.99943543	0.03918954	0.613744292	0.99943543	0.067200257	-0.166351501
ATMIN	0.504352778	0.945798935	0.407700882	0.613101145	0.945798935	0.392876994	0.108748367
NONO	0.317595834	0.924561884	0.677445624	0.612648738	0.924561884	0.647037783	0.295052905
TAF1	0.559692212	0.960873048	0.35466535	0.611123834	0.960873048	0.35466535	0.051431622
ANKRD52	0.392471217	0.919276861	0.538245639	0.610599015	0.919276861	0.36346902	0.218127798
SMC6	0.167952582	0.820466401	0.999345574	0.609708773	0.886668239	0.684501774	0.441756191
MTOR	0.367836152	0.97405185	0.483736938	0.608388275	0.97405185	0.246902131	0.240552123
CHD4	0.349677869	0.948970665	0.557518574	0.60731505	0.948970665	0.318866757	0.257637181
ALKBH2	0.746975538	0.987312972	0.123447394	0.603786018	0.987312972	0.163587799	-0.14318952
SMARCB1	0.37323629	0.958125566	0.727687149	0.59841862	0.958125566	0.618036036	0.225182331
APOBEC1	0.734016869	0.956864874	0.234856141	0.597171999	0.956864874	0.234856141	-0.13684487
INO80E	0.599795954	0.915057453	0.305161286	0.589979126	0.915057453	0.305161286	-0.009816828
NCAPH2	0.319972736	0.958320243	0.757017051	0.588922948	0.958320243	0.485389183	0.268950212
NOTCH2	0.510715064	0.91600724	0.344733419	0.588493958	0.91600724	0.344733419	0.077778894
PBRM1	0.687943917	1	0.135051244	0.586353275	1	0.135202919	-0.101590643
CSNK2A2	0.50986497	0.999868116	0.163497721	0.586137615	0.999868116	0.138047626	0.076272644
PDS5A	0.223515701	0.881387988	0.943428028	0.583780693	0.903669151	0.747192437	0.360264992
DTX4	0.768386081	0.999941958	0.048127349	0.582824383	0.999941958	0.100502891	-0.185561697
COPS2	0.568854641	0.972442529	0.21942953	0.582187508	0.972442529	0.21942953	0.013332867
BRD4	0.366077075	0.954687836	0.459386861	0.580963612	0.954687836	0.228469914	0.214886537
USP11	0.538775995	0.977479353	0.153262321	0.58058747	0.977479353	0.153262321	0.041811475
BCAS2	0.393516836	0.952015502	0.519345734	0.579187998	0.952015502	0.321132075	0.185671162
NELFB	0.326455677	0.92473282	0.614812545	0.57875234	0.92473282	0.614812545	0.252296664
SIRT7	0.247455597	0.999664558	0.268494609	0.575320168	0.999664558	0.161013986	0.327864571
XRCC2	0.467780347	0.962583472	0.408856284	0.57498531	0.962583472	0.408856284	0.107204963
MORF4L2	0.399172218	0.909420079	0.401249076	0.573253985	0.909420079	0.401249076	0.174081767
SIRT1	0.31689217	0.999600581	0.201449853	0.57198745	0.999600581	0.143449576	0.255095279
SPTBN1	0.886349276	1	0.039491377	0.57189824	1	0.114241101	-0.314451036
WRNIP1	0.32049541	0.995688479	0.305766406	0.568113115	0.995688479	0.188067147	0.247617705
SMARCD1	0.525308641	0.999812917	0.137079121	0.567089118	0.999812917	0.137079121	0.041780477
CCNB3	0.717691187	0.999788155	0.076506761	0.5626955	0.999788155	0.128605479	-0.154995688
TIMELESS	0.402455917	0.904159214	0.506353162	0.5614994	0.904159214	0.453628084	0.159043483

POLM	0.707251649	0.999967463	0.066705271	0.559886889	0.999967463	0.098898365	-0.14736476
USP51	0.515818535	0.999505252	0.193741697	0.55982461	0.999505252	0.193024582	0.044006075
KAT5	0.255786644	0.939740242	0.67560114	0.55391209	0.939740242	0.347298061	0.298125446
RAD54L2	0.528436525	0.99939853	0.175195409	0.552639103	0.99939853	0.175195409	0.024202578
APOBEC2	0.606607318	0.999739009	0.145825187	0.550721098	0.999739009	0.155543975	-0.05588622
SCAF8	0.490131615	0.997827855	0.175836763	0.547630531	0.997827855	0.172985518	0.057498916
NonTargetingCo	0.67970672	0.999344463	0.161848152	0.546956029	0.999344463	0.174973777	-0.132750691
HNRNPUL1	0.391382272	0.981160424	0.318235111	0.543892879	0.981160424	0.318235111	0.152510606
KLHL15	0.269454997	0.992613477	0.306523469	0.542364329	0.992613477	0.212715082	0.272909333
COL1A1	0.366080096	0.911479638	0.541344177	0.539478509	0.911479638	0.460714715	0.173398413
UBE2K	0.253967734	1	0.303014228	0.537837763	1	0.167608679	0.283870029
ABL1	0.672014131	0.999996573	0.098284978	0.537551188	0.999996573	0.153482962	-0.134462944
NEIL2	0.473125247	0.900745624	0.319866714	0.535697886	0.900745624	0.319866714	0.062572639
CIB1	0.618150028	0.992548413	0.139868079	0.534148962	0.992548413	0.139868079	-0.084001066
UBE2R2	0.855975926	1	0.067788305	0.529879809	1	0.145224292	-0.326096118
NonTargetingCo	0.531076367	0.999999115	0.15579312	0.525815767	0.999999115	0.15579312	-0.0052606
NFATC2IP	0.464750009	0.947512601	0.218206324	0.521167851	0.947512601	0.218206324	0.056417842
CUL7	0.546102568	0.999988816	0.163441994	0.519258063	0.999988816	0.163441994	-0.026844505
GPI	0.215464397	0.999992441	0.31817114	0.518411299	0.999992441	0.178502918	0.302946901
PMP22	0.633250013	0.999994455	0.152606457	0.517318081	0.999994455	0.155612006	-0.115931932
DTX3L	0.495498776	0.99393549	0.250939498	0.517158469	0.99393549	0.250939498	0.021659693
UBE2NL	0.309468499	0.944566022	0.338582809	0.517101159	0.944566022	0.279276013	0.207632661
NonTargetingCo	0.607242373	0.999896743	0.199662611	0.516328981	0.999896743	0.199662611	-0.090913393
PHF11	0.5548391	0.968480013	0.214912858	0.512641038	0.968480013	0.214912858	-0.042198062
CLSPN	0.352877128	0.890889164	0.569936767	0.509822768	0.890889164	0.569936767	0.15694564
SIRT6	0.580681507	0.933946592	0.319914192	0.506626237	0.933946592	0.325524863	-0.07405527
WDR70	0.274001952	0.919984796	0.444759693	0.504255918	0.919984796	0.444759693	0.230253966
RFC1	0.418056179	0.870530865	0.493337784	0.504129285	0.870530865	0.493337784	0.086073105
CTCF	0.122634174	0.784405204	0.999918614	0.503715478	0.868529592	0.614396517	0.381081305
POLI	0.458026212	0.870502638	0.359127809	0.501061541	0.870502638	0.359127809	0.043035328
ALKBH1	0.349034622	0.999961205	0.247811976	0.498782096	0.999961205	0.204675693	0.149747474
TOP3A	0.319739642	0.888644981	0.617350779	0.498632731	0.888644981	0.617350779	0.178893089
POLD2	0.256301144	0.945471268	0.733883653	0.496586335	0.945471268	0.428514497	0.240285191
UBE2D1	0.526864285	0.999939613	0.17954647	0.495053981	0.999939613	0.17954647	-0.031810304
OR1E1	0.493094137	0.985974094	0.248132441	0.49251492	0.985974094	0.248132441	-5.79217E-04
CBX3	0.373231435	0.85241978	0.418979627	0.491329506	0.85241978	0.418979627	0.118098071
POT1	0.320688413	0.855717782	0.689061257	0.487958919	0.855717782	0.689061257	0.167270506
PPP6C	0.216168934	0.901738276	0.895944022	0.487417832	0.927447893	0.543269057	0.271248897
CHFR	0.405361716	0.999662265	0.215805398	0.486359466	0.999662265	0.200026196	0.080997749
NonTargetingCo	0.340278519	0.999944922	0.231304551	0.486265394	0.999944922	0.17984537	0.145986874
ALDH2	0.537953486	0.97275521	0.275798753	0.485824378	0.97275521	0.275798753	-0.052129107
CDK7	-0.071350577	0.578927962	0.999996104	0.483990454	0.819337633	0.882138893	0.555341031
KAT2B	0.68996412	0.998273194	0.149539643	0.478171073	0.998273194	0.190016003	-0.211793048
RRM2	0.04018955	0.686176125	0.999998419	0.474539539	0.837413672	0.82022985	0.434349989
POLN	0.60916456	0.999765812	0.160303789	0.474371384	0.999765812	0.203772318	-0.134793176
EP400	0.507184212	0.878030871	0.605255147	0.473479589	0.878030871	0.605255147	-0.033704623
TRAIP	0.031801186	0.679698557	0.999999649	0.472694744	0.84737765	0.999999649	0.440893558
ATM	0.726936134	1	0.168865327	0.469572463	1	0.262666884	-0.257363671
RAD9B	0.460246134	0.907235566	0.334368469	0.468056927	0.907235566	0.334368469	0.007810793
SIRT4	0.257673676	0.909510653	0.374848148	0.462724124	0.909510653	0.309220548	0.205050448
SERBP1	0.531703972	0.936111565	0.358438756	0.461614707	0.936111565	0.358438756	-0.070089265
PHF3	0.455625991	0.999371961	0.143769059	0.461470369	0.999371961	0.143769059	0.005844379
PLRG1	0.309439362	0.857516336	0.68552123	0.460723146	0.857516336	0.68552123	0.151283783
MGMT	0.499961864	0.992856975	0.198492016	0.457827531	0.992856975	0.201493378	-0.042134332
FBXO18	0.529714634	0.999245999	0.182890444	0.456930124	0.999245999	0.182890444	-0.07278451
RNF111	0.504709692	0.999944988	0.188176928	0.454449697	0.999944988	0.188176928	-0.050259995
SIRT5	0.510897261	0.999831869	0.149802239	0.453350026	0.999831869	0.164763799	-0.057547234
NonTargetingCo	0.471570905	0.999257052	0.158280513	0.452439031	0.999257052	0.158280513	-0.019131874
NonTargetingCo	0.462116891	0.998943602	0.209028753	0.446095563	0.998943602	0.209028753	-0.016021328
MCM10	0.464674147	0.90263807	0.293246413	0.445940293	0.90263807	0.293246413	-0.018733854
MLH3	0.347832787	0.999862757	0.264575591	0.444329427	0.999862757	0.235879208	0.096496641
RNF138	0.457038629	0.999989483	0.198265834	0.443825224	0.999989483	0.198265834	-0.013213405
NonTargetingCo	0.314520653	0.999748986	0.285754435	0.441006929	0.999748986	0.239880679	0.126486276
NOTCH4	0.534518463	0.977380485	0.170484673	0.439284253	0.977380485	0.175613395	-0.09523421
LIG3	0.011577723	0.999904028	0.489055158	0.433525695	0.999904028	0.209181304	0.421947972
USP15	0.757389347	1	0.065138382	0.432773252	1	0.149444377	-0.324616096
CHD1L	0.280722827	0.999838881	0.293622209	0.430428018	0.999838881	0.250804319	0.149705191
RAD51D	0.324252353	0.892670296	0.59099305	0.430182478	0.892670296	0.524784962	0.105930124
CDC25A	0.355230262	0.999910282	0.237963608	0.429454786	0.999910282	0.237963608	0.074224525
SALL4	0.364380296	0.991028909	0.305548539	0.428955112	0.991028909	0.305548539	0.064574816
MVP	0.316961898	0.881549393	0.324692981	0.42768818	0.881549393	0.324692981	0.110726281
CDC25B	0.342002859	0.844476651	0.635585585	0.42616	0.844476651	0.635585585	0.084157141
NonTargetingCo	0.554486916	0.999963084	0.155978914	0.425393527	0.999963084	0.155978914	-0.129093389
RAD51AP1	0.456931665	0.853380663	0.405176852	0.42336151	0.853380663	0.405176852	-0.033570155
FAM175A	0.475283203	0.987271407	0.244612063	0.423237489	0.987271407	0.244612063	-0.052045714
RAD54B	0.632748934	0.984425058	0.210337492	0.422705853	0.984425058	0.227586521	-0.210043081
PER3	0.330918674	0.849608299	0.489903783	0.422482176	0.849608299	0.489903783	0.091563502
NUDT1	0.514664269	0.946357521	0.256553735	0.422297776	0.946357521	0.268982162	-0.092366493
XPC	0.499630599	0.991484933	0.201804197	0.421488332	0.991484933	0.201804197	-0.078142267
NonTargetingCo	0.298967265	0.999895055	0.275815284	0.418374834	0.999895055	0.246418794	0.119407569
USP13	0.344368252	0.999322517	0.2603818	0.417389849	0.999322517	0.2603818	0.073021597
DCUN1D5	0.461718052	0.999889397	0.278144345	0.415475729	0.999889397	0.278144345	-0.046242323

OPRM1	0.401464041	0.999960465	0.208737076	0.41459864	0.999960465	0.208737076	0.013134599
INO80D	0.264091668	0.995796808	0.322263207	0.414217239	0.995796808	0.300051338	0.15012557
RAG2	0.626378518	0.937786552	0.240309256	0.407025391	0.937786552	0.240309256	-0.219353127
MUM1	0.314494111	0.998613554	0.275787866	0.404294631	0.998613554	0.259256963	0.08980052
REV3L	0.210023169	0.868753474	0.932761344	0.403427825	0.868753474	0.788736013	0.193404656
INO80B	0.116820451	0.761572409	0.998019997	0.403031862	0.789809779	0.998019997	0.286211411
CUL9	0.419968504	0.91141591	0.465315529	0.401930022	0.91141591	0.465315529	-0.018038483
CBX1	0.233113527	0.818043684	0.73796149	0.397965353	0.818043684	0.73796149	0.164851825
NonTargetingCo	0.804925962	0.999981145	0.09448797	0.392329033	0.999981145	0.199749228	-0.412596929
DLGAP5	0.480816324	0.886341913	0.404700279	0.391979414	0.886341913	0.404700279	-0.08883691
COPS5	-0.244384407	0.404433415	0.999999992	0.39075595	0.812575703	0.961241786	0.635140358
RNF8	0.16014603	0.802892438	0.996162079	0.385586498	0.802892438	0.960191821	0.225440468
SMG6	-0.005461663	0.636351351	0.975220406	0.385116078	0.812123968	0.975220406	0.390577741
UBE2D4	0.462303142	0.907990743	0.308397143	0.384685324	0.907990743	0.308397143	-0.077617819
WDR76	0.279239542	0.892541247	0.274239745	0.384672844	0.892541247	0.274239745	0.105433301
MSH4	0.364146544	0.993583438	0.259161096	0.381616126	0.993583438	0.259161096	0.017469582
TIPIN	0.245494149	0.889867239	0.384848746	0.380421394	0.889867239	0.384848746	0.134927245
PPM1G	0.127716356	0.727096542	0.977161392	0.379885461	0.804984645	0.977161392	0.252169105
HELLS	0.179866498	0.807778785	0.971985663	0.379525907	0.807778785	0.914990729	0.199659409
CHTF18	0.356636942	0.982124975	0.28965022	0.372851403	0.982124975	0.28965022	0.016214462
UBE2D2	0.393105956	0.926997804	0.271229486	0.372065648	0.926997804	0.271229486	-0.021040308
POLB	0.43192381	0.978148625	0.284457033	0.370537426	0.978148625	0.284457033	-0.061386383
FBXW7	0.574566033	0.999999997	0.085417617	0.368266552	0.999999997	0.155916677	-0.20629948
USP20	0.347646686	0.997002414	0.283895858	0.359199101	0.997002414	0.283895858	0.011552415
NonTargetingCo	0.442509568	0.860063864	0.436971171	0.358485562	0.860063864	0.436971171	-0.084024006
MORF4L1	0.563658653	0.994177809	0.199108881	0.358447101	0.994177809	0.284673044	-0.205211552
EME1	0.526170666	0.900026124	0.209613513	0.357232765	0.900026124	0.286857971	-0.168937901
POLD4	0.325040377	0.846632852	0.684444735	0.355934722	0.846632852	0.684444735	0.030894345
FEN1	0.123433362	0.79899342	0.999973193	0.352818081	0.799238777	0.914509293	0.229384719
POLR2C	0.127829777	0.757168982	0.999999547	0.352789433	0.811996895	0.999999547	0.224959657
TRRAP	0.328885638	0.881436828	0.64564017	0.350149298	0.881436828	0.64564017	0.021263661
APLF	0.171434195	0.999572699	0.363502534	0.349403424	0.999572699	0.27377354	0.177969229
ETAA1	0.322595837	0.999902643	0.221874002	0.347254243	0.999902643	0.221874002	0.024658406
CDC5L	0.137101956	0.81731613	0.999999994	0.342944453	0.81731613	0.94976868	0.205842497
DDB1	0.051937277	0.703881747	1	0.339825989	0.843925082	0.986091054	0.287888712
OTUD7B	0.297632198	0.966178755	0.309427349	0.338111736	0.966178755	0.309427349	0.040479537
ATXN7	0.608538726	0.999322392	0.185430777	0.337749114	0.999322392	0.272883116	-0.270789613
SENP2	0.235677481	0.974847315	0.384750348	0.337380603	0.974847315	0.384750348	0.101703122
CCND2	0.291705106	0.999700615	0.311027717	0.336727776	0.999700615	0.311027717	0.04502267
H3F3B	0.341607808	0.771063803	0.762949784	0.335336501	0.771063803	0.762949784	-0.006271307
USP47	0.446509119	0.996708864	0.31463378	0.333616957	0.996708864	0.31463378	-0.112892162
TDG	0.248283136	0.776038219	0.622908194	0.330918044	0.776038219	0.622908194	0.082634908
NABP2	0.592938669	0.995463463	0.162132468	0.329018532	0.995463463	0.257108345	-0.263920136
NonTargetingCo	0.50853398	0.999346524	0.207882263	0.32812489	0.999346524	0.242091075	-0.18040909
PML	0.317368004	0.999831852	0.230662228	0.32773183	0.999831852	0.230662228	0.010363826
MAU2	-0.147011198	0.476696072	0.999999903	0.326689848	0.829245983	0.999999903	0.473701046
HLTF	0.416922155	0.842836197	0.400106702	0.325657169	0.842836197	0.400106702	-0.091264986
DDX1	-0.23667862	0.387931432	1	0.322280278	0.760905597	1	0.558958898
CUL4B	-0.107486351	0.99947849	0.586378269	0.321489287	0.99947849	0.338852979	0.428975638
KMT5C	0.619178579	0.999795972	0.133164186	0.320847875	0.999795972	0.270707591	-0.298330705
DCUN1D2	0.333394694	0.967274579	0.312938999	0.320701093	0.967274579	0.312938999	-0.012693602
HDAC2	0.402738613	0.869520373	0.350883165	0.318957473	0.869520373	0.350883165	-0.08378114
BARD1	0.109171041	0.778589206	0.99981174	0.317172212	0.778589206	0.99981174	0.208001171
ARID1B	0.359173691	0.970376264	0.301973032	0.315793487	0.970376264	0.301973032	-0.043380204
PRKCG	0.307436638	0.999019977	0.26646088	0.314885711	0.999019977	0.26646088	0.007449074
ATP23	0.28894874	0.941599552	0.436241072	0.314457384	0.941599552	0.436241072	0.025508645
SCAI	0.398552836	0.999862613	0.216875457	0.31287916	0.999862613	0.238601495	-0.085673676
RAD9A	-0.470775683	0.2339057	0.999222767	0.310417717	0.724768978	0.999222767	0.7811934
RRM2B	0.137291676	0.999997564	0.374142036	0.307500433	0.999997564	0.302887972	0.170208758
RECQL5	0.364150897	0.807844349	0.447635835	0.303579955	0.807844349	0.447635835	-0.060570942
TPP1	0.473110787	0.998535295	0.168111978	0.303061756	0.998535295	0.238775227	-0.170049031
CSNK1E	0.284173167	0.996433343	0.282415934	0.302930571	0.996433343	0.282415934	0.018757404
NonTargetingCo	0.214876411	0.999999994	0.31495842	0.301834677	0.999999994	0.31495842	0.086958266
RIF1	0.050419085	0.70734721	0.999998123	0.301655759	0.837438824	0.999998123	0.251236674
NonTargetingCo	0.379861196	0.998153711	0.268790737	0.299171604	0.998153711	0.294528743	-0.080689592
HPF1	0.396970933	0.942247654	0.482518472	0.298627357	0.942247654	0.482518472	-0.098343577
NonTargetingCo	0.359949368	0.999534742	0.252566243	0.298032568	0.999534742	0.252566243	-0.061916801
NonTargetingCo	0.399940064	0.99906883	0.28639908	0.297658846	0.99906883	0.28639908	-0.102281218
RNF2	0.427654003	0.999627895	0.27250104	0.294628844	0.999627895	0.285554332	-0.133025159
TOPBP1	0.172817156	0.749373197	0.999999996	0.292567416	0.756878038	0.999999996	0.119750259
DCUN1D1	0.413050362	0.999999878	0.314919159	0.291088434	0.999999878	0.314919159	-0.121961928
HFM1	0.349526351	0.993815046	0.276872453	0.289986725	0.993815046	0.276872453	-0.059539626
NSMCE3	0.048877426	0.698453842	0.999991203	0.289393785	0.825734077	0.999991203	0.240516358
SFR1	0.401276155	0.81670404	0.6184974	0.289223915	0.81670404	0.6184974	-0.112052241
SUMO1	0.188213129	0.848506551	0.352701213	0.287473228	0.848506551	0.352701213	0.099260099
FAN1	0.289960407	0.997111193	0.267264115	0.285268425	0.997111193	0.267264115	-0.004691982
PRDM10	0.113669381	0.750825113	0.67521091	0.284730562	0.750825113	0.67521091	0.171061181
APTX	0.33897098	0.902305794	0.297388906	0.281886138	0.902305794	0.315636768	-0.057084843
UBE2A	0.242774433	0.966338213	0.370554378	0.281342855	0.966338213	0.370554378	0.038568423
SENP6	-0.286711438	0.322686644	0.99993276	0.281300052	0.744935638	0.99993276	0.56801149
SMARCA4	0.37031933	0.921918975	0.347630633	0.281229728	0.921918975	0.372150019	-0.089089601
UBE2V1	0.246067744	0.994675609	0.311815552	0.281089026	0.994675609	0.311815552	0.035021282

NonTargetingCo	0.323106605	0.993980969	0.287545259	0.280953768	0.993980969	0.287545259	-0.042152837
ATXN3	0.298619174	0.999887003	0.248271682	0.27978673	0.999887003	0.248271682	-0.018832445
NABP1	0.284152881	0.959632317	0.345913405	0.279452417	0.959632317	0.345913405	-0.004700465
UNG	0.505883328	0.879170242	0.711741337	0.278222649	0.879170242	0.711741337	-0.22766068
SMARCAD1	0.336684001	0.902049214	0.473019693	0.277619876	0.902049214	0.473019693	-0.059064125
PARP4	0.287562937	0.999779181	0.272654857	0.277170649	0.999779181	0.272654857	-0.010392288
PRIMPOL	0.233167036	0.97661071	0.334150094	0.275762336	0.97661071	0.334150094	0.0425953
RMI1	0.088313273	0.779794902	0.999979412	0.273491881	0.821870283	0.951183412	0.185178608
MDC1	0.321779889	0.7975822	0.732251606	0.272894906	0.7975822	0.732251606	-0.048884983
FANCE	0.089604266	0.750727108	0.999512955	0.271965705	0.785751133	0.999512955	0.182361439
SETMAR	0.328957864	0.987364155	0.317835521	0.271506072	0.987364155	0.323505813	-0.057451792
RING1	0.420651615	1	0.220555776	0.265710526	1	0.273389315	-0.154941089
SUV39H2	0.17767884	0.994902355	0.317153685	0.263910814	0.994902355	0.317153685	0.086231974
NonTargetingCo	0.366537602	0.999451714	0.280807461	0.263158863	0.999451714	0.296424935	-0.103378739
SLBP	0.144814752	0.84926528	0.520300724	0.262637854	0.84926528	0.520300724	0.117823102
RPA4	0.269746202	0.926587876	0.347017442	0.260844413	0.926587876	0.347017442	-0.008901789
SUMO3	0.223064655	0.994900124	0.328498082	0.260134127	0.994900124	0.328498082	0.037069472
NonTargetingCo	0.327835915	0.999999893	0.249756542	0.258901382	0.999999893	0.276269994	-0.068934533
MEN1	-0.020974036	0.619235737	0.983314517	0.257409713	0.712323746	0.983314517	0.278383749
TYMS	0.162326344	0.989232021	0.373620608	0.256170237	0.989232021	0.373620608	0.093843894
NSMCE4A	0.16462439	0.797276073	0.999942809	0.255369407	0.797276073	0.999942809	0.090745017
COPS7A	0.160935669	0.999970404	0.376272799	0.254930687	0.999970404	0.349247598	0.093995019
BRAT1	0.192455024	0.764885569	1	0.254676499	0.764885569	1	0.062221475
TOP2A	0.130692025	0.810893181	0.622751665	0.254609451	0.810893181	0.622751665	0.123917426
RPA2	-0.21376361	0.432295693	0.999999998	0.253970309	0.702065047	0.999999998	0.467733919
CASP3	0.107890271	0.92594083	0.520395807	0.25051429	0.92594083	0.457113336	0.14262402
RECQL4	0.613534021	0.880369061	0.595715041	0.249142842	0.877680198	0.595715041	-0.364391179
CETN2	0.297006696	0.995655769	0.37745133	0.246762896	0.995655769	0.37745133	-0.0502438
PRDM9	0.232303207	0.943546646	0.367872819	0.2462107	0.943546646	0.367872819	0.013907494
SLX4	0.134821732	0.708659367	0.999341474	0.245495944	0.72475368	0.999341474	0.110674212
NCAPG	-0.034200251	0.598434212	0.999983682	0.244747076	0.775976151	0.999983682	0.278947327
CDKN1B	0.32112048	0.999985514	0.28000831	0.244400577	0.999985514	0.299831019	-0.076719903
NEK9	0.476432151	0.99995695	0.192826201	0.243968607	0.99995695	0.261878806	-0.232463544
OR6B1	0.369405735	0.780133397	0.543041925	0.243770756	0.780133397	0.543041925	-0.125634979
SSBP2	0.477726997	0.999223979	0.29651219	0.243240097	0.999223979	0.29651219	-0.2344869
ATF2	0.204044217	0.990828682	0.307924958	0.242596009	0.990828682	0.307924958	0.038551792
NonTargetingCo	0.235156649	0.998153433	0.304050787	0.241890122	0.998153433	0.304050787	0.006733474
MPZ	0.233931752	0.783285652	0.514905795	0.241397115	0.783285652	0.514905795	0.007465363
SMARCAL1	0.286381239	0.760780742	0.748013154	0.240007721	0.760780742	0.748013154	-0.046373519
NonTargetingCo	0.231527536	0.999971612	0.299195533	0.239957248	0.999971612	0.299195533	0.008429712
HMGB2	0.529962903	0.999925107	0.189092663	0.239609392	0.999925107	0.294548092	-0.290353511
BAZ1A	0.145901898	0.733462775	0.45138603	0.239569294	0.733462775	0.45138603	0.093667396
PIAS1	0.239954108	0.730146097	0.478187399	0.23956084	0.730146097	0.478187399	-3.93269E-04
RHO	0.159588291	0.867938538	0.43694721	0.239256803	0.867938538	0.43694721	0.079668512
SKIV2L2	0.10922438	0.791033887	0.788549952	0.238461501	0.791033887	0.788549952	0.129237121
EID3	0.170894052	0.993920362	0.38559444	0.23843719	0.993920362	0.368745894	0.067543138
CCNB2	0.364482867	0.989274411	0.262865149	0.237681763	0.989274411	0.349399958	-0.126801104
PPP6R3	0.198306861	0.99966489	0.346160016	0.230222089	0.99966489	0.346160016	0.031915229
MSH3	0.349040835	0.986451479	0.310510777	0.230086217	0.986451479	0.328355923	-0.118954618
PPP6R2	0.154498939	0.793930204	0.51836679	0.229997991	0.793930204	0.51836679	0.075499052
MBD4	0.346396449	0.99826714	0.294597572	0.227598825	0.99826714	0.294597572	-0.118797625
FANCM	-0.026907834	0.605209051	0.999902234	0.220675893	0.73068862	0.999902234	0.247583726
TP73	0.228221807	0.721214667	0.496816724	0.217701868	0.721214667	0.496816724	-0.010519938
PIF1	0.289386808	0.789502562	0.452710548	0.217233042	0.789502562	0.452710548	-0.072153766
DCAF11	0.34057827	0.900717935	0.386361477	0.21626799	0.900717935	0.386361477	-0.12431028
GABBR1	0.152584097	0.830415951	0.443223333	0.215827262	0.830415951	0.443223333	0.063243165
PIAS2	0.174949454	0.972756723	0.373570722	0.215446755	0.972756723	0.373570722	0.040497302
EXO5	0.193381234	0.775154374	0.966614507	0.214351367	0.775154374	0.966614507	0.020970133
HELQ	-0.028334907	0.53104413	0.86709702	0.214052942	0.694556398	0.86709702	0.242387849
ZRANB3	0.179837509	0.858872109	0.384695382	0.212341904	0.858872109	0.384695382	0.032504395
MAPK14	0.27530326	0.999999645	0.374315111	0.212086655	0.999999645	0.374315111	-0.063216605
NIPBL	0.306525747	0.754348284	0.998963233	0.210823162	0.754348284	0.998963233	-0.095702585
SMARCC1	0.022106108	0.999999991	0.479243695	0.210334113	0.999999991	0.360935491	0.188228004
DTX3	0.098059875	0.999520968	0.402899465	0.209054233	0.999520968	0.388267478	0.110994358
NUDT16L1	0.132170695	0.821254066	0.439119507	0.207721136	0.821254066	0.439119507	0.075550441
NonTargetingCo	0.376914598	0.990797611	0.311783685	0.205609028	0.990797611	0.312148404	-0.171305569
KAT2A	0.056820247	0.699444162	0.992094734	0.204592701	0.699444162	0.992094734	0.147772454
TRIP12	0.509089587	0.999977382	0.190500439	0.204431419	0.999977382	0.327148801	-0.304658168
ERCC6	0.038199894	0.742080257	0.463305052	0.203975228	0.742080257	0.461681238	0.165775334
KMT5A	0.044776008	0.741562051	0.574073591	0.203807832	0.741562051	0.574073591	0.159031824
PAGR1	0.198099944	0.703693388	0.916817828	0.202803743	0.703693388	0.916817828	0.004703799
HDAC1	0.238744524	0.853806783	0.358107678	0.202786863	0.853806783	0.358107678	-0.035957661
EXD2	0.195805746	0.986875983	0.445430619	0.20170656	0.986875983	0.445430619	0.005900813
PINX1	-0.12540294	0.4890233	0.974286015	0.201252104	0.683101813	0.974286015	0.326655044
PARP2	0.301501907	0.943985904	0.309226463	0.200860676	0.943985904	0.309226463	-0.100641231
UIMC1	0.225093982	0.861488402	0.390302293	0.199566106	0.861488402	0.390302293	-0.025527876
IP6K3	0.12028865	0.985510177	0.420443513	0.199388785	0.985510177	0.414284209	0.079100135
CLK2	0.071729317	0.937955813	0.53407626	0.19870005	0.937955813	0.496150193	0.126970733
INO80C	0.245621527	0.99225101	0.408909174	0.198253664	0.99225101	0.408909174	-0.047367863
H2AFY2	0.186008731	0.763884749	0.465235999	0.196110382	0.763884749	0.465235999	0.010101651
RNF169	0.171406662	0.972630813	0.445966562	0.194683429	0.972630813	0.445966562	0.023276767
FIGNL1	-0.016811797	0.606793026	0.998935428	0.193966159	0.67263919	0.998935428	0.210777956

USP45	0.290465849	0.96395309	0.348616929	0.193480256	0.96395309	0.348616929	-0.096985592
CENPS	0.210625614	0.809540827	0.504680041	0.192107366	0.809540827	0.504680041	-0.018518248
SIRT2	0.281448634	0.996559267	0.27428979	0.190776549	0.996559267	0.312800279	-0.090672085
RBBP7	0.288182063	0.976664116	0.416652738	0.190758643	0.976664116	0.416652738	-0.09742342
RAD18	0.268618645	0.998249125	0.318397932	0.189786742	0.998249125	0.318397932	-0.078831902
POLE	0.005568224	0.65044863	0.865959085	0.186585804	0.767358674	0.865959085	0.18101758
PARP9	0.370294465	0.997612841	0.358199205	0.186371163	0.997612841	0.43324421	-0.183923302
SENP7	0.171343024	0.8161503	0.467620277	0.185445931	0.8161503	0.467620277	0.014102907
POLR2B	-0.216481377	0.468988107	0.998193741	0.184470603	0.659020709	0.998193741	0.400951979
TOP2B	0.100925367	0.894281573	0.517418298	0.182356958	0.894281573	0.517418298	0.081431592
ANP32E	0.156182167	0.877808356	0.388795789	0.180876547	0.877808356	0.388795789	0.02469438
NonTargetingCo	0.236617153	0.975822499	0.356101424	0.180718675	0.975822499	0.356101424	-0.055898478
SMARCA5	0.01820058	0.665372902	0.999784118	0.179928313	0.751199328	0.999784118	0.161727733
UBE2V2	0.423879572	0.999897557	0.188967762	0.178368788	0.999897557	0.345894655	-0.245510783
NonTargetingCo	0.202147548	0.999854713	0.331837147	0.177679184	0.999854713	0.331837147	-0.024468364
PARK2	0.159903876	0.744557492	0.508448011	0.175246668	0.744557492	0.508448011	0.015342792
USP44	0.151529559	0.66852974	0.962981781	0.174560436	0.66852974	0.962981781	0.023030877
ANKRD28	0.344712209	0.964281934	0.377704218	0.172785874	0.964281934	0.377704218	-0.171926334
APBB1	0.072882493	0.998373594	0.421358868	0.170778616	0.998373594	0.368351676	0.097896124
SMC3	-0.098608192	0.532186486	0.999896419	0.169402041	0.66233072	0.999896419	0.268010234
NonTargetingCo	0.355351287	0.999695194	0.275977059	0.167967878	0.999695194	0.34865466	-0.187383409
OR1E2	-0.179013757	0.776359	0.646068915	0.166444109	0.776359	0.639285089	0.345457867
TNKS	0.126349217	0.667495342	0.844252915	0.165199313	0.667495342	0.844252915	0.038850096
BOD1L1	-0.032829853	0.60517879	0.999999296	0.164328481	0.714055888	0.999999296	0.197158334
NonTargetingCo	0.31815717	0.999245228	0.296567827	0.163957125	0.999245228	0.350041004	-0.154200045
XRCC3	0.05203835	0.701483566	1	0.163840043	0.723177898	1	0.111801693
SET	-0.084422359	0.548548085	0.9998963	0.162002677	0.635075834	0.9998963	0.246425036
PINK1	0.133626093	0.859205561	0.480296597	0.161693155	0.859205561	0.480296597	0.028067062
POLQ	0.206025128	0.707187804	0.452518333	0.160927477	0.707187804	0.452518333	-0.045097651
MSH2	0.269148225	0.974192869	0.401188919	0.158716909	0.974192869	0.401188919	-0.110431316
MTA3	-0.030980498	0.998930186	0.547359712	0.156317881	0.998930186	0.472414848	0.187298379
NEIL3	0.262646778	0.830465663	0.459576238	0.154469848	0.830465663	0.459576238	-0.108176929
C9orf142	0.431925396	0.955815087	0.345532622	0.154014393	0.955815087	0.371053383	-0.277911002
DTX1	0.234206059	0.802545681	0.457077757	0.15323491	0.802545681	0.457077757	-0.08097115
USP22	0.156814152	0.642641712	0.653544646	0.148331124	0.642641712	0.653544646	-0.008483028
NonTargetingCo	0.245055782	0.999117535	0.350377074	0.148248239	0.999117535	0.362643208	-0.096807544
NonTargetingCo	0.285915648	0.998539304	0.315053553	0.147943066	0.998539304	0.38688018	-0.137972582
IGHMBP2	0.074253192	0.733461585	0.477616102	0.147809134	0.733461585	0.477616102	0.073555942
NonTargetingCo	0.499186756	0.999991775	0.217961669	0.144991406	0.999991775	0.383256157	-0.35419535
PARK7	0.197329461	0.994823768	0.356819735	0.144233111	0.994823768	0.356819735	-0.05309635
SHFM1	0.06493968	0.999991064	0.45381777	0.143637797	0.999991064	0.446457726	0.078698116
HDAC4	0.101608408	0.952460343	0.448885076	0.143559086	0.952460343	0.448885076	0.041950678
NonTargetingCo	0.140635653	0.998830219	0.372629334	0.143143418	0.998830219	0.372629334	0.002507765
APOBEC3A	0.178830077	0.949371552	0.402239037	0.14197017	0.949371552	0.402239037	-0.036859907
PAPD7	0.026422408	0.791645969	0.607132583	0.141606657	0.791645969	0.529345001	0.115184249
NonTargetingCo	0.184370111	0.99994745	0.42039104	0.140083152	0.99994745	0.42039104	-0.044286959
CCNO	0.112287059	0.98679286	0.393804847	0.139633915	0.98679286	0.393804847	0.027346856
PPP5C	0.041976523	0.956631895	0.457858901	0.13830775	0.956631895	0.442428591	0.096331228
NonTargetingCo	0.165686803	0.939658178	0.359655223	0.137113958	0.939658178	0.359655223	-0.028572846
TERF2IP	0.239063688	0.747038604	0.740824367	0.135992388	0.747038604	0.740824367	-0.1030713
NonTargetingCo	0.248073406	0.998182876	0.349017695	0.133920552	0.998182876	0.375299197	-0.114152854
CDKN2A	0.323500887	0.999994328	0.26627578	0.132502962	0.999994328	0.412837869	-0.190997925
RHNO1	-0.11414187	0.976984352	0.598425131	0.132379189	0.976984352	0.501028007	0.246521059
NonTargetingCo	0.074845753	0.999499894	0.446367433	0.130582545	0.999499894	0.446367433	0.055736792
CDC34	0.234787574	0.943082939	0.317670536	0.130091008	0.943082939	0.372836029	-0.104696566
HNRNPUL2	0.19112298	0.999853973	0.361544483	0.129560081	0.999853973	0.381769483	-0.061562898
UCHL5	-0.404248878	0.236702792	0.999999896	0.126944347	0.622926319	0.999999896	0.531193225
PSIP1	0.160209525	0.882014247	0.407987723	0.125041277	0.882014247	0.407987723	-0.035168248
NonTargetingCo	0.233662123	0.9463425	0.377586763	0.123764007	0.9463425	0.377586763	-0.109898116
MRE11	0.30082283	0.806380107	0.999979051	0.118029192	0.78700842	0.999979051	-0.182793638
POLE4	-0.041769721	0.59141024	0.999981281	0.116542184	0.609192821	0.999981281	0.158311905
ERCC8	0.151748201	0.716506865	0.709966902	0.116078139	0.716506865	0.709966902	-0.035670062
NonTargetingCo	0.122333369	0.99991058	0.441098104	0.115942881	0.99991058	0.441098104	-0.006390488
EME2	-0.058043618	0.998886994	0.583093659	0.115628631	0.998886994	0.583093659	0.173672249
NonTargetingCo	0.033124009	0.999960589	0.470147617	0.115476952	0.999960589	0.470147617	0.082352943
HMGB1	0.791723087	0.994845796	0.425398111	0.115466441	0.994845796	0.469061389	-0.676256646
OGG1	-0.008340151	0.848582944	0.508307522	0.115346694	0.848582944	0.508307522	0.123686845
RAP1A	0.19255877	0.998612783	0.393863608	0.114086686	0.998612783	0.409908534	-0.078472084
NonTargetingCo	0.042761908	0.998422901	0.457736564	0.112704276	0.998422901	0.457736564	0.069942368
KDM1A	-0.079761611	0.935769267	0.576498871	0.112013403	0.935769267	0.48560199	0.191775014
NonTargetingCo	0.1619288	0.999975913	0.446068832	0.111386577	0.999975913	0.446068832	-0.050542223
CSNK2A1	-0.262970831	0.59893175	0.749365565	0.111357772	0.59893175	0.744935698	0.374328603
STAG1	0.227472047	0.723799903	0.633347551	0.109624145	0.723799903	0.633347551	-0.117847902
RNF40	0.172548026	0.729677955	0.999986349	0.108899014	0.729677955	0.999986349	-0.063649012
SMC1B	0.274894788	0.999741633	0.333848527	0.107651166	0.999741633	0.39971864	-0.167243622
REV1	0.083720514	0.951147894	0.418264435	0.106932987	0.951147894	0.418264435	0.023212473
NonTargetingCo	0.296627755	0.999974703	0.315982043	0.10565409	0.999974703	0.399229992	-0.190973664
CDK2	-0.302984953	0.355245308	0.991668433	0.10517448	0.67148519	0.991668433	0.408159433
ERCC5	0.172530907	0.788299656	0.480513536	0.104315441	0.788299656	0.480513536	-0.068215466
AICDA	0.030042485	0.884412741	0.47259631	0.103981221	0.884412741	0.47259631	0.073938737
USP3	0.352998415	0.90412076	0.449800464	0.103296304	0.90412076	0.449800464	-0.249702111
NLK	0.207005543	0.981217976	0.473667152	0.10037435	0.981217976	0.473667152	-0.106631193

BAZ1B	0.196188049	0.677081241	0.831773684	0.100075894	0.677081241	0.831773684	-0.096112155
NonTargetingCo	0.10721369	0.999028141	0.437768735	0.099053281	0.999028141	0.437768735	-0.008160409
MSH6	0.336586656	0.807076469	0.633023141	0.098424167	0.77028725	0.633023141	-0.238162488
APOBEC3G	0.172558944	0.800085083	0.404673257	0.097794993	0.800085083	0.404673257	-0.074763951
PRMT6	0.001627464	0.998934623	0.498427432	0.097508662	0.998934623	0.462884498	0.095881198
ALKBH3	0.204496952	0.999874058	0.340861998	0.097096815	0.999874058	0.402184634	-0.107400137
CRY2	0.081785464	0.8956699	0.466013717	0.096751867	0.8956699	0.466013717	0.014966403
NOTCH1	0.161498064	0.99799131	0.40855067	0.094979928	0.99799131	0.40855067	-0.066518136
POLH	0.147576642	0.817609978	0.414541812	0.092886523	0.817609978	0.414541812	-0.054690119
NonTargetingCo	0.067907148	0.99999086	0.476318929	0.092723087	0.99999086	0.476318929	0.024815939
CCNA2	0.005150099	0.649111021	0.999949601	0.091905399	0.656303391	0.999949601	0.0867553
NonTargetingCo	0.178838353	0.997641235	0.416399926	0.08987514	0.997641235	0.416399926	-0.088963213
WDR48	0.143072651	0.618490932	0.999368917	0.089525909	0.618490932	0.999368917	-0.053546742
NSMCE2	-0.197583236	0.402159958	0.996527617	0.088765279	0.581523688	0.996527617	0.286348515
NonTargetingCo	0.248671566	0.995299415	0.370924813	0.088666127	0.995299415	0.415645803	-0.16000544
NonTargetingCo	0.18444402	0.965584874	0.434281159	0.084889796	0.965584874	0.434281159	-0.099554224
OTUB2	0.00231718	0.999750694	0.497927565	0.083390052	0.999750694	0.497927565	0.081072873
PARP14	0.128894718	0.999626837	0.470970352	0.082890299	0.999626837	0.470970352	-0.046004419
WHSC1	0.090989869	0.984510192	0.423713962	0.08259638	0.984510192	0.423713962	-0.008393489
PPP4R4	0.285672558	0.999944276	0.376532614	0.082416921	0.999944276	0.423630814	-0.203255637
NonTargetingCo	0.094635038	0.999971942	0.477072241	0.081785473	0.999971942	0.477072241	-0.012849565
BEND3	0.126494563	0.782060364	0.418467606	0.080444058	0.782060364	0.418467606	-0.046050506
NFRKB	-0.066215911	0.57136474	0.983903022	0.08032033	0.57136474	0.983903022	0.146536242
SHPRH	0.098958681	0.726763686	0.552152367	0.077119567	0.726763686	0.552152367	-0.021839114
SLF1	0.105642745	0.957297648	0.419842852	0.077101292	0.957297648	0.419842852	-0.028541453
ATAD5	-0.227787361	0.639201937	0.719766489	0.076304936	0.639201937	0.719766489	0.304092297
NonTargetingCo	0.223745852	0.999998311	0.370998384	0.073703669	0.999998311	0.431434635	-0.150042183
UHRF2	0.150949908	0.933087821	0.456677267	0.073231661	0.933087821	0.481163607	-0.077718247
APOBEC3B	0.495681136	0.999967008	0.236724223	0.072803602	0.999967008	0.439631995	-0.422877534
COPS7B	-0.028425894	0.999189187	0.530865771	0.071324268	0.999189187	0.530865771	0.099750163
NonTargetingCo	0.01743834	0.999049499	0.483241338	0.070988352	0.999049499	0.483241338	0.053550012
CCNB1	0.137667683	0.634479609	0.998111376	0.068262306	0.634018473	0.998111376	-0.069405377
PPP6R1	0.094075231	0.772941429	0.646705834	0.067919262	0.772941429	0.646705834	-0.026155969
APOBEC3D	0.211079234	0.974141819	0.417259904	0.067875679	0.974141819	0.441172526	-0.143203555
TNP1	0.361322998	0.962981376	0.371141252	0.067462979	0.962981376	0.439422263	-0.293860019
TRIM29	0.189422766	0.983559316	0.416560922	0.067242188	0.983559316	0.433498953	-0.122180579
MLH1	0.005062914	0.942751324	0.556658798	0.065992863	0.942751324	0.556658798	0.060929949
RMI2	-0.165800103	0.436135851	0.971086796	0.064624998	0.564797388	0.971086796	0.230425101
APOBEC3F	0.223065013	0.96743583	0.474663017	0.063944441	0.96743583	0.501546132	-0.159120572
MCPH1	-0.015420607	0.586576959	0.999999494	0.062809071	0.586576959	0.999999494	0.078229678
PXMP2	0.128311372	0.923308842	0.444325346	0.060566703	0.923308842	0.444325346	-0.067744669
RASSF7	0.188515544	0.997777622	0.450251198	0.060147647	0.997777622	0.450251198	-0.128367897
CCNA1	0.034679891	0.810951228	0.598707029	0.058685624	0.810951228	0.598707029	0.024005734
ADH5	0.217448393	0.997682785	0.454255411	0.055027897	0.997682785	0.454255411	-0.162420496
XPA	0.198370699	0.954356687	0.473829968	0.05268071	0.954356687	0.473829968	-0.145689989
NonTargetingCo	0.222434374	0.999989034	0.374467506	0.051899445	0.999989034	0.448699368	-0.170534929
NonTargetingCo	-0.068327269	0.984970515	0.567578657	0.049997001	0.984970515	0.567578657	0.11832427
GEN1	0.276229726	0.754153117	0.671192216	0.04769194	0.754153117	0.680332541	-0.228537787
APOBEC3H	0.170452151	0.843921742	0.402261229	0.044590678	0.843921742	0.460698652	-0.125861474
WRN	0.131974248	0.936131005	0.479474015	0.042583582	0.936131005	0.515359827	-0.089390666
NonTargetingCo	0.100703259	0.999838243	0.461086203	0.041196446	0.999838243	0.461086203	-0.059506813
MUTYH	0.114817047	0.663194739	0.683401713	0.040645969	0.663194739	0.683401713	-0.074171078
MCM3AP	-0.286180313	0.308827261	0.973219488	0.036863167	0.535656581	0.973219488	0.323043481
EXO1	0.079384069	0.626652201	0.875452844	0.031063341	0.626652201	0.875452844	-0.048320729
H3F3A	0.226807795	0.576658748	0.533961199	0.030838678	0.576658748	0.533961199	-0.195969117
PMS1	0.210088274	0.958274699	0.395162706	0.030467873	0.958274699	0.471369499	-0.179620401
PARP3	-0.189061477	0.999043034	0.676938494	0.030361073	0.999043034	0.604239028	0.21942255
PER2	-0.097272424	0.999727149	0.594350844	0.028219027	0.999727149	0.535196289	0.125491451
SLF2	0.017301604	0.968887803	0.484472338	0.028168707	0.968887803	0.484472338	0.010867103
MUS81	0.262045319	0.73378913	0.99287909	0.02795188	0.612924944	0.99287909	-0.234093439
MTA1	-0.212200519	0.620309887	0.799156054	0.027537536	0.620309887	0.740035073	0.239738055
BMI1	0.072267586	0.997754667	0.473439774	0.027322754	0.997754667	0.473439774	-0.044944832
MMS19	-0.176260766	0.438297367	0.99999986	0.026661134	0.59052151	0.99999986	0.202921899
MBTD1	0.330697551	0.982125174	0.388244541	0.026545393	0.982125174	0.534368121	-0.304152158
NonTargetingCo	0.186983093	0.9999448	0.437487325	0.025662743	0.9999448	0.47723812	-0.16132035
BRIP1	-0.141799403	0.47669902	0.882716175	0.023747323	0.522385756	0.882716175	0.165546726
NonTargetingCo	0.17001704	0.999998025	0.445386196	0.02287021	0.999998025	0.478553585	-0.14714683
PARPBP	0.230639358	0.997597669	0.369543954	0.022696047	0.997597669	0.477570025	-0.207943311
ANKRD44	0.066732909	0.998536699	0.477003499	0.022320155	0.998536699	0.477003499	-0.044412754
NonTargetingCo	-0.016312358	0.995893787	0.516918944	0.021134109	0.995893787	0.516918944	0.037446467
PIAS3	-0.017344841	0.955902472	0.518574108	0.019972651	0.955902472	0.518574108	0.037317492
ERCC2	-0.49491335	0.187000355	1	0.016257288	0.520286283	1	0.511170639
USP26	0.152007057	0.977805328	0.439122437	0.015538564	0.977805328	0.485622771	-0.136468493
SMARCA2	-0.028202709	0.964445153	0.590235601	0.01530662	0.964445153	0.590235601	0.043509329
FANCB	-0.496912034	0.256489302	0.995133965	0.012910738	0.511800817	0.995133965	0.509822772
RFC4	-0.325879669	0.291544092	0.999840568	0.007338403	0.506785614	0.999840568	0.333218072
TCEB3	0.04505574	0.60703653	0.990465878	0.006638889	0.60703653	0.990465878	-0.038416851
BTG2	0.262777446	0.999849211	0.355808262	0.005319547	0.999849211	0.495504378	-0.257457899
ASF1B	0.03716606	0.852870623	0.49571593	0.004380178	0.852870623	0.49571593	-0.032785882
CUL4A	-0.252242157	0.655076567	0.74258042	0.001188571	0.655076567	0.689545238	0.253430728
MPG	0.02048292	0.678395155	0.64260504	2.03046E-04	0.678395155	0.64260504	-0.020279874
GADD45A	0.161994458	0.999990609	0.449042256	-0.002898601	0.999990609	0.50282161	-0.164893059

DCUN1D4	0.203768083	0.997906465	0.37770114	-0.003509477	0.997906465	0.503222977	-0.20727756
TCEA1	-0.032200996	0.635881387	0.597959364	-0.004020063	0.635881387	0.597959364	0.028180932
DNMT1	-0.323635804	0.309144761	0.999965741	-0.00542591	0.494476034	0.999965741	0.318209894
NTHL1	0.115199037	0.931538222	0.496313114	-0.007206169	0.931538222	0.507212164	-0.122405206
USP1	-0.178477004	0.590243354	0.848664132	-0.007316072	0.590243354	0.848664132	0.171160931
RAD54L	-0.067512892	0.553927821	0.930512659	-0.00761728	0.553927821	0.930512659	0.059895612
CCNC	-0.079634918	0.999898713	0.643277447	-0.008339125	0.999898713	0.643277447	0.071295793
NonTargetingCo	0.042081856	0.999913624	0.572381097	-0.008851837	0.999913624	0.572381097	-0.050933693
NonTargetingCo	0.233506459	0.999999634	0.388790269	-0.009613137	0.999999634	0.508604389	-0.243119597
RAD23B	-0.203060898	0.726194025	0.689054646	-0.009835824	0.726194025	0.689054646	0.193225074
UVSSA	0.097944023	0.69812623	0.613241301	-0.009961717	0.69812623	0.613241301	-0.107905739
TDP2	0.069773341	0.674335764	0.917993286	-0.012763567	0.674335764	0.917993286	-0.082536908
TREX1	0.193696223	0.968436391	0.370772458	-0.013178293	0.968436391	0.513313881	-0.206874516
USP4	0.281471169	0.805362863	0.589526684	-0.013510374	0.805362863	0.589526684	-0.294981543
OTUB1	-0.253278478	0.59043536	0.800128386	-0.014819568	0.59043536	0.800128386	0.23845891
ATRX	-0.223235115	0.584883682	0.796610207	-0.015072152	0.584883682	0.796610207	0.208162963
SETD2	-0.179302521	0.99309399	0.672358721	-0.017574371	0.99309399	0.665279736	0.16172815
RBM7	-0.098994913	0.988203047	0.584967972	-0.018384617	0.988203047	0.579838284	0.080610296
APEX1	-0.164506127	0.975643502	0.654696958	-0.018606272	0.975643502	0.654696958	0.145899856
HMGN1	-0.068084139	0.991290138	0.570215911	-0.01866383	0.991290138	0.570215911	0.049420309
NonTargetingCo	-0.208488508	0.99765574	0.693830415	-0.020245779	0.99765574	0.668450185	0.18824273
BUB1B	-0.402122358	0.336105544	0.999987313	-0.022028273	0.539107392	0.999987313	0.380094085
SPO11	0.026064919	0.999054627	0.522824139	-0.02283228	0.999054627	0.522824139	-0.0488972
NonTargetingCo	-0.107054688	0.999999992	0.59688114	-0.026148089	0.999999992	0.59618914	0.080906599
RFWD3	-0.165143786	0.445843971	0.946496535	-0.026576992	0.475789095	0.946496535	0.138566794
CDK12	0.20957843	0.699279618	0.972174261	-0.02679629	0.610150803	0.972174261	-0.23637472
NonTargetingCo	-0.154190756	0.999962639	0.639036963	-0.028920279	0.999962639	0.633891715	0.125270477
NonTargetingCo	0.011533528	0.980263038	0.59738111	-0.030943018	0.980263038	0.59738111	-0.042476546
HUS1B	0.128084867	0.999041355	0.489202098	-0.031077675	0.999041355	0.529101758	-0.159162542
NonTargetingCo	0.099973709	0.999999492	0.516849778	-0.031378864	0.999999492	0.530138163	-0.131352573
RNF168	0.106702335	0.686855358	0.768789476	-0.03396969	0.686855358	0.768789476	-0.140672025
NonTargetingCo	0.326262759	0.999829527	0.263208602	-0.036388887	0.999829527	0.537102755	-0.362651646
NonTargetingCo	-0.138457431	0.99999849	0.618000193	-0.038021567	0.99999849	0.599975444	0.100435864
UBE2B	0.01174031	0.967780942	0.537212607	-0.04074934	0.967780942	0.537212607	-0.05248965
FAAP20	0.04531898	0.545811951	0.704574993	-0.042167031	0.529341341	0.704574993	-0.087486012
DNTT	0.020176515	0.999905117	0.539049228	-0.042769599	0.999905117	0.539049228	-0.062946115
RAD23A	-0.281339552	0.635087306	0.805323122	-0.043689608	0.685247005	0.805323122	0.237649945
DTX2	-0.216824845	0.671581355	0.696367427	-0.047402807	0.671581355	0.696367427	0.169422038
NonTargetingCo	0.323773806	0.997856576	0.39414485	-0.053859257	0.997856576	0.552324939	-0.377633063
RAD17	-0.12485428	0.503630424	0.99993315	-0.054487327	0.506668585	0.99993315	0.070366953
RAD52	0.069762424	0.728971579	0.559429461	-0.057170394	0.728971579	0.559429461	-0.126932818
EYA3	-0.248226171	0.490007368	0.978716184	-0.061897876	0.537003538	0.978716184	0.186328295
CENPX	0.127619606	0.828940722	0.621083846	-0.06256522	0.828940722	0.625916836	-0.190184826
BLM	0.137441067	0.840181435	0.470355048	-0.06294413	0.840181435	0.566089673	-0.200385197
COL21A1	-0.079655005	0.921825514	0.629774398	-0.063123225	0.921825514	0.629774398	0.016531781
ACTR8	0.022464979	0.520837149	0.99999942	-0.067420663	0.520837149	0.99999942	-0.089885642
RAD51C	-0.323902805	0.39136104	0.997588655	-0.06830009	0.494673041	0.997588655	0.255602714
NonTargetingCo	0.085174159	0.963105599	0.474021678	-0.068545734	0.963105599	0.569857509	-0.153719893
PPP4R1	-0.014994947	0.856665652	0.662714626	-0.071834033	0.856665652	0.662714626	-0.056839086
ATRIP	-0.430669068	0.203753298	0.998218448	-0.074454101	0.419343219	0.998218448	0.356214967
NonTargetingCo	-0.151836407	0.999427371	0.645580156	-0.074501536	0.999427371	0.645580156	0.077334871
NonTargetingCo	0.011664054	0.998717176	0.549290299	-0.077153816	0.998717176	0.57724664	-0.088817869
PMS2P3	0.113501082	0.943456195	0.540776061	-0.078039733	0.943456195	0.563219438	-0.191540815
CRY1	-0.083618706	0.920529515	0.580422196	-0.078536307	0.920529515	0.580422196	0.005082399
DCLRE1C	-0.115781035	0.999665045	0.605788186	-0.082100745	0.999665045	0.605788186	0.03368029
NonTargetingCo	-0.174044727	0.985115366	0.664975186	-0.082130058	0.985115366	0.664975186	0.091914669
SIRT3	0.044493062	0.979592947	0.513082548	-0.082310999	0.979592947	0.581317926	-0.126804061
NonTargetingCo	-0.038938678	0.999287288	0.584495058	-0.082791854	0.999287288	0.584495058	-0.043853177
SMARCC2	0.003612468	0.997555566	0.581758943	-0.083544245	0.997555566	0.581758943	-0.087156713
NonTargetingCo	0.002317818	0.999999721	0.640099925	-0.088312815	0.999999721	0.650712797	-0.090630633
POLG2	-0.189875925	0.981114272	0.681840553	-0.089534683	0.981114272	0.661667142	0.100341242
ESCO2	0.017999061	0.582427273	0.992629276	-0.090319536	0.524945953	0.992629276	-0.108318597
ZDHHC16	-0.15006496	0.956923154	0.713194275	-0.093779588	0.956923154	0.713194275	0.056285372
ENDOV	-0.20974255	0.999296873	0.717721773	-0.099576443	0.999296873	0.717721773	0.110166107
SWI5	-0.168908419	0.998147498	0.639690468	-0.101241186	0.998147498	0.639690468	0.067667232
NonTargetingCo	-0.095008934	0.966309425	0.627350751	-0.101481113	0.966309425	0.627350751	-0.00647218
KDM4D	-0.099761613	0.999517962	0.626749494	-0.10347926	0.999517962	0.626749494	-0.003717647
PER1	0.098799031	0.990077097	0.514606643	-0.105058018	0.990077097	0.605258762	-0.203857049
RFC3	0.014504918	0.572970282	0.999999623	-0.110352138	0.528668119	0.999999623	-0.124857056
HES1	-0.027615052	0.76809946	0.612258629	-0.112465904	0.76809946	0.612258629	-0.084850852
INO80	-0.316400948	0.26996301	0.998880602	-0.117223123	0.378822049	0.998880602	0.199177825
RFC5	-0.343450701	0.321844312	1	-0.11992326	0.461291153	1	0.22352744
CCNE1	-0.087163357	0.972601188	0.624351389	-0.121880534	0.972601188	0.624351389	-0.034717177
NonTargetingCo	0.001714446	0.878180299	0.628679769	-0.122751404	0.878180299	0.628679769	-0.12446585
HDAC10	0.045044759	0.997973562	0.508985692	-0.122987103	0.997973562	0.630188828	-0.168031861
ORC2	-0.106338257	0.481268607	0.87352768	-0.123683713	0.481268607	0.87352768	-0.017345456
SPIDR	-0.06379337	0.476235924	0.816668104	-0.123927058	0.476235924	0.816668104	-0.060133688
ACTR5	-0.280987237	0.309331697	0.999664378	-0.126950838	0.394510139	0.999664378	0.1540364
NEK8	0.188480188	0.999004224	0.410909534	-0.128595022	0.999004224	0.625124536	-0.31707521
H2AFY	0.176274938	0.985621785	0.372894174	-0.12872809	0.985621785	0.62538959	-0.305003027
MYBBP1A	-0.197797672	0.40555722	1	-0.132564684	0.425627013	1	0.065232987
TADA3	-0.102741899	0.433691801	0.915647428	-0.135177736	0.433691801	0.915647428	-0.032435837

RTEL1	-0.330234985	0.248836053	0.999998909	-0.135830601	0.403609845	0.999998909	0.194404384
TRIM28	-0.318105925	0.696727965	0.791868369	-0.136616202	0.696727965	0.743038716	0.181489723
AMN1	-0.090166737	0.99801046	0.637246295	-0.138100627	0.99801046	0.637246295	-0.04793389
RNF20	-0.351332795	0.230650755	0.999999519	-0.138556007	0.393438068	0.999999519	0.212776787
NCAPH	-0.538643734	0.127392844	0.99898725	-0.139349713	0.356986697	0.99898725	0.39929402
NonTargetingCo	0.050549676	0.850087936	0.533634841	-0.143105711	0.850087936	0.643417709	-0.193655387
ERCC6L2	-0.08184418	0.872367225	0.646306863	-0.144387297	0.872367225	0.646306863	-0.062543117
TOP3B	-0.079061265	0.997428561	0.650585715	-0.146925205	0.997428561	0.650585715	-0.06786394
TCEB1	0.160536218	0.600507844	1	-0.147892757	0.526846187	1	-0.308428975
CUL2	-0.43007583	0.180360854	0.999999866	-0.15254424	0.345880545	0.999999866	0.27753159
SETDB1	-0.024883536	0.99959465	0.588933526	-0.153666509	0.99959465	0.642357532	-0.128782973
NAE1	-0.464061867	0.106455892	0.999999565	-0.155554875	0.319207002	0.999999565	0.308506992
PALB2	-0.149867519	0.501162855	0.956352073	-0.156631389	0.501162855	0.956352073	-0.006763869
FAAP100	-0.23706679	0.348324268	0.999216741	-0.157192908	0.384275466	0.999216741	0.079873882
NonTargetingCo	0.220282152	0.995046821	0.372114596	-0.158038419	0.995046821	0.652193201	-0.378320572
PARP15	0.062636979	0.998960655	0.514397665	-0.159400433	0.998960655	0.64254074	-0.222037413
PAXIP1	0.124689613	0.640313842	0.733419247	-0.165483819	0.640313842	0.733419247	-0.290173432
DSCC1	-0.531996416	0.140551596	0.999994766	-0.170333897	0.33511414	0.999994766	0.361662519
FANCG	-0.471611377	0.19714898	0.999845823	-0.171477865	0.374626323	0.999845823	0.300133512
WRAP53	-0.530918051	0.206508048	0.999668421	-0.174942405	0.346982738	0.999668421	0.355975646
CEP57	-0.724040032	0.081750529	0.999999863	-0.175839559	0.349820542	0.999999863	0.548200473
SSBP1	-0.24047795	0.828033245	0.768758977	-0.177548046	0.828033245	0.768758977	0.062929903
NonTargetingCo	-0.189504919	0.999999932	0.720769173	-0.189012223	0.999999932	0.720769173	4.92696E-04
TTI1	-0.573352558	0.174725054	1	-0.189262016	0.396935071	1	0.384090542
NonTargetingCo	-0.114289432	0.999823905	0.686442141	-0.191520391	0.999823905	0.686442141	-0.077230959
RAD51B	-0.504569208	0.161939293	0.9999845	-0.195945166	0.311246654	0.9999845	0.308624042
POLK	-0.190678596	0.999979036	0.682608088	-0.196547301	0.999979036	0.682608088	-0.005868705
SMUG1	-0.241451733	0.926775706	0.722752663	-0.198764655	0.926775706	0.722752663	0.042687078
TREX2	0.049093165	0.89181467	0.589818312	-0.2035565	0.89181467	0.696388402	-0.252649665
ZSWIM7	-0.211411608	0.735231576	0.724270237	-0.203682179	0.735231576	0.724270237	0.007729428
MSH5	-0.185385827	0.738573839	0.706570482	-0.204700128	0.738573839	0.706570482	-0.019314301
RNF4	-0.341582966	0.51553963	0.863172383	-0.207547961	0.51553963	0.863172383	0.134035005
ERCC1	-0.761019077	0.121299122	0.999920277	-0.210039984	0.320759508	0.999920277	0.550979093
SUV39H1	-0.240812088	0.686927959	0.727706492	-0.213337842	0.686927959	0.727706492	0.027474246
ARID1A	-0.26679015	0.459801678	0.960738841	-0.215089776	0.459801678	0.960738841	0.051700373
SUMO2	-0.055497564	0.592600641	0.874235475	-0.215503346	0.592600641	0.874235475	-0.160005782
XRCC1	-0.106298568	0.503469724	0.83560372	-0.215936402	0.443528978	0.83560372	-0.109637833
CHRAC1	-0.165555297	0.470805861	0.883613746	-0.223600938	0.470805861	0.883613746	-0.058045641
DDB2	-0.132236323	0.968589624	0.712817449	-0.228168693	0.968589624	0.715183319	-0.09593237
TP63	-0.037612615	0.982719463	0.659207594	-0.238062284	0.982719463	0.739874739	-0.200449669
NonTargetingCo	-0.110602421	0.999988159	0.74150653	-0.242975996	0.999988159	0.74150653	-0.132373575
MPLKIP	-0.281904592	0.417071503	0.839815793	-0.244925047	0.417071503	0.839815793	0.036979545
RAG1	0.0278725	0.998190338	0.609191893	-0.249445625	0.998190338	0.722315365	-0.277318125
POLE3	-0.236645108	0.308110286	0.999987142	-0.254790943	0.308110286	0.999987142	-0.018145836
HINFP	-0.289465065	0.315293475	0.999999995	-0.263096349	0.315293475	0.999999995	0.026368716
UVRAG	-0.111994747	0.432851819	0.999970332	-0.264030964	0.319541234	0.999970332	-0.152036217
MAD2L2	-0.310795125	0.337235147	0.999997565	-0.265201861	0.337235147	0.999997565	0.045593265
KDM4A	-0.53778644	0.166800392	0.999685556	-0.279034984	0.261393687	0.999685556	0.258751456
CDKN2D	-0.075545086	0.997688613	0.685570329	-0.285502212	0.997688613	0.747486115	-0.209957126
FANCA	-0.503828788	0.209442566	0.968847838	-0.309835357	0.212293296	0.968847838	0.193993431
SIN3A	-0.448706121	0.136922181	0.999999614	-0.310842184	0.211087626	0.999999614	0.137863936
FANCL	-0.396020418	0.280568326	0.999999866	-0.313798766	0.280568326	0.999999866	0.082221652
CNOT7	-0.295707409	0.288024187	0.942650234	-0.314410792	0.288024187	0.942650234	-0.018703383
PIAS4	-0.091510459	0.530232231	0.788581482	-0.317203993	0.530232231	0.788581482	-0.225693534
ERCC4	-0.398931986	0.252285106	0.999998625	-0.317434566	0.262326445	0.999998625	0.081497421
PDS5B	-0.564826034	0.164773	0.997655936	-0.333372893	0.248176773	0.997655936	0.231453141
TERT	-1.120561076	0.043657438	0.999994311	-0.338573436	0.262906278	0.999994311	0.781987641
FAAP24	-0.258183287	0.289786957	0.999280513	-0.338904435	0.262097914	0.999280513	-0.080721148
KDM2A	-0.558518598	0.434804887	0.910732661	-0.351084033	0.434804887	0.910732661	0.207434565
NFE2L2	-0.251395388	0.300917887	0.994462838	-0.352666261	0.300917887	0.994462838	-0.101270872
TFPT	-0.301295778	0.297516508	0.890885344	-0.354046883	0.297516508	0.890885344	-0.052751105
UBB	-0.408509311	0.712171643	0.810120028	-0.369070703	0.712171643	0.810120028	0.039438609
TDP1	-0.296059632	0.743472684	0.813004354	-0.374266685	0.743472684	0.813004354	-0.078207052
BAP1	-0.861019258	0.06781337	0.991006485	-0.377923266	0.25143855	0.991006485	0.483095992
HUS1	-0.231085161	0.3202775	0.999975309	-0.383060076	0.302094643	0.999975309	-0.151974916
CTC1	-0.646536128	0.171305894	0.999977979	-0.38840447	0.270798243	0.999977979	0.258131658
TCEB2	-0.67807386	0.220472453	1	-0.389656589	0.32884493	1	0.288417272
GTF2H5	-0.329634928	0.299807685	0.999989346	-0.414480078	0.299807685	0.999989346	-0.084845149
TELO2	-0.789127642	0.081905094	0.999999997	-0.424255838	0.196901763	0.999999997	0.364871804
POLG	-0.383028325	0.400960382	0.874455448	-0.425626497	0.400960382	0.874455448	-0.042598172
CREBBP	-0.529525138	0.200253782	0.977017433	-0.433716988	0.200253782	0.977017433	0.09580815
UHRF1	-0.384034522	0.261600482	0.99999626	-0.456693592	0.254843006	0.99999626	-0.07265907
XRCC4	-0.692794146	0.091989725	0.983404757	-0.470787491	0.154492811	0.983404757	0.222006655
FZR1	-0.388999548	0.182286415	1	-0.484611118	0.156141661	1	-0.09561157
NBN	0.129128469	0.797503888	0.750377074	-0.487505531	0.562629286	0.937556694	-0.616634
NHEJ1	-0.731347402	0.121990341	0.989815203	-0.49821906	0.18793881	0.989815203	0.233128341
FANCF	-0.540715666	0.115596019	0.999997085	-0.508393866	0.115596019	0.999997085	0.0323218
PRKDC	-1.052365726	0.107027335	0.997540738	-0.513309908	0.243221648	0.997540738	0.539055817
LMNA	-1.019814402	0.106849512	0.988127832	-0.539698478	0.183523833	0.988127832	0.480115925
PARP1	-0.497157357	0.279310195	0.90920163	-0.551684532	0.279310195	0.90920163	-0.054527175
RAD50	-0.612330237	0.043572166	0.999999891	-0.559317575	0.048090896	0.999999891	0.053012663
ENY2	-0.971981534	0.148082476	0.971646103	-0.582950593	0.218434077	0.971646103	0.389030941

UBE2N	-1.016751085	0.01951038	0.999808198	-0.610289182	0.068995853	0.999808198	0.406461904
RNASEH2A	-0.985021172	0.059056933	0.999838311	-0.632305411	0.106612141	0.999838311	0.35271576
ZMPSTE24	-0.369169724	0.278722686	0.99078592	-0.636975557	0.182120681	0.99078592	-0.267805832
FANCC	-0.655601424	0.084856054	0.999998236	-0.658633483	0.084856054	0.999998236	-0.003032059
UBE2M	-0.859090131	0.119797607	0.99993481	-0.72567155	0.119797607	0.99993481	0.133418581
LIG4	-0.80476088	0.089990965	0.997992962	-0.757120665	0.089990965	0.997992962	0.047640215
TEN1	-1.379092553	0.007574556	1	-0.911606024	0.048887649	1	0.467486529

Appendix Table 6 Raw data from JACKS analysis of RPE-1 WRN-/- *G7-C5 2nM CPT treated*

RPE-1 WRN-/- G7-C5, DMSO and 2nM CPT treated enrichment compared to the day 14 control. fdr=false discovery rate.

Gene	Enrichment in DMSO treated	neg_fdr1	pos_fdr1	Enrichment in 2nM CPT treated	neg_fdr2	pos_fdr2	Difference in Enrichment
TP53	3.637109045	1	5.46E-11	4.419451518	1	4.16E-15	0.782342473
CAND1	4.183380117	1	1.11E-13	3.132955448	1	2.38E-08	-1.050424669
CDKN1A	1.924779332	1	0.001048617	2.448484547	1	9.32E-05	0.523705215
KEAP1	2.699222891	1	1.25E-05	2.44652434	1	5.48E-05	-0.25269855
H2AFZ	2.337796569	1	1.45593E-04	2.064925972	1	4.34633E-04	-0.272870597
RNF146	1.613932235	1	0.002145623	1.82378186	1	7.17001E-04	0.209849624
DCUN1D1	1.913524529	0.999999878	0.001247478	1.669027209	0.999999878	0.005822329	-0.24449732
SHFM1	1.249332624	0.999991064	0.043570209	1.64713178	0.999991064	0.008886461	0.397799156
PTEN	2.062337291	1	8.08E-05	1.549065134	1	0.00216206	-0.513272157
CHEK2	1.229560498	1	0.009185668	1.435746473	1	0.003619417	0.206185975
USP28	1.762497827	1	6.49627E-04	1.430325046	1	0.003641298	-0.33217278
THRAP3	1.810836217	1	0.002800992	1.428189331	1	0.020693888	-0.382646886
DCUN1D3	1.408137125	1	0.003451057	1.419206881	1	0.003451057	0.011069756
ENDOV	0.754041756	0.999296873	0.092010657	1.395377416	0.999296873	0.004744135	0.64133566
CUL3	0.840845144	1	0.034681949	1.338961146	1	0.002718399	0.498116001
UBE2F	1.337548482	1	0.012666928	1.325802917	1	0.012666928	-0.011745565
BRD7	1.489069964	1	0.010066749	1.277715667	1	0.018878619	-0.211354297
GADD45G	0.883990326	0.999993748	0.109459973	1.222322068	0.999993748	0.041460106	0.338331742
NonTargetingC	1.115776499	0.999999721	0.024735777	1.220818747	0.999999721	0.020960806	0.105042248
ARID2	1.162854276	1	0.016857352	1.21791499	1	0.016563163	0.055060714
BABAM1	1.173245523	1	0.008274041	1.200070548	1	0.006162554	0.026825025
MAPK14	0.185072057	0.999999645	0.376640212	1.179456144	0.999999645	0.031913612	0.994384087
RNF7	1.415388362	1	0.003231386	1.153328231	1	0.011142591	-0.262060131
TP53BP1	1.215534642	1	0.019079977	1.144680494	1	0.019079977	-0.070854149
POLD3	0.870732149	0.999843055	0.017371545	1.137858109	0.999843055	0.009074953	0.267125961
NonTargetingC	1.085840933	0.999999994	0.018460583	1.136184892	0.999999994	0.018460583	0.05034396
NonTargetingC	1.087590023	0.999989034	0.020152083	1.10524716	0.999989034	0.020152083	0.017657137
NonTargetingC	0.942578583	0.999999634	0.041218556	1.077546489	0.999999634	0.031770949	0.134967905
MAPKAPK2	1.397347909	1	0.011555573	1.077481678	1	0.033510011	-0.31986623
GTF2H2	1.961668809	0.983875327	0.267484538	1.074963012	0.983875327	0.298260716	-0.886705797
ALKBH3	1.03208538	0.999874058	0.018670212	1.071606352	0.999874058	0.016989885	0.039520972
UBE2R2	1.492722275	1	0.007215625	1.066847242	1	0.051198162	-0.425875032
CDC25A	0.702769648	0.999910282	0.128917776	1.063434141	0.999910282	0.04050902	0.360664493
NonTargetingC	0.935723402	0.999944922	0.050467137	1.028436902	0.999944922	0.033843428	0.0927135
MLH3	0.703739216	0.999862757	0.198237753	1.025975051	0.999862757	0.079853147	0.322235835
SCAF4	1.556523332	1	0.001688265	1.02002515	1	0.02861133	-0.536498182
DCUN1D5	1.012400106	0.999889397	0.055911449	1.009958814	0.999889397	0.055911449	-0.002441292
APEX1	0.65644442	0.986387666	0.15599156	1.001139974	0.986387666	0.065603277	0.344695554
DNTT	0.593982275	0.999905117	0.199584509	0.99845473	0.999905117	0.042664065	0.404472456
CUL4B	0.899230132	0.99947849	0.082157943	0.991105566	0.99947849	0.079295321	0.091875434
NonTargetingC	0.737982307	0.99999303	0.075778326	0.962959885	0.99999303	0.044109855	0.224977578
NonTargetingC	0.841536407	0.999998311	0.059923502	0.958248072	0.999998311	0.056064085	0.116711665
USP15	1.204233595	1	0.005702571	0.955727311	1	0.023808551	-0.248506284
RAP1A	0.79085845	0.998612783	0.094062905	0.944740099	0.998612783	0.060393377	0.15388165
UBE2V2	0.866885109	0.999897557	0.067595817	0.935976249	0.999897557	0.058887722	0.069091139
DMC1	0.97365822	0.999556483	0.040784214	0.934853111	0.999556483	0.040784214	-0.038805108
NonTargetingC	0.788548297	0.999991775	0.080257338	0.913523639	0.999991775	0.05583858	0.124975342
NonTargetingC	0.706495225	0.999974703	0.108990837	0.906095497	0.999974703	0.06010541	0.199600271
PHIP	1.555423036	1	0.002998833	0.901569002	1	0.037564294	-0.653854034
ALKBH1	0.764467305	0.999961205	0.074890232	0.894976706	0.999961205	0.06579161	0.1305094
ADH5	0.649487858	0.997682785	0.200187542	0.881587223	0.997682785	0.132963441	0.232099365
STAG2	0.910011189	0.999999998	0.04127621	0.872694811	0.999999998	0.053813247	-0.037316378
HDAC10	0.575578682	0.997973562	0.150096766	0.867220266	0.997973562	0.059408089	0.291641584
GPI	0.903424872	0.999992441	0.067431384	0.865478577	0.999992441	0.097925025	-0.037946296
KDM4D	0.586380313	0.999517962	0.145442715	0.865240119	0.999517962	0.073901812	0.278859806
CUL5	0.947067415	1	0.024841794	0.863849097	1	0.034917742	-0.083218318
CHD3	0.860047447	0.991912216	0.03497551	0.863097043	0.991912216	0.03497551	0.003049596
BCLAF1	1.258631342	1	0.05446127	0.859766431	1	0.096179445	-0.398864911
PBRM1	0.538902517	1	0.135202919	0.857354921	1	0.076475389	0.318452403
UBB	0.940360605	0.998261617	0.070544342	0.848197903	0.998261617	0.096012842	-0.092162702
OPRM1	0.638831562	0.999960465	0.17818549	0.836470421	0.999960465	0.104987069	0.197638858
KMT5B	0.555582098	0.999968266	0.103565356	0.836104112	0.999968266	0.058861614	0.280522014
APC	0.957395823	1	0.018941734	0.831975132	1	0.029096505	-0.125420692
NonTargetingC	0.603489486	0.999981145	0.137054504	0.823480419	0.999981145	0.09448797	0.219990933
CCNC	0.989700421	0.999898713	0.038233546	0.821383817	0.999898713	0.071515853	-0.168316603
NonTargetingC	0.881331038	0.999913624	0.054235963	0.819015233	0.999913624	0.059356689	-0.062315805
DCLRE1A	0.444507797	0.999578127	0.19438612	0.805795347	0.999578127	0.054793111	0.36128755
NEK8	0.648001286	0.999004224	0.12826138	0.78792341	0.999004224	0.097016192	0.139922125
MORF4L1	0.863124411	0.994177809	0.115523685	0.78164414	0.994177809	0.125312048	-0.081480272
SWI5	1.269691047	0.998147498	0.017408436	0.777569192	0.998147498	0.087297344	-0.492121855
RRM2B	0.818345656	0.999997564	0.057020947	0.777525681	0.999997564	0.057020947	-0.040819975

FBXW7	0.657002771	0.999999997	0.053402788	0.776078442	0.999999997	0.034006552	0.11907567
LIG3	0.958547004	0.999904028	0.049596982	0.770592546	0.999904028	0.101936788	-0.187954458
CIB1	1.12793543	0.992548413	0.025260605	0.759379027	0.992548413	0.116390644	-0.368556404
PARK7	0.545330686	0.994823768	0.18605194	0.757489933	0.994823768	0.093968135	0.212159247
NonTargetingC	0.970242748	0.999999893	0.040242436	0.756090544	0.999999893	0.106425244	-0.214152204
WRNIP1	0.867869928	0.995688479	0.068674602	0.754740093	0.995688479	0.094922128	-0.113129835
COPS7A	0.52883645	0.999970404	0.26042997	0.75331933	0.999970404	0.216411231	0.224482879
NonTargetingC	0.645572386	0.997641235	0.146197913	0.750912508	0.997641235	0.146197913	0.105340122
PARP15	0.747436582	0.998960655	0.111632352	0.747373176	0.998960655	0.111632352	-6.34E-05
SETX	0.622007128	0.956660985	0.104585117	0.746319196	0.956660985	0.104585117	0.124312069
HNRNPUL2	0.539293252	0.999853973	0.170076124	0.745773901	0.999853973	0.096429535	0.206480649
EP300	0.920734605	1	0.040019774	0.743966822	1	0.07019854	-0.176767783
NonTargetingC	0.827318964	0.999999932	0.09844609	0.738864773	0.999999932	0.130085938	-0.08845419
AMN1	0.424605461	0.99801046	0.323548996	0.728948559	0.99801046	0.111304787	0.304343097
SIRT1	0.564277419	0.999600581	0.143449576	0.727098804	0.999600581	0.095579646	0.162821385
RING1	1.022707347	1	0.042515799	0.726982875	1	0.133823247	-0.295724471
NonTargetingC	0.772001259	0.999999115	0.093009819	0.726109736	0.999999115	0.099706887	-0.045891523
CCND2	1.155280239	0.999700615	0.030604037	0.722768889	0.999700615	0.165212122	-0.43251135
NonTargetingC	1.144701666	0.99991058	0.017856836	0.718665386	0.99991058	0.130325742	-0.42603628
POLM	0.801592713	0.999967463	0.066705271	0.714121999	0.999967463	0.097842657	-0.087470714
NonTargetingC	0.429882391	0.999963084	0.155978914	0.71191403	0.999963084	0.145117706	0.282031639
UBE2K	0.758379402	1	0.09853474	0.707851177	1	0.100765604	-0.050528226
HDAC9	0.877381213	0.999999739	0.047327388	0.707746053	0.999999739	0.072304092	-0.169635161
RHNO1	0.421562628	0.976984352	0.373780185	0.702651507	0.976984352	0.224533712	0.281088879
VCP	0.431072228	0.999408308	0.249430452	0.701182096	0.999408308	0.138655802	0.270109868
BTG2	0.510983469	0.999849211	0.213299326	0.700937781	0.999849211	0.155672065	0.189954313
NonTargetingC	0.574456905	0.999499894	0.21770554	0.700767603	0.999499894	0.169740492	0.126310698
NonTargetingC	0.445567268	0.999838243	0.307673837	0.699521131	0.999838243	0.137210699	0.253953862
CHD1L	0.484239835	0.999838881	0.232137854	0.695355324	0.999838881	0.150055814	0.211115488
SCAF8	0.371369871	0.997827855	0.239387643	0.690964507	0.997827855	0.162676815	0.319594636
SETD2	0.273034952	0.99309399	0.513673877	0.690455684	0.99309399	0.202534748	0.417420733
NonTargetingC	0.742149713	0.999988159	0.129180192	0.68951654	0.999988159	0.129288874	-0.052633173
SSBP3	0.548660955	0.993437983	0.16441545	0.684736982	0.993437983	0.124852644	0.136076027
NonTargetingC	0.874359175	0.999962639	0.08666355	0.683871456	0.999962639	0.158511496	-0.19048772
MGMT	0.5893579	0.992856975	0.198492016	0.683168129	0.992856975	0.198492016	0.093810229
BRE	0.611588262	0.999999447	0.110837116	0.679816485	0.999999447	0.094768601	0.068228223
PARP4	0.392938001	0.999779181	0.272654857	0.679559674	0.999779181	0.14485674	0.286621673
POLN	0.268999203	0.999765812	0.268906068	0.679246118	0.999765812	0.160303789	0.410246915
MTA2	0.646520614	0.999859602	0.093462295	0.679207279	0.999859602	0.089278041	0.032686664
CSNK1D	0.545477831	0.998727585	0.105453163	0.667517767	0.998727585	0.105453163	0.122039936
SMARCD1	0.47605373	0.999812917	0.137079121	0.666710623	0.999812917	0.137079121	0.190656892
NonTargetingC	0.662323769	0.999998025	0.099334073	0.664419004	0.999998025	0.099334073	0.002095235
CUL7	0.628216038	0.999988816	0.163441994	0.65894483	0.999988816	0.163441994	0.030728792
HMGB1	1.694407556	0.994845796	0.415375388	0.656166342	0.994845796	0.425398111	-1.038241213
NonTargetingC	0.397105327	0.999896743	0.199662611	0.653278894	0.999896743	0.186011917	0.256173567
DTX3	0.737634812	0.999520968	0.119553352	0.647522684	0.999520968	0.150091408	-0.090112128
RNF169	0.481951257	0.972630813	0.366785716	0.640488181	0.972630813	0.283651505	0.158536924
RBBP7	0.536164888	0.976664116	0.293233037	0.636998869	0.976664116	0.275603875	0.100833981
DDB2	0.720493292	0.968589624	0.160772799	0.634941137	0.968589624	0.160772799	-0.085552154
NonTargetingC	0.784391457	0.99994745	0.127178242	0.630700522	0.99994745	0.172966586	-0.153690935
SPO11	0.663956501	0.999054627	0.170621179	0.626498847	0.999054627	0.176194418	-0.037457654
NonTargetingC	0.842905405	0.99999849	0.080526688	0.625637162	0.99999849	0.12981327	-0.217268243
NonTargetingC	0.655786659	0.999999492	0.134195552	0.622757804	0.999999492	0.134195552	-0.033028855
NonTargetingC	0.383025967	0.999829527	0.259075986	0.621562338	0.999829527	0.220187151	0.238536371
DCLRE1C	0.543979667	0.999665045	0.176864689	0.619746328	0.999665045	0.176864689	0.075766661
SIRT2	0.390986491	0.996559267	0.249293392	0.616328123	0.996559267	0.204201368	0.225341632
SETDB1	0.718518165	0.99959465	0.136331363	0.613335451	0.99959465	0.173017035	-0.105182713
NonTargetingC	0.276893181	0.993980969	0.287545259	0.608470957	0.993980969	0.226999156	0.331577776
DTX4	0.87622649	0.999941958	0.039358656	0.607227651	0.999941958	0.100502891	-0.268998839
TEP1	0.374019303	0.9949726	0.237436036	0.596955138	0.9949726	0.114384796	0.222935834
CLK2	0.509362595	0.937955813	0.278473867	0.596019401	0.937955813	0.278473867	0.086656806
RNF138	0.576114373	0.999989483	0.198265834	0.595763207	0.999989483	0.198265834	0.019648835
KMT5C	0.59658192	0.999795972	0.133164186	0.593814699	0.999795972	0.133164186	-0.002767221
CDKN2A	0.557702545	0.999994328	0.121225582	0.590888218	0.999994328	0.121225582	0.033185673
PRKCG	0.785255421	0.999019977	0.081378241	0.584353198	0.999019977	0.179427851	-0.200902223
NonTargetingC	0.56944774	0.997856576	0.218475022	0.580453646	0.997856576	0.218475022	0.011005907
SMARCC1	0.782707832	0.999999991	0.063694768	0.576877453	0.999999991	0.147043368	-0.205830379
UBE2A	0.729293709	0.966338213	0.202457118	0.571200805	0.966338213	0.235013798	-0.158092905
SPTBN1	0.964621729	1	0.039491377	0.569070109	1	0.114241101	-0.39555162
APAF1	0.610550203	0.999769105	0.083972321	0.566042609	0.999769105	0.104031181	-0.044507594
NonTargetingC	0.574133995	0.999823905	0.175982262	0.559811466	0.999823905	0.175982262	-0.014322529
CSNK1E	0.571772806	0.996433343	0.238423719	0.559306324	0.996433343	0.238423719	-0.012466482
NonTargetingC	0.432852845	0.9999448	0.251025669	0.557691706	0.9999448	0.197425308	0.124838861
PER1	0.573266394	0.990077097	0.206151482	0.549827899	0.990077097	0.206151482	-0.023438496
NOTCH4	0.428439293	0.977380485	0.175613395	0.548574333	0.977380485	0.170484673	0.120135041
PHF3	0.474240672	0.999371961	0.143769059	0.546285628	0.999371961	0.143769059	0.072044956
NonTargetingC	0.42221828	0.999534742	0.250390998	0.545449526	0.999534742	0.214881587	0.123231247
NonTargetingC	0.615209971	0.999257052	0.158280513	0.54315201	0.999257052	0.158280513	-0.072057961
USP13	0.530616015	0.999322517	0.259214001	0.539095272	0.999322517	0.259214001	0.008479257
RAG1	0.201577337	0.998190338	0.471223399	0.538275325	0.998190338	0.290667958	0.336697989
RASSF7	0.780672	0.997777622	0.132805625	0.536353228	0.997777622	0.29600717	-0.244318772
PMS2P3	0.753672138	0.943456195	0.238305977	0.535839944	0.943456195	0.366467735	-0.217832195

ETAA1	0.520689404	0.999902643	0.215226257	0.535724118	0.999902643	0.215226257	0.015034714
NonTargetingC	0.562209165	0.999999992	0.175381736	0.5336008	0.999999992	0.187047653	-0.028608365
NOTCH1	0.40927441	0.99799131	0.362305799	0.532465972	0.99799131	0.299947195	0.123191562
XPC	0.40177247	0.991484933	0.201804197	0.532446875	0.991484933	0.201804197	0.130674405
TPP1	0.374238031	0.998535295	0.210486575	0.531910258	0.998535295	0.168111978	0.157672227
POLK	0.655462282	0.999979036	0.139778175	0.5315357	0.999979036	0.163570562	-0.123926582
DTX3L	0.608383799	0.99393549	0.250939498	0.530919818	0.99393549	0.250939498	-0.077463982
NonTargetingC	0.451394425	0.999028141	0.261998587	0.530905506	0.999028141	0.249237726	0.079511081
CDKN2D	0.218410673	0.997688613	0.451990342	0.523799382	0.997688613	0.345746038	0.305388709
PMP22	0.509906221	0.999994455	0.155612006	0.523674552	0.999994455	0.155612006	0.013768332
FBXO18	0.368446992	0.999245999	0.230101554	0.522274759	0.999245999	0.182890444	0.153827767
MBTD1	0.45330823	0.982125174	0.318080321	0.52191348	0.982125174	0.318080321	0.068605249
PARP3	0.483256554	0.999043034	0.280436872	0.520313593	0.999043034	0.280436872	0.037057039
PARPBP	0.642183018	0.997597669	0.16658308	0.519001302	0.997597669	0.16658308	-0.123181716
NonTargetingC	0.616944964	0.999695194	0.246673432	0.515168563	0.999695194	0.255795637	-0.101776401
SETMAR	0.467507602	0.987364155	0.30982586	0.513821275	0.987364155	0.30982586	0.046313673
NonTargetingC	0.615222345	0.99906883	0.231426952	0.513175072	0.99906883	0.249456668	-0.102047272
EME1	0.240399694	0.900026124	0.323672826	0.511270615	0.900026124	0.209613513	0.270870921
CCNB3	0.420477938	0.999788155	0.164253439	0.509888716	0.999788155	0.128605479	0.089410778
APOBEC3C	0.502549543	0.995992372	0.161640284	0.50931792	0.995992372	0.161640284	0.006768377
OTUB2	0.219326652	0.999750694	0.461871695	0.505340629	0.999750694	0.257785958	0.286013976
RAD18	0.430555916	0.998249125	0.240765977	0.505303235	0.998249125	0.223023743	0.074747319
POLR2J	0.697300413	0.996488758	0.151021882	0.502906991	0.996488758	0.19139029	-0.194393422
NonTargetingC	0.400855796	0.999245228	0.283514144	0.499830634	0.999245228	0.283514144	0.098974839
NonTargetingC	0.533101985	0.998153711	0.268790737	0.499039531	0.998153711	0.268790737	-0.034062455
TRIM29	0.596549482	0.983559316	0.2416772	0.498917126	0.983559316	0.264995431	-0.097632356
ALKBH2	0.224700618	0.987312972	0.302122659	0.49859343	0.987312972	0.197386863	0.273892812
APBB1	0.551155499	0.998373594	0.226218434	0.497371905	0.998373594	0.226218434	-0.053783594
SCAI	0.469562418	0.999862613	0.19869465	0.496843174	0.999862613	0.19869465	0.027280756
NonTargetingC	0.34298216	0.998539304	0.29558584	0.495160116	0.998539304	0.29558584	0.152177956
NonTargetingC	0.404776442	0.998943602	0.209028753	0.491409802	0.998943602	0.209028753	0.08663336
UBE2NL	0.497566341	0.944566022	0.279276013	0.489996532	0.944566022	0.279276013	-0.007569808
NonTargetingC	0.686722804	0.999854713	0.159474854	0.483352549	0.999854713	0.25340258	-0.203370255
RNF111	0.441368269	0.999944988	0.188176928	0.48044543	0.999944988	0.188176928	0.039077161
PHF11	0.332481806	0.968480013	0.295161343	0.480167494	0.968480013	0.214912858	0.147685688
IP6K3	0.53701283	0.985510177	0.288481443	0.479787981	0.985510177	0.288481443	-0.057224849
KAT2B	0.42985505	0.998273194	0.200766073	0.478286948	0.998273194	0.190016003	0.048431898
FAN1	0.301635968	0.997111193	0.267264115	0.478023524	0.997111193	0.267264115	0.176387557
MDM2	0.745521652	0.999296181	0.097379709	0.477444649	0.999296181	0.182974552	-0.268077003
SIRT3	0.404523722	0.979592947	0.363779079	0.476295174	0.979592947	0.363779079	0.071771452
HMGN1	0.4192672	0.991290138	0.37957964	0.47618887	0.991290138	0.37957964	0.05692167
NonTargetingC	0.691064923	0.998182876	0.25151439	0.471000114	0.998182876	0.282525502	-0.220064809
NonTargetingC	0.46303319	0.998153433	0.278982803	0.47088869	0.998153433	0.278982803	0.0078555
NonTargetingC	0.51641731	0.995893787	0.201545788	0.470878267	0.995893787	0.201545788	-0.045539044
NonTargetingC	0.264286784	0.995046821	0.372114596	0.470633481	0.995046821	0.372114596	0.206346697
PML	0.488228284	0.999831852	0.218708286	0.468552129	0.999831852	0.218708286	-0.019676155
SMARCC2	0.410964454	0.997555566	0.354861922	0.468354447	0.997555566	0.354861922	0.057389993
CHFR	0.165861963	0.999662265	0.363249416	0.46807362	0.999662265	0.200026196	0.302211657
COPS7B	0.611463743	0.999189187	0.167304159	0.460364341	0.999189187	0.278102552	-0.151099402
NonTargetingC	0.626507886	0.999975913	0.153631625	0.458975915	0.999975913	0.201741731	-0.167531971
ANKRD44	0.16699919	0.998536699	0.477003499	0.458728677	0.998536699	0.266477136	0.291729487
NOTCH3	0.325262779	0.994536715	0.209763614	0.458123839	0.994536715	0.179718803	0.13286106
PARG	0.020726856	0.995565538	0.622838059	0.456644728	0.995565538	0.385421367	0.435917871
TRIP12	0.560416204	0.999977382	0.190500439	0.456631153	0.999977382	0.201815044	-0.103785051
OTUD7B	0.386903391	0.966178755	0.309427349	0.455064676	0.966178755	0.309427349	0.068161284
NonTargetingC	0.332722267	0.999344463	0.204766592	0.454930772	0.999344463	0.174973777	0.122208505
MSH3	0.026441893	0.986451479	0.474160079	0.454169464	0.986451479	0.310510777	0.427727571
SIRT7	0.54942449	0.999664558	0.161013986	0.45107144	0.999664558	0.184380409	-0.098353049
TREX1	0.394221984	0.968436391	0.369414995	0.447250178	0.968436391	0.369414995	0.053028194
SLF1	0.331791474	0.957297648	0.353040755	0.446807449	0.957297648	0.353040755	0.115015975
SIRT5	0.325008676	0.999831869	0.199559323	0.446786604	0.999831869	0.162101104	0.121777928
BRCA2	0.592009836	0.996405184	0.09897257	0.446394884	0.996405184	0.1621038	-0.145614951
NonTargetingC	0.495866089	0.999971942	0.263850838	0.445091973	0.999971942	0.263850838	-0.050774116
NonTargetingC	0.287755961	0.999287288	0.397960225	0.442644833	0.999287288	0.362981881	0.154888872
HELB	0.175850019	0.99823044	0.346842636	0.441062781	0.99823044	0.173793352	0.265212762
PXMP2	0.3207126	0.923308842	0.444325346	0.436667673	0.923308842	0.444325346	0.115955073
RBM7	0.339287006	0.988203047	0.519220154	0.435074116	0.988203047	0.515253133	0.09578711
ATXN3	0.449466818	0.999887003	0.235765562	0.429514311	0.999887003	0.235765562	-0.019952507
TYMS	0.419183302	0.989232021	0.359659598	0.425976972	0.989232021	0.359659598	0.00679367
MSH2	0.154440696	0.974192869	0.401188919	0.423366563	0.974192869	0.401188919	0.268925867
MSH4	0.13750266	0.993583438	0.376483249	0.415122076	0.993583438	0.259161096	0.277619416
RAD54B	0.471432234	0.984425058	0.227586521	0.413843268	0.984425058	0.227586521	-0.057588967
MAPK8	0.507464271	0.999525364	0.154640654	0.413722088	0.999525364	0.184534957	-0.093742183
NonTargetingC	0.456158885	0.999427371	0.378668407	0.412023138	0.999427371	0.378668407	-0.044135747
NonTargetingC	0.412725737	0.999971612	0.247231389	0.411376662	0.999971612	0.247231389	-0.001349075
UBE2B	0.451727534	0.967780942	0.392128864	0.410982706	0.967780942	0.392128864	-0.040744828
EME2	-0.099482512	0.998886994	0.583093659	0.408470392	0.998886994	0.3321133	0.507952905
CSNK2A2	0.646189847	0.999868116	0.137312201	0.407699656	0.999868116	0.182703161	-0.238490191
UBE2D2	0.182881841	0.926997804	0.390062159	0.405907499	0.926997804	0.271229486	0.223025658
NonTargetingC	0.418244042	0.999049499	0.300327216	0.40514397	0.999049499	0.300327216	-0.013100072
RAD54L2	0.664238302	0.99939853	0.162887868	0.400571613	0.99939853	0.260367602	-0.263666689
PARP2	0.345429586	0.943985904	0.309226463	0.398061421	0.943985904	0.309226463	0.052631834

CCNB2	0.376528949	0.989274411	0.262865149	0.397750621	0.989274411	0.262865149	0.021221672
CDKN1B	0.677757422	0.999985514	0.201300535	0.397069302	0.999985514	0.277651111	-0.28068812
WDR76	0.30878335	0.892541247	0.274239745	0.390062068	0.892541247	0.274239745	0.081278718
BRCC3	0.664420303	0.99999999	0.129582776	0.388382964	0.99999999	0.255489982	-0.276037339
APLF	0.655931164	0.999572699	0.268687357	0.384863065	0.999572699	0.27377354	-0.271068098
SUMO3	0.197318756	0.994900124	0.328498082	0.38453705	0.994900124	0.328498082	0.187218294
NABP2	0.257027611	0.995463463	0.268568282	0.384230148	0.995463463	0.241334357	0.127202537
ARID1B	0.437270751	0.970376264	0.301973032	0.382051584	0.970376264	0.301973032	-0.055219167
REV1	0.28110326	0.951147894	0.357975676	0.380428671	0.951147894	0.321946653	0.099325411
USP45	0.350124502	0.96395309	0.348616929	0.37826907	0.96395309	0.348616929	0.028144567
APOBEC3B	0.455785012	0.999967008	0.236724223	0.376857898	0.999967008	0.236724223	-0.078927113
MVP	0.370491355	0.881549393	0.324692981	0.372667385	0.881549393	0.324692981	0.00217603
NonTargetingC	0.439750883	0.999117535	0.344349493	0.370486312	0.999117535	0.344349493	-0.069264571
KDM1A	0.126091589	0.935769267	0.48560199	0.369710622	0.935769267	0.48560199	0.243619034
HMGB2	0.610550215	0.999925107	0.189092663	0.366230624	0.999925107	0.267173602	-0.244319591
NEK9	0.379792037	0.99995695	0.203498892	0.364414308	0.99995695	0.203498892	-0.015377729
TET2	0.92998819	0.999998163	0.053624086	0.360776459	0.999998163	0.242515829	-0.569211731
NonTargetingC	0.61658203	0.999960589	0.219092132	0.360179291	0.999960589	0.391518669	-0.256402739
UBA3	0.392609834	0.994051665	0.225515477	0.355250245	0.994051665	0.225515477	-0.037359589
NonTargetingC	0.469740183	0.985115366	0.413667613	0.354506413	0.985115366	0.46541422	-0.11523377
ASF1A	0.384600608	0.992322994	0.189662944	0.353617343	0.992322994	0.20076454	-0.030983265
POLG2	0.262933392	0.981114272	0.378952066	0.351476926	0.981114272	0.378952066	0.088543534
POLL	0.398054248	0.995018218	0.277494893	0.351231205	0.995018218	0.278194075	-0.046823043
H2AFY	0.382537403	0.985621785	0.33088071	0.350773271	0.985621785	0.33088071	-0.031764132
PRIMPOL	0.364305535	0.97661071	0.334150094	0.349123989	0.97661071	0.334150094	-0.015181546
SF3B1	0.482900631	0.985254946	0.16687755	0.346819767	0.985254946	0.221569382	-0.136080864
APOBEC3D	0.508483866	0.974141819	0.330086098	0.342770008	0.974141819	0.369387537	-0.165713858
OGG1	0.019844109	0.848582944	0.508307522	0.341602815	0.905134815	0.508307522	0.321758706
RNF2	0.444681803	0.999627895	0.27250104	0.340723931	0.999627895	0.283344358	-0.103957872
SLF2	0.281679594	0.968887803	0.484472338	0.340229842	0.968887803	0.484472338	0.058550248
ALDH2	0.486546867	0.97275521	0.275798753	0.33901215	0.97275521	0.293154395	-0.147534717
INO80C	0.351330512	0.99225101	0.408909174	0.337524099	0.99225101	0.408909174	-0.013806413
UBE2D1	0.376058569	0.999939613	0.225241959	0.336397705	0.999939613	0.225688434	-0.039660864
ATM	1.201579498	1	0.032047214	0.334287078	1	0.323193756	-0.86729242
ABL1	0.479701063	0.999996573	0.153482962	0.32569033	0.999996573	0.223556899	-0.154010733
NonTargetingC	0.36075394	0.99765574	0.332556735	0.319896864	0.99765574	0.332556735	-0.040857076
ATF2	0.28052765	0.990828682	0.307924958	0.317288998	0.990828682	0.307924958	0.036761348
SALL4	0.211574193	0.991028909	0.311969916	0.31433645	0.991028909	0.305548539	0.102762257
NonTargetingC	0.450400929	0.995299415	0.36581474	0.313060714	0.995299415	0.370924813	-0.137340215
NonTargetingC	0.716584864	0.99999086	0.162519131	0.312501616	0.99999086	0.371721322	-0.404083248
PRMT6	0.595771426	0.998934623	0.20570671	0.311601101	0.998934623	0.405066951	-0.284170324
NonTargetingC	0.281308535	0.999346524	0.242091075	0.310968158	0.999346524	0.242091075	0.029659623
NonTargetingC	0.291871577	0.990797611	0.311783685	0.30834454	0.990797611	0.311783685	0.016472964
USP47	0.340678368	0.996708864	0.31463378	0.308208677	0.996708864	0.31463378	-0.032469691
NTHL1	0.242248578	0.931538222	0.398161732	0.306280651	0.931538222	0.398161732	0.064032073
NonTargetingC	0.66793684	0.998830219	0.201771406	0.305431058	0.998830219	0.372629334	-0.362505783
NonTargetingC	0.16588145	0.963105599	0.474021678	0.298881325	0.963105599	0.474021678	0.132999875
USP20	0.570717433	0.997002414	0.24448993	0.298748207	0.997002414	0.297860276	-0.271969226
PARP14	-0.052090885	0.999626837	0.55035571	0.296650416	0.999626837	0.422550735	0.348741301
USP11	0.29021863	0.977479353	0.267347445	0.292297743	0.977479353	0.267347445	0.002079113
PINK1	-0.232957626	0.859205561	0.7120578	0.292016342	0.859205561	0.480296597	0.524973968
SENP8	0.793514012	1	0.117722982	0.29177947	1	0.300314728	-0.501734542
NABP1	0.425386447	0.959632317	0.345913405	0.291399708	0.959632317	0.345913405	-0.133986739
PPP5C	0.111652577	0.956631895	0.442428591	0.288826821	0.956631895	0.442428591	0.177174244
RAG2	0.130665655	0.937786552	0.382911203	0.288541948	0.937786552	0.279899438	0.157876293
APOBEC3A	0.295508196	0.949371552	0.402239037	0.287559727	0.949371552	0.402239037	-0.007948469
RHO	0.17738965	0.867938538	0.43694721	0.286215907	0.867938538	0.43694721	0.108826257
SSBP2	0.30010202	0.999223979	0.29651219	0.283602099	0.999223979	0.29651219	-0.016499921
APOBEC2	0.219990172	0.999739009	0.307701603	0.280765648	0.999739009	0.307701603	0.060775476
PMS1	0.231855822	0.958274699	0.395162706	0.279624556	0.958274699	0.395162706	0.047768733
NonTargetingC	0.316415105	0.980263038	0.392473977	0.276595121	0.980263038	0.392473977	-0.039819984
SMUG1	0.266987691	0.926775706	0.400235835	0.275533631	0.926775706	0.400235835	0.008545941
ERCC6	0.109759631	0.742080257	0.463305052	0.272885837	0.742080257	0.461681238	0.163126206
PPP6R3	0.427865803	0.99966489	0.323761886	0.272166394	0.99966489	0.346160016	-0.155699409
RPA4	0.10962224	0.926587876	0.418620376	0.271949767	0.926587876	0.347017442	0.162327527
NonTargetingC	0.112659323	0.966309425	0.585852947	0.27182476	0.966309425	0.563951342	0.159165437
SERBP1	-0.055402979	0.936111565	0.549367782	0.271075829	0.936111565	0.436697139	0.326478808
NUDT1	0.09702177	0.946357521	0.410731261	0.268617241	0.946357521	0.322648734	0.171595472
TNP1	0.162474561	0.962981376	0.406564069	0.268559553	0.962981376	0.371141252	0.106084993
PIAS3	0.220998256	0.955902472	0.518574108	0.265580921	0.955902472	0.518574108	0.044582665
MUM1	0.586028663	0.998613554	0.166129122	0.264817817	0.998613554	0.275787866	-0.321210846
MBD4	0.308408146	0.99826714	0.294597572	0.262546439	0.99826714	0.294597572	-0.045861707
NEIL2	0.079645045	0.900745624	0.42471125	0.261775171	0.900745624	0.380534521	0.182130126
CCNO	0.107660869	0.98679286	0.393804847	0.258422772	0.98679286	0.393804847	0.150761903
NonTargetingC	0.298982513	0.984970515	0.390025888	0.257662825	0.984970515	0.390025888	-0.041319688
CCND3	0.223063909	0.99943543	0.257562988	0.257309752	0.99943543	0.257562988	0.034245843
USP51	0.300470978	0.999505252	0.300943535	0.256327081	0.999505252	0.303779222	-0.044143897
RECQL	0.491747529	0.991266977	0.227210593	0.255184663	0.991266977	0.346060971	-0.236562866
USP26	0.303958027	0.977805328	0.414615829	0.253714322	0.977805328	0.414615829	-0.050243705
NonTargetingC	0.279661214	0.998717176	0.426064512	0.253466775	0.998717176	0.426064512	-0.026194439
NonTargetingC	0.373422582	0.99983586	0.219087331	0.253053387	0.99983586	0.273662572	-0.120369195
CENPS	-0.165737356	0.809540827	0.654784225	0.251987209	0.809540827	0.504680041	0.417724565

SUV39H1	0.035520359	0.686927959	0.727706492	0.251722001	0.816719917	0.727706492	0.216201642
OR1E2	-0.046680827	0.776359	0.639285089	0.250135218	0.776359	0.639285089	0.296816044
GADD45A	0.237855855	0.999990609	0.416522956	0.248290086	0.999990609	0.416522956	0.010434231
INO80D	0.124782837	0.995796808	0.385321677	0.246581288	0.995796808	0.322263207	0.121798451
APOBEC3H	0.230781046	0.843921742	0.402261229	0.243273363	0.843921742	0.402261229	0.012492317
C9orf142	0.226359013	0.955815087	0.345532622	0.239141833	0.955815087	0.345532622	0.012782819
ATXN7	0.629376656	0.999322392	0.185430777	0.235773668	0.999322392	0.300331243	-0.393602988
LMNA	0.137809714	0.703254743	0.988127832	0.235251507	0.703254743	0.988127832	0.097441793
CRY2	0.274015564	0.8956699	0.466013717	0.23469537	0.8956699	0.466013717	-0.039320194
HES1	0.06007948	0.76809946	0.612258629	0.233702749	0.801786985	0.612258629	0.173623269
NonTargetingC	0.349701776	0.999451714	0.280807461	0.233483269	0.999451714	0.296424935	-0.116218507
NonTargetingC	0.163785092	0.9463425	0.377586763	0.230307412	0.9463425	0.377586763	0.066522319
CDC34	0.227487745	0.943082939	0.317670536	0.229082209	0.943082939	0.317670536	0.001594464
UBE2V1	0.676775662	0.994675609	0.203828569	0.228322742	0.994675609	0.311815552	-0.44845292
HDAC4	0.264719905	0.952460343	0.448885076	0.227808383	0.952460343	0.448885076	-0.036911521
SUV39H2	0.381515643	0.994902355	0.317153685	0.227320766	0.994902355	0.317153685	-0.154194876
XPA	0.459401382	0.954356687	0.428896985	0.226625495	0.954356687	0.473829968	-0.232775887
GABBR1	0.116340011	0.830415951	0.443223333	0.22158859	0.830415951	0.443223333	0.105248579
HUS1B	0.153822685	0.999041355	0.489202098	0.220769523	0.999041355	0.489202098	0.066946838
CCNE1	0.314320619	0.972601188	0.463674971	0.219653256	0.972601188	0.463674971	-0.094667364
NonTargetingC	0.251793551	0.939658178	0.359655223	0.216847108	0.939658178	0.359655223	-0.034946444
NonTargetingC	0.164850469	0.975822499	0.356101424	0.216614764	0.975822499	0.356101424	0.051764296
NonTargetingC	0.412477701	0.995789702	0.156773149	0.214065217	0.995789702	0.301779753	-0.198412484
BMI1	0.423723041	0.997754667	0.342022959	0.213148011	0.997754667	0.45990931	-0.210575031
DCUN1D4	0.375164322	0.997906465	0.339737976	0.209996603	0.997906465	0.37770114	-0.165167719
POLB	0.387642184	0.978148625	0.284457033	0.208822909	0.978148625	0.362603932	-0.178819275
HDAC1	0.017750919	0.853806783	0.481902706	0.206801755	0.853806783	0.358107678	0.189050836
NEIL1	0.47341097	0.967157443	0.197009555	0.206092534	0.967157443	0.321605993	-0.267318436
NonTargetingC	0.065607191	0.965584874	0.434281159	0.203833701	0.965584874	0.434281159	0.138226511
ANKRD28	0.279343555	0.964281934	0.377704218	0.203733426	0.964281934	0.377704218	-0.075610129
PSIP1	0.182814347	0.882014247	0.407987723	0.202226528	0.882014247	0.407987723	0.01941218
SCAF11	0.578619509	0.986336654	0.170906471	0.198772805	0.986336654	0.377734284	-0.379846704
ATMIN	0.146735323	0.945798935	0.623082988	0.196221937	0.945798935	0.623082988	0.049486614
NonTargetingC	0.426426405	0.999895055	0.246418794	0.191663436	0.999895055	0.327708527	-0.234762968
PRDM9	0.278200216	0.943546646	0.367872819	0.191049834	0.943546646	0.367872819	-0.087150382
PNN	-0.193308689	0.997902515	0.687712017	0.190054384	0.997902515	0.399103118	0.383363073
SMARCA2	-0.183015484	0.964445153	0.662672832	0.189519252	0.964445153	0.590235601	0.372534736
MTA3	0.497542296	0.998930186	0.238585568	0.189440643	0.998930186	0.472414848	-0.308101653
PPP4R4	0.354292349	0.999944276	0.355000241	0.186939341	0.999944276	0.415491344	-0.167353008
NonTargetingC	0.177854682	0.878180299	0.570687847	0.185133451	0.878180299	0.570687847	0.007278769
TP63	0.323737216	0.982719463	0.431918923	0.184529845	0.982719463	0.471691556	-0.139207372
TOP3B	0.187319284	0.997428561	0.478796616	0.181748161	0.997428561	0.478796616	-0.005571123
L3MBTL1	0.193188911	0.999081574	0.329772844	0.175355944	0.999081574	0.329772844	-0.017832967
ZSWIM7	0.27737294	0.743131832	0.724270237	0.172618176	0.743131832	0.724270237	-0.104754765
MLH1	-0.083837356	0.942751324	0.581493012	0.172563029	0.942751324	0.556658798	0.256400385
DCAF11	0.011343408	0.900717935	0.487812003	0.170446097	0.900717935	0.386361477	0.159102689
HDAC2	0.242624258	0.869520373	0.350883165	0.166968371	0.869520373	0.350883165	-0.075655887
NonTargetingC	0.220571779	0.999748986	0.331340985	0.164977284	0.999748986	0.357644257	-0.055594495
WRN	0.194002836	0.936131005	0.479474015	0.163784773	0.936131005	0.479474015	-0.030218064
HNRNPUL1	0.065258696	0.981160424	0.437871191	0.163553397	0.981160424	0.388394168	0.098294701
SUMO1	0.209439311	0.848506551	0.352701213	0.159560717	0.848506551	0.352701213	-0.049878594
IGHMBP2	0.051354525	0.733461585	0.477616102	0.159362388	0.733461585	0.477616102	0.108007863
CRY1	0.109280694	0.920529515	0.580422196	0.157846794	0.920529515	0.580422196	0.048566101
ANP32E	0.090454976	0.877808356	0.403546598	0.157621012	0.877808356	0.388795789	0.067166036
MCM10	0.018534883	0.90263807	0.48159913	0.156753517	0.90263807	0.396343306	0.138218634
RAD23B	0.125553414	0.726194025	0.689054646	0.155677338	0.726194025	0.689054646	0.030123924
ZDHHC16	-0.619488517	0.841054331	0.906549519	0.15437286	0.957586173	0.713194275	0.773861376
MSH5	-0.152193068	0.738573839	0.706570482	0.153969319	0.810969531	0.706570482	0.306162388
H2AFY2	0.148010251	0.763884749	0.465235999	0.149223636	0.763884749	0.465235999	0.001213385
COL21A1	0.147885849	0.921825514	0.550247241	0.147630492	0.921825514	0.550247241	-2.55358E-04
SUMO4	-0.2977552	0.958853859	0.703876238	0.14750239	0.958853859	0.448380721	0.44525759
WHSC1	0.324311081	0.984510192	0.413699041	0.147316887	0.984510192	0.423713962	-0.176994195
POLH	0.221447455	0.817609978	0.414541812	0.143453016	0.817609978	0.414541812	-0.077994439
BLM	-0.044631219	0.840181435	0.566089673	0.143088336	0.840181435	0.470355048	0.187719554
PAXIP1	0.004171241	0.640313842	0.733419247	0.140747098	0.640313842	0.733419247	0.136575857
RAD52	0.052618481	0.728971579	0.559429461	0.139358087	0.728971579	0.559429461	0.086739606
APOBEC3F	-0.069098036	0.96743583	0.558607065	0.137463363	0.96743583	0.495537325	0.206561399
ASF1B	0.2770417	0.852870623	0.479460419	0.135389719	0.852870623	0.479460419	-0.14165198
EXO1	0.0038375	0.626652201	0.875452844	0.133688975	0.626652201	0.875452844	0.129851475
SMC1B	0.406920037	0.999741633	0.330922427	0.132101041	0.999741633	0.39971864	-0.274818997
TIPIN	-0.066041576	0.889867239	0.561447242	0.131938246	0.889867239	0.431000282	0.197979822
APOBEC3G	0.172594923	0.800085083	0.404673257	0.130130582	0.800085083	0.404673257	-0.042464341
NBN	0.323243153	0.877525563	0.750377074	0.127117548	0.797503888	0.750377074	-0.196125605
EID3	0.245719157	0.993920362	0.368745894	0.126087803	0.993920362	0.389930596	-0.119631355
RAD9B	0.092239963	0.907235566	0.416475499	0.125768599	0.907235566	0.416475499	0.033528636
CUL4A	0.155945046	0.655076567	0.689545238	0.125635587	0.655076567	0.689545238	-0.030309459
HFM1	0.370797409	0.993815046	0.276872453	0.125293337	0.993815046	0.383542611	-0.245504072
SENP2	0.335707035	0.974847315	0.384750348	0.124786415	0.974847315	0.384750348	-0.210920621
H3F3A	0.239065004	0.576658748	0.533961199	0.123420012	0.576658748	0.533961199	-0.115644991
MORF4L2	-0.08291946	0.909420079	0.609511379	0.12316091	0.909420079	0.584895047	0.20608037
COPS4	-0.369197186	0.962367229	0.784286744	0.123057171	0.962367229	0.715195378	0.492254357
FAM175A	0.288665055	0.987271407	0.317198107	0.122177976	0.987271407	0.412046859	-0.166487079

TRIM28	-0.035181148	0.696727965	0.743038716	0.120099747	0.696727965	0.743038716	0.155280895
UNG	-0.151604107	0.879170242	0.711741337	0.119793468	0.879170242	0.711741337	0.271397575
DCUN1D2	0.483637729	0.967274579	0.312938999	0.119728117	0.967274579	0.397567792	-0.363909612
UBE2D4	0.530167178	0.907990743	0.308397143	0.117439635	0.907990743	0.445140961	-0.412727543
DTX1	0.353444764	0.802545681	0.457077757	0.115984764	0.802545681	0.457077757	-0.237460001
AICDA	0.223795156	0.884412741	0.47259631	0.113797368	0.884412741	0.47259631	-0.109997789
SMARCA4	0.07564986	0.921918975	0.428203393	0.113699745	0.921918975	0.428203393	0.038049885
LIG1	-0.323826434	0.526211125	0.979584009	0.113695322	0.903825925	0.894261113	0.437521757
RECQL4	-0.704082691	0.477553355	0.944230596	0.103531557	0.877680198	0.595715041	0.807614248
NonTargetingC	0.0252258	0.850087936	0.533634841	0.103184482	0.850087936	0.533634841	0.077958682
PER2	0.190416275	0.999727149	0.535196289	0.098989114	0.999727149	0.535196289	-0.091427161
NFATC2IP	0.402180172	0.947512601	0.218206324	0.097418092	0.947512601	0.414063697	-0.30476208
XRCC5	0.135621641	0.986959415	0.419954995	0.09500498	0.986959415	0.419954995	-0.040616661
XRCC1	0.138081457	0.636133304	0.83560372	0.093587426	0.636133304	0.83560372	-0.044494031
RECQL5	0.063694102	0.807844349	0.449528537	0.09254501	0.807844349	0.449528537	0.028850908
NonTargetingC	0.227566212	0.998422901	0.457736564	0.091697192	0.998422901	0.457736564	-0.13586902
PIF1	0.053836296	0.789502562	0.452710548	0.091245429	0.789502562	0.452710548	0.037409133
CBX3	0.182938952	0.85241978	0.418979627	0.090643746	0.85241978	0.418979627	-0.092295206
BEND3	0.131089838	0.782060364	0.418467606	0.087865329	0.782060364	0.418467606	-0.043224508
TOP2A	0.036454574	0.810893181	0.622751665	0.086579172	0.810893181	0.622751665	0.050124599
CHTF18	-0.044743262	0.982124975	0.541052539	0.08562101	0.982124975	0.470831958	0.130364272
POLQ	0.068675702	0.707187804	0.452518333	0.084371766	0.707187804	0.452518333	0.015696064
MTA1	0.027925211	0.620309887	0.740035073	0.083837069	0.620309887	0.740035073	0.055911858
RFC1	-0.008355058	0.870530865	0.507184656	0.08255101	0.870530865	0.507184656	0.090906068
RAD51AP1	0.282305351	0.853380663	0.405176852	0.076032306	0.853380663	0.509234634	-0.206273046
TCEA1	-0.041161416	0.635881387	0.597959364	0.074564313	0.635881387	0.597959364	0.115725729
USP22	-0.028193361	0.642641712	0.653544646	0.074009799	0.642641712	0.653544646	0.10220316
NLK	0.152660664	0.981217976	0.473667152	0.073554147	0.981217976	0.473667152	-0.079106517
PPP6R1	-0.180540057	0.772941429	0.696452101	0.070165085	0.772941429	0.646705834	0.250705142
ERCC6L2	0.257779422	0.872367225	0.646306863	0.06056496	0.872367225	0.646306863	-0.197214462
UIMC1	0.246243792	0.861488402	0.390302293	0.059326254	0.861488402	0.444985534	-0.186917537
MSH6	0.049096949	0.77028725	0.633023141	0.056577325	0.77028725	0.633023141	0.007480376
RNF168	0.249943224	0.723921583	0.768789476	0.054766667	0.686855358	0.768789476	-0.195176557
DTX2	0.074069585	0.671581355	0.696367427	0.05381061	0.671581355	0.696367427	-0.020258975
PPP6R2	-0.243076337	0.793930204	0.728714928	0.045462184	0.793930204	0.582901683	0.288538521
SENP7	0.330744832	0.8161503	0.467620277	0.044435137	0.8161503	0.467620277	-0.286309695
ATAD5	-0.056820094	0.639201937	0.719766489	0.043432205	0.639201937	0.719766489	0.100252299
SLBP	-0.199307395	0.84926528	0.689545481	0.039423417	0.84926528	0.520300724	0.238730812
BAZ1A	0.152587803	0.733462775	0.45138603	0.039047852	0.733462775	0.474065524	-0.113539951
PRDM10	0.018883294	0.750825113	0.67521091	0.032405396	0.750825113	0.67521091	0.013522102
MPG	-0.149772922	0.678395155	0.722356284	0.03185652	0.678395155	0.64260504	0.181629442
PARP9	0.194337967	0.997612841	0.43324421	0.026209723	0.997612841	0.476439733	-0.168128245
UCHL3	0.13091457	0.990060866	0.431779794	0.017147081	0.990060866	0.484845025	-0.11376749
TP73	0.003021666	0.721214667	0.496816724	0.016865918	0.721214667	0.496816724	0.013844253
RNF126	0.03207365	0.98261248	0.48642391	0.015435248	0.98261248	0.48642391	-0.016638402
PIAS2	0.433295828	0.972756723	0.373570722	0.011042594	0.972756723	0.489889098	-0.422253234
HLTF	0.215943345	0.842836197	0.400106702	0.008822015	0.842836197	0.491351357	-0.20712133
APOBEC1	6.31454E-04	0.956864874	0.499361168	0.008738493	0.956864874	0.499361168	0.008107039
ASCC1	0.771740111	0.999128493	0.059553489	0.006423457	0.999128493	0.494072896	-0.765316655
OR1E1	0.38709719	0.985974094	0.259163815	0.006129547	0.985974094	0.49547548	-0.380967643
SSBP1	0.190719099	0.828033245	0.733551418	0.005723336	0.828033245	0.7423631	-0.184995763
CSNK2A1	0.114166939	0.59893175	0.744935698	0.004215594	0.59893175	0.744935698	-0.109951345
BAZ1B	-0.285309055	0.677081241	0.831773684	0.002834699	0.677081241	0.831773684	0.288143755
CCND1	-0.135735032	0.869752987	0.68862852	9.76677E-04	0.869752987	0.641848467	0.136711709
TREX2	0.328076149	0.89181467	0.529610279	-0.00218478	0.89181467	0.589818312	-0.330260929
ZRANB3	0.267796074	0.858872109	0.384695382	-0.004053803	0.858872109	0.503880464	-0.271849876
ERCC4	-0.582410528	0.171687831	0.999998625	-0.006311267	0.49479728	0.999998625	0.576099261
OR6B1	-0.020739962	0.780133397	0.543041925	-0.006429892	0.780133397	0.543041925	0.01431007
SMARCAL1	0.085000324	0.760780742	0.748013154	-0.011956131	0.760780742	0.748013154	-0.096956455
SIRT6	0.16482436	0.933946592	0.491069507	-0.027412561	0.933946592	0.526319988	-0.192236921
RNF40	-1.144754447	0.019481974	0.999986349	-0.028827287	0.710868279	0.999986349	1.11592716
KLHL15	0.40765917	0.992613477	0.275391024	-0.031211822	0.992613477	0.525682708	-0.438870991
DLGAP5	-0.091161529	0.886341913	0.585898305	-0.040257893	0.886341913	0.585898305	0.050903635
EYA1	0.096844369	0.990056724	0.455516153	-0.04049906	0.990056724	0.53979723	-0.137343429
SIRT4	-0.115909667	0.909510653	0.616954509	-0.040541048	0.909510653	0.607658791	0.075368619
OTUB1	0.08380161	0.59043536	0.800128386	-0.040880799	0.59043536	0.800128386	-0.124682409
USP3	0.232671829	0.90412076	0.449800464	-0.048132813	0.90412076	0.545462659	-0.280804642
STAG1	0.074002938	0.723799903	0.633347551	-0.049438275	0.723799903	0.705338843	-0.123441213
UHRF2	0.187028524	0.933087821	0.456677267	-0.049617575	0.933087821	0.541887984	-0.236646099
COL1A1	0.249914919	0.911479638	0.561336024	-0.056901749	0.911479638	0.616873471	-0.306816668
APTX	0.053021535	0.902305794	0.503230052	-0.058995877	0.902305794	0.55735868	-0.112017412
UBC	-0.801976588	0.305068474	0.98099411	-0.059050896	0.680768834	0.98099411	0.742925692
PARK2	0.168701095	0.744557492	0.508448011	-0.059535046	0.744557492	0.558212871	-0.228236141
NEIL3	0.170400308	0.830465663	0.459576238	-0.062925562	0.830465663	0.559838615	-0.23332587
ERCC5	0.067635461	0.788299656	0.480513536	-0.07624458	0.788299656	0.579596243	-0.14388004
ANKRD52	0.05420815	0.830515882	0.982790897	-0.077679179	0.763937201	0.982790897	-0.131887329
TADA3	-0.363449042	0.433691801	0.915647428	-0.078706003	0.433691801	0.915647428	0.28474304
EXD2	0.467668765	0.986875983	0.445430619	-0.079378146	0.986875983	0.577746051	-0.547046911
PPP4R3B	-0.085563086	0.993541008	0.583369414	-0.082536945	0.993541008	0.583369414	0.003026141
SHPRH	0.008478531	0.726763686	0.552152367	-0.082853496	0.726763686	0.585907914	-0.091332026
NonTargetingC	0.005532232	0.860063864	0.556267724	-0.085311621	0.860063864	0.58586819	-0.090843853
PPP4R1	-0.188117089	0.856665652	0.694032596	-0.085795205	0.856665652	0.662714626	0.102321884

CHRAC1	-0.145499585	0.470805861	0.883613746	-0.086188938	0.470805861	0.883613746	0.059310647
PIAS1	-0.046448663	0.730146097	0.594026501	-0.094716277	0.730146097	0.594026501	-0.048267615
RNASEH2A	-0.433064026	0.182239122	0.999838311	-0.100734202	0.407589848	0.999838311	0.332329824
USP1	-0.268746332	0.590243354	0.848664132	-0.101292794	0.590243354	0.848664132	0.167453538
ECT2	-0.416490353	0.601225405	0.863494177	-0.104058134	0.601225405	0.863494177	0.312432218
TDP1	0.063966399	0.868239207	0.786153488	-0.108869623	0.868239207	0.813004354	-0.172836022
UVSSA	-0.080539004	0.69812623	0.613241301	-0.109398277	0.69812623	0.613241301	-0.028859273
HPF1	0.202930995	0.942247654	0.495465149	-0.114787885	0.942247654	0.598148943	-0.31771888
CBX1	0.108481757	0.818043684	0.73796149	-0.115511477	0.732768406	0.73796149	-0.223993234
MDM4	-0.272131062	0.999708607	0.750459003	-0.120556767	0.999708607	0.701052302	0.151574295
CASP3	0.045602456	0.92594083	0.520395807	-0.122515028	0.92594083	0.595479011	-0.168117484
KMT5A	0.069387497	0.741562051	0.574073591	-0.124254304	0.741562051	0.589666108	-0.193641801
USP4	0.095010668	0.805362863	0.589526684	-0.124857406	0.805362863	0.619356451	-0.219868073
NOTCH2	0.039655919	0.91600724	0.518683693	-0.127144125	0.91600724	0.625304146	-0.166800044
GEN1	0.135956313	0.754153117	0.671192216	-0.127435798	0.754153117	0.717346874	-0.263392111
PER3	0.078220487	0.849608299	0.489903783	-0.132105967	0.849608299	0.626409073	-0.210326454
TOP1	-0.787746898	0.304162692	0.965118595	-0.133298574	0.593986618	0.965118595	0.654448324
NUDT16L1	0.181216111	0.821254066	0.439119507	-0.136536639	0.821254066	0.626962619	-0.317752749
CREBBP	0.052174079	0.548938199	0.977017433	-0.138574936	0.420105411	0.977017433	-0.190749015
TERF2IP	-0.177971527	0.747038604	0.740824367	-0.139410868	0.747038604	0.740824367	0.038560659
SMARCAD1	0.053450148	0.902049214	0.573219163	-0.153093248	0.902049214	0.648090642	-0.206543396
PMS2	0.305918679	0.962221154	0.340576221	-0.154685312	0.962221154	0.638062213	-0.460603991
PAPD7	-0.181913822	0.791645969	0.677664409	-0.154780646	0.791645969	0.677664409	0.027133176
SUMO2	-0.81598687	0.592600641	0.874235475	-0.158564629	0.592600641	0.874235475	0.657422242
INO80E	-0.338749577	0.854418796	0.789865255	-0.159554037	0.854418796	0.709819692	0.17919554
FAAP20	-0.051728204	0.529341341	0.704574993	-0.163049879	0.529341341	0.704574993	-0.111321675
EYA3	0.024634086	0.537003538	0.978716184	-0.164652103	0.537003538	0.978716184	-0.189286189
HNRNPK	-0.15426426	0.998457502	0.62563868	-0.166001737	0.998457502	0.62563868	-0.011737477
CHD4	0.064941475	0.842817081	0.901051259	-0.169529344	0.617171486	0.901051259	-0.234470819
PLRG1	-0.180752334	0.511586171	0.948788813	-0.17983506	0.511586171	0.948788813	9.17274E-04
POLI	0.013854053	0.870502638	0.548205948	-0.18215919	0.870502638	0.664697319	-0.196013243
UBE2W	-0.291609078	0.991327705	0.777638042	-0.184987553	0.991327705	0.75196683	0.106621525
RAD51C	-0.2608917	0.39136104	0.997588655	-0.187334279	0.417094838	0.997588655	0.073557421
TOP2B	-0.211270017	0.894281573	0.707130718	-0.202720287	0.894281573	0.707130718	0.00854973
POLE	-0.330480148	0.65044863	0.865959085	-0.203500907	0.65044863	0.865959085	0.126979241
MUTYH	-0.163272742	0.663194739	0.683401713	-0.203807178	0.663194739	0.683401713	-0.040534436
BRIP1	-0.627539607	0.360874066	0.9361424	-0.206801674	0.47669902	0.882716175	0.420737933
PRKDC	-0.27479796	0.322483042	0.997540738	-0.207842338	0.337385664	0.997540738	0.066955622
DNMT1	-0.696213569	0.099572518	0.999965741	-0.208180516	0.398664484	0.999965741	0.488033053
CETN2	0.17810407	0.995655769	0.37745133	-0.21355994	0.995655769	0.688944595	-0.39166401
EP400	-0.246309596	0.584723843	0.934499724	-0.214073555	0.584723843	0.934499724	0.032236041
RMI2	-0.282193033	0.436135851	0.971086796	-0.21437492	0.436135851	0.971086796	0.067818113
KDM2A	-0.243077433	0.434804887	0.910732661	-0.215050117	0.434804887	0.910732661	0.028027317
POLD4	-0.081457374	0.72269126	0.774671345	-0.21602438	0.72269126	0.774671345	-0.134567006
TDG	-0.030070008	0.776038219	0.622908194	-0.221651095	0.776038219	0.69564578	-0.191581087
TIMELESS	-0.753367836	0.095802368	0.999719417	-0.231443128	0.465176593	0.999719417	0.521924709
NPM1	-0.121955727	0.971362538	0.666090951	-0.236842999	0.971362538	0.666090951	-0.114887273
SPIDR	-0.022112482	0.476235924	0.816668104	-0.238385035	0.476235924	0.816668104	-0.216272554
WRAP53	-0.397013136	0.268762888	0.999668421	-0.245486584	0.346982738	0.999668421	0.151526551
PMS2P5	0.011898812	0.642106223	0.567006492	-0.246312061	0.642106223	0.567006492	-0.258210873
RBBP8	-0.069836369	0.642743577	0.850956524	-0.253103248	0.483882031	0.850956524	-0.183266879
SMG6	-0.265206384	0.420174475	0.975220406	-0.263211491	0.420174475	0.975220406	0.001994893
CENPX	0.025693368	0.828940722	0.621083846	-0.26866434	0.828940722	0.713266541	-0.294357708
ERCC8	-0.195362159	0.716506865	0.739113123	-0.272484995	0.716506865	0.739113123	-0.077122836
GTF2H5	-0.366482448	0.299807685	0.999989346	-0.276417372	0.299807685	0.999989346	0.090065076
HELQ	-0.07609044	0.53104413	0.86709702	-0.27830037	0.53104413	0.86709702	-0.20220993
PARP1	-0.123123771	0.420140741	0.90920163	-0.280067512	0.361300018	0.90920163	-0.156943742
PIAS4	-0.073605927	0.530232231	0.788581482	-0.281359099	0.530232231	0.788581482	-0.207753171
MRE11	-0.459386299	0.159442554	0.999979051	-0.287002511	0.308853834	0.999979051	0.172383787
CBX5	-0.077902855	0.913303254	0.641256109	-0.3079524	0.913303254	0.743051663	-0.230049545
ENY2	-0.286884167	0.262644554	0.971646103	-0.311861656	0.262644554	0.971646103	-0.024977489
ATP23	0.047240205	0.941599552	0.509040395	-0.312384151	0.941599552	0.771902937	-0.359624355
PPP4R2	0.027219553	0.780268214	0.884977733	-0.321735999	0.570779587	0.884977733	-0.348955552
FANCI	-0.573468796	0.250591065	0.995192091	-0.325300647	0.380371193	0.995192091	0.248168149
CCNA1	0.193270341	0.810951228	0.598707029	-0.327567746	0.810951228	0.772818133	-0.520838087
POLR2D	-0.656392465	0.767441941	0.897448418	-0.333372204	0.774231543	0.897448418	0.323020261
H3F3B	-0.287782191	0.596271997	0.851687166	-0.33407007	0.596271997	0.851687166	-0.046287879
TNKS	-0.073346311	0.632422958	0.844252915	-0.335362567	0.632422958	0.844252915	-0.262016256
SUPT5H	0.014366953	0.999366891	0.54817901	-0.340921473	0.999366891	0.76591109	-0.355288426
POLR2A	-0.990280666	0.2211972	0.975422533	-0.34321534	0.763345102	0.854275904	0.647065327
MPZ	-0.150188406	0.783285652	0.721277278	-0.348634103	0.783285652	0.79012249	-0.198445696
RNF20	-0.482384041	0.169146504	0.999999519	-0.348933319	0.230650755	0.999999519	0.133450722
CDK12	-0.380291063	0.461626646	0.972174261	-0.349726391	0.461626646	0.972174261	0.030564672
ATRX	-0.270503893	0.584883682	0.796610207	-0.358354038	0.584883682	0.796610207	-0.087850145
FANCB	-0.234435856	0.334949315	0.995133965	-0.359238293	0.324218933	0.995133965	-0.124802437
CDCA5	-0.482313731	0.84546838	0.843402935	-0.366377621	0.84546838	0.843402935	0.11593611
RAD54L	-0.213438121	0.553927821	0.930512659	-0.368570607	0.553927821	0.930512659	-0.155132486
BAP1	-0.058185386	0.452201464	0.991006485	-0.36955053	0.25405261	0.991006485	-0.311365144
CNOT7	-0.07746357	0.430372424	0.942650234	-0.376370911	0.288024187	0.942650234	-0.298907342
SMG1	-0.142718598	0.671159782	0.889597163	-0.383043016	0.65746305	0.889597163	-0.240324418
USP44	-0.290345117	0.5445791	0.973182489	-0.38402573	0.5445791	0.973182489	-0.093680613
RAD23A	-0.237262111	0.635087306	0.805323122	-0.385837997	0.635087306	0.805323122	-0.148575886

POLD2	-0.259372698	0.407668588	0.982634944	-0.386508862	0.334274577	0.982634944	-0.127136164
NFE2L2	-0.349002704	0.300917887	0.994462838	-0.394113255	0.300917887	0.994462838	-0.045110551
POLD1	-0.07078397	0.657827464	0.971842685	-0.404476043	0.346799236	0.971842685	-0.333692073
FANCA	-0.397122824	0.209442566	0.968847838	-0.4064322	0.209442566	0.968847838	-0.009309375
POLA1	-0.030920581	0.992727618	0.791658424	-0.406565914	0.83158969	0.809082136	-0.375645333
NFRKB	-0.554723843	0.295007312	0.983903022	-0.411184381	0.390152558	0.983903022	0.143539462
SFR1	0.295270277	0.81670404	0.6184974	-0.415250096	0.640166994	0.894819057	-0.710520373
NSMCE2	-0.574637705	0.193492295	0.996527617	-0.418030714	0.25462394	0.996527617	0.156606991
XRCC4	-0.379964724	0.175353771	0.983404757	-0.418575907	0.175353771	0.983404757	-0.038611183
MPLKIP	0.023924658	0.523320306	0.839815793	-0.418786098	0.417071503	0.839815793	-0.442710756
ATRIP	-0.321344961	0.241456283	0.998218448	-0.422427568	0.203753298	0.998218448	-0.101082607
DUT	-0.720547004	0.198585301	0.992138582	-0.43176538	0.358134174	0.992138582	0.288781624
PDS5B	-0.604185155	0.164773	0.997655936	-0.43965332	0.191064986	0.997655936	0.164531835
BRCA1	-0.439426985	0.240341187	0.988927882	-0.442884549	0.240341187	0.988927882	-0.003457564
SMARCA5	-0.781953997	0.089334214	0.999784118	-0.444778386	0.332306224	0.999784118	0.337175611
SMC4	-0.600801606	0.725181501	0.91147312	-0.448302506	0.725181501	0.91147312	0.1524991
CDK2	-0.292723056	0.355245308	0.991668433	-0.454953795	0.355245308	0.991668433	-0.162230739
POLE3	-0.665859111	0.130317511	0.999987142	-0.459125558	0.234506104	0.999987142	0.206733553
NAE1	-0.778033725	0.011012103	0.999999565	-0.459312284	0.106455892	0.999999565	0.318721441
ORC2	-0.18252488	0.481268607	0.87352768	-0.460619321	0.481268607	0.87352768	-0.278094441
POLG	0.163107171	0.665474388	0.874455448	-0.467272193	0.400960382	0.874455448	-0.630379363
PPM1G	-0.702791598	0.202151406	0.977161392	-0.470878614	0.348028758	0.977161392	0.231912985
RAD51	-0.796837665	0.096633806	0.99987961	-0.472373821	0.237502187	0.99987961	0.324463845
TINF2	-1.028007517	0.063877364	0.999488823	-0.486489463	0.298488608	0.999488823	0.541518054
HELLS	-0.349264632	0.378136086	0.971985663	-0.490390349	0.378136086	0.971985663	-0.141125717
MUS81	-0.266691818	0.394675737	0.99287909	-0.494046882	0.261371504	0.99287909	-0.227355064
RAD9A	-0.846315292	0.082922686	0.999222767	-0.494088297	0.2339057	0.999222767	0.352226995
DSCC1	-0.546825262	0.140551596	0.999994766	-0.496870933	0.167690344	0.999994766	0.049954329
CLSPN	-0.896090088	0.111173048	0.995842411	-0.508595584	0.313806293	0.995842411	0.387494504
RNF4	-0.088933354	0.51553963	0.863172383	-0.521311604	0.51553963	0.863172383	-0.432378249
SKIV2L2	-0.529143601	0.430956169	0.899222865	-0.524483166	0.430956169	0.899222865	0.004660435
FIGNL1	-0.262646066	0.401254241	0.998935428	-0.531311839	0.256950171	0.998935428	-0.268665774
TFPT	-0.45742285	0.297516508	0.890885344	-0.532598399	0.297516508	0.890885344	-0.075175549
NSMCE1	-0.598416985	0.133137564	0.99991118	-0.542011303	0.133137564	0.99991118	0.056405682
TERF1	-0.992601749	0.149199926	0.989034776	-0.544728384	0.329831688	0.989034776	0.447873365
INO80B	-0.561273872	0.204278007	0.998019997	-0.549015665	0.204278007	0.998019997	0.012258207
NONO	-0.753868163	0.076990814	0.999999975	-0.549691125	0.13960147	0.999999975	0.204177038
FANCG	-0.794734076	0.082113337	0.999845823	-0.55395964	0.189304986	0.999845823	0.240774436
RBX1	-0.140676752	0.98131896	0.778330918	-0.560172399	0.98131896	0.852992763	-0.419495646
ESCO2	-0.402338495	0.248389248	0.992629276	-0.560417497	0.196685607	0.992629276	-0.158079002
ERCC1	-0.311874506	0.26756681	0.999920277	-0.56073461	0.174877559	0.999920277	-0.248860104
POLR2K	-0.547115875	0.283843607	0.987262845	-0.5610864	0.283843607	0.987262845	-0.013970525
CDC25B	-0.247796174	0.43383429	0.990217901	-0.566451208	0.252367631	0.990217901	-0.318655034
SKP1	-0.702689721	0.14306062	0.999801217	-0.5706111	0.177808843	0.999801217	0.132078622
RAD50	-0.489597988	0.063442841	0.999999891	-0.583400633	0.050991002	0.999999891	-0.093802644
RFC2	-1.064713944	0.047321048	0.999995591	-0.599979962	0.142577215	0.999995591	0.464733982
RTEL1	-1.11978688	0.007576526	0.999998909	-0.602639123	0.111441801	0.999998909	0.517147757
WDR48	-0.231509292	0.45692757	0.999368917	-0.602990246	0.169767239	0.999368917	-0.371480954
MMS22L	-0.793495734	0.03248745	0.99993567	-0.603354765	0.101274561	0.99993567	0.190140969
KAT2A	-0.36384287	0.423700318	0.992094734	-0.604800975	0.262923643	0.992094734	-0.240958106
CSNK2B	-0.773429184	0.098440714	0.999938691	-0.61731956	0.172515794	0.999938691	0.156109625
PALB2	-0.641031163	0.21624328	0.956352073	-0.620629099	0.21624328	0.956352073	0.020402064
ERCC6L	0.007079137	0.995790705	0.555695391	-0.623186355	0.995790705	0.885943006	-0.630265492
XAB2	-0.926183863	0.047322107	0.99997275	-0.623250272	0.176883581	0.99997275	0.302933591
CCNB1	-0.529895584	0.191625285	0.998111376	-0.633722182	0.191625285	0.998111376	-0.103826598
FANCM	-0.876834687	0.030852823	0.999902234	-0.635320229	0.122080628	0.999902234	0.241514458
ACTR5	-0.87055273	0.087369321	0.999664378	-0.638139641	0.215516903	0.999664378	0.232413089
POLR2F	0.121671562	0.924083994	0.863874008	-0.648241283	0.216537678	0.932523806	-0.769912845
MAU2	-1.187186929	0.010802878	0.999999903	-0.653013289	0.083182623	0.999999903	0.534173639
RIF1	-0.757641121	0.07591614	0.999998123	-0.659779458	0.084137059	0.999998123	0.097861663
FZR1	-1.588116053	0.00038546	1	-0.662356468	0.113022711	1	0.925759585
RPAIN	-0.414738535	0.250850992	0.977445656	-0.666151419	0.205984554	0.977445656	-0.251412885
MTOR	-0.920480362	0.02129748	0.999949697	-0.670037909	0.069209453	0.999949697	0.250442453
PCID2	-0.884616949	0.040644676	0.999999883	-0.672258493	0.131259	0.999999883	0.212358456
NHEJ1	-0.213508435	0.341147889	0.989815203	-0.676938549	0.121990341	0.989815203	-0.463430114
POLR2B	-1.237591596	0.015752097	0.998193741	-0.67906433	0.164797606	0.998193741	0.558527266
KDM4A	-0.49933554	0.166800392	0.999685556	-0.682373284	0.125797803	0.999685556	-0.183037743
TCEB3	-0.188593485	0.502933479	0.990465878	-0.684066061	0.201967185	0.990465878	-0.495472576
WAPL	-0.522721443	0.200987195	0.99976222	-0.687034511	0.159477215	0.99976222	-0.164313069
EXO5	0.003804552	0.755495107	0.99160132	-0.690318315	0.173995496	0.99160132	-0.694122867
MCM3AP	-0.683803436	0.210290216	0.973219488	-0.697906683	0.210290216	0.973219488	-0.014103247
WEE1	-0.824870782	0.069213929	0.994310613	-0.706964784	0.102905994	0.994310613	0.117905998
MDC1	-0.633752064	0.122963509	0.986434394	-0.712525084	0.122963509	0.986434394	-0.07877302
PINX1	-0.429198595	0.343672826	0.974286015	-0.727670555	0.148550039	0.974286015	-0.298471961
CEP57	-0.773227332	0.0800124	0.999999863	-0.740468004	0.081750529	0.999999863	0.032759328
FANCD2	-1.088568212	0.026977856	0.999999968	-0.740484905	0.087721872	0.999999968	0.348083307
XRCC2	-1.741692264	1.81706E-04	1	-0.756996584	0.095199366	1	0.98469568
DNA2	-0.723821688	0.129489668	0.997085571	-0.759194908	0.120860467	0.997085571	-0.03537322
SLX4	-0.22461791	0.431754272	0.999341474	-0.764041416	0.102953521	0.999341474	-0.539423506
TONSL	-1.091450007	0.015216284	0.999999969	-0.788608386	0.064721645	0.999999969	0.30284162
INO80	-0.770050885	0.072838474	0.998880602	-0.792653027	0.072838474	0.998880602	-0.022602142
UBE2N	-0.615617321	0.068995853	0.999808198	-0.798045422	0.068995853	0.999808198	-0.182428101

RAD51B	-0.588208221	0.161939293	0.9999845	-0.803178354	0.090436675	0.9999845	-0.214970134
RFC3	-1.378255029	0.006771308	0.999999623	-0.81157798	0.082919225	0.999999623	0.566677049
ARID1A	-0.618188406	0.226680273	0.960738841	-0.812530373	0.184496925	0.960738841	-0.194341967
ZMPSTE24	-0.558575163	0.201849785	0.99078592	-0.812754609	0.15261029	0.99078592	-0.254179446
PLK1	-0.88297001	0.062117327	0.999800348	-0.82665493	0.062117327	0.999800348	0.05631508
FANCF	-0.880508953	0.057681808	0.999997085	-0.828182287	0.072455227	0.999997085	0.052326666
FANCL	-0.931558177	0.060321741	0.999999866	-0.848813544	0.075039619	0.999999866	0.082744633
FANCC	-0.967553578	0.033990772	0.999998236	-0.859797121	0.063798999	0.999998236	0.107756457
BCCIP	-0.90379916	0.076493307	0.998808704	-0.877725026	0.076493307	0.998808704	0.026074134
POLE2	-1.150349447	0.010574456	0.999980808	-0.879842489	0.048521821	0.999980808	0.270506958
TRIP13	-1.3216832	0.011234718	0.999999981	-0.881127716	0.082199218	0.999999981	0.440555484
SET	-0.465083823	0.178291556	0.9998963	-0.88318351	0.057764581	0.9998963	-0.418099686
H2AFX	-1.091814939	0.022759205	0.998820878	-0.88477279	0.075135148	0.998820878	0.207042149
COPS3	-0.654159443	0.155518309	0.998901311	-0.885562102	0.092317752	0.998901311	-0.231402658
SIN3A	-0.484052363	0.136922181	0.999999614	-0.899553376	0.026352754	0.999999614	-0.415501013
PAGR1	-0.038248802	0.690643539	0.995113011	-0.899703365	0.076743601	0.995113011	-0.861454563
TOPBP1	-1.165191087	0.004157882	0.999999996	-0.90770613	0.02212246	0.999999996	0.257484957
SPRTN	-1.058543444	0.030000709	0.993980344	-0.908052049	0.030000709	0.993980344	0.150491395
MEN1	-0.4611888	0.27247094	0.983314517	-0.911678551	0.09665337	0.983314517	-0.450489751
DAXX	-0.346772858	0.439790132	0.982592441	-0.916448612	0.145857946	0.982592441	-0.569675754
ACD	-0.647378812	0.475876179	0.956128584	-0.92148248	0.394842748	0.956128584	-0.274103668
CDK7	-0.792099281	0.095364152	0.999996104	-0.928166635	0.08089796	0.999996104	-0.136067355
CUL9	-0.160142107	0.761002897	0.98584922	-0.937779347	0.117847898	0.98584922	-0.777637239
NCAPH	-0.39841296	0.208162732	0.99898725	-0.939882303	0.029502951	0.99898725	-0.541469343
BRD4	-0.813463944	0.021255954	0.999964741	-0.94164872	0.009627659	0.999964741	-0.128184776
RMI1	-0.874985046	0.011457508	0.999979412	-0.944868933	0.011457508	0.999979412	-0.069883887
BOD1L1	-1.35686258	0.007127861	0.999999296	-0.950526083	0.05004508	0.999999296	0.406336497
SMC6	-0.749373936	0.115589293	0.999345574	-0.951857428	0.069491368	0.999345574	-0.202483492
UCHL5	-0.848664058	0.04510004	0.999999896	-0.967003466	0.028532625	0.999999896	-0.118339408
BRAT1	-1.36580548	0.011198467	1	-0.971405489	0.051218805	1	0.394399991
POLR2C	-1.170845748	0.002845873	0.999999547	-0.97772117	0.018445818	0.999999547	0.193124578
XRCC6	-0.275399909	0.454490881	0.996737637	-0.981191285	0.174617053	0.996737637	-0.705791375
FEN1	-0.842482854	0.041761688	0.999973193	-0.982866703	0.031779646	0.999973193	-0.14038385
UVRAG	-0.747707651	0.053359959	0.999970332	-0.985840327	0.019068122	0.999970332	-0.238132676
MAD2L2	-0.647439858	0.123894209	0.999997565	-0.989182582	0.04891888	0.999997565	-0.341742724
RAD51D	-1.204626601	3.57746E-04	0.999999993	-0.996679735	0.002946491	0.999999993	0.207946866
RFC4	-0.678043817	0.10153731	0.999840568	-1.016422469	0.039813359	0.999840568	-0.338378651
CCNH	-1.098149855	0.041573014	0.999833994	-1.017280978	0.041573014	0.999833994	0.080868877
BARD1	-1.101677725	0.012679529	0.99981174	-1.019574485	0.012679529	0.99981174	0.08210324
MCPH1	-1.170602984	0.024615128	0.999999494	-1.025635243	0.060706551	0.999999494	0.144967741
TDP2	-1.032263923	0.077108027	0.983092246	-1.028173277	0.077108027	0.983092246	0.004090647
SMC2	-1.307130038	0.011944405	0.998050525	-1.02818608	0.027175902	0.998050525	0.278943958
NSMCE4A	-0.757125785	0.142025292	0.999942809	-1.03116117	0.069580756	0.999942809	-0.274035385
NOP10	-1.798550851	4.39915E-04	0.999999242	-1.033936912	0.027159473	0.999999242	0.764613939
LIG4	-0.679846136	0.093721735	0.997992962	-1.043615304	0.069856744	0.997992962	-0.363769168
TELO2	-1.0466678	0.020409205	0.999999997	-1.04415919	0.026209223	0.999999997	0.002508609
TRRAP	-0.432937763	0.220991377	0.997020082	-1.048408028	0.050000856	0.997020082	-0.615470265
RUVBL2	-0.946541451	0.027503608	0.999999577	-1.049570572	0.022568603	0.999999577	-0.103029121
RFWD3	-0.112206586	0.445843971	0.946496535	-1.058130786	0.037563129	0.992271177	-0.945924199
FAAP100	-0.512444848	0.224899745	0.999216741	-1.060241098	0.018813012	0.999216741	-0.54779625
COPS2	-0.756981794	0.104368911	0.992713471	-1.065427188	0.065578765	0.992713471	-0.308445394
PNKP	-1.136093305	0.014696263	0.999999942	-1.067761284	0.014696263	0.999999942	0.06833202
TERF2	-1.115888815	0.068957806	0.996613913	-1.080329436	0.068957806	0.996613913	0.035559378
SMC3	-0.72417382	0.067091927	0.999896419	-1.09232109	0.022195719	0.999896419	-0.36814727
CUL1	-0.90409899	0.044775354	0.99998777	-1.093015737	0.01572293	0.99998777	-0.188916747
RNF8	-0.628339642	0.182009248	0.996162079	-1.098184297	0.044856782	0.996162079	-0.469844654
MMS19	-1.125260016	0.011497232	0.99999986	-1.099794684	0.011497232	0.99999986	0.025465332
PRMT1	-0.766863791	0.057656701	0.999836497	-1.110068541	0.028165463	0.999836497	-0.34320475
SFPQ	-0.797533619	0.08729688	0.99600134	-1.117727153	0.047558183	0.99600134	-0.320193534
STN1	-1.88081306	1.41E-05	1	-1.122406617	0.007663879	1	0.758406444
MCRS1	-0.198485558	0.962567628	0.872466732	-1.148282773	0.064286512	0.992857054	-0.949797215
TCEB1	-2.669195655	6.17E-05	1	-1.149358747	0.062229635	1	1.519836908
RPA3	-1.067680934	0.018489401	0.999948141	-1.150671855	0.015560347	0.999948141	-0.082990921
CCNA2	-1.211916047	0.007778821	0.999949601	-1.153710844	0.008711261	0.999949601	0.058205203
USP5	-0.658834391	0.120216542	0.999889437	-1.157335238	0.015286393	0.999889437	-0.498500847
TOP3A	-1.285875929	0.002395589	0.999999999	-1.161114816	0.006062652	0.999999999	0.124761113
SMARCE1	-0.491514325	0.30174795	0.990164848	-1.164894581	0.045333147	0.990164848	-0.673380256
PDS5A	-1.064705268	0.0216274	0.999995695	-1.164927729	0.021278258	0.999995695	-0.10022246
POLE4	-1.178396344	0.008462805	0.999981281	-1.179143396	0.008462805	0.999981281	-7.47052E-04
REV3L	-0.719340895	0.128238355	0.995825835	-1.185438941	0.037567482	0.995825835	-0.466098046
NIPBL	-0.021505529	0.723613776	0.998963233	-1.187241645	0.03039099	0.998963233	-1.165736117
DCLRE1B	-1.475193697	0.005452934	0.999992796	-1.188381406	0.026447696	0.999992796	0.286812292
CUL2	-1.201813259	0.004118064	0.999999866	-1.191513602	0.004118064	0.999999866	0.010299658
FANCE	-0.374700006	0.291835479	0.999512955	-1.212084086	0.018464133	0.999512955	-0.83738408
CDK9	-0.900017544	0.060387965	0.999986787	-1.213756632	0.022903835	0.999986787	-0.313739088
XRCC3	-1.781357524	5.11E-05	1	-1.218389766	0.007189884	1	0.562967759
KAT5	-0.743932276	0.035189382	0.999736495	-1.22279869	0.002133019	0.999736495	-0.478866414
WDR70	-0.666586827	0.258358485	0.99662953	-1.237391643	0.030334227	0.99662953	-0.570804817
NCAPH2	-1.78970588	4.32932E-04	0.999999184	-1.257723465	0.01515208	0.999999184	0.531982415
BCAS2	-1.578471705	4.00525E-04	0.999999806	-1.25909061	0.002490513	0.999999806	0.319381096
POT1	-1.181794295	0.008773476	0.999990622	-1.261567322	0.008759856	0.999990622	-0.079773027
USP37	-0.966626136	0.033446632	0.999898899	-1.266010258	0.009538152	0.999898899	-0.299384123

DDX11	-0.697966048	0.099787007	0.999667691	-1.272050669	0.016553886	0.999667691	-0.574084621
CHAF1A	-1.184469777	0.009374157	0.998605523	-1.283797124	0.009374157	0.998605523	-0.099327347
NCAPG2	-1.174082813	0.014953177	0.999979983	-1.292271738	0.009892353	0.999979983	-0.118188925
PRPF19	-1.361645177	0.005370152	0.999912334	-1.299906695	0.006445654	0.999912334	0.061738482
CTC1	-1.377217576	0.016902436	0.999977979	-1.338439423	0.017874802	0.999977979	0.038778152
ACTR8	-1.15863525	0.006640216	0.99999942	-1.342805207	0.006640216	0.99999942	-0.184169957
SUPT6H	-1.30210622	0.003204183	0.999391397	-1.346508394	0.002192787	0.999391397	-0.044402174
CHEK1	-1.093926255	0.042520934	0.9943534	-1.349115942	0.030196048	0.9943534	-0.255189687
NSMCE3	-0.894120324	0.049769056	0.999991203	-1.3505984	0.004434808	0.999991203	-0.456478076
CTCF	-1.100229591	0.017737472	0.999918614	-1.360838827	0.004521795	0.999918614	-0.260609236
PPM1D	-1.369722623	0.002520059	0.999999741	-1.372427049	0.00339156	0.999999741	-0.002704425
RPA1	-0.727411903	0.113189097	0.99954152	-1.378780295	0.012422433	0.99954152	-0.651368392
GTF2H3	-1.519340119	0.001156798	1	-1.382376736	0.002539689	1	0.136963383
POLR2L	-1.117776771	0.104012539	0.993747536	-1.393657294	0.056272173	0.993747536	-0.275880524
SENP6	-0.966817294	0.031025098	0.99993276	-1.399317383	0.003163164	0.99993276	-0.432500089
NCAPG	-1.05251781	0.009488512	0.999983682	-1.40934757	7.91929E-04	0.999983682	-0.356829759
RPA2	-1.762918732	4.44E-05	0.999999998	-1.411851302	0.00071642	0.999999998	0.351067431
RRM2	-1.204187425	0.011680714	0.999998419	-1.424287046	0.005798221	0.999998419	-0.22009962
HUS1	-1.073470889	0.023548946	0.999975309	-1.425281073	0.008665098	0.999975309	-0.351810185
NCAPD2	-1.09751632	0.011498671	0.999998189	-1.426483828	0.00370183	0.999998189	-0.328967508
POLR2E	-1.228713453	0.02472649	0.999997744	-1.431356536	0.01599537	0.999997744	-0.202643083
POLR2I	-1.222019544	0.008578353	0.999989168	-1.438908304	0.002173743	0.999989168	-0.21688876
TCEB2	-2.259599213	6.44071E-04	1	-1.445869727	0.020401517	1	0.813729486
POLR2G	-0.966309782	0.08584976	0.997446221	-1.449288038	0.02298401	0.997446221	-0.482978256
GAR1	-1.239506831	0.004803577	0.99968861	-1.455748526	0.001938396	0.99968861	-0.216241696
RUVBL1	-1.207594764	0.011953263	0.999640183	-1.457363316	0.006023867	0.999640183	-0.249768551
TERT	-0.93550575	0.043657438	0.999994311	-1.46148728	0.011895478	0.999994311	-0.52598153
THOC1	-1.117748795	0.008044671	1	-1.477450377	0.0008028	1	-0.359701582
DKC1	-1.723840294	0.00093827	1	-1.480855467	0.002915943	1	0.242984827
RAD1	-0.656703975	0.157551584	0.999593394	-1.494929447	0.009070256	0.999593394	-0.838225472
UBE2M	-0.205219669	0.349407984	0.99993481	-1.520406397	0.013448764	0.99993481	-1.315186728
NELFB	-1.417982038	0.001030236	1	-1.531413779	4.06312E-04	1	-0.113431741
DNAJC2	-1.191751575	0.033749097	0.99865042	-1.538257656	0.012146219	0.99865042	-0.346506081
USP7	-1.593965581	0.001227715	0.999984213	-1.549029393	0.002057157	0.999984213	0.044936187
PCNA	-1.412811519	0.003589444	0.999618781	-1.568113786	0.002009772	0.999618781	-0.155302268
UHRF1	-1.065785415	0.049728807	0.99999626	-1.587701079	0.009246655	0.99999626	-0.521915664
HUWE1	-0.702532895	0.078641477	0.999999817	-1.596982179	1.34554E-04	0.999999817	-0.894449284
BUB1B	-1.434479359	0.00267785	0.999987313	-1.60912752	9.15767E-04	0.999987313	-0.174648161
SMARCB1	-1.716772614	6.22164E-04	0.999998637	-1.617203561	8.83765E-04	0.999998637	0.099569053
FAAP24	-0.582044687	0.222473765	0.999280513	-1.621957738	0.004598138	0.999280513	-1.039913051
SMC5	-1.925713208	2.01292E-04	0.999999999	-1.630922062	0.001524546	0.999999999	0.294791146
COPS5	-2.028623032	3.88E-05	0.999999992	-1.646664021	3.90347E-04	0.999999992	0.381959011
UBA1	-1.24526508	0.002783611	0.99999971	-1.654802776	1.41407E-04	0.99999971	-0.409537696
RAD21	-0.519600211	0.357823622	0.999354912	-1.676750447	0.005329002	0.999354912	-1.157150236
GTF2H1	-0.829130719	0.053833741	0.999999996	-1.678853589	0.00030453	0.999999996	-0.849722871
COPS8	-1.663333664	0.006818796	0.99994207	-1.682113005	0.006818796	0.99994207	-0.018779341
CDC5L	-1.42965042	2.59402E-04	0.999999994	-1.71613481	1.26E-05	0.999999994	-0.286484391
MNAT1	-1.311795888	0.014918815	0.999979182	-1.73333385	0.001325347	0.999979182	-0.421537963
RAD17	-0.880442422	0.053973242	0.99993315	-1.737684228	6.01653E-04	0.99993315	-0.857241806
MASTL	-0.833094228	0.148431181	0.999652537	-1.744976627	0.00312717	0.999652537	-0.911882399
CDK4	-1.473893228	0.004491811	0.999987981	-1.749106476	0.001354917	0.999987981	-0.275213248
SUPT4H1	-1.516636128	0.004245821	0.999999516	-1.749716082	0.001090094	0.999999516	-0.233079954
TICRR	-1.448249424	5.50578E-04	0.999999997	-1.753394181	4.27E-05	0.999999997	-0.305144758
NCAPD3	-1.233330497	0.015783266	0.999902021	-1.763442244	8.81809E-04	0.999902021	-0.530111747
HINFP	-1.706086417	3.27379E-04	0.999999995	-1.76827554	2.85187E-04	0.999999995	-0.062189124
UBE2D3	-1.207927626	0.080523003	0.997770826	-1.775148831	0.020062569	0.997770826	-0.567221206
UPF1	-1.19957807	0.015677525	0.999880087	-1.775906133	0.00107922	0.999880087	-0.576328063
RRM1	-1.636329246	0.00109815	0.999991166	-1.782620212	0.00109815	0.999991166	-0.146290967
NHP2	-1.639825021	0.002643368	1	-1.786761276	0.002025525	1	-0.146936254
PPP6C	-1.998909197	5.32E-07	1	-1.797060991	1.06E-05	1	0.201848206
YBX1	-1.379274439	0.022518939	0.999992389	-1.798431746	0.007244031	0.999992389	-0.419157307
KAT8	-1.437697142	0.002727836	0.999999975	-1.807534096	0.00050914	0.999999975	-0.369836954
TRAIP	-1.209129942	0.007893198	0.999999649	-1.812264011	2.30569E-04	0.999999649	-0.603134069
RFC5	-2.425112489	5.90E-06	1	-1.823390275	0.00046692	1	0.601722215
DDX1	-1.378724108	0.001313713	1	-1.82719798	4.66E-05	1	-0.448473871
ERCC3	-1.760516956	5.42456E-04	0.999999988	-1.850893063	4.87564E-04	0.999999988	-0.090376107
COPS6	-1.70234368	1.70337E-04	0.999999928	-1.851681278	7.18E-05	0.999999928	-0.149337598
UBE2I	-1.857194193	3.52961E-04	0.999999985	-1.852599508	3.52961E-04	0.999999985	0.004594685
GTF2H4	-1.698199808	5.56E-05	1	-1.923618712	2.12E-05	1	-0.225418904
ATR	-2.065496376	2.43E-05	0.999999984	-1.931260496	7.88E-05	0.999999984	0.13423588
DDB1	-1.966787967	1.88E-05	1	-1.932212746	2.80E-05	1	0.034575221
UBE2T	-1.46189205	0.002758927	1	-1.94316124	3.02241E-04	1	-0.48126919
ACTL6A	-1.45375353	0.001180502	0.999999998	-1.959770588	3.31E-05	0.999999998	-0.506017059
POLR2H	-1.686699446	6.92E-05	0.999999145	-1.977422406	5.65E-06	0.999999145	-0.290722959
APEX2	-1.497452787	0.002050515	1	-1.995979125	2.83E-05	1	-0.498526338
TAF1	-1.707180647	7.05455E-04	0.999999984	-2.004350022	1.10472E-04	0.999999984	-0.297169375
TTI1	-1.948727945	1.48665E-04	1	-2.010812949	1.48665E-04	1	-0.062085004
UBA2	-2.227382007	3.47E-06	1	-2.159435995	1.48E-05	1	0.067946012
TEN1	-1.747074838	0.00100213	1	-2.172888685	1.12756E-04	1	-0.425813847
RPS27L	-0.55064821	0.278173592	0.999927292	-2.236196283	6.53192E-04	0.999927292	-1.685548074
MYBBP1A	-1.945216456	2.34E-06	1	-2.306948637	3.40E-08	1	-0.361732181
GPS1	-1.485381024	0.003835013	1	-2.342625635	4.32E-06	1	-0.857244612

HDAC3	-1.800735298	0.00131368	0.999994236	-2.358322124	5.19E-05	0.999994236	-0.557586826
ERCC2	-2.031793893	8.59E-06	1	-2.3761029	2.62E-07	1	-0.344309007
TTI2	-1.574691533	7.25004E-04	1	-2.394994331	5.29E-07	1	-0.820302798
PPP4C	-1.876858279	4.78466E-04	1	-2.516808574	4.21E-06	1	-0.639950295
SMC1A	-2.224393211	1.48E-05	1	-2.588422409	2.15E-06	1	-0.364029198
THOC2	-2.254248673	5.15E-06	1	-3.002180348	1.85E-09	1	-0.747931676
NEDD8	-2.550288055	1.10133E-04	1	-3.029734725	5.40E-06	1	-0.47944667
SOD1	-2.481368529	2.69E-05	1	-3.037825906	4.71E-07	1	-0.556457377

Appendix Table 7 Raw data from JACKS analysis of RPE-1 WRN-/- E5-C6 2nM CPT treated

RPE-1 *WRN-/-* E5-C6 DMSO and 2nM CPT treated enrichment compared to the day 14 control. fdr=false discovery rate

Gene	Enrichment in DMSO treated	neg_fdr1	pos_fdr1	Enrichment in 2nM CPT treated	neg_fdr2	pos_fdr2	Difference in Enrichment
TP53	3.918153179	1	2.64E-12	5.306634686	1	0	1.388481507
CDKN1A	2.036870903	1	6.24645E-04	3.295639221	1	1.86E-07	1.258768318
RNF146	3.56227894	1	2.12E-09	2.453289102	1	2.36E-05	-1.108989837
KEAP1	2.594822889	1	1.25E-05	2.339274939	1	5.48E-05	-0.25554795
CHEK2	1.247259903	1	0.009185668	1.99436911	1	1.41196E-04	0.747109207
USP28	1.603918558	1	8.32433E-04	1.716103418	1	6.49627E-04	0.11218486
CAND1	3.231152638	1	6.81E-09	1.642912406	1	0.001106907	-1.588240232
SMARCC1	1.003112762	0.999999991	0.021047167	1.568040976	0.999999991	9.12208E-04	0.564928214
BRD7	1.416358089	1	0.010986801	1.480277336	1	0.010066749	0.063919247
H2AFZ	1.777501455	1	0.001542282	1.463637824	1	0.005033477	-0.313863631
PBRM1	1.193528155	1	0.01852567	1.461257554	1	0.005421536	0.267729398
CUL5	1.818181804	1	1.68233E-04	1.439142198	1	0.002760659	-0.379039605
EME2	0.986820686	0.998886994	0.052980102	1.411284412	0.998886994	0.010547111	0.424463726
MAPKAPK2	1.460605137	1	0.01130881	1.327556216	1	0.013529806	-0.133048921
PER2	1.045032969	0.999727149	0.022100274	1.249239073	0.999727149	0.008183094	0.204206104
THRAP3	1.291547318	1	0.021767884	1.23048065	1	0.02444419	-0.061066668
DCUN1D3	1.666081912	1	0.00108847	1.217957235	1	0.010333614	-0.448124677
TET2	0.991425845	0.999998163	0.053624086	1.213573395	0.999998163	0.031904811	0.22214755
UBE2K	1.043207285	1	0.025280854	1.162241367	1	0.014994861	0.119034082
MAPK14	0.8277983	0.999999645	0.083696301	1.136631036	0.999999645	0.031913612	0.308832736
SUPT5H	1.403929047	0.999366891	0.003472975	1.123641901	0.999366891	0.008598454	-0.280287147
ARID2	1.066631776	1	0.018974867	1.078537466	1	0.018974867	0.01190569
APOBEC2	1.059793339	0.999739009	0.035022547	1.074336874	0.999739009	0.035022547	0.014543536
RRM2B	0.899647429	0.999997564	0.049546731	1.048482702	0.999997564	0.036143911	0.148835272
TP53BP1	0.962612578	1	0.022022593	1.047478064	1	0.019079977	0.084865486
PARP14	1.010372447	0.999626837	0.023795514	1.04081158	0.999626837	0.022964683	0.030439134
POLD3	0.553705154	0.999843055	0.065463816	1.039863382	0.999843055	0.009218103	0.486158228
CDKN2A	1.076312674	0.999994328	0.016039924	1.028589858	0.999994328	0.022886344	-0.047722816
PTEN	2.745001951	1	3.15E-07	0.99244664	1	0.029941261	-1.752555311
L3MBTL1	0.987041605	0.999081574	0.025714311	0.957674863	0.999081574	0.025714311	-0.029366742
MDM2	1.449800679	0.999296181	0.004918483	0.94067799	0.999296181	0.041152517	-0.50912269
GADD45A	0.830832025	0.999990609	0.044147667	0.928466177	0.999990609	0.044147667	0.097634152
PHIP	1.071003407	1	0.025331803	0.927840362	1	0.037564294	-0.143163044
RNF7	1.428066461	1	0.003231386	0.9206441	1	0.030025696	-0.507422362
KMT5B	0.895130964	0.999968266	0.057891409	0.916719205	0.999968266	0.057891409	0.021588241
APC	0.75159499	1	0.032557745	0.909708036	1	0.019712713	0.158113046
UBE2W	0.90753358	0.991327705	0.029246599	0.898846268	0.991327705	0.029246599	-0.008687312
HMGB1	1.143875284	0.994845796	0.425398111	0.893215535	0.994845796	0.425398111	-0.250659749
SPTBN1	0.909714479	1	0.039491377	0.888133264	1	0.041254712	-0.021581214
TOP3B	0.749867675	0.997428561	0.062329899	0.868364988	0.997428561	0.048787354	0.118497313
RNF111	0.874928609	0.999944988	0.091761042	0.85562231	0.999944988	0.093278795	-0.019306299
SUMO4	0.927410874	0.958853859	0.147639042	0.852880268	0.958853859	0.147639042	-0.074530606
PML	0.757810702	0.999831852	0.10294274	0.837361395	0.999831852	0.093532818	0.079550693
SWI5	0.885942314	0.998147498	0.077222507	0.828727023	0.998147498	0.077222507	-0.057215291
MAPK8	0.91134231	0.999525364	0.041435367	0.827212106	0.999525364	0.048598135	-0.084130205
MTA3	0.709332894	0.998930186	0.13087276	0.824647197	0.998930186	0.13087276	0.115314304
UBE2R2	0.84921193	1	0.067788305	0.819486332	1	0.067788305	-0.029725598
HELB	0.525719853	0.99823044	0.173793352	0.809748126	0.99823044	0.106849088	0.284028274
CSNK2A2	0.450420098	0.999868116	0.166395409	0.78975449	0.999868116	0.105983738	0.339334392
NonTargeting	0.757368612	0.999998025	0.082040893	0.782913609	0.999998025	0.082040893	0.025544997
ZDHHC16	0.800769612	0.995336677	0.129119902	0.767079937	0.995336677	0.129119902	-0.033689675
SF3B1	0.732419476	0.985254946	0.055963987	0.751230631	0.985254946	0.055963987	0.018811154
PMP22	0.749758006	0.999994455	0.152606457	0.738716729	0.999994455	0.152606457	-0.011041277
PARP4	0.54574345	0.999779181	0.221653661	0.736429078	0.999779181	0.14485674	0.190685628
SENP8	1.476254336	1	0.01590188	0.714325011	1	0.124909829	-0.761929325
BRCC3	1.121708966	0.99999999	0.057265626	0.711568943	0.99999999	0.129582776	-0.410140023
NonTargeting	0.7523863	0.999999992	0.112474331	0.710651358	0.999999992	0.112474331	-0.041734942
UBE2V1	0.577155183	0.994675609	0.225568527	0.708928566	0.994675609	0.203828569	0.131773384
ABL1	0.915654896	0.999996573	0.071496935	0.701898426	0.999996573	0.098284978	-0.21375647
NonTargeting	0.583968942	0.999971612	0.173463696	0.700089144	0.999971612	0.130600039	0.116120203
PPP6R3	0.651890428	0.99966489	0.179871004	0.698864735	0.99966489	0.179871004	0.046974307
NonTargeting	0.36061044	0.999999721	0.312403609	0.697320733	0.999999721	0.121340675	0.336710293
UBE2D1	0.522238267	0.999939613	0.17954647	0.69710035	0.999939613	0.17954647	0.174862083
SHFM1	0.632024737	0.999991064	0.190015166	0.695232516	0.999991064	0.190015166	0.063207779
NonTargeting	0.79606286	0.99999849	0.091522014	0.694255218	0.99999849	0.122819381	-0.101807642
NABP2	0.750616787	0.995463463	0.148398876	0.693377237	0.995463463	0.148398876	-0.05723955
FAN1	0.698880577	0.997111193	0.153197142	0.67878919	0.997111193	0.153197142	-0.020091387
BABAM1	0.88700819	1	0.026096888	0.67207442	1	0.067618745	-0.214933769
KLHL15	0.62007801	0.992613477	0.200722476	0.666783402	0.992613477	0.200722476	0.046705392
RNF2	0.694381393	0.999627895	0.223458862	0.666278151	0.999627895	0.223458862	-0.028103242
NUDT1	0.49296662	0.946357521	0.256553735	0.66427748	0.946357521	0.243187598	0.171310861
SIRT7	0.493944552	0.999664558	0.17410725	0.663679594	0.999664558	0.161013986	0.169735042
HNRNPUL2	0.783864031	0.999853973	0.094660594	0.663675253	0.999853973	0.102242903	-0.120188778

SUMO3	0.41165291	0.994900124	0.328498082	0.66321678	0.994900124	0.205953361	0.251563869
ALKBH1	0.93779704	0.999961205	0.063956104	0.662387961	0.999961205	0.106630108	-0.27540908
CCNO	0.490503341	0.98679286	0.256102712	0.661197939	0.98679286	0.175819175	0.170694598
EID3	0.564534238	0.993920362	0.192573057	0.659204179	0.993920362	0.178650241	0.094669941
CHFR	0.591545976	0.999662265	0.171961903	0.655337968	0.999662265	0.171961903	0.063791992
BTG2	0.722338577	0.999849211	0.155672065	0.650109149	0.999849211	0.155672065	-0.072229429
USP51	0.826300765	0.999505252	0.13682832	0.648850429	0.999505252	0.162255581	-0.177450335
SMC4	0.484554713	0.997535657	0.242196184	0.64462712	0.997535657	0.181319391	0.160072407
SIRT5	0.521069681	0.999831869	0.149802239	0.644552509	0.999831869	0.149802239	0.123482827
NonTargeting	0.414252765	0.999999932	0.260927114	0.644310723	0.999999932	0.13690271	0.230057958
NonTargeting	0.530303035	0.999975913	0.191127262	0.639141923	0.999975913	0.153631625	0.108838889
TPP1	0.574471158	0.998535295	0.168111978	0.638128406	0.998535295	0.168111978	0.063657248
UBE2V2	0.484862322	0.999897557	0.183107207	0.625348673	0.999897557	0.162851504	0.140486351
DCUN1D4	0.72934462	0.997906465	0.17463028	0.622340222	0.997906465	0.193257327	-0.107004398
HUS1B	0.680796965	0.999041355	0.143658564	0.620828126	0.999041355	0.158282988	-0.059968839
NonTargeting	0.50781918	0.99999086	0.231225941	0.620529147	0.99999086	0.200711474	0.112709967
CUL3	1.849361366	1	6.74E-05	0.615986277	1	0.091624684	-1.233375089
OTUB2	0.475933019	0.999750694	0.257785958	0.615105594	0.999750694	0.255736908	0.139172574
UCHL3	0.618015717	0.990060866	0.114264449	0.613269838	0.990060866	0.114264449	-0.004745878
PARP9	0.693401931	0.997612841	0.168838305	0.606122223	0.997612841	0.184516048	-0.087279708
CHTF18	0.591117725	0.982124975	0.268349384	0.603670755	0.982124975	0.268349384	0.01255303
MLH3	0.51888002	0.999862757	0.218820537	0.597743987	0.999862757	0.198237753	0.078863967
RAD18	0.482957799	0.998249125	0.223023743	0.593543142	0.998249125	0.223023743	0.110585342
CDKN1B	0.628867119	0.999985514	0.201300535	0.587037245	0.999985514	0.201300535	-0.041829875
SETDB1	0.247599246	0.99959465	0.435121798	0.582601829	0.99959465	0.173017035	0.335002583
APAF1	0.827337792	0.999769105	0.061545504	0.581450918	0.999769105	0.104031181	-0.245886874
COPS7A	0.47308801	0.999970404	0.26042997	0.577403665	0.999970404	0.26042997	0.104315655
BCLAF1	0.894307703	1	0.096179445	0.576575488	1	0.162566663	-0.317732215
INO80D	0.476855636	0.995796808	0.300051338	0.573929008	0.995796808	0.278782051	0.097073372
GTF2H2	0.714451821	0.983875327	0.298260716	0.570046575	0.983875327	0.301401438	-0.144405246
RING1	0.652205231	1	0.133823247	0.566536411	1	0.164469045	-0.08566882
MUM1	0.616114465	0.998613554	0.166129122	0.565557937	0.998613554	0.166129122	-0.050556528
PNN	0.602925912	0.997902515	0.128412393	0.560371122	0.997902515	0.146268002	-0.04255479
KDM4D	0.544056041	0.999517962	0.145442715	0.556364522	0.999517962	0.145442715	0.012308481
NonTargeting	0.555166515	0.9999448	0.197425308	0.553713911	0.9999448	0.197425308	-0.001452604
DCLRE1C	0.340740794	0.999665045	0.307463955	0.546163025	0.999665045	0.176864689	0.205422231
CCND3	0.71823042	0.99943543	0.03918954	0.542933541	0.99943543	0.086114234	-0.175296879
ERCC6L	0.601470647	0.995790705	0.213520175	0.535496423	0.995790705	0.213520175	-0.065974224
PARPBP	0.525003161	0.997597669	0.16658308	0.532843984	0.997597669	0.16658308	0.007840823
APTX	0.377140893	0.902305794	0.297388906	0.524834373	0.902305794	0.297388906	0.14769348
NonTargeting	0.606338154	0.999748986	0.234064461	0.523252681	0.999748986	0.239880679	-0.083085472
POLK	0.668530595	0.999979036	0.139778175	0.522146731	0.999979036	0.163570562	-0.146383864
RAG2	0.426627012	0.937786552	0.240309256	0.520062256	0.937786552	0.240309256	0.093435244
NonTargeting	0.650845773	0.99999303	0.084068939	0.519502841	0.99999303	0.121721249	-0.131342932
NonTargeting	0.557721552	0.999981145	0.137054504	0.51794066	0.999981145	0.139321668	-0.039780892
HMGB2	0.523032318	0.999925107	0.189092663	0.517448609	0.999925107	0.189092663	-0.005583709
BRE	0.84278433	0.999999447	0.068616703	0.517120351	0.999999447	0.133672493	-0.325663979
APOBEC3D	0.42801509	0.974141819	0.330086098	0.515727801	0.974141819	0.330086098	0.087712711
UBE2F	1.249749988	1	0.012666928	0.513994505	1	0.16837439	-0.735755483
NonTargeting	0.369197226	0.995893787	0.263359967	0.513767138	0.995893787	0.201545788	0.144569912
APLF	0.48168315	0.999572699	0.27194838	0.512647978	0.999572699	0.27194838	0.030964828
NonTargeting	0.602750216	0.999963084	0.155978914	0.510866653	0.999963084	0.155978914	-0.091883564
FBXW7	0.788213727	0.999999997	0.030633553	0.50843447	0.999999997	0.090879926	-0.279779257
NonTargeting	0.527007543	0.999988159	0.182175157	0.507416791	0.999988159	0.182175157	-0.019590752
GADD45G	0.667800743	0.999993748	0.118839552	0.507259531	0.999993748	0.170070962	-0.160541212
NonTargeting	0.444841736	0.999346524	0.207882263	0.504199225	0.999346524	0.207882263	0.059357489
PRMT6	0.666582208	0.998934623	0.174713701	0.504186053	0.998934623	0.20570671	-0.162396155
GPI	0.404094552	0.999992441	0.202680477	0.499911233	0.999992441	0.178502918	0.095816681
TOP2B	0.448178862	0.894281573	0.408842915	0.499691792	0.894281573	0.408842915	0.05151293
LIG3	0.424258743	0.999904028	0.209181304	0.499533674	0.999904028	0.209181304	0.075274931
RNF126	0.477337748	0.98261248	0.164481931	0.496043021	0.98261248	0.164481931	0.018705273
NonTargeting	0.548980939	0.998422901	0.258809733	0.495610511	0.998422901	0.258809733	-0.053370428
FAM175A	0.479566935	0.987271407	0.244612063	0.495577105	0.987271407	0.244612063	0.01601017
SSBP2	0.375054001	0.999223979	0.29651219	0.49443671	0.999223979	0.29651219	0.119382709
NonTargeting	0.564446193	0.999534742	0.214881587	0.494207226	0.999534742	0.214881587	-0.070238966
USP15	0.627588579	1	0.102165018	0.493932028	1	0.137014551	-0.133656551
CUL7	0.37652266	0.999988816	0.186250394	0.493344358	0.999988816	0.163441994	0.116821698
ETAA1	0.405330558	0.999902643	0.221874002	0.492504954	0.999902643	0.215226257	0.087174396
SPO11	0.562913556	0.999054627	0.179772372	0.489827256	0.999054627	0.198459518	-0.073086301
SMARCA4	0.34360244	0.921918975	0.347630633	0.487533933	0.921918975	0.339227283	0.143931493
MDM4	0.477970149	0.999708607	0.168291238	0.487202731	0.999708607	0.168291238	0.009232582
SIRT1	0.396614738	0.999600581	0.161515408	0.487087576	0.999600581	0.143449576	0.090472838
NonTargeting	0.589573042	0.999999492	0.134195552	0.485434502	0.999999492	0.190222317	-0.10413854
CHD3	0.242909638	0.991912216	0.264105085	0.482869816	0.991912216	0.128179922	0.239960178
APOBEC3F	0.483666491	0.96743583	0.35574373	0.480259593	0.96743583	0.35574373	-0.003406898
CIB1	0.50685177	0.992548413	0.150193736	0.479898864	0.992548413	0.150193736	-0.026952906
HMGN1	0.298857582	0.991290138	0.433557475	0.479401924	0.991290138	0.37957964	0.180544342
SIRT2	0.548724477	0.996559267	0.204201368	0.477407467	0.996559267	0.229177017	-0.07131701
NonTargeting	0.334662434	0.999999634	0.321780292	0.473600731	0.999999634	0.241786496	0.138938296
NonTargeting	0.446477396	0.999829527	0.239639066	0.463617073	0.999829527	0.239639066	0.017139677
CETN2	0.550808786	0.995655769	0.37745133	0.462078631	0.995655769	0.37745133	-0.088730156
NFATC2IP	0.424640164	0.947512601	0.218206324	0.460692265	0.947512601	0.218206324	0.036052101

NonTargeting	0.333635745	0.999854713	0.282497522	0.457435076	0.999854713	0.25340258	0.12379933
STAG2	0.948955124	0.999999998	0.039133738	0.457273909	0.999999998	0.169663828	-0.491681215
PPP4R4	0.565859999	0.999944276	0.252353018	0.457054465	0.999944276	0.297974671	-0.108805535
NCAPD3	0.470509736	0.985103036	0.277419456	0.456601991	0.985103036	0.277419456	-0.013907745
SMARCA2	0.323640881	0.964445153	0.590235601	0.456079374	0.964445153	0.590235601	0.132438493
HDAC9	0.797607268	0.999999739	0.04781332	0.453199665	0.999999739	0.152346015	-0.344407603
ATP23	0.678772718	0.941599552	0.274281335	0.451301117	0.941599552	0.421044528	-0.227471602
NonTargeting	0.364431758	0.999971942	0.292363149	0.449849986	0.999971942	0.263850838	0.085418228
NonTargeting	0.508930766	0.999944922	0.17984537	0.449767395	0.999944922	0.17984537	-0.059163372
TDP1	0.484311582	0.868239207	0.538929836	0.448222365	0.868239207	0.538929836	-0.036089217
NonTargeting	0.449510902	0.999257052	0.158280513	0.446400573	0.999257052	0.158280513	-0.003110329
NEIL1	0.317900485	0.967157443	0.24442714	0.444497599	0.967157443	0.197009555	0.126597114
CASP3	0.475013433	0.92594083	0.457113336	0.44447113	0.92594083	0.457113336	-0.030542303
NonTargeting	0.502512543	0.995789702	0.150159785	0.443832896	0.995789702	0.150159785	-0.058679647
NonTargeting	0.345059881	0.939658178	0.359655223	0.443297732	0.939658178	0.359655223	0.098237851
ALKBH2	0.377003054	0.987312972	0.219222666	0.442771765	0.987312972	0.197386863	0.065768711
OR1E1	0.531306773	0.985974094	0.248132441	0.440759392	0.985974094	0.248132441	-0.09054738
NonTargeting	0.483664369	0.999999893	0.235386492	0.436349719	0.999999893	0.235386492	-0.047314649
EYA1	0.48690574	0.990056724	0.176995001	0.434747212	0.990056724	0.183770167	-0.052158528
RAG1	0.361012759	0.998190338	0.338792589	0.433814601	0.998190338	0.321678892	0.072801843
POLR2J	0.568604356	0.996488758	0.15697495	0.433098966	0.996488758	0.19139029	-0.135505389
SENP2	0.214275131	0.974847315	0.384750348	0.432673991	0.974847315	0.384750348	0.21839886
DNTT	0.4047412	0.999905117	0.259683811	0.429312566	0.999905117	0.259683811	0.024571365
ACD	0.544021638	0.982712271	0.293678069	0.427247312	0.982712271	0.326101539	-0.116774326
SSBP3	0.623986766	0.993437983	0.124852644	0.427056566	0.993437983	0.185494114	-0.1969302
SCAI	0.471900266	0.999862613	0.19869465	0.42231885	0.999862613	0.199032325	-0.049581415
ASCC1	0.534403215	0.999128493	0.143995512	0.420767794	0.999128493	0.196789527	-0.11363542
HNRNPUL1	0.216378027	0.981160424	0.388394168	0.419144869	0.981160424	0.318235111	0.202766842
NEK8	0.285219297	0.999004224	0.346263726	0.418819836	0.999004224	0.262314706	0.133600539
PER1	0.241221496	0.990077097	0.397443467	0.418202201	0.990077097	0.255339764	0.176980706
ANKRD44	0.406450716	0.998536699	0.266477136	0.416666823	0.998536699	0.266477136	0.010216107
REV1	0.448386697	0.951147894	0.321946653	0.415013411	0.951147894	0.321946653	-0.033373286
COL21A1	0.36952199	0.921825514	0.428542352	0.410865251	0.921825514	0.428542352	0.041343261
MBD4	0.440550445	0.99826714	0.294597572	0.409673065	0.99826714	0.294597572	-0.03087738
TP63	0.26780186	0.982719463	0.431918923	0.408332276	0.982719463	0.423601302	0.140530416
PPP4R1	0.306569255	0.856665652	0.489049591	0.407658857	0.856665652	0.489049591	0.101089601
NLK	0.393970517	0.981217976	0.403358995	0.406648325	0.981217976	0.403358995	0.012677808
PPP5C	0.125275454	0.956631895	0.442428591	0.406459459	0.956631895	0.442428591	0.281184005
POLM	0.40810916	0.999967463	0.144842318	0.406259208	0.999967463	0.144842318	-0.001849953
DCLRE1A	0.306682872	0.999578127	0.22869833	0.406009474	0.999578127	0.19438612	0.099326602
SMC1B	0.377737938	0.999741633	0.330922427	0.405007968	0.999741633	0.330922427	0.027270029
POLG2	0.299286936	0.981114272	0.378952066	0.401533495	0.981114272	0.378952066	0.102246559
NonTargeting	0.201352276	0.99991058	0.441098104	0.400881779	0.99991058	0.315682899	0.199529502
MLH1	0.348836987	0.942751324	0.556658798	0.400023892	0.942751324	0.556658798	0.051186906
APOBEC3B	0.478030331	0.999967008	0.236724223	0.398346609	0.999967008	0.236724223	-0.079683722
ATF2	0.337588499	0.990828682	0.307924958	0.397948363	0.990828682	0.307924958	0.060359864
TRIP12	0.801437788	0.999977382	0.115849535	0.39735146	0.999977382	0.216413463	-0.404086328
SALL4	0.301770579	0.991028909	0.305548539	0.394879304	0.991028909	0.305548539	0.093108725
HFM1	0.284045827	0.993815046	0.276872453	0.393087445	0.993815046	0.276872453	0.109041618
OPRM1	0.4538093	0.999960465	0.208737076	0.391884358	0.999960465	0.208737076	-0.061924942
ASF1A	0.550189138	0.992322994	0.122385749	0.391550945	0.992322994	0.189662944	-0.158638193
ALKBH3	0.332055597	0.999874058	0.315633542	0.39144764	0.999874058	0.315633542	0.059392042
NonTargeting	0.294801763	0.999974703	0.315982043	0.390952258	0.999974703	0.315982043	0.096150495
NonTargeting	0.431468873	0.999998311	0.259655304	0.390332111	0.999998311	0.259655304	-0.041136762
POLN	0.42466064	0.999765812	0.203772318	0.387524619	0.999765812	0.203772318	-0.037136021
CDKN2D	0.362619019	0.997688613	0.353913927	0.387047896	0.997688613	0.353913927	0.024428877
UBE2D2	0.114218376	0.926997804	0.397916567	0.385938519	0.926997804	0.271229486	0.271720143
CCND2	0.417080908	0.999700615	0.311027717	0.385216796	0.999700615	0.311027717	-0.031864112
NonTargeting	0.396707043	0.998153711	0.268790737	0.382535706	0.998153711	0.268790737	-0.014171336
WRN	0.362875233	0.936131005	0.40821908	0.382226945	0.936131005	0.40821908	0.019351713
CCNB3	0.190681699	0.999788155	0.302991582	0.380762076	0.999788155	0.164253439	0.190080377
RHNO1	0.297401652	0.976984352	0.373780185	0.371283103	0.976984352	0.373780185	0.073881451
NonTargeting	0.294568275	0.999989034	0.357554583	0.370787905	0.999989034	0.333393895	0.076219629
NonTargeting	0.345251499	0.999049499	0.300327216	0.368578545	0.999049499	0.300327216	0.023327046
NOTCH2	0.36232832	0.91600724	0.344733419	0.364655833	0.91600724	0.344733419	0.002327513
POLB	0.106171882	0.978148625	0.403850581	0.364038274	0.978148625	0.284457033	0.257866392
KAT2B	0.183397715	0.998273194	0.324216922	0.361353815	0.998273194	0.211898774	0.1779561
NonTargeting	0.231425763	0.999028141	0.396127636	0.361063402	0.999028141	0.300418543	0.129637639
ANP32E	0.304716415	0.877808356	0.388795789	0.360316242	0.877808356	0.388795789	0.055599827
NonTargeting	0.498496568	0.99983586	0.177729949	0.359044809	0.99983586	0.219087331	-0.139451759
USP26	0.310404761	0.977805328	0.414615829	0.358409275	0.977805328	0.414615829	0.048004514
CBX5	0.148659182	0.913303254	0.48031268	0.35653221	0.913303254	0.48031268	0.207873028
NonTargeting	0.242438657	0.999962639	0.434635276	0.356098646	0.999962639	0.377849709	0.113659989
NonTargeting	0.445261074	0.999344463	0.174973777	0.356076837	0.999344463	0.201913395	-0.089184238
BMI1	0.429925984	0.997754667	0.342022959	0.355973035	0.997754667	0.350783085	-0.073952949
CUL4B	0.342742539	0.99947849	0.338852979	0.35556182	0.99947849	0.338852979	0.012819281
WDR70	0.43188158	0.919984796	0.444759693	0.354631358	0.919984796	0.444759693	-0.077250223
NonTargeting	0.402464367	0.999896743	0.199662611	0.354066939	0.999896743	0.199712305	-0.048397428
NonTargeting	0.435479611	0.999245228	0.283514144	0.353314281	0.999245228	0.286029607	-0.082165331
CHD1L	0.103814303	0.999838881	0.399243654	0.352625162	0.999838881	0.250804319	0.248810859
NonTargeting	0.362470662	0.99994745	0.306802465	0.352156676	0.99994745	0.306802465	-0.010313986
NonTargeting	0.643911897	0.999895055	0.16967695	0.351951523	0.999895055	0.246418794	-0.291960374

ATXN3	0.383082758	0.999887003	0.235765562	0.351386974	0.999887003	0.235765562	-0.031695783
NonTargeting	0.45488947	0.999695194	0.255795637	0.350795929	0.999695194	0.275977059	-0.104093542
UHRF2	0.411501315	0.933087821	0.456677267	0.350134221	0.933087821	0.456677267	-0.061367094
NEK9	0.516847455	0.99995695	0.192826201	0.349908293	0.99995695	0.203498892	-0.166939163
BLM	0.347615033	0.840181435	0.436421852	0.349758741	0.840181435	0.436421852	0.002143708
PHF3	0.653772108	0.999371961	0.143769059	0.348247775	0.999371961	0.20887769	-0.305524333
CDC34	0.297428344	0.943082939	0.317670536	0.345126037	0.943082939	0.317670536	0.047697693
SMARCD1	0.527142353	0.999812917	0.137079121	0.343642472	0.999812917	0.199872653	-0.183499881
NonTargeting	0.261199814	0.965584874	0.434281159	0.343457743	0.965584874	0.434281159	0.082257929
NonTargeting	0.335233999	0.999838243	0.307673837	0.343322402	0.999838243	0.307673837	0.008088402
TREX2	0.210309864	0.89181467	0.551032501	0.341698954	0.89181467	0.529610279	0.13138909
NonTargeting	0.280676615	0.9463425	0.377586763	0.341239998	0.9463425	0.377586763	0.060563384
POLR2A	0.562711975	0.999743729	0.274893427	0.338475222	0.999743729	0.440454401	-0.224236753
NonTargeting	0.340452217	0.999451714	0.280807461	0.337867041	0.999451714	0.280807461	-0.002585176
USP13	0.245060932	0.999322517	0.281251701	0.336442633	0.999322517	0.2603818	0.091381701
C9orf142	0.238422044	0.955815087	0.345532622	0.336274866	0.955815087	0.345532622	0.097852822
PIAS2	0.245566043	0.972756723	0.373570722	0.334215491	0.972756723	0.373570722	0.088649448
NonTargeting	0.341944374	0.998539304	0.29558584	0.332801479	0.998539304	0.29558584	-0.009142895
RAD9B	0.26516734	0.907235566	0.345670085	0.332643662	0.907235566	0.334368469	0.067476322
H2AFY	0.310571824	0.985621785	0.33088071	0.331540806	0.985621785	0.33088071	0.020968982
POLI	0.269547295	0.870502638	0.359127809	0.331118884	0.870502638	0.359127809	0.061571588
RNF138	0.479140873	0.999989483	0.198265834	0.330356928	0.999989483	0.234045998	-0.148783944
CENPX	0.449410477	0.828940722	0.621083846	0.329958607	0.828940722	0.621083846	-0.119451869
NonTargeting	0.285850146	0.999117535	0.344349493	0.328830777	0.999117535	0.344349493	0.042980631
NonTargeting	0.401850783	0.998182876	0.282525502	0.327858204	0.998182876	0.305339414	-0.073992579
MTA2	0.279366666	0.999859602	0.254401532	0.323991756	0.999859602	0.254135987	0.044625089
RBX1	0.612450769	0.98131896	0.258394512	0.323007721	0.98131896	0.425444544	-0.289443048
RAD23A	0.153860624	0.732912694	0.805323122	0.322161905	0.787557378	0.805323122	0.16830128
NTHL1	0.274808226	0.931538222	0.398161732	0.317382998	0.931538222	0.398161732	0.042574772
PAPD7	0.322462555	0.791645969	0.529345001	0.31648681	0.791645969	0.529345001	-0.005975745
TYMS	0.181356302	0.989232021	0.373620608	0.31617895	0.989232021	0.373620608	0.134822648
NonTargeting	0.312051819	0.99765574	0.332556735	0.31428562	0.99765574	0.332556735	0.0022338
NonTargeting	0.288458787	0.999999115	0.233332762	0.314134508	0.999999115	0.233332762	0.025675721
USP4	0.353579339	0.805362863	0.589526684	0.313983876	0.805362863	0.589526684	-0.039595463
WHSC1	0.32143443	0.984510192	0.413699041	0.313391228	0.984510192	0.413699041	-0.008043203
SUMO1	0.234644661	0.848506551	0.352701213	0.313272344	0.848506551	0.352701213	0.078627683
NonTargeting	0.292574188	0.999999994	0.31495842	0.308103597	0.999999994	0.31495842	0.015529409
RAD54L2	0.274891876	0.99939853	0.260367602	0.305897435	0.99939853	0.260367602	0.031005559
APOBEC1	0.181532586	0.956864874	0.431690689	0.304047257	0.956864874	0.391040725	0.12251467
NonTargeting	0.321881252	0.984970515	0.390025888	0.303338514	0.984970515	0.390025888	-0.018542738
NEIL2	0.155575779	0.900745624	0.397738309	0.303114871	0.900745624	0.380534521	0.147539092
DCUN1D1	0.648972147	0.999999878	0.200346762	0.301212246	0.999999878	0.314919159	-0.347759901
TNP1	0.421060159	0.962981376	0.371141252	0.300943354	0.962981376	0.371141252	-0.120116805
NUDT16L1	0.323249415	0.821254066	0.439119507	0.30017573	0.821254066	0.439119507	-0.023073685
DDB2	0.198809745	0.968589624	0.450929984	0.300047383	0.968589624	0.404525838	0.101237638
ATXN7	0.448044251	0.999322392	0.266701844	0.297861007	0.999322392	0.274036909	-0.150183244
NonTargeting	0.318560959	0.990797611	0.311783685	0.297692572	0.990797611	0.311783685	-0.020868387
APOBEC3A	0.194000969	0.949371552	0.402239037	0.296551136	0.949371552	0.402239037	0.102550168
CRY1	0.158222825	0.920529515	0.580422196	0.29601171	0.920529515	0.580422196	0.137788885
CCNE1	0.192712876	0.972601188	0.463674971	0.295325936	0.972601188	0.463674971	0.10261306
SUV39H2	0.317757697	0.994902355	0.317153685	0.292419783	0.994902355	0.317153685	-0.025337914
KMT5A	-0.012395479	0.741562051	0.574073591	0.290783927	0.741562051	0.574073591	0.303179406
XRCC5	0.342041613	0.986959415	0.306909583	0.288543698	0.986959415	0.306909583	-0.053497915
KMT5C	0.24853645	0.999795972	0.270707591	0.288355953	0.999795972	0.270707591	0.039819503
IP6K3	0.268021518	0.985510177	0.381365811	0.287722155	0.985510177	0.381365811	0.019700637
CDC25A	0.360648794	0.999910282	0.237963608	0.28706602	0.999910282	0.259541979	-0.073582774
MSH4	0.40594813	0.993583438	0.259161096	0.2837673	0.993583438	0.282124354	-0.122180831
NonTargeting	0.317911015	0.999823905	0.348407925	0.28361007	0.999823905	0.348407925	-0.034300945
MSH3	0.357705032	0.986451479	0.310510777	0.283592992	0.986451479	0.310510777	-0.07411204
ZRANB3	0.299009878	0.858872109	0.384695382	0.281418897	0.858872109	0.384695382	-0.017590981
NonTargeting	0.383920257	0.999991775	0.24927865	0.28133581	0.999991775	0.29031418	-0.102584447
EP300	0.849834377	1	0.042418571	0.280490026	1	0.264578303	-0.569344351
NonTargeting	0.237891321	0.998943602	0.279968177	0.280420832	0.998943602	0.274483067	0.042529511
FBXO18	0.299554974	0.999245999	0.240653207	0.280327849	0.999245999	0.240653207	-0.019227125
WDR76	0.242738902	0.892541247	0.274239745	0.279850942	0.892541247	0.274239745	0.03711204
RAP1A	0.372657024	0.998612783	0.358073562	0.27932769	0.998612783	0.38918289	-0.093329334
DNAJC2	0.335537311	0.994253356	0.528340234	0.277621554	0.994253356	0.528340234	-0.057915757
SLF1	0.301911579	0.957297648	0.353040755	0.276060938	0.957297648	0.353040755	-0.025850641
SMARCC2	0.333888351	0.997555566	0.354861922	0.273864256	0.997555566	0.375418645	-0.060024095
APBB1	0.20667197	0.998373594	0.368351676	0.268406143	0.998373594	0.368351676	0.061734173
XPC	0.263205128	0.991484933	0.266992798	0.267165043	0.991484933	0.266992798	0.003959915
MCRS1	0.141427235	0.962567628	0.660978706	0.266643451	0.962567628	0.577988276	0.125216217
POLR2L	0.222073915	0.987939077	0.577094208	0.265233557	0.987939077	0.577094208	0.043159642
TRIM29	0.252292908	0.983559316	0.396849196	0.263037621	0.983559316	0.396849196	0.010744713
NonTargeting	0.29660753	0.998153433	0.304050787	0.261882097	0.998153433	0.304050787	-0.034725433
NonTargeting	0.191787141	0.850087936	0.533634841	0.261750129	0.850087936	0.533634841	0.069962988
SUMO2	0.049117805	0.592600641	0.874235475	0.261093149	0.644335166	0.874235475	0.211975344
SSBP1	0.0668574	0.828033245	0.7423631	0.256864945	0.828033245	0.733551418	0.190007545
NonTargeting	0.183715823	0.998830219	0.372629334	0.256776702	0.998830219	0.372629334	0.073060879
MPZ	0.308026472	0.783285652	0.514905795	0.255731597	0.783285652	0.514905795	-0.052294875
MASTL	0.883630519	0.997129735	0.081320799	0.2549841	0.997129735	0.526068432	-0.62864642
NonTargeting	0.275823959	0.975822499	0.356101424	0.25493944	0.975822499	0.356101424	-0.020884519

NonTargeting	0.293254702	0.980263038	0.392473977	0.254153841	0.980263038	0.392473977	-0.039100861
NonTargeting	0.287012647	0.999499894	0.402289811	0.253456627	0.999499894	0.402289811	-0.033556021
DTX3L	0.143921107	0.99393549	0.378693194	0.25189452	0.99393549	0.333028172	0.107973413
DCAF11	0.154268696	0.900717935	0.386361477	0.24956088	0.900717935	0.386361477	0.095292184
SMUG1	0.312520351	0.926775706	0.400235835	0.248607357	0.926775706	0.400235835	-0.063912995
ERCC6	0.249360089	0.742080257	0.461681238	0.247996607	0.742080257	0.461681238	-0.001363482
DCUN1D5	0.358675655	0.999889397	0.278144345	0.247872547	0.999889397	0.293437971	-0.110803108
HDAC4	0.179418356	0.952460343	0.448885076	0.245672844	0.952460343	0.448885076	0.066254488
KDM1A	0.235802164	0.935769267	0.48560199	0.245526299	0.935769267	0.48560199	0.009724135
DTX3	0.261791691	0.999520968	0.388267478	0.244130959	0.999520968	0.388267478	-0.017660731
DCUN1D2	0.306471221	0.967274579	0.312938999	0.243264191	0.967274579	0.343729976	-0.063207029
NonTargeting	0.329036991	0.999287288	0.397960225	0.243255653	0.999287288	0.397960225	-0.085781338
DTX4	0.534429167	0.999941958	0.116024582	0.24256298	0.999941958	0.279954388	-0.291866188
NonTargeting	0.323021327	0.999960589	0.391518669	0.240993467	0.999960589	0.425428312	-0.08202786
NonTargeting	0.079018771	0.997856576	0.47694779	0.240609246	0.997856576	0.417835492	0.161590475
MSH2	0.320010717	0.974192869	0.401188919	0.240570668	0.974192869	0.401188919	-0.079440049
INO80C	0.014942282	0.99225101	0.485442928	0.240040087	0.99225101	0.408909174	0.225097804
SERBP1	0.021064294	0.936111565	0.541077159	0.239644209	0.936111565	0.436697139	0.218579916
PARP2	0.249235535	0.943985904	0.309226463	0.239431905	0.943985904	0.309226463	-0.009803631
PMS1	0.258294827	0.958274699	0.395162706	0.239067185	0.958274699	0.395162706	-0.019227642
TIPIN	0.31039752	0.889867239	0.384848746	0.238033357	0.889867239	0.384848746	-0.072364162
GABBR1	0.054176411	0.830415951	0.443223333	0.235800469	0.830415951	0.443223333	0.181624058
MSH5	0.140696851	0.810969531	0.706570482	0.228687888	0.810969531	0.706570482	0.087991037
NonTargeting	0.254885887	0.99906883	0.28639908	0.227902327	0.99906883	0.28639908	-0.02698356
ANKRD28	0.090820312	0.964281934	0.405411693	0.227067987	0.964281934	0.377704218	0.136247675
PIF1	0.308361184	0.789502562	0.452710548	0.225785047	0.789502562	0.452710548	-0.082576136
SETD2	-0.114424351	0.99309399	0.672358721	0.225461408	0.99309399	0.513673877	0.339885759
CSNK1E	0.359561972	0.996433343	0.282415934	0.224393108	0.996433343	0.288671942	-0.135168864
RASSF7	0.091390315	0.997777622	0.450251198	0.223541113	0.997777622	0.450251198	0.132150798
POLR2D	0.20681174	0.994575267	0.61575968	0.222743476	0.994575267	0.61575968	0.015931736
NonTargeting	0.347271657	0.998717176	0.426064512	0.222526197	0.998717176	0.426064512	-0.12474546
NonTargeting	0.46145596	0.993980969	0.287545259	0.221327649	0.993980969	0.296908024	-0.24012831
NonTargeting	0.2176404	0.963105599	0.474021678	0.221101728	0.963105599	0.474021678	0.003461328
SIRT4	0.375615099	0.909510653	0.309220548	0.221070185	0.909510653	0.374848148	-0.154544915
NonTargeting	0.195065807	0.966309425	0.563951342	0.219416584	0.966309425	0.563951342	0.024350777
PPP6R1	0.101003442	0.772941429	0.646705834	0.218368227	0.773394928	0.646705834	0.117364786
MGMT	0.218978288	0.992856975	0.313217262	0.216487967	0.992856975	0.313217262	-0.002490321
USP1	0.024186031	0.590243354	0.848664132	0.213801799	0.696120545	0.848664132	0.189615768
PHF11	0.196859794	0.968480013	0.31960288	0.212622165	0.968480013	0.31960288	0.015762371
APOBEC3G	0.220990788	0.800085083	0.404673257	0.211510399	0.800085083	0.404673257	-0.009480388
HDAC2	0.247099876	0.869520373	0.350883165	0.211469392	0.869520373	0.350883165	-0.035630484
RAD54B	0.283304926	0.984425058	0.274302318	0.210107769	0.984425058	0.303339357	-0.073197157
PARP3	0.283701376	0.999043034	0.436919409	0.209173366	0.999043034	0.455114251	-0.07452801
NonTargeting	0.227570329	0.995299415	0.370924813	0.208483062	0.995299415	0.370924813	-0.019087267
NEIL3	0.187890614	0.830465663	0.459576238	0.207078229	0.830465663	0.459576238	0.019187615
HDAC3	-0.050780051	0.836458763	0.963541237	0.206054887	0.950775197	0.823837204	0.256834939
TERF2IP	0.034358778	0.747038604	0.740824367	0.205419131	0.747038604	0.740824367	0.171060353
NonTargeting	0.178323363	0.985115366	0.493287977	0.204577607	0.985115366	0.493287977	0.026254244
USP3	0.236840047	0.90412076	0.449800464	0.204257416	0.90412076	0.449800464	-0.032582631
PARP15	0.217914831	0.998960655	0.477792218	0.204229197	0.998960655	0.477792218	-0.013685634
AMN1	0.20519385	0.99801046	0.457817368	0.202608216	0.99801046	0.457817368	-0.002585634
POLA1	0.092590672	0.992727618	0.751616353	0.202502085	0.992727618	0.737074663	0.109911413
ASF1B	0.190560893	0.852870623	0.479460419	0.199910858	0.852870623	0.479460419	0.009349965
USP11	0.339891841	0.977479353	0.267347445	0.196739558	0.977479353	0.299292053	-0.143152283
PSIP1	0.107449096	0.882014247	0.407987723	0.196660676	0.882014247	0.407987723	0.08921158
PIAS1	0.180534579	0.730146097	0.478187399	0.195791403	0.730146097	0.478187399	0.015256825
PINK1	0.142806541	0.859205561	0.480296597	0.195335499	0.859205561	0.480296597	0.052528958
DMC1	0.4960421	0.999556483	0.128005462	0.194553459	0.999556483	0.317474323	-0.301488641
ERCC5	0.193455577	0.788299656	0.480513536	0.193324345	0.788299656	0.480513536	-1.31232E-04
RECQL4	0.051804521	0.877680198	0.595715041	0.193149989	0.877680198	0.595715041	0.141345468
MCM10	0.339184671	0.90263807	0.293246413	0.192509367	0.90263807	0.394994315	-0.146675305
SIRT3	0.102638457	0.979592947	0.513082548	0.192111243	0.979592947	0.513082548	0.089472786
PPP6R2	0.230479083	0.793930204	0.51836679	0.19153953	0.793930204	0.51836679	-0.038939553
NonTargeting	0.178788056	0.860063864	0.436971171	0.187915267	0.860063864	0.436971171	0.009127211
UVSSA	0.202607389	0.69812623	0.613241301	0.187799928	0.69812623	0.613241301	-0.014807461
TREX1	0.176890245	0.968436391	0.370772458	0.186492946	0.968436391	0.370772458	0.009602701
UBE2NL	0.171814002	0.944566022	0.366758691	0.185500637	0.944566022	0.366758691	0.013686635
NonTargeting	0.277800767	0.999427371	0.44594415	0.184313989	0.999427371	0.495138712	-0.093486778
KDM2A	-0.143111278	0.451542273	0.910732661	0.183116806	0.680644401	0.910732661	0.326228084
ARID1B	0.103647065	0.970376264	0.395840165	0.182717563	0.970376264	0.363498145	0.079070498
SCAF8	0.070530316	0.997827855	0.427710487	0.18264722	0.997827855	0.356655799	0.112116904
SMARCAD1	0.30035202	0.902049214	0.473019693	0.180094551	0.902049214	0.483473467	-0.12025747
APOBEC3C	0.317211694	0.995992372	0.264095215	0.179379647	0.995992372	0.335288309	-0.137832048
UBA3	0.477811961	0.994051665	0.225515477	0.177551812	0.994051665	0.337183058	-0.300260149
NPM1	0.228364612	0.971362538	0.666090951	0.17740322	0.971362538	0.666090951	-0.050961392
CRY2	0.177601091	0.8956699	0.466013717	0.176646684	0.8956699	0.466013717	-9.54407E-04
NonTargeting	0.226435304	0.995046821	0.372114596	0.17628256	0.995046821	0.372114596	-0.050152744
HDAC1	0.212494995	0.853806783	0.358107678	0.174707043	0.853806783	0.358107678	-0.037787952
PMS2	0.150503098	0.962221154	0.400871549	0.173102264	0.962221154	0.400871549	0.022599166
PRIMPOL	0.183810092	0.97661071	0.334150094	0.172617552	0.97661071	0.334150094	-0.01119254
COPS7B	0.189604923	0.999189187	0.476153164	0.172573142	0.999189187	0.476153164	-0.01703178
DLGAP5	0.253387846	0.886341913	0.404700279	0.172241313	0.886341913	0.422190703	-0.081146533

SCAF4	1.325007422	1	0.004812026	0.16826768	1	0.363009218	-1.156739742
NonTargeting	0.214674387	0.999913624	0.505860767	0.16817032	0.999913624	0.505860767	-0.046504067
NonTargeting	0.221323901	0.997641235	0.416399926	0.1670684	0.997641235	0.416399926	-0.054255501
USP20	0.149593467	0.997002414	0.352491499	0.163548311	0.997002414	0.352491499	0.013954844
BAZ1A	0.169490984	0.733462775	0.45138603	0.162771296	0.733462775	0.45138603	-0.006719688
OR1E2	0.031494679	0.776359	0.639285089	0.161866345	0.776359	0.639285089	0.130371666
CBX3	0.124908817	0.85241978	0.418979627	0.161719234	0.85241978	0.418979627	0.036810417
RBM7	0.170017875	0.988203047	0.538082584	0.160336863	0.988203047	0.538082584	-0.009681012
APOBEC3H	0.245912685	0.843921742	0.402261229	0.15950453	0.843921742	0.402261229	-0.086408155
UIMC1	0.293940925	0.861488402	0.390302293	0.159137612	0.861488402	0.390302293	-0.134803313
TCEA1	0.107978306	0.635881387	0.597959364	0.158382789	0.635881387	0.597959364	0.050404484
ENDOV	0.236910853	0.999296873	0.470078315	0.157013489	0.999296873	0.505355303	-0.079897365
PRKCG	0.308605373	0.999019977	0.26646088	0.155734414	0.999019977	0.348687818	-0.152870958
PPP4R3B	0.18626974	0.993541008	0.444203171	0.154957265	0.993541008	0.444203171	-0.031312475
MUTYH	-0.051843351	0.663194739	0.683401713	0.154697633	0.663194739	0.683401713	0.206540984
EME1	0.503476096	0.900026124	0.209613513	0.151809809	0.900026124	0.35856155	-0.351666287
NOTCH3	0.347803895	0.994536715	0.209763614	0.147983046	0.994536715	0.346213408	-0.19982085
PARK7	0.162411492	0.994823768	0.356819735	0.146151782	0.994823768	0.356819735	-0.016259709
USP45	0.277689591	0.96395309	0.348616929	0.144852222	0.96395309	0.355162977	-0.132837369
DTX2	0.02331751	0.671581355	0.696367427	0.139547395	0.671581355	0.696367427	0.116229885
MPG	0.068866513	0.678395155	0.64260504	0.138438328	0.678395155	0.64260504	0.069571815
MORF4L1	0.121746272	0.994177809	0.39585355	0.136957891	0.994177809	0.39585355	0.015211618
HNRNPK	0.526083294	0.998457502	0.296670182	0.133953218	0.998457502	0.603972521	-0.392130076
SLBP	0.139355251	0.84926528	0.520300724	0.13327944	0.84926528	0.520300724	-0.006075811
SLF2	0.013611913	0.968887803	0.484472338	0.133209372	0.968887803	0.484472338	0.119597459
CCNB2	0.113270481	0.989274411	0.381245164	0.132743084	0.989274411	0.381245164	0.019472603
CCNC	0.161689526	0.999898713	0.571692998	0.132473348	0.999898713	0.571692998	-0.029216179
USP47	0.222621293	0.996708864	0.335923692	0.132084192	0.996708864	0.376874263	-0.0905371
TFPT	0.18230516	0.674985546	0.890885344	0.131803399	0.674985546	0.890885344	-0.050501761
SCAF11	0.154415351	0.986336654	0.377734284	0.129559681	0.986336654	0.377734284	-0.024855669
ALDH2	0.205288599	0.97275521	0.360095874	0.128638342	0.97275521	0.389625096	-0.076650257
ADH5	0.300261747	0.997682785	0.454255411	0.127568439	0.997682785	0.454255411	-0.172693307
OGG1	0.123653224	0.848582944	0.508307522	0.125193004	0.848582944	0.508307522	0.00153978
NonTargeting	0.112091075	0.878180299	0.570687847	0.124616003	0.878180299	0.570687847	0.012524928
ATRX	0.020093607	0.584883682	0.796610207	0.122231692	0.620375092	0.796610207	0.102138085
NOTCH1	0.160431152	0.99799131	0.40855067	0.122009758	0.99799131	0.40855067	-0.038421394
VCP	0.171777739	0.999408308	0.397997887	0.12198891	0.999408308	0.397997887	-0.049788829
UBE2B	0.089930816	0.967780942	0.537212607	0.113808699	0.967780942	0.537212607	0.023877883
POLH	0.082071271	0.817609978	0.414541812	0.113645775	0.817609978	0.414541812	0.031574504
RECQL	0.204531622	0.991266977	0.346060971	0.110290712	0.991266977	0.394390206	-0.094240911
NABP1	0.130917209	0.959632317	0.37841813	0.109498228	0.959632317	0.37841813	-0.021418982
CCNA1	0.22803564	0.810951228	0.598707029	0.108449837	0.810951228	0.598707029	-0.119585803
BEND3	0.191734163	0.782060364	0.418467606	0.108326766	0.782060364	0.418467606	-0.083407397
ATM	0.943915105	1	0.081241606	0.106493679	1	0.466444914	-0.837421426
EXD2	0.212897749	0.986875983	0.445430619	0.106370928	0.986875983	0.445430619	-0.106526822
BRCA2	0.144455879	0.996405184	0.390630433	0.104315302	0.996405184	0.390630433	-0.040140576
HES1	0.063669629	0.76809946	0.612258629	0.099168713	0.76809946	0.612258629	0.035499084
CDCA5	0.209257724	0.953015111	0.687248839	0.098594465	0.953015111	0.733014267	-0.110663259
SETMAR	0.130645154	0.987364155	0.40481647	0.0952048	0.987364155	0.40481647	-0.035440354
TDP2	0.259346777	0.711202432	0.917993286	0.094098262	0.674335764	0.917993286	-0.165248515
PARK2	-0.002213953	0.744557492	0.558212871	0.091904438	0.744557492	0.519731198	0.094118391
XPA	0.39221296	0.954356687	0.428896985	0.091243623	0.954356687	0.473829968	-0.300969337
OTUD7B	0.181131674	0.966178755	0.371732999	0.091099419	0.966178755	0.413043431	-0.090032255
HDAC10	0.10296821	0.997973562	0.508985692	0.089846358	0.997973562	0.508985692	-0.013121852
CSNK1D	0.455645118	0.998727585	0.147949752	0.089806427	0.998727585	0.407814328	-0.365838691
NOTCH4	0.146490144	0.977380485	0.393068506	0.089508113	0.977380485	0.406041051	-0.056982031
USP22	-0.08988158	0.642641712	0.653544646	0.087887047	0.642641712	0.653544646	0.177768626
CCND1	0.097377397	0.869752987	0.641848467	0.087067703	0.869752987	0.641848467	-0.010309694
HLTF	0.21653935	0.842836197	0.400106702	0.086164078	0.842836197	0.462500405	-0.130375272
BUB1B	-0.219697257	0.468920428	0.999987313	0.084848879	0.576205996	0.999987313	0.304546136
CENPS	0.176204454	0.809540827	0.504680041	0.084507524	0.809540827	0.504680041	-0.09169693
TRIM28	-0.020763468	0.696727965	0.743038716	0.083263708	0.696727965	0.743038716	0.104027176
RPA4	0.246804945	0.926587876	0.347017442	0.08264088	0.926587876	0.418620376	-0.164164065
TDG	0.171354519	0.776038219	0.622908194	0.081982776	0.776038219	0.622908194	-0.089371742
POLL	0.139099851	0.995018218	0.414511884	0.078584312	0.995018218	0.42431045	-0.060515538
RAD23B	-0.049204152	0.726194025	0.689054646	0.074848626	0.726194025	0.689054646	0.124052777
PIAS3	0.059787001	0.955902472	0.518574108	0.074456	0.955902472	0.518574108	0.014668999
SENP7	0.030641338	0.8161503	0.467620277	0.07047571	0.8161503	0.467620277	0.039834372
RAD52	0.107879973	0.728971579	0.559429461	0.06997367	0.728971579	0.559429461	-0.037906303
PXMP2	0.063277829	0.923308842	0.444325346	0.067883797	0.923308842	0.444325346	0.004605968
PER3	0.063532836	0.849608299	0.489903783	0.065916041	0.849608299	0.489903783	0.002383204
RHO	-0.094953519	0.867938538	0.600412196	0.065020096	0.867938538	0.484596608	0.159973616
SKIV2L2	0.133767643	0.791033887	0.788549952	0.06338899	0.791033887	0.788549952	-0.070378653
CUL9	0.022738544	0.851605881	0.855499456	0.06283844	0.851605881	0.855499456	0.040099895
INO80E	0.075453653	0.854418796	0.665537272	0.06000491	0.854418796	0.665537272	-0.015448743
HPF1	0.34620325	0.942247654	0.482518472	0.059949205	0.942247654	0.576728887	-0.286254045
ERCC6L2	0.082971582	0.872367225	0.646306863	0.059204415	0.872367225	0.646306863	-0.023767167
UBE2D4	0.201658186	0.907990743	0.395428014	0.055146625	0.907990743	0.445565858	-0.146511561
RUVBL1	-0.153454706	0.662185567	0.999640183	0.054300845	0.820973379	0.999640183	0.207755551
POLG	-0.010706466	0.665474388	0.874455448	0.053156036	0.665474388	0.874455448	0.063862501
AICDA	0.092415873	0.884412741	0.47259631	0.052877257	0.884412741	0.47259631	-0.039538617
POLQ	0.163186408	0.707187804	0.452518333	0.052289266	0.707187804	0.452518333	-0.110897142

RECQL5	0.306297541	0.807844349	0.447635835	0.051651412	0.807844349	0.449528537	-0.254646128
PRDM9	0.168769325	0.943546646	0.367872819	0.04784386	0.943546646	0.449775634	-0.120925464
DTX1	0.046182582	0.802545681	0.457077757	0.044109694	0.802545681	0.457077757	-0.002072888
OTUB1	-0.228427007	0.59043536	0.800128386	0.037539574	0.59043536	0.800128386	0.265966582
SHPRH	0.121492533	0.726763686	0.552152367	0.037051661	0.726763686	0.552152367	-0.084440872
TP73	0.153404834	0.721214667	0.496816724	0.035157299	0.721214667	0.496816724	-0.118247535
IGHMBP2	0.022171585	0.733461585	0.477616102	0.03294178	0.733461585	0.477616102	0.010770195
ERCC8	0.078879398	0.716506865	0.709966902	0.028140536	0.716506865	0.709966902	-0.050738862
CLK2	-0.110313539	0.937955813	0.60099048	0.026897751	0.937955813	0.53407626	0.13721129
ARID1A	-0.004515786	0.524709241	0.960738841	0.026415831	0.524709241	0.960738841	0.030931617
H3F3B	-0.069808624	0.771063803	0.851687166	0.024440463	0.771063803	0.851687166	0.094249087
PMS2P3	0.047253518	0.943456195	0.540776061	0.023999063	0.943456195	0.540776061	-0.023254455
PARG	-0.381310333	0.995565538	0.775369659	0.02111252	0.995565538	0.622838059	0.402422853
CTC1	-0.604107134	0.186351673	0.999977979	0.020211568	0.51582487	0.999977979	0.624318701
SUV39H1	-0.171821126	0.686927959	0.727706492	0.013962166	0.686927959	0.727706492	0.185783291
PMS2P5	0.137426805	0.642106223	0.567006492	0.0133464	0.642106223	0.567006492	-0.124080405
CSNK2A1	-0.195308596	0.59893175	0.749365565	0.011347324	0.59893175	0.744935698	0.20665592
PRDM10	-0.023312679	0.750825113	0.67521091	0.007033971	0.750825113	0.67521091	0.03034665
RNF4	0.016632553	0.51553963	0.863172383	0.00622785	0.51553963	0.863172383	-0.010404703
MTA1	-0.061503087	0.620309887	0.740035073	0.005178521	0.620309887	0.740035073	0.066681608
COPS4	0.172337992	0.962367229	0.715195378	-0.00226884	0.962367229	0.752958171	-0.174606832
USP44	-0.035793351	0.66852974	0.962981781	-0.003191434	0.66852974	0.962981781	0.032601917
RFC1	0.187239317	0.870530865	0.493337784	-0.004610795	0.870530865	0.507184656	-0.191850113
MVP	-0.003233065	0.881549393	0.509313399	-0.008949586	0.881549393	0.509313399	-0.005716522
UBB	0.131580167	0.998261617	0.703563445	-0.011506907	0.998261617	0.764261501	-0.143087074
ATAD5	-0.180263996	0.639201937	0.719766489	-0.012020629	0.639201937	0.719766489	0.168243367
RNF169	-0.178212041	0.972630813	0.673874758	-0.012568394	0.972630813	0.576521082	0.165643647
SIRT6	0.115883981	0.933946592	0.491069507	-0.012902396	0.933946592	0.526319988	-0.128786376
POLD4	-0.152430023	0.72269126	0.774671345	-0.018536418	0.72269126	0.774671345	0.133893605
COL1A1	-0.008019083	0.911479638	0.616873471	-0.021235504	0.911479638	0.616873471	-0.013216421
POLR2B	-0.267503378	0.468988107	0.998193741	-0.025249103	0.611948588	0.998193741	0.242254275
CHEK1	-0.210828802	0.613334613	0.9943534	-0.028889947	0.717628982	0.9943534	0.181938854
CTCF	-0.278839908	0.470432027	0.999918614	-0.031313419	0.707214958	0.999918614	0.247526489
APEX1	0.04505838	0.975643502	0.654696958	-0.032401345	0.975643502	0.654696958	-0.077459725
RBBP7	-0.173001878	0.976664116	0.670460655	-0.037495341	0.976664116	0.605891961	0.135506536
RAD51AP1	0.261280461	0.853380663	0.405176852	-0.043143269	0.853380663	0.540512803	-0.30442373
TEP1	0.298852919	0.9949726	0.275978287	-0.046895012	0.9949726	0.544646231	-0.345747931
OR6B1	0.034434096	0.780133397	0.543041925	-0.048782563	0.780133397	0.543041925	-0.083216659
MBTD1	0.123132222	0.982125174	0.487072459	-0.049491053	0.982125174	0.549045505	-0.172623275
REV3L	-0.195390357	0.586466619	0.995825835	-0.053169669	0.677729369	0.995825835	0.142220689
SETX	-0.061594389	0.956660985	0.560406733	-0.056988341	0.956660985	0.560406733	0.004606048
TOP2A	-0.104540464	0.810893181	0.622751665	-0.061311358	0.810893181	0.622751665	0.043229106
PIAS4	-0.027867095	0.530232231	0.788581482	-0.064941031	0.530232231	0.788581482	-0.037073936
CUL4A	-0.088287072	0.655076567	0.689545238	-0.065496881	0.655076567	0.689545238	0.022790191
ORC2	-0.169288907	0.481268607	0.87352768	-0.067722992	0.481268607	0.87352768	0.101565915
WRNIP1	-0.039180542	0.995688479	0.564859139	-0.068806024	0.995688479	0.564859139	-0.029625482
SMC5	-0.613505342	0.187778569	0.999999999	-0.076743469	0.649455476	0.999999999	0.536761873
DAXX	-0.297105535	0.439790132	0.982592441	-0.077652638	0.641892997	0.982592441	0.219452897
PARP1	-0.098941001	0.420140741	0.90920163	-0.080462653	0.420140741	0.90920163	0.018478348
CDK2	-0.357679166	0.355245308	0.991668433	-0.083488204	0.539835242	0.991668433	0.274190962
UBE2A	-0.134213747	0.966338213	0.624669305	-0.090238379	0.966338213	0.624669305	0.043975368
MPLKIP	-0.050214801	0.504591767	0.839815793	-0.090727672	0.504591767	0.839815793	-0.040512871
POLE	-0.19943263	0.65044863	0.865959085	-0.093914916	0.65044863	0.865959085	0.105517715
MSH6	-0.017441367	0.77028725	0.633023141	-0.095550842	0.77028725	0.633023141	-0.078109475
RAD54L	0.065435368	0.565077241	0.930512659	-0.097263653	0.553927821	0.930512659	-0.162699021
UNG	-0.140507607	0.879170242	0.711741337	-0.097954022	0.879170242	0.711741337	0.042553586
TNKS	-0.113515915	0.632422958	0.844252915	-0.102750963	0.632422958	0.844252915	0.010764952
PALB2	-0.017023307	0.507357419	0.956352073	-0.109382034	0.501162855	0.956352073	-0.092358726
H2AFY2	-0.101809783	0.763884749	0.608864689	-0.112067979	0.763884749	0.608864689	-0.010258196
BRIP1	-0.085205865	0.47669902	0.882716175	-0.112335334	0.47669902	0.882716175	-0.027129469
KAT5	-0.131731425	0.544346065	0.999736495	-0.113515061	0.544346065	0.999736495	0.018216364
TOP1	-0.250919421	0.593986618	0.965118595	-0.113775851	0.593986618	0.965118595	0.13714357
DUT	-0.148361159	0.579846774	0.992138582	-0.11814688	0.579846774	0.992138582	0.030214279
FAAP20	-0.029570021	0.529341341	0.704574993	-0.12000869	0.529341341	0.704574993	-0.090438669
MORF4L2	-0.054651735	0.909420079	0.609511379	-0.123335851	0.909420079	0.609511379	-0.068684116
UPF1	0.156450488	0.948328204	0.827507694	-0.129993137	0.701914317	0.999880087	-0.286443626
FANCC	-0.472839968	0.141034121	0.999998236	-0.130770543	0.376495571	0.999998236	0.342069425
H3F3A	-0.066562921	0.576658748	0.533961199	-0.13224946	0.576658748	0.533961199	-0.065686538
COPS2	-0.081647004	0.620978721	0.992713471	-0.132313589	0.620978721	0.992713471	-0.050666585
GEN1	0.121114146	0.754153117	0.671192216	-0.133598753	0.754153117	0.717346874	-0.254712899
NHEJ1	-0.275904963	0.320688385	0.989815203	-0.137074163	0.368523332	0.989815203	0.1388308
KAT2A	-0.258826185	0.451517864	0.992094734	-0.140848258	0.536768849	0.992094734	0.117977927
CHRAC1	-0.146265724	0.470805861	0.883613746	-0.141548985	0.470805861	0.883613746	0.004716739
HELQ	-0.117832957	0.53104413	0.86709702	-0.148396953	0.53104413	0.86709702	-0.030563996
SMG1	-0.001027006	0.748581794	0.889597163	-0.154371649	0.671159782	0.889597163	-0.153344643
SPIDR	-0.160869561	0.476235924	0.816668104	-0.163306594	0.476235924	0.816668104	-0.002437032
CBX1	-0.322394083	0.732768406	0.73796149	-0.165062075	0.732768406	0.73796149	0.157332007
ECT2	-0.285309725	0.601225405	0.863494177	-0.16529244	0.601225405	0.863494177	0.120017286
CDK12	-0.12669623	0.564415163	0.972174261	-0.168720419	0.564415163	0.972174261	-0.042024189
HELLS	-0.3323148	0.378136086	0.971985663	-0.169311399	0.508538198	0.971985663	0.163003401
TERF1	-0.13534812	0.599924359	0.989034776	-0.173441923	0.599924359	0.989034776	-0.038093803
ZMPSTE24	-0.271713141	0.31252721	0.99078592	-0.18626921	0.342656174	0.99078592	0.085443931

SMARCE1	-0.302947089	0.467321058	0.990164848	-0.189759385	0.506807517	0.990164848	0.113187704
RNF168	-0.167531462	0.686855358	0.768789476	-0.190727785	0.686855358	0.768789476	-0.023196323
RFWD3	-0.123203367	0.445843971	0.946496535	-0.19492709	0.445843971	0.946496535	-0.071723723
NFE2L2	-0.33470849	0.300917887	0.994462838	-0.19573084	0.315725366	0.994462838	0.13897765
ZSWIM7	-0.083677693	0.743131832	0.724270237	-0.196197051	0.735231576	0.724270237	-0.112519358
SFPQ	-0.57681843	0.185355112	0.99600134	-0.205258684	0.483148886	0.99600134	0.371559746
MEN1	-0.496261129	0.27247094	0.983314517	-0.208255789	0.482053675	0.983314517	0.28800534
WEE1	-0.155452837	0.513030134	0.994310613	-0.211778417	0.513030134	0.994310613	-0.056325581
POLR2G	-0.019972112	0.726226515	0.997446221	-0.212864322	0.608440782	0.997446221	-0.19289221
CDC25B	-0.240849288	0.43383429	0.990217901	-0.217992272	0.43383429	0.990217901	0.022857016
CCNB1	-0.431339642	0.244388192	0.998111376	-0.219921533	0.43057925	0.998111376	0.211418108
PPM1G	-0.26147433	0.439542171	0.977161392	-0.220610115	0.439542171	0.977161392	0.040864215
PINX1	-0.287599591	0.411515389	0.974286015	-0.221432877	0.437576953	0.974286015	0.066166714
ACTR8	-0.411475434	0.290246766	0.99999942	-0.224807063	0.442959091	0.99999942	0.186668371
NCAPH2	-0.571878906	0.191663105	0.999999184	-0.228129586	0.461935274	0.999999184	0.34374932
SPRTN	-0.325328722	0.359037223	0.993980344	-0.228243527	0.401269127	0.993980344	0.097085195
RAD21	-0.197435806	0.524806212	0.999354912	-0.232340701	0.524806212	0.999354912	-0.034904895
DCLRE1B	-0.428985616	0.368748407	0.999992796	-0.233025953	0.491971737	0.999992796	0.195959663
BAZ1B	-0.161895191	0.677081241	0.831773684	-0.236830325	0.677081241	0.831773684	-0.074935134
SMC2	-0.435588738	0.306500359	0.998050525	-0.246408633	0.445587659	0.998050525	0.189180105
PAXIP1	-0.162524062	0.640313842	0.733419247	-0.247736084	0.640313842	0.733419247	-0.085212022
CHAF1A	-0.320935796	0.408536458	0.998605523	-0.254401494	0.417980079	0.998605523	0.066534302
CLSPN	-0.362088605	0.350724578	0.995842411	-0.25568384	0.400633478	0.995842411	0.106404765
UBE2D3	-0.164298771	0.584918544	0.997770826	-0.256125828	0.584918544	0.997770826	-0.091827057
SMARCAL1	-0.191703632	0.734519105	0.748013154	-0.258188722	0.734519105	0.748013154	-0.06648509
RNF8	-0.420300366	0.309963928	0.996162079	-0.264000625	0.403392721	0.996162079	0.156299741
FAAP100	-0.350651232	0.348295658	0.999216741	-0.265090255	0.348324268	0.999216741	0.085560977
EXO5	-0.250611934	0.483459042	0.99160132	-0.267014669	0.483459042	0.99160132	-0.016402734
NFRKB	-0.019030058	0.57136474	0.983903022	-0.269946772	0.457232904	0.983903022	-0.250916714
STAG1	0.097146543	0.723799903	0.633347551	-0.271542088	0.723799903	0.800676248	-0.36868863
SMARCA5	-0.259388098	0.390297438	0.999784118	-0.276523034	0.390297438	0.999784118	-0.017134937
ATMIN	-0.073792073	0.945798935	0.687818418	-0.281206628	0.945798935	0.717556338	-0.207414554
CNOT7	-0.426368207	0.288024187	0.942650234	-0.284916952	0.288024187	0.942650234	0.141451255
TADA3	-0.580141432	0.433691801	0.915647428	-0.287635052	0.433691801	0.915647428	0.29250638
NIPBL	-0.327330488	0.525388835	0.998963233	-0.295695572	0.525388835	0.998963233	0.031634916
CHD4	-0.516423917	0.501435684	0.901051259	-0.302107709	0.501435684	0.901051259	0.214316207
EXO1	-0.265627482	0.626652201	0.875452844	-0.316215182	0.626652201	0.875452844	-0.0505877
TCEB3	-0.360643752	0.392677042	0.990465878	-0.326566923	0.392677042	0.990465878	0.034076829
PPP4R2	-0.244939295	0.570779587	0.884977733	-0.331330644	0.570779587	0.884977733	-0.086391349
ACTR5	-0.260340651	0.309331697	0.999664378	-0.335459641	0.309331697	0.999664378	-0.07511899
SMG6	-0.6453912	0.290383003	0.975220406	-0.336765894	0.420174475	0.975220406	0.308625306
NBN	0.08695752	0.797503888	0.750377074	-0.337560003	0.618038755	0.937556694	-0.424517523
GTF2H4	-0.422854362	0.275615179	1	-0.341758269	0.293305429	1	0.081096092
UCHL5	-0.577541186	0.133405401	0.999999896	-0.34195548	0.248764813	0.999999896	0.235585706
RFC4	-0.716468546	0.10153731	0.999840568	-0.342002964	0.291544092	0.999840568	0.374465582
EP400	-0.107096777	0.603096792	0.934499724	-0.342791618	0.584723843	0.934499724	-0.235694841
INO80	-0.448952636	0.225029413	0.998880602	-0.344610666	0.26996301	0.998880602	0.10434197
RBBP8	-0.342988327	0.462614282	0.850956524	-0.347030497	0.462614282	0.850956524	-0.00404217
CUL1	-0.305524858	0.340697374	0.99998777	-0.347179148	0.340697374	0.99998777	-0.041654289
COPS3	-0.227953783	0.442367828	0.998901311	-0.348516407	0.384372956	0.998901311	-0.120562624
TAF1	-0.327362859	0.387331098	0.999999984	-0.355485229	0.387331098	0.999999984	-0.02812237
FANCM	-0.475851292	0.163779083	0.999902234	-0.355635242	0.235438146	0.999902234	0.12021605
GAR1	-0.304532452	0.362184186	0.99968861	-0.365152671	0.343440901	0.99968861	-0.060620218
XRCC1	-0.223303714	0.443528978	0.83560372	-0.373783118	0.443528978	0.83560372	-0.150479403
RMI2	-0.384013037	0.359083547	0.971086796	-0.375905162	0.359083547	0.971086796	0.008107876
RAD1	-0.762895421	0.148316872	0.999593394	-0.376440405	0.325790703	0.999593394	0.386455016
POLR2C	-0.50033028	0.157098961	0.999999547	-0.380740339	0.223820267	0.999999547	0.119589942
LIG1	-0.512431584	0.526211125	0.979584009	-0.384275107	0.526211125	0.979584009	0.128156477
SENP6	-0.352317624	0.287750183	0.99993276	-0.385500519	0.287750183	0.99993276	-0.033182896
EYA3	-0.456112416	0.442394633	0.978716184	-0.387686053	0.442394633	0.978716184	0.068426364
SFR1	-0.156771023	0.81670404	0.894819057	-0.390192821	0.640166994	0.894819057	-0.233421798
POLR2F	-0.562227633	0.216537678	0.932523806	-0.397437876	0.294463502	0.932523806	0.164789757
NSMCE2	-0.556001856	0.193492295	0.996527617	-0.399262842	0.25462394	0.996527617	0.156739013
USP7	-0.391609257	0.305594303	0.999984213	-0.402061931	0.305594303	0.999984213	-0.010452674
BRCA1	-0.407897117	0.240341187	0.988927882	-0.403056485	0.240341187	0.988927882	0.004840632
BARD1	-0.245556819	0.383219376	0.99981174	-0.404384838	0.263085177	0.99981174	-0.158828019
RNF40	-0.53170703	0.314960506	0.999986349	-0.409308039	0.377800215	0.999986349	0.12239899
POT1	-0.473156679	0.27823922	0.999990622	-0.410456241	0.289223339	0.999990622	0.062700438
RNASEH2A	-0.774272995	0.074537796	0.999838311	-0.412804047	0.182239122	0.999838311	0.361468949
UBE2I	-0.498894992	0.273549919	0.999999985	-0.41353856	0.311095516	0.999999985	0.085356432
MCM3AP	-0.571487276	0.210290216	0.973219488	-0.414577182	0.245791437	0.973219488	0.156910094
RMI1	-0.453799452	0.143321541	0.999979412	-0.416007829	0.15028984	0.999979412	0.037791622
UVRAG	-0.571651452	0.117036679	0.999970332	-0.416051718	0.187861322	0.999970332	0.155599734
TICRR	-0.797400874	0.045540757	0.999999997	-0.416743566	0.230127031	0.999999997	0.380657308
PAGR1	-0.325517228	0.344956722	0.995113011	-0.417768757	0.301574201	0.995113011	-0.092251529
FANCI	-0.586703828	0.250591065	0.995192091	-0.425331133	0.341551623	0.995192091	0.161372695
MDC1	-0.260384407	0.368398642	0.986434394	-0.427783586	0.235619766	0.986434394	-0.167399179
ATRIP	-0.443349339	0.203753298	0.998218448	-0.427978459	0.203753298	0.998218448	0.01537088
FANCA	-0.628314974	0.209442566	0.968847838	-0.435673566	0.209442566	0.968847838	0.192641408
FANCF	-0.781412813	0.058292815	0.999997085	-0.444210884	0.134503467	0.999997085	0.337201928
CSNK2B	-0.726343327	0.098440714	0.999938691	-0.4474661	0.202035915	0.999938691	0.278877227
CREBBP	-0.584821188	0.200253782	0.977017433	-0.447778848	0.200253782	0.977017433	0.13704234

FAAP24	-0.340509812	0.262097914	0.999280513	-0.448306062	0.262097914	0.999280513	-0.10779625
FEN1	-0.623830581	0.100825771	0.999973193	-0.450553621	0.196283072	0.999973193	0.17327696
SMC1A	-0.740754463	0.131619159	1	-0.453336412	0.275896418	1	0.287418051
RAD51B	-0.549552869	0.161939293	0.9999845	-0.456481337	0.161939293	0.9999845	0.093071533
PDS5B	-0.599265121	0.164773	0.997655936	-0.458760261	0.191064986	0.997655936	0.14050486
COPS8	-0.531819356	0.295386634	0.99994207	-0.459321251	0.315067169	0.99994207	0.072498105
MTOR	-0.414611926	0.179431512	0.999949697	-0.461006804	0.179431512	0.999949697	-0.046394878
RPAIN	-0.736503038	0.205984554	0.977445656	-0.463024302	0.250850992	0.977445656	0.273478736
SLX4	-0.446272706	0.231739994	0.999341474	-0.4639301	0.231739994	0.999341474	-0.017657394
PDS5A	-0.875842427	0.042144701	0.999995695	-0.468175233	0.208321058	0.999995695	0.407667195
PRMT1	-0.776165098	0.057656701	0.999836497	-0.469090598	0.169360935	0.999836497	0.3070745
NSMCE4A	-0.633510441	0.144094622	0.999942809	-0.470068139	0.221355976	0.999942809	0.163442302
TERF2	-0.434257981	0.320585828	0.996613913	-0.47126373	0.320585828	0.996613913	-0.037005749
UBC	-0.500661645	0.319689711	0.98099411	-0.475523583	0.319689711	0.98099411	0.025138062
POLD2	-0.318331019	0.334274577	0.982634944	-0.479593426	0.334274577	0.982634944	-0.161262406
ENY2	-0.375068238	0.262644554	0.971646103	-0.482395224	0.218434077	0.971646103	-0.107326987
POLR2K	-0.599130386	0.283843607	0.987262845	-0.482978015	0.283843607	0.987262845	0.116152371
PCNA	-0.525227676	0.210773824	0.999618781	-0.484398215	0.210773824	0.999618781	0.040829461
POLR2H	-0.311275572	0.3367429	0.999999145	-0.491210287	0.189479666	0.999999145	-0.179934715
KDM4A	-0.666794788	0.125797803	0.999685556	-0.494144558	0.166800392	0.999685556	0.17265023
PRPF19	-0.368776851	0.304999985	0.999912334	-0.495298886	0.234990742	0.999912334	-0.126522036
RAD17	-0.429162084	0.243071081	0.99993315	-0.496070957	0.22734203	0.99993315	-0.066908873
PLRG1	-0.412979263	0.343606608	0.948788813	-0.501635898	0.343606608	0.948788813	-0.088656635
ESCO2	-0.574482163	0.196685607	0.992629276	-0.502442957	0.196685607	0.992629276	0.072039206
HINFP	-0.79221487	0.06620008	0.999999995	-0.503922395	0.198246862	0.999999995	0.288292475
XAB2	-0.511185044	0.176883581	0.99997275	-0.506123258	0.176883581	0.99997275	0.005061786
SMARCB1	-0.566741201	0.195990515	0.999998637	-0.509017206	0.195990515	0.999998637	0.057723996
CDK4	-0.889478248	0.06897007	0.999987981	-0.510104937	0.238138286	0.999987981	0.379373311
LMNA	-0.569427782	0.183523833	0.988127832	-0.510726506	0.183910288	0.988127832	0.058701276
NCAPG	-0.706636908	0.057577289	0.999983682	-0.512604221	0.144898496	0.999983682	0.194032687
COPS6	-0.470339935	0.212521005	0.999999928	-0.51767767	0.211926691	0.999999928	-0.047337735
NOP10	-0.476179328	0.209605617	0.999999242	-0.521170097	0.209605617	0.999999242	-0.044990769
POLE4	-0.42725172	0.219300567	0.999981281	-0.522554491	0.190544578	0.999981281	-0.095302771
FIGNL1	-0.635831087	0.256950171	0.998935428	-0.525543682	0.256950171	0.998935428	0.110287405
FANCE	-0.364772348	0.291835479	0.999512955	-0.528331463	0.247125549	0.999512955	-0.163559115
MUS81	-0.249320524	0.394675737	0.99287909	-0.531680644	0.261371504	0.99287909	-0.28236012
CCNA2	-0.465565996	0.191396525	0.999949601	-0.533169747	0.173826648	0.999949601	-0.067603751
SUPT6H	-0.369824995	0.259662653	0.999391397	-0.533852523	0.171471244	0.999391397	-0.164027529
USP37	-0.630890187	0.138351985	0.999898899	-0.535352006	0.185518057	0.999898899	0.095538181
RRM1	-1.032482639	0.034982101	0.999991166	-0.537000329	0.206941584	0.999991166	0.49548231
RTEL1	-0.717936118	0.059114878	0.999998909	-0.537148512	0.123143958	0.999998909	0.180787606
WRAP53	-0.856791271	0.086903678	0.999668421	-0.539435383	0.206508048	0.999668421	0.317355888
TOP3A	-1.001860485	0.011708291	0.999999999	-0.543032157	0.147739849	0.999999999	0.458828328
XRCC6	-0.493731367	0.30899219	0.996737637	-0.548909689	0.30899219	0.996737637	-0.055178322
TRRAP	-0.722812973	0.093073137	0.997020082	-0.549214967	0.176588043	0.997020082	0.173598006
PRKDC	-0.662192669	0.214157339	0.997540738	-0.550745767	0.243221648	0.997540738	0.111446902
H2AFX	-0.444842418	0.204068226	0.998820878	-0.550884741	0.16413212	0.998820878	-0.106042324
CCNH	-0.607541695	0.192832043	0.999833994	-0.553776106	0.20405674	0.999833994	0.053765589
BCCIP	-0.799570442	0.076493307	0.998808704	-0.570549457	0.162389922	0.998808704	0.229020985
ANKRD52	-0.613407251	0.231288577	0.982790897	-0.575989171	0.231288577	0.982790897	0.037418081
COPS5	-0.528190762	0.189865129	0.999999992	-0.577799119	0.177449129	0.999999992	-0.049608356
ATR	-0.409950543	0.29311123	0.999999984	-0.582986911	0.222781367	0.999999984	-0.173036368
RPA2	-0.611746352	0.103269561	0.999999998	-0.585976995	0.103269561	0.999999998	0.025769357
FZR1	-0.833828486	0.046563153	1	-0.586179003	0.113022711	1	0.247649484
UBA1	-1.044494546	0.009561138	0.99999971	-0.587854726	0.11056439	0.99999971	0.45663982
DNMT1	-0.700092374	0.099572518	0.999965741	-0.591410006	0.133473953	0.999965741	0.108682367
MNAT1	-0.645490908	0.157051272	0.999979182	-0.603328955	0.157051272	0.999979182	0.042161953
RAD51C	-0.761398497	0.113616994	0.997588655	-0.604908202	0.152715579	0.997588655	0.156490296
INO80B	-0.595322664	0.204278007	0.998019997	-0.605130526	0.204278007	0.998019997	-0.009807862
LIG4	-0.719846315	0.089990965	0.997992962	-0.6368925	0.093721735	0.997992962	0.082953815
XRCC4	-0.822417214	0.091989725	0.983404757	-0.640573753	0.091989725	0.983404757	0.181843462
NCAPD2	-0.825278566	0.039432398	0.999998189	-0.653554924	0.085051438	0.999998189	0.171723642
FANCB	-0.543948709	0.243223748	0.995133965	-0.656515485	0.233938209	0.995133965	-0.112566777
DDB1	-0.808233965	0.049577004	1	-0.659886016	0.091273938	1	0.14834795
RIF1	-0.81251909	0.056789732	0.999998123	-0.662089165	0.079041381	0.999998123	0.150429925
ERCC1	-0.953958407	0.050180246	0.999920277	-0.663101208	0.122859932	0.999920277	0.290857198
RAD50	-0.83067853	0.015008192	0.999999891	-0.664566307	0.037270877	0.999999891	0.166112223
RFC2	-0.70393894	0.139953401	0.999995591	-0.667040553	0.139953401	0.999995591	0.036898388
UHRF1	-0.85512478	0.088687066	0.99999626	-0.668005213	0.157106615	0.99999626	0.187119568
RRM2	-0.775229811	0.072519205	0.999998419	-0.672004664	0.103864803	0.999998419	0.103225146
DSCC1	-0.92511543	0.034456733	0.999994766	-0.680968072	0.104580418	0.999994766	0.244147359
UBE2N	-0.667674535	0.068995853	0.999808198	-0.685292861	0.068995853	0.999808198	-0.017618326
BOD1L1	-0.598619201	0.141601523	0.999999296	-0.689650975	0.118693167	0.999999296	-0.091031774
FANCG	-0.884314386	0.064052494	0.999845823	-0.689936771	0.097001355	0.999845823	0.194377615
SMC6	-0.62827312	0.132391657	0.999345574	-0.692233339	0.126184411	0.999345574	-0.063960219
TRAIP	-0.671298382	0.096031914	0.999999649	-0.694102841	0.096031914	0.999999649	-0.022804458
CUL2	-0.875200656	0.023571088	0.999999866	-0.698554752	0.057999767	0.999999866	0.176645904
NCAPH	-0.606933255	0.102639616	0.99898725	-0.699930989	0.083483881	0.99898725	-0.092997734
TIMELESS	-0.503827473	0.193906466	0.999719417	-0.708976581	0.095802368	0.999719417	-0.205149108
CDC5L	-0.760661737	0.037544845	0.999999994	-0.714861575	0.041418212	0.999999994	0.045800162
ERCC2	-1.218816117	0.004226068	1	-0.71876319	0.07463958	1	0.500052928
TINF2	-1.052697794	0.062390672	0.999488823	-0.718827813	0.161866225	0.999488823	0.333869981

TERT	-1.119248487	0.02682869	0.999994311	-0.724382429	0.095245018	0.999994311	0.394866058
NONO	-0.88124444	0.046848806	0.999999975	-0.72967408	0.078795352	0.999999975	0.15157036
WAPL	-0.636602806	0.159477215	0.99976222	-0.730159163	0.159477215	0.99976222	-0.093556357
UBE2M	-1.011751636	0.065861773	0.99993481	-0.731412428	0.119797607	0.99993481	0.280339207
POLR2I	-0.8634729	0.055039592	0.999989168	-0.737157999	0.082150629	0.999989168	0.126314902
TOPBP1	-0.80870758	0.031817037	0.999999996	-0.737404821	0.040861579	0.999999996	0.071302759
RPA1	-0.881774299	0.106025686	0.99954152	-0.744955761	0.113189097	0.99954152	0.136818538
MCPH1	-0.83176374	0.075980889	0.999999494	-0.744990395	0.091723762	0.999999494	0.086773346
BAP1	-1.029589117	0.055763061	0.991006485	-0.748150896	0.073380185	0.991006485	0.281438221
SUPT4H1	-1.00091772	0.040545034	0.999999516	-0.753356508	0.108986745	0.999999516	0.247561211
POLD1	-0.59733313	0.23555842	0.971842685	-0.7635773	0.180360624	0.971842685	-0.16624417
MRE11	-0.830435636	0.025047042	0.999979051	-0.76726737	0.026157005	0.999979051	0.063168266
HUS1	-1.050795745	0.023548946	0.999975309	-0.76941399	0.070467648	0.999975309	0.281381755
PPM1D	-0.818972432	0.056433841	0.999999741	-0.776477356	0.066088169	0.999999741	0.042495076
MMS22L	-0.737394842	0.03248745	0.99993567	-0.781802697	0.03248745	0.99993567	-0.044407855
POLE2	-0.798156747	0.056564907	0.999980808	-0.782549004	0.056564907	0.999980808	0.015607742
NCAPG2	-0.5285561	0.165792029	0.999979983	-0.783565264	0.071478728	0.999979983	-0.255009164
NSMCE1	-0.942989575	0.026233199	0.99991118	-0.789847179	0.04901269	0.99991118	0.153142396
FANCL	-1.147402801	0.028245279	0.999999866	-0.795178247	0.075039619	0.999999866	0.352224554
RAD51D	-0.552894054	0.065205148	0.999999993	-0.812298023	0.01025387	0.999999993	-0.259403969
USP5	-1.150485989	0.011361343	0.999889437	-0.817007808	0.050377951	0.999889437	0.333478181
RPA3	-0.872642189	0.035653258	0.999948141	-0.822775077	0.038869502	0.999948141	0.049867112
SET	-0.769576973	0.061630068	0.9998963	-0.828279842	0.057764581	0.9998963	-0.058702869
BCAS2	-0.744492885	0.04473404	0.999999806	-0.831270247	0.02787142	0.999999806	-0.086777362
TTI2	-0.992372638	0.027257807	1	-0.844982689	0.044712493	1	0.147389949
RFC3	-0.934650532	0.054169331	0.999999623	-0.850623585	0.065608785	0.999999623	0.084026948
PLK1	-0.96255131	0.037840371	0.999800348	-0.852781467	0.060230761	0.999800348	0.109769843
MAD2L2	-0.958167287	0.04891888	0.999997565	-0.854889164	0.060539348	0.999997565	0.103278123
NSMCE3	-0.683360615	0.092704172	0.999991203	-0.857143886	0.049769056	0.999991203	-0.173783271
PNKP	-0.80267637	0.039702197	0.999999942	-0.882698709	0.029025251	0.999999942	-0.080022339
GTF2H5	-1.1004463	0.046745333	0.999989346	-0.885029409	0.089697707	0.999989346	0.215416891
RPS27L	-0.79402782	0.175372193	0.999927292	-0.888757007	0.161479949	0.999927292	-0.094729186
RAD9A	-0.927458863	0.067132826	0.999222767	-0.899193871	0.067132826	0.999222767	0.028264992
TELO2	-1.172716219	0.013985229	0.999999997	-0.904726878	0.026209223	0.999999997	0.26798934
SMC3	-0.799894537	0.049865107	0.999896419	-0.904917567	0.031973568	0.999896419	-0.10502303
STN1	-0.782629209	0.041530494	1	-0.90720345	0.026988165	1	-0.124574241
MYBBP1A	-1.025202232	0.010018794	1	-0.907860429	0.021683468	1	0.117341803
RAD51	-0.92356063	0.050711825	0.99987961	-0.918172083	0.050711825	0.99987961	0.005388548
DNA2	-0.928731648	0.081324841	0.997085571	-0.923324836	0.081324841	0.997085571	0.005406812
CEP57	-0.930663582	0.050797872	0.999999863	-0.923494477	0.050797872	0.999999863	0.007169105
CDK7	-1.363152748	0.015968789	0.999996104	-0.924442309	0.08089796	0.999996104	0.438710439
RUVBL2	-1.026203446	0.016083642	0.999999577	-0.926984443	0.021748041	0.999999577	0.099219003
RNF20	-1.019072896	0.010500752	0.999999519	-0.940470732	0.012461345	0.999999519	0.078602164
POLE3	-1.136498113	0.016674233	0.999987142	-0.942941383	0.037850299	0.999987142	0.193556729
NAE1	-0.902197182	0.003232546	0.999999565	-0.945431998	0.002753912	0.999999565	-0.043234815
DKC1	-1.364076727	0.004014222	1	-0.94665081	0.038135829	1	0.417425917
PCID2	-1.117308148	0.017776905	0.999999883	-0.948072863	0.038148711	0.999999883	0.169235285
KAT8	-1.064025104	0.016068004	0.999999975	-0.956548954	0.026863206	0.999999975	0.10747615
MAU2	-0.759045329	0.065961298	0.999999903	-0.956681973	0.027342485	0.999999903	-0.197636644
DDX11	-0.702699161	0.099787007	0.999667691	-0.965268804	0.039129554	0.999667691	-0.262569643
TTI1	-0.981426123	0.035783619	1	-0.971939182	0.035783619	1	0.00948694
BRD4	-0.978677301	0.00735117	0.999964741	-0.97966693	0.00735117	0.999964741	-9.89629E-04
THOC1	-1.135449125	0.00467572	1	-0.980254858	0.009298454	1	0.155194267
ERCC4	-1.17532617	0.021366124	0.999998625	-0.996613955	0.027251309	0.999998625	0.178712215
TRIP13	-1.157043288	0.018400542	0.999999981	-1.00968538	0.04055486	0.999999981	0.147357908
XRCC2	-1.428955421	0.001033272	1	-1.039231745	0.014944617	1	0.389723677
TCEB1	-1.148363345	0.062229635	1	-1.039256167	0.064334891	1	0.109107178
MMS19	-0.955069116	0.015777023	0.99999986	-1.047373414	0.011497232	0.99999986	-0.092304299
GPS1	-1.318401276	0.005457301	1	-1.053639719	0.022171922	1	0.264761557
BRAT1	-1.313133015	0.011780141	1	-1.062487689	0.034624716	1	0.250645326
THOC2	-0.887437463	0.057304135	1	-1.063706268	0.030945577	1	-0.176268805
CDK9	-1.244433753	0.014249275	0.999986787	-1.091568735	0.022903835	0.999986787	0.152865019
POLR2E	-0.940954896	0.049066423	0.999997744	-1.097184709	0.030720381	0.999997744	-0.156229814
ACTL6A	-0.883006151	0.034442895	0.999999998	-1.126201443	0.007771734	0.999999998	-0.243195292
XRCC3	-1.044307076	0.008138937	1	-1.133775622	0.008138937	1	-0.089468546
WDR48	-0.805916784	0.083168093	0.999368917	-1.137592992	0.019257388	0.999368917	-0.331676209
SKP1	-1.083960198	0.030424549	0.999801217	-1.147246997	0.027967785	0.999801217	-0.0632868
NHP2	-1.16013315	0.024016887	1	-1.1522589	0.029844428	1	0.00787425
GTF2H1	-0.788830166	0.053833741	0.999999996	-1.152725526	0.00674735	0.999999996	-0.36389536
HUWE1	-1.257218042	0.002142485	0.999999817	-1.205818042	0.003067944	0.999999817	0.0514
GTF2H3	-1.258468818	0.003311299	1	-1.207175857	0.003468343	1	0.051292961
TONSL	-1.084045325	0.015216284	0.999999969	-1.299648315	0.006929571	0.999999969	-0.21560299
ERCC3	-1.2986242	0.005283572	0.999999988	-1.30640378	0.005283572	0.999999988	-0.00777958
UBA2	-1.305414106	0.003216039	1	-1.309865231	0.003216039	1	-0.004451125
SIN3A	-1.271089547	0.001289953	0.999999614	-1.336380532	0.001179733	0.999999614	-0.065290985
FANCD2	-1.316814696	0.005691331	0.999999968	-1.337736594	0.005691331	0.999999968	-0.020921898
PPP4C	-1.406453222	0.004950314	1	-1.35771761	0.007296962	1	0.048735611
DDX1	-1.320938371	0.001313713	1	-1.381278713	0.001067527	1	-0.060340342
TEN1	-2.140373648	9.97E-05	1	-1.422936264	0.006507468	1	0.717437384
UBE2T	-1.655701088	0.00159295	1	-1.433609433	0.002758927	1	0.222091656
APEX2	-1.562788136	4.97825E-04	1	-1.455040441	0.001166236	1	0.107747694
PPP6C	-1.387606335	2.98722E-04	1	-1.529751089	6.39E-05	1	-0.142144754

NELFB	-1.261256265	0.00158733	1	-1.551796828	0.00021724	1	-0.290540563
YBX1	-1.42193616	0.022518939	0.999992389	-1.650778084	0.010570368	0.999992389	-0.228841924
RFC5	-1.827748116	0.00031227	1	-1.88080396	0.00031227	1	-0.053055844
TCEB2	-1.694335472	0.005673604	1	-1.933593904	0.002100758	1	-0.239258432
SOD1	-1.90269645	6.62355E-04	1	-1.958146027	6.62355E-04	1	-0.055449577
NEDD8	-1.946809783	0.001163337	1	-2.594518288	7.17E-05	1	-0.647708504

Appendix Table 8 Raw data from JACKS analysis of combined WRN-/- clones

JACKS analysis of both RPE-1 WRN-/- knockouts combined. DMSO and 2nM CPT treated enrichments compared to day 14 control. fdr=false discovery rate.

Gene	Enrichment in DMSO treated	neg_fdr1	pos_fdr1	Enrichment in 2nM CPT treated	neg_fdr2	pos_fdr2	Difference in Enrichment
TP53	3.780649719	1	0	4.882959231	1	0	1.102309512
CAND1	3.71483349	1	0	2.397332707	1	0	-1.317500784
KEAP1	2.664762701	1	0	2.375701355	1	0	-0.289061346
RNF146	2.561658263	1	0	2.018131327	1	0	-0.543526936
PTEN	2.400244039	1	0	1.284624803	1	0	-1.115619236
H2AFZ	2.075238905	1	0	1.814288593	1	0	-0.260950312
CDKN1A	1.981593159	1	0	2.866886267	1	0	0.885293109
USP28	1.629193356	1	0	1.530397607	1	0	-0.098795749
THRAP3	1.574434371	1	0	1.261210653	1	1.77E-09	-0.313223719
DCUN1D3	1.525251596	1	0	1.326244967	1	0	-0.199006629
MAPKAPK2	1.433026426	1	0	1.22082305	1	3.20E-10	-0.212203376
HMGB1	1.420952668	0.994845796	0.04638784	0.805133723	0.994845796	0.304018437	-0.615818946
BRD7	1.414047873	1	0	1.397732382	1	1.15E-13	-0.016315491
SCAF4	1.380476377	1	0	0.581517162	1	9.32560E-04	-0.798959214
RNF7	1.3766905	1	0	1.048062627	1	1.50E-11	-0.328627873
CUL3	1.351041982	1	0	0.973057337	1	1.12E-12	-0.377984645
CUL5	1.345666481	1	0	1.158972336	1	7.21E-11	-0.186694146
PHIP	1.326156713	1	0	0.843872759	1	3.96E-06	-0.482283954
UBE2F	1.308285667	1	0	0.954460831	1	1.36E-08	-0.353824836
DCUN1D1	1.211584188	0.999999878	1.10E-06	0.853288222	0.999999878	0.001247478	-0.358295966
UBE2R2	1.147405648	1	1.80E-14	0.958229954	1	1.08E-08	-0.189175694
CHEK2	1.14285313	1	1.50E-14	1.668447564	1	0	0.525594434
GTF2H2	1.107164199	0.983875327	0.145122058	0.623143049	0.983875327	0.298260716	-0.484021151
SENP8	1.096096436	1	6.02E-10	0.556490357	1	0.010517296	-0.539606079
MDM2	1.077640404	0.999296181	0.004918483	1.012205373	0.999296181	0.004918483	-0.06543503
TP53BP1	1.076412296	1	8.99E-15	1.143918732	1	2.70E-12	0.067506437
ATM	1.070934019	1	2.20E-14	0.190049773	1	0.179495883	-0.880884246
BABAM1	1.059587988	1	9.09E-14	0.93035329	1	2.51E-09	-0.129234698
BCLAF1	1.056312331	1	2.58E-09	0.74306358	1	1.33712E-04	-0.313248751
ARID2	1.026393204	1	1.72E-11	1.141843247	1	5.66E-10	0.115450042
STAG2	0.925733828	0.999999998	1.68E-08	0.681305843	0.999999998	5.51359E-04	-0.244427985
SPTBN1	0.92352555	1	1.18E-11	0.799794767	1	7.57E-08	-0.123730783
TET2	0.868679723	0.999998163	1.65E-05	0.734337162	0.999998163	4.93467E-04	-0.134342561
UBE2K	0.86602612	1	5.33E-10	0.911106868	1	9.30E-09	0.045080748
RING1	0.860412284	1	3.16E-10	0.681559998	1	1.27E-05	-0.178852286
EP300	0.858144239	1	2.69E-09	0.545855075	1	0.001349538	-0.312289164
USP15	0.856921972	1	2.26E-09	0.705523916	1	1.28E-05	-0.151398056
APC	0.848068732	1	9.15E-13	0.852200408	1	5.15E-09	0.004131676
HDAC9	0.843939239	0.999999739	2.35E-06	0.589104319	0.999999739	0.002259987	-0.25483492
PBRM1	0.838419351	1	5.26E-10	1.153112979	1	4.16E-12	0.314693628
BRCC3	0.83648652	0.99999999	8.91E-08	0.557806123	0.99999999	0.003909831	-0.278680397
SHFM1	0.804097548	0.999991064	9.83826E-04	1.05601668	0.999991064	8.04E-05	0.251919132
SWI5	0.753642647	0.998147498	0.016672518	0.677646015	0.998147498	0.017408436	-0.075996632
GADD45G	0.747285192	0.999993748	3.24E-05	0.866979208	0.999993748	3.24E-05	0.119694016
RRM2B	0.743096063	0.999997564	2.19E-05	0.760344611	0.999997564	5.17E-05	0.017248548
ALKBH1	0.720454955	0.999961205	3.49156E-04	0.63961773	0.999961205	0.001822755	-0.080837225
BRE	0.720307951	0.999999447	4.98E-06	0.584352947	0.999999447	4.65350E-04	-0.135955004
NonTargetingC	0.70259513	0.99999849	1.36E-05	0.65319339	0.99999849	1.34198E-04	-0.04940174
NonTargetingC	0.692004312	0.999999994	5.83E-08	0.698904228	0.999999994	1.21E-05	0.006899916
NonTargetingC	0.67753482	0.999999893	9.60E-07	0.604846657	0.999999893	9.67E-05	-0.072688163
NonTargetingC	0.674066369	0.999999992	7.33E-08	0.685819306	0.999999992	2.88E-06	0.011752936
CDKN2A	0.666188865	0.999994328	5.11E-05	0.564315547	0.999994328	0.002634496	-0.101873318
FBXW7	0.665627843	0.999999997	2.26E-08	0.584264808	0.999999997	4.52E-06	-0.081363036
SMARCC1	0.660232787	0.999999991	4.92E-05	1.063346715	0.999999991	8.23E-08	0.403113928
GPI	0.655552422	0.999992441	6.80E-05	0.76658223	0.999992441	7.11E-05	0.111029807
PMP22	0.639085119	0.999994455	4.99E-05	0.587115184	0.999994455	0.001038143	-0.051969934
NonTargetingC	0.636888948	0.999999492	4.57E-06	0.55023286	0.999999492	6.42542E-04	-0.086656088
KMT5B	0.626968491	0.999968266	2.00202E-04	0.734895267	0.999968266	2.00202E-04	0.107926776
DCUN1D5	0.624999801	0.999889397	9.95428E-04	0.601770462	0.999889397	0.002315351	-0.023229339
TRIP12	0.62444937	0.999977382	2.03559E-04	0.369383832	0.999977382	0.080042355	-0.255065539
POLD3	0.621145838	0.999843055	0.0116702	1.035401475	0.999843055	0.001412508	0.414255637
DMC1	0.621051635	0.999556483	0.00399165	0.595023953	0.999556483	0.006828284	-0.026027682
LIG3	0.620940502	0.999904028	8.32202E-04	0.632635319	0.999904028	8.32202E-04	0.011694817
NonTargetingC	0.618577823	0.999999932	6.14E-07	0.683543433	0.999999932	1.23E-05	0.06496561
NonTargetingC	0.617473452	0.99999303	5.09E-05	0.690088401	0.99999303	5.09E-05	0.072614949
CDKN1B	0.61709428	0.999985514	1.30372E-04	0.577411957	0.999985514	0.001065661	-0.039682322
NonTargetingC	0.612021749	0.999999721	9.86E-05	0.867697389	0.999999721	2.51E-06	0.255675639
HNRNPUL2	0.610040971	0.999853973	0.001095076	0.691219338	0.999853973	0.001095076	0.081178367
CCND2	0.605520818	0.999700615	0.002694468	0.550500518	0.999700615	0.016504253	-0.055020301
BTG2	0.604172203	0.999849211	0.001357102	0.558642667	0.999849211	0.006648606	-0.045529536

SUPT5H	0.599016965	0.999366891	0.043557499	0.383837843	0.999366891	0.165792744	-0.215179121
POLK	0.595002737	0.999979036	1.88678E-04	0.497133746	0.999979036	0.004474451	-0.097868991
NonTargetingC	0.593831844	0.999998311	1.52E-05	0.501258018	0.999998311	0.001617568	-0.092573826
ABL1	0.593230388	0.999996573	3.08E-05	0.459653883	0.999996573	0.003047945	-0.133576505
MLH3	0.593204773	0.999862757	0.002090355	0.752323181	0.999862757	0.001235189	0.159118408
NonTargetingC	0.585254329	0.999999634	1.22E-05	0.763611874	0.999999634	3.29E-06	0.178357545
SF3B1	0.579396337	0.985254946	0.055963987	0.612393346	0.985254946	0.055963987	0.032997009
NonTargetingC	0.577477456	0.999988159	1.06571E-04	0.55961053	0.999988159	9.89499E-04	-0.017866926
NonTargetingC	0.577379538	0.999944922	4.95698E-04	0.635084653	0.999944922	6.02202E-04	0.057705115
APOBEC2	0.572565752	0.999739009	0.002348917	0.574366439	0.999739009	0.019162219	0.001800686
MAPK8	0.566340281	0.999525364	0.004271726	0.46250209	0.999525364	0.023054877	-0.103838191
NonTargetingC	0.566209689	0.999989034	6.56E-05	0.636497585	0.999989034	6.56E-05	0.070287896
APAF1	0.564224284	0.999769105	0.002078053	0.465141959	0.999769105	0.027624344	-0.099082325
ALKBH3	0.562823813	0.999874058	0.001002856	0.588225467	0.999874058	0.001002856	0.025401653
NonTargetingC	0.553759191	0.999998025	2.24E-05	0.681089059	0.999998025	1.78E-05	0.127329867
OPRM1	0.552603887	0.999960465	3.55817E-04	0.58495829	0.999960465	4.25577E-04	0.032354403
CCNC	0.546436096	0.999898713	9.11581E-04	0.498547821	0.999898713	0.005136349	-0.047888275
DTX4	0.545644156	0.999941958	5.22375E-04	0.361762644	0.999941958	0.039358656	-0.183881511
PML	0.545069654	0.999831852	9.13534E-04	0.651063165	0.999831852	9.13534E-04	0.105993511
POLM	0.540611668	0.999967463	2.92833E-04	0.35615257	0.999967463	0.066705271	-0.184459098
COPS7A	0.540010627	0.999970404	2.13912E-04	0.635992245	0.999970404	2.13912E-04	0.095981618
RNF138	0.534510623	0.999989483	9.47E-05	0.459899632	0.999989483	0.004480214	-0.074610991
CSNK2A2	0.532594871	0.999868116	0.001186958	0.544573956	0.999868116	0.003030681	0.011979086
POLR2J	0.532341188	0.996488758	0.031601176	0.351443951	0.996488758	0.151021882	-0.180897237
APLF	0.529142949	0.999572699	0.003845712	0.347901121	0.999572699	0.140914785	-0.181241828
NonTargetingC	0.529023829	0.999991775	5.93E-05	0.562528026	0.999991775	5.93E-05	0.033504198
RNF111	0.525412441	0.999944988	4.95109E-04	0.516009999	0.999944988	0.004738232	-0.009402442
HMGB2	0.522127063	0.999925107	6.74039E-04	0.399134148	0.999925107	0.023984364	-0.122992915
NonTargetingC	0.52075134	0.99991058	8.04781E-04	0.525905224	0.99991058	0.003421882	0.005153884
UBB	0.519589051	0.998261617	0.015645446	0.459802721	0.998261617	0.034310504	-0.059786329
NonTargetingC	0.516617099	0.99999086	8.23E-05	0.434920375	0.99999086	0.005591504	-0.081696724
NonTargetingC	0.505012743	0.999999115	7.96E-06	0.5327731	0.999999115	4.29E-05	0.027760358
NonTargetingC	0.503587214	0.999962639	2.70110E-04	0.539397878	0.999962639	2.70110E-04	0.035810664
USP51	0.501717557	0.999505252	0.004452736	0.360309703	0.999505252	0.114374938	-0.141407854
RAP1A	0.500532375	0.998612783	0.011681693	0.536763786	0.998612783	0.011681693	0.03623141
ASCC1	0.49811437	0.999128493	0.00594499	0.384261298	0.999128493	0.033274023	-0.113853071
ADH5	0.497604805	0.997682785	0.020854938	0.433824815	0.997682785	0.075431164	-0.06377999
UBE2V2	0.495062267	0.999897557	0.008744066	0.709706194	0.999897557	9.21987E-04	0.214643927
MUM1	0.492953984	0.998613554	0.012478017	0.404227019	0.998613554	0.079069859	-0.088726965
NonTargetingC	0.488759769	0.999913624	7.77386E-04	0.465584214	0.999913624	0.002495472	-0.023175555
PPP6R3	0.488312575	0.99966489	0.00301599	0.545409792	0.99966489	0.005075611	0.057097217
NonTargetingC	0.487240044	0.999981145	2.81435E-04	0.603360524	0.999981145	1.69695E-04	0.11612048
RNF2	0.486421736	0.999627895	0.003348943	0.397403402	0.999627895	0.044668243	-0.089018334
NonTargetingC	0.484884898	0.9999448	4.23622E-04	0.528295185	0.9999448	4.23622E-04	0.043410286
PRMT6	0.483663265	0.998934623	0.009588391	0.359151993	0.998934623	0.101765205	-0.124511273
SIRT7	0.482690951	0.999664558	0.008296838	0.679147777	0.999664558	0.00301898	0.196456826
NonTargetingC	0.480336807	0.99994745	4.72952E-04	0.39963753	0.99994745	0.007824834	-0.080699277
PARP14	0.475955977	0.999626837	0.003226101	0.546448914	0.999626837	0.003226101	0.070492937
CIB1	0.475729751	0.992548413	0.025260605	0.510048948	0.992548413	0.025260605	0.034319197
PER2	0.47495386	0.999727149	0.00339372	0.638425871	0.999727149	0.002455659	0.163472011
APOBEC3B	0.471566128	0.999967008	2.96928E-04	0.344691696	0.999967008	0.029337291	-0.126874432
NonTargetingC	0.469784036	0.999975913	2.16780E-04	0.48839396	0.999975913	0.001041003	0.018609924
NonTargetingC	0.465077379	0.999974703	2.25329E-04	0.555771499	0.999974703	2.25329E-04	0.09069412
NEK9	0.464138712	0.99995695	3.87452E-04	0.392599903	0.99995695	0.005484981	-0.071538808
MTA2	0.459937769	0.999859602	9.21074E-04	0.549706268	0.999859602	9.21074E-04	0.089768499
NonTargetingC	0.45962608	0.999963084	0.00114248	0.5735945	0.999963084	3.32241E-04	0.11396842
CUL4B	0.458145133	0.99947849	0.02373075	0.627326828	0.99947849	0.00469359	0.169181694
KDM4D	0.457881597	0.999517962	0.004285615	0.546130405	0.999517962	0.004285615	0.088248808
L3MBTL1	0.448549201	0.999081574	0.008265831	0.438369968	0.999081574	0.025714311	-0.010179234
UBE2D1	0.446005868	0.999939613	3.71956E-04	0.532087137	0.999939613	3.71956E-04	0.086081269
DTX3	0.445993898	0.999520968	0.004311289	0.462618887	0.999520968	0.004929058	0.016624989
RAD54L2	0.441613523	0.99939853	0.005413231	0.366415641	0.99939853	0.077274196	-0.075197882
PARP4	0.441207455	0.999779181	0.003532065	0.588376143	0.999779181	0.001987368	0.147168688
SPO11	0.440523093	0.999054627	0.008508354	0.39419453	0.999054627	0.03058186	-0.046328562
DCLRE1C	0.439258507	0.999665045	0.003014598	0.511329958	0.999665045	0.003039399	0.072071452
SMARCD1	0.439054503	0.999812917	8.99585E-04	0.477127937	0.999812917	8.99585E-04	0.038073433
GADD45A	0.438377593	0.999990609	3.44089E-04	0.58719145	0.999990609	8.45E-05	0.148813857
ATXN7	0.438054318	0.999322392	0.006098476	0.234934797	0.999322392	0.185430777	-0.203119521
NonTargetingC	0.435850165	0.999960589	3.54701E-04	0.294254513	0.999960589	0.074023295	-0.141595652
PPP4R4	0.434472337	0.999944276	5.01513E-04	0.333106255	0.999944276	0.020397537	-0.101366083
CUL7	0.433422121	0.999988816	0.012468535	0.63763587	0.999988816	1.00655E-04	0.204213749
MAPK14	0.432621729	0.999999645	0.031913612	1.051226212	0.999999645	3.19E-06	0.618604483
NonTargetingC	0.432438554	0.999534742	0.004187319	0.470671385	0.999534742	0.004846813	0.038232831
ENDOV	0.431718755	0.999296873	0.05576269	0.706112442	0.999296873	0.004744135	0.274393687
PHF3	0.429249272	0.999371961	0.005652352	0.24354206	0.999371961	0.143769059	-0.185707212
ETAA1	0.425787409	0.999902643	8.76214E-04	0.460235881	0.999902643	0.001088294	0.034448472
PARPBP	0.424973272	0.997597669	0.015217751	0.451113463	0.997597669	0.015217751	0.026140191
TOP3B	0.424643615	0.997428561	0.014521913	0.453857253	0.997428561	0.014521913	0.029213638
NonTargetingC	0.424113318	0.999895055	9.44504E-04	0.24491873	0.999895055	0.148125069	-0.179194588
NonTargetingC	0.422820494	0.999971942	2.52520E-04	0.469815113	0.999971942	4.41038E-04	0.046994619
SSBP3	0.421469778	0.993437983	0.043362548	0.443163633	0.993437983	0.043362548	0.021693855
UBE2V1	0.420652204	0.994675609	0.047919518	0.401848007	0.994675609	0.098856355	-0.018804197

SCAI	0.420522941	0.999862613	8.99863E-04	0.47343267	0.999862613	8.99863E-04	0.052909728
NonTargetingC	0.420055402	0.999971612	3.34138E-04	0.534444927	0.999971612	2.55488E-04	0.114389524
CSNK1D	0.419082963	0.998727585	0.008019149	0.392565503	0.998727585	0.008019149	-0.02651746
OR1E1	0.413202416	0.985974094	0.126233158	0.211729227	0.985974094	0.248132441	-0.201473189
NonTargetingC	0.411416588	0.999854713	0.001307583	0.407017463	0.999854713	0.011271617	-0.004399126
PRKCG	0.410102594	0.999019977	0.00464534	0.426009496	0.999019977	0.00464534	0.015906902
CDC25A	0.408003566	0.999910282	0.008634941	0.637391526	0.999910282	8.07461E-04	0.229387961
NonTargetingC	0.40757624	0.999695194	0.002743251	0.455177167	0.999695194	0.002987649	0.047600927
DCUN1D4	0.40680066	0.997906465	0.018841813	0.28593611	0.997906465	0.173372281	-0.12086455
DTX3L	0.405785974	0.99393549	0.054580589	0.31124357	0.99393549	0.218128527	-0.094542404
ATXN3	0.404211008	0.999887003	0.001016977	0.398205588	0.999887003	0.00727392	-0.00600542
NonTargetingC	0.397068013	0.99983586	0.001477259	0.330735188	0.99983586	0.013059877	-0.066332825
NonTargetingC	0.396289499	0.999823905	0.001584858	0.408618897	0.999823905	0.001635808	0.012329398
SMC1B	0.395636349	0.999741633	0.002325299	0.268317428	0.999741633	0.179939828	-0.127318922
DNTT	0.395335601	0.999905117	0.021585552	0.669130393	0.999905117	8.53944E-04	0.273794792
PARP15	0.392727398	0.998960655	0.009475103	0.490895442	0.998960655	0.009354107	0.098168044
COPS7B	0.392335746	0.999189187	0.007297314	0.30570364	0.999189187	0.093333243	-0.086632105
USP13	0.391000319	0.999322517	0.005109626	0.484376913	0.999322517	0.005109626	0.093376595
NonTargetingC	0.389232728	0.999748986	0.002259127	0.344988384	0.999748986	0.031354421	-0.044244344
SIRT2	0.388601478	0.996559267	0.030678412	0.526506191	0.996559267	0.030678412	0.137904713
EME2	0.388490505	0.998886994	0.052980102	0.694460128	0.998886994	0.01001705	0.305969623
NonTargetingC	0.388253539	0.999838243	0.00125695	0.474133612	0.999838243	0.00125695	0.085880073
HUS1B	0.388115183	0.999041355	0.004398793	0.434485439	0.999041355	0.004398793	0.046370256
FAM175A	0.387743296	0.987271407	0.093731501	0.427498771	0.987271407	0.093731501	0.039755475
CSNK1E	0.385829527	0.996433343	0.0209335	0.414738216	0.996433343	0.0209335	0.028908689
MBD4	0.38429344	0.99826714	0.01559574	0.286849987	0.99826714	0.124263594	-0.097443453
NonTargetingC	0.382843694	0.999257052	0.004565265	0.435331252	0.999257052	0.004565265	0.052487558
CCND3	0.381878377	0.99943543	0.00508113	0.368383988	0.99943543	0.014618537	-0.01349439
NonTargetingC	0.381707216	0.999499894	0.004500951	0.383985712	0.999499894	0.012446087	0.002278496
VCP	0.380663469	0.999408308	0.115960073	0.445378003	0.999408308	0.115960073	0.064714534
PARP9	0.380135273	0.997612841	0.02148443	0.292829225	0.997612841	0.116161208	-0.087306048
NABP2	0.379958104	0.995463463	0.040828833	0.401198838	0.995463463	0.053278296	0.021240734
KMT5C	0.377729386	0.999795972	0.002133781	0.468576244	0.999795972	0.00183625	0.090846858
PARP3	0.377534789	0.999043034	0.008612698	0.364711571	0.999043034	0.014761129	-0.012823218
TPP1	0.374375486	0.998535295	0.033884411	0.52196074	0.998535295	0.013182345	0.147585254
RASSF7	0.373452444	0.997777622	0.016291481	0.478504465	0.997777622	0.016291481	0.105052021
NonTargetingC	0.373050855	0.997641235	0.021228882	0.355295326	0.997641235	0.037950373	-0.017755529
HMGN1	0.372967155	0.991290138	0.07502529	0.494512239	0.991290138	0.07502529	0.121545084
NonTargetingC	0.371211128	0.998182876	0.016354114	0.204345213	0.998182876	0.282525502	-0.166865915
NonTargetingC	0.371181524	0.99906883	0.008380531	0.332940118	0.99906883	0.030198034	-0.038241405
NonTargetingC	0.370487942	0.999896743	0.004318142	0.487847147	0.999896743	9.29316E-04	0.117359206
BRCA2	0.370112981	0.996405184	0.042518312	0.315360738	0.996405184	0.056377273	-0.054752243
NonTargetingC	0.367605282	0.998153711	0.01006237	0.403316133	0.998153711	0.01006237	0.035710851
NonTargetingC	0.36658831	0.999427371	0.005153663	0.298052854	0.999427371	0.086884385	-0.068535456
MORF4L1	0.363938231	0.994177809	0.067987997	0.486329144	0.994177809	0.052399719	0.122390913
NonTargetingC	0.362734997	0.999049499	0.006297343	0.406441463	0.999049499	0.006297343	0.043706465
KLHL15	0.360490538	0.992613477	0.066478705	0.37644078	0.992613477	0.0844281	0.015950242
ERCC6L	0.358707564	0.995790705	0.213520175	0.049922004	0.995790705	0.555695391	-0.30878556
NonTargetingC	0.357578289	0.999245228	0.003725956	0.424121648	0.999245228	0.003725956	0.066543359
XPA	0.357339003	0.993392091	0.059471178	0.141780998	0.954356687	0.428896985	-0.215558005
HNRNPK	0.356378549	0.998457502	0.261427864	-0.015565502	0.998457502	0.62563868	-0.371944051
NonTargetingC	0.355844712	0.999451714	0.004934576	0.334330826	0.999451714	0.023971943	-0.021513886
USP20	0.355692311	0.997002414	0.026978272	0.286162769	0.997002414	0.162864684	-0.069529542
APBB1	0.355131855	0.998373594	0.014637654	0.354006385	0.998373594	0.015964916	-0.00112547
CETN2	0.35460406	0.995655769	0.039098081	0.068307935	0.995655769	0.37745133	-0.286296125
SIRT5	0.354220257	0.999831869	0.013453383	0.516763721	0.999831869	0.00151318	0.162543464
BMI1	0.352369933	0.997754667	0.020207996	0.204463573	0.997754667	0.308308753	-0.14790636
DCLRE1A	0.351353819	0.999578127	0.037537926	0.635528611	0.999578127	0.003796861	0.284174792
NonTargetingC	0.350770169	0.998830219	0.010528025	0.271999942	0.998830219	0.092824935	-0.078770227
MTA3	0.348877561	0.998930186	0.028972608	0.497897982	0.998930186	0.009628326	0.149020422
NonTargetingC	0.348404496	0.999344463	0.005899834	0.358950532	0.999344463	0.012576335	0.010546036
WRNIP1	0.34775209	0.995688479	0.038803687	0.279885654	0.995688479	0.068674602	-0.067866436
EID3	0.345537235	0.993920362	0.033445914	0.454098837	0.993920362	0.033445914	0.108561601
NonTargetingC	0.345091361	0.999346524	0.005881284	0.352098914	0.999346524	0.014500667	0.007007552
SSBP2	0.344780471	0.999223979	0.005553309	0.440524355	0.999223979	0.005553309	0.095743884
SETDB1	0.338835545	0.99959465	0.025967371	0.530761453	0.99959465	0.003648154	0.191925909
NonTargetingC	0.336333096	0.999028141	0.008746729	0.373952829	0.999028141	0.011058207	0.037619733
FAN1	0.334292717	0.997111193	0.04354769	0.445414878	0.997111193	0.025999263	0.111122161
NonTargetingC	0.33273271	0.995789702	0.03789268	0.317835317	0.995789702	0.064401746	-0.014897393
NonTargetingC	0.332020731	0.998422901	0.014193895	0.235994229	0.998422901	0.167837849	-0.096026502
FBXO18	0.331325496	0.999245999	0.016078336	0.446257693	0.999245999	0.006786008	0.114932198
NonTargetingC	0.330069122	0.998153433	0.008364475	0.400529292	0.998153433	0.008364475	0.07046017
NonTargetingC	0.327650085	0.998943602	0.007157745	0.391017486	0.998943602	0.007157745	0.063367401
XPC	0.326291855	0.991484933	0.073349615	0.363972356	0.991484933	0.073349615	0.037680501
NonTargetingC	0.325914855	0.999117535	0.007942183	0.380848028	0.999117535	0.009004957	0.054933173
TEP1	0.324913872	0.9949726	0.039248942	0.273729046	0.9949726	0.060813472	-0.051184827
APOBEC3C	0.322713832	0.995992372	0.024509088	0.341754004	0.995992372	0.024509088	0.019040172
SMARCC2	0.322416404	0.997555566	0.035640779	0.414638668	0.997555566	0.021999903	0.092222264
NonTargetingC	0.322082532	0.998717176	0.011545412	0.193601174	0.998717176	0.224472566	-0.128481358
NonTargetingC	0.320907077	0.998539304	0.010744462	0.391545649	0.998539304	0.010744462	0.070638572
ASF1A	0.319272519	0.992322994	0.052847818	0.281847308	0.992322994	0.078059183	-0.037425211
PER1	0.31881728	0.990077097	0.046747196	0.370799589	0.990077097	0.046747196	0.051982309

POLN	0.318643353	0.999765812	0.036343344	0.53615097	0.999765812	0.002107696	0.217507617
USP47	0.318408794	0.996708864	0.029620225	0.2157136	0.996708864	0.287164197	-0.102695194
MGMT	0.317540213	0.992856975	0.099133255	0.455019015	0.992856975	0.064287229	0.137478802
NOTCH1	0.316544751	0.99799131	0.018078207	0.333733918	0.99799131	0.029665091	0.017189167
NonTargetingC	0.31491605	0.993980969	0.047783905	0.39284619	0.993980969	0.047783905	0.07793014
TRIM29	0.31386602	0.983559316	0.100666804	0.33745407	0.983559316	0.100666804	0.02358805
DCUN1D2	0.312723456	0.984290555	0.141385004	0.177600562	0.967274579	0.312938999	-0.135122894
XRCC5	0.309914669	0.986959415	0.107422336	0.323023533	0.986959415	0.107422336	0.013108863
NEK8	0.309596514	0.999004224	0.042093234	0.474675121	0.999004224	0.008961985	0.165078608
KAT2B	0.307057539	0.998273194	0.028104344	0.389908742	0.998273194	0.015541253	0.082851204
NonTargetingC	0.306757887	0.99765574	0.021098336	0.310791598	0.99765574	0.04698073	0.004033711
RAD54B	0.304162007	0.984425058	0.140174476	0.274528116	0.984425058	0.177073626	-0.029633892
NonTargetingC	0.302522343	0.999287288	0.006414411	0.311348573	0.999287288	0.014131042	0.008826231
WHSC1	0.302353485	0.984510192	0.139408268	0.216286702	0.984510192	0.413699041	-0.086066783
CHFR	0.301523902	0.999662265	0.153952361	0.615694513	0.999662265	0.003039611	0.314170611
NEIL1	0.301168815	0.967157443	0.189189276	0.265750256	0.967157443	0.189189276	-0.03541856
HFM1	0.30109423	0.993815046	0.055664585	0.217983263	0.993815046	0.251415801	-0.083110967
APEX1	0.300810019	0.986387666	0.065603277	0.360220973	0.986387666	0.065603277	0.059410954
RECQL	0.298974779	0.991266977	0.078597211	0.140569235	0.991266977	0.2470642	-0.158405544
CDKN2D	0.298209479	0.997688613	0.042023876	0.437850069	0.997688613	0.020802479	0.13964059
RAD18	0.298142599	0.998249125	0.050929143	0.450371639	0.998249125	0.015757876	0.15222904
OTUB2	0.297765795	0.999750694	0.037376045	0.548732809	0.999750694	0.002243756	0.250967013
NonTargetingC	0.295640379	0.999829527	0.034993675	0.528281388	0.999829527	0.001534256	0.232641009
INO80D	0.293555004	0.995796808	0.030140106	0.374182358	0.995796808	0.030140106	0.080627354
CCNB3	0.293298687	0.999788155	0.022138254	0.456908576	0.999788155	0.001906605	0.16360989
HELB	0.29299867	0.99823044	0.106849088	0.538636834	0.99823044	0.015926043	0.245638164
CHD1L	0.292987055	0.999838881	0.073850499	0.5300549	0.999838881	0.001450073	0.237067845
UBE2W	0.292891339	0.991327705	0.029563568	0.364210194	0.991327705	0.029246599	0.071318855
NonTargetingC	0.29231445	0.997856576	0.03606656	0.392809727	0.997856576	0.019290817	0.100495276
SETX	0.291782851	0.956660985	0.104585117	0.317566368	0.956660985	0.104585117	0.025783517
SUV39H2	0.2903352	0.994902355	0.045878801	0.290941911	0.994902355	0.061952346	6.06712E-04
SETMAR	0.290158846	0.987364155	0.113722601	0.265677857	0.987364155	0.185355033	-0.024480989
SUMO3	0.284507942	0.994900124	0.058241085	0.414948814	0.994900124	0.045898881	0.130440871
H2AFY	0.284487746	0.985621785	0.147696522	0.36418835	0.985621785	0.129403932	0.079700604
APOBEC3D	0.283831042	0.974141819	0.179150259	0.298232319	0.974141819	0.179150259	0.014401276
RBM7	0.282116241	0.988203047	0.063805676	0.306439256	0.988203047	0.063805676	0.024323015
CCNO	0.281015056	0.98679286	0.11886426	0.340015929	0.98679286	0.175819175	0.059000873
ATF2	0.27989972	0.990828682	0.045309388	0.325797682	0.990828682	0.045309388	0.045897962
NOTCH3	0.279051841	0.994536715	0.049169561	0.237636011	0.994536715	0.114422057	-0.04141583
NonTargetingC	0.278342969	0.995299415	0.042305269	0.207110735	0.995299415	0.196013782	-0.071232233
SIRT1	0.278034755	0.999600581	0.081784444	0.469954879	0.999600581	0.003594773	0.191920124
NBN	0.276836002	0.987415375	0.113261628	-0.060881643	0.724451774	0.937556694	-0.337717644
CHD3	0.273891523	0.991912216	0.048094907	0.436939112	0.991912216	0.028208578	0.16304759
MBTD1	0.273463496	0.982125174	0.160873438	0.222705313	0.982125174	0.290413856	-0.050758182
DDB2	0.2731059	0.968589624	0.160772799	0.273755276	0.968589624	0.160772799	6.49376E-04
RHNO1	0.270739638	0.976984352	0.179474098	0.389184167	0.976984352	0.179474098	0.11844453
SALL4	0.269472786	0.991028909	0.066567689	0.342949621	0.991028909	0.066567689	0.073476835
EYA1	0.268738498	0.990056724	0.085153923	0.195426153	0.990056724	0.132520655	-0.073312345
SCAF11	0.26811892	0.986336654	0.065113885	0.079104103	0.986336654	0.377734284	-0.189014818
HDAC10	0.267719267	0.997973562	0.059408089	0.428646326	0.997973562	0.018237943	0.160927059
CHTF18	0.267446266	0.982124975	0.268635277	0.418264792	0.982124975	0.160875227	0.150818525
CCNB2	0.264641371	0.989274411	0.06775385	0.304612589	0.989274411	0.06775385	0.039971218
PIAS2	0.264414624	0.972756723	0.160096169	0.272418686	0.972756723	0.160096169	0.008004062
EXD2	0.260114925	0.986875983	0.118116153	0.11481086	0.986875983	0.445430619	-0.145304065
ALDH2	0.258837975	0.97275521	0.153001844	0.288262464	0.97275521	0.153001844	0.029424489
ALKBH2	0.255972649	0.987312972	0.123447394	0.411091039	0.987312972	0.11418325	0.15511839
UBE2B	0.255472975	0.967780942	0.289971524	0.233775701	0.967780942	0.304857666	-0.021697274
NFATC2IP	0.252042261	0.947512601	0.218206324	0.121382344	0.947512601	0.275703548	-0.130659917
NonTargetingC	0.248729409	0.990797611	0.082821504	0.251502022	0.990797611	0.09384638	0.002772613
IP6K3	0.24869553	0.985510177	0.261311076	0.366627851	0.985510177	0.130408409	0.117932321
USP26	0.247892988	0.977805328	0.149971481	0.264518575	0.977805328	0.149971481	0.016625587
RNF126	0.246198189	0.98261248	0.109412227	0.251276394	0.98261248	0.164481931	0.005078205
UBE2A	0.246079362	0.966338213	0.202457118	0.226299418	0.966338213	0.215018048	-0.019779944
SENP2	0.246070925	0.974847315	0.146240917	0.264530422	0.974847315	0.146240917	0.018459497
POLB	0.244658146	0.978148625	0.174796863	0.265622816	0.978148625	0.174796863	0.02096467
UCHL3	0.24363087	0.990060866	0.101431848	0.374510574	0.990060866	0.089452209	0.130879705
MSH4	0.242499292	0.993583438	0.109662339	0.354194538	0.993583438	0.057749062	0.111695246
ANKRD44	0.242222142	0.998536699	0.082898651	0.391287426	0.998536699	0.013169709	0.149065284
PARK7	0.242084991	0.994823768	0.093968135	0.397829964	0.994823768	0.046586084	0.155744973
PRIMPOL	0.242040708	0.97661071	0.210503611	0.17725626	0.97661071	0.334150094	-0.064784448
HPF1	0.241950447	0.95693271	0.387605613	-0.041836997	0.942247654	0.598148943	-0.283787444
TREX1	0.241874686	0.968436391	0.22084864	0.284359476	0.968436391	0.22084864	0.042484789
NLK	0.241516324	0.981217976	0.164190091	0.23979725	0.981217976	0.164190091	-0.001719074
TYMS	0.240775365	0.989232021	0.11574737	0.365677549	0.989232021	0.096911808	0.124902184
TP63	0.240091417	0.982719463	0.090971624	0.275620695	0.982719463	0.090971624	0.035529278
NonTargetingC	0.239816851	0.985115366	0.133961703	0.225228609	0.985115366	0.177444699	-0.014588243
AMN1	0.239650803	0.99801046	0.076797633	0.39469997	0.99801046	0.01790586	0.155049168
SUMO4	0.239471242	0.958853859	0.153849462	0.336405766	0.958853859	0.147639042	0.096934524
ARID1B	0.239336629	0.970376264	0.161373934	0.299220747	0.970376264	0.161373934	0.059884118
NonTargetingC	0.238327345	0.984970515	0.135265368	0.213970822	0.984970515	0.207121895	-0.024356522
POLL	0.236422868	0.995018218	0.159188182	0.179110228	0.995018218	0.277494893	-0.057312641
PMS2P3	0.236185822	0.943456195	0.238305977	0.306158536	0.943456195	0.238305977	0.069972713

ATP23	0.235994159	0.941599552	0.274281335	0.070621624	0.941599552	0.436241072	-0.165372535
MSH2	0.233902642	0.974192869	0.177064168	0.308988389	0.974192869	0.177064168	0.075085747
NonTargetingC	0.231359382	0.980263038	0.177632659	0.200372817	0.980263038	0.272549319	-0.030986565
USP45	0.229490877	0.96395309	0.324422189	0.190311299	0.96395309	0.348616929	-0.039179579
OTUD7B	0.227653101	0.966178755	0.232707468	0.224016278	0.966178755	0.232707468	-0.003636823
NonTargetingC	0.22727685	0.990930841	0.081622427	0.221574407	0.990930841	0.119824781	-0.005702443
UBA3	0.227110791	0.994051665	0.225515477	0.194253218	0.994051665	0.225515477	-0.032857572
CASP3	0.226501624	0.92594083	0.457113336	0.108437048	0.92594083	0.457113336	-0.118064576
RAG1	0.223570868	0.998190338	0.160315949	0.428302169	0.998190338	0.016286954	0.204731302
PHF11	0.222249927	0.968480013	0.154324222	0.273383743	0.968480013	0.154324222	0.051133816
PMS1	0.221985715	0.978795846	0.134546777	0.29158645	0.978795846	0.134546777	0.069600735
NABP1	0.221793017	0.959632317	0.345913405	0.19988208	0.959632317	0.345913405	-0.021910938
SLF1	0.220285557	0.957297648	0.306099134	0.245619091	0.957297648	0.306099134	0.025333535
USP11	0.217504752	0.977479353	0.153262321	0.286116402	0.977479353	0.153262321	0.068611651
MCM10	0.215114907	0.90263807	0.293246413	0.149431244	0.90263807	0.293246413	-0.065683663
APOBEC3A	0.215090634	0.949371552	0.238896378	0.274141769	0.949371552	0.238896378	0.059051135
NonTargetingC	0.215052384	0.995893787	0.201545788	0.366193733	0.995893787	0.036955918	0.151141349
CCNE1	0.214694849	0.972601188	0.146505559	0.264904043	0.972601188	0.146505559	0.050209194
CDC34	0.209531106	0.946296811	0.317670536	0.153817668	0.943082939	0.317670536	-0.055713438
PARP2	0.208953479	0.943985904	0.297513822	0.211901002	0.943985904	0.297513822	0.002947523
NonTargetingC	0.208693395	0.995046821	0.136350417	0.324611356	0.995046821	0.044578614	0.115917961
INO80C	0.207558446	0.99225101	0.187459633	0.371020118	0.99225101	0.069740913	0.163461671
SLF2	0.205178958	0.968887803	0.156328463	0.221612245	0.968887803	0.156328463	0.016433287
EME1	0.203600489	0.900026124	0.209613513	0.211420226	0.900026124	0.209613513	0.007819737
REV1	0.202925071	0.951147894	0.271200076	0.241681523	0.951147894	0.271200076	0.038756452
RAG2	0.200055096	0.937786552	0.240309256	0.258659168	0.937786552	0.240309256	0.058604073
CLK2	0.198658705	0.937955813	0.278473867	0.262170316	0.937955813	0.278473867	0.06351161
TNP1	0.197293209	0.962981376	0.371141252	0.318391006	0.962981376	0.333167618	0.121097798
WDR76	0.196970169	0.892541247	0.274239745	0.224860815	0.892541247	0.274239745	0.027890646
PMS2	0.195093203	0.962221154	0.15340566	0.13657562	0.962221154	0.340576221	-0.058517583
ZRANB3	0.194522664	0.938815439	0.384695382	0.098666971	0.858872109	0.384695382	-0.095855693
C9orf142	0.193324192	0.955815087	0.316585533	0.271802852	0.955815087	0.316585533	0.07847866
UHRF2	0.193013849	0.933087821	0.456677267	0.066623524	0.933087821	0.456677267	-0.126390324
NTHL1	0.18867166	0.931538222	0.38384766	0.233612229	0.931538222	0.38384766	0.044940569
MSH3	0.186463019	0.986451479	0.247644469	0.320912521	0.986451479	0.121936687	0.134449502
TIPIN	0.183204973	0.889867239	0.384848746	0.265142106	0.889867239	0.384848746	0.081937132
TREX2	0.183004734	0.89181467	0.529610279	0.12557543	0.89181467	0.529610279	-0.057429304
POLG2	0.180518051	0.981114272	0.343501744	0.311396422	0.981114272	0.169971554	0.130878371
SIRT3	0.178576941	0.979592947	0.233911855	0.292432662	0.979592947	0.183663475	0.113855722
PRDM9	0.17826664	0.943546646	0.34954151	0.20412231	0.943546646	0.34954151	0.025855671
WRN	0.177266638	0.936131005	0.40821908	0.151011892	0.936131005	0.40821908	-0.026254747
SMARCAD1	0.174777969	0.936207121	0.473019693	-0.017353946	0.902049214	0.622217972	-0.192131915
SCAF8	0.171836859	0.997827855	0.168020195	0.40334465	0.997827855	0.019549306	0.231507791
PIAS3	0.17155595	0.958700981	0.316221072	0.251899811	0.958700981	0.316221072	0.080343861
KDM1A	0.16823756	0.935769267	0.48560199	0.253609091	0.935769267	0.48560199	0.085371531
USP3	0.167786814	0.917147685	0.449800464	0.043360556	0.90412076	0.449800464	-0.124426258
COL21A1	0.167778746	0.921825514	0.428542352	0.119986131	0.921825514	0.428542352	-0.047792615
RPA4	0.167017561	0.926587876	0.347017442	0.181410584	0.926587876	0.347017442	0.014393024
NOTCH4	0.166960522	0.977380485	0.170484673	0.266921016	0.977380485	0.170484673	0.099960495
UBE2NL	0.166633867	0.944566022	0.279276013	0.251374784	0.944566022	0.279276013	0.084740917
NonTargetingC	0.165261062	0.966373778	0.202973428	0.213548714	0.966373778	0.202973428	0.048287652
APOBEC3H	0.162242019	0.904946719	0.402261229	0.095607824	0.843921742	0.402261229	-0.066634195
AICDA	0.161501069	0.884412741	0.47259631	0.138016618	0.884412741	0.47259631	-0.023484452
APOBEC3F	0.159174248	0.96743583	0.35574373	0.314082977	0.96743583	0.293077531	0.154908729
PSIP1	0.156430306	0.93413416	0.407987723	0.211061805	0.93413416	0.407987723	0.054631499
UIMC1	0.154384826	0.883241569	0.390302293	0.098556143	0.861488402	0.390302293	-0.055828683
NonTargetingC	0.153967297	0.963105599	0.390496479	0.24093281	0.963105599	0.332049606	0.086965513
ANP32E	0.153300459	0.877808356	0.388795789	0.187589064	0.877808356	0.388795789	0.034288606
ANKRD28	0.152893569	0.964281934	0.377704218	0.251201613	0.964281934	0.321462594	0.098308043
PPP4R3B	0.151566138	0.993541008	0.289907362	0.124838129	0.993541008	0.41143344	-0.026728009
NonTargetingC	0.151342002	0.965584874	0.357298286	0.221640334	0.965584874	0.309736136	0.070298332
CCNA1	0.150725106	0.89570662	0.598707029	-0.098121843	0.810951228	0.772818133	-0.248846949
SIRT4	0.149045264	0.909510653	0.309220548	0.152027514	0.909510653	0.309220548	0.00298225
ERCC6L2	0.148076626	0.872367225	0.646306863	0.107302968	0.872367225	0.646306863	-0.040773658
RAD9B	0.147544194	0.907235566	0.334368469	0.192702924	0.907235566	0.334368469	0.045158729
SMUG1	0.1472134	0.926775706	0.400235835	0.248068567	0.926775706	0.400235835	0.100855166
MDM4	0.146831288	0.999708607	0.287065518	0.261281725	0.999708607	0.168291238	0.114450438
NonTargetingC	0.146573353	0.939658178	0.359655223	0.216129305	0.939658178	0.359655223	0.069555952
APTX	0.144711795	0.902305794	0.297388906	0.161522247	0.902305794	0.297388906	0.016810452
HDAC4	0.143203584	0.973538072	0.386053811	0.245737917	0.973538072	0.238157352	0.102534333
TDP1	0.142542786	0.868239207	0.538929836	0.097960217	0.868239207	0.673210986	-0.044582569
NEIL3	0.142031465	0.896172364	0.459576238	0.027930553	0.830465663	0.467663953	-0.114100912
RBX1	0.141672537	0.98131896	0.425444544	-0.148053283	0.98131896	0.794602751	-0.28972582
APOBEC3G	0.140118289	0.90021691	0.404673257	0.050768097	0.800085083	0.404673257	-0.089350192
UBE2D4	0.138821871	0.907990743	0.308397143	0.104870014	0.907990743	0.395428014	-0.033951857
HDAC2	0.1370304	0.869520373	0.350883165	0.115575604	0.869520373	0.350883165	-0.021454797
TOP2B	0.135564847	0.894281573	0.408842915	0.117990479	0.894281573	0.517418298	-0.017574368
RBBP7	0.135333979	0.976664116	0.33148424	0.301965475	0.976664116	0.210022957	0.166631496
RAD51AP1	0.132745745	0.853380663	0.405176852	0.018187688	0.853380663	0.509234634	-0.114558058
NUDT16L1	0.131287501	0.821254066	0.439119507	0.046686767	0.821254066	0.439119507	-0.084600733
CRY2	0.129611472	0.8956699	0.466013717	0.172439114	0.8956699	0.466013717	0.042827643
BLM	0.129371988	0.840181435	0.436421852	0.13648684	0.840181435	0.436421852	0.007114852

SENP7	0.123584502	0.8161503	0.467620277	0.056526078	0.8161503	0.467620277	-0.067058424
NUDT1	0.122611348	0.946357521	0.275364442	0.325970243	0.946357521	0.243187598	0.203358895
SETD2	0.121207959	0.99309399	0.513673877	0.426999537	0.99309399	0.062154088	0.305791578
PXMP2	0.120340814	0.923308842	0.444325346	0.215942139	0.923308842	0.444325346	0.095601326
UBE2D2	0.118536728	0.926997804	0.271229486	0.382316171	0.992420459	0.068215873	0.263779443
RNF169	0.117617402	0.972630813	0.414805696	0.30086676	0.972630813	0.246322687	0.183249359
ASF1B	0.116777237	0.852870623	0.479460419	0.051367014	0.852870623	0.479460419	-0.065410223
PPP5C	0.110552053	0.956631895	0.442428591	0.281103806	0.973158705	0.241571653	0.170551753
ERCC5	0.103642324	0.848849287	0.480513536	0.057582936	0.788299656	0.480513536	-0.046059388
RECQL5	0.102736796	0.807844349	0.447635835	0.08806141	0.807844349	0.447635835	-0.014675385
POLH	0.102428561	0.817609978	0.414541812	0.1000875	0.817609978	0.414541812	-0.002341061
NonTargetingC	0.101472603	0.9463425	0.377586763	0.20227871	0.9463425	0.377586763	0.100806107
CRY1	0.1010152	0.920529515	0.580422196	0.223529528	0.964071396	0.32335744	0.122514328
DLGAP5	0.100321714	0.886341913	0.404700279	0.097130312	0.886341913	0.404700279	-0.003191402
CENPX	0.098720051	0.828940722	0.621083846	0.083969871	0.828940722	0.621083846	-0.014750179
SUMO1	0.097856858	0.848506551	0.352701213	0.142370419	0.848506551	0.352701213	0.04451356
HDAC1	0.096414509	0.853806783	0.358107678	0.154248431	0.853806783	0.358107678	0.057833922
HNRNPUL1	0.096412513	0.981160424	0.345787108	0.320727583	0.981160424	0.169556184	0.22431507
NonTargetingC	0.095661587	0.90585647	0.570687847	0.163250246	0.90585647	0.570687847	0.067588659
PPP4R1	0.095560872	0.856665652	0.489049591	0.147535793	0.856665652	0.489049591	0.051974921
MORF4L2	0.094237103	0.909420079	0.494279508	0.177075585	0.909420079	0.401249076	0.082838482
HLTF	0.093128655	0.842836197	0.400106702	0.06514597	0.842836197	0.400106702	-0.027982685
SIRT6	0.091291004	0.933946592	0.459625065	0.114097657	0.933946592	0.459625065	0.022806653
ZSWIM7	0.08698657	0.743131832	0.724270237	0.041751048	0.743131832	0.724270237	-0.045235522
H3F3A	0.086270988	0.576658748	0.533961199	-0.004415697	0.576658748	0.533961199	-0.090686685
POLI	0.086103946	0.870502638	0.359127809	0.092447095	0.870502638	0.359127809	0.006343149
PNN	0.083741379	0.997902515	0.399103118	0.157535298	0.997902515	0.399103118	0.073793919
GEN1	0.083582114	0.754153117	0.671192216	-0.176486198	0.754153117	0.864396786	-0.260068312
ERCC6	0.082830531	0.742080257	0.461681238	0.092587625	0.742080257	0.461681238	0.009757094
MLH1	0.082806956	0.942751324	0.556658798	0.275851238	0.955400396	0.401396437	0.193044282
PMS2P5	0.074679353	0.642106223	0.567006492	-0.116507271	0.642106223	0.567006492	-0.191186623
NonTargetingC	0.074084781	0.860063864	0.436971171	0.048634142	0.860063864	0.436971171	-0.025450639
SMARCA4	0.072900555	0.921918975	0.377932557	0.198592881	0.921918975	0.339227283	0.125692327
RAD52	0.072831603	0.728971579	0.559429461	0.052162223	0.728971579	0.559429461	-0.020669381
RFC1	0.071794516	0.870530865	0.493337784	0.108414506	0.870530865	0.493337784	0.03661999
CBX5	0.07170902	0.913303254	0.48031268	0.104542209	0.913303254	0.48031268	0.032833189
SSBP1	0.071095589	0.828033245	0.733551418	0.153453365	0.860183173	0.733551418	0.082357776
RHO	0.071087397	0.867938538	0.43694721	0.166538785	0.909660554	0.43694721	0.095451389
NEIL2	0.071063685	0.900745624	0.380534521	0.181492715	0.900745624	0.319866714	0.11042903
COL1A1	0.070699394	0.911479638	0.561336024	-0.04826752	0.911479638	0.616873471	-0.118966914
SMARCA2	0.070306953	0.964445153	0.590235601	0.322357521	0.974002741	0.233975331	0.252050568
KMT5A	0.069522462	0.741562051	0.574073591	0.153058425	0.741562051	0.574073591	0.083535963
SHPRH	0.067273972	0.726763686	0.552152367	0.047209532	0.726763686	0.552152367	-0.020064439
MVP	0.066447168	0.881549393	0.399734471	0.166258094	0.881549393	0.324692981	0.099810927
PARK2	0.062026844	0.744557492	0.508448011	0.0638596	0.744557492	0.508448011	0.001832755
POLG	0.061416315	0.665474388	0.874455448	-0.13190285	0.437368476	0.874455448	-0.193319165
POLQ	0.061363685	0.707187804	0.452518333	0.017129579	0.707187804	0.452518333	-0.044234106
NonTargetingC	0.059979106	0.850087936	0.533634841	0.151755925	0.914641727	0.533634841	0.091776818
BAZ1A	0.059171876	0.733462775	0.45138603	0.010258444	0.733462775	0.474065524	-0.048913432
DTX2	0.059149442	0.671581355	0.696367427	0.059870984	0.671581355	0.696367427	7.21542E-04
ACD	0.05905609	0.982712271	0.619669651	-0.119693955	0.982712271	0.822760624	-0.178750045
DTX1	0.058132955	0.802545681	0.457077757	0.131552243	0.802545681	0.457077757	0.073419289
UVSSA	0.057129501	0.69812623	0.613241301	-0.039138155	0.69812623	0.613241301	-0.096267656
BEND3	0.056015667	0.782060364	0.418467606	0.110372716	0.784672403	0.418467606	0.054357049
CENPS	0.054459324	0.809540827	0.504680041	0.203240104	0.862437361	0.504680041	0.14878078
USP4	0.054275234	0.805362863	0.589526684	-0.008597673	0.805362863	0.589526684	-0.062872907
PER3	0.053455331	0.849608299	0.489903783	0.023467064	0.849608299	0.489903783	-0.029988267
APOBEC1	0.051404986	0.956864874	0.431690689	0.177653356	0.956864874	0.234856141	0.12624837
DCAF11	0.051353841	0.900717935	0.386361477	0.209398226	0.928979972	0.386361477	0.158044384
H2AFY2	0.050363606	0.763884749	0.465235999	0.096400817	0.763884749	0.465235999	0.046037211
NOTCH2	0.050195055	0.91600724	0.441506818	0.078694461	0.91600724	0.441506818	0.028499406
OGG1	0.047976145	0.848582944	0.508307522	0.177432534	0.905574911	0.508307522	0.129456389
PAPD7	0.047281708	0.791645969	0.529345001	0.114457158	0.791645969	0.529345001	0.06717545
STAG1	0.04708998	0.723799903	0.633347551	-0.160781946	0.723799903	0.800676248	-0.207871927
IGHMBP2	0.043940273	0.733461585	0.477616102	0.103525082	0.740019751	0.477616102	0.059584809
CBX3	0.043742116	0.85241978	0.418979627	0.114289415	0.85241978	0.418979627	0.070547299
TP73	0.041507452	0.721214667	0.496816724	0.055569235	0.721214667	0.496816724	0.014061783
SERBP1	0.038793009	0.936111565	0.518464993	0.220617858	0.936111565	0.358438756	0.181824848
SLBP	0.033742092	0.84926528	0.520300724	0.173241302	0.853138404	0.520300724	0.13949921
MPZ	0.032867989	0.783285652	0.569902016	0.020854632	0.783285652	0.569902016	-0.012013356
TDG	0.031650583	0.776038219	0.622908194	-0.019491399	0.776038219	0.622908194	-0.051141982
SFR1	0.031078724	0.81670404	0.746105984	-0.292719309	0.640166994	0.928438731	-0.323798032
HES1	0.02421712	0.76809946	0.612258629	0.171440941	0.873871288	0.612258629	0.147223822
OR6B1	0.021637562	0.780133397	0.543041925	0.018962446	0.780133397	0.543041925	-0.002675116
PIAS1	0.020815564	0.730146097	0.55679566	0.067473984	0.730146097	0.478187399	0.04665842
GABBR1	0.020545675	0.830415951	0.443223333	0.184983578	0.901884705	0.443223333	0.164437902
PIF1	0.020289941	0.789502562	0.452710548	0.018396824	0.789502562	0.452710548	-0.001893117
MCRS1	0.012858545	0.962567628	0.702009461	-0.423860616	0.149047656	0.992857054	-0.436719161
PIAS4	0.011073816	0.534303065	0.788581482	-0.093289501	0.530232231	0.788581482	-0.104363316
NPM1	0.006458503	0.971362538	0.666090951	-0.17786433	0.971362538	0.666090951	-0.184322833
CUL4A	1.27857E-04	0.655076567	0.689545238	0.060368814	0.655076567	0.689545238	0.060240957
TCEA1	-0.001069823	0.635881387	0.597959364	-0.022496842	0.635881387	0.597959364	-0.021427019

ATRX	-0.008123802	0.584883682	0.796610207	-0.035329702	0.584883682	0.796610207	-0.0272059
ZDHHC16	-0.017123259	0.956923154	0.713194275	0.48690153	0.995336677	0.041969904	0.504024789
MUTYH	-0.023928773	0.663194739	0.683401713	-0.02014341	0.663194739	0.683401713	0.003785363
OR1E2	-0.025011978	0.776359	0.639285089	0.197193827	0.852952844	0.639285089	0.222205804
PINK1	-0.025210376	0.859205561	0.651866215	0.244384851	0.96440717	0.320335471	0.269595227
MSH5	-0.025418707	0.738573839	0.706570482	0.12375609	0.825296938	0.706570482	0.149174798
PPP6R2	-0.026983184	0.793930204	0.658974471	0.105752555	0.793930204	0.51836679	0.13273574
INO80E	-0.027526916	0.854418796	0.709819692	0.029373156	0.854418796	0.665537272	0.056900072
RNF4	-0.033967332	0.51553963	0.863172383	-0.124752913	0.51553963	0.863172383	-0.090785581
MSH6	-0.036633742	0.77028725	0.633023141	0.01904652	0.77028725	0.633023141	0.055680262
SUV39H1	-0.039423558	0.686927959	0.727706492	0.115434501	0.816719917	0.727706492	0.154858059
ATMIN	-0.046955331	0.945798935	0.687818418	0.04392406	0.945798935	0.623082988	0.09087939
RNF168	-0.047566662	0.686855358	0.768789476	-0.164856187	0.686855358	0.830175809	-0.117289524
WDR70	-0.050524705	0.848053481	0.934631013	-0.281808111	0.258358485	0.99662953	-0.231283407
RAD23B	-0.052195755	0.726194025	0.689054646	0.115874171	0.763368188	0.689054646	0.168069926
PAXIP1	-0.052223525	0.640313842	0.733419247	-0.016965229	0.640313842	0.733419247	0.035258296
PARG	-0.052295033	0.995565538	0.710100661	0.328664906	0.995565538	0.08609987	0.380959939
NIPBL	-0.054320967	0.690169452	0.998963233	-0.664244679	0.009330906	0.998963233	-0.609923712
PPP6R1	-0.054649076	0.772941429	0.696452101	0.090973048	0.773394928	0.646705834	0.145622124
TNKS	-0.054790498	0.632422958	0.844252915	-0.129374758	0.632422958	0.844252915	-0.074584259
SMC4	-0.056325241	0.997535657	0.765303894	0.043632767	0.997535657	0.644779088	0.099958008
TRIM28	-0.057614478	0.696727965	0.743038716	0.078759989	0.712365564	0.743038716	0.136374467
SMARCAL1	-0.062285927	0.734519105	0.748013154	-0.059324134	0.734519105	0.748013154	0.002961793
TOP2A	-0.066506104	0.810893181	0.622751665	0.0102456	0.810893181	0.622751665	0.076751705
ORC2	-0.070942293	0.481268607	0.87352768	-0.159008641	0.481268607	0.87352768	-0.088066348
PRDM10	-0.072691583	0.750825113	0.688004874	-0.056324044	0.750825113	0.688004874	0.016367539
FAAP20	-0.079637557	0.529341341	0.704574993	-0.036089269	0.529341341	0.704574993	0.043548288
XRCC1	-0.081948717	0.443528978	0.83560372	-0.126488948	0.443528978	0.83560372	-0.04454023
ATAD5	-0.08405132	0.639201937	0.719766489	0.134662609	0.805147372	0.719766489	0.218713929
CUL9	-0.086283682	0.694477132	0.98584922	-0.322826362	0.117847898	0.98584922	-0.23654268
ERCC8	-0.087778064	0.716506865	0.739113123	0.053983414	0.716506865	0.709966902	0.141761477
CBX1	-0.089547682	0.732768406	0.73796149	-0.105540314	0.732768406	0.73796149	-0.015992632
MPLKIP	-0.103811915	0.417071503	0.839815793	-0.132896713	0.417071503	0.839815793	-0.029084798
RFWD3	-0.105139018	0.445843971	0.946496535	-0.551501004	0.037563129	0.992271177	-0.446361986
KDM2A	-0.107119257	0.434804887	0.910732661	0.024361476	0.635097672	0.910732661	0.131480733
TFPT	-0.107978674	0.297516508	0.890885344	-0.171899425	0.297516508	0.890885344	-0.063920751
SPIDR	-0.108790252	0.476235924	0.816668104	-0.110521777	0.476235924	0.816668104	-0.001731525
CDCA5	-0.111481331	0.84546838	0.843402935	-0.0494265	0.907590288	0.843402935	0.062054831
CSNK2A1	-0.115433546	0.59893175	0.749365565	0.014463681	0.59893175	0.744935698	0.129897227
RAD23A	-0.11667256	0.635087306	0.805323122	0.040814137	0.732912694	0.805323122	0.157486697
RAD54L	-0.126592922	0.553927821	0.930512659	-0.251373537	0.553927821	0.930512659	-0.124780615
PARP1	-0.127914059	0.279310195	0.90920163	-0.187085541	0.279310195	0.90920163	-0.059171482
MPG	-0.128031749	0.678395155	0.824092206	0.074923027	0.678395155	0.64260504	0.202954776
MTA1	-0.132868177	0.620309887	0.876758892	0.040637312	0.620309887	0.740035073	0.173505489
POLA1	-0.134563873	0.83158969	0.809082136	-0.193146133	0.83158969	0.809082136	-0.05858226
EXO1	-0.137875464	0.626652201	0.875452844	-0.037928988	0.626652201	0.875452844	0.099946476
POLD4	-0.142312237	0.72269126	0.811369298	-0.080783908	0.72269126	0.774671345	0.061528329
COPS4	-0.144612611	0.962367229	0.784286744	-0.05340531	0.962367229	0.773073404	0.091207301
TERF2IP	-0.14896781	0.747038604	0.873688043	-0.018517477	0.747038604	0.740824367	0.130450334
EP400	-0.150950959	0.584723843	0.934499724	-0.316936187	0.584723843	0.934499724	-0.165985229
RBBP8	-0.151290976	0.462614282	0.850956524	-0.197376254	0.462614282	0.850956524	-0.046085278
CHD4	-0.151945071	0.501435684	0.901051259	-0.171329026	0.501435684	0.901051259	-0.019383955
UNG	-0.154785905	0.879170242	0.843624469	0.039821732	0.879170242	0.711741337	0.194607637
HELQ	-0.160854123	0.53104413	0.86709702	-0.164474864	0.53104413	0.86709702	-0.003620741
PAGR1	-0.165923582	0.281102876	0.995113011	-0.54044677	0.043982902	0.995113011	-0.374523187
CHRAC1	-0.168534433	0.470805861	0.883613746	-0.124666104	0.470805861	0.883613746	0.04386833
ECT2	-0.171151274	0.601225405	0.863494177	-0.074990814	0.601225405	0.863494177	0.09616046
USP1	-0.176650435	0.590243354	0.881468859	0.006881274	0.590243354	0.848664132	0.183531709
LMNA	-0.176655961	0.183523833	0.988127832	-0.025482483	0.561094561	0.988127832	0.151173478
SKIV2L2	-0.180172562	0.430956169	0.899222865	-0.177050851	0.430956169	0.899222865	0.003121711
USP22	-0.183838769	0.642641712	0.845438996	0.016899146	0.642641712	0.653544646	0.200737915
POLR2A	-0.188104143	0.763345102	0.854275904	-0.144072004	0.763345102	0.854275904	0.044032139
POLE	-0.190543829	0.65044863	0.865959085	-0.030158808	0.65044863	0.865959085	0.160385021
H3F3B	-0.196597617	0.596271997	0.851687166	-0.195591112	0.596271997	0.851687166	0.001006505
CNOT7	-0.19949701	0.288024187	0.942650234	-0.339063476	0.288024187	0.942650234	-0.139566466
OTUB1	-0.203434471	0.59043536	0.901421273	0.039150756	0.59043536	0.800128386	0.242585227
CCND1	-0.207573164	0.869752987	0.817524746	0.018562789	0.869752987	0.641848467	0.226135953
POLD2	-0.208542476	0.334274577	0.982634944	-0.432094866	0.156285504	0.982634944	-0.223552389
SMG1	-0.222482737	0.65746305	0.889597163	-0.177078894	0.65746305	0.889597163	0.045403843
MASTL	-0.223354855	0.386713651	0.999652537	-0.639203315	0.094058397	0.999652537	-0.41584846
USP44	-0.227671854	0.241357596	0.973182489	-0.170397989	0.5445791	0.973182489	0.057273865
POLR2F	-0.230876499	0.216537678	0.932523806	-0.331050991	0.216537678	0.932523806	-0.100174492
DAXX	-0.234092082	0.370287653	0.982592441	-0.477385848	0.145857946	0.982592441	-0.243293766
PLRG1	-0.236438298	0.343606608	0.948788813	-0.264427117	0.343606608	0.948788813	-0.027988819
CREBBP	-0.238700169	0.200253782	0.977017433	-0.188856336	0.200253782	0.977017433	0.049843833
PALB2	-0.24104358	0.21624328	0.956352073	-0.176502208	0.274097763	0.956352073	0.064541372
MUS81	-0.241066367	0.112188123	0.99287909	-0.42869439	0.064088194	0.99287909	-0.187628023
ENY2	-0.245632696	0.218434077	0.971646103	-0.343604578	0.148082476	0.971646103	-0.097971882
COPS2	-0.250094945	0.104368911	0.992713471	-0.33552651	0.104368911	0.992713471	-0.085431565
POLD1	-0.250258657	0.301446908	0.971842685	-0.581528504	0.180360624	0.971842685	-0.331269846
EXO5	-0.251552149	0.104557156	0.99160132	-0.396324564	0.075588121	0.99160132	-0.144772415
TCEB3	-0.25591657	0.201967185	0.990465878	-0.510498133	0.085807102	0.990465878	-0.254581563

PPP4R2	-0.258368916	0.570779587	0.884977733	-0.24878398	0.570779587	0.884977733	0.009584936
POLR2D	-0.260322916	0.767441941	0.897448418	-0.048427783	0.984172942	0.843884706	0.211895132
XRCC4	-0.265056586	0.091989725	0.983404757	-0.304627427	0.091989725	0.983404757	-0.03957084
BRIP1	-0.268506001	0.360874066	0.9361424	-0.077691499	0.47669902	0.882716175	0.190814502
CDC25B	-0.270526747	0.054812273	0.990217901	-0.361589008	0.054812273	0.990217901	-0.091062261
TADA3	-0.276603476	0.433691801	0.915647428	-0.092572502	0.433691801	0.915647428	0.184030973
NFRKB	-0.27995273	0.08237066	0.983903022	-0.357797074	0.08237066	0.983903022	-0.077844344
BAZ1B	-0.280345078	0.496971196	0.944780978	-0.029115166	0.677081241	0.831773684	0.251229912
FANCE	-0.282976853	0.158677652	0.999512955	-0.811396026	0.004383402	0.999512955	-0.528419174
MDC1	-0.283865123	0.102756888	0.986434394	-0.400415896	0.102756888	0.986434394	-0.116550774
REV3L	-0.2873757	0.128238355	0.995825835	-0.504624834	0.040619012	0.995825835	-0.217249134
ARID1A	-0.288305518	0.184496925	0.960738841	-0.245123096	0.308653699	0.960738841	0.043182423
EYA3	-0.291394047	0.191554347	0.978716184	-0.158867981	0.442394633	0.978716184	0.132526066
CDK12	-0.29236442	0.250431647	0.972174261	-0.24979598	0.354350191	0.972174261	0.042568439
DNAJC2	-0.295825188	0.294286911	0.99865042	-0.5565439	0.134663326	0.99865042	-0.260718712
RMI2	-0.299420629	0.260218835	0.971086796	-0.205945675	0.359083547	0.971086796	0.093474953
NHEJ1	-0.302506788	0.09166317	0.989815203	-0.285530055	0.121990341	0.989815203	0.016976733
KAT2A	-0.306548812	0.071147396	0.992094734	-0.216879083	0.262923643	0.992094734	0.08966973
TDP2	-0.309533973	0.130991125	0.983092246	-0.366988197	0.130991125	0.983092246	-0.057454224
HELLS	-0.311522354	0.252129036	0.971985663	-0.161144545	0.378136086	0.971985663	0.150377809
SUMO2	-0.323885876	0.592600641	0.874235475	-0.069132051	0.592600641	0.874235475	0.254753825
PINX1	-0.325346997	0.148550039	0.974286015	-0.369962275	0.148550039	0.974286015	-0.044615277
FANCA	-0.325681171	0.209442566	0.968847838	-0.241885307	0.209442566	0.968847838	0.083795864
LIG1	-0.327713059	0.179085725	0.980101586	-0.080180537	0.57090815	0.979584009	0.247532523
ZMPSTE24	-0.330617725	0.054864878	0.99078592	-0.375909008	0.054864878	0.99078592	-0.045291282
ATRIP	-0.362903422	0.013917203	0.998218448	-0.438694531	0.013917203	0.998218448	-0.075791109
CDK2	-0.367593312	0.074984106	0.991668433	-0.208285683	0.355245308	0.991668433	0.15930763
MCM3AP	-0.371072936	0.210290216	0.973219488	-0.222155907	0.245791437	0.973219488	0.148917029
BRCA1	-0.374522909	0.099649059	0.988927882	-0.260872849	0.240341187	0.988927882	0.113650061
SLX4	-0.37594172	0.006668479	0.999341474	-0.540291908	0.005926732	0.999341474	-0.164350188
SMG6	-0.383253541	0.223016344	0.975220406	-0.254386024	0.290383003	0.975220406	0.128867517
NFE2L2	-0.384092026	0.049834458	0.994462838	-0.222560303	0.300917887	0.994462838	0.161531723
ANKRD52	-0.384924158	0.154881923	0.982790897	-0.268656035	0.235897498	0.982790897	0.116268123
ESCO2	-0.40137917	0.066336516	0.992629276	-0.403177491	0.089727079	0.992629276	-0.001798321
TOP1	-0.40296529	0.304162692	0.965118595	-0.19365018	0.593986618	0.965118595	0.209315111
FANCB	-0.403402649	0.037634452	0.995133965	-0.46657312	0.037634452	0.995133965	-0.063170471
RAD21	-0.406114979	0.186882038	0.999354912	-0.964551829	0.005329002	0.999354912	-0.55843685
CCNB1	-0.407993398	0.016997613	0.998111376	-0.393095395	0.043718332	0.998111376	0.014898003
MEN1	-0.413336532	0.09665337	0.983314517	-0.427910931	0.09665337	0.983314517	-0.0145744
SMARCE1	-0.42066373	0.045333147	0.990164848	-0.408545593	0.146678665	0.990164848	0.012118136
PPM1G	-0.423367672	0.202151406	0.977161392	-0.330068097	0.202151406	0.977161392	0.093299575
PRKDC	-0.424578433	0.02213336	0.997540738	-0.282321823	0.132195725	0.997540738	0.14225661
FIGNL1	-0.42895911	0.009581148	0.998935428	-0.20521407	0.256950171	0.998935428	0.22374504
BAP1	-0.43689325	0.055763061	0.991006485	-0.492074184	0.06781337	0.991006485	-0.055180934
NCAPD3	-0.43785277	0.091343379	0.999902021	-0.642718683	0.051026323	0.999902021	-0.204865913
FAAP24	-0.439601311	0.008315086	0.999280513	-0.800356355	0.004598138	0.999280513	-0.360755044
DUT	-0.442240628	0.07075276	0.992138582	-0.306662989	0.198585301	0.992138582	0.135577639
FAAP100	-0.44520896	0.006553714	0.999216741	-0.623841474	0.006553714	0.999216741	-0.178632513
UPF1	-0.445585181	0.069818791	0.999880087	-0.878174722	0.009081953	0.999880087	-0.432589541
RECQL4	-0.463617245	0.477553355	0.944230596	0.049375513	0.877680198	0.595715041	0.512992758
INO80	-0.46532329	0.010074584	0.998880602	-0.41133481	0.030687121	0.998880602	0.053988481
KAT5	-0.465335388	0.003449885	0.999736495	-0.690271907	0.002133019	0.999736495	-0.224936519
XRCC6	-0.472190397	0.045700529	0.996737637	-0.804499098	0.029361264	0.996737637	-0.332308701
SPRTN	-0.475781513	0.030000709	0.993980344	-0.480296074	0.030000709	0.993980344	-0.004514561
TRRAP	-0.484532015	0.026819265	0.997020082	-0.503288197	0.050000856	0.997020082	-0.018756181
NCAPH	-0.489256463	0.017134412	0.99898725	-0.761227683	0.009114748	0.99898725	-0.27197122
POLR2L	-0.491628573	0.150546855	0.993747536	-0.657855516	0.110634723	0.993747536	-0.166226943
COPS3	-0.495542472	0.006412714	0.998901311	-0.635829813	0.006412714	0.998901311	-0.14028734
LIG4	-0.503665564	0.018063341	0.997992962	-0.534381482	0.034925692	0.997992962	-0.030715918
RPAIN	-0.503958507	0.202989095	0.977445656	-0.450691353	0.205984554	0.977445656	0.053267154
WDR48	-0.50522505	0.008246915	0.999368917	-0.723194509	0.005679749	0.999368917	-0.21796946
CLSPN	-0.50941712	0.037418297	0.995842411	-0.280286077	0.290846178	0.995842411	0.229131043
NSMCE2	-0.512167482	0.031251449	0.996527617	-0.308959512	0.193492295	0.996527617	0.20320797
INO80B	-0.515890768	0.017820024	0.998019997	-0.53249095	0.02661184	0.998019997	-0.016600182
CUL1	-0.519515423	0.001867307	0.99998777	-0.760790779	1.10066E-04	0.99998777	-0.241275356
ACTR5	-0.521510069	0.003020597	0.999664378	-0.429203977	0.043490312	0.999664378	0.092306093
RAD51C	-0.524020216	0.021702105	0.997588655	-0.364352083	0.113616994	0.997588655	0.159668133
UBC	-0.53399397	0.17105301	0.98099411	-0.240221572	0.319689711	0.98099411	0.293772398
SMARCA5	-0.539063506	0.001942941	0.999784118	-0.317331177	0.089334214	0.999784118	0.221732328
SFPQ	-0.539353578	0.035987943	0.99600134	-0.472652434	0.049026311	0.99600134	0.066701144
MRE11	-0.552045358	1.88543E-04	0.999979051	-0.416697937	0.003387275	0.999979051	0.135347421
WEE1	-0.553347577	0.051204483	0.994310613	-0.55979839	0.069213929	0.994310613	-0.006450813
WRAP53	-0.555013619	0.002984207	0.999668421	-0.344633636	0.086903678	0.999668421	0.210379983
PDS5B	-0.556626107	0.021096573	0.997655936	-0.379042656	0.097722757	0.997655936	0.17758345
KDM4A	-0.55794361	0.00283	0.999685556	-0.42784437	0.032069603	0.999685556	0.13009924
RAD17	-0.559543711	0.004165578	0.99993315	-0.901408686	6.03347E-04	0.99993315	-0.341864975
RNF8	-0.559882093	0.034541288	0.996162079	-0.589318186	0.050428236	0.996162079	-0.029436093
RMI1	-0.570967126	1.40335E-04	0.999979412	-0.641622427	1.40335E-04	0.999979412	-0.070655302
SET	-0.571000357	0.004028212	0.9998963	-0.918574764	9.33297E-04	0.9998963	-0.347574406
WAPL	-0.572820907	0.001391377	0.99976222	-0.674462372	0.001391377	0.99976222	-0.101641465
POLR2G	-0.584625034	0.079959761	0.997446221	-0.820139653	0.045334103	0.997446221	-0.235514619
POLR2K	-0.59571162	0.084374199	0.987262845	-0.629564716	0.084374199	0.987262845	-0.033853096

RAD51B	-0.595792757	1.39498E-04	0.9999845	-0.631913209	0.001183107	0.9999845	-0.036120452
SMC6	-0.596548189	0.003379865	0.999345574	-0.810964001	0.003379865	0.999345574	-0.214415812
UVRAG	-0.598472671	2.67008E-04	0.999970332	-0.67358317	5.31623E-04	0.999970332	-0.075110499
MTOR	-0.599883978	4.52729E-04	0.999949697	-0.519913795	0.004064661	0.999949697	0.079970184
FANCI	-0.605414404	0.043271177	0.995192091	-0.383691008	0.250591065	0.995192091	0.221723397
UBE2N	-0.605661129	0.001335053	0.999808198	-0.672414641	0.001335053	0.999808198	-0.066753512
TIMELESS	-0.605961603	0.002525248	0.999719417	-0.58850862	0.008488559	0.999719417	0.017452983
DNMT1	-0.606238396	3.08331E-04	0.999965741	-0.347424933	0.055334608	0.999965741	0.258813463
TERF1	-0.606902174	0.098687015	0.989034776	-0.380461603	0.149199926	0.989034776	0.226440571
CHAF1A	-0.607760097	0.009374157	0.998605523	-0.616528298	0.014738668	0.998605523	-0.008768202
ERCC1	-0.608959397	7.17505E-04	0.999920277	-0.618593574	0.003684935	0.999920277	-0.009634178
DDX11	-0.612202105	0.003677219	0.999667691	-0.867831673	0.00299078	0.999667691	-0.255629568
RAD50	-0.619088614	9.78E-07	0.999999891	-0.525851959	0.002264283	0.999999891	0.093236655
RNASEH2A	-0.633098337	0.001455201	0.999838311	-0.315842774	0.074537796	0.999838311	0.317255563
MMS22L	-0.637095931	5.78971E-04	0.99993567	-0.544054541	0.022522814	0.99993567	0.09304139
UBE2M	-0.642867839	0.001539701	0.99993481	-0.942652837	5.86712E-04	0.99993481	-0.299784997
RFC4	-0.643045643	0.001434892	0.999840568	-0.492300714	0.039813359	0.999840568	0.150744929
FANCM	-0.648945492	8.79891E-04	0.999902234	-0.472884958	0.020160665	0.999902234	0.176060534
NAE1	-0.651524075	3.92E-06	0.999999565	-0.567564635	1.89E-05	0.999999565	0.08395944
UBE2D3	-0.657876035	0.080523003	0.997770826	-0.840914225	0.068166793	0.997770826	-0.18303819
SMC2	-0.659453252	0.011944405	0.998050525	-0.631655212	0.025619039	0.998050525	0.02779804
H2AFX	-0.661130878	0.010612095	0.998820878	-0.645226422	0.017080208	0.998820878	0.015904456
SENP6	-0.6637173	6.05160E-04	0.99993276	-0.80674806	6.69474E-04	0.99993276	-0.14303076
RAD1	-0.673110354	0.003659453	0.999593394	-0.76978318	0.008876769	0.999593394	-0.096672826
SMC3	-0.689872104	9.32226E-04	0.999896419	-0.831304401	0.001562601	0.999896419	-0.141432297
FANCG	-0.69122434	0.001387593	0.999845823	-0.461730573	0.040873382	0.999845823	0.229493767
DNA2	-0.701327248	0.034541048	0.997085571	-0.888864407	0.026229862	0.997085571	-0.187537159
GAR1	-0.703137931	0.002365365	0.99968861	-0.869079322	0.001938396	0.99968861	-0.165941391
FANCC	-0.704821451	1.59E-05	0.999998236	-0.365285594	0.033990772	0.999998236	0.339535858
RIF1	-0.706251531	1.69E-05	0.999998123	-0.595986728	5.08760E-04	0.999998123	0.110264803
CHEK1	-0.707462919	0.030196048	0.9943534	-0.670544483	0.042520934	0.9943534	0.036918436
NSMCE1	-0.709858081	7.47286E-04	0.99991118	-0.64069105	7.47286E-04	0.99991118	0.06916703
BRD4	-0.711113154	7.10488E-04	0.999964741	-0.893007158	3.17332E-04	0.999964741	-0.181894004
RPS27L	-0.71657304	0.032752451	0.999927292	-1.466963551	6.53192E-04	0.999927292	-0.750390511
DSCC1	-0.717425194	4.71E-05	0.999994766	-0.465510166	0.027457823	0.999994766	0.251915028
PRMT1	-0.718984959	0.00147153	0.999836497	-0.549841624	0.028663352	0.999836497	0.169143334
POLE4	-0.724956104	1.68468E-04	0.999981281	-0.665003351	0.003794188	0.999981281	0.059952752
NSMCE4A	-0.726873567	5.14719E-04	0.999942809	-0.785133146	0.001095579	0.999942809	-0.058259579
RNF20	-0.728301274	4.33E-06	0.999999519	-0.526992805	0.002913086	0.999999519	0.201308468
SIN3A	-0.730538101	2.41E-05	0.999999614	-1.013703366	3.47E-06	0.999999614	-0.283165265
RNF40	-0.73881293	1.22863E-04	0.999986349	-0.029221108	0.710868279	0.999986349	0.709591822
BARD1	-0.738839984	0.001083637	0.99981174	-0.770984988	0.001083637	0.99981174	-0.032145004
RUVBL1	-0.739972476	0.001637605	0.999640183	-0.815365688	0.001637605	0.999640183	-0.075393212
UCHL5	-0.742440726	9.36E-07	0.999999896	-0.625684018	4.32089E-04	0.999999896	0.116756708
CTCF	-0.744663808	7.32478E-04	0.999918614	-0.661548381	0.004102201	0.999918614	0.083115427
CSNK2B	-0.745571525	5.51784E-04	0.999938691	-0.335199514	0.098440714	0.999938691	0.41037201
SUPT6H	-0.746657561	0.002192787	0.999391397	-0.861343914	0.002192787	0.999391397	-0.114686353
POLR2B	-0.752953743	0.015752097	0.998193741	-0.414558124	0.164797606	0.998193741	0.338395619
RPA1	-0.759143778	0.00730068	0.99954152	-0.982863907	0.00412632	0.99954152	-0.223720129
FEN1	-0.760073358	2.41264E-04	0.999973193	-0.740843131	0.005210954	0.999973193	0.019230227
UHRF1	-0.771743133	8.46514E-04	0.99999626	-1.190513475	3.37E-05	0.99999626	-0.418770341
USP37	-0.774675195	9.09908E-04	0.999898899	-0.882488746	0.001557334	0.999898899	-0.107813551
BCCIP	-0.775237049	0.010231943	0.998808704	-0.783068992	0.010231943	0.998808704	-0.007831943
XAB2	-0.77755665	2.45249E-04	0.99997275	-0.537115832	0.04553182	0.99997275	0.240440817
MAD2L2	-0.778527676	2.19E-05	0.999997565	-0.905986965	5.05308E-04	0.999997565	-0.127459289
NCAPG	-0.785677183	1.46863E-04	0.999983682	-0.878838743	5.21785E-04	0.999983682	-0.09316156
GTF2H5	-0.786441457	9.59E-05	0.999989346	-0.519688318	0.018317109	0.999989346	0.266753138
RAD9A	-0.787602975	0.0069951	0.999222767	-0.529611682	0.067132826	0.999222767	0.257991293
ACTR8	-0.811343162	5.22E-06	0.99999942	-0.70880241	7.62257E-04	0.99999942	0.102540752
RAD51D	-0.815465721	5.97E-08	0.999999993	-0.843700159	1.18E-06	0.999999993	-0.028234438
BUB1B	-0.815530539	1.14180E-04	0.999987313	-0.673143636	0.002955252	0.999987313	0.142386904
FANCF	-0.81909573	2.62E-05	0.999997085	-0.431643108	0.037613913	0.999997085	0.387452622
CCNA2	-0.820320278	4.53595E-04	0.999949601	-0.74001539	0.003496758	0.999949601	0.080304889
CEP57	-0.820384317	1.23E-06	0.999999863	-0.804457113	2.33039E-04	0.999999863	0.015927203
PCNA	-0.823563296	0.003476035	0.999618781	-0.950407408	0.002009772	0.999618781	-0.126844112
POLE3	-0.825123736	1.15721E-04	0.999987142	-0.592634187	0.005320778	0.999987142	0.232489549
RPA3	-0.836425466	4.26491E-04	0.999948141	-1.055987547	4.26491E-04	0.999948141	-0.219562081
ERCC4	-0.841939163	1.24E-05	0.999998625	-0.458190294	0.027251309	0.999998625	0.383748869
NONO	-0.848853275	2.26E-07	0.999999975	-0.721935339	2.63559E-04	0.999999975	0.126917936
MNAT1	-0.854794009	1.87358E-04	0.999979182	-1.059231572	2.63248E-04	0.999979182	-0.204437563
CUL2	-0.857561838	1.21E-06	0.999999866	-0.772105909	1.21596E-04	0.999999866	0.085455929
POLR2C	-0.866047847	4.08E-06	0.999999547	-0.656255437	0.001678245	0.999999547	0.20979241
TERF2	-0.871423011	0.030474781	0.996613913	-0.656041054	0.068957806	0.996613913	0.215381957
USP5	-0.873813393	9.95063E-04	0.999889437	-0.921589222	0.001830971	0.999889437	-0.047775829
RAD51	-0.879470827	0.00108351	0.99987961	-0.505067813	0.050711825	0.99987961	0.374403014
TERT	-0.890344915	5.12E-05	0.999994311	-0.776186557	0.011895478	0.999994311	0.114158358
SKP1	-0.890751182	0.001789046	0.999801217	-0.838565608	0.003508149	0.999801217	0.052185574
HDAC3	-0.890895992	0.002931244	0.999994236	-0.932773817	0.009628739	0.999994236	-0.041877825
RFC2	-0.892677464	3.97E-05	0.999995591	-0.450196195	0.047321048	0.999995591	0.442481269
RTEL1	-0.897650218	9.82E-06	0.999998909	-0.466794288	0.021191095	0.999998909	0.43085593
POT1	-0.898140107	8.44E-05	0.999990622	-0.679050932	0.008759856	0.999990622	0.219089175
HUS1	-0.902720807	2.22223E-04	0.999975309	-1.08362732	3.67523E-04	0.999975309	-0.180906513

NSMCE3	-0.905593203	7.92E-05	0.999991203	-1.106826843	1.47235E-04	0.999991203	-0.20123364
GTF2H1	-0.919259143	1.35E-07	0.999999996	-1.303689509	3.59E-08	0.999999996	-0.384430366
POLR2H	-0.922983558	4.22E-05	0.999999145	-1.171365717	5.65E-06	0.999999145	-0.248382158
NCAPD2	-0.923381072	1.63E-05	0.999998189	-0.98297521	2.92483E-04	0.999998189	-0.059594138
TOPBP1	-0.925758858	3.98E-08	0.999999996	-0.767975488	1.49E-05	0.999999996	0.15778337
PDS5A	-0.926834728	3.87E-05	0.999995695	-0.773964263	0.005073667	0.999995695	0.152870465
RUVBL2	-0.927458697	3.81E-06	0.999999577	-0.849480065	2.75882E-04	0.999999577	0.077978632
CCNH	-0.934723175	0.001494055	0.999833994	-0.95105308	0.005074572	0.999833994	-0.016329905
BOD1L1	-0.943571931	6.34E-06	0.999999296	-0.745247096	4.45225E-04	0.999999296	0.198324835
POLE2	-0.944057041	1.72725E-04	0.999980808	-0.752997217	0.010574456	0.999980808	0.191059823
MMS19	-0.950005689	1.26E-06	0.99999986	-0.883233076	2.04447E-04	0.99999986	0.066772613
PLK1	-0.951993708	0.001796867	0.999800348	-0.787926557	0.021661373	0.999800348	0.164067151
PNKP	-0.964557122	5.20E-07	0.999999942	-0.851711551	2.19999E-04	0.999999942	0.112845571
MAU2	-0.96832087	8.70E-07	0.999999903	-0.70706527	8.99236E-04	0.999999903	0.2612556
NCAPG2	-0.97170784	1.80149E-04	0.999979983	-0.971596494	7.17926E-04	0.999979983	1.11346E-04
CTC1	-0.974149564	1.98191E-04	0.999977979	-0.590325184	0.016902436	0.999977979	0.38382438
POLR2I	-0.975017693	9.75E-05	0.999989168	-1.046959267	2.45639E-04	0.999989168	-0.071941575
PCID2	-0.981880826	1.06E-06	0.999999883	-0.630060278	0.009347545	0.999999883	0.351820548
PRPF19	-0.988881213	7.88992E-04	0.999912334	-0.90149646	0.003343997	0.999912334	0.087384752
RRM2	-0.989679496	1.42E-05	0.999998419	-0.923249047	6.28091E-04	0.999998419	0.066430449
COPS8	-0.990173499	5.21373E-04	0.99994207	-0.914636479	0.006818796	0.99994207	0.07553702
MCPH1	-0.991052357	4.56E-06	0.999999494	-0.71936576	0.003862328	0.999999494	0.271686598
HUWE1	-0.996059806	6.02E-06	0.999999817	-1.321807026	1.65E-06	0.999999817	-0.32574722
POLR2E	-1.010734931	2.03E-05	0.999997744	-1.106857688	9.49E-05	0.999997744	-0.096122757
USP7	-1.012593368	1.42086E-04	0.999984213	-0.939610607	0.002888682	0.999984213	0.072982761
UBA1	-1.02293677	2.61E-06	0.99999971	-1.089239714	9.92E-06	0.99999971	-0.066302944
ACTL6A	-1.024202976	1.12E-06	0.999999998	-1.484751078	2.18E-08	0.999999998	-0.460548103
TINF2	-1.027020011	0.004600589	0.999488823	-0.854854318	0.060804359	0.999488823	0.172165692
CDC5L	-1.029656352	5.30E-08	0.999999994	-1.232466119	1.80E-07	0.999999994	-0.202809767
TRAIP	-1.033210521	3.16E-06	0.999999649	-1.16154149	1.37497E-04	0.999999649	-0.128330969
CDK9	-1.055727381	1.18917E-04	0.999986787	-1.156210503	1.93697E-04	0.999986787	-0.100483122
FANCL	-1.070090152	1.21E-06	0.999999866	-0.778514536	6.44640E-04	0.999999866	0.291575616
TAF1	-1.079666714	1.42E-07	0.999999984	-1.216174351	6.19E-07	0.999999984	-0.136507638
RFC3	-1.085430692	3.39E-06	0.999999623	-0.819789301	0.002226218	0.999999623	0.265641392
TELO2	-1.090506084	2.31E-08	0.999999997	-0.643763677	0.002380353	0.999999997	0.446742407
BCAS2	-1.095781321	1.75E-06	0.999999806	-0.940137707	1.72958E-04	0.999999806	0.155643614
SMARCB1	-1.123693211	1.23E-05	0.999998637	-0.912760447	4.14381E-04	0.999998637	0.210932764
COPS6	-1.12380299	6.47E-07	0.999999928	-1.188384001	4.03E-05	0.999999928	-0.064581011
TOP3A	-1.129628629	1.15E-08	0.999999999	-0.873527182	7.97348E-04	0.999999999	0.256101448
NOP10	-1.129730869	6.82E-06	0.999999242	-0.67370674	0.016102566	0.999999242	0.456024129
FANCD2	-1.134188172	2.89E-07	0.999999968	-1.051699737	3.17E-05	0.999999968	0.082488435
TICRR	-1.13479981	2.90E-08	0.999999997	-1.035849042	7.46E-06	0.999999997	0.098950769
THOC1	-1.146114008	2.32E-10	1	-1.160490799	2.51E-07	1	-0.014376792
TONSL	-1.157474749	2.83E-07	0.999999969	-0.984835513	3.49403E-04	0.999999969	0.172639236
CDK7	-1.158117741	3.51E-05	0.999996104	-0.83226292	0.006740316	0.999996104	0.325854821
DCLRE1B	-1.159531775	6.48E-05	0.999992796	-0.859535013	0.003297575	0.999992796	0.299996762
RRM1	-1.163855663	7.95E-05	0.999991166	-1.066559007	0.00122264	0.999991166	0.097296656
PPM1D	-1.17032895	2.33E-06	0.999999741	-1.086653491	5.19758E-04	0.999999741	0.083675459
COPS5	-1.173461324	6.96E-08	0.999999992	-1.174918054	1.18E-06	0.999999992	-0.00145673
KAT8	-1.192625092	2.28E-07	0.999999975	-1.309115872	4.62E-06	0.999999975	-0.11649078
NCAPH2	-1.203770205	7.34E-06	0.999999184	-0.674458158	0.021290023	0.999999184	0.529312046
GTF2H4	-1.209308858	3.39E-11	1	-0.995347295	9.85E-07	1	0.213961564
FZR1	-1.211366218	1.19E-11	1	-0.6669526	3.85460E-04	1	0.544413617
TRIP13	-1.212553425	1.70E-07	0.999999981	-0.98454926	3.85278E-04	0.999999981	0.228004165
SUPT4H1	-1.226964967	4.36E-06	0.999999516	-1.184084867	9.36E-05	0.999999516	0.042880101
HINFP	-1.228375501	4.37E-08	0.999999995	-1.041099163	2.85187E-04	0.999999995	0.187276339
CDK4	-1.229252468	1.08175E-04	0.999987981	-1.054519737	0.00223532	0.999987981	0.174732731
RPA2	-1.247560967	1.89E-08	0.999999998	-1.010994076	6.29E-05	0.999999998	0.23656689
UBE2I	-1.268176607	1.31E-07	0.999999985	-0.977469343	7.06388E-04	0.999999985	0.290707264
DDB1	-1.268930991	1.72E-09	1	-1.155184823	2.18E-06	1	0.113746168
TTI2	-1.286990104	6.12E-11	1	-1.539749541	3.73E-09	1	-0.252759438
ATR	-1.291043485	1.41E-07	0.999999984	-1.210676503	2.43E-05	0.999999984	0.080366982
STN1	-1.307813463	1.01E-09	1	-1.041584562	2.62E-05	1	0.266228901
SMC5	-1.372502462	1.24E-08	0.999999999	-0.717572023	0.002850351	0.999999999	0.654930439
NHP2	-1.37492816	1.73E-09	1	-1.376299318	3.26E-05	1	-0.001371158
DDX1	-1.378347942	5.38E-13	1	-1.536340219	1.38E-10	1	-0.157992277
BRAT1	-1.384128988	1.35E-09	1	-1.015259778	2.63E-05	1	0.36886921
YBX1	-1.392920742	3.80E-05	0.999992389	-1.740350813	3.80E-05	0.999992389	-0.347430071
GPS1	-1.397191665	8.90E-11	1	-1.668772551	3.87E-09	1	-0.271580886
SMC1A	-1.401416682	1.36E-09	1	-1.397096706	2.15E-06	1	0.004319976
NELFB	-1.410347624	1.07E-14	1	-1.347416491	4.09E-09	1	0.062931133
TTI1	-1.429240394	4.07E-11	1	-1.377682204	3.90E-07	1	0.05155819
GTF2H3	-1.441793994	1.14E-12	1	-1.270428534	2.15E-08	1	0.171365461
XRCC3	-1.443889834	1.51E-13	1	-1.088064552	3.18E-07	1	0.355825282
MYBBP1A	-1.448519931	2.69E-13	1	-1.532077732	3.06E-10	1	-0.0835578
ERCC3	-1.488842436	1.06E-07	0.999999988	-1.474146327	8.00E-07	0.999999988	0.014696109
DKC1	-1.540157248	2.39E-09	1	-1.09704993	2.55E-05	1	0.443107317
UBE2T	-1.545201154	5.11E-10	1	-1.635110774	3.54E-08	1	-0.08990962
PPP4C	-1.5485548	3.11E-10	1	-1.818304254	2.77E-08	1	-0.269749454
XRCC2	-1.552260107	1.04E-12	1	-0.739173379	8.75793E-04	1	0.813086728
ERCC2	-1.571883538	3.46E-12	1	-1.550486756	5.20E-09	1	0.021396781
APEX2	-1.610227732	9.31E-13	1	-1.58286698	1.17E-09	1	0.027360752

PPP6C	-1.632962193	3.12E-19	1	-1.474868263	3.09E-11	1	0.158093931
THOC2	-1.665220487	4.45E-11	1	-2.006963324	2.15E-10	1	-0.341742837
UBA2	-1.766771251	2.37E-16	1	-1.523906595	5.57E-10	1	0.242864656
TCEB1	-1.83403278	6.32E-11	1	-1.025927353	3.54E-05	1	0.808105427
TEN1	-1.902750858	4.01E-14	1	-1.547284435	8.69E-08	1	0.355466423
TCEB2	-2.008223442	3.54E-11	1	-1.656887611	3.14E-06	1	0.351335831
RFC5	-2.101292684	1.35E-18	1	-1.703344812	7.02E-09	1	0.397947871
NEDD8	-2.124387862	1.56E-13	1	-2.679174078	4.45E-12	1	-0.554786216
SOD1	-2.186500447	3.61E-15	1	-2.536809145	2.88E-13	1	-0.350308697

Appendix Table 9 List of genes showing greater enrichment in CPT treated samples than DMSO treated samples compared to the day 14 control (from related JACKS analysis).

Genes showing greater enrichment in CPT treated compared to DMSO treated (difference>0.3, FDR<10%)				
WT 5nM CPT	**WT 2nM CPT**	**E5 2nM CPT**	**G7 2nM CPT**	**Both knockouts 2nM CPT**
TP53	TP53	TP53	MAPK14	TP53
UBE2D3	RPS27L	CDKN1A	TP53	CDKN1A
POLR2A	CDKN1A	CHEK2	ENDOV	MAPK14
UBC	SOD1	SMARCC1	CDKN1A	CHEK2
CDKN1A	POLR2A	POLD3	CUL3	ZDHHC16
APEX2	UBE2D3	EME2	DNTT	POLD3
PPP4C	PPP4C	MAPK14	SHFM1	SMARCC1
FANCD2	THOC2		DCLRE1A	PBRM1
RPS27L	MDM2		CDC25A	CHFR
PCNA	GPS1		APEX1	EME2
BRD7	TINF2		GADD45G	SETD2
THOC2	APEX2		MLH3	
TTI2	TTI2		PBRM1	
MDM2	FANCD2			
DNAJC2	PCNA			
PPM1D	USP7			
SOD1	POLR2D			
RRM1	UBC			
RUVBL2	SMC5			
TINF2	PPM1D			
GPS1	TICRR			
NCAPD3	NCAPD3			
POLR2E	CCND1			
MDM4	PLK1			
NEDD8	RRM1			
CCND1	NEDD8			
POLE2	USP37			
PLK1	RUVBL2			
RPAIN	USP5			
MASTL	SF3B1			
POLR2D	MASTL			
USP5	RAD21			
CHEK2	CCNH			
DCLRE1B	DKC1			
BRCA2	MMS22L			
POLR2G	POLR2L			
SF3B1	DNAJC2			
TOP1	CDK4			
XAB2	DCLRE1B			
TICRR	RPAIN			
RAD21	COPS6			
UPF1	RUVBL1			
USP7	POLR2G			
SMC5	XAB2			
UBE2I	BRD7			
POLR2L	CHEK2			
RUVBL1	POLD3			
	COPS4			
	UPF1			
	BRCA2			
	POLR2H			
	H2AFX			
	NHP2			
	HNRNPK			
	PNN			